THE DEFORMATION AND DISSOLUTION OF SUBSURFACE SALT: EXPLORATION AND ENGINEERING IMPLICATIONS

compiled by

Neil L. Anderson*

(1992)

* Kansas Geological Survey, University of Kansas, Lawrence, Kansas
# The University of Calgary, Calgary, Alberta

TABLE OF CONTENTS

INTRODUCTION

1) CHEMICAL COMPOSITION AND MINERAL ASSEMBLAGES

A) Overview:

Evaporitic deposits are widely distributed - both stratigraphically and geographically. They range in age from Precambrian to Quaternary and are preserved in the rock record on all seven continents as outcrop and/or deeply buried strata.

A comprehensive overview of the distribution of Paleozoic salt deposits is provided by Yanshin (1984). Large-scale maps depicting the locations of the major salt basins are presented by Halbouty (1979). For recent and comprehensive overviews of evaporite sedimentology the reader is referred to Warren (1989) and Melvin (1991). For information about specific evaporitic basins the reader is referred to the bibliography (Chapter X).

Main components of ocean waters (after Braitsch 1962; 1971, table 1)

Ions	Weight %	Mol. in 1000 mol. H_2O	Fictive compounds weight % of sum of components
Na^+	1.056	8.567	78.03 NaCl
Mg^{2+}	0.127	0.976	9.21 $MgCl_2$
Ca^{2+}	0.040	0.186	3.48 $CaSO_4$
K^+	0.038	0.181	2.11 KCl
Cl^-	1.898	9.988	
SO_4^{2-}	0.265	0.514	6.53 $MgSO_4$
HCO_3^-	0.014	0.043	0.33 $CaCO_3$

Figure I:1:1 (Table 2-I; Baar, 1977)

Although the chemical composition of the sea water source (Figure I:1:1) has remained relatively constant since Precambrian time (Braitsch, 1971; Warren, 1989), evaporites exhibit a variability in their present composition unknown in other sediments (Figure I:1:2). This is attributable to several factors:

1) The original components of sea water have different solubilities. Upon the evaporation of water, the highly soluble components remain in the concentrating solution while the less soluble components precipitate. During the initial stages of the isothermal evaporation of sea water a small amount of carbonates is precipitated. Subsequently calcium sulfate and thereafter rock salt crystallizes. In the final phase of evaporation, various Na-K-Mg sulfates and chlorides are precipitated (Figure I:1:2).

Main components of salt and potash deposits in approximate order of abundance (selected from table 3 in Braitsch, 1971)

Mineral	Formula	Color (normal)	Solubility (20° C)	Remarks
Chlorides:				
Halite	NaCl	colorless to grey	26.4%	primary or secondary; rare colors: red, blue
Sylvite	KCl	white, reddish	25.6%	primary or secondary
Carnallite	$KMgCl_3 \cdot 6\ H_2O$	red, white	27.3% hygroscopic [1]	primary, secondary in pockets, fissures
Bischofite	$MgCl_2 \cdot 6\ H_2O$	colorless to white	35.1% very hygroscopic [1]	primary terminal mineral secondary in fissures
Tachhydrite	$CaMg_2Cl_6 \cdot 12\ H_2O$	yellow	very hygroscopic [1]	considered secondary
Sulphates:				
Kieserite	$MgSO_4 \cdot H_2O$	colorless to white	hygroscopic [1]	transforms into other $MgSO_4$ hydrates
Langbeinite	$K_2SO_4 \cdot MgSO_4$	colorless	slowly dissolving	usually secondary
Epsomite	$MgSO_4 \cdot 7\ H_2O$	white	26.2%	often forming in mines after kieserite
Polyhalite	$K_2MgCa_2(SO_4)_4 \cdot 2\ H_2O$	red	slowly dissolving	usually secondary
Chloride-sulphate:				
Kainite	$4\ (KClMgSO_4) \cdot 11\ H_2O$	reddish		primary or secondary

[1] Hygroscopic = deliquescent, adsorbing water from moist air.

Figure I:1:2 (Table 2-III; Baar, 1977)

2) The environmental conditions of sea water evaporation differ. The temperature, pressure and composition of evaporating seawater can vary appreciably, and particularly so in a restricted environment. These variables are a function of climate (precipitation, air humidity, air movement), basin configuration and patterns of water circulation.

3) Post-depositional changes occur to the original composition of the precipitates. (These include the conversion of carnallite to sylvite; the conversion of gypsum to anhydrite or vice-versa; the conversion of anhydrite to calcite and sulfur).

Information regarding the evaporation and post-evaporation processes can often be gleaned from the study bromine concentrations and isotope ratios. These techniques are briefly summarized in Sections I:C and I:D.

B) Isothermal evaporation of sea water:

Figure I:1:3 is a simple model from Baar (1977) which demonstrates the effects of isothermal evaporation of sea water in a conical vessel. The conical vessel could be regarded as representing the regular natural basin of evaporation; each circle indicating the remaining surface area after evaporation of water during the various phases of precipitation of solids.

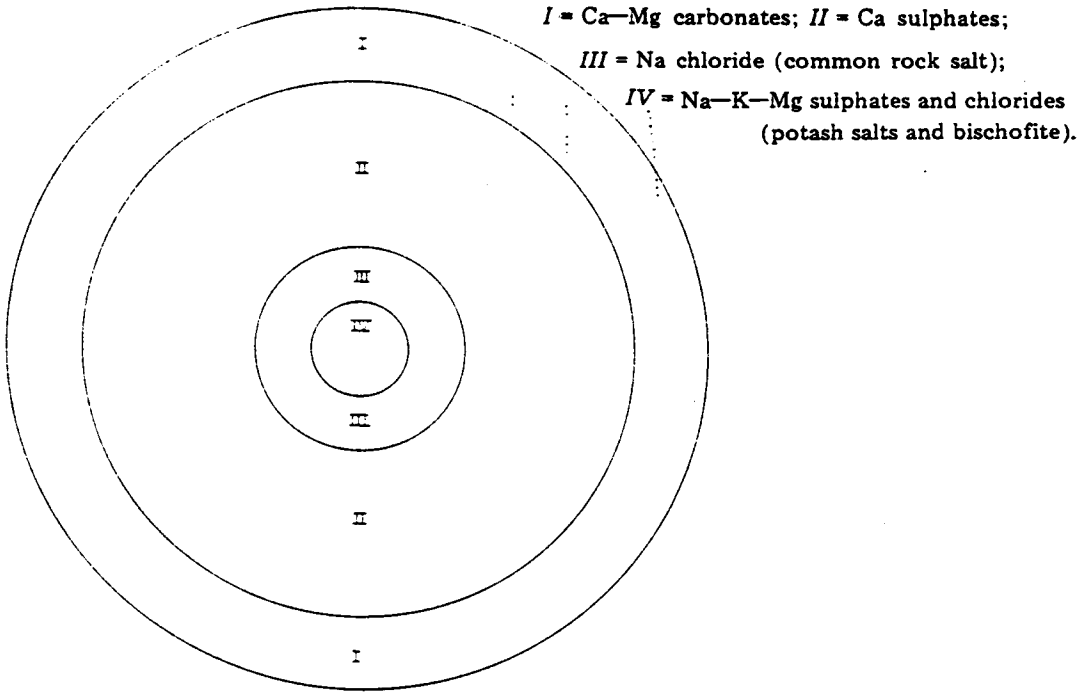

Fig. 2-1. Successive phases in the progressive evaporation of sea water. The areas of the circles represent the volume of brine at the beginning of various phases of precipitation. (After Borchert and Muir, 1964).

Figure I:1:3 (Figure 2-1; Baar, 1977)

During phase I (initiated at about 50% of original volume), small amounts of Fe_2O_3 and $CaCO_3$ (carbonate) precipitate (about 1% of the total solid precipitate). Precipitation continues to dryness. (Some researchers think that carbonate is seldom if ever chemically precipitated in nature; they suggest that the carbonate in the rock record is either an alteration product or biological in origin.)

During phase II (initiated at about 20% of original volume), $CaSO_4$ is precipitated (about 3% of the total solid precipitate). Depending upon the temperature and pressure, either gypsum ($CaSO_4.2H_2O$) or anhydrite ($CaSO_4$) will be precipitated (Figure I:1:4). These minerals cease precipitating at about 3% of the original volume.

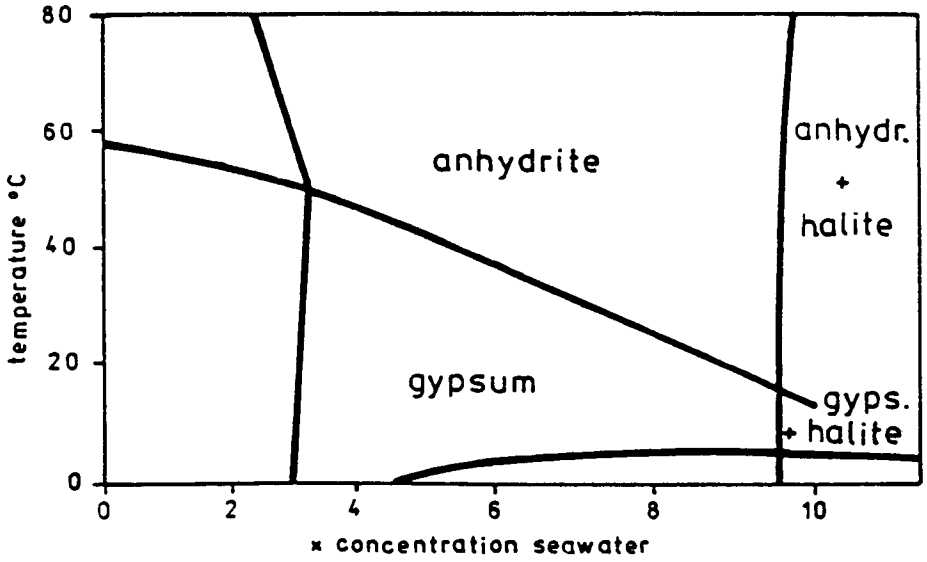

Fig. 1. Stability of gypsum and anhydrite in dependence on temperature and concentration (after Hardie, 1967).

Figure I:1:4 (Figure 1; Langbein, 1987)

During stage III (initiated at about 10% of original volume), halite is precipitated (no less than 69% of the total solid precipitate). Precipitation continues to dryness.

During stage IV (initiated at about 4% of original volume), various Na-K-Mg sulphates and chlorides crystallize. The salts of phase IV represent the remaining 27% of solid precipitate.

These laboratory proportions would be obtained in the real world only if a marginal sea evaporated to complete dryness and was completely cut off from the open sea. (These conditions have probably never been fulfilled.) The ideal natural evaporitic cycle, the result of evaporation to dryness, would consist of a thin clastic member at the base - the result of the initial marine incursion - followed upwards by limestone ($CaCO_3$), dolomite ($CaCO_3.MgCO_3$), anhydrite ($CaSO_4$), halite (NaCl) and various Mg and K bittern salts.

As a result of preferential deposition, diagenesis and post-depositional dissolution, the most commanly occurring salts are the calcium sulfates: gypsum and anhydrite. Next in order of abundance comes halite. The potash salts are much scarcer. Among this group, sylvite, carnallite, langbeinite and kainite are the most important.

C) Bromine:

A fraction of the bromine present in concentrated sea water enters crystallizing chlorides (B^- substitutes for Cl^-). Inasmuch as the bromine content of sea

water has not changed since Precambrian times, the Br/NaCl ratio in rock salt can be used to deduce the course of evaporation processes.

The bromine content of primary halite in evaporites of normal marine origin falls within the range of 50 to 100 ppm. Bromime content in excess of 100 ppm suggests precipitation from stage IV brines (Section I:B); concentrations of less than 50% suggest solution and repricipitation. If the water involved in the re-solution are not of marine origin, the bromine content may be near-zero.

Figure I:1:5 from Baar (1977), shows the normal, regular bromine profiles of the Zechstein 2 rock salt (wt% Br/NaCl as a function of depth). According to Baar, in the central portion of the basin, the regular bromine profile commences with values of 0.007 wt.% (70 ppm) at the salt base and increases slowly upwards indicating the slowly increasing concentration of the huge body of brines from which the salts were precipitated. In the shallower portions of the basin, the profiles show higher values at the base of the salt and much faster increases (Figure I:1:5), indicating that the brine moved from the shore into deeper parts of the basin where halite crystallized due to cooling (at lower salinities).

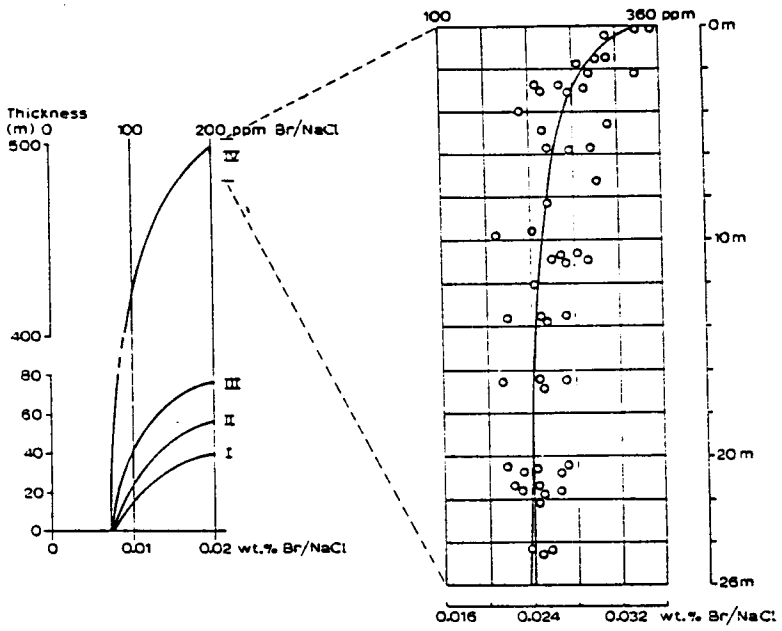

Fig. 2-6. Regular bromine profiles, Zechstein 2 rock salt (Baar, 1954b).
I—III = marginal areas; *IV* = main basin.

Fig. 2-7. Irregular bromine contents in deformed rock salt. (After Simon and Haltenhof, 1970.)
26-m section at the top of profile *IV* of Fig. 2-6.

Figure I:1:5 (Figures 2-6 and 2-7; Baar, 1977)

Baar demonstrates how normal bromine profiles of rock-salt sequences from regular progressive evaporation reflect the original depths of the basins. This author also emphasizes that only regular bromine profiles must be used in

such calculations. He points out that in salt domes and other extensively deformed structures, the original bromine concentration may have been altered by extensive recrystallization in the presence of brines with different bromine concentrations. Baar also notes that irregular bromine profiles can result from processes such as rainstorms during temporary exposure.

D) Isotope ratios (From: Posey, 1986; and Posey et al., 1987):

Posey (1986) in a study of the Hockley salt dome, describes how strontium, carbon, and oxygen isotope ratios were used to help determine the sources of fluids that formed the cap rocks (Figure I:1:6). In this study, carbon and oxygen isotope pairs were measured from calcite, whereas strontium isotopes were measured from calcite, gypsum, anhydrite, and barite. In addition, strontium concentrations were measured on most of the samples except barite.

The intrinsic properties of the isotopes of carbon, oxygen, and strontium were utilized by Posey in his investigation into the sources of salt dome cap rocks. This author notes that the isotopes of carbon and oxygen have a relatively large percent-mass differences between the light and heavy isotopes ($^{13}C/^{12}C$; $^{18}O/^{16}$); hence, they are subject to fractionation (segregation from one another) during processes such as heating or bacterially mediated reactions. Strontium isotopes, in contrast, do not fractionate measurably during natural processes; hence the strontium isotope ratio in a mineral is a direct indicator of the strontium isotope ratio of the fluid from which it formed. The characteristic properties of carbon, oxygen and strontium enabled Posey to make parallel studies of both source and process (Figure I:1:6).

Carbon and Oxygen Isotopes: According to Posey, in most solid-fluid reactions the heavy isotope of either carbon (^{13}C) or oxygen (^{18}O) partitions more effectively into the solid, and the lighter isotope (^{12}C and ^{16}O respectively) into the liquid. Similarly, for liquid-gas reactions, the light isotope partitions into the gas phase. Generally, bacterial processes promote fractionation to a higher degree than simple condensation or precipitation; as a result, bacterial processes are commonly recognizable in minerals that exhibit wide isotopic ranges. This is especially true for carbon.

Posey also states that regardless of the element, fractionation of isotopes between solid and liquid or liquid and gas decreases as temperature increases. The degree of fractionation differs for each element as well as each mineral, and the rate of change with respect to temperature is different. In addition, compared with oxygen derived from seawater, rock-derived oxygen is significantly heavier; compared with seawater-oxygen, oxygen derived from meteoric water is significantly lighter. According to Posey, these features of oxygen isotopes may be used to determine the source of a carbonate rock for which the parent fluid is not known.

According to Posey, carbon isotopes have features similar to oxygen, in that

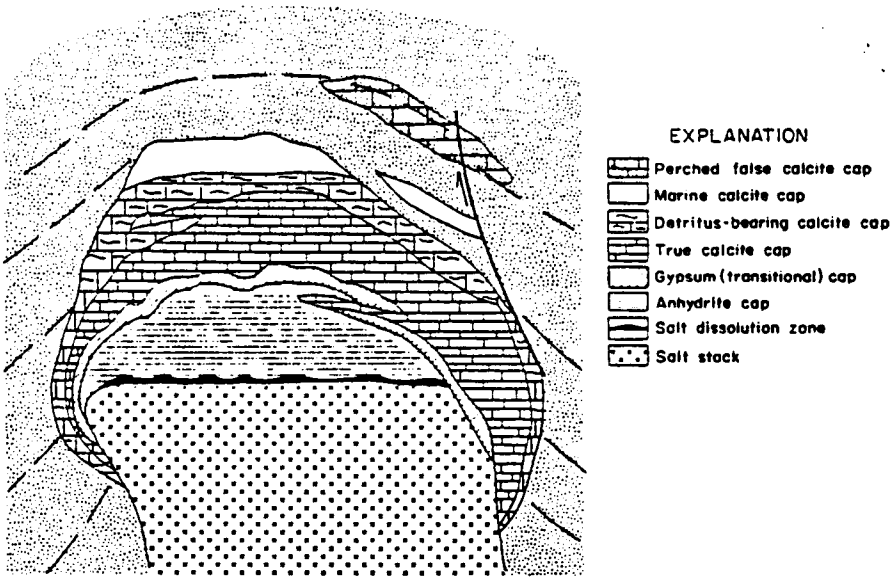

FIG. 2. Generalized cross-section of salt dome cap rocks. No scale. After POSEY (1986).

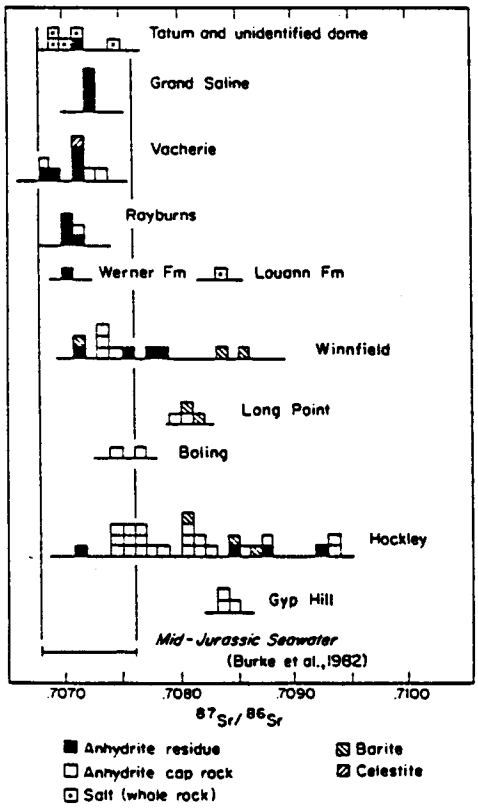

FIG. 3. $^{87}Sr/^{86}Sr$ ratios of Gulf Coast salt dome SO_4 minerals. Compilation of data from POSEY (1986), PUSHKAR *et al.* (1983), STUEBER *et al.* (1984), and RUSSELL (1985). Mid-Jurassic seawater range (BURKE *et al.*, 1981) includes all of error envelope for Middle Jurassic values.

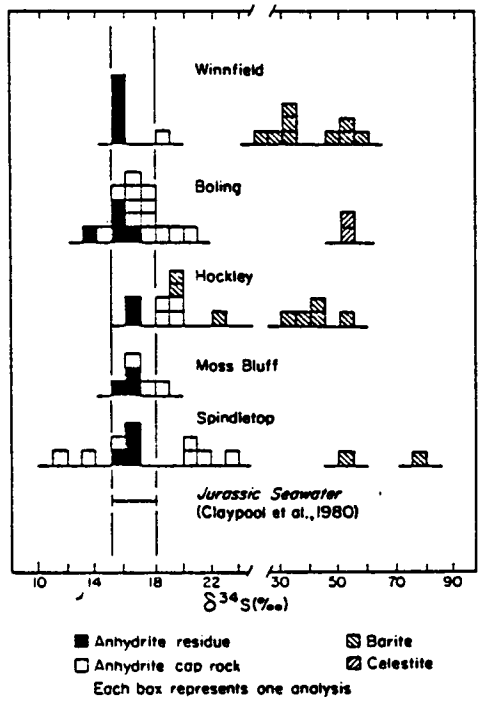

FIG. 4. Sulfur isotope composition of Gulf Coast salt dome SO_4 minerals. Note break in scale at 30‰. Compilation of data from FEELY and KULP (1957), KYLE and PRICE (1986), and unpublished data. FEELY and KULP's (1957) $^{32}S/^{34}S$ data have been re-calculated to $\delta^{34}S$ values using their CDT standard value of 22.20. Jurassic seawater $\delta^{34}S$ from CLAYPOOL *et al.* (1980).

Figure I:1:4 (Figures 2, 3 and 4; Posey et al., 1987)

fractionation decreases with increasing temperature and different carbon reservoirs have distinct carbon isotope ranges. For instance, the two most abundant carbon sources in hydrothermal solutions are CH_4 and CO_2. Carbonates precipitated from a reservoir richer in CH_4 than CO_2 will be isotopically lighter than those produced from one richer in CO_2.

Strontium Isotopes: According to Posey (1986), of the four naturally occurring isotopes of strontium (^{88}Sr, ^{87}Sr, ^{86}Sr, and ^{84}Sr) only ^{87}Sr has a radioactive parent (^{87}Rb) with a half-life brief enough to produce conventionally measurable differences in the ^{87}Sr concentration through geological time. Because the abundance of ^{87}Sr is close to that of ^{86}Sr, these two are always paired in studies of strontium isotopes. Because the abundance of ^{87}Sr increases through time it is important either to measure only those materials that contain none of the radioactive parent Rb or to correct for the amount added since a mineral was formed. All of the minerals used in Posey's study (calcite, anhydrite, gypsum, and barite) contain no Rb and thus record the $^{87}Sr/^{86}Sr$ of the fluid from which they formed at the time they formed. Minerals that have mostly mantle strontium have lower $^{87}Sr/^{86}Sr$ ratios than minerals that have mostly continental strontium (radiogenic strontium formed from the decay of ^{87}Rb).

2) ROCK SALT MECHANICS

A) General:

Rock salt and the potash salts exhibit unique physical properties and mechanical behaviour. Insitu, they are remarkably soluable, relatively impermeable and non-porous, almost incompressible, highly ductile, and rather easily deformed by creep (Figures I:2:1 and I:2:2). The plastic behaviour of rock salt is demonstrated by salt glaciers and by flowage patterns observed in salt domes.

While salt rocks in-situ exhibit plastic behaviour even in low-pressure, low-temperature regimes, the very same rocks in the laboratory exhibit elastic behaviour under most testing conditions. There are two principal reasons for this discrepancy: 1) laboratory strain rates are too high to allow for Solution Precipitation creep; and 2) laboratory samples are too dry to allow for Solution Precipitation creep (see section I:2:B). When loaded too fast and in excess of their strength, salt rocks are destroyed without any measurable deformation.

The other comman evaporites (particularly anhydrite), in contrast, exhibit near elastic behaviour. They typically deform elastically until their strength is exceeded; failure occurs more-or-less suddenly and violently without any noticeable preceding plastic deformation (Figures I:2:1 and I:2:2).

According to Baar (1977), after failure and intensive fracturing, formations which consist of elastic rock may exhibit what is often called pseudo-plastic

behaviour. Displacements between individual fragments and blocks may occur rather easily, particularly in response to tensional and/or shear stresses. Such displacements cannot be easily predicted from laboratory investigations on drill cores as the fracture patterns rather than the strength of individual cores determine the mechanical behaviour of the formation.

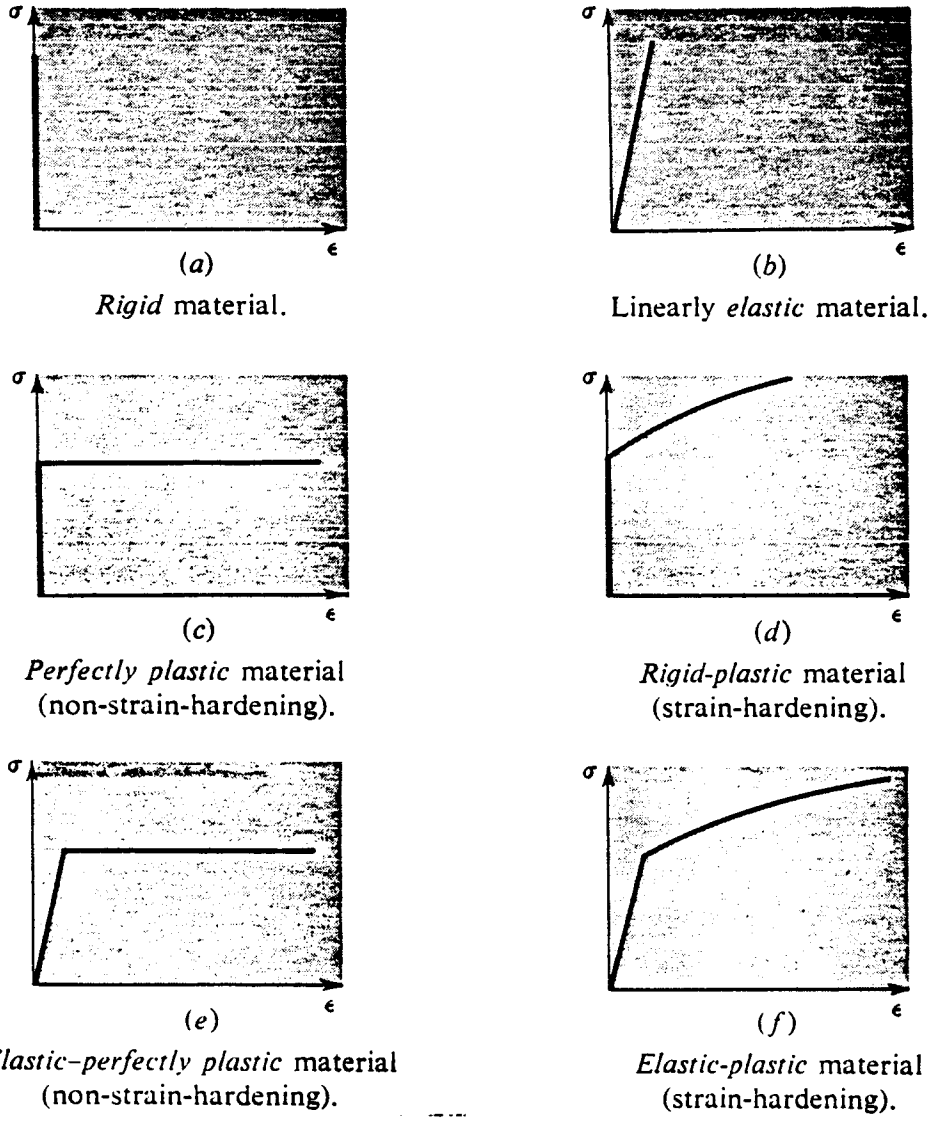

Fig. 5.7 Idealized models of material behavior.

Figure I:2:1 (Figure 5.7; Crandall et al., 1972)

This author states that at or near the surface, rational design can be based with some confidence on information provided by modern methods in geological engineering. In mining operations deep below the surface, information required for the rational prediction of overburden formations to extraction mining is frequently not available. This is particularly true for the initial mining activities in a new area. Alternatively, in areas where mining has been going on for long periods of time, careful observations and measurements can

provide the information needed for the reliable prediction of overburden reactions.

Below, some of the properties of rock salts are summarized:

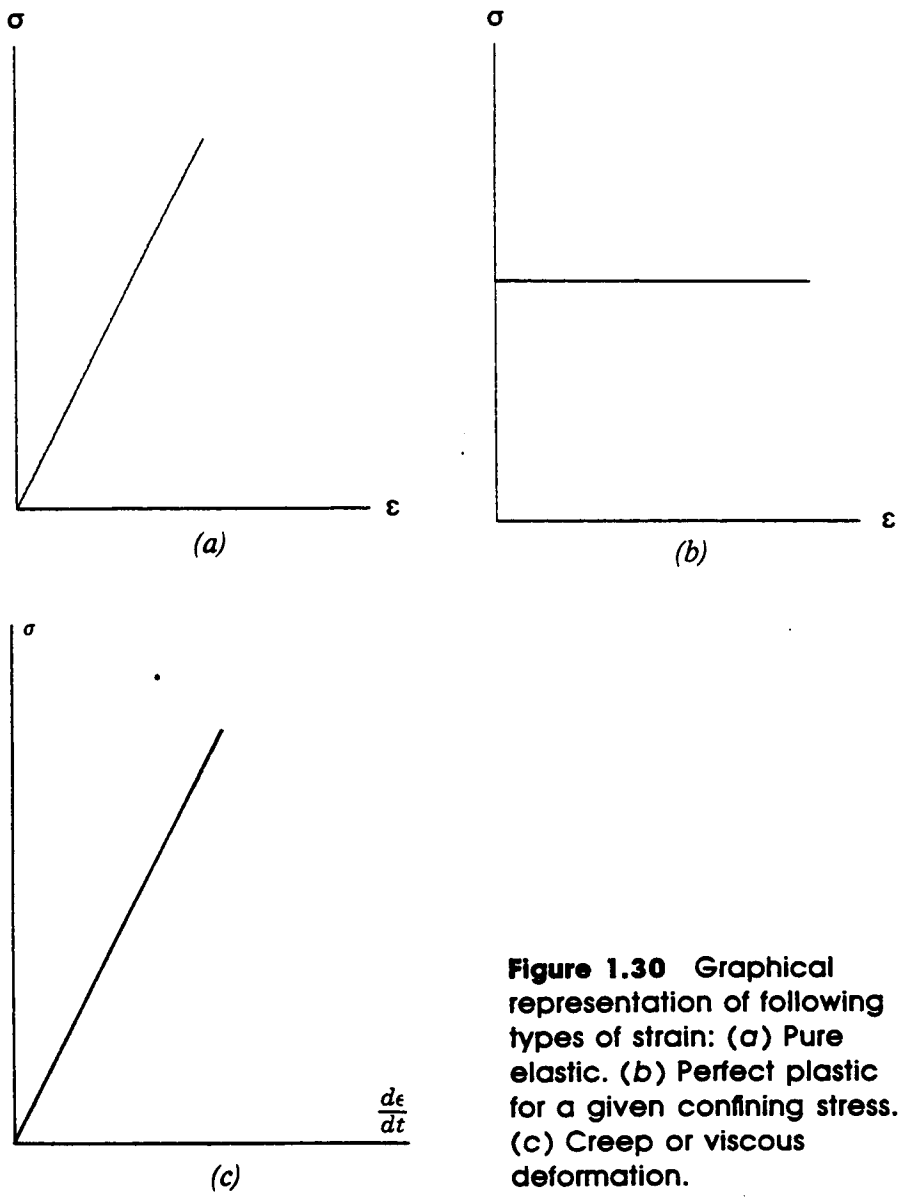

Figure 1.30 Graphical representation of following types of strain: (*a*) Pure elastic. (*b*) Perfect plastic for a given confining stress. (*c*) Creep or viscous deformation.

Figure I:2:2 (Figure 1.30; Johnson and DeGraff, 1988)

B) Mechanisms of creep in rock salt:

The total strain of any material is given by:

$$e = e_e + e_p + e_t + e_s + e_a$$

where e_e is the elastic strain upon loading, e_p is the plastic strain produced during loading, e_t is the transient or primary creep strain, e_s is the secondary or steady state creep strain and e_a is the accelerating or tertiary creep strain. According to Carter and Hansen (1983), e_e and e_p are generally less than one percent (<1%) and are not particularly significant with respect to the long-term creep of rock salt. These authors also state that the accelerating creep strain e_a is generally observed at stresses above one-half of the short-term breaking strength in unconfined creep tests and in low-temperature, low-temperature triaxial creep tests. Under these conditions, microfracturing leads to macroscopic failure by faulting (Glide mechanism; Figure I:2:3).

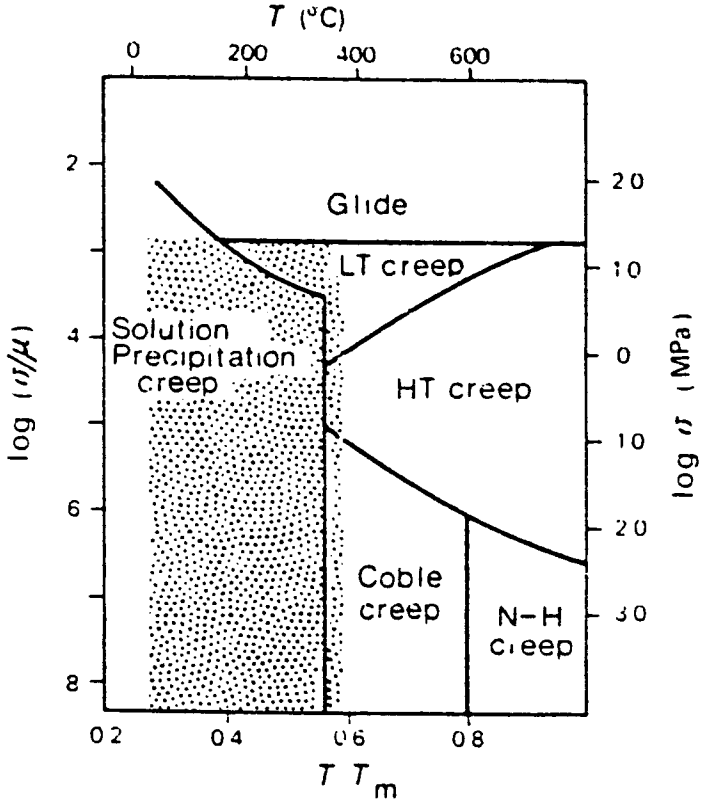

Fig. 5 Deformation mechanism map for halite (after ref. 28), modified to include solution-precipitation creep as described by the model given in the text (equation (1)). Values of the parameters *A*, *B* and *C* were chosen as for Figs 2 and 4. The map was constructed for a grain size of 1 mm and intergranular fluid pressure of 10 MPa. The extent of the solution-precipitation or solution-transfer creep field towards higher temperatures is assumed to be limited by the liquid-vapour phase transition. Stippling indicates the range of conditions relevant for halokinesis and radioactive waste repositories (the latter ranging up to only 200 °C). LT, low-temperature; HT, high-temperature; N-H, Nabarro-Herring.

Figure I:2:3 (Figure 5; Urai et al., 1985)

Transient creep e_t (LT creep mechanism; Figure I:2:3) is described by Carter and Hansen (1983) as non-recoverable and decelerating. According to these authors, this type of creep stems from the constraints placed on dislocation glide at low temperatures, where diffusion rates are low and dislocations cannot surmount obstacles to glide and climb by cross-slip. Each increment of strain makes further motion more difficult (strain hardening) and thus the creep rate decreases continuously with time.

According to Carter and Hansen (1983), steady state creep e_s encompasses Solution Precipitation creep, HT creep, Cobble creep and N-H creep (Figure I:2:3). HT creep can be thought of as non-decelerating LT creep. With respect to the former mechanism, vacancy diffusion in the higher temperature regime is thought to allow for climb by dislocation intersection processes. In the same temperature regime, but at very low stresses, stress-induced bulk vacancy diffusion (Nabarro-Herring creep) or grain-boundary diffusion are thought to occur.

In the presence of water, Solution Precipitation creep (Figure I:2:3) can occur within the low-temperature, low-pressure regime. This mechanism is described by Urai et al. (1986) as solution transfer creep; a dynamic recrystallization process.

C) Creep:

The natural creep limits - limits of elastic behaviour - of rock salts are extraordinarily small compared to most other rocks and difficult to determine in the laboratory. (Indeed many researchers think that rock salt does not have a yield point; they conclude that over time, rock salt will eventually exhibit plastic deformation; Figures I:2:1 and I:2:2).

With respect to mining, **from a practical perspective**, rock salt behaviour in-situ and over the short term can be considered to be elasto-plastic; this means that the behaviour can be modelled as elastic (in the short term) unless differences in the principal stresses are excessive and deformation occurs (LT creep and/or Glide creep; section I:2:B). If and when the stress difference exceeds the short-term, practical elastic limit, rock salt in-situ begins to deform plastically, and continues to creep until the limit of elastic behaviour is re-established. (Note: In the long term, salt behaves as a plastic even in low-temperature, low-pressure conditions.)

D) Plastic deformation:

The plastic deformation of rock salt in-situ does not cause structural damage or fractures; rock salt is self-annealing. Indeed one of the fundamental principles in salt-mining operations is to ensure that plastic deformation as opposed to fracturing or structural damage occurs (Figures I:2:1 and I:2:2).

Dilatency and failure due to accelerating creep strain e_a is generally observed

at stresses above one-half of the short-term breaking strength in unconfined creep tests and in low-temperature, low-temperature triaxial creep tests. Under these conditions, microfracturing leads to macroscopic failure by faulting (Glide mechanism; Figure I:2:3).

E) Strain hardening:

In laboratory testing, strain hardening (Figures I:2:1) of rock salt typically occurs; as a consequence decreasing creep rates (Transient creep; section I:2:B) are observed. In-situ, the long term creep deformation of salt rocks is not affected by strain hardening and steady state creep occurs until elastic behaviour is re-established. There are two principal reasons for the discrepancy between laboratory and in-situ observations: 1) laboratory strain rates are generally too high to allow for Solution Precipitation creep; and 2) laboratory samples are too dry to allow for Solution Precipitation creep (section I:2:G). In-situ, the deformation of rock salt generally occurs in the presence of trace brine and under low stress differentials.

According to Jackson and Talbot (1986), the strain rates for the in-situ deformation of rock salt vary by over 8 orders of magnitude from $10^{-8}s^{-1}$ to $10^{-16}s^{-1}$. According to these authors, the most rapid rates are those of borehole closure during accelerating creep ($10^{-8}s^{-1}$), mine closures and steady state borehole closures ($10^{-9}s^{-1}$ to $10^{-11}s^{-1}$) and namakiers (salt glaciers; $10^{-8}s^{-1}$ to $10^{-11}s^{-1}$). The rates of diapiric extrusion assisted by folding ($10^{-13}s^{-1}$) and the rates for the most active phase of gravity driven diapiric growth are significantly lower ($10^{-8}s^{-1}$ to $10^{-11}s^{-1}$). These rates are significantly lower than the strain rates at which laboratory specimans are typically tested ($>10^{-7}s^{-1}$).

F) Temperature effects:

Thermal activation plays a major role in creep phenomona in-situ. As is indicated in Figure I:2:3, the mechanisms of creep are a partial function of temperature. As the temperature of rock salt (in the presence of trace brine and under low stress differential) is increased, the dominant creep mechanism changes from Solution Precipitation creep to HT creep, Cobble creep or N-H creep. From a practical perspective, this transformation allows for a greater rate of strain (Figure I:2:4).

G) Pressure effects:

Differential pressure plays a major role in creep phenomona in laboratory experiments. As is indicated in Figure I:2:3, the mechanisms of creep are a partial function of differential pressure. As the differential pressure of rock salt (in the presence of trace brine) is increased, the dominant creep mechanism changes from either Solution Precipitation creep, LT creep, HT creep, Cobble creep or N-H creep (depending upon the temperature) to Glide. From a practical perspective, an increase in the differential stress, during laboratory testing, results in: 1) a greater rate of strain; 2) a decrease in the

time-to-failure; and 3) a decrease in total strain prior to failure (Figure I:2:5). Generally rock salts in-situ are deformed under relatively low differential pressures; hence Solution Precipitation creep, LT creep, HT creep, Cobble creep or N-H creep predominates (depending upon the temperature).

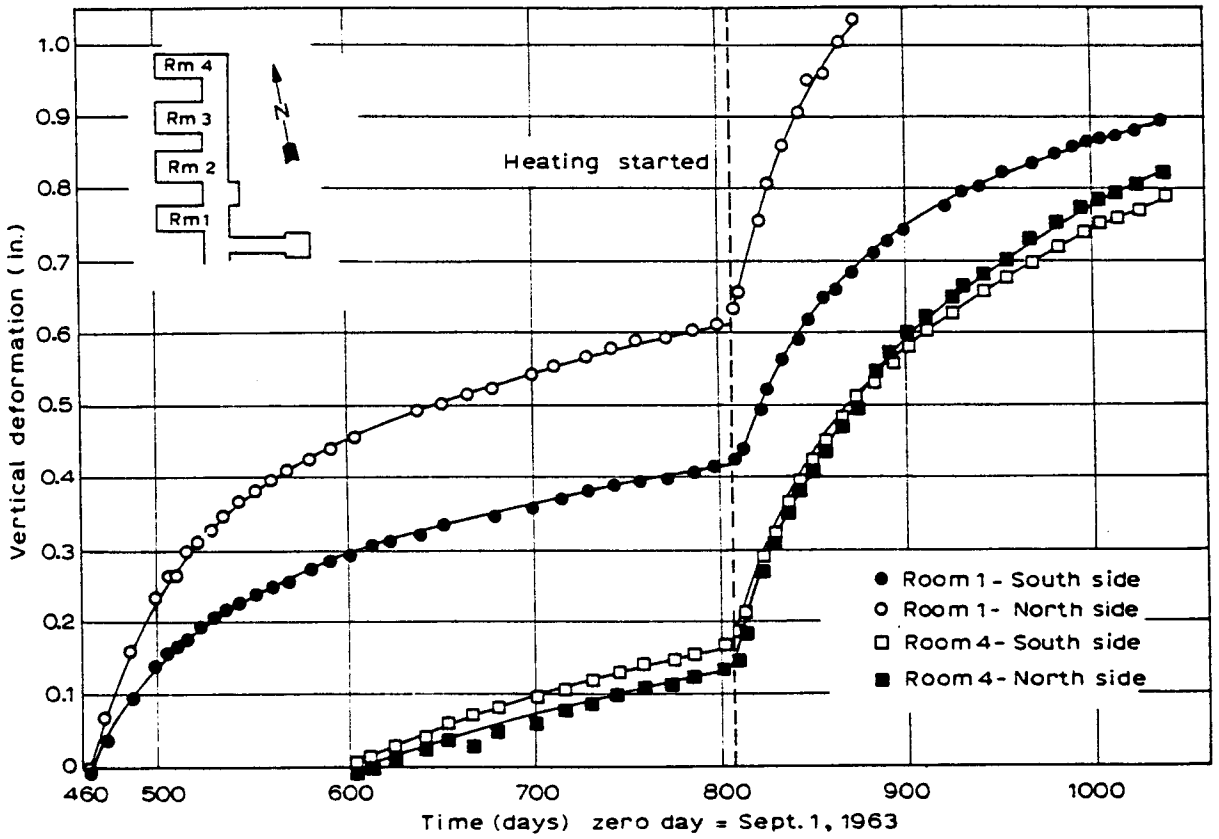

Fig. 3-10. Accelerated creep caused by heating of a salt-mine pillar; peak temperatures were about 150°C. (After Empson et al., 1970.)

Figure I:2:4 (Figure 3-10; Baar, 1977)

H) Effect of time:

Time plays a major role in creep phenomona in laboratory experiments. As is indicated in Figure I:2:6, greater differential pressures are required to cause failure over shorter time intervals, and result in higher strain rates prior to failure. These results are consistent with the thesis that rock salt does not have a yield point; and that over time, rock salt under differential stress will eventually exhibit measurable plastic deformation (Figure I:2:6). These results also support the premise that the creep mechanisms are a function of differential pressure and strain rate.

Again, while salt rocks in-situ exhibit plastic behaviour even in low-pressure, low-temperature regimes, the very same rocks in the laboratory exhibit elastic

behaviour under most testing conditions. There are two principal reasons for this discrepancy: 1) laboratory strain rates are too high to allow for Solution

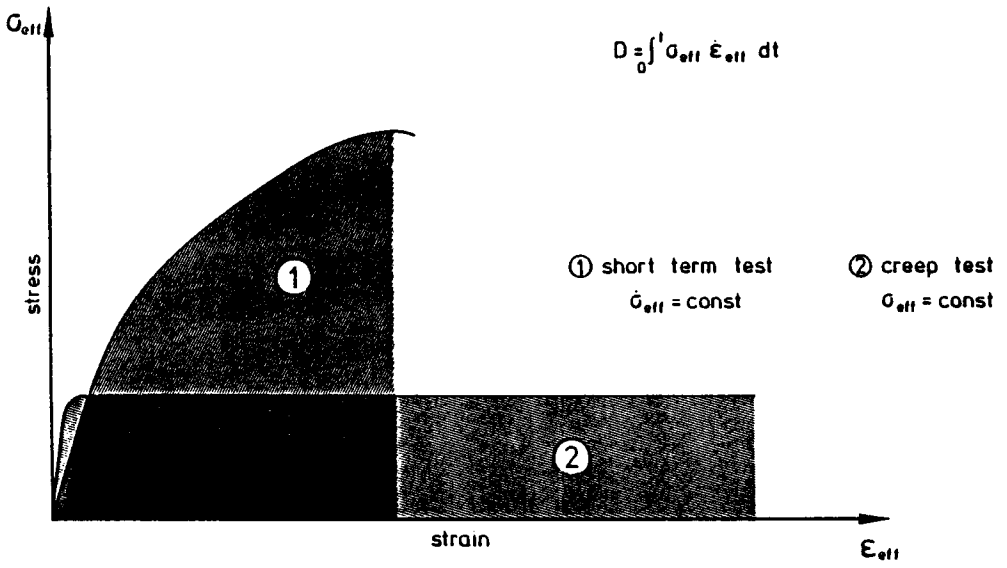

Figure 2. Determination of the Plastic Deformation Energy

Figure I:2:5 (Figure 2; Rokar and Staudtmeister, 1985)

Precipitation creep (Section I:2:B); and 2) laboratory samples are too dry to allow for Solution Precipitation creep (Section I:2:B). When loaded too fast and in excess of their strength, salt rocks are destroyed without any measurable deformation.

Generally rock salts in-situ are deformed under relatively low differential pressures and at low strain rates; hence Solution Precipitation creep, LT creep, HT creep, Cobble creep or N-H creep predominate (depending upon the temperature).

I) Effect of water:

The presence of even trace amounts of brine has a marked effect on the deformation of rock salt in laboratory tests (Figures I:2:8 and I:2:9). Tests on dry dilated salt show more-or-less conventional dislocation creep behaviour (Glide); brine-bearing samples, in contrast, show a marked weakening at low strain rates (low differential stress). According to Urai et al. (1986) this is associated with dynamic recrystallization and a change of deformation mechanism to Solution Precipitation creep.

These authors surmise that trace amounts of brine are present in rock salt in-situ, and that the presence of such fluid accounts for the observed discrepency between typical laboratory and in-situ observations. Rock salt under typical laboratory conditions (dry) deforms as an elasto-plastic; rock salt in-situ deforms as a plastic. Indeed the salt glaciers in Iran flow under gravitational

stresses alone.

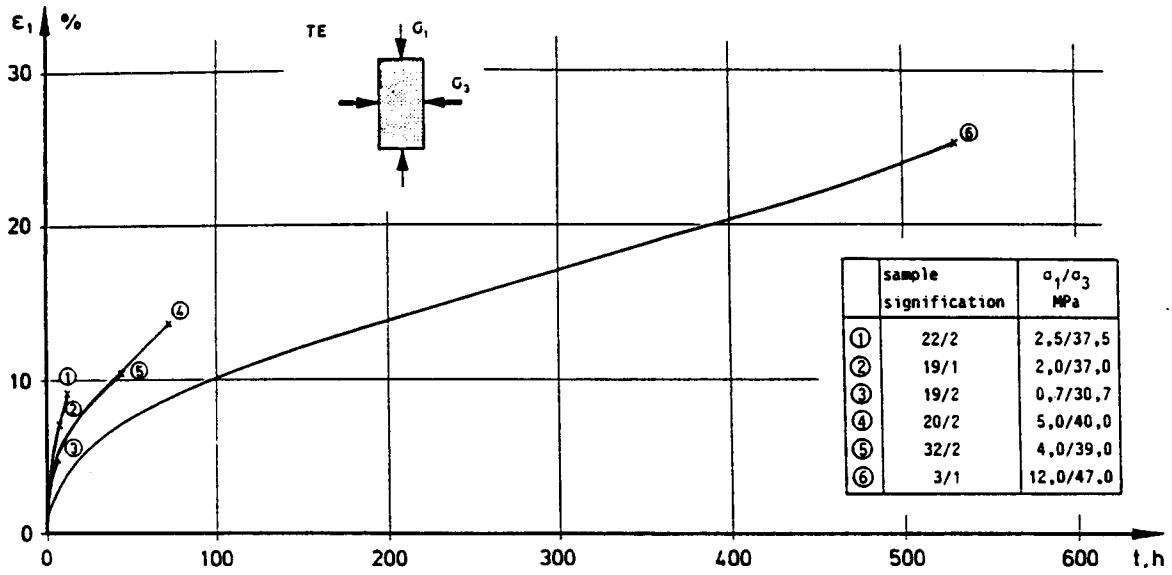

Figure 7. Results of Creep Rupture Tests, Location Asse

Figure I:2:6 (Figure 7; Rokar and Staudtmeister, 1985)

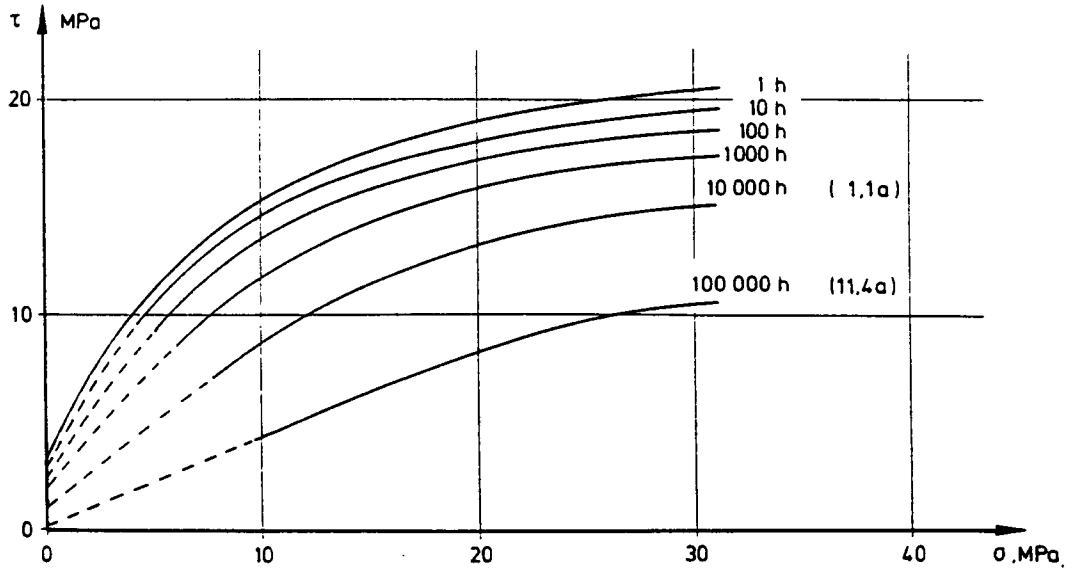

Figure 10. Time-dependent triaxial strength, Mohr's envelope

Figure I:2:7 (Figure 10; Rokar and Staudtmeister, 1985)

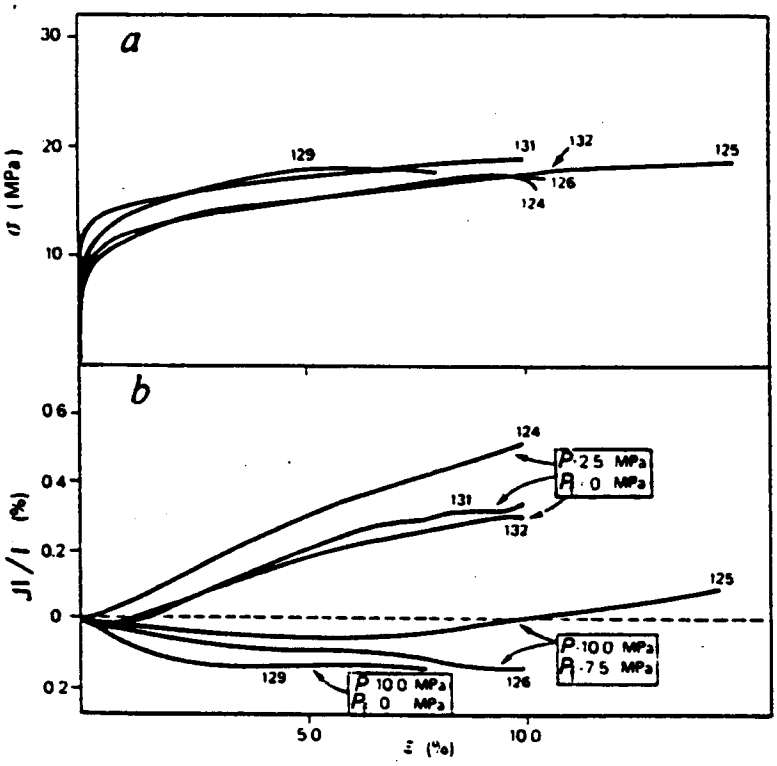

Fig. 1 *a*, Differential stress (σ) and *b*, volume change ($\Delta V/V$) plotted against strain (ε) for the pre-relaxation stage of the deformation experiments on natural (Asse) samples. $T = 150$ °C; $\dot{\varepsilon} = 3 \times 10^{-5}\ s^{-1}$. The confining pressure (P) and pore fluid (brine) pressure (P_f) used in each test are indicated. Note that samples deformed at $P = 2.5$ MPa show substantial dilatancy (volume increase) compared with those deformed at $P = 10$ MPa.

Figure I:2:8 (Figure 1; Urai et al., 1985)

3) OTHER PROPERTIES OF SALT ROCKS

A) Porosity and permeability:

According to Baar (1977), consolidation of salt deposits by diagenetic crystallization and recrystallization takes place relatively rapidly. The author cites a typical example: 40% initial porosity, 30% when under 0.15 m of salt, 20% under 0.3 m of salt, 15-20% under 0.6 m of salt, 5-10% under 6-12 m of salt, and then eventually to nearly zero with deeper covering. He further states that vertical permeability ceases at depths of between 20-30 m; lateral permeability may exist at depths of up to 300 m if non-evaporitic facies are present in the section. Despite the near absence of porosity and permeability, rock salt always contains some brine. This fluid facilitates Solution Precipitation creep at low temperatures and low differential prssure regimes.

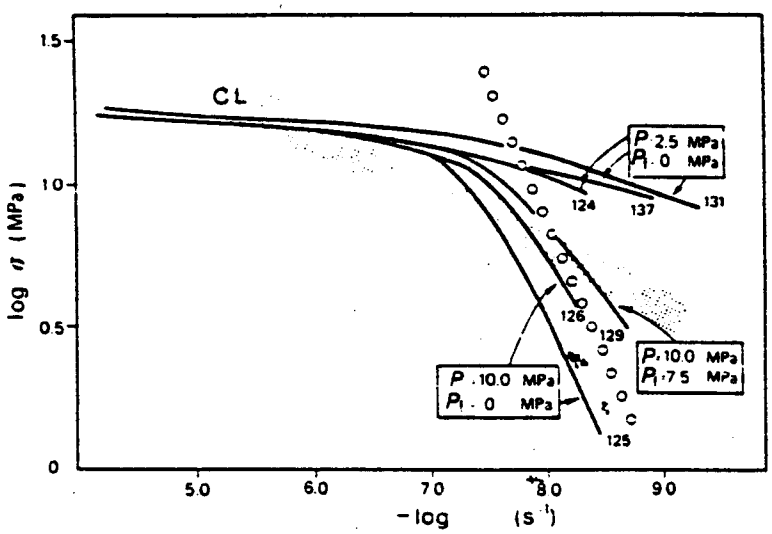

Fig. 2 Differential stress (σ) plotted against strain rate ($\dot{\varepsilon}$) (solid curves) for the stress relaxation stage of the experiments shown in Fig. 1. Note the dramatic weakening effect seen in samples deformed in non-dilatant conditions ($P = 10.0$ MPa), at strain rates of $<10^{-7}$ s^{-1}. This low-strain-rate behaviour can be described by a power-law creep equation, $\dot{\varepsilon} = A\sigma^n$, where the stress exponent (or stress sensitivity of strain rate, n) has a value of 1–2. Samples deformed in dilatant conditions ($P = 2.5$ MPa) are stronger than predicted by previously existing creep laws[1,3,4,25] (stippled area, Cl) but exhibit similar stress sensitivity (n values) at the lower strain rates. Note that the weakening behaviour observed in non-dilatant conditions ($P = 10.0$ MPa) agrees well with predictions based on the solution-precipitation creep model given in the text (equation (1)). This model was applied to the recrystallized samples using $d = 3$ mm, $a = 44$ (ref. 18) and $C = 8 \times 10^{-8}$ m (ref. 8). The diffusivity parameter B was estimated from published data[8].

Figure I:2:9 (Figure 2; Urai et al., 1985)

B) Thermal conductivity:

Rock salt has a higher thermal conductivity (about 6 W/m/°C) than that of comman clastic rock types (in the range of 1.5-2.5 W/m/°C). As a consequence an enhanced heat flux is associated with salt deposits and with salt domes in particular.

In a their study of the influence of salt domes on paleotemperature distributions, O'Brien and Lerche (1984) present a simple analytical model of heat flow in the vicinity of an isolated salt dome (Figure I:3:1). In addition to an enhanced surface heat flow, their model shows that on the upper flanks of a

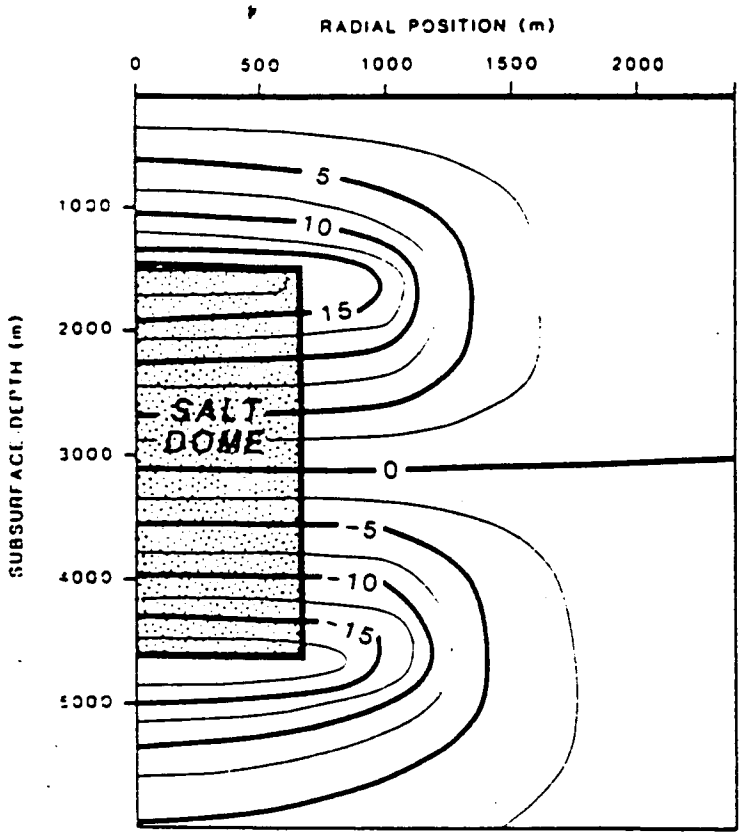

Figure 7. Contour plot of subsurface temperature anomaly (°C) for a salt dome of height 3,000 m and radius 600 m. Horizontal exaggeration is 2:1.

Figure I:3:1 (Figure 7; O'Brien and Lerche, 1984)

salt dome a temperature higher than the regional trend is predicted, thus enhancing hydrocarbon maturation at these depths. On the lower flanks of the salt dome a temperature lower than the regional trend is predicted, thus inhibiting overmaturation.

C) Density:

The density of comman clastic rocks generally increases with depth of burial as a result of both chemical and physical compaction (Figure I:2:10). The density of rock salt in contrast, at depths of greater than about 30 m (see section), decreases with increasing depth of burial. This characteristic of salt is attributable to thermal expansion at depth.

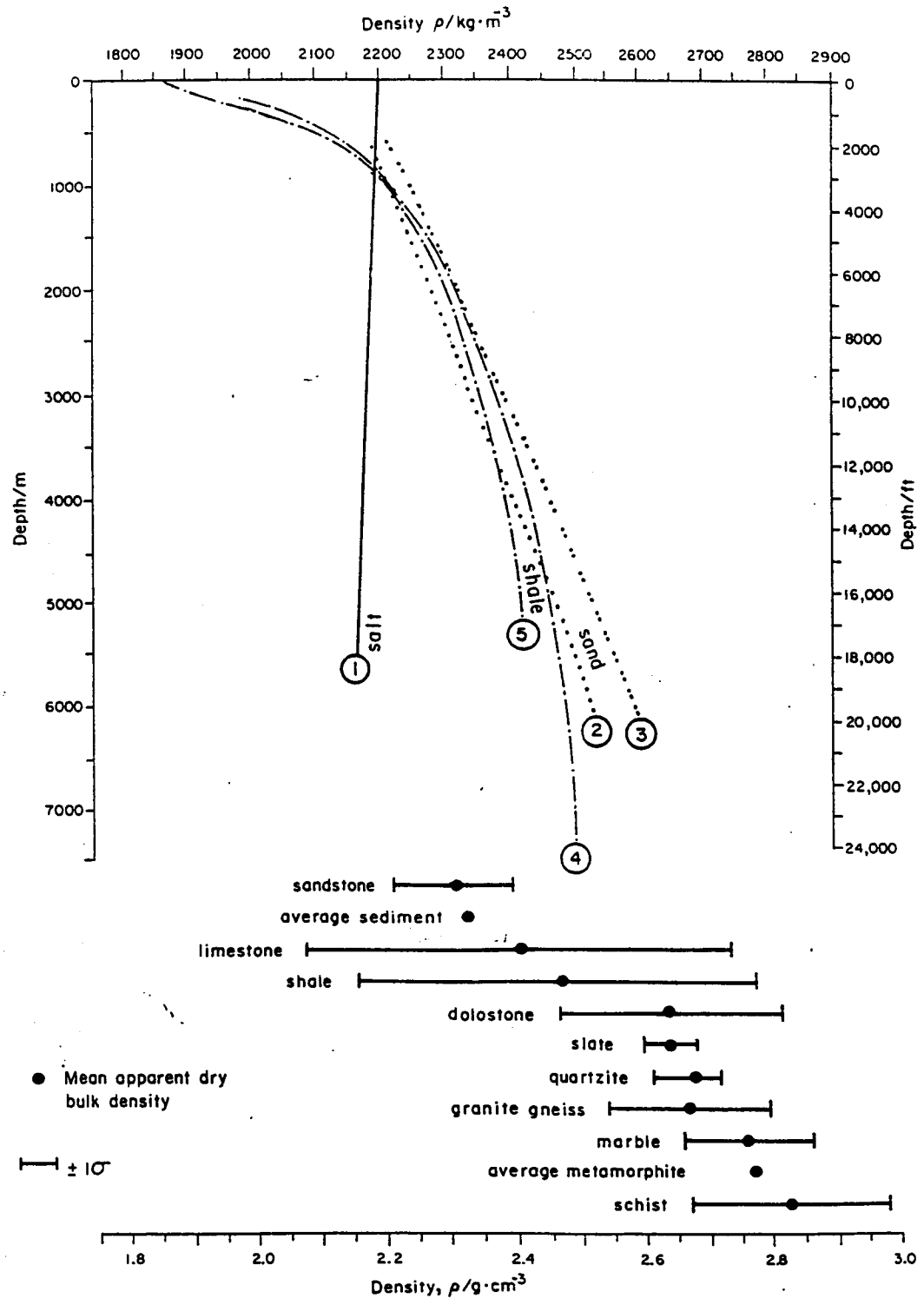

Figure 6. Relation between bulk density and depth in salt and associated terrigenous clastics in the United States Gulf Coast. 1. Rock salt with a few percent anhydrite has a density close to 2,200 kg · m^{-3}, but on burial with a geothermal gradient of 30 °C · km^{-1}, it expands by heat more than it contracts by confining pressure, thus lowering the density slightly (Clark, 1966; Gussow, 1968). 2, 3. 4,393 and 3,171 specimens of brine-filled nonmatrix and matrix lower Tertiary sandstone, calculated from porosity data of Loucks and others (1979) by equation 1 of Chapman (1974), assuming grain density of 2,650 kg · m^{-3} and brine density of 1,070 kg · m^{-3}. 4. Brine-filled Tertiary shale (Dickinson, 1953). 5. Brine-filled shale (Gardner and others, 1974). Mean apparent dry bulk densities of common sedimentary and metamorphic rocks (impermeable mass/bulk volume) ± 1 standard deviation. Sample size of individual rock types averages 184 (Touloukian and others, 1981).

Figure I:3:2 (Figure 6; Jackson and Talbot, 1986)

4) REFERENCES

Baar, C.A., 1977, Applied salt-rock mechanics 1: Elsevier Scientific Publishing Company, 294 p.

Braitsch, O., 1971, Salt deposits - their origin and composition: Springer, 297 p.

Carter, N.L. and Hansen, F.D., 1983, Creep of rock salt: Tectonophysics 92, 275-333.

Crandall, S.H., Dahl, N.C. and Lardner, T.J., 1972, An Introduction to the Mechanics of Solids: McGraw-Hill, New York, 628 p.

Friedman, G.M., 1978, Principles of sedimentology: John Wiley and Sons, 792 p.

Halbouty, M.T., 1979, Salt domes: Gulf Publishing Company, Houston, 561 p.

Jackson, M.P.A. and Talbot, C.J., 1986, External shapes, strain rates, and dynamics of salt structures: Bulletin Geological Society of America 97, 305-323.

Johnson, R.B. and DeGraff, J.V., 1988, Principles of Engineering Geology: John Wiley and Sons, New York, 497 p.

Melvin, J.L. (Editor), 1991, Evaporites, Petroleum and Mineral Resources; Elsevier, New York, 556 p.

O'Brien, J.J. and Lerche, I., 1984, The influence of salt domes on paleo-temperature distributions, Geophysics 49, 2032-2043.

Posey, H.H., 1986, Isotope geochemistry of the Hockley Dome cap rock, *in* Comparison of cap rocks, mineral resources, and surface features of salt domes in the Houston diapir province: Geological Society of America and Society of Economic Geology Special Publication, 185-207.

Posey, H.H, Kyle, J. R., Jackson, T.J. and Hurst, S.D., 1987, Multiple fluid components of salt diapirs and salt dome cap rocks, Gulf Coast, U.S.A.: Applied Geochemistry 2, 523-534.

Rokar, R.B. and Staudtmeister, K., 1985, Creep rupture criteria for rock salt, *in* Schreiber, B.C. and Harner, H.L., Eds., Sixth International Symposium on Salt: Salt Institute Inc., Virginia, 1, 455-462.

Urai, J.L., Spiers, C.J., Zwart, H.J. and Lister, G.S., 1986, Weakening of rock salt by water during long-term creep: Nature 324, 554-557.

Warren, J.K., 1989, Evaporite Sedimentology: Prentice-Hall, Eaglewood Cliffs, N.J., 285 p.

Yanshin, A.L., Ed., 1984, Paleozoic Salt Bearing Formations of the World: Springer-Verlag, 427 p. (Original text authored by Zharkov, M.A.).

II: DISSOLUTION OF ROCK SALT

1) OVERVIEW

The dissolution of salts can occur as a result of a number of different processes including:

1) faulting;

2) folding;

3) flow (due to isostatic or tectonic forces, gravity, thermal convection)

4) chemical transformations (for examples: the conversion of carnallite to sylvite (Figure IV:1:1); the conversion of gypsum to anhydrite or vice-versa (Figures IV:1:2 and IV:1:3) etc.).

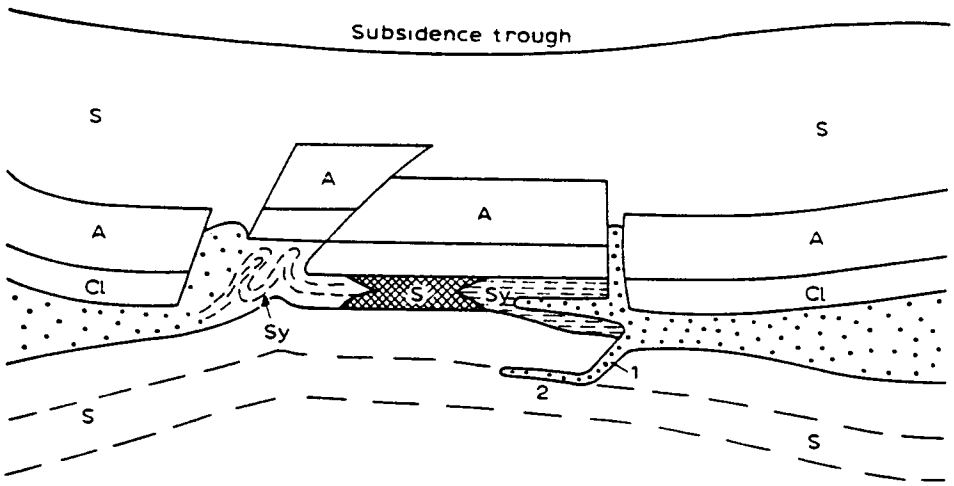

Fig. 2-20. Deformations caused by carnallite conversion to sylvite (Baar, 1958).
Final state after re-consolidation, shown in a schematic section of geological conditions encountered after events schematized in Fig. 2-19.
Carnallite stippled; *Sy* = sylvinite; *1* = former shear fracture; *2* = former bed separation void.

Figure II:1:1 (Figure 2-20; Baar, 1977)

2) DISSOLUTION AND MASS TRANSPORT OF HALITE

The solubility of halite (359 g NaCl/l H_2O at 25 °C) varies somewhat (depending upon temperature, pressure, and the concentrations of other solutes), but it is one to three orders of magnitude higher than the solubilities of anhydrite and limestone under normal groundwater conditions. The dissolution of halite (rock salt) is essentially instantaneous relative to the time scale of the transport process in the

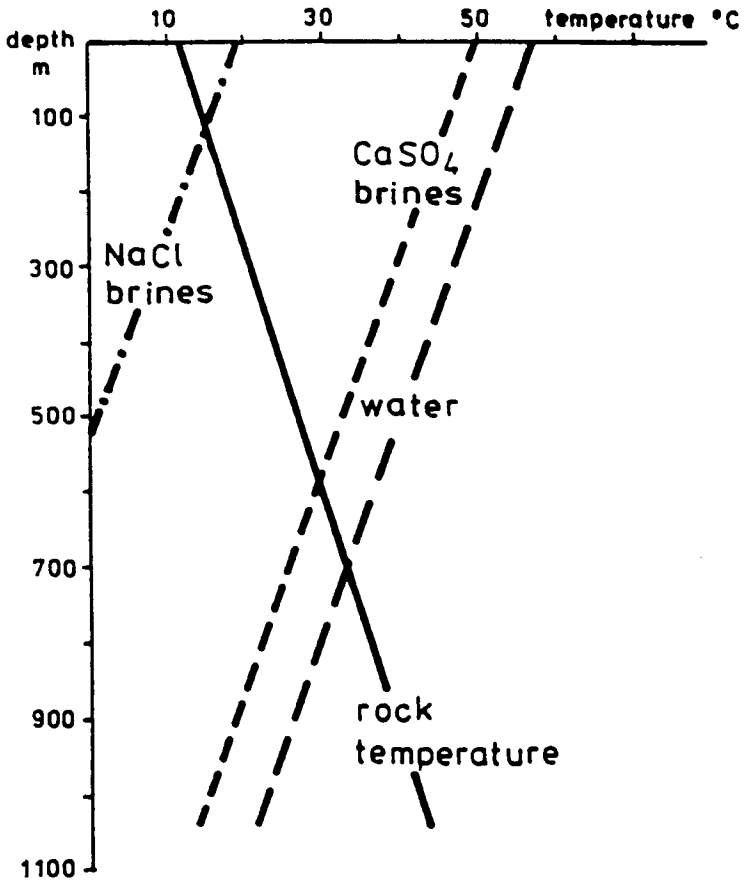

Fig. 2. The point of the changing of anhydrite and gypsum in dependence on temperature, depth, and the types of brines.

Figure II:1:2 (Figure 2; Langbein, 1987)

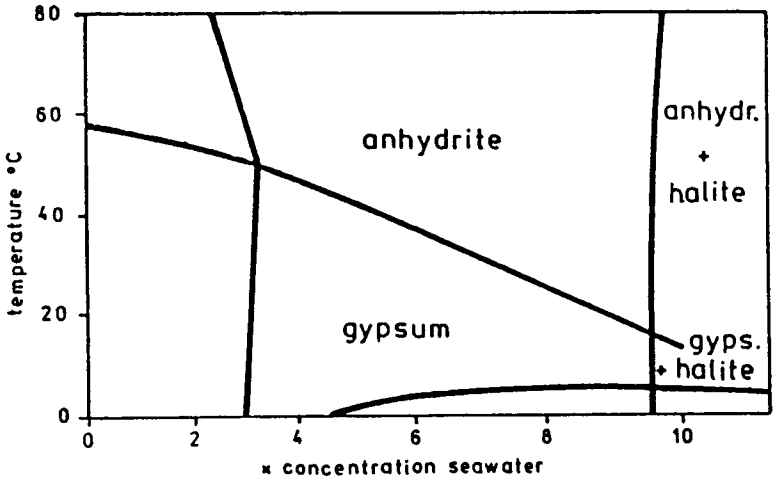

Fig. 1. Stability of gypsum and anhydrite in dependence on temperature and concentration (after Hardie, 1967).

Figure II:1:3 (Figure 1; Langbein, 1987)

presence of unsaturated water; the rate of solid rock salt removal is therefor controlled by the convective and/or diffusive flux of sodium and chloride ions away from a halite-bearing formation. Transport mechanisms include molecular diffusion, free convection and by forced convection.

Mass transport by diffusion is a very slow process. Davies (1989) cites the following example: in the situation where a halite unit is separated from an underlying fresh-water aquifer by a 10 m thick aquiclude having a *De* value of 10^{-11} m^2/s, the regional halite removal rate is on the order of 5 microns per year. In most natural situations, the water in the aquifer has higher initial salinities and the *De* values of the aquiclude are most likely a few orders of magnitude lower. Therefore, in most situations, halite removal rates controlled by diffusion are much less than one micron per year (Davies, 1989).

According to Davies (1989), mass transport by free convection (driven by gravity acting on an inverted fluid density gradient), is much faster than transport by diffusion alone. Davies cites as an example, a situation where a 1-m wide fracture zone with a hydraulic conductivity of 10^{-4} cm/s transects the aquiclude described in the previous paragraph. The localized halite removal rate for this scenario is on the order of a few centimeters per year, which is orders of magnitude higher than the removal rate for diffusion alone (Davies, 1989).

According to Davies (1989), once salt-rich brine passes from a fracture zone into an underlying aquifer, the mode of mass transport is altered significantly. Forced convection through the aquifer, driven by a regional head gradient, becomes the primary transport mechanism. However, if the vertical component of the external head gradient is small, the vertical component of flow may still be primarily driven by buoyancy (Davies, 1989).

3) LARGE-SCALE MECHANISMS OF NATURAL DISSOLUTION

A) Overview:

Anderson (1992) studied the dissolution of the main Devonian salts in western Canada (Chapters VII and VIII) and concluded that, in general, the inferred major episodes of dissolution were initiated and/or enhanced by one or more of the following seven principal processes: 1) the centrifugal flow of unsaturated groundwater from the basin interior and towards the basin margin; 2) the near-surface exposure of the salts as a result of erosion; 3) the centripetal (basinward) flow of unsaturated waters from the basin margin and towards the basin interior; 3) regional faulting/fracturing; 4) pressure dissolution/localized fracturing; 5) glacial loading and/or unloading; 6) dissolution of the underlying salt; and 7) salt flow. In addition the researchers conclude that leaching is often self-perpetuating; a process whereby fractures, created by the collapse of overlying strata, provide conduits for water thereby facilitating further dissolution.

B) Centrifugal-flow: (Figure II:2:1)

Sediments in the shallow subsurface of a subsiding, juvenile basin are subjected to diagenesis; the sum total of all physical, chemical and biochemical changes in a sedimentary deposit after burial (excluding metamorphism). Many facets of diagenesis involve the expulsion of interstitial waters of various origin (eg. physical compaction of sediment, dehydration of clay minerals, the conversion of gypsum to anhydrite).

According to Perrodon (1983), in normally-pressured sediment, this interstitial water is progressively expelled from the deepest zones subjected to the highest pressures, and migrates towards zones with a weaker potential, laterally towards the edges and vertically through the beds into the surface layers. As a result of the thermal expansion of the deep aquifers, interstial water at depth also flows from the warmer basin center towards the colder basin margins Figure II:2:1). Generally, as a result of electrofiltration, the expelled waters are less saline than the interstitial waters that remain.

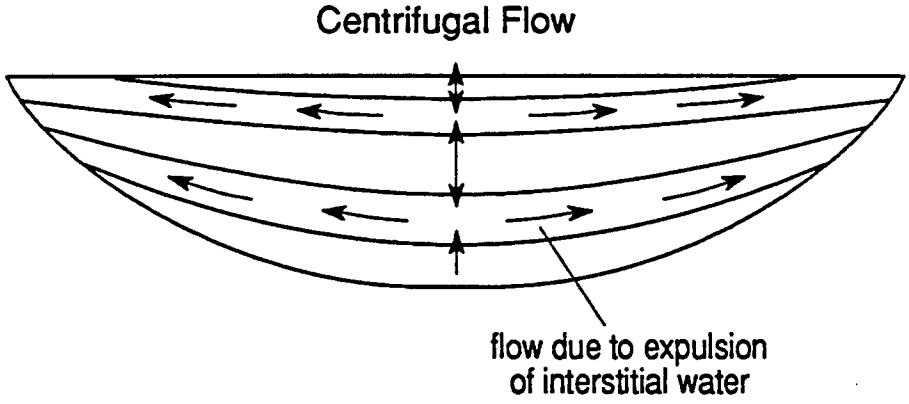

Figure II:2:1 (Anderson, 1991)

The outward flow of unsaturated interstitial waters in response to burial, could result in the dissolution of subsurface salt. For example, leaching, as a result of the lateral flow of fluids, could occur along the upper and lower surfaces of salt beds in those places where the salt beds and aquifers were juxtaposed. Perhaps the most extensive dissolution would occur near the outer margins of the salt bed, as a result of the increased relative vertical permeability and the focusing of vertically migrating waters.

C) Near-surface exposure: (Figure II:2:2)

Salt is chemically unstable at the earth's surface and under typical atmospheric conditions is readily dissolved. As a result, it is rarely preserved in either outcrop or subcrop. The inference is that dissolution will generally

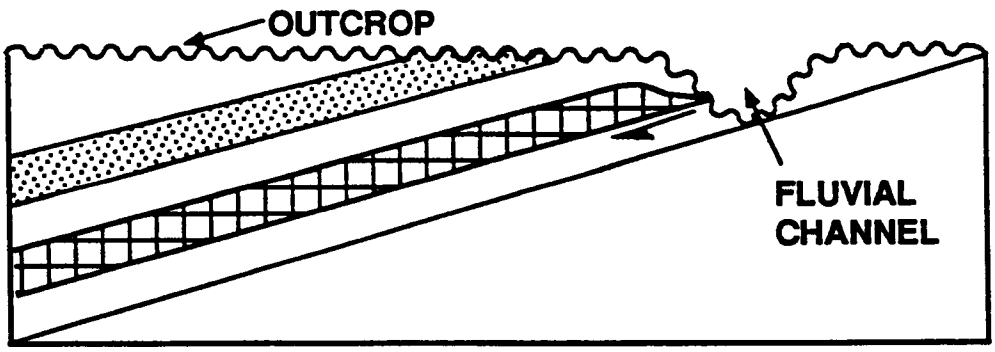

STAGE 1

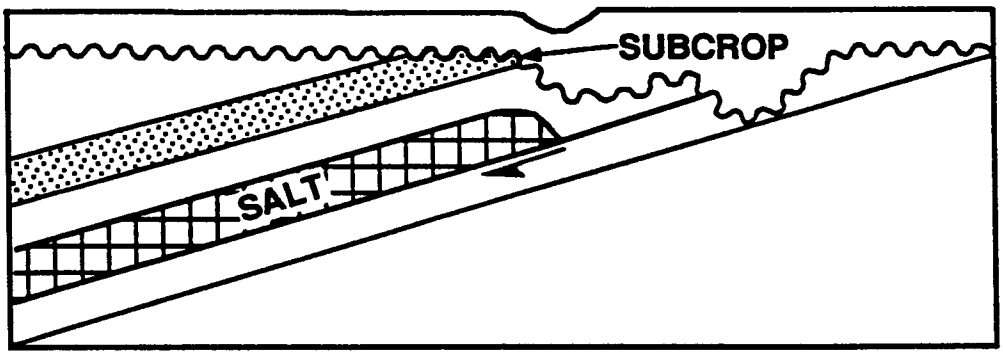

STAGE 2

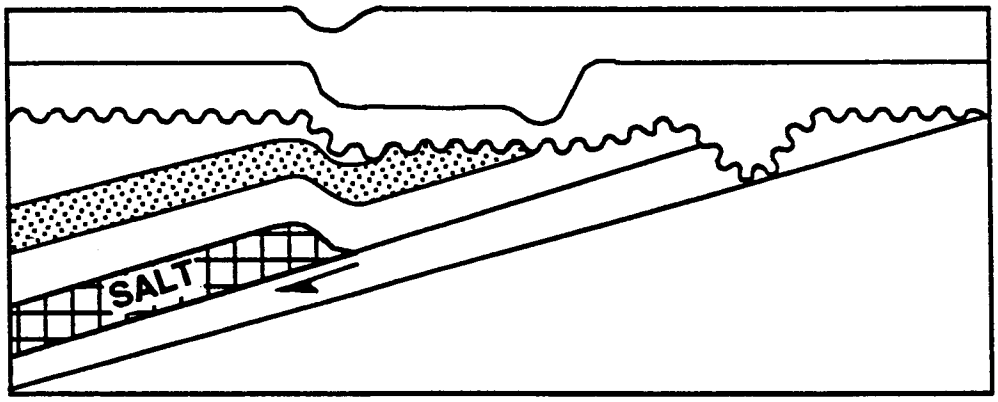

STAGE 3

Figure II:2:2 (Anderson, 1991)

occur in response to the erosion of the overlying sediment and the resultant near-surface exposure of the salt. Physical, chemical and biochemical changes in the adjacent sediments, as a consequence of erosion and near-surface exposure, could also facilitate leaching.

D) Centripetal-flow: (Figure II:2:3)

According to Perrodon (1983), in a mature basin of great structural stability and relatively low geothermal gradient, hydrological flow will be from the highland areas towards the basin center. This influx of water could cause extensive dissolution of subsurface salts, particularly in places where the salts are in direct contact with unsaturated aquifers. The earliest phases of centripetal-flow induced dissolution could be expected to occur along the edges of the salt nearest the basin margins where the salinity of the water would be at a minimum, and the relative vertical permeability of the sediment would be the maximun.

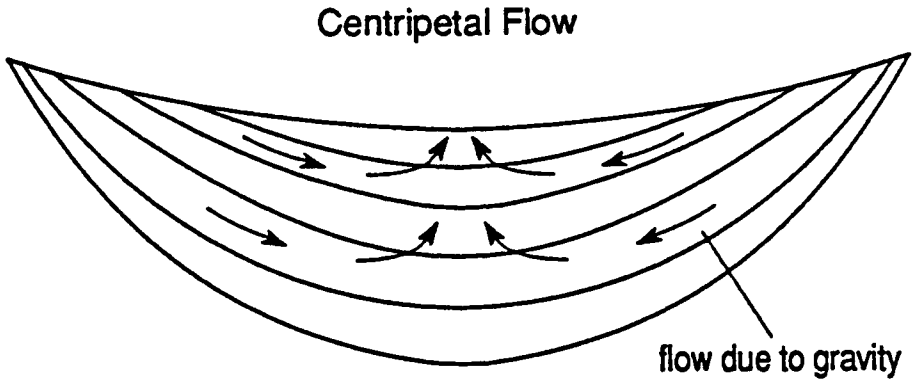

Figure II:2:3 (Anderson, 1991)

E) Regional faulting/fracturing: (Figure II:2:4)

Regional tectonism can cause widespread fracturing and/or faulting of varying intensity. These fault/fracture planes can act as conduits in the subsurface and enhance both the lateral and vertical flow of fluids, thereby facilitating the dissolution of salt.

It is also recognized that regional tectonism can result in uplift and erosion, rapid subsidence and/or major changes in the geothermal gradient. Such processes could significantly affect the hydrological environment of some or all salt. Any resultant leaching could be classified as due to near-surface exposure, centripetal flow, centrifugal flow, etc.

F) Pressure dissolution/localized fracturing: (Figure II:2:5)

The differential compaction of juxtaposed sediments such as reef and off-reef shales, and crystalline basement and sedimentary fill generally introduces post-

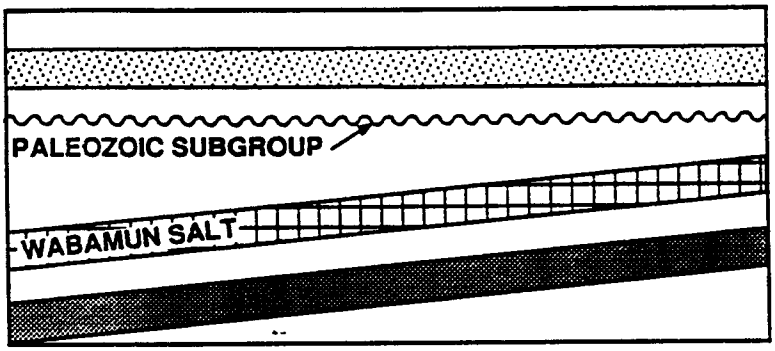

STAGE 1

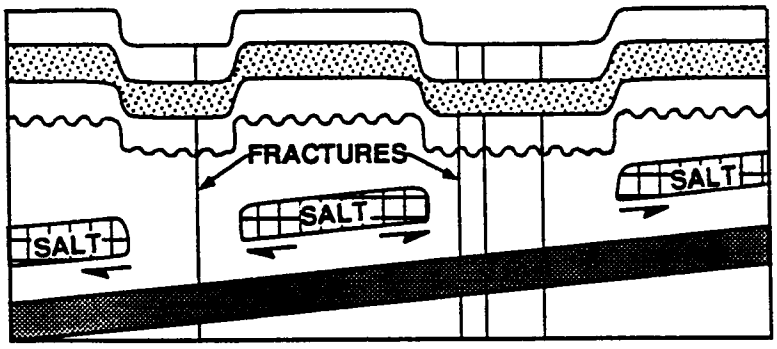

STAGE 2

Figure II:2:4 (Anderson, 1991)

depositional structure into the subsurface. Localized tensional fracturing and/or pressure dissolution could occur in the overlying strata in response to this gradual deformation. (Pressure dissolution is a process in which a solid dissolves along its contact with another solid, and in the presence of water, because increased pressure has increased its solubility.)

There are many situations in western Canada where, as a result of the differential compaction of underlying sediments, salts are draped across underlying structures. It is conceivable that such salts could be subjected to pressure dissolution and/or leached as a result of the the introduction of fracture permeability into the adjacent strata.

G) Glacial loading and/or unloading: (Figure II:2:6)

The process of glacial loading could significantly affect the hydrological environment of the subsurface. The rapidly applied load would cause further compaction and necessitate the expulsion of additional interstitial water. An increase in the geothermal gradient and the thermal expansion of the deep aquifers could result as well. Conceivably the rate of centrifugal flow within the basin could be significantly increased and the associated dissolution of salts could be accentuated.

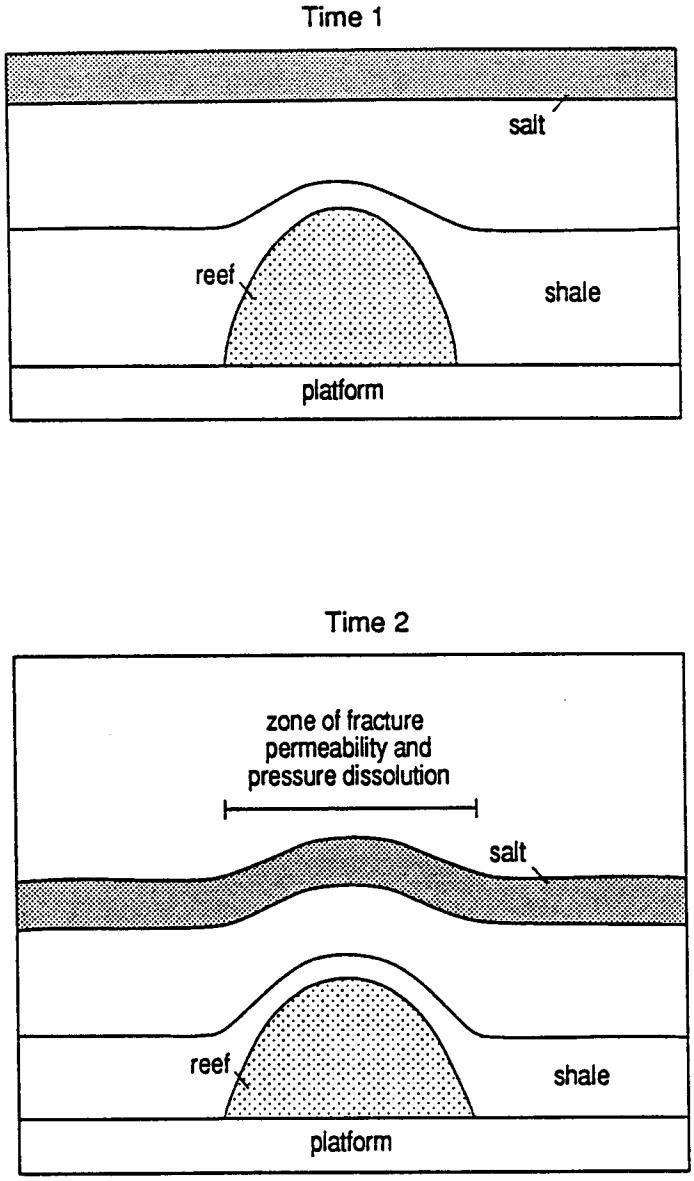

Figure II:2:5 (Anderson, 1991)

The process of glacial unloading could also significantly affect sub-surface salts. The relatively rapid decrease in applied load would be manifested as glacial rebound. This process could result in a net increase in the gross porosity and fracture permeability of the sub-surface, and a net decrease in the geothermal gradient. As a consequence, the rate of centripetal flow could be significantly enhanced. (It is conceivable that the flow regime could change from centrifugal to centripetal.) This postulated increase in flow rates and the potential influx of unsaturated glacial melt-waters could significantly enhance the rate of salt dissolution.

H) Dissolution of the underlying salt: (Figure II:2:7)

The subsurface in heterogeeous, both with respect to lithology and hydrology.

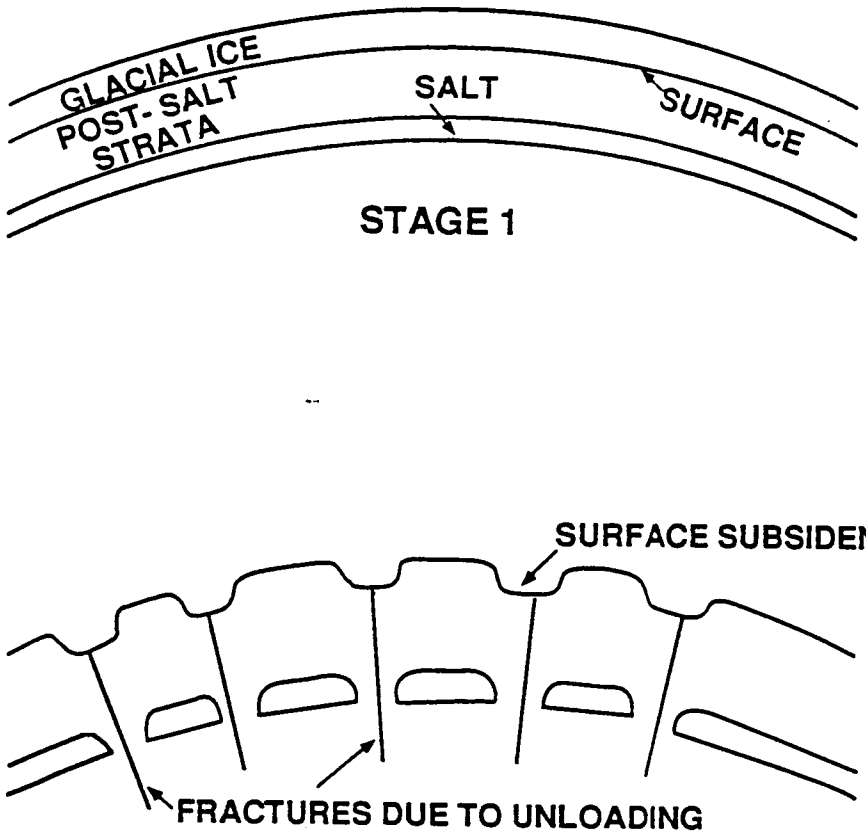

Figure II:2:6 (Anderson, 1991)

As a result, certain bodies of salt could be more susceptible to dissolution than others. In those situations where underlying salts are preferentially leached , the resultant collapse of the overlying strata could create fracture permeability and initiate or accentuate the dissolution of the upper salts.

I) Salt movement: (Figure II:2:8)

The movement of salt is generally thought to occur in response to the density differential between salt and the adjacent strata, differential loading, and lateral stresses, and to be enhanced by the presence of water. Salt flow has been documented at the earth's surface, but more typically occurs at depth and in a higher temperature/higher pressure environment. Such movement stresses the overlying strata and is likely to cause the development of fracture permeability and to result in the leaching of the salts.

J) Dissolution - a self-perpetuating process: (Figure II:2:9)

The dissolution of subsurface salts is thought to be triggered by numerous

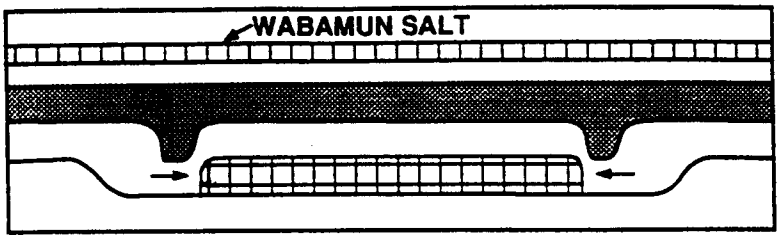

STAGE 1

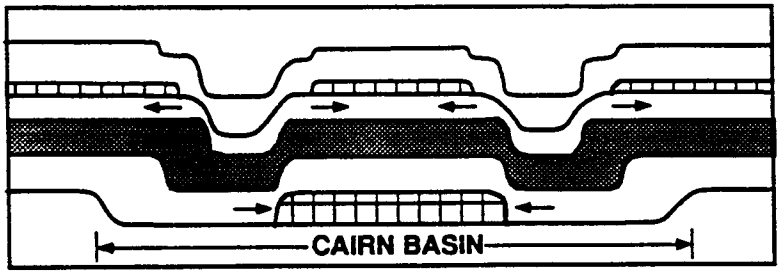

STAGE 2

Figure II:2:7 (Anderson, 1991)

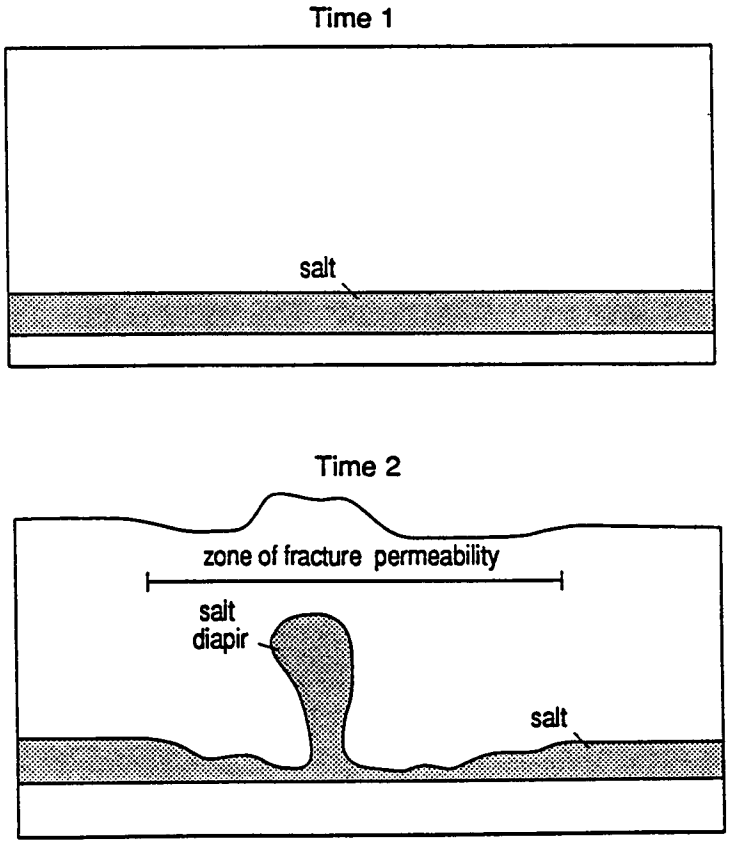

Figure II:2:8 (Anderson, 1991)

dependent and independent mechanisms, (some of which are discussed above). Once leaching has been initiated at a specific site, however, the associated salt-dissolution front appears to migrate over time indicating that leaching is self-perpetuating; a process whereby fractures, created by the collapse of overlying strata, provide conduits for water thereby facilitating further dissolution.

4) BRITTLE VERSUS DUCTILE SUBSIDENCE

Salt is characterized by its ability to deform either in a ductile (plastic) or brittle manner, depending on temperature, stress state, and deformation rate (section I:2). At temperatures expected for the salt dissolution-subsidence process, the primary ductile deformation mechanisms for rock salt are dislocation glide (Glide creep) at moderate differential stresses and moderate deformation rates, and Solution Precipitation creep at low differential stresses and low deformation rates. If intercrystalline water penetrates the subsiding salt mass, deformation by intergranular liquid diffusion (Solution Precipitation creep) is capable of producing strain rates that are orders of magnitude higher than are possible in relatively dry salt at the same stress states (Davies, 1989).

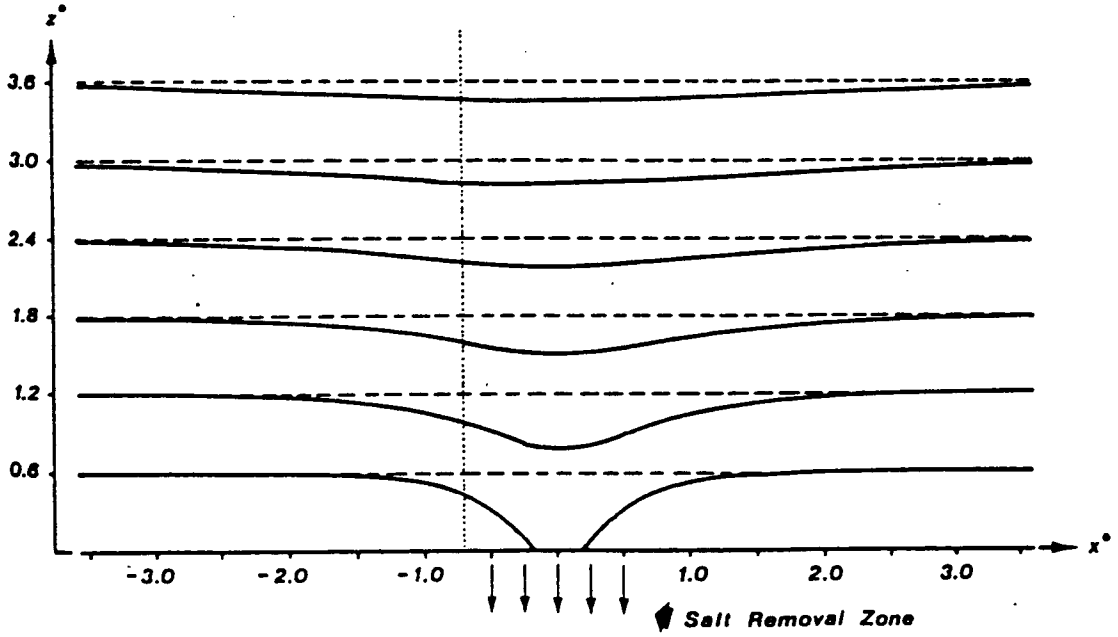

Fig.5. Ductile subsidence model results showing deformation of a set of marker horizons (solid lines) that were originally horizontal (dashed lines). The vertical dotted line shows how a vertical borehole could be located within the subsidence depression, yet miss hitting the salt-removal zone.

Figure II:3:1 (Figure 5; Davies, 1989)

According to Davies (1989), there are two basic types of subsidence: (1) very slow subsidence characterized by predominantly ductile deformation; and (2) relatively rapid subsidence characterized by predominantly brittle deformation. These two types of subsidence represent the ends of a continuous range of subsidence

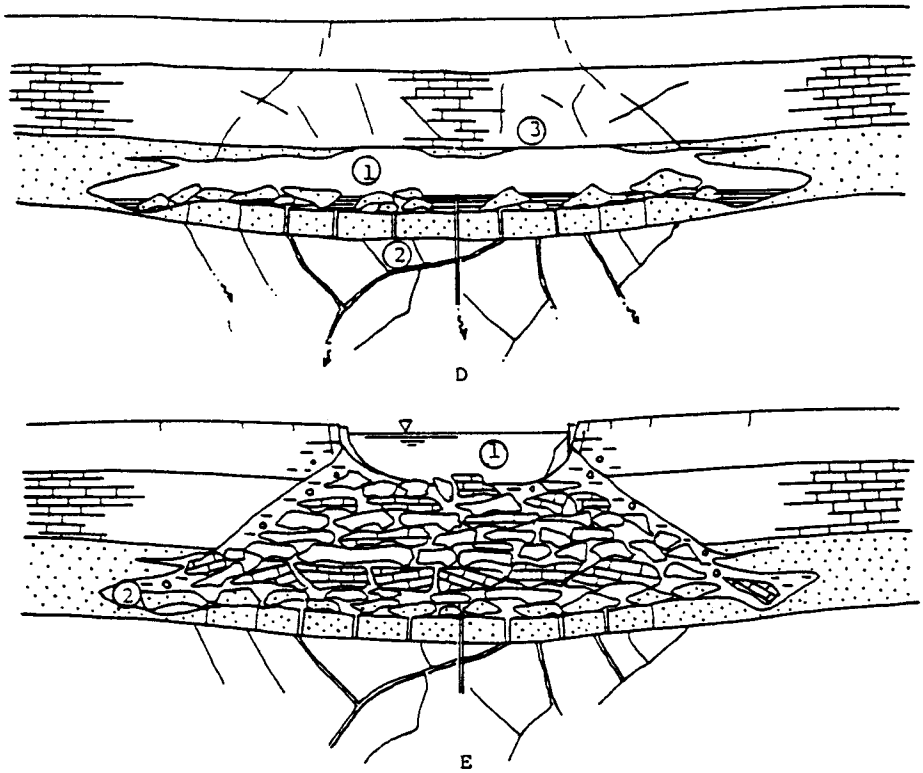

Figure II:3:2 (Figure 9; Nieto et al., 1985)

processes. As is illustrated in Figures II:3:1 and II:3:2, ductile deformation typically generates an expanding cone of subsidence; brittle deformation in contrast is characterized by inverted cone-shaped, collapse cavity. Whether or not the subsidence feature is expressed at the surface depends upon several factors including the areal extent, volume and depth of the dissolved salt, and the response of the overburden. For example if sufficient porosity develops within the overburden (due to stoping), the vertical migration of subsidence could effectively cease, pending additional dissolution. In a second scenario, the strength of the overburden and depth to the collapse cavity could be such that the inverted cone-shaped, collapse cavity beomes effectively bridged in the subsurface.

5) MAN-MADE CAUSES OF UNINTENTIONAL SALT DISSOLUTION

A) Overview:

Several man-made activities can cause the unintentional dissolution of salts: salt mining, the use of salt-water disposal wells, and drilling. As illustrated in the following case histories, mining activities and the unintentional disposal of oil industry brines into saliferous formations through corroded pipe can result

in significant dissolution, and in some instances catastrophic collapse. Drilling, in contrast, generally only results in the dissolution of salts in the immediate vicinity of the borehole. Improper casing techniques however, could result in extensive leaching due to the vertical migration of fluids into and out of the saliferous zone.

B) Salt mining:

Baar (1977), refers to numerous examples of flooding in dry salt mines. According to Baar, greater than expected creep deformation around mined-out openings in salt deposits are the main cause of groundwater inflow that, sooner or later, results in disastrous surface damages; a continuous flow of groundwater which, before it is pumped back to the surface dissolves salt, must result in uncontrollable rock mechanic reactions in the overburden (such as rockbursts, differential subsidence, and sinkhole formation). In most of these cases, when mining operations underneath salt deposits resulted in subsidence and made the salt formations permeable, the solubility of rock salts was underestimated, or ignored. Frequently, the distances over which groundwater flow systems are affected by such events are underestimated.

The following three examples from Baar (1977) illustrate three different causes of dissolution and collapse. In each case, large areas of German cities fell victim to the uncontrolled dissolution of salt deposits by groundwater, the dissolution being initiated by mining operations.

Example 1: The city of Staafurt, suffered severe damage from conventional potash mining. Several mines operating within the city limits were lost by flooding during the first decades of potash mining as the strength of mine pillars were underestimated. At least one of the large surface craters which formed in residential areas is now in use as a lake resort area. Large areas in the city center had to be abandoned.

Example 2: The city of Eisleben, suffered similar damage from copper-shale mining activities which initiated the dissolution of salt deposits above the mining levels. Groundwater from considerable distances was flowing for decades into the mines, dissolving overlying salt, and was pumped back to the surface to be channeled into major rivers.

Example 3: The city of Luneburg, suffered damage as a result of inadequate solution mining techniques; natural salt dissolution by groundwater may also have played a minor role."

Baar describes numerous other incidents of flooding. He attributes most of these problems to inadequate designs based on the theories of elasticity and the premise that strain hardening of rock salt will occur. Baar stresses in his textbook that, until recently (1970's), salt mines were designed on the erroneous assumption that steady state creep did not occur.

C) Salt-water disposal wells:

There are relatively few documented instances in which extensive dissolution of subsurface salts has been attributed to salt-water disposal (or other oil and gas related) wells; several such case histories are discussed in Walters (1978). The potential severity of this situation however, under the proper geological conditions must not be discounted.

In order to illustrate the potential consequences of this problem, the Panning sinkhole case history (from Walters, 1978) is summarized below.

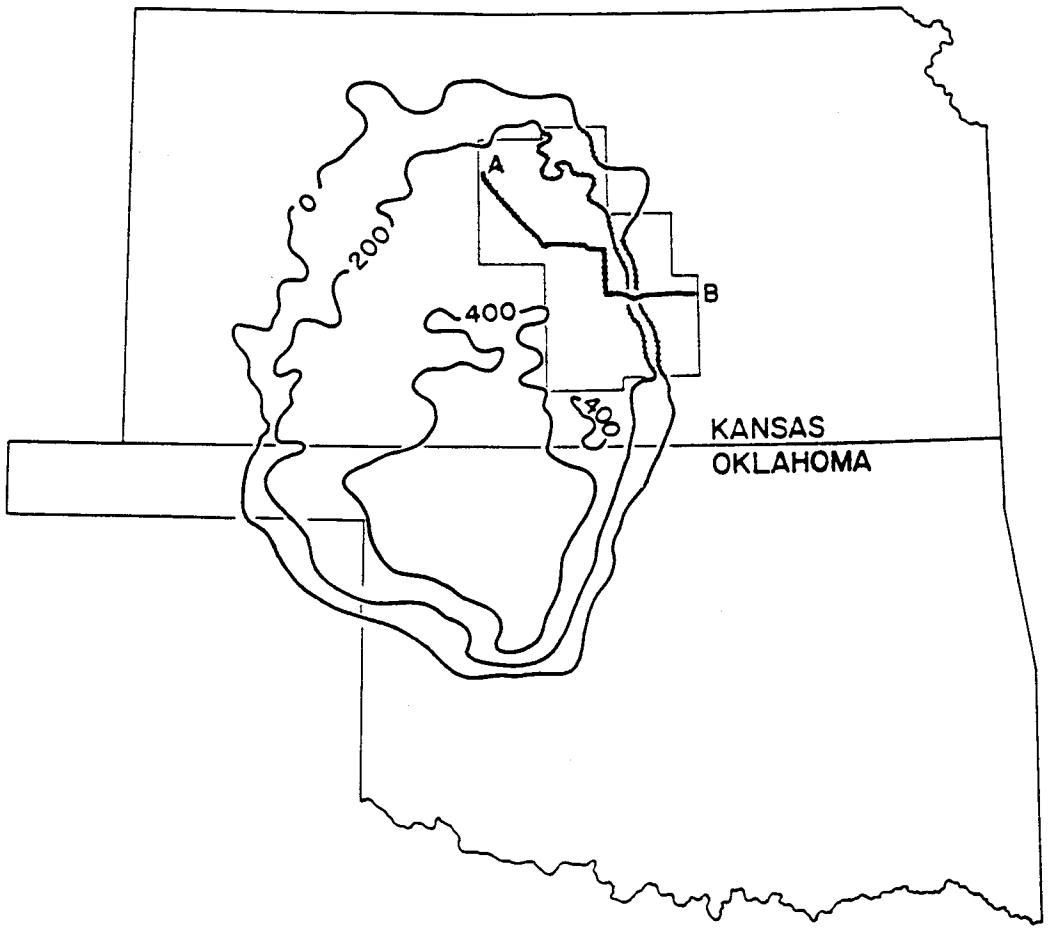

FIGURE 1.—Extent and thickness in feet of the Hutchinson Salt Member of the Wellington Formation, Permian System. Kansas portion modified from Schumaker (1966). Oklahoma portion by Johnson (1976). The location of Cross Section A-B (Fig. 2) is indicated within the shaded study area (Fig. 3).

Figure II:4:1 (Figure 1; Walters, 1979)

1) Background geological and hydrological information:

The Hutchinson Salt Member of the Permian Wellington Formation underlies 70,000 km_2 in south and central Kansas (Figure II:4:1). In the Panning sink area the top of the salt is at a depth of about 300 m (Figure II:4:1); it has a gross thickness on the order of 100 m, including shale and anhydrite interbeds totaling 20 percent of the section. The salt is overlain by impermeable shales and typically, by a shallow fresh-water aquifer(s).

The principal reservoir facies in the Panning area, the Lower Ordivician Arbuckle dolomite (at about 3000 m depth; Figure II:4:2), is an enormously large aquifer; hence the Arbuckle reservoirs have a strong water drive. Scores of wells in the Panning area produced 500 barrels or more of salt water per day. Most of this salt is re-injected into the Arbuckle through high volume, gravity-fed injection wells.

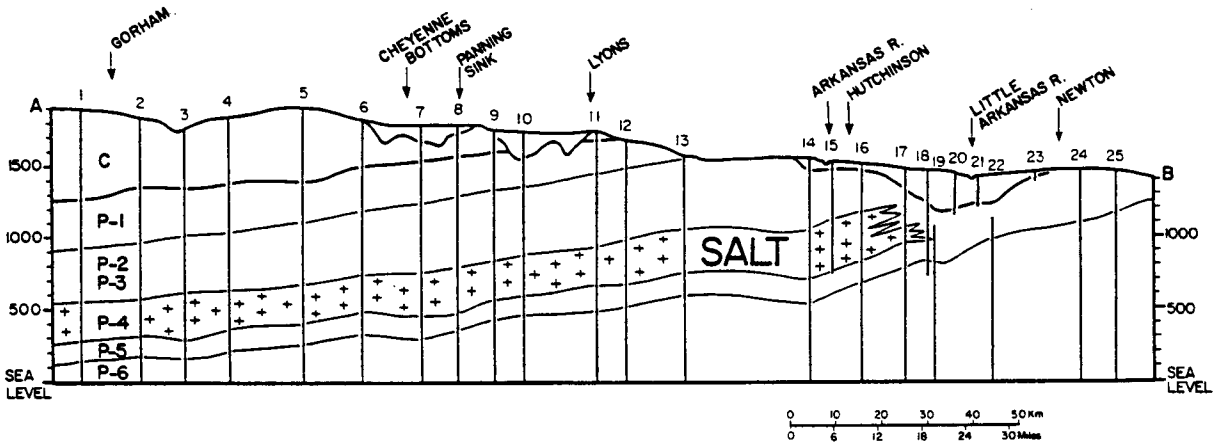

FIGURE 2.—Cross Section A-B. Length of section depicted is 150 miles. Vertical exaggeration × 100. Figures indicate elevation in feet above mean sea level. Location of cross section indicated in Figures 1 and 3. Control borings drilled for oil, gas, salt, or water, numbered 1 to 25, are listed in Appendix B. Stippled areas = unconsolidated beds, water-bearing; R = river.

STRATA			
C			Cretaceous
P			Permian
	P-1		Nippewalla Group
	P-2 to P-5		Sumner Group
		P-2	Ninnescah Shale
		P-3	Wellington Shale
		P-4	Hutchinson Salt Member
		P-5	Wellington Shale-Anhydrite
	P-6		Chase Group

Figure II:4:2 (Figure 2; Walters, 1979)

The disposed brine is unsaturated with respect to sodium chlorides (average of 13,870 ppm chlorides as opposed saturated brine at 260,000 ppm) and corrosive to metals; the Arbuckle brines characteristically contain dissolved H_2S. Hence within the disposal wells there is the potential for appreciable salt dissolution - high energy input, large volumes of water unsaturated with respect to chlorides, and an enormous brine outlet in the Arbuckle dolomite.

2) Reconstructed well history:

The Panning sinkhole (Figure II:4:3) developed around an abandoned oil well (Panning 11A) then in use as a salt-water disposal well. The following excerpt from Walters (1978) represent that author's reconstruction of the sequence of events that led to the formation of the Panning sinkhole.

FIGURE 28.—Photograph by Larry Panning, April 24, 1959. Panning Sinkhole, view toward the northwest. Vertical water well casing of Figure 27 at left center. Figure of man, left foreground. The light areas in the sides of the pit are water flows.

Figure II:4:3 (Figure 28; Walters, 1979)

September 1938 (Figure II:4:4): During the drilling of the Panning 11A, the fresh-water drilling fluid dissolved salt to a diameter of 54 inches (1.37 m). Note that the production casing did not proceed up hole this high.

1938-1943 (Figure II:4:4): No dissolution of salt took place while over 100,000 barrels of oil were being processed through tubing. Shale interbeds in the shale section collapsed and fell, accumulating in the void space from 1200 to 1275 feet (367 to 389 m), just above the constriction in the hole size at the first anhydrite bed.

1943-1946 (Figure II:4:4): A cased hole gamma-ray neutron log recorded in a nearby hole showed the static fluid level of the Arbuckle aquifer to be

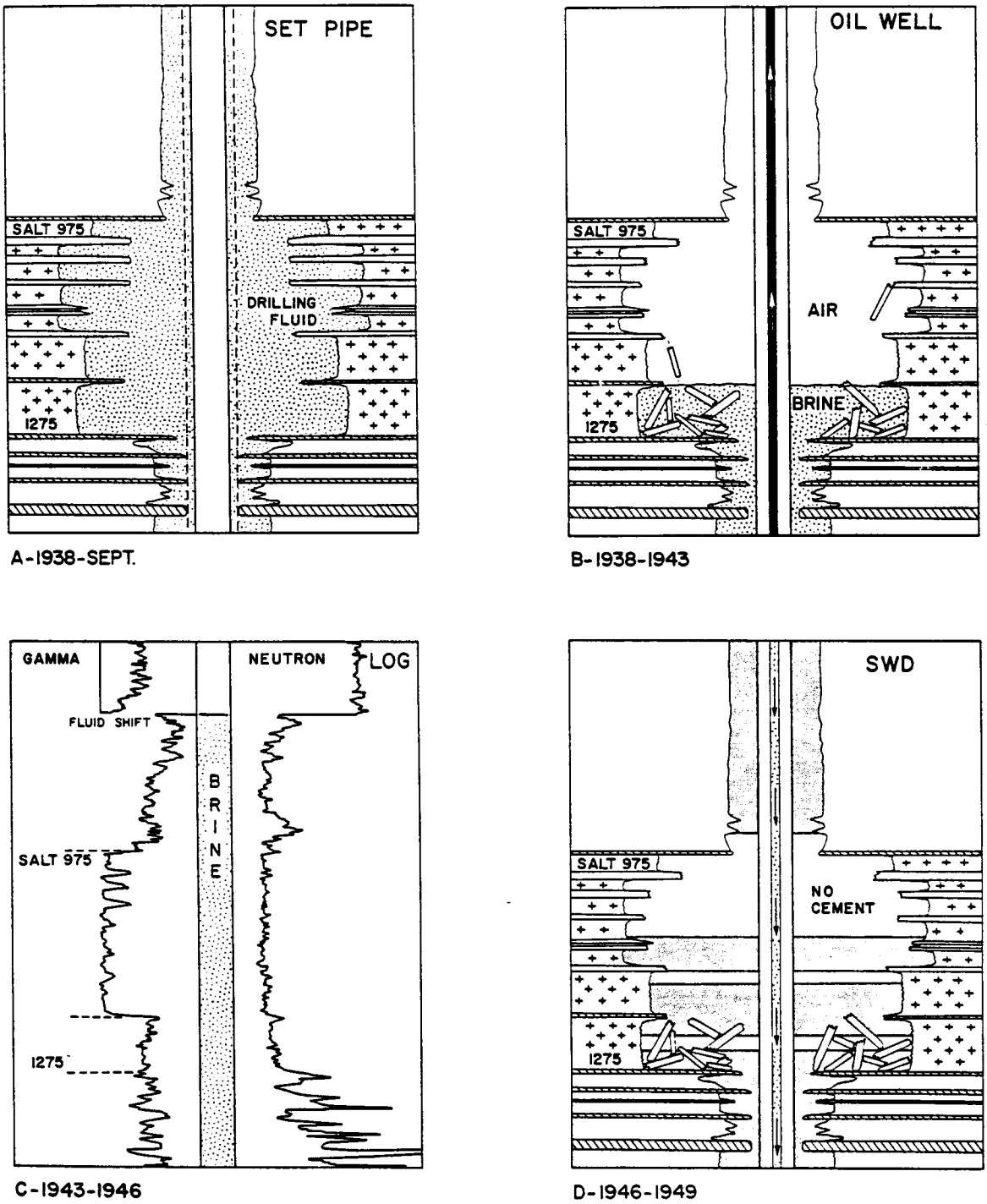

FIGURE 29.—Diagram; salt section in Panning 11-A.
A. After setting 6-inch oil string casing.
B. Oil well. Oil is pumped up 2-inch tubing.
C. Gamma-neutron log; tubing removed.
D. Salt water disposal well (SWD). Waste brine moving down 3-inch plastic-lined tubing.

Figure II:4:4 (Figure 29; Walters, 1979)

912 feet (278 m) from the top of the hole. No salt dissolved in these years during which the well was temporarily abandoned as non-commercial after pumping 99% water due to the depletion of oil.

1946-1949 (Figure II:4:4): The well was converted for use as a salt water disposal well by recementing the casing. Note the presence of cement opposite the lower salt section and the absence of cement opposite the upper salt section. No salt dissolved. Brine was disposed through tubing by gravity flow.

1949-1953 (Figure II:4:5): Tubing was removed from this disposal well and brine was disposed directly down the casing. Corrosion resulted in casing leaks, permitting access for 72 gallons per minute of brine, 14,000ppm chlorides, to circulate across the salt face, then downward into the Arbuckle aquifer. A huge cavern dissolved in the salt,larger than 300 feet (90 m) in diameter. Progressive falls of the shale interbeds and shale roof rocks partially filled the cavern. Succesive roof falls caused the void space to gradually migrate upward to near the Stone Corral Anhydrite, depth 465 feet (142 m) causing in turn, surface subsidence, ponding of water, and tilting of the derrick.

1959-January (Figure II:4:5): The Panning A-11 was abandoned but not plugged. The derrick was removed because surface subsidence caused it to tilt dangerously. With disposal brine flow discontinued, salt dissolution ceased.

1959-April (Figure II:4:5): The Panning 11-A was plugged with 150 sacks of cementin the surface pipe to a depth of 190 feet (58 m), and the Arbuckle was bridged: There was no other plugging. The underground void space at shallow depth was now isolated from both the near surface and Arbuckle aquifers. Brine in the void space drained downward gradually to reach equilibrium with the intermediate aquifers leaving the near-surface void space unsupported by fluid and under vacuum.

1959-April 24 (Figure II:4:5): When the uppermost keystone bedrock at a depth of 106 feet (32 m) fell into the newly drained shallow void space, the surface sinkhole formed rapidly in three hours from 9:00 a.m. until noon, with some subsidence continuing until about 9:00 p.m. As the shallow void space filled with fresh water and air, falling material such as concrete derrick corner blocks fell into the narrow aperature and compressed, then ejected, the air. The casing collapsed and fell. At first , the loose sand and gravel moved downward in a freshwater slurry at a rate faster than the flow of the aquifer, forming a deep cone-shaped pit. As the void space filled, water accumulated in the surface sinkhole.

1959-April to 1978 (Figure II:4:5): The circular sinkhole diameter near 330 feet (100 m), stabilized forming a fresh water pond 64 feet (20 m) deep, volume near 2,000,000 cubic feet (57,000 m^3). In 17 years, the

surrounding fence buckled downward and inward only about two feet (0.6 m) on each side, indicating resumption of stable subsurface conditions. Transported sand and gravel fills the shallow space voided by roof falls. The former cavern in the salt is filled and plugged with fallen Permian shale and redbeds; hence it is thought that no further dissolution is occurring.

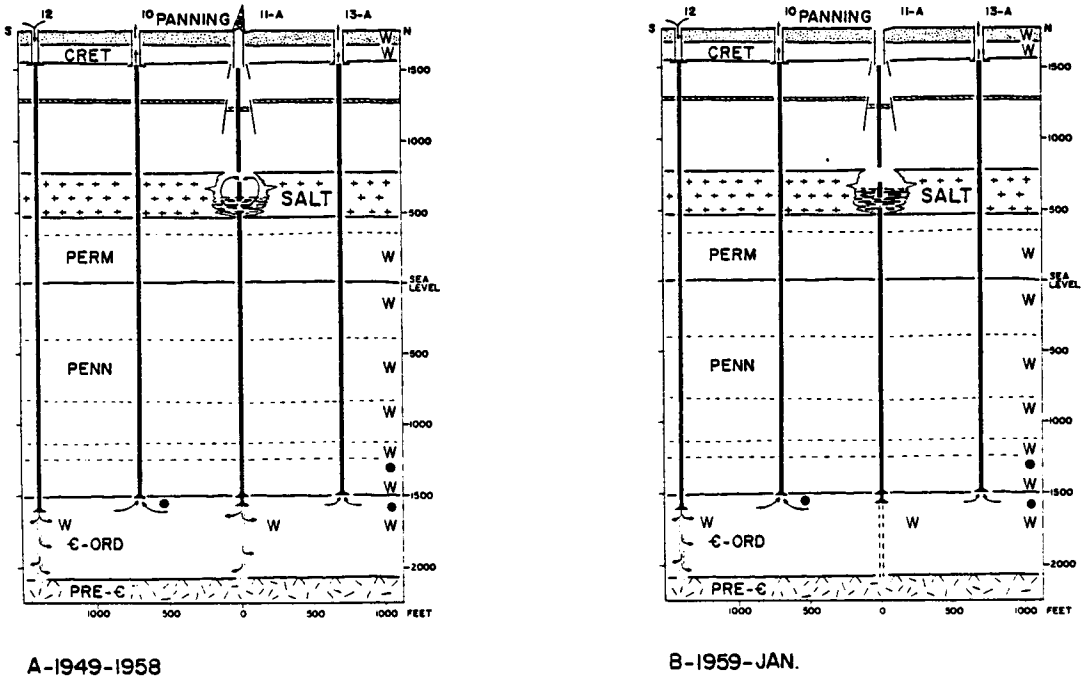

FIGURE 30.—Cross section through Panning 11-A disposal well.
A. Waste brine moving down inside 6-inch casing (plastic-lined tubing removed) and circulating by Permian salt section through holes in casing.
B. Well abandoned; derrick removed.

Figure II:4:4 (Figure 29; Walters, 1979)
(continued on next page)

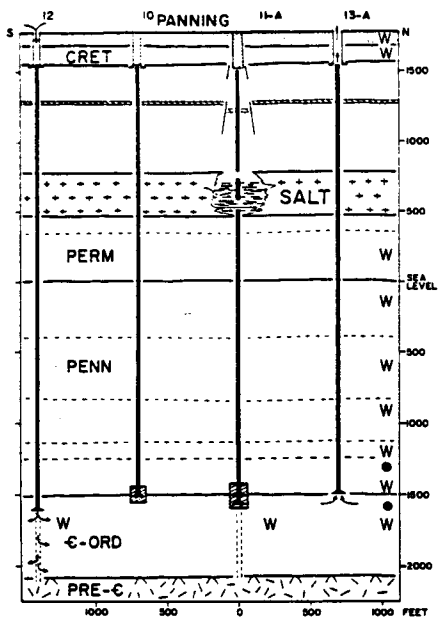

C-1959-APRIL 14

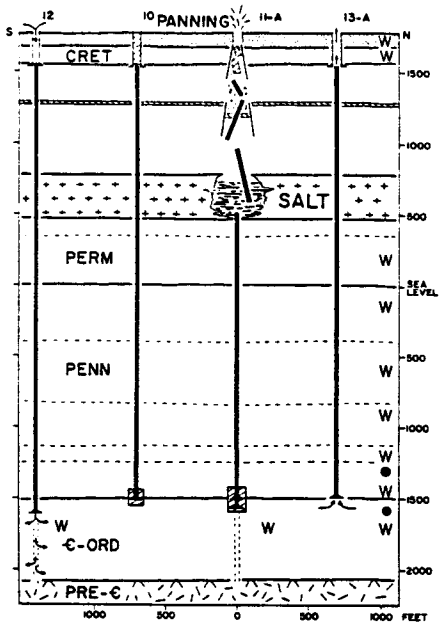

D-1959-APRIL 24

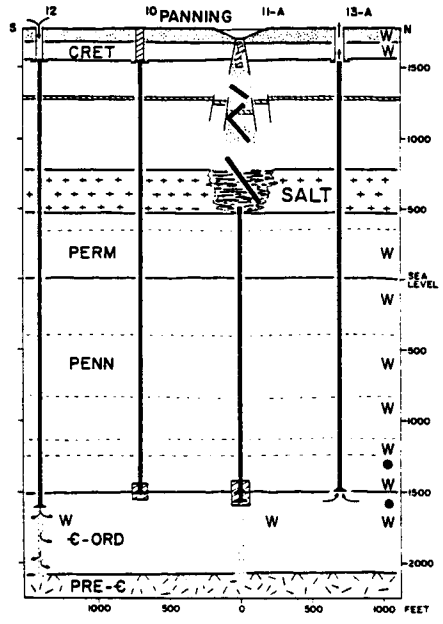

E-1959-PRESENT (1976)

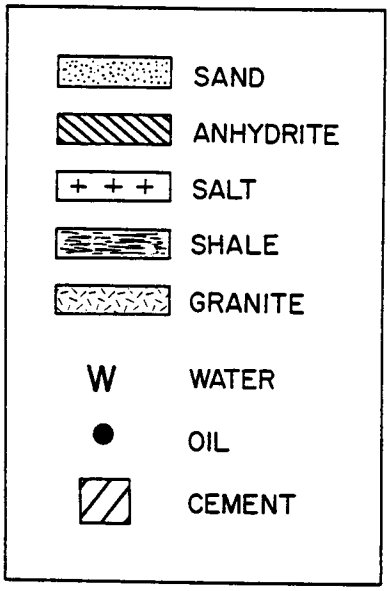

F- LEGEND

FIGURE 30 (continued).—Cross section through Panning 11-A disposal well.
C. Well plugged with cement in surface pipe, and "bridged" in Cambro-Ordovician Arbuckle Dolomite.
D. Sinkhole forming April 24, 1959.
E. Panning Sinkhole with pond.
F. Legend for Figure 30.

Figure II:4:4 - continued (Figure 29; Walters, 1979)

6) EXPLORATION IMPLICATIONS OF SALT DISSOLUTION

A) Hydrocarbon entrapment:

The dissolution of bedded salt is of interest to the explorationist for several reasons (Figures II:5:1-II:5:6): 1) stratigraphic traps can form where reservoir facies were either preferentially deposited or preserved in salt-dissolution lows; 2) reservoir facies can develop in high energy environments such as topographic highs that are controlled by salt edges or remnants; 3) structural traps can form where reservoir facies are draped across salt remnants or collapse features; and 4) salt remnants can be misinterpreted as reefs, faults or other structural features.

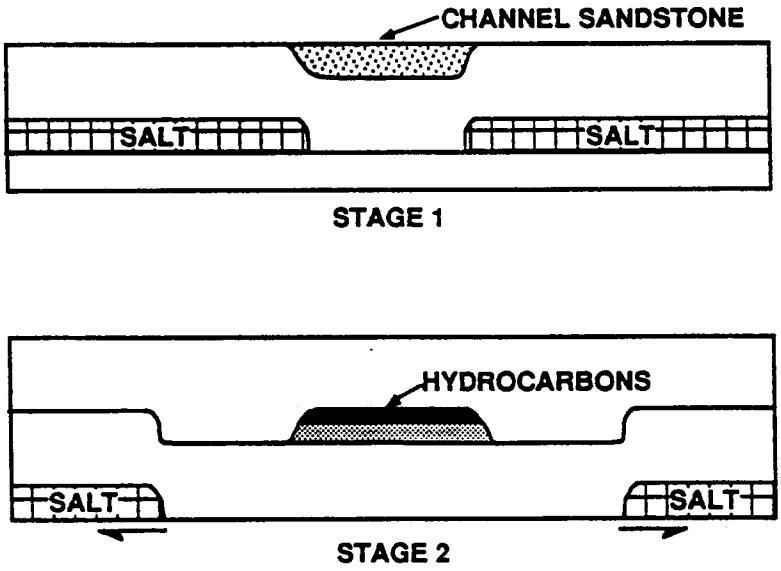

Figure II:5:1 (Anderson, 1990)

B) Misinterpretation of salt dissolution features:

Dissolution can cause time-structual relief along both reflections that are pre-salt (velocity pull-up or push-down) and on those that are post-salt (collapse structure). As suggested by Figure II:5:7, such relief could be misinterpreted as indicative of reefal buildups or deep-seated structure. The explorationist, working in an area of salt dissolution, must carefully evaluate the seismic data, keeping in mind the several possible interpretations - and testing each - in order to determine the most probable cause of any time-structural relief.

In Figure II:5:8, a modified version of Figure II:5:7 is presented. Manual static corrections were applied to these data by a processor who was not aware that spectacular collapse features occurred in this area. Had it not been for both the anomolous relief at a two-way traveltime of about 20 milliseconds and the discontinuity near trace 102, this processing error might have gone

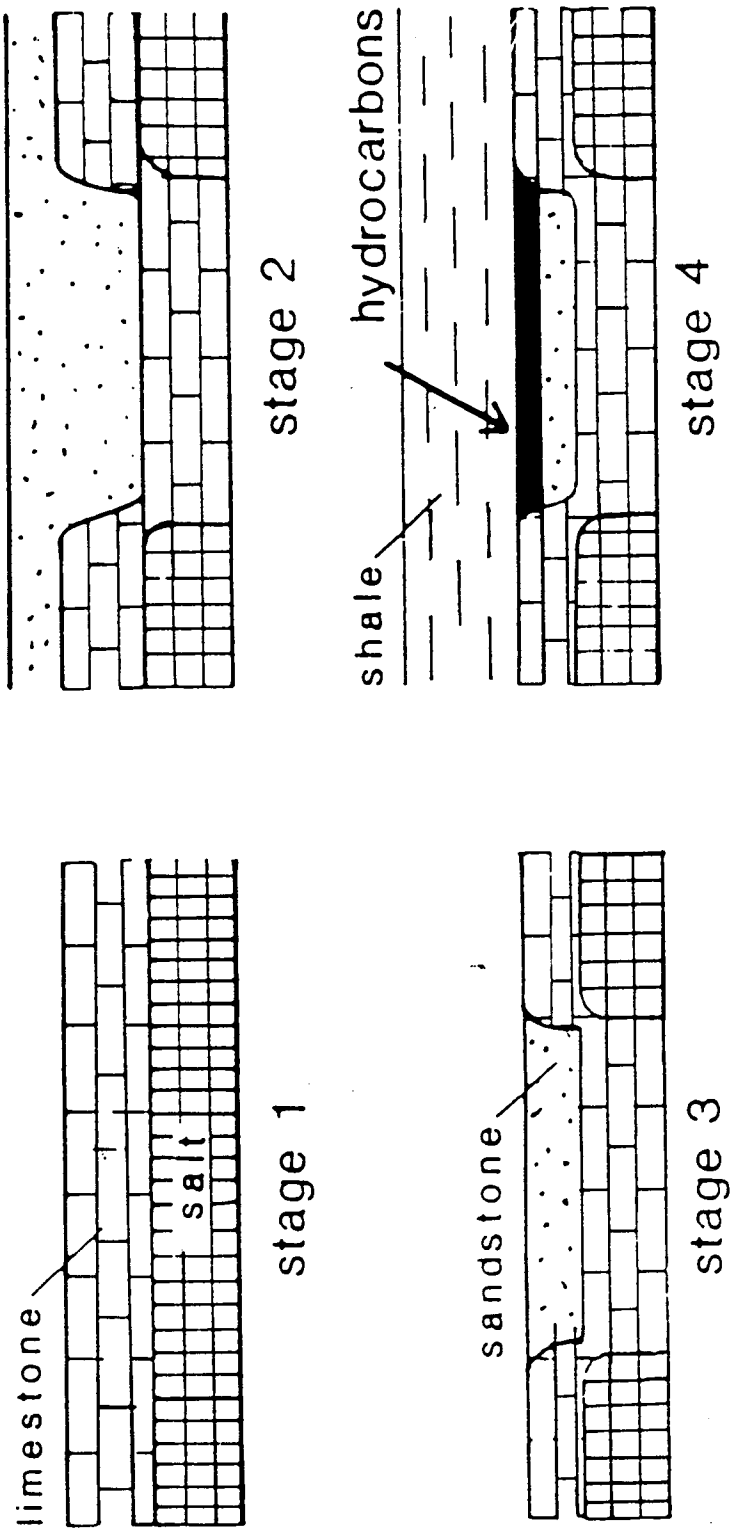

Figure II:5:2 (Anderson, 1990)

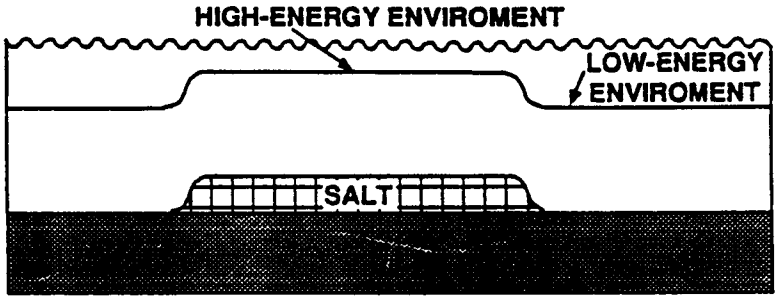

STAGE 1

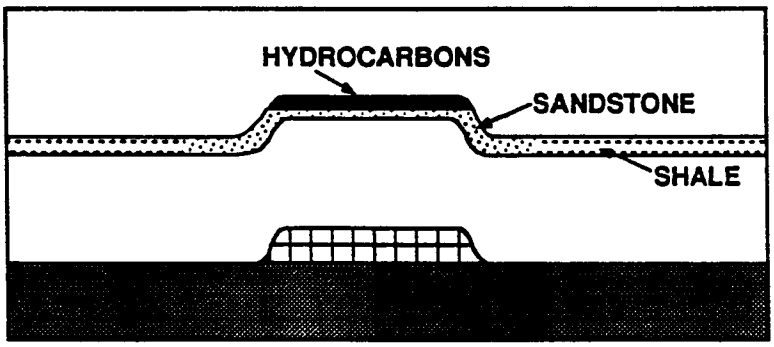

STAGE 2

Figure II:5:3 (Anderson, 1990)

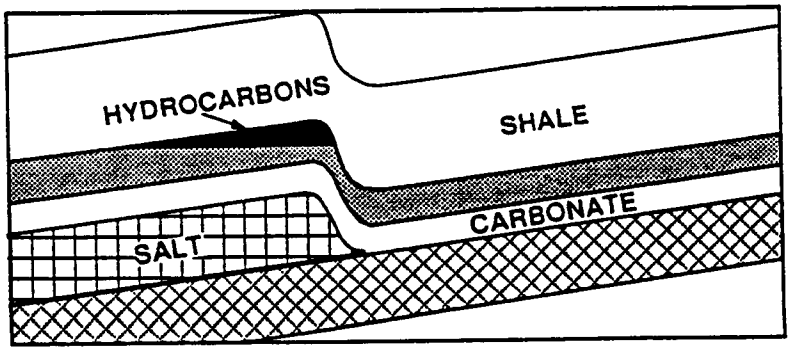

Figure II:5:4 (Anderson, 1990)

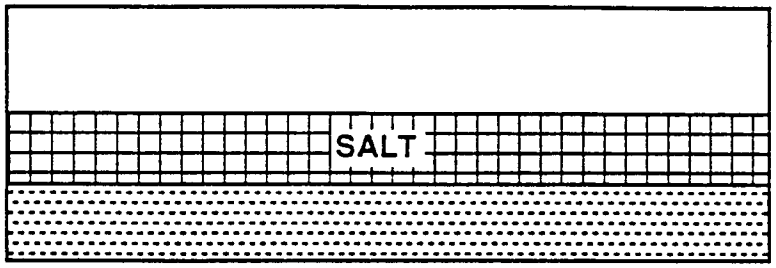

STAGE 1

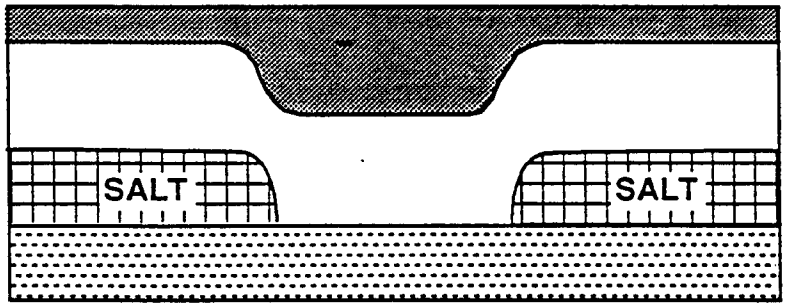

STAGE 2

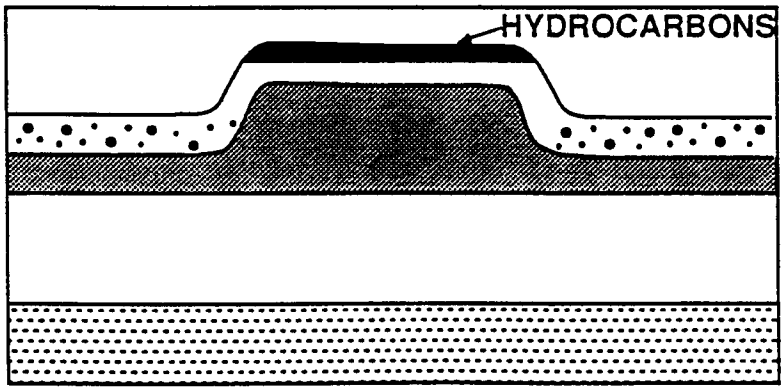

STAGE 3

Figure II:5:5 (Anderson, 1990)

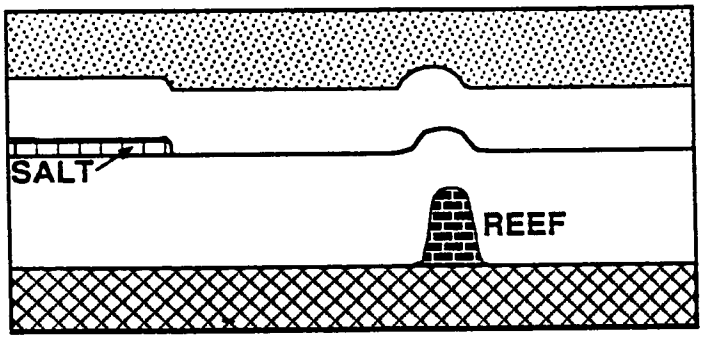

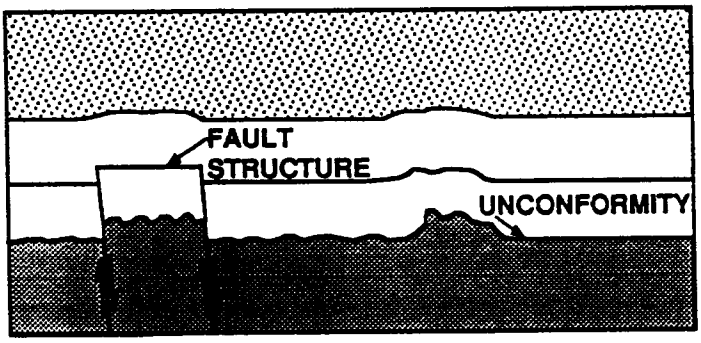

Figure II:5:6 (Anderson, 1990)

unchallenged by the interpreter. In any case it is not difficult to conceive of seismic sections that are equally misprocessed but do not display such telltale evidence of it. These data, on the basis of apparent velocity pullup and the thinning of the Wabamun to Ireton interval, could have been misinterpreted as indicative of reef and/or faults, resulting possibly in the acquisition of additional seismic control, an acreage position, and/or unwarranted drilling.

C) Drilling problems:

Because of the high solubility of salt, specially designed salt-based or oil-based drilling muds are required in order to prevent extensive dissolution. In addition to the specialized mud requirements, drilling into deep salt domes presents additional difficulties associated with:

1) lost ciculation;

2) heaving shale;

3) salt water flows;

4) abnormally high pressure zones; and

5) high temperatures.

According to Halbouty, standard borehole logging techniques are also adversely affected by salts and by the use of specialty muds (Figure II:5:9).

Effect of Mud System on Logging Devices

Log	Salt-Water	Oil or Invert Emulsion
SP	Poor	Useless
Normal Resist.	Depressed	Useless
Micro-Resist.	Poor-Qualitative Value Only	Useless
Induction/Dual Induction	Good	Good
Dual Laterolog	Good	Useless
Acoustic-Velocity	Good if gauged hole	Good
Density	Good if gauged hole	Good
Gamma Ray	Good	Good
Neutron	Good if gauged hole	Good
Nuclear Magnetism	Good	Good
Dipmeter	Good	Good

Figure II:5:7 (Table 9-1; Halbouty, 1979)

7) REFERENCES

Anderson, N.L., 1990, Exploration implications of salt dissolution: Kansas Geological Survey Open File Report 90-37.

Anderson, N.L., 1991, Large scale mechanisms of salt dissolution: illustrated case histories: Kansas Geological Survey Open File Report 91-57.

Baar, C.A., 1977, Applied salt-rock mechanics 1: Elsevier Scientific Publishing Company, 294 p.

Davies, P.B., 1989, Assessing deep-seated dissolution-subsidence hazards at radioactive-waste repository sites in bedded salt, *in* Johnson, A.M., Burnham, C.W., Allen, C.R. and Muehberger, W., Eds., Richard H. Jahns Memorial Volume: Engineering Geology 27, 467-487.

Halbouty, M.T., 1979, Salt domes: Gulf Publishing Company, Houston, 561 p.

Langbein, R., 1987, The Zechstein sulfates: the state of the art, *in* Peryt, T.M., Ed., The Zechstein facies in Europe: Springer-Verlag, New York, 143-188.

Nieto, A.S., Stump, D. and Russell, D.G., 1985, A mechanism for sinkhole development above brine cavities in the Windsor-Detroit area, *in* Schreiber, B.C. and Harner, H.L., Eds., Sixth International Symposium on Salt: Salt Institute Inc., Virginia, 1, 351-367.

Walters, R.F., 1978, Land subsidence in central Kansas related to salt dissolution: Kansas Geological Survey Bulletin 214, 82p.

III: SALT DOMES

1) OVERVIEW

Salt domes are generally attributed to isostatic and/or tectonic forces. These principal driving forces can be accentuated by the gravity flow of salt and thermal convection (Figure III:1:1).

In the isostatic model (Figure III:1:1), the flow of salt is driven by the density differences between the salt (average density of 2.2 g/cc) and the adjacent sediment. In this model, flow will cease when the buoyancy and restraining forces are effectively balanced. This can occur for one or more of several reasons: 1) Generally the density of the adjacent sediment decreases at shallower depths, hence the buoyancy forces decrease as the salt rises; 2) Temperature and pressure, and hence the viscosity of the salt, generally decreases at shallower depths; 3) The rising salt may encounter more competent strata; 4) The source body of salt may become depleted. The downbuilding hypothesis, a variation of the isostatic model, is illustrated in Figure III:1:2.

In the tectonic model (Figure III:1:1), the flow of salt is driven by a combination of compressive and isostatic forces. In this model, the cessation of movement can be the result of: 1) decreasing buoyancy forces; 2) the decreased viscosity of the salt; 3) the presence of competent shallow strata; 4) the depletion of the source salt; and 5) the relaxation of the compressive stresses.

Alternatively, salt flow can be re-initiated (or accentuated) by further burial, increased compressive stresses, faulting or fracturing, and increased heat flow (thermal convective halokinesis).

In some instances, as a result of dissolution or erosion, the net movement of salt may be nil or recessive, even though vertical flow continues. In other places, the environment is favourable for the extrusion of salt onto the earth's surface. In Iran for example, extruded salt glaciers are positive features, which flow under their own weight (Gravity halokinesis; Figure III:1:3).

With respect to the initiation of salt flow, modelling and case history data suggest that movement can occur in response to one or more of several different features:

1) External stresses which produce faults or folds, and hence lateral pressure differentials within the salt.

2) Natural variations in the density of the overburden.

3) Variations in the thickness of the overburden as a result of depositional, erosional, and/or compactional processes.

4) Internal stresses caused by the partial dissolution of the salt.

The initiation and growth of a sallow salt dome is described by Halbouty as a 6 stage process (Figure III:1:4). In stage 1, salt flow is initiated. In stage 2, a salt pillow (or plug) and peripheral sink form. At stage 3, the salt diapir has pierced the overlying strata and the salt supply flowing to the dome is cut off by the drop in the peripheral sink. Further growth is at the expense of the material within the peripheral sink and salt core. At stage 4, most of the original material over the salt dome has been removed by erosion. At stage 5, the rocks carried up by the diapir have been almost completely eroded; circulating groundwaters have produced

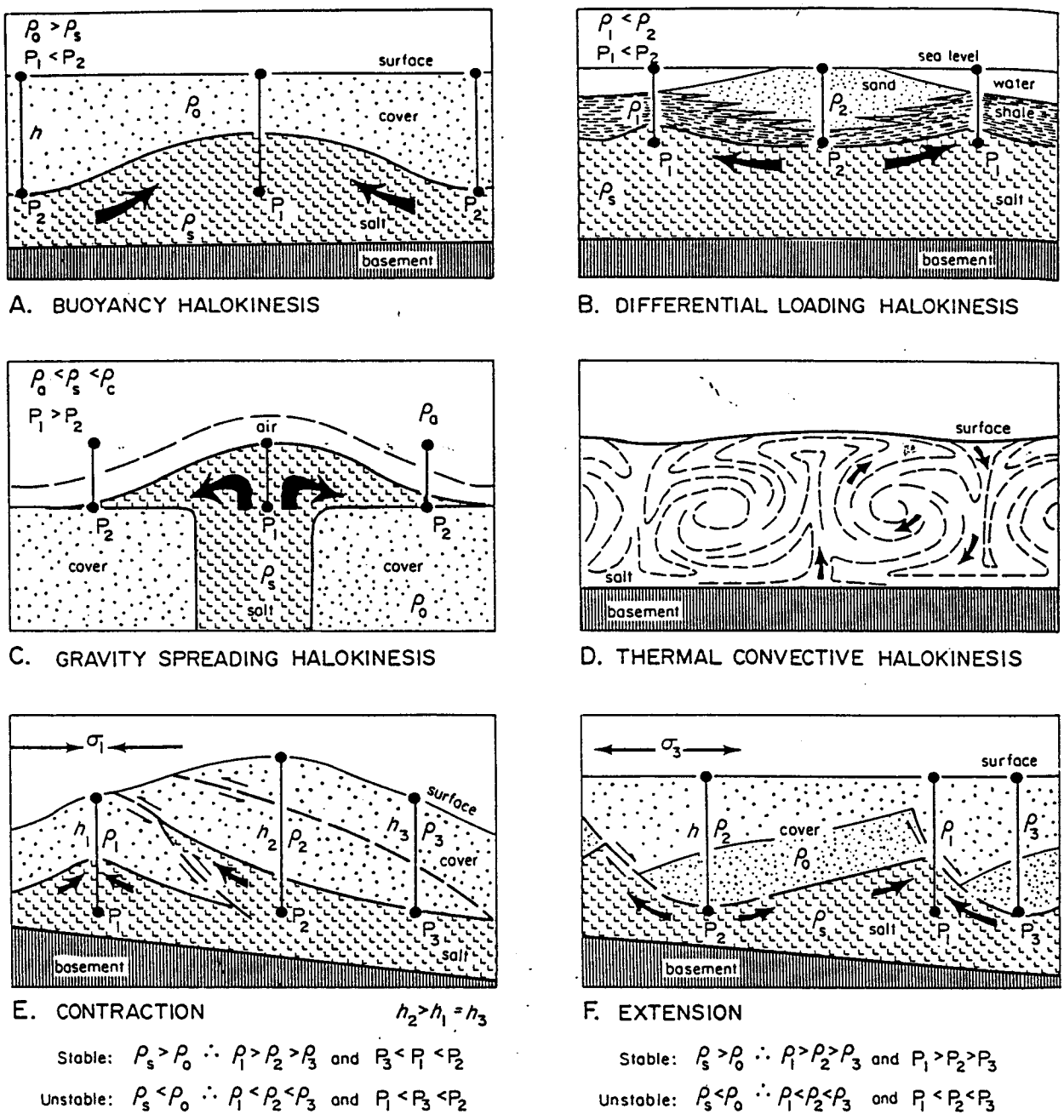

Figure 5. Six principal mechanisms of salt tectonics. All types can combine. P refers to a point or to the lithostatic pressure at that point, based on thickness and density of the overburden; ρ refers to the mean bulk density of a unit where the symbol is isolated or to the mean bulk density of a complete crustal section where the symbol is adjacent to a vertical line defining the section. A. Buoyancy halokinesis. B. Differential loading halokinesis. The salt does not need to be overlain by denser cover, as in case A. C. Gravity spreading halokinesis. An extrusive dome spreads sideways, completing the cycle of overturn. Dashed line shows hypothetical profile of extrusive salt without erosional attrition. D. Thermal convective halokinesis. The convection cell has overturned several times; dashed lines represent partly homogenized layering. E. Contraction halotectonics. Salt acts as a detachment zone for an overlying fold-and-thrust belt; lithostatic pressures can retard the shortening (stable contraction) with normal density stratification or augment it (unstable contraction) if densities are inverted. F. Extension halotectonics. Salt rollers form a decoupling zone below listric normal faults in extending cover; lithostatic pressures can retard or augment this flow, depending on whether a density inversion is absent (stable extension) or present (unstable extension), respectively.

Figure III:1:1 (Figure 5; Jackson and Talbot, 1986)

the caprock. At stage 6, sediments are shown to have collapsed into the peripheral sink.

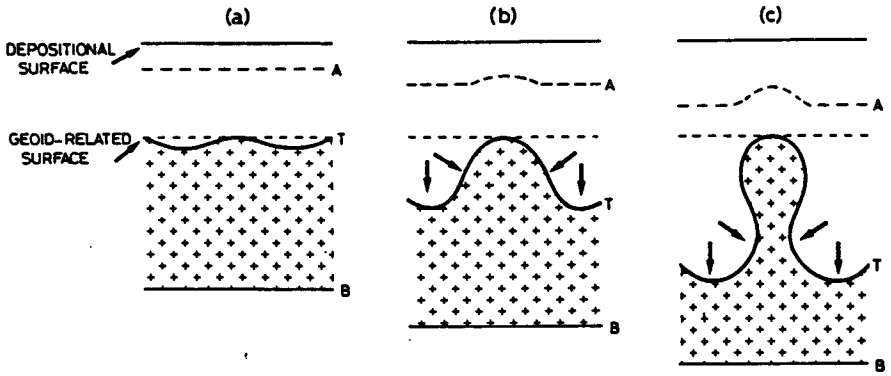

Fig. 4.2 Schematic diagrams summarising Barton's (1933) downbuilding hypothesis for the development of salt diapirs. Key: cross symbol, salt; overburden left blank; upper dashed line A is a reference horizon within the overburden; lower dashed line is the trace of a reference surface related to the geoid; solid lines B, T, are base and top salt levels. The sequence of events suggested is (a) a salt swell begins to develop for unspecified reasons; (b) basinal subsidence occurs beneath the load of continuing deposition, while crest of salt swell remains at same level as in (a), and components of overburden load stress perpendicular to salt flanks tend to compress the plastic salt mass laterally. (c) Salt diapir develops as an inverted 'teardrop' shape. Crest remains at the same level as the salt subsides, with flow into diapir continuing. Greater compaction effects above the salt 'lows' flanking the diapir lead to apparent uplift of horizon A above the diapir.

Figure III:1:2 (Figure 4.2; Jenyon, 1986)

Fig. 2-36. Salt glacier flowing out of crater, Iran. (After Lotze, 1957.)

Figure III:1:3 (Figure 2-36; Baar, 1977)

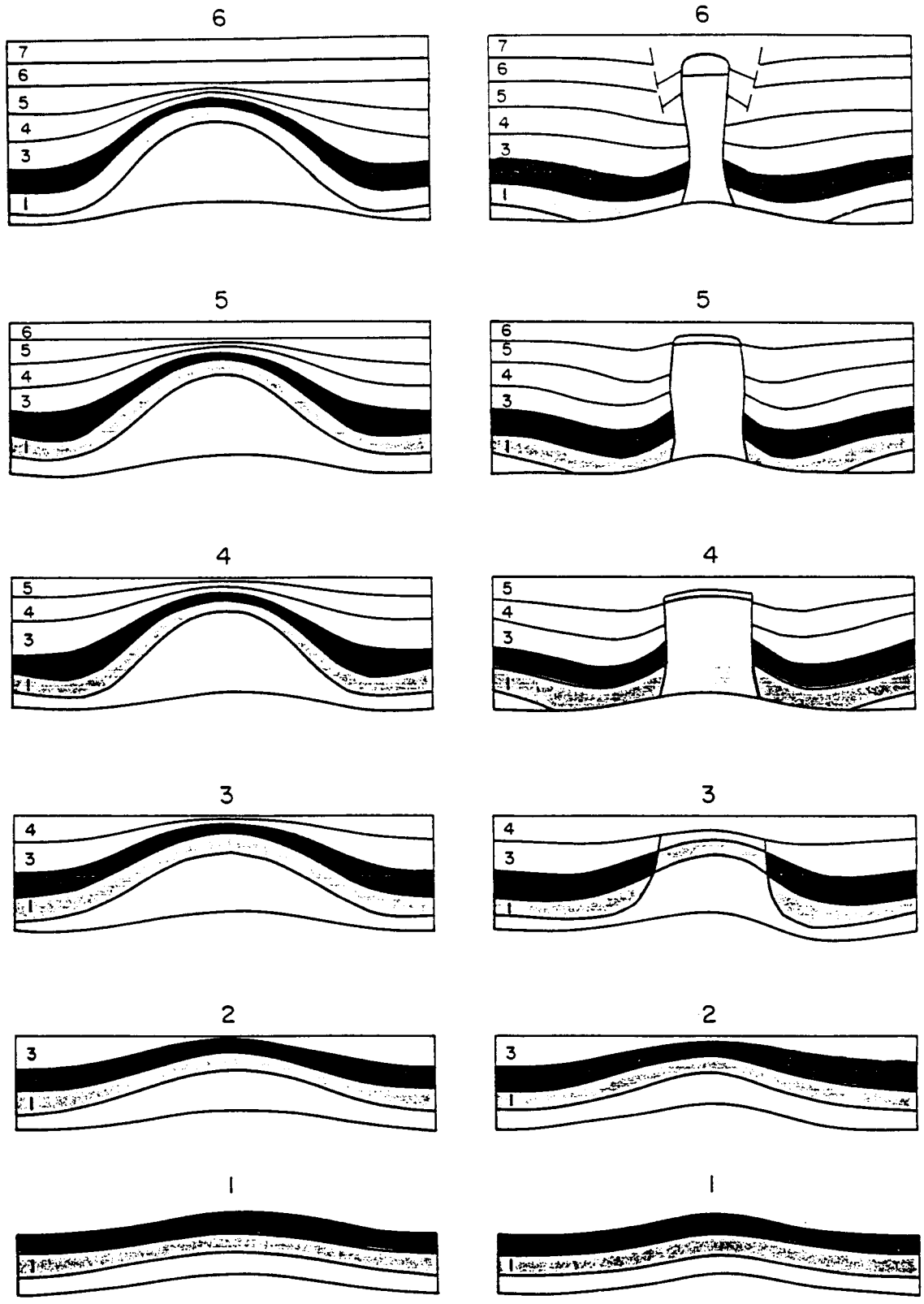

Figure 3-2. Stage development of a shallow piercement dome (right) and deep-seated, non-piercement dome (left). (After Nettleton, 1934).

Figure III:1:4 (Figure 3-2; Halbouty, 1979)

2) CLASSIFICATION OF SALT FLOW STRUCTURES

A) Depth of burial:

Several classification schemes for salt domes, based on the depth to the top of the cap rock or salt, have been suggested (Figure III:2:1):

Shallow	Intermediate	Deep
<2000 ft	2000-4000 ft	>4000 ft
<4000 ft	4000-10000 ft	>10000 ft

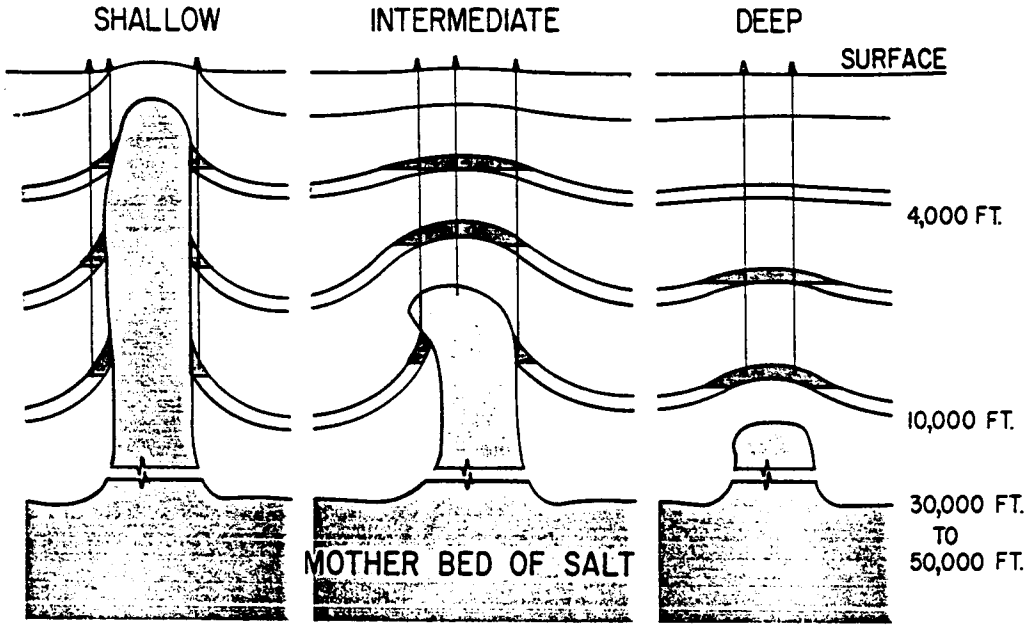

Figure 5-1. Diagrammatic section of typical piercement domes classified according to depth of burial. Note that the domes have been greatly foreshortened between the upper part of the salt stock and source layer.

Figure III:2:1 (Figure 5-1; Halbouty, 1979)

B) Form:

Various forms of salt flow structures have been documented in the literature. These include salt rollers (domes), salt anticlines (domes), salt pillows (domes), diapiric stocks, diapiric salt walls (ridges or massifs), detached diapirs, dikes, sills, and extruded glaciers or namakiers (Figure III:2:2).

C) Domes vrs. diapirs:

The term salt dome is used in reference to a flow-related convexity or buldge along the upper surface of a body of salt. If this feature pierces the overlying strata, the dome is referred to as a diapir (Figure III:2:3).

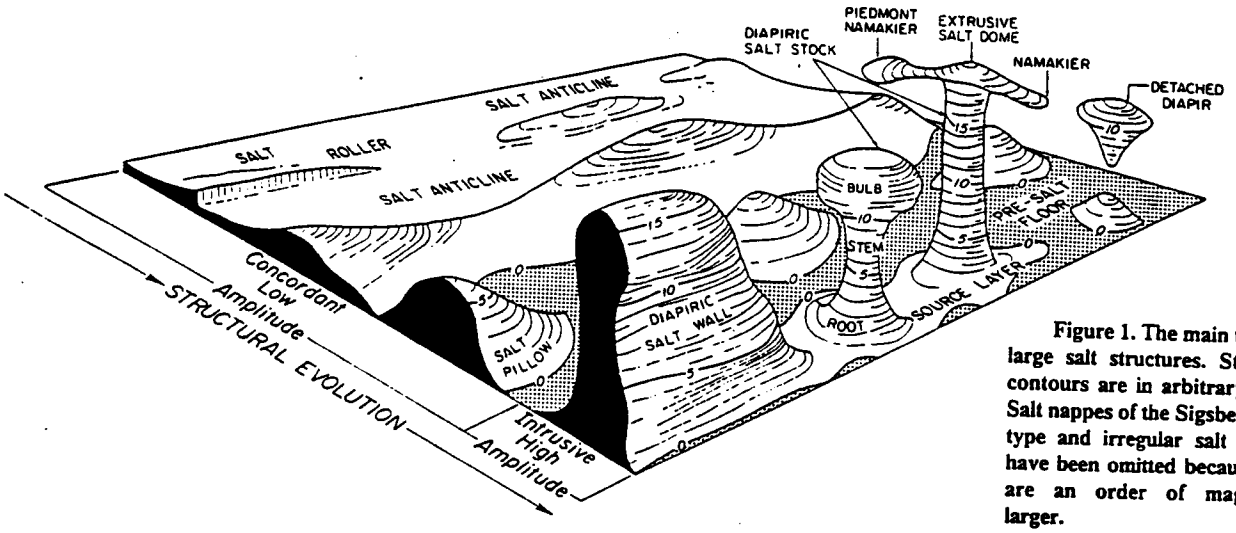

Figure 1. The main types of large salt structures. Structure contours are in arbitrary units. Salt nappes of the Sigsbee Scarp type and irregular salt massifs have been omitted because they are an order of magnitude larger.

Figure III:2:2 (Figure 1; Jackson and Talbot, 1986)

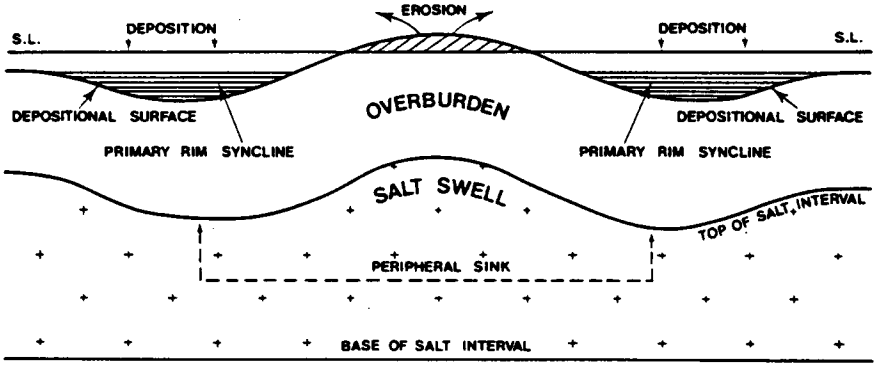

(a)

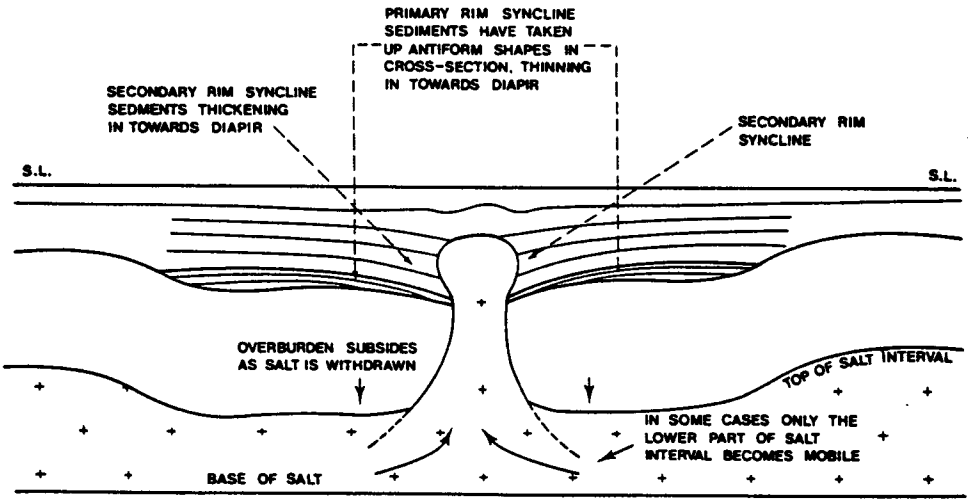

(b)

Fig. 7.17 Diagrammatic representations of the pre-piercement (a) and piercement (b) stages of diapirism, showing the peripheral sink and the development of primary and secondary rim synclines. Note the position of the depositional surface contemporary with salt movement in (a).

Figure III:2:3 (Figure 7.17; Jenyon, 1986)

D) Peripheral sinks:

A salt dome is typically initiated by the lateral flow of peripheral salt into a localized, central area of net salt accumulation (pillow or buldge). The area of salt depletion, the peripheral sink, is frequently manifested as an encircling salt thin. As the salt pierces the overlying strata and flows vertically, the primary peripheral sink progressively shifts towards the diapir. If the development of the diapir is more-or-less continuous, and contemporaneous with sedimentation, the speed of the salt movement can be estimated from the shifting of the thickness maxima in the post-salt sediment (Figure III:2:4).

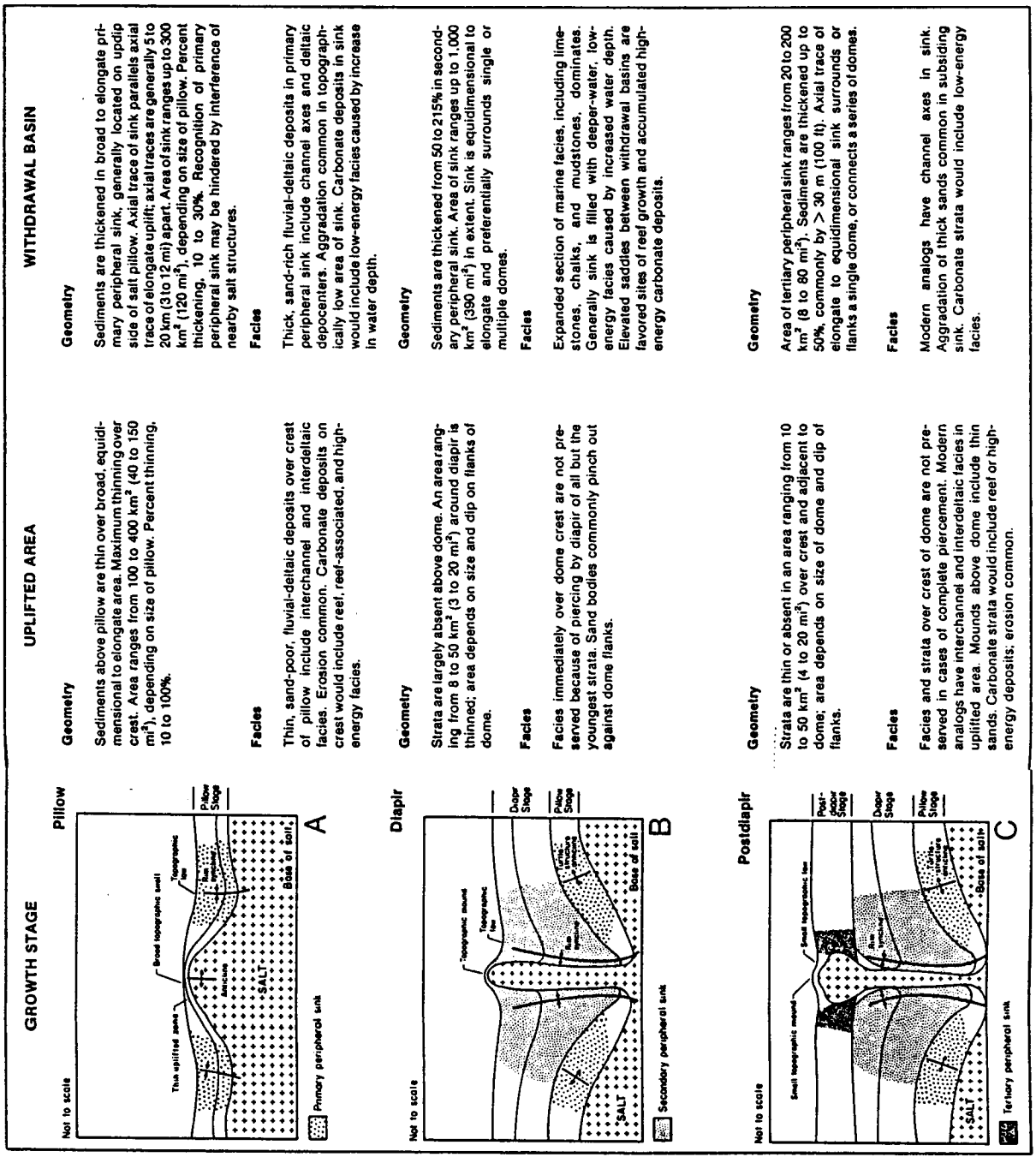

Figure III:2:4 (Figure 8; Jackson and Talbot, 1986)

E) Genetic relationships:

Following Halbouty's terminology, an isolated salt dome, or one near the center of an arc or circle formed by other domes, anticlines or ridges is generally considered to be primary (Figure III:2:5). The features comprising the arc are regarded as secondary salt structures. The relationship between the primary and secondary domes is addressed in the following summary of their development:

1) A primary dome and peripheral sink develop. A series of graben fractures contemporaneously form about the margins of the sink.

2) The equilibrium between the salt and the overlying beds is disturbed and the growth of domes is initiated on the edge of the sink. Generally these secondary domes are smaller.

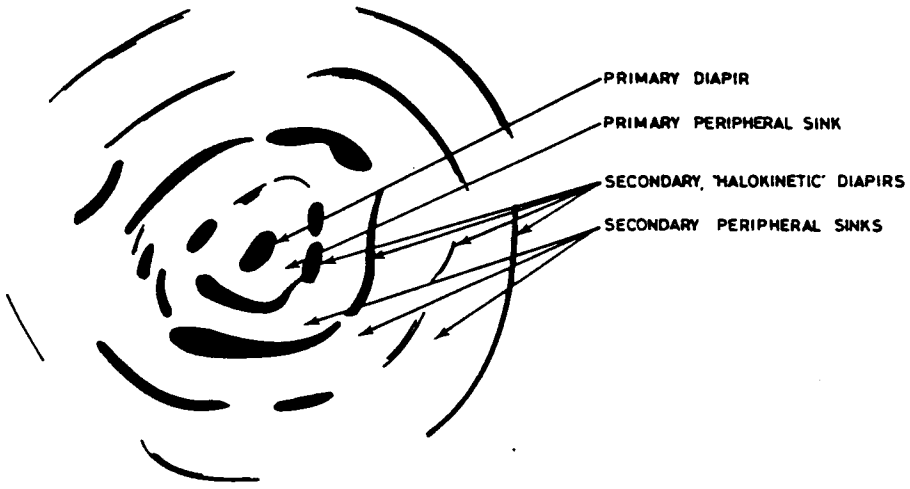

Fig. 4.11 Freehand sketch of a photograph of later-stage developments in one of the concentric diapir groups in Parker and McDowell's model studies, as shown in Fig. 4.10 (After Parker and McDowell, 1955.)

Figure III:2:5 (Figure 4.11; Jenyon, 1986)

3) CAP ROCKS

Anhydritic cap rock is generally considered to be the accumulated insoluable residues precipitated from ground waters acting on the dome's salt mass. Gypsum, calcite, sulphur and other minerals are products of anhydritic alteration (Figure III:3:1). These cap rocks are of economic interest because of their association with hydrocarbon traps and potential commercial mineral accumulations (sulfur, ion, lead, zinc, uranium; Light and Posey (1987)).

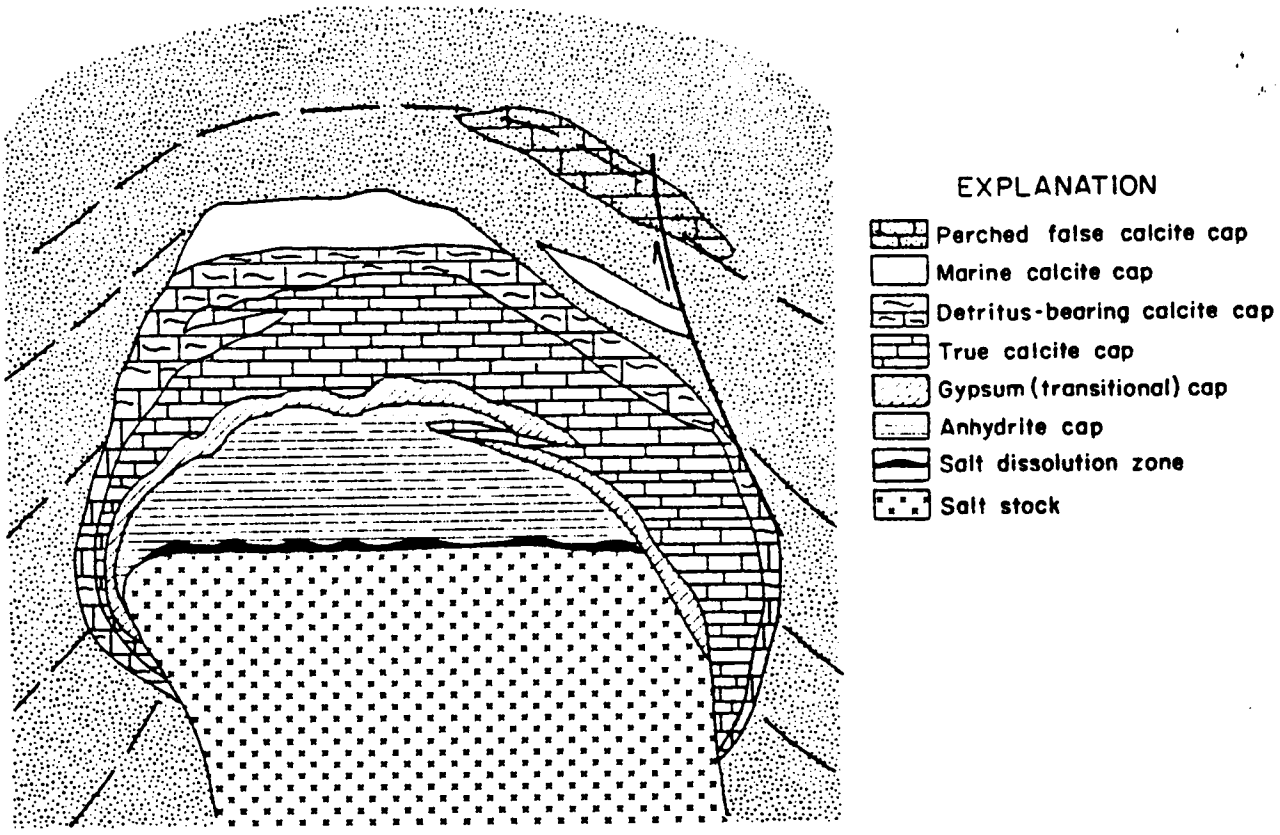

FIG. 2. Generalized cross-section of salt dome cap rocks. No scale. After POSEY (1986).

Figure III:3:1 (Figure 2; Posey et al., 1987)

According to Posey et al. (1987), salt diapirs contain a few percent of anhydrite that accumulated as residue to form anhydrite cap rocks during salt dissolutions. Reported $^{87}Sr/^{86}Sr$ ratios of these salt-hosted and cap rock anhydrites in the Gulf Coast U.S.A., indicate their derivation from Middle Jurrasic seawater. However a much wider range of $^{87}Sr/^{86}Sr$ ratios, incorporqating a highly radiogenic component in addition to the Middle Jurrasic component, has been foun din several Gulf Coast salt domes. This wide range of $^{87}Sr/^{86}Sr$ ratios of anhydrite within the salt stock records Sr contributions from both marine water and formation water that has equilibrated with siliclastics. During cap rock formation this anhydrite either recrystallized in the presence of, or was cemented by, a low-Sr fluid with a Late Cretaceous seawater type Sr isotope ratio or simply lost Sr during recrystallization. Later, the cap rock was invaded by warm saline brines with high Sr isotope ratios from which barite and metal sulfides were precipitated. Subsequently, low salinity water hydrated part of the anhydrite bringing to six the total number of fluids that interacted throughout the history of salt dome and cap rock growth. The proginator of these salt diapirs, the Louann Formation, is generally thought to have formed from marine waters evaporated to halite and rarely, higher evaporite facies. Salt domes in East Texas, North Louisiana, and Mississippian Basins have $^{87}Sr/^{86}Sr$ and ^{34}S values that corroborate a mid-Jurassic age for the mother salt. However salt domes in the Houston and Rio Grande Embayments of the Gulf Coast Basin have $^{87}Sr/^{86}Sr$ ratios ranging to higher than both Middle Jurassic seawater and all Rb-free Phanerozoic rocks. These anomalous $^{87}Sr/^{86}Sr$ ratios are probanly

derived from radiogenic Sr-bearing fluids that equilibrated with siliclastic rocks and invaded the salt either prior to, or during, diapirism. Potential sources of the radiogenic ^{87}Sr component include clay or feldspar (located in either older units below the Louann Formation or younger units flanking the salt diapirs) and K-salts within the Louann evaporites. Because partial Sr exchange in anhydrite had to take place in a fluid medium, admittance of radiogenic ^{87}Sr-bearing fluids into the salt may have led to diapirism by lowering the shear stregnth of the crystalline salt. The slight number of anomalous $^{87}Sr/^{86}Sr$ values in the interior basins indicates that the anomalous values are related to areally discrete structural or stratigraphic controls that affected only the Gulf Coast Basin.

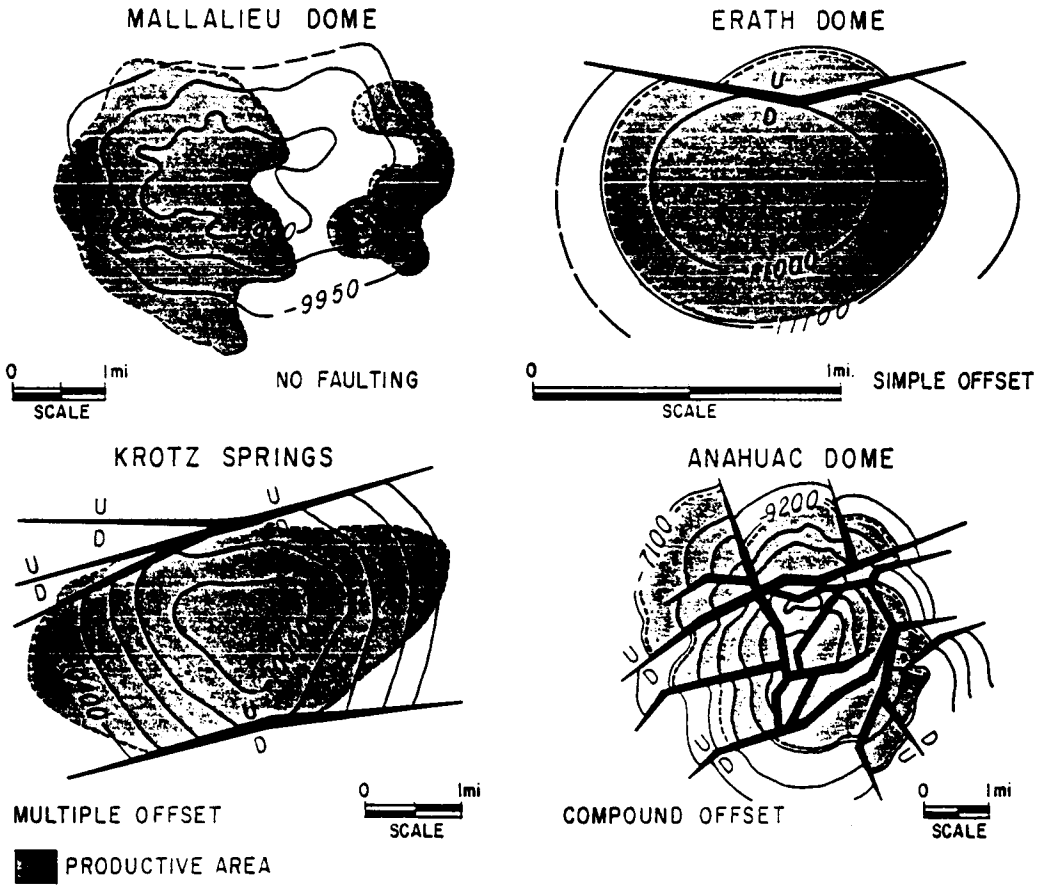

Figure 5-10. Structure contour maps of principal types of offset fault patterns defined by Wallace (1944). The simplest form is a domal type structure with no major faulting, such as Mallalieu field, Lincoln County, Mississippi. Erath field, Vermilion Parish, Louisiana is an example of a domal type structure with simple offset faulting. A multiple offset fault pattern is characterized by more than one major fault downthrown in the same direction, as exemplified by Krotz Springs field, St. Landry Parish, Louisiana. Compound offset faulting forms a complex pattern in which no particular type is dominant, as in the case of Anahuac field, Chambers County, Texas. (After Murray, Steig, Bader and Louisiana Department of Conservation in Murray, 1961).

Figure III:4:1 (Figure 5-10; Halbouty, 1979)

4) ASSOCIATED FAULTING

According to Halbouty, typical fault patterns associated with salt domes include (Figures III:4:1-III:4:3):

A) Over or adjacent to salt dome:

1) Offset - 3 classifications:

a) Simple offset - single major fault.

b) Multiple offset - more than one major fault in same direction.

c) Compound offsets - many major and minor faults with no particular orientation.

2) Radial - normal faults emanating from apex or flanks of dome.

3) Graben - prominent pattern over apex of many domes.

4) Horst - uncomman fault pattern sometimes formed by multiple offset.

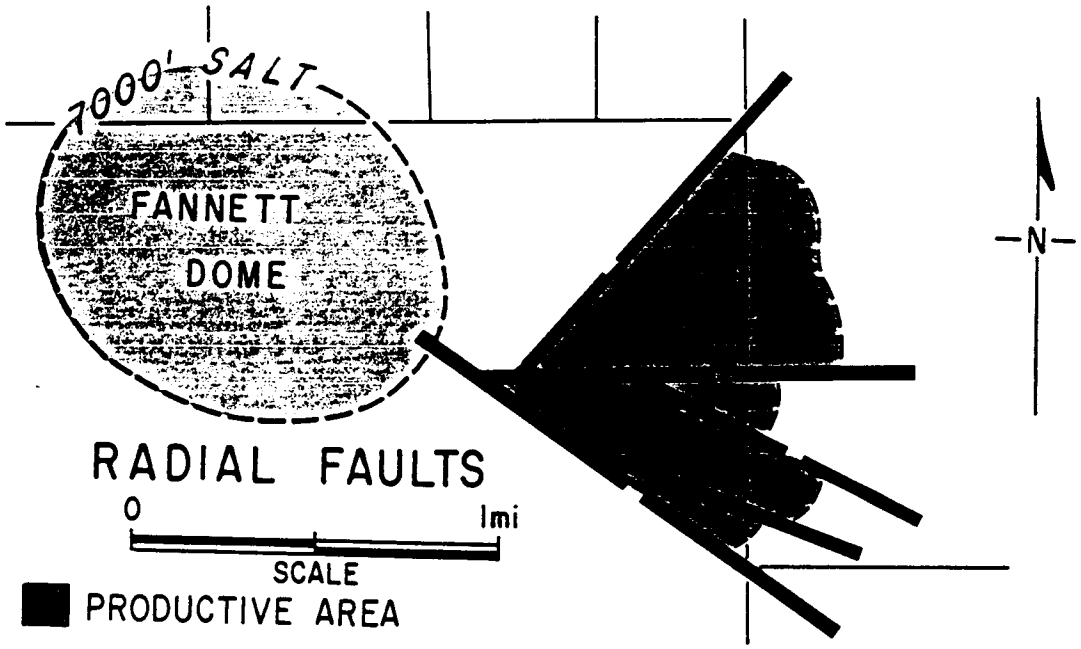

Figure 5-11. Radial fault pattern (greatly simplified), Fannett dome, Jefferson County, Texas.

Figure III:4:1 (Figure 5-10; Halbouty, 1979)

B) Away from dome:

1) Tangential or peripheral - normal faults up- or down-thrown toward dome some distance away from the salt plug.

2) Regional - major fault may influence structure on more than one dome.

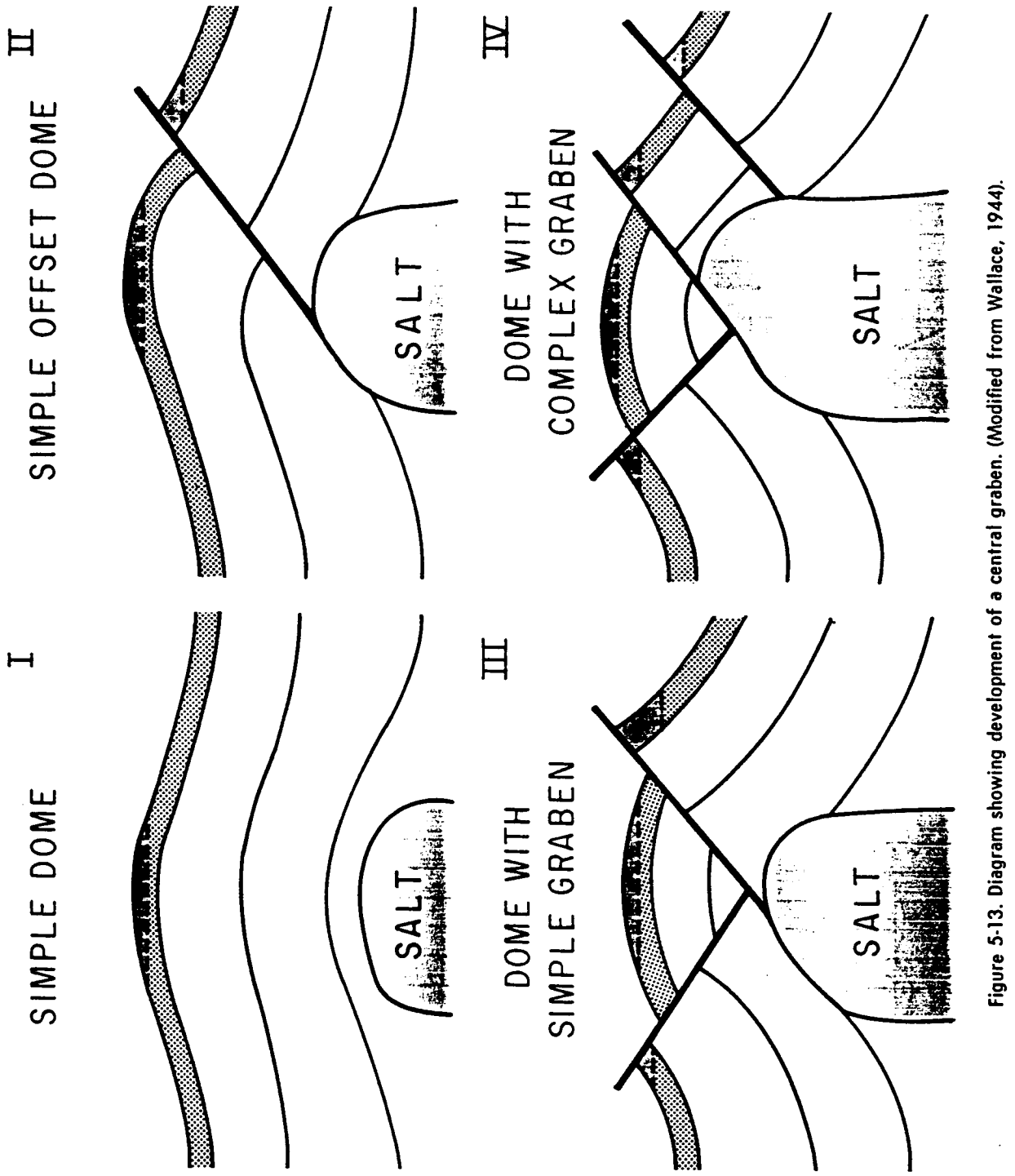

Figure 5-13. Diagram showing development of a central graben. (Modified from Wallace, 1944).

Figure III:4:3 (Figure 5-13; Halbouty, 1979)

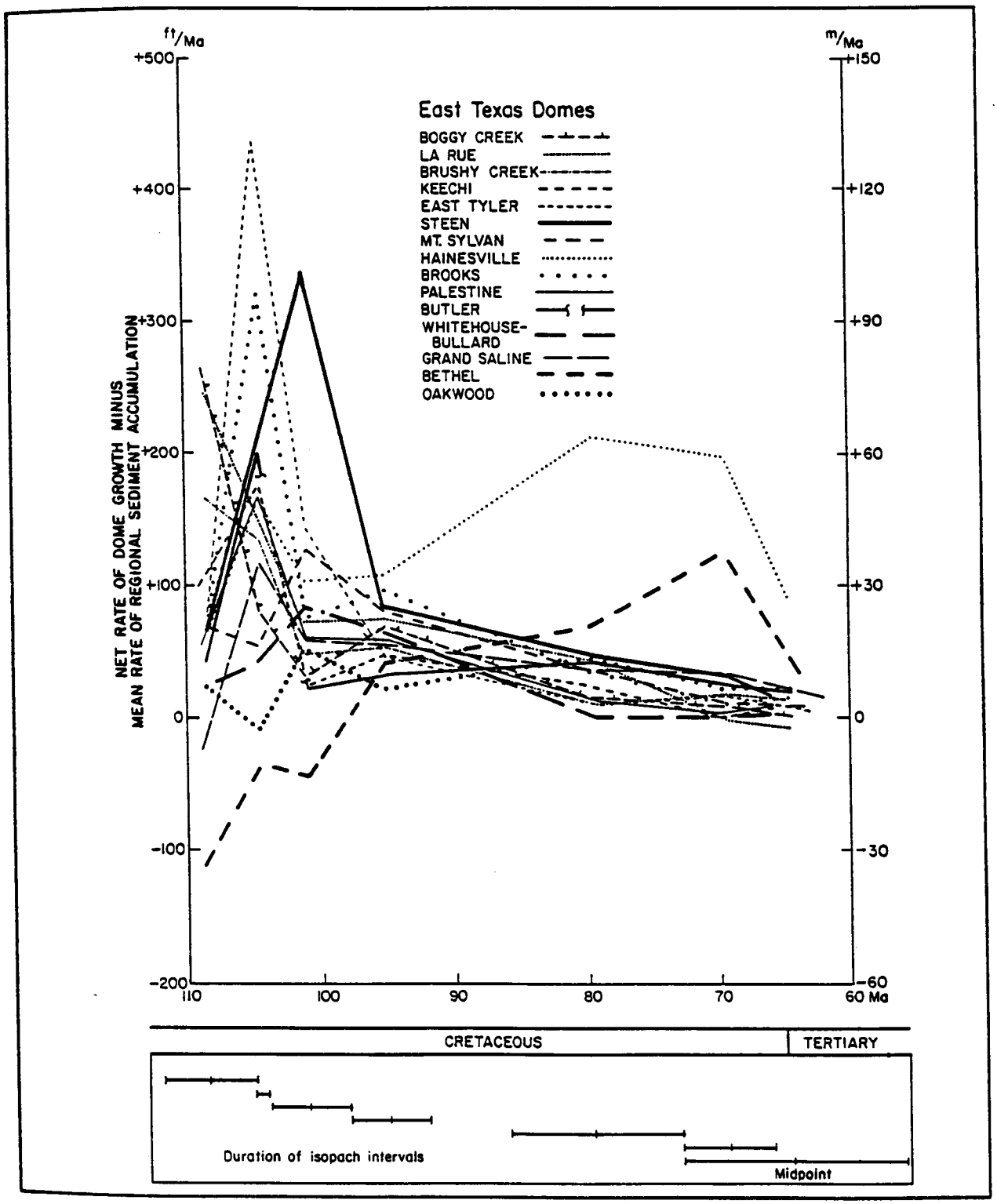

FIGURE 54. Residual rates of dome growth for 16 East Texas salt domes calculated by subtracting mean rate of regional sediment accumulation from net rate of dome growth. Residual rates of dome growth are independent of regional sediment-accumulation rates. Even with removal of high rates of regional sedimentation (compare fig. 53), most domes grew fastest during the Early Cretaceous.

Figure III:5:1 (Figure 54; Seni and Jackson, 1984)

5) RATE OF FLOW (Figure III:5:1)

According to Jackson and Talbot (1986), the strain rates for the in-situ deformation of rock salt vary by over 8 orders of magnitude from $10^{-8}s^{-1}$ to $10^{-16}s^{-1}$. According to these authors, the most rapid rates are those of borehole closure during accelerating creep ($10^{-8}s^{-1}$), mine closures and steady state borehole closures ($10^{-9}s^{-1}$ to $10^{-11}s^{-1}$) and namakiers (salt glaciers; $10^{-8}s^{-1}$ to $10^{-11}s^{-1}$). The rates of diapiric extrusion assisted by folding ($10^{-13}s^{-1}$) and the rates for the most active phase of gravity driven diapiric growth are significantly lower ($10^{-8}s^{-1}$ to $10^{-11}s^{-1}$).

The natural rates of strain for in-situ salts are significantly lower than those typically used in laboratory stress tests (on the order of $10^{-7}s^{-1}$ or greater); this relationship and the use of dry laboratory rock salt test samples probably explains why rock salts were assumed to deform elastically. Recall that in laboratory testing, strain hardening (Figure I:2:1) of rock salt typically occurs; as a consequence decreasing creep rates (Transient creep; Section I:2:B) are observed. In-situ, the long term creep deformation of salt rocks is not affected by strain hardening and steady state creep occurs until elastic behaviour is re-established. There are two principal reasons for the discrepancy between laboratory and in-situ observations: 1) laboratory strain rates are generally too high to allow for Solution Precipitation creep; and 2) laboratory samples are too dry to allow for Solution Precipitation creep (Section I:2:G). In-situ, the deformation of rock salt generally occurs in the presence of trace brine and under low stress differentials.

Jackson and Talbot (1986) present estimated relative strain rates during the growth of a model diapir are presented. The peak strain rates of between $10^{-14}s^{-1}$ and $10^{-15}s^{-1}$ were estimated on the basis of: 1) the maximum height of the diapir; 2) the density contrast between the rock salt and adjacent sediment; 3) the length of time over which the diapir formed; and 4) the buoyancy forces operative at various stages of growth.

6) EXPLORATION IMPLICATIONS: SALT DOMES

A) Hydrocarbon entrapment:

Halbouty prepared an idealized section through a salt dome in order to illustrate some of the comman types of traps (Figure III:6:1). A single dome may have several, if not all, of these types of traps.

1) Simple domal anticline

2) Graben fault trap over dome

3) Porous cap rock (limestone or dolomite)

4) Flank sand pinchout and sand lens

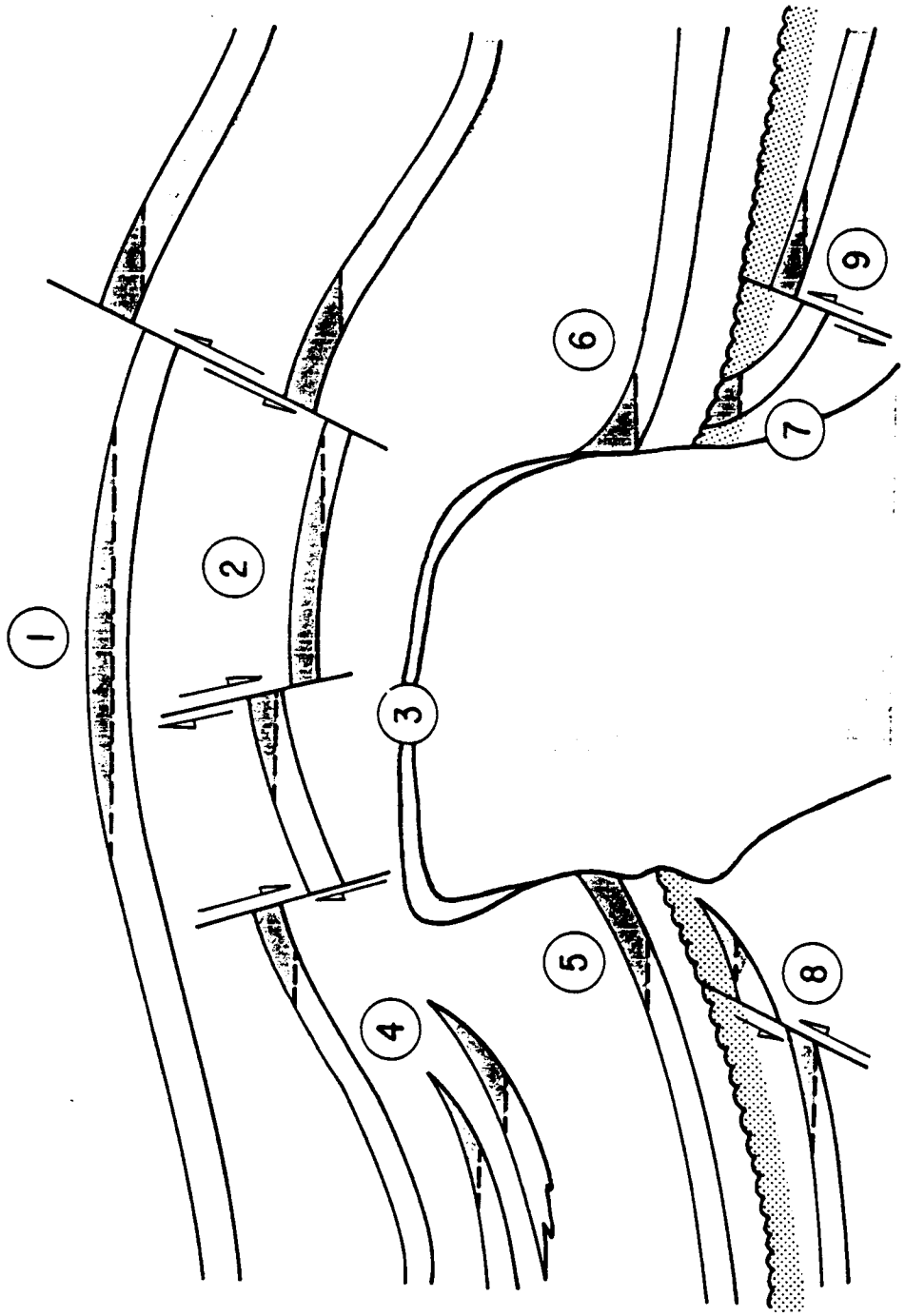

Figure 6-1. Idealized section showing common types of hydrocarbon traps associated with salt domes. Various traps include (1) simple domal anticline draped over salt; (2) graben fault trap over dome; (3) porous cap rock; (4) flank sand pinchout and sand lens; (5) trap beneath overhang; (6) trap uplifted and buttressed against salt plug; (7) unconformity; (8) fault trap downthrown away from dome; (9) fault trap downthrown toward dome.

Figure III:6:1 (Figure 6-1; Halbouty, 1979)

5) Trap beneath overhang

6) Trap uplifted and buttressed against salt plug

7) Unconformity

8) Fault trap downthrown away from dome

9) Fault trap downthrown towards dome

B) Factors affecting reservoir quality:

1) Oil catchment area.

2) Structural closure.

3) Structural character of the area.

4) Shape of domal mass.

5) Pattern and complexity of faulting above and around the dome.

6) Occurance and magnitude of unconformities.

7) Dip of the flank beds.

8) Occurance of caprock and supredomal accumulations.

9) Timing and rate of doming.

10) Source rock quality and proximity.

12) Reservoir quality.

C) Misinterpretation of salt dome features:

The seismic signature of a salt dome can be misinterpreted as indicative of faulting or of a poor data quality area. Alternatively, the diffraction patterns from faults and a localized poor data quality area can be inadvertantly interpreted as salt dome features.

D) Heat flow anomalies:

Rock salt has a higher thermal conductivity (about 6 W/m/°C) than that of comman clastic rock types (in the range of 1.5-2.5 W/m/°C). As a consequence an enhanced heat flux is associated with salt deposits and with salt domes in particular.

In a their study of the influence of salt domes on paleotemperature distributions, O'Brien and Lerche (1984) present a simple analytical model of heat flow in the vicinity of an isolated salt dome. In addition to an enhanced surface heat flow, their model shows that on the upper flanks of a salt dome a temperature higher than the regional trend is predicted, thus enhancing hydrocarbon maturation at these depths. On the lower flanks of the salt dome a temperature lower than the regional trend is predicted, thus inhibiting overmaturation.

7) REFERENCES

Baar, C.A., 1977, Applied salt-rock mechanics 1: Elsevier Scientific Publishing Company, 294 p.

Halbouty, M.T., 1979, Salt domes: Gulf Publishing Company, Houston, 561 p.

Jackson, M.P.A. and Talbot, C.J., 1986, External shapes, strain rates, and dynamics of salt structures: Bulletin Geological Society of America 97, 305-323.

Jenyon, M.K., 1986, Salt tectonics: Elsevier Applied Science Publishers, 191 p.

Light, M.P.R. and Posey, H.H., 1987, Model for the origins of geopressured brines, hydrocarbons, cap rocks and metallic mineral deposits: Gulf Coast, U.S.A.: Dynamical Geology of Salt and Related Structures, 787-830.

Posey, H.H, Kyle, J. R., Jackson, T.J. and Hurst, S.D., 1987, Multiple fluid components of salt diapirs and salt dome cap rocks, Gulf Coast, U.S.A.: Applied Geochemistry 2, 523-534.

Seni, S.J. and Jackson, M.P.A., 1984, Sedimentary record of Cretaceous and Tertiary salt movement, East Texas Basin: Times, rates, and volumes of salt flow and their implications to nuclear wate isolation and petroleum exploration: The University of Texas at Austin Bureau of Economic Geology Report of Investigations 139, 89 p.

Talbot, C.J. and Jackson, M.P.A., 1987, Internal Kinematics of salt diapirs: Bulletin American Association Petroleum Geologists 71, 1068-1093.

IV: STORAGE AND WASTE DISPOSAL

1) OVERVIEW

The materials being stored in salt cavities fall into four broad categories (Figure IV:1:1-IV:1:2):

A) Hydrocarbon storage.

B) Radioactive waste.

C) Industrial waste.

D) Air storage for peaking power.

E) Documents, records, etc.

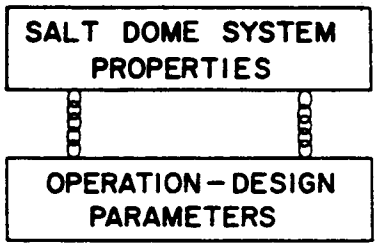

EXAMPLE:

OPERATION–DESIGN PARAMETER	CRITICAL SALT DOME CHARACTERISTIC
• Rate of Cavity Development	Character of Salt and Included Material
• Shape of Cavity	Internal Domal Structure
• Stability of Cavity	Mechanical Properties of Domal Material
• Blowouts	Gas and Stress Conditions
• Contamination	Gas and Liquid Inclusions
• Optimization of Domal Use	Geometric Configuration and System Properties
• Future Adaptation	All Possible
• Environmental	Complete Geomechanical System

Figure 3. Salt dome system properties as a basis for operation-design parameters.

Figure IV:1:1 (Figure 3; Martinez, 1985)

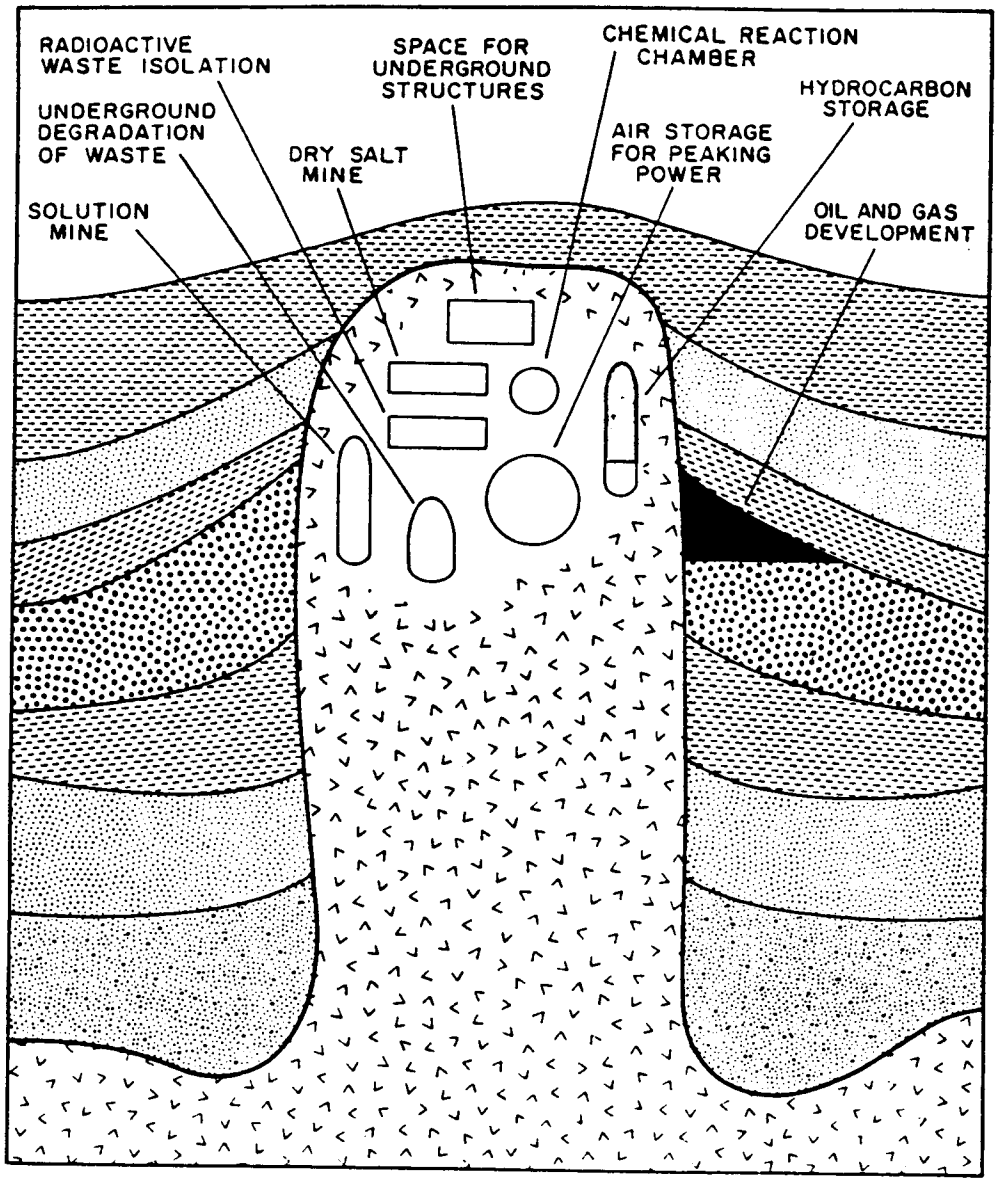

Figure 1. Potential demands for salt dome utilization. From Martinez and Thoms (1978).

Figure IV:1:2 (Figure 3; Martinez, 1985)

2) HYDROCARBON STORAGE

A) Overview:

The hydrocarbons being stored in salt cavities fall into two broad categories:

1) Liquid petroleum products such as gasoline, fuel oil, and crude oil.

2) Natural gas.

B) Storage of liquid petroleum products:

Liquid petroleum products can be economically stored on a long-term basis in subsurface salt cavities. The process of creating, filling, and emptying such caverns can be thought of as a three stage process.

In the initial phase of this process, a solution cavity of pre-designed shape and size is created (Figures IV:2:1-IV:2:5). In a typical operation, fresh water is injected through the middle casing string under pressure. The subsurface salt is dissolved producing a dense brine which sinks to the bottom of the

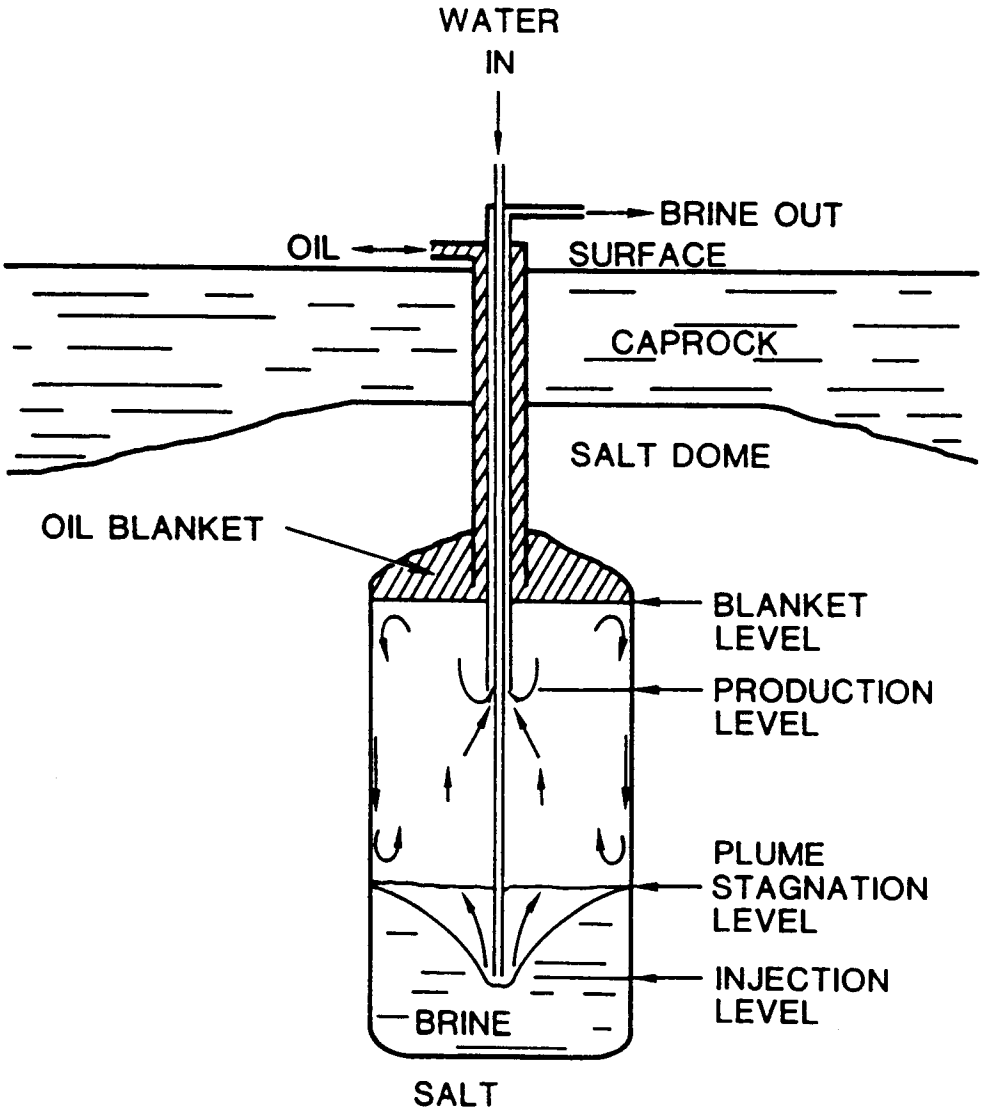

Figure 1. Cavern Geometry and Flow Regions for Direct Leaching

Figure IV:2:1 (Figure 1; Russo, 1985)

cavity where it is pumped or flows to the surface through the smallest casing. To prevent fresh water from dissolving the salt around the casing seat, an inert blanket of oil or gasoline is often maintained at the top of the cavity.

After the cavern has been completed, pressurized liquid petroleum is injected at the top of the cavity; the brine is displaced and removed through tubing at the base. In practice, steps one and two may be overlapped in order to: 1) accelerate the process; and 2) control the lateral extent of leaching at any given level within the cavity. In step three, brine or fresh water is injected into the base of the cavity; displaced liquid petroleum is removed at the top. Steps two and three are repeated each time the cavity is emptied and then refilled with liquid petroleum products (Figures IV:2:1-IV:2:5).

The storage of liquid petroleum products in salt cavities is attractive for several reasons:

1) A subsurface waste containment unit is not easily accessible, and therefor less likely to be accidentally damaged or intentionally sabotaged.

2) Salt cavities are relatively easy to construct and are lower in cost than other containment units of comparable size. This is particularly true if the removed salt is mined.

3) Salt is impervious to the passage of water and liquid petroleum products because of its plasticity and crystalline structure.

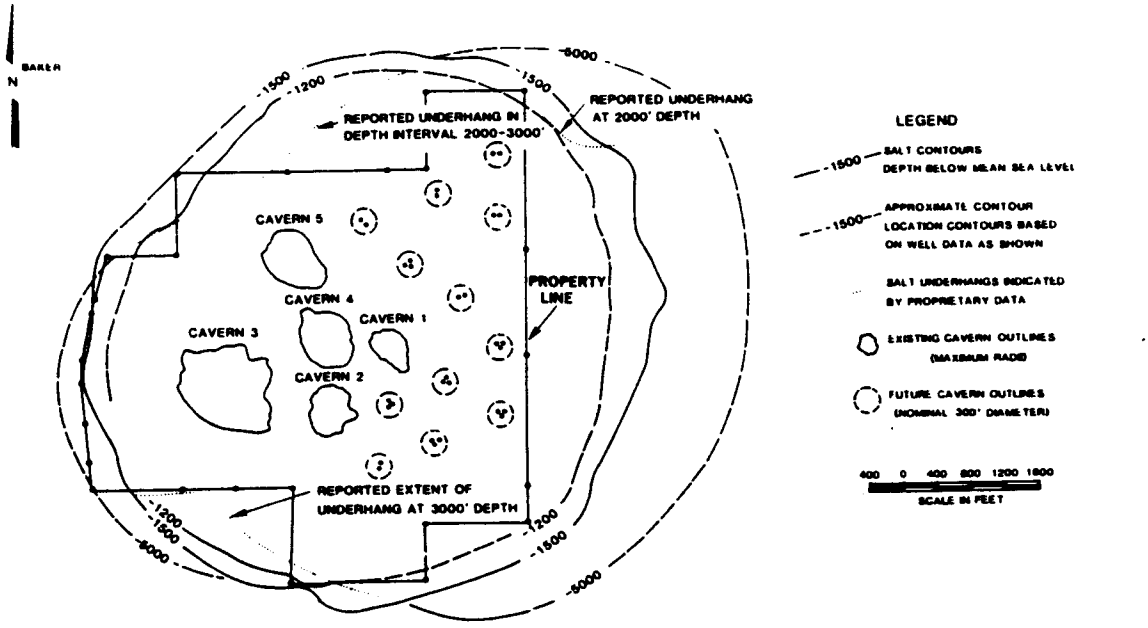

Figure 1. Plan View of Bryan Mound Salt Dome.

Figure IV:2:2 (Figure 1; Preece and Foley, 1985)

4) Salts generally deform plastically; fractures that do occur usually heal rapidly as a result of recrystallization. Permanent fractures do form in other rock types.

The are some disadvantages to the use of salt cavities for the storage of liquid petroleum products:

1) Additional dissolution will occur each and every time the cavity is emptied. If the cavern is emptied and re-filled repetitively, it will eventually fail. As a result, the caverns can be economically used only for long term storage.

2) Salt is corrosive.

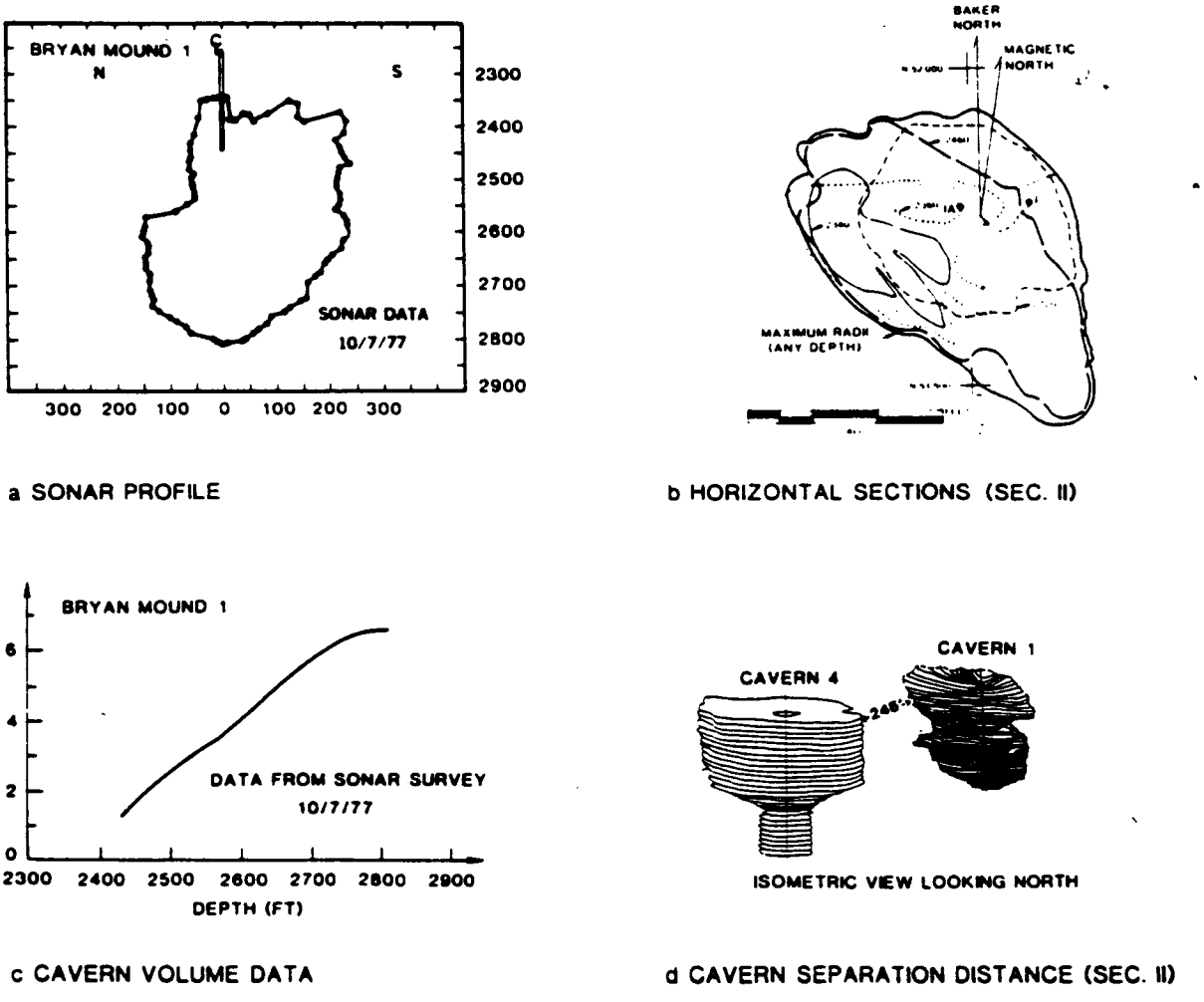

Figure 10. Bryan Mound Cavern One.

Figure IV:2:3 (Figure 10; Preece and Foley, 1985)

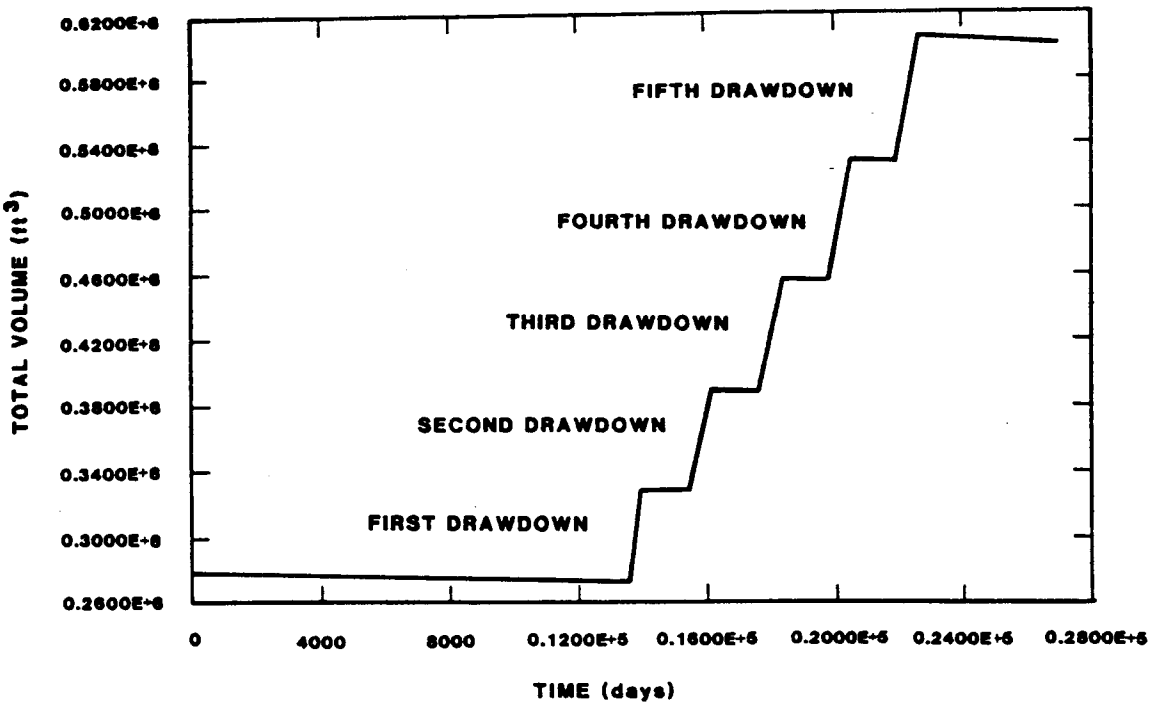

Figure 8. Volumetric Response of Cavern One.

Figure IV:2:4 (Figure 8; Preece and Foley, 1985)

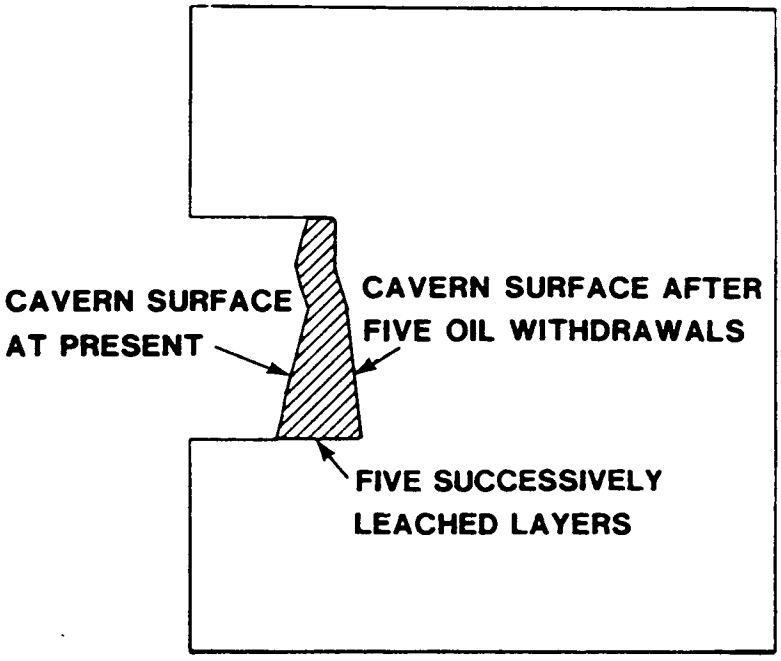

Figure 7. Bryan Mound Cavern One with Leached Layers Crosshatched.

Figure IV:2:5 (Figure 7; Preece and Foley, 1985)

C) Storage of natural gas:

Natural gas can be economically stored in shallow, subsurface salt cavities (Figure IV:2:6). The process of creating, filling, emptying, and re-filling such caverns can be thought of as a four stage process.

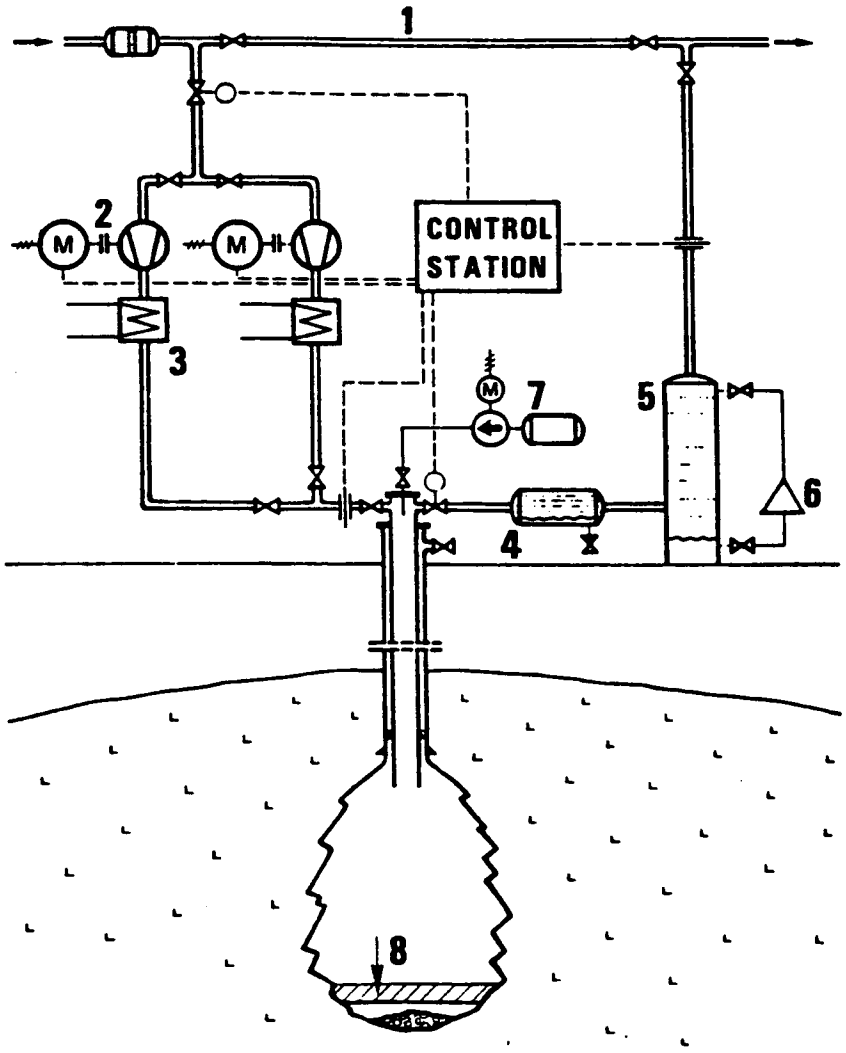

Figure 10. Schematic diagram of a high pressure gas cavern storage.

Figure IV:2:6 (Figure 10; Haddenhorst and Quast, 1985)

In the initial phase of this process, a solution cavity of pre-designed shape and size is created. After the cavern has been completed, pressurized natural gas is injected at the top of the cavity; the brines is displaced and removed through tubing at the base. The residual brine may be overlain by a special fluid in order to prevent a rise in the water vapour content and thereby in the water dewpoint of the stored gas. In step three, pressurized gas is

released from the cavern as required; the internal pressure of the residual gas drops accordingly. In step four, pressurized gas is re-injected into the cavern until the desired internal pressure is re-established. Steps three and four are repeated each time the cavity is emptied and then refilled.
The storage of natural gas in salt cavities is attractive for several reasons:

1) A subsurface waste containment unit is not easily accessible, and therefor less likely to be accidentally damaged or intentionally sabotaged.

2) Salt cavities are relatively easy to construct and are lower in cost than other containment units of comparable size. This is particularly true if the removed salt is mined.

3) Salt is impervious to the passage of water and gas because of its plasticity and crystalline structure.

4) Salts generally deform plastically; fractures that do occur usually heal rapidly as a result of recrystallization. Permanent fractures do form in other rock types.

5) Unlike aquifer storage, no friction pressure losses occur in the salt cavern; therefor relatively high production rates can be achieved.

6) The gas can be withdrawn and re-injected in accordance with daily or other peak and low consumption periods.

The are some disadvantages to the use of salt cavities for the storage of natural gas:

1) The storage capacity of the cavity will decrease as a result of long-term creep.

2) Salt is corrosive.

3) Secondary H_2S can occur as a result of unintentional innoculation with sulfate reducing bacteria or by hydrolysis of carbonyl-sulfide (COS). percentages in the stored gas.

3) RADIOACTIVE WASTE

A) Protective cannisters:

Hazardous waste can often be encased in non-corrosive, protective cannisters or other material and stored within a subsurface salt cavity. Such storage is attractive for several reasons:

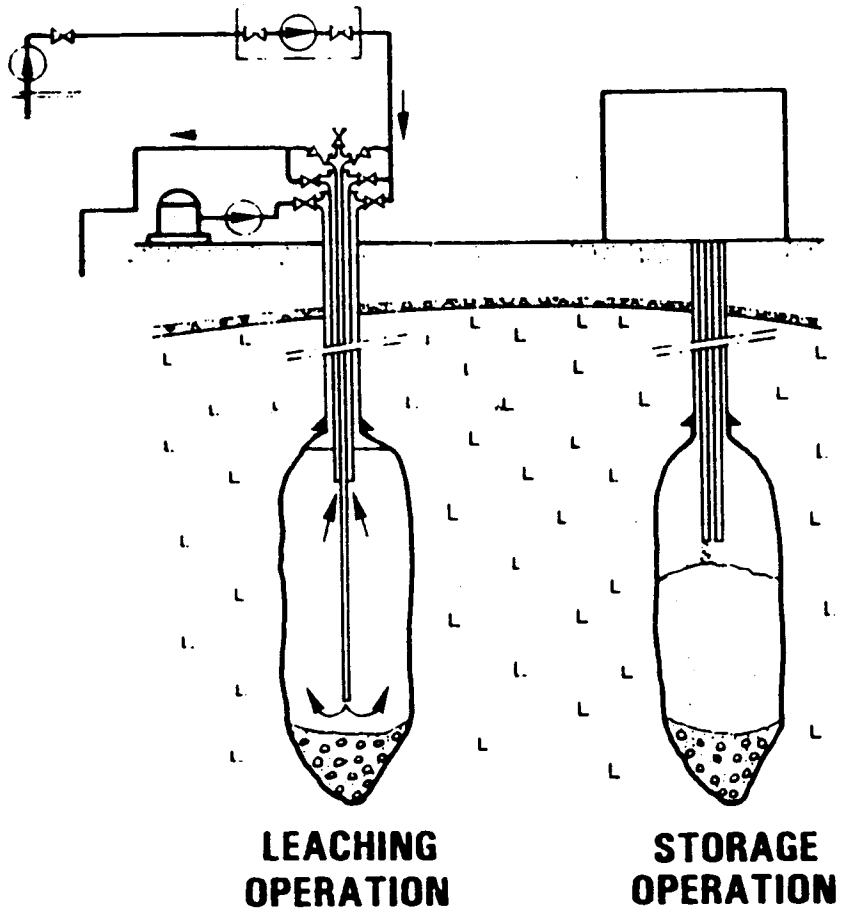

Figure 27. Disposal of MLW/LLW principle leaching and storage diagram

Figure IV:3:1 (Figure 27; Quast and Schmidt, 1985)

1) A subsurface waste containment unit is not easily accessible, and therefor less likely to be accidentally damaged or intentionally sabotaged.

2) Salt cavities are relatively easy to construct and are lower in cost than other containment units of comparable size. This is particularly true if the removed salt is mined.

3) Salt is impervious to the passage of water because of its plasticity and crystalline structure.

4) Salts generally deform plastically; fractures that do occur usually heal rapidly as a result of recrystallization. Permanent fractures do form in other rock types.

5) Salt has a sufficiently high melting point and a comparatively high

thermal conductivity so that the heat generated by radioactive wastes can be dissipated in the salt without exceeding pre-determined temperature rises if care is taken in the design of the size, shape and spacing of the cannisters.

The are some disadvantages to the use of salt containment units:

1) A subsurface waste containment unit is not easily accessible.

2) The cavity within the salt will eventually close as a result of long-term creep; the enclosed cannisters could rupture. With respect to radioactive wastes, it is important to ensure that the cavity will be an effective containment unit as long as the waste remains hazardous.

3) Salt is corrosive.

B) Pellet/cement slurry:

Quast and Schmidt (1985) describe the leaching of five caverns with initial volumes of 10 m^3 each. These caverns were filled with medium- and low-level radioactive wastes (MLW/LLW). The waste was deposited as pellets in a cement slurry. The construction, filling procedure and temperature measurements conducted during and after curing of the cement is described (Figure IV:3:1).

4) WASTE

The use of salt cavities for the disposal of environmentally toxic waste (chemicals, saline drilling muds) can be practical and cost-effective. Karably (1985) and Wassmann (1985) discuss the use of salt cavities as waste disposal units (Figures IV:4:1-IV:4:3).

5) AIR STORAGE FOR PEAKING POWER

Gustin (1985) discusses the concept of storing compressed air in salt cavities for periods of peak power demand.

6) DOCUMENTS, RECORDS, ETC.

Important documents can be stored in the rooms of dry salt mines. Such storage is attractive primarily because a subsurface waste containment unit is not easily accessible, and therefor less likely to be accidentally damaged or intentionally sabotaged. As well, salts generally deform plastically and cavities are not likely to fail during earthquakes. In comparison to secured surface structures, salt

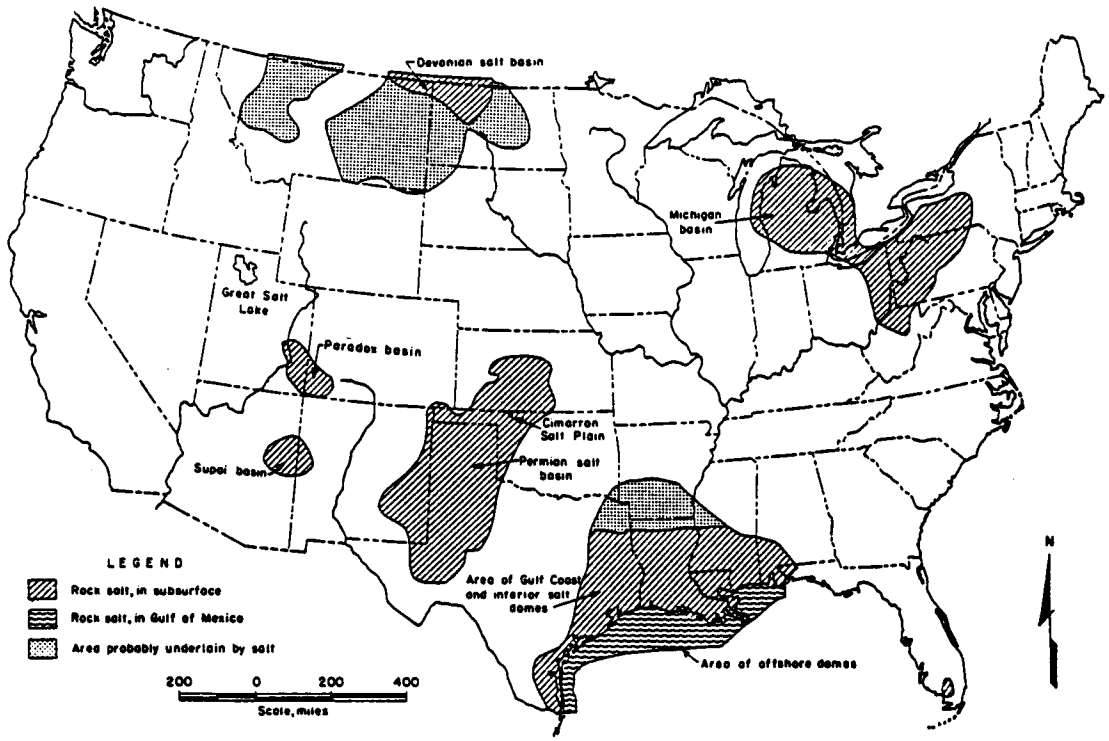

Figure 1. Salt Deposits in the United States

Figure IV:4:1 (Figure 1; Karably, 1985)

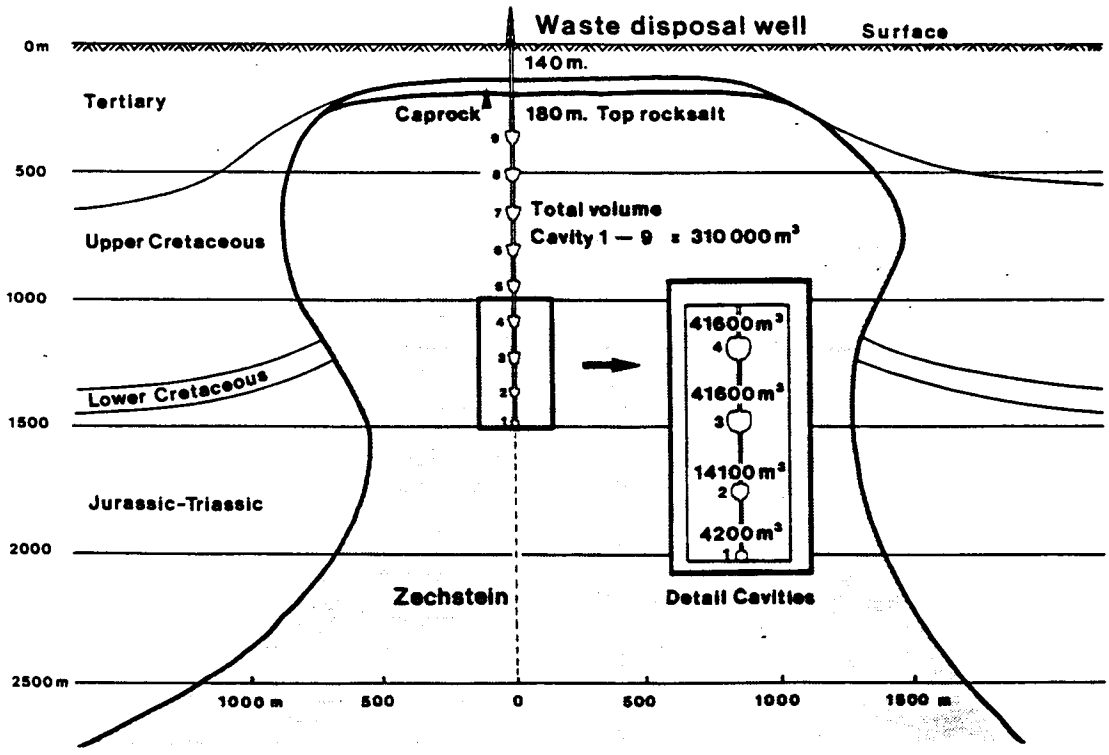

Figure 10. Suggestions for chemical waste disposal in a salt dome.

Figure IV:4:2 (Figure 1; Wassman, 1985)

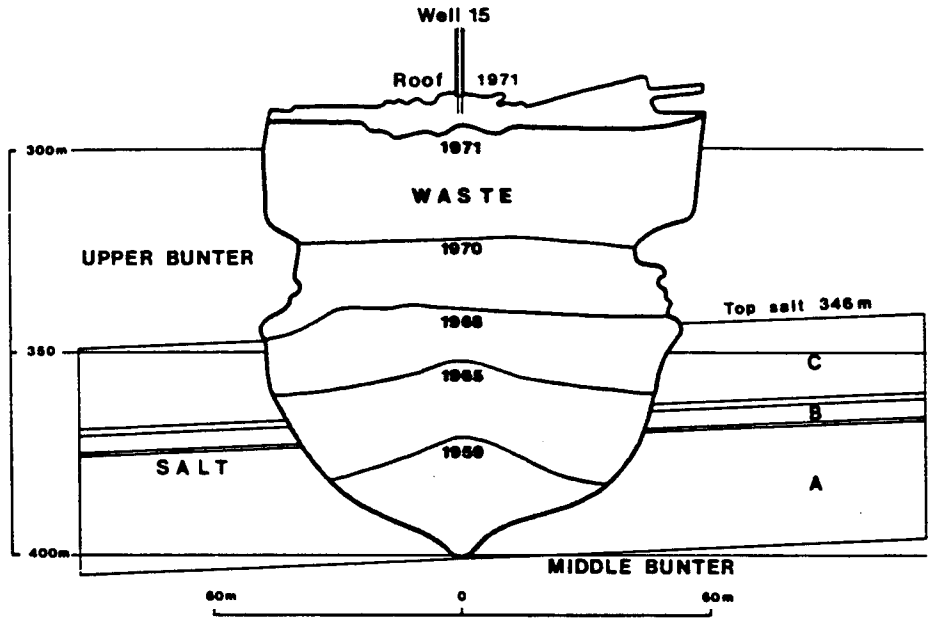

Figure 5. Summary of the filling rate of the waste disposal Well 15, Hengelo.

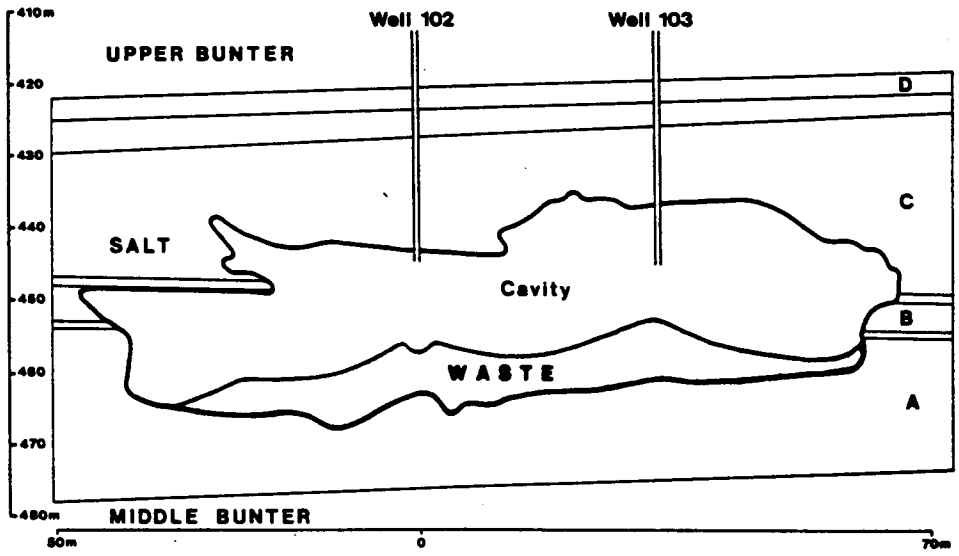

Figure 6. Waste disposal in a Hydraulic-Fracturing connected well system in the Hengelo area.

Figure IV:4:2 (Figure 1; Wassman, 1985)

containment units are less susceptible to fire, theft, sabotage, lightening, hurricanes, damage due to high humidity, etc.

According to Baar (1977), most dry salt mines are room and pillar operations (Figures V:2:1 and V:2:2) in which the salt is removed in a checkerboard pattern, leaving pillars for roof support. Mining techniques are not standardized; both old techniques and new techniques are in use. The oldest mines were designed on the basis of previous experience and, to a certain extent, on a trial and error basis. Later mines were designed on the basis of the rock mechanic elasticity theories. (The plasticity of rock salt was not taken into consideration). These design citeria proved satisfactory for some of the shallower mines where the affects of long-term creep proved to be minimal, but cannot be safely applied to deeper mines where long-term creep must be taken into consideration (Figures V:2:3 and V:2:4).

One of the main drawbacks to the standard room and pillar mining is that the restrictions on extraction ratios and pillar sizes - widths and heights - become increasingly stringent with increasing depths. These restrictions translate into cutbacks in the profitability and lifetime of the mine. There are however, several cost-effective alternatives to the standard room and pillar technique (Baar, 1977).

One alternative is controlled subsidence. In one variation of this method, after first mining in standard room-and-pillar patterns, the pillars are mined, leaving only those pillars required to ensure the structural integrity during the second phase of mining. Thereafter the subsiding overburden slowly crushes the pillar remnants. The use of backfill can reduce the surface subsidence so that controlled subsidence becomes feasible in mining beds of considerable thickness (Baar, 1977).

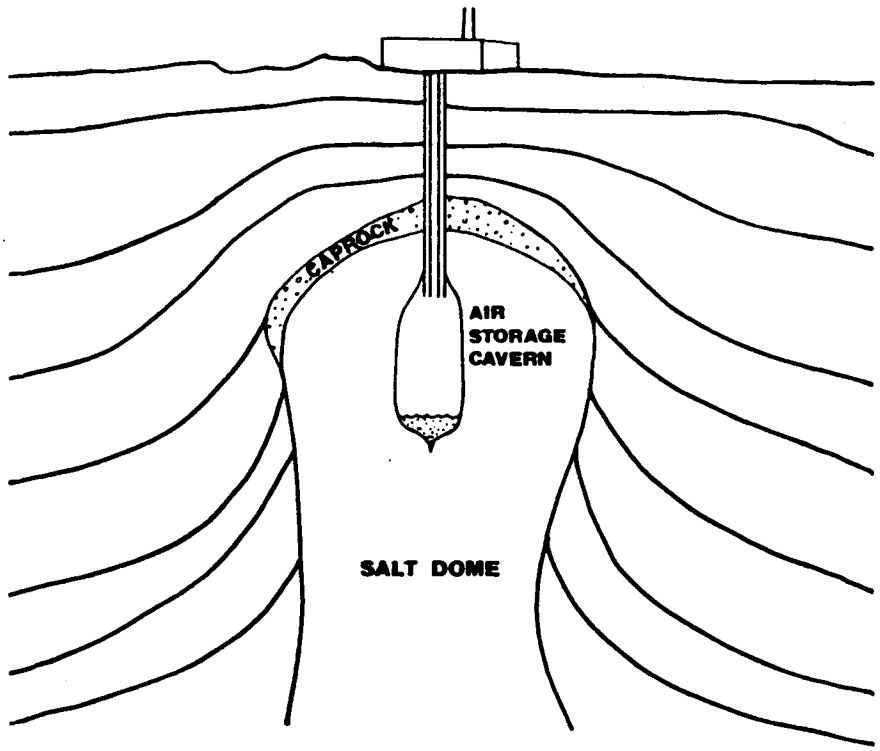

Figure 1. Cross-Sectional View of a Compressed Air Energy Storage Plant in a Salt Dome

Figure IV:5:1 (Figure 1; Gustin, 1985)

Another alternative method involves the backfilling of rooms with refinery waste. The waste is transported hydraulically, using saturated brines. After the brines have drained off, the backfill becomes rather solid due to crystallization processes. Some of the standing pillars are subsequently mined; the new rooms are backfilled to minimze subsidence (Baar, 1977).

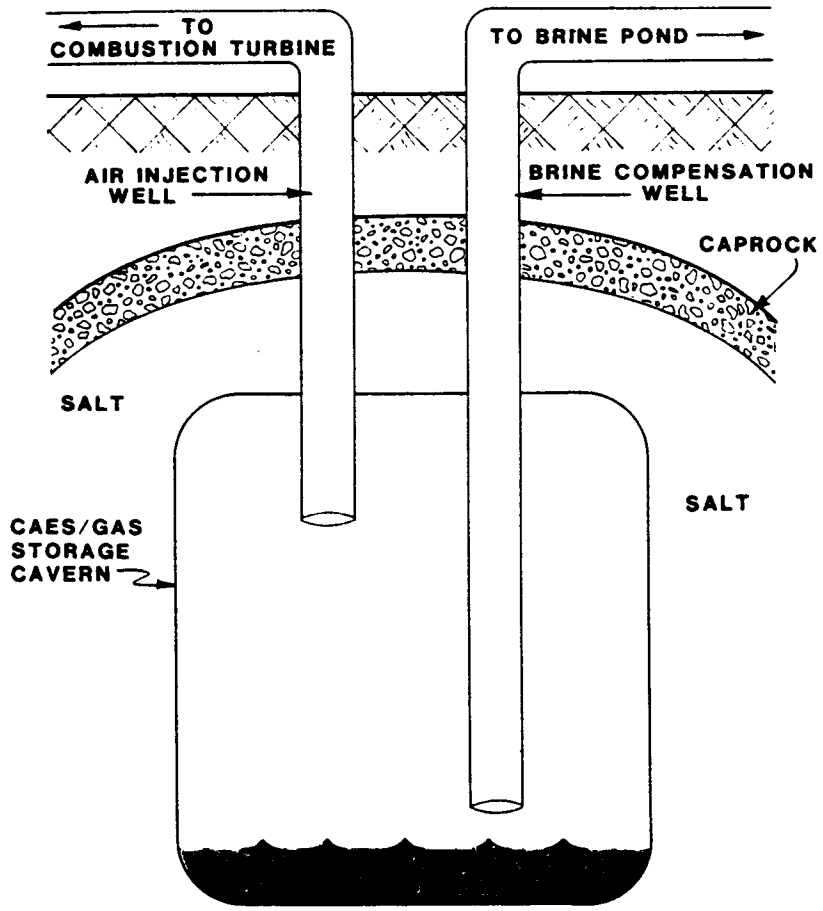

Figure 4. Cross-Sectional View of a Brine-Compensated Compressed Air Storage Cavern in Salt

Figure IV:5:2 (Figure 4; Gustin, 1985)

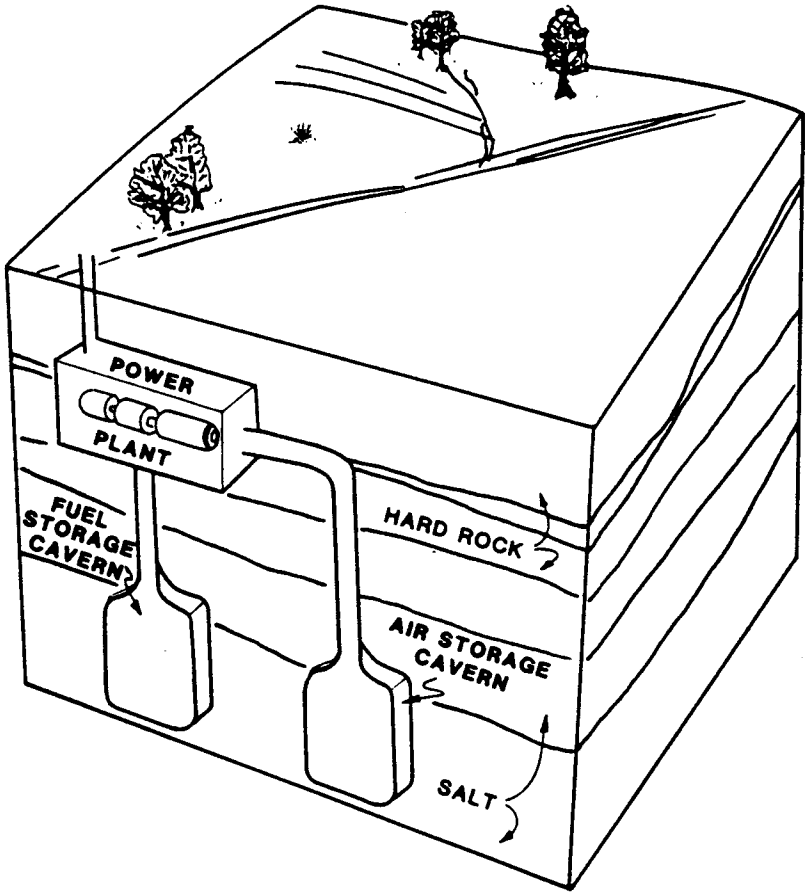

Figure 6. Block Diagram of a Compressed Air Energy Storage Plant Modified for Military or Civil Defense Purposes

Figure IV:5:3 (Figure 6; Gustin, 1985)

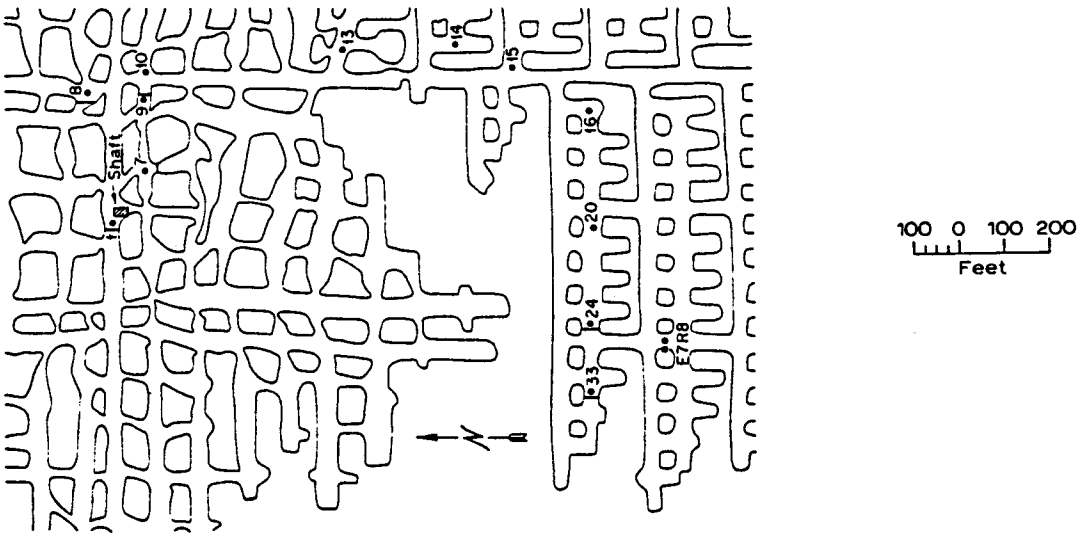

Fig. 5-28. Partial plan of Lyons mine, Kansas, showing locations of convergence measuring stations. (After Bradshaw et al., 1964, fig. 3; Hedley, 1967, fig. 8.)

Figure IV:6:1 (Figure 5-28; Baar, 1977)

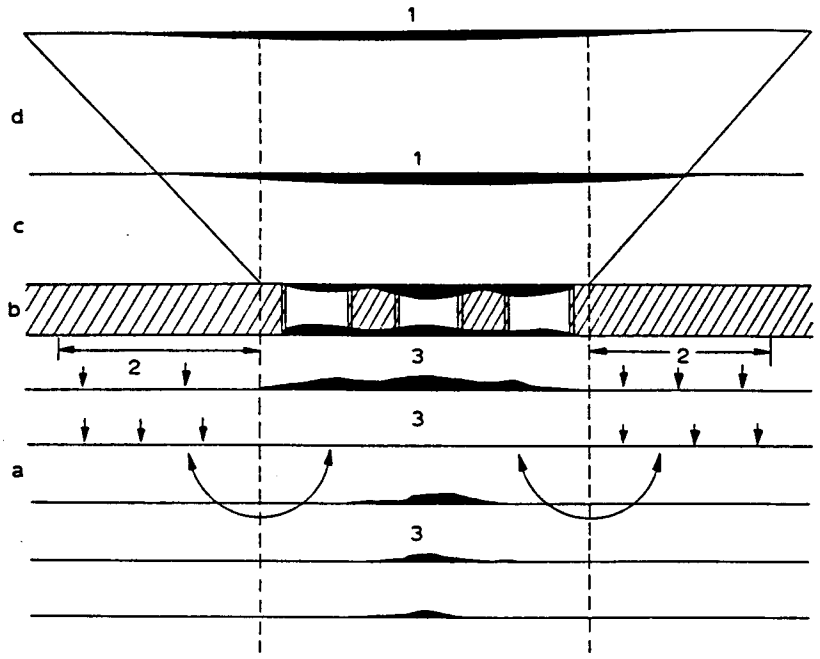

Fig. 5-13A. Schematic summary of measured deformations around a developing potash extraction panel. (Modified after Gimm and Meyer, 1962, who obviously reproduced fig. 24 of Wilkening, 1958.)

Based on measurement data shown in Figs. 5-10 to 5-12. a. rock salt with bedding planes; b. Stassfurt potash bed; c. shale (saliferous clay); d. anhydrite; *1* = roof subsidence; *2* = abutment load; *3* = floor uplift; arrows indicate directions of creep deformations.

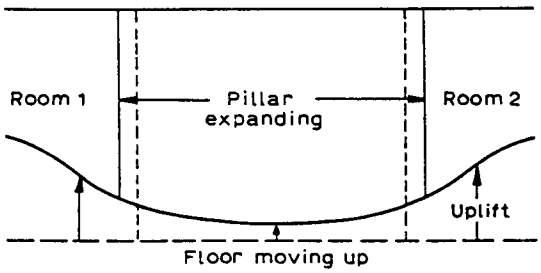

Fig. 5-13B. Floor uplift under conditions of Fig. 5-13A. (After Wilkening, 1958, fig. 22.) Lateral creep deformations as shown in Fig. 5-12 allow floor uplift which is ignored in the original of Fig. 5-13A (Gimm and Meyer, 1962).

Figure IV:6:1 (Figure 5-13A&B; Baar, 1977)

7) REFERENCES

Baar, C.A., 1977, Applied salt-rock mechanics 1: Elsevier Scientific Publishing Company, 294 p.

Braitsch, O., 1971, Salt deposits - their origin and composition: Springer, New York, N.Y., 297 p.

Gustin, J.D., 1985, Energy storage in salt, *in* Schreiber, B.C. and Harner, H.L., Eds., Sixth International Symposium on Salt: Salt Institute Inc., Virginia, 2, 177-182.

Haddenhorst, H.G., and Quast, P., 1985, Underground storage of natural gas in West Germany, *in* Schreiber, B.C. and Harner, H.L., Eds., Sixth International Symposium on Salt: Salt Institute Inc., Virginia, 2, 203-210.

Karably, L.S., 1985, High integrity isolation of industrial waste in salt, *in* Schreiber, B.C. and Harner, H.L., Eds., Sixth International Symposium on Salt: Salt Institute Inc., Virginia, 2, 211-216.

Martinez, J.D., 1985, Energy programs - a contribution to salt dome knowledge, *in* Schreiber, B.C. and Harner, H.L., Eds., Sixth International Symposium on Salt: Salt Institute Inc., Virginia, 2, 235-248.

Preece, D.S. and Foley, J.T., 1985, Finite element analysis of salt caverns employed in the strategic petroleum reserve, *in* Schreiber, B.C. and Harner, H.L., Eds., Sixth International Symposium on Salt: Salt Institute Inc., Virginia, 2, 49-64.

Russo, A.J., 1985, Solution mining calculations for SPR caverns, *in* Schreiber, B.C. and Harner, H.L., Eds., Sixth International Symposium on Salt: Salt Institute Inc., Virginia, 1, 101-109.

Quast, P. and Schmidt, M.W., 1985, Disposal of medium- and low-level radioactive waste (MLW/LLW) in leached caverns, *in* Schreiber, B.C. and Harner, H.L., Eds., Sixth International Symposium on Salt: Salt Institute Inc., Virginia, 2, 217-234.

Wassmann, T.H., 1985, Cavity utilization in the Netherlands, *in* Schreiber, B.C. and Harner, H.L., Eds., Sixth International Symposium on Salt: Salt Institute Inc., Virginia, 2, 191-201.

Walters, R.F., 1978, Land subsidence in central Kansas related to salt dissolution: Kansas Geological Survey Bulletin 214, 82p.

Yuanxiong, L. and Ghengxun, N., 1985, Technical development of solution mining in thinly bedded rock salt deposits of Ziliujing, Sichuan, China, *in* Schreiber, B.C. and Harner, H.L., Eds., Sixth International Symposium on Salt: Salt Institute Inc., Virginia, 1, 87-99.

V: GEOPHYSICAL SIGNATURES OF SALT BODIES

1) SALT DOMES SIGNATURES

A) Overview:

A salt dome is generally emplaced within clastic strata. It typically has physical properties that are different from those of the surrounding sediments and which enable its detection by geophysical methods. These properties are: A) relatively low density; B) negative magnetic susceptibility; C) a high electrical resistivity; and D) a relatively high propagation velocity for seismic waves.

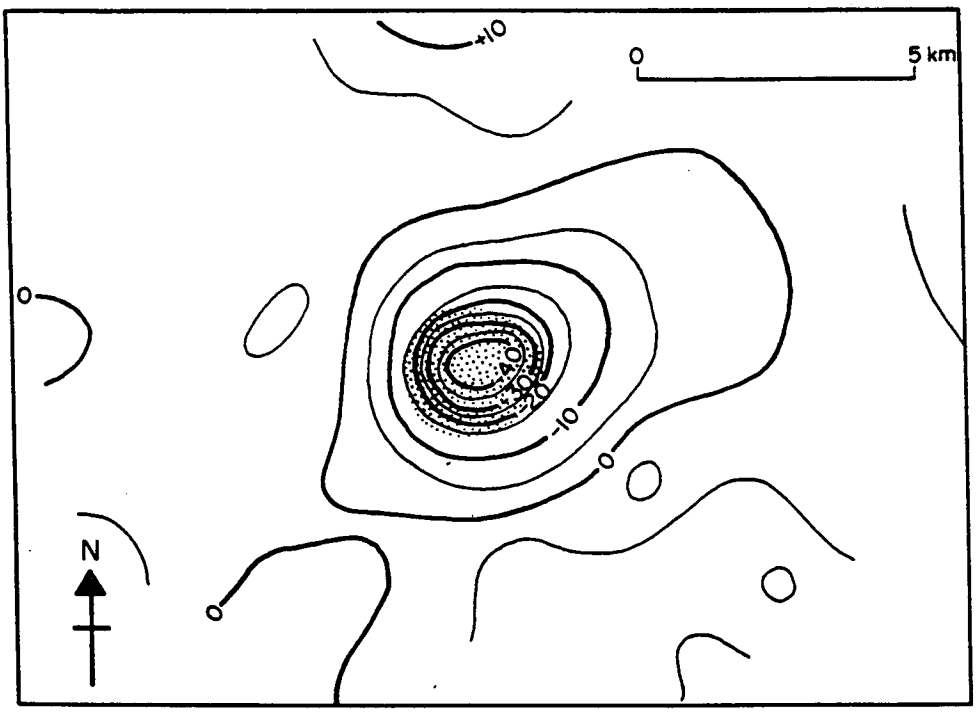

Fig. 1.1. The gravity anomaly over the Grand Saline Salt Dome, Texas, USA (contours in gravity units – see Chapter 6). The stippled area represents the subcrop of the dome. (Redrawn from Peters & Dugan 1945.)

Figure V:1:1 (Figure 1.1; Keary and Brooks)

B) Relatively low density:

Salt has a relatively low density and is consequently a zone of anomalously low mass. It therefor gives rise to a gravity anomaly that is negative with respect to the surrounding areas. The readings in Figure V:1:1 have been corrected for effects which result from the earth's rotation, irregular surface relief, and regional geology.

C) Negative magnetic susceptibility:

The low magnetic susceptibility of salt causes a local decrease in the strength of the earth's magnetic field in the vicinity of a salt dome. The readings in Figure V:1:2 have been corrected for effects which result for large scale variations of the magnetic field with latitude, longtitude and time.

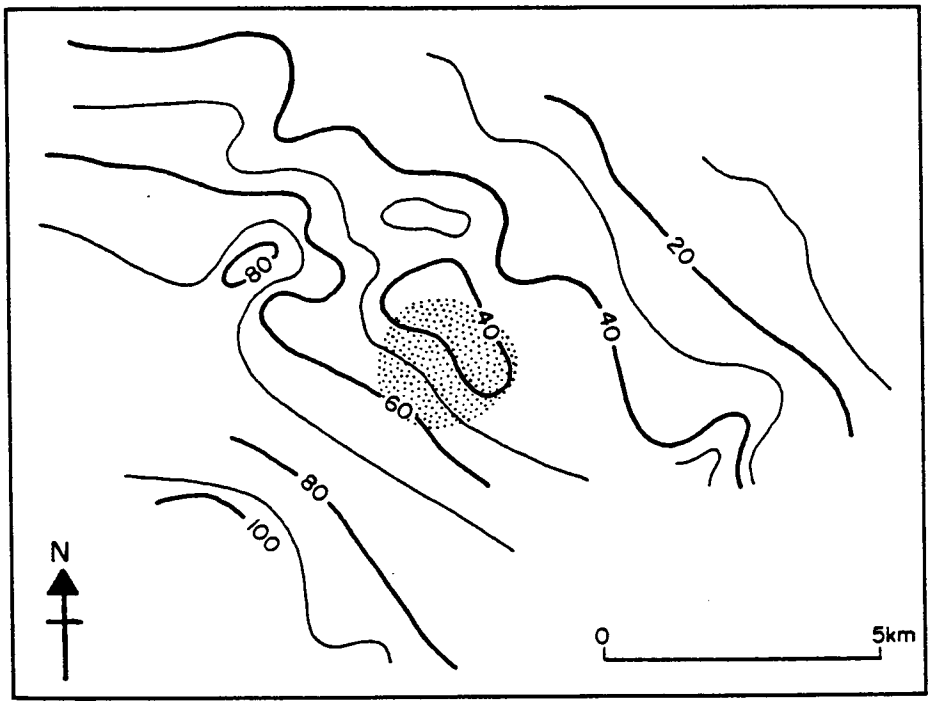

Fig. 1.2. Magnetic anomalies over the Grand Saline Dome, Texas, USA (contours in nT – see Chapter 7). The stippled area represents the subcrop of the dome. (Redrawn from Peters & Duggan 1945.)

Figure V:1:2 (Figure 1.2; Keary and Brooks)

D) High electrical resistivity:

Salt domes have a high electrical resistivity and electric currents preferentially flow around and over the top of such a structure rather than through it. This pattern of flow creates a distortion in the potential gradient of the natural telluric currents at the earth's surface (Figure V:1:3).

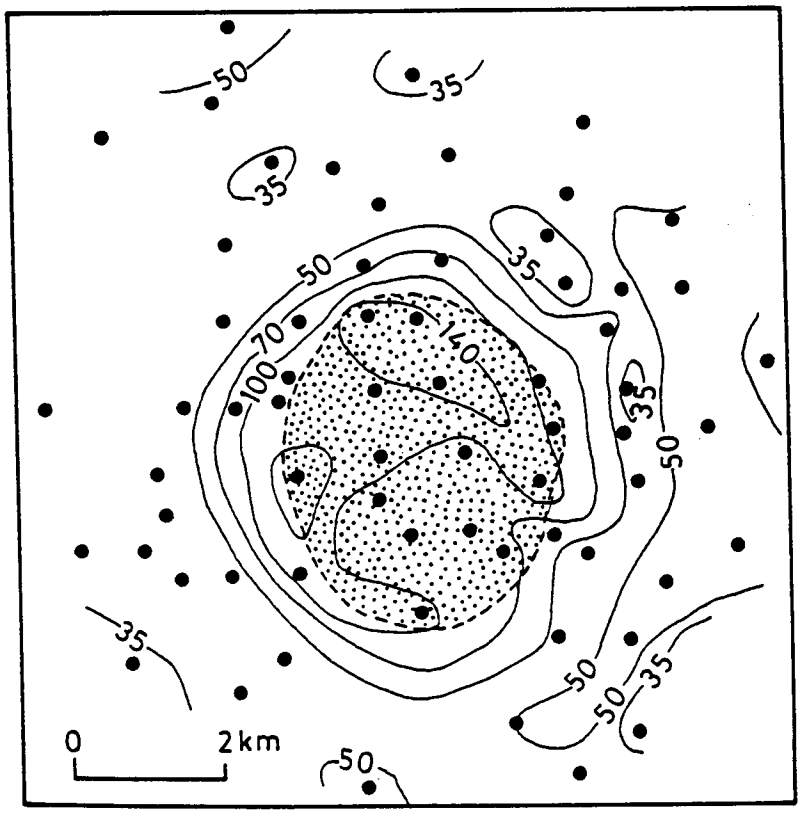

Fig. 1.4. Perturbation of telluric currents over the Haynesville Salt Dome, Texas, USA (for explanation of units see Chapter 9). The stippled area represents the subcrop of the dome. (Redrawn from Boissonas & Leonardon 1948.)

Figure V:1:3 (Figure 1.4; Keary and Brooks)

E) Relatively high propagation velocity for seismic waves:

Salt domes generally have a higher seismic velocity than the surrounding sediments. As a consequence any seismic energy that is incident on the boundary of the salt is partitioned into a refracted and a reflected phase.

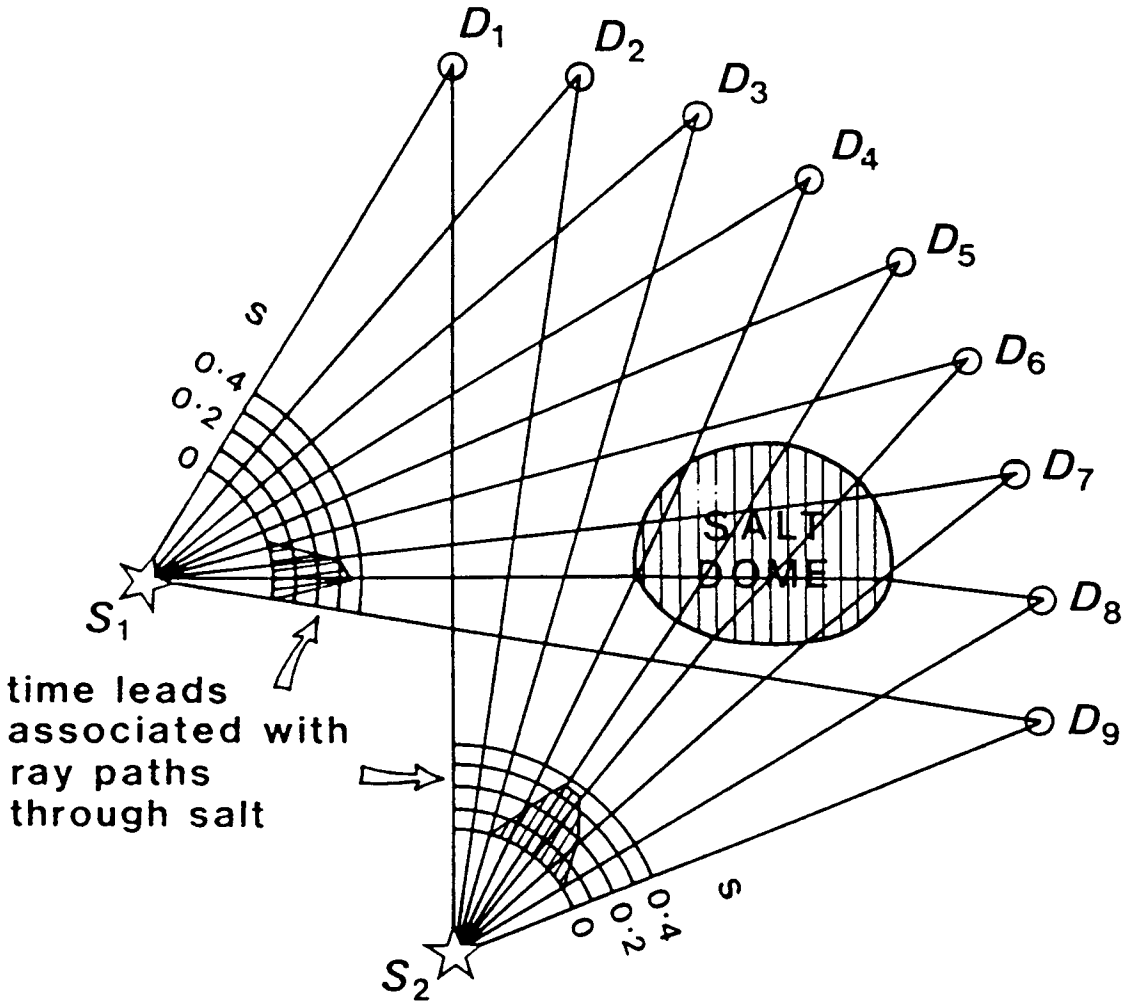

Fan-shooting for the detection of localized zones of anomalous velocity.

Figure V:1:4 (Figure 5.21; Keary and Brooks)

Salt domes are therefor characterized on refraction surveys as areas of anomalously high velocity and fast arrival time (Figure V:1:4).

On reflection surveys the salt boundary, except where steeply inclined, is characterized by a high-amplitude event. The seismic image of the more-or-less homogeneous salt body is characterized by an absence of internal reflections. The reflections originating from within the adjacent strata are truncated against the flanks of the seismic image of the salt (Figure V:1:5).

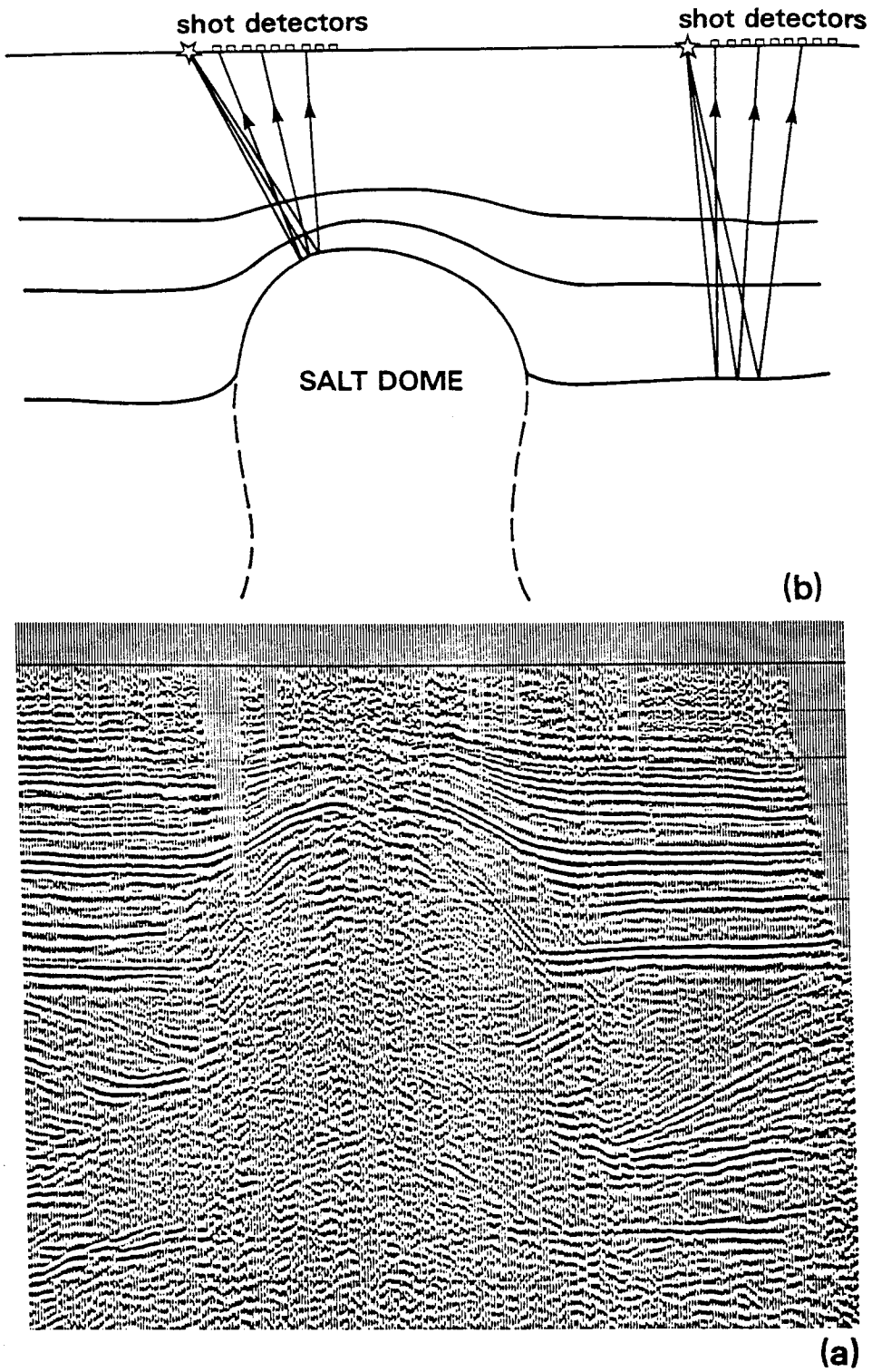

Fig. 1.3. (a) Seismic reflection section across a buried salt dome (courtesy Prakla-Seismos GMBH). (b) Simple structural interpretation of the seismic section, illustrating some possible raypaths for reflected rays.

Figure V:1:5 (Figure 1.3; Keary and Brooks)

2) DISSOLUTION FEATURE SIGNATURES

A) Wabamun example: Red Deer River area

ABSTRACT

Analyses of well log and seismic data suggest that about 40 m of rock salt were uniformly deposited within the Famennian-age Wabamun Group in the Stettler study area, southeastern Alberta. Subsequent to deposition, these original rock salts have been leached to the extent that they are now preserved only as isolated to contiguous bodies of irregular shape and variable thickness. Investigation suggests that in the immediate study area, the dissolution of these rock salts was initiated by regional faulting and/or fracturing during the mid-Late Cretaceous, and accentuated thereafter by various mechanisms including glacial loading and unloading. Leaching, once initiated, appears to have been self-perpetuating; a process whereby fractures, created by the collapse of overlying strata, provide a conduit for unsaturated waters, thereby facilitating further dissolution.

Seismic data suggests that some of the salt-dissolution features in the Stettler study area retain a marked linear orientation (SSW-NNE). In short cross-section (on west-east oriented seismic lines), these structures are manifested as upward-expanding conical-shaped zones of "measurable" subsidence. These zones of subsidence are characterized by decreasing structural relief at shallower depths (due principally to the timing of the leaching, stoping and lateral strain within post-salt strata), and seismic chatter (due to small-amplitude vertical offsets).

The character of these subsidence features is consistent with: 1) the onset of dissolution as a result of regional faulting and/or fracturing during mid-Late Cretaceous time; 2) the plastic deformation of rock salt; 3) the relatively slow subsidence of the post-salt strata; and 4) accelerated rates of leaching in response to glacial loading and unloading.

INTRODUCTION

Rock salts exhibit unique physical properties and mechanical behaviour. Insitu, they are remarkably soluable, relatively impermeable and non-porous, almost incompressible, highly ductile, and rather easily deformed by creep. In the presence of unsaturated waters, the dissolution of rock salt is essentially instantaneous relative to the time-scale of the transport mechanisms (molecular diffusion, free convection and forced convection). The plastic behaviour of rock salt is demonstrated by salt glaciers and by flowage patterns observed in salt domes (Talbot and Jarvis, 1984; Richter-Bernburg, 1987).

The dissolution of rock salts in the subsurface can create pore space, differential stresses, creep and ultimately subsidence. There are two basic types (end members) of subsidence: (1) very slow subsidence characterized by the ductile deformation of rock salt; and (2) relatively rapid subsidence characterized by the brittle deformation of rock salt (Figures II:3:1 and II:3:2). Ductile deformation is typified by upward-expanding zones of subsidence; in contrast, brittle deformation by a vertically propagating cavity or collapse chimney. Particularly in this later case, measurable surface subsidence may not occur; pending further dissolution, the cavity may be effectively bridged and/or infilled as a consequence of stoping.

The seismic data suggest that the linear salt-collapse features in the Stettler study area (T30-T32, R20-R22W4M) can exhibit, in short cross-section, an upward-expanding zone of measurable subsidence. This zone of subsidence is characterized by a decrease in the amplitude of structural relief at shallower depths (primarily as a result of the timing of the leaching, stoping and lateral strain within post-salt strata), and seismic chatter (due to small-amplitude vertical offsets). The character of these collapse features is consistent with the plastic deformation of rock salt and the relatively slow subsidence of the post-salt strata.

ROCK SALT MECHANICS

The natural creep limits - limits of elastic behaviour - of rock salts are extraordinarily small compared to most other rocks and difficult to determine in the laboratory. Indeed most researchers think that rock salt does not have a yield point; they conclude that over time, rock salt will eventually exhibit plastic deformation (ie. creep; Figure I:2:3).

The total strain of rock salt is given by:

$$e = e_e + e_p + e_t + e_s + e_a$$

where e_e is the elastic strain upon loading, e_p is the plastic strain produced during loading, e_t is the transient or primary creep strain, e_s is the secondary or steady state creep strain and e_a is the accelerating or tertiary creep strain. According to Carter and Hansen (1983), e_e and e_p are generally less than one percent (<1%) and are not particularly significant with respect to the long-term creep of rock salt. These authors also state that the accelerating creep strain e_a is generally observed at stresses above one-half of the short-term breaking strength in unconfined creep tests and in low-temperature, low-temperature triaxial creep tests. Under these conditions, microfracturing leads to macroscopic failure by faulting (Glide mechanism; Figure I:2:3).

Transient creep e_t (LT creep mechanism) is non-recoverable and deccelerating.

This type of creep stems from the constraints placed on dislocation glide at low temperatures, where diffusion rates are low and dislocations cannot surmount obstacles to glide and climb by cross-slip. Each increment of strain makes further motion more difficult (strain hardening) and thus the creep rate decreases continuously with time.

According to Carter and Hansen (1983), steady state creep e_s encompasses Solution Precipitation creep, HT creep, Cobble creep and N-H creep (Figure I:2:3). HT creep can be thought of as non-decelerating LT creep. With respect to the former mechanism, vacancy diffusion in the higher temperature regime is thought to allow for climb by dislocation intersection processes. In the same temperature regime, but at very low stresses, stress-induced bulk vacancy diffusion (Nabarro-Herring creep) or grain-boundary diffusion are thought to occur.

In the presence of water, Solution Precipitation creep (Figure I:2:3) can occur within the low-temperature, low-pressure regime. This mechanism is described by Urai et al. (1986) as solution transfer creep; a dynamic recrystallization process. The presence of even trace amounts of brine has a marked effect on the deformation of rock salt in laboratory tests. Tests on dry dilated salt show more-or-less conventional dislocation creep behaviour (Glide); brine-bearing samples, in contrast, show a marked weakening at low strain rates (low differential stress). According to Urai et al. (1986) this is associated with dynamic recrystallization and a change of deformation mechanism to Solution Precipitation creep. These authors surmise that trace amounts of brine are present in rock salt in-situ, and that the presence of such fluid accounts for the observed discrepency between typical laboratory and in-situ observations. Rock salt under typical laboratory conditions (dry) deforms as an elasto-plastic; rock salt in-situ deforms as a plastic. Indeed the salt glaciers in Iran flow under gravitational stresses alone.

According to Jackson and Talbot (1986), the strain rates for the in-situ deformation of rock salt vary by over 8 orders of magnitude from $10^{-8}s^{-1}$ to $10^{-16}s^{-1}$. The most rapid rates are those of borehole closure during accelerating creep ($10^{-8}s^{-1}$), mine closures and steady state borehole closures ($10^{-9}s^{-1}$ to $10^{-11}s^{-1}$) and namakiers (salt glaciers; $10^{-8}s^{-1}$ to $10^{-11}s^{-1}$). The rates of diapiric extrusion assisted by folding ($10^{-13}s^{-1}$) and the rates for the most active phase of gravity driven diapiric growth are significantly lower ($10^{-8}s^{-1}$ to $10^{-11}s^{-1}$). These rates are significantly lower than the strain rates at which laboratory specimens are typically tested ($>10^{-7}s^{-1}$).

DISSOLUTION AND MASS TRANSPORT OF HALITE

The solubility of halite (359 g NaCl/l H_2O at 25 ^{0}C) varies somewhat (depending upon temperature, pressure, and the concentrations of other

solutes), but it is one to three orders of magnitude higher than the solubilities of anhydrite and limestone under normal groundwater conditions. The dissolution of rock salt is essentially instantaneous relative to the time scale of the transport process in the presence of unsaturated water; the rate of solid rock salt removal is therefor controlled by the convective and/or diffusive flux of sodium and chloride ions away from a halite-bearing formation. Transport mechanisms include molecular diffusion, free convection and forced convection.

Mass transport by diffusion is a very slow process. Davies (1989) cites the following example: in the situation where a halite unit is separated from an underlying fresh-water aquifer by a 10 m thick aquiclude having a *De* value of 10^{-11} m^2/s, the regional halite removal rate is on the order of 5 microns per year. In most natural situations, the water in the aquifer has higher initial salinities and the *De* values of the aquiclude are most likely a few orders of magnitude lower. Therefore, in most situations, halite removal rates controlled by diffusion are much less than one micron per year.

According to Davies (1989), mass transport by free convection (driven by gravity acting on an inverted fluid density gradient), is much faster than transport by diffusion alone. Davies cites as an example, a situation where a 1-m wide fracture zone with a hydraulic conductivity of 10^{-4} cm/s transects the aquiclude described in the previous paragraph. The localized halite removal rate for this scenario is on the order of a few centimeters per year, which is orders of magnitude higher than the removal rate for diffusion alone.

Once salt-rich brine passes from a fracture zone into an underlying aquifer, the mode of mass transport is altered significantly. Forced convection through the aquifer, driven by a regional head gradient, becomes the primary transport mechanism. However, if the vertical component of the external head gradient is small, the vertical component of flow may still be primarily driven by buoyancy (Davies, 1989).

BRITTLE VERSUS DUCTILE SUBSIDENCE

Salt is characterized by its ability to deform either in a ductile (plastic) or brittle manner, depending on temperature, stress state, and deformation rate. At temperatures expected for the salt dissolution-subsidence process, the primary ductile deformation mechanisms for rock salt are dislocation glide (Glide creep) at moderate differential stresses and moderate deformation rates, and Solution Precipitation creep at low differential stresses and low deformation rates (Figure I:2:3). If intercrystalline water penetrates the subsiding salt mass, deformation by intergranular liquid diffusion (Solution Precipitation creep) is capable of producing strain rates that are orders of magnitude higher than are possible in relatively dry salt at the same stress states (Davies, 1989).

There are two basic types of subsidence: (1) very slow subsidence characterized by predominantly ductile deformation; and (2) relatively rapid subsidence characterized by predominantly brittle deformation (Figures II:3:1 and II:3:2). These two types of subsidence represent the ends of a continuous range of subsidence processes. As is illustrated in Figures II:3:1 and II:3:2, ductile deformation typically generates an upward-expanding zone of subsidence; brittle deformation in contrast is characterized by inverted cone-shaped, vertically-migrating collapse cavity (chimney). Whether or not measurable subsidence is expressed at the surface depends upon several factors including the timing of the dissolution, the areal extent and volume of the leached rock salt, the depth to the rock salt, and the response of the overburden. For example subsidence may not be exhibited within those sediments deposited after dissolution and collapse has ceased. In a second scenario, as a result of either stoping or bridging, the vertical migration of measurable subsidence could effectively cease, pending additional dissolution. Particularly in the former case, structural relief could be induced in the subsurface as a result of the compaction of the "compensation" sediments (Oliver and Cowper, 1983).

EXAMPLE SEISMIC DATA

The rock salts of the Wabamun Group (Upper Devonian) in the Stettler study area (T30-T32, R20-R22W4M) of southern Alberta are interbedded within an anhydrite/carbonate sequence and have been leached to the point that they are now preserved only as discontinuous remnants of variable thickness and areal extent (Figures V:2:1-V:2:4). Several authors including Anderson (1992) and Anderson and Brown (1991, 1992) and Anderson et al. (1988) suggest that the dissolution of these rock salts, in the immediate study area, was initiated by regional faulting/fracturing during the mid-Late Cretaceous, and accentuated thereafter by various mechanisms including glacial loading and unloading. They have also reported that leaching is often self-perpetuating; a process whereby fractures, created by the collapse of overlying strata, provide a conduit for unsaturated waters, thereby facilitating further dissolution.

In support of these hypothesis, Anderson (1992) presents the interpreted seismic line shown as Figure V:2:5. According to this author, the time-structural anomaly on these data is principally due to the dissolution of Wabamun rock salt. It is suggested that 40 m of rock salt are present to the east and west of traces 39 and 145 respectively, and that there is little, if any, remnant rock salt in the vicinity of trace 89.

In general terms, the collapse feature highlighted on Figure V:2:6, can be described as an upward-expanding conical-shaped zone of measurable subsidence; a feature characteristic of the ductile deformation of salt and gradual related subsidence. Seismic "chatter" is observed within the zone of

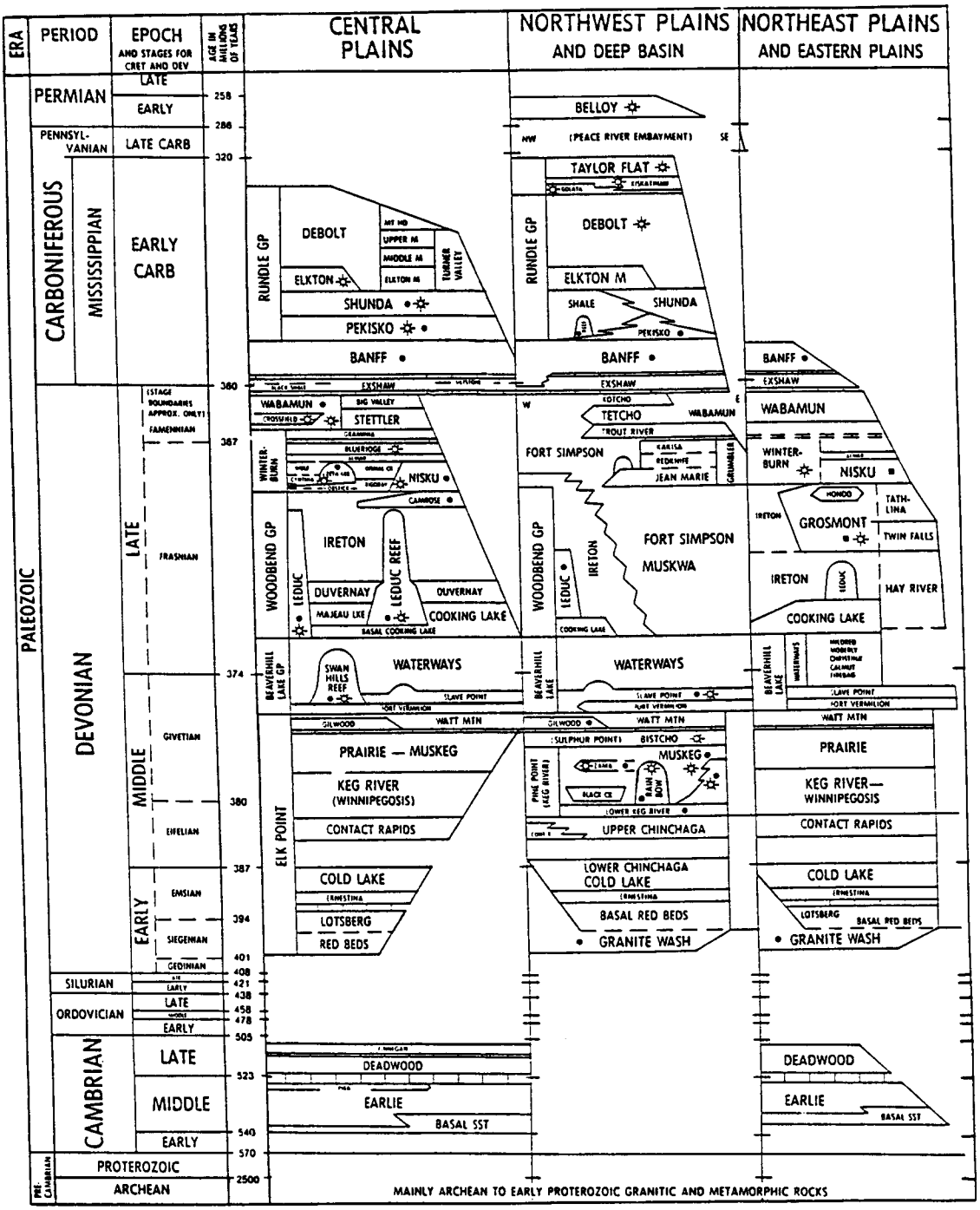

Figure V:2:1. Stratigraphic chart of the Paleozoic in the south-central mountains, northern mountains and southern plains areas of Alberta (modified after AGAT Laboratories, 1988).

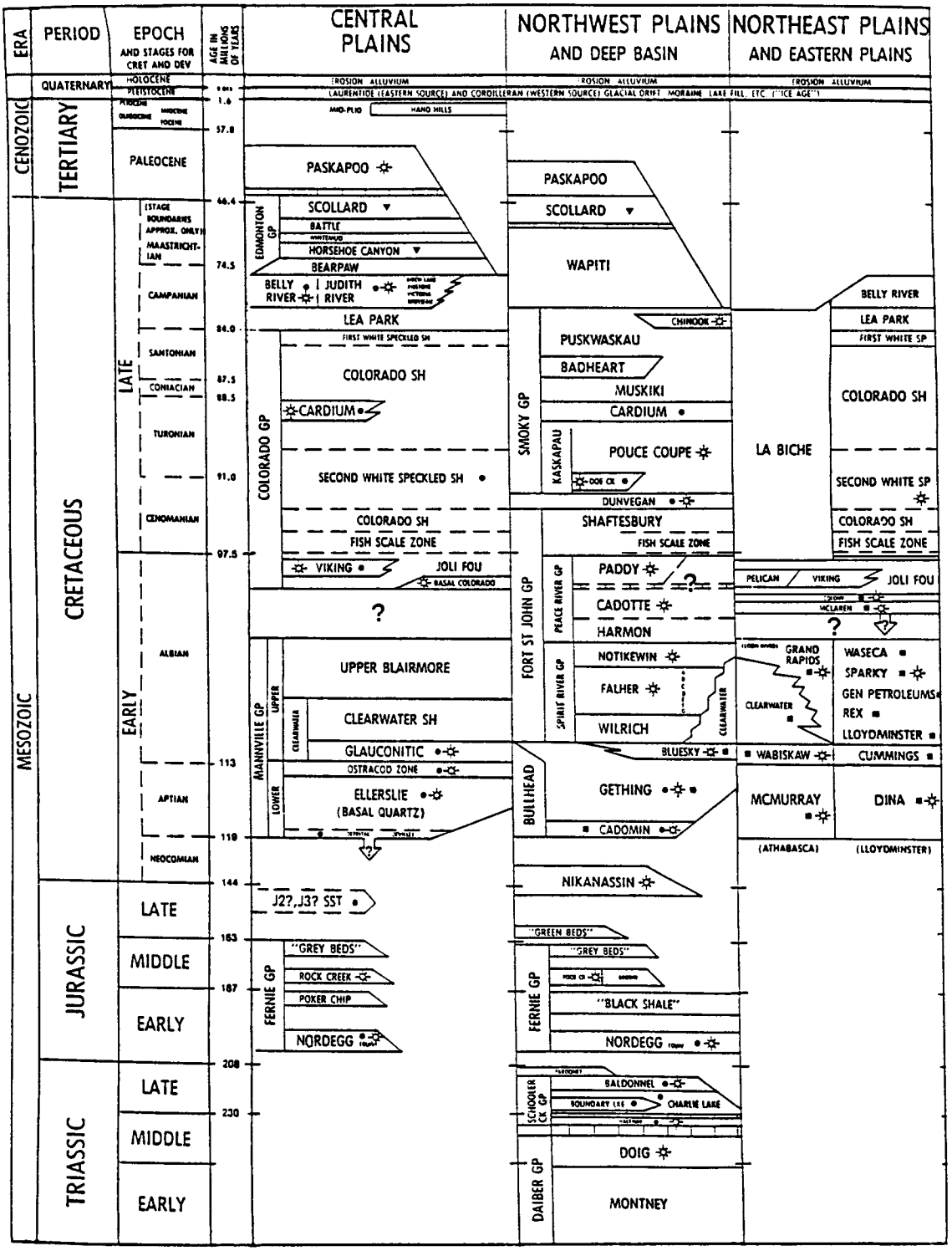

Figure V:2:2. Stratigraphic chart of the Mesozoic in the south-central mountains, northern mountains and southern plains areas of Alberta (modified after AGAT Laboratories, 1988).

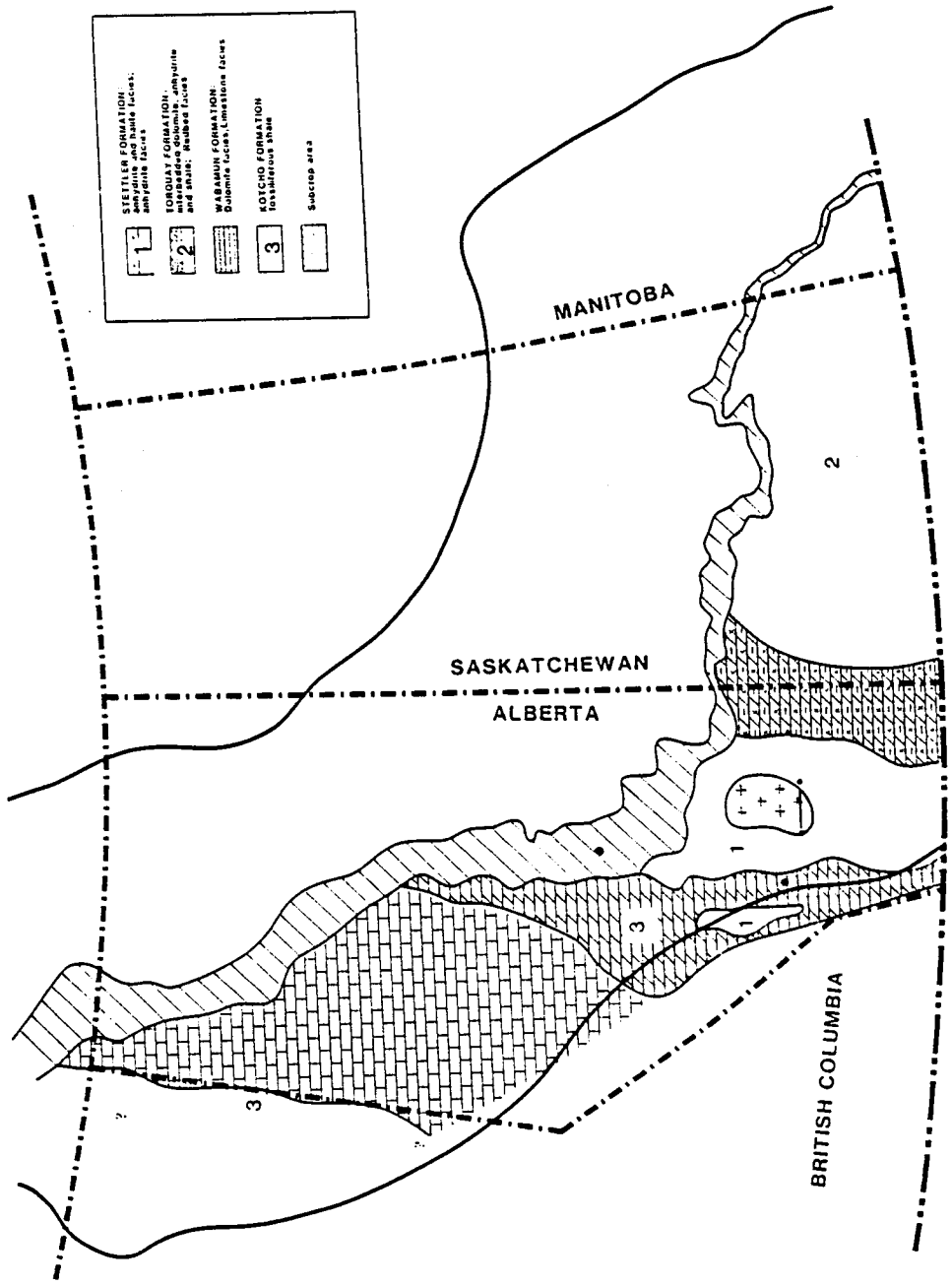

Figure V:2:3. Distribution of the Stettler Formation (Wabamun Group) and its equivalents in the western Interior Plains (modified after Belyea, 1966; Meijer Drees, 1986). The Stettler study area (T30-T32, R20-R22W4M) is situated within the cross-hatched area denoted as comprised partially of anhydrite and halite facies.

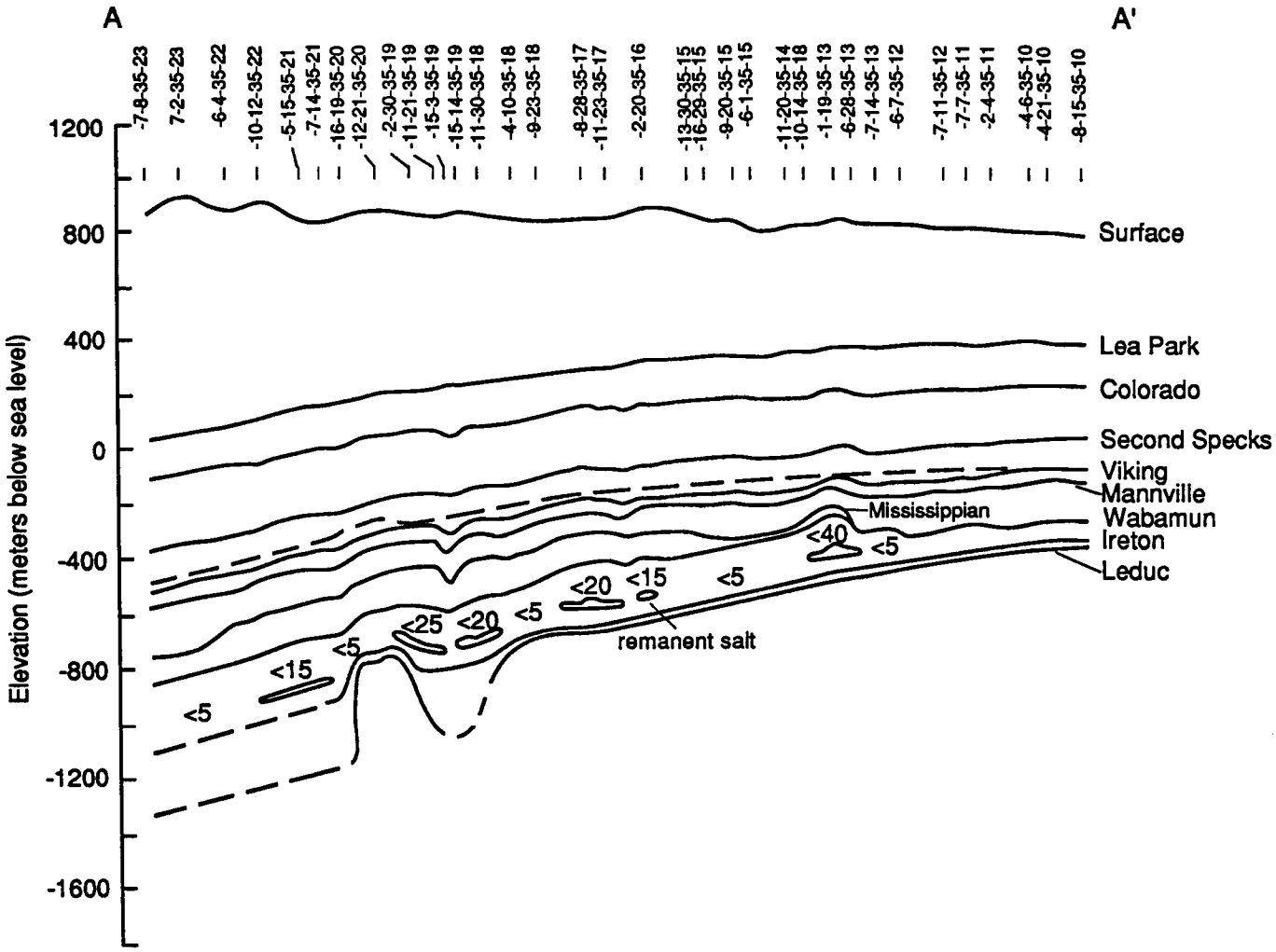

Figure V:2:4. West-to-east geologic cross-sections illustrating the discontinuous nature of the Wabamun Group rock salts in south-central Alberta (Figure 3). As is indicated on the cross-sections, these rock salts attain a maximun net thickness on the order of 40 m. Both present-day and reconstructed profiles for the Viking horizon are displayed on the cross-sections. Ideally, the reconstructed profile represents the pattern of structural relief which would be observed if partial dissolution of the Wabamun rock salt had not occurred after the deposition of the Viking Formation. Near the Wabamun subcrop, the dissolution of the rock salt is thought to have been initiated by the near-surface exposure of these evaporites; further to the west, leaching is thought to have triggered by faulting and/or fracturing during the mid-Late Cretaceous (Anderson and Brown, 1992).

subsidence suggesting that numerous low-amplitude vertical displacements are present within the zone of subsidence. Note that the zone of subsidence as drafted, is intended to encompass only those regions of seismically measurable subsidence. Minor subsidence has probably occured outside of this zone and in response to both lateral creep and dissolution.

Anderson (1992) also discusses the absence of significant relief (less than 20 ms) along the Colorado and post-Colorado levels, and the linear nature of this collapse feature (as evidenced on a suite of parallel seismic lines). These relationships are cited as support for the thesis that the dissolution of Wabamun rock salt in the Stettler study area was initiated during upper Colorado time (mid-Late Cretaceous) by regional faulting and/or fracturing (Figure V:2:7). During the mid-Late Cretaceous, the depth to the rock salt was on the order of 850 m.

In a geologically-oriented study of the Wabamun salt-dissolution, Anderson and Brown (1988, 1992) note the marked correlation between the locations of lakes, rivers and the present day near-zero edges of remnant salt. This apparent relationship is presented in support of an accelerated late-Pleistocene/Holocene phase(s) of dissolution. These authors suggest that this latest phase(s) of accelerated leaching could have been caused by: 1) glacial loading and a resultant increase in temperature and differential pressure; 2) glacial unloading and potential influx of fresh-water; and 3) the potential reversal in regional hydrologic environment from centrifugal-flow to centripetal flow as a consequence of sediment rebound in response to de-glaciation (Figure V:2:7).

In Figures V:2:5 and V:2:6, the shallowest, correlatable reflections on the example seismic line are time-structurally low within the zone of measurable subsidence, supporting the thesis of late-Pleistocene/ Holocene phase(s) of dissolution. Alternatively, it is possible that this relief is due to the glacial-induced compaction of "compensation" sediments.

SUMMARY

On the basis of the interpretation of the incorporated seismic data, it is suggested that the dissolution of the Wabamun rock salt in the study area was initiated by regional faulting and/or fracturing in mid-Late Cretaceous time. The fault/fracture planes provided conduits between the evaporitic beds (at a depth of about 850 m) and adjacent aquifers; leaching and subsidence were thereby initiated.

The shape of the zone of measurable subsidence suggests that the rock salts in the vicinity of the fault/fracture planes deformed plastically (ie. flowed towards the zone of dissolution even as the main edge of the rock salt moved

away). Partially as a consequence of the plasticity of rock salt, dissolution appears to have been self-perpetuating; a process whereby fractures, created by the collapse of overlying strata, provide a conduit for unsaturated waters, thereby facilitating further dissolution. The rate of dissolution is thought to have been controlled by the rate at which the saturated brines were transported out of the system. As the main edge of the rock salt (edge of the zone of measurable subsidence) migrated away from the fault/fracture conduit, the rates of dissolution and subsidence are thought to have slowed.

The most recent (post-Pleistocene) episode(s) of relatively rapid leaching appears to have been triggered by glacial loading and/or unloading. It is suggested that this latest phase(s) of accelerated leaching could have been caused by: 1) glacial loading and the resultant increase in both temperature and stress differential; 2) glacial unloading and potential influx of fresh-water; and 3) the possible reversal in regional hydrologic environment from centrifugal-flow to centripetal flow as a consequence of sediment rebound in response to de-glaciation.

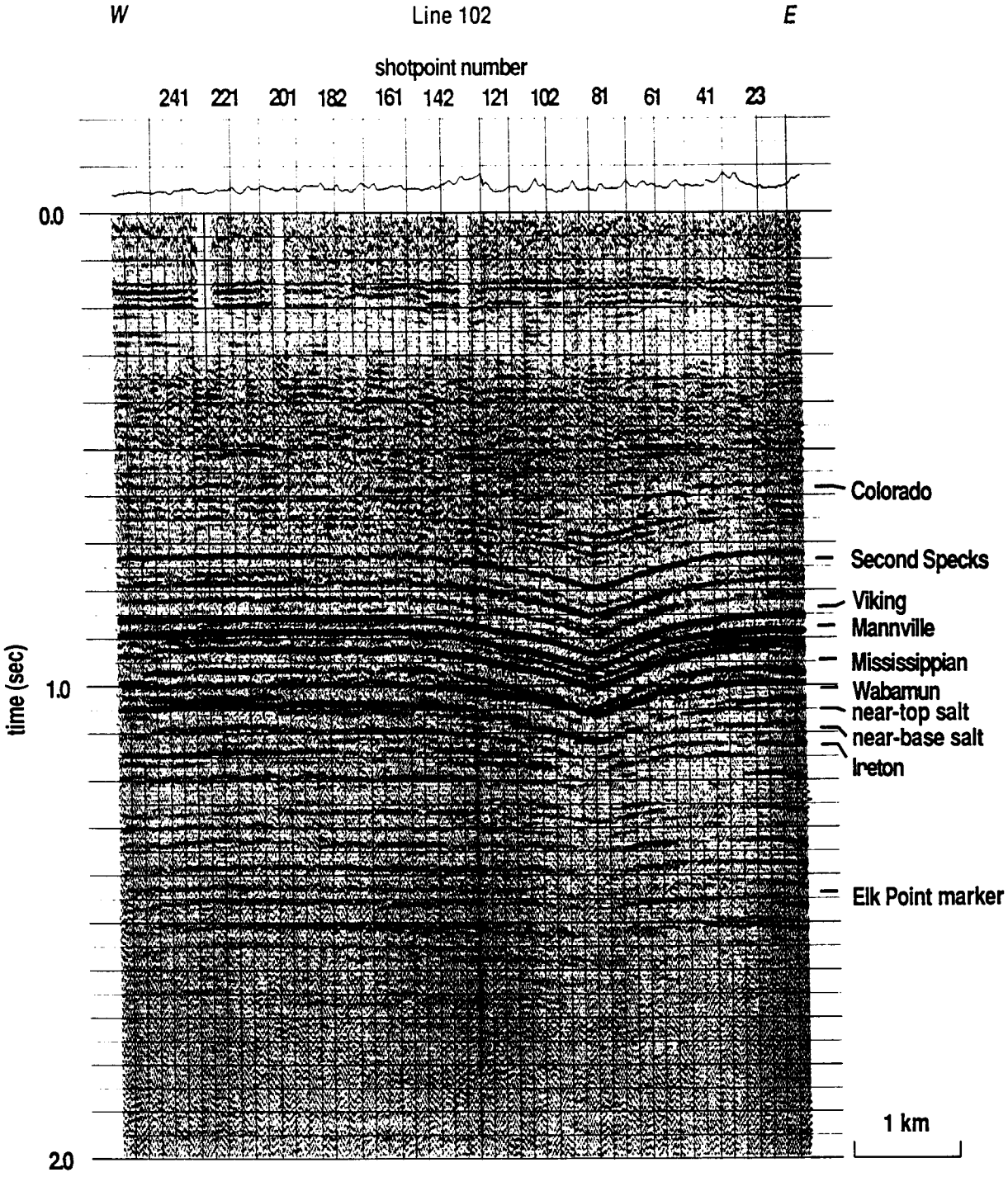

Figure V:2:5. Interpreted seismic line across a salt-collapse feature in the Stettler study area. Anderson (1992) indicates that this structure is oriented NNE/SSW, and can be correlated across several parallel seismic lines. These interpretations support the thesis that the dissolution Wabamun rock salt in the Stettler study area was initiated during upper Colorado time (mid-Late Cretaceous) by regional faulting and/or fracturing. At this time, the depth to the rock salt was on the order of 850 m.

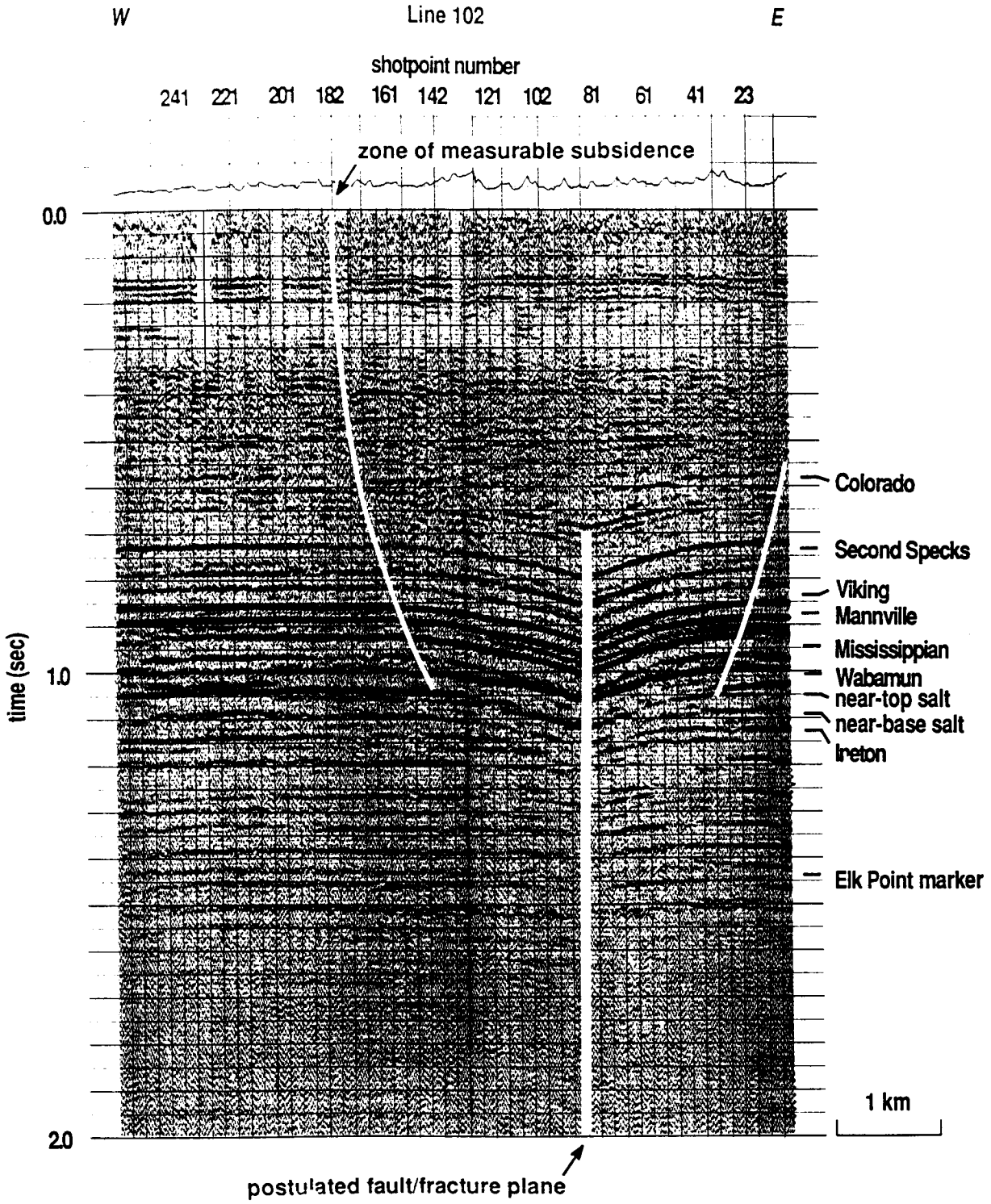

Figure V:2:6. The hypothesized fault and/or fracture plane and the envisioned upward-expanding zone of subsidence are superposed on the interpreted seismic line of Figure V:2:5. The curved nature of the zone of subsidence on the seismic line is partially a product of the acoustic velocity function within the subsurface; as demonstrated by Anderson (1992), the acoustic velocity increases more-or-less continuously with depth. As noted in the text, minor subsidence has probably occured outside of this zone, in response to both lateral creep and dissolution.

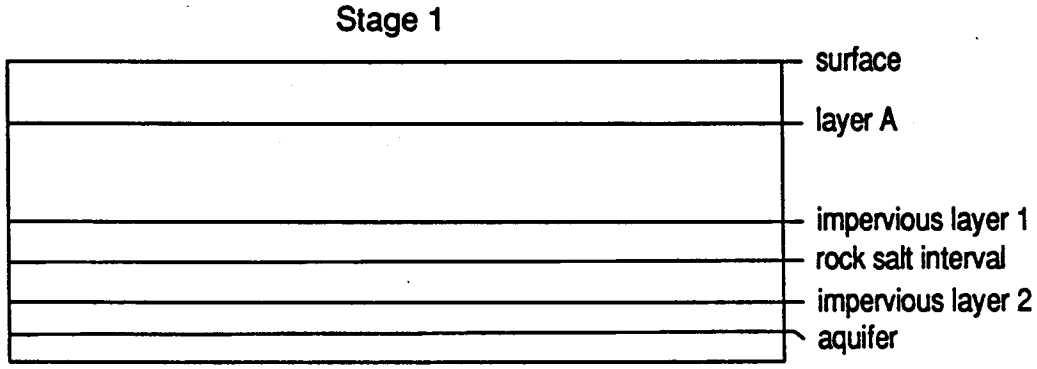

Figures V:2:7a-V:2:7f. Schematic illustration of the dissolution of rock salt in response to regional faulting and/or fracturing, and glacial loading and unloading.

In Figure V:2:7a (analogous to early-Late Cretaceous time in the Stettler study area) the rock salt is shown to be uniformly deposited and relatively undisturbed. At this time there is no effective communication between the rock salt and the underlying aquifer.

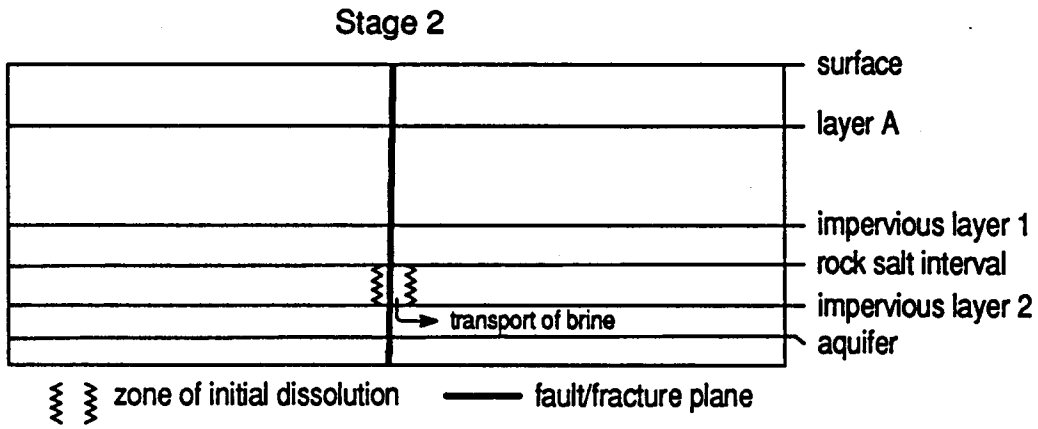

In Figure V:2:7b (analogous to mid-Late Cretaceous) regional faulting and/or fracturing has occurred. A conduit between the rock salt and the underlying aquifer has been created; the transport of brine waters by free and forced convection has been initiated. The initial rate of dissolution is relatively rapid. Leaching, once initiated, appears to have been self-perpetuating; a process whereby fractures, created by the collapse of overlying strata, provide a conduit for unsaturated waters, thereby facilitating further dissolution.

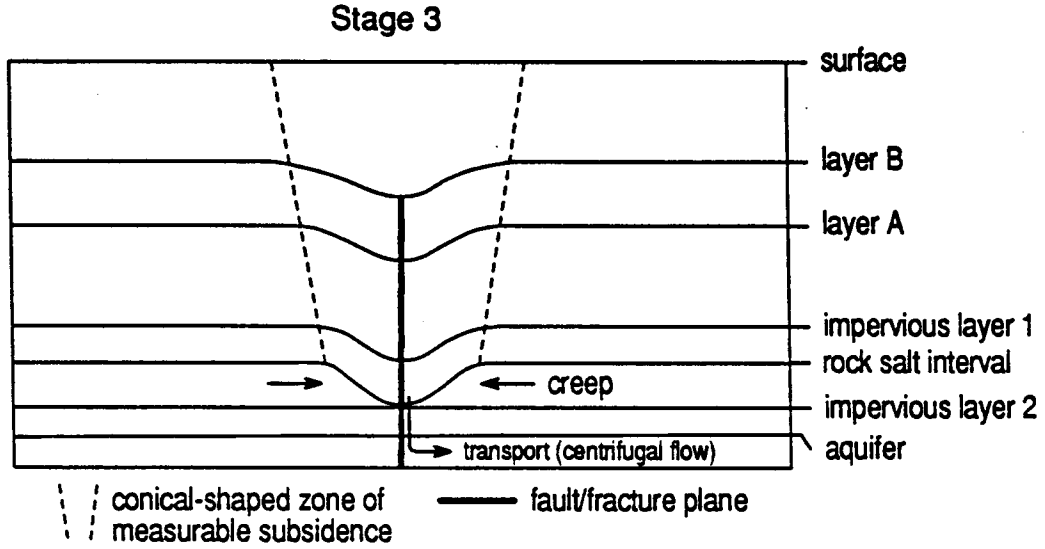

In Figure V:2:7c (analogous to mid-Late Cretaceous) the post-salt strata are shown to have subsided in response to the dissolution of rock salt. The collapse feature is manifested as an upward-expanding conical-shaped zone of subsidence which suggests that the rock salt is creeping towards the zones of active dissolution, even as the main salt-edge (edge of zone of measurable subsidence) is regressing. Solution-precipitation creep is envisioned as the dominant mechanism; the rate of movement is probably accentuated by the presence of the dissolving brines.

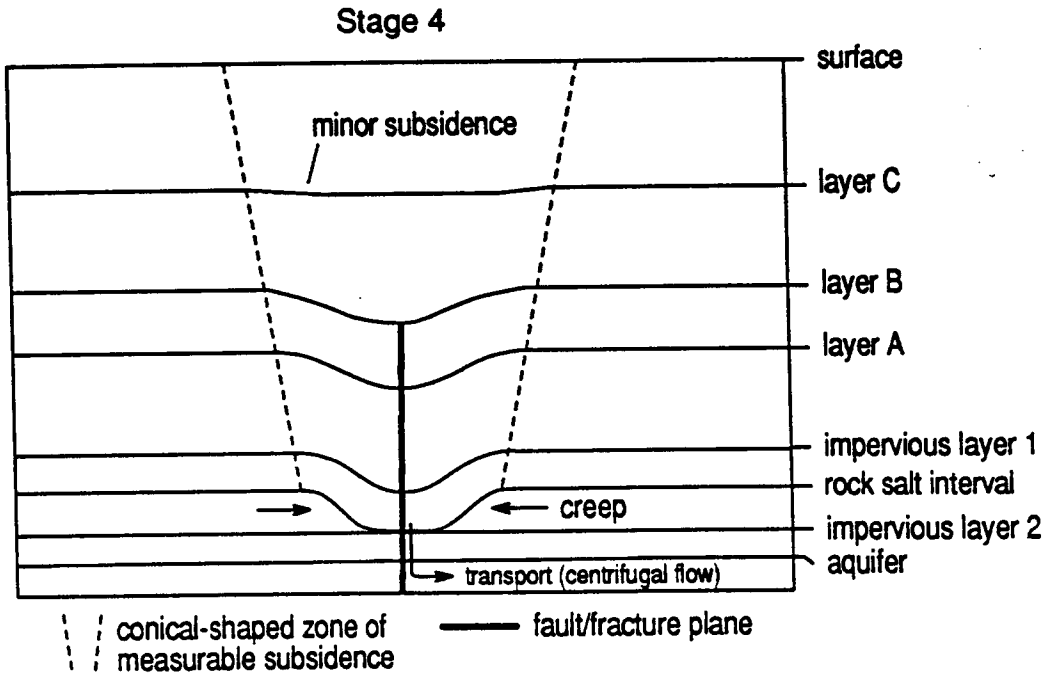

In Figure V:2:7d (analogous to upper-Late Cretaceous and Tertiary) the zone of measurable subsidence has migrated a significant distance from the fault/fracture plane; hence the rate of dissolution (effectively controlled by the rate at which dissolved salts are transported out of the system) is relatively low. As a result, the regressive migration of the zone of measurable subsidence and the creep of the residual rock salt have slowed considerably.

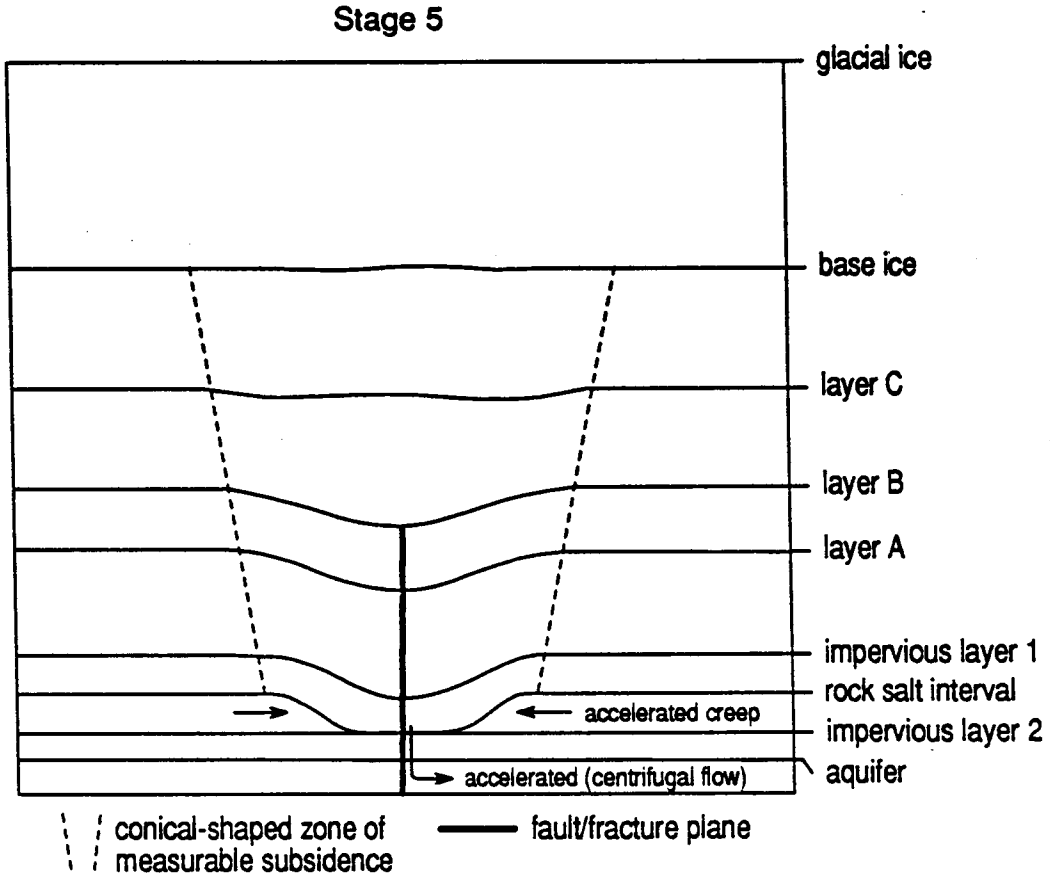

In Figure V:2:7e (analogous to Pleistocene) the study area is overlain by several kilometers of glacial ice. This additional load is envisioned as having increased both the temperature of the rock salt and the rate of centripetal-flow (basin to margin flow of fluids). These changes increase both the rate at which the rock salt creeps (increased temperature and stress differential) and the rate of transport. As a result the rates of dissolution and subsidence are relatively high.

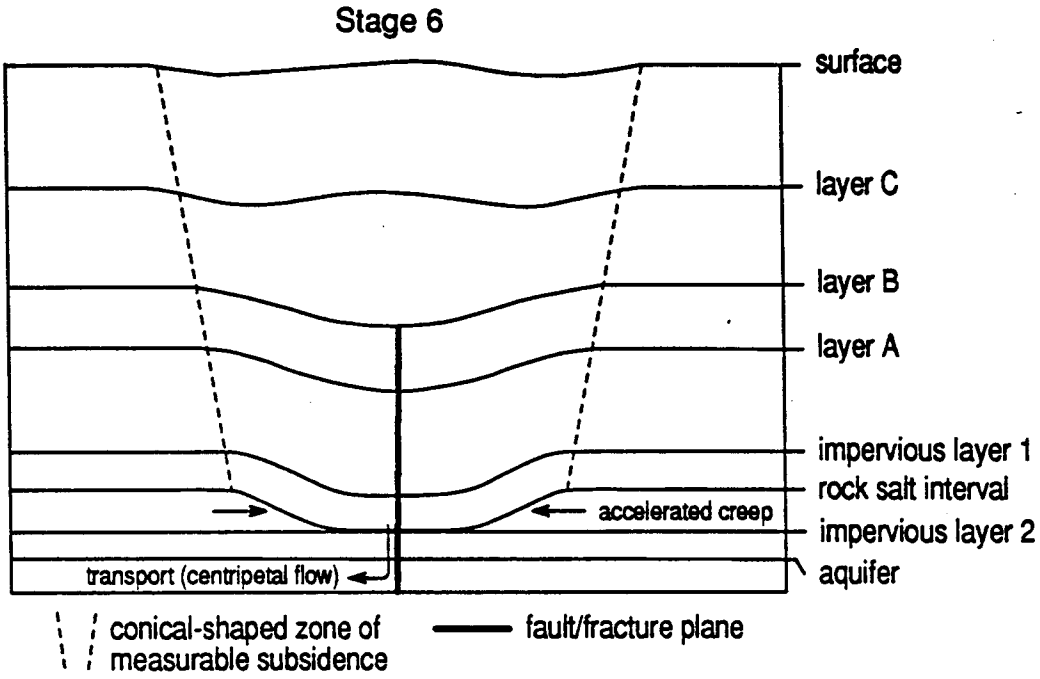

In Figure V:2:7f (analogous to Holocene) the glacial ice has retreated. This rapid removal of this load is envisioned as having changed the hydrologic environment in the study area; from centripetal-flow to centrifugal flow (margin to basin flow of fluids). As a consequence of the sudden influx of relatively fresh waters (some of glacial origin), the rates of dissolution and subsidence remain relatively high. In the schematic model, the permeability (and rate of fluid flow) within the fault/fracture plane is envisioned as having increased due to rebound-induced fracturing along the pre-existing planes of weakness.

3) REFERENCES

AGAT Laboratories, 1988, Table of formations of Alberta: AGAT Laboratories, Calgary.

Anderson, N.L., 1992, Dissolution of the Wabamun Group salt: exploration implications, *in* Cavanaugh, T.D., Ed., Integrated exploration case histories, North America: The Geophysical Society of Tulsa Special Publication, in press.

Anderson, N.L. and Brown, R.J., 1992, Reconstruction of the Wabamun Group salts, southern Alberta, Canada, *in* Cavanaugh, T.D., Ed., Integrated exploration case histories, North America: The Geophysical Society of Tulsa Special Publication, in press.

Anderson, N.L. and Brown, R.J., 1991, Dissolution of the Wabamun and Black Creek salts: a seismic analysis: Geophysics 56, 618-627.

Anderson, N.L., Brown, R.J. and Hinds, R.C., 1988, Geophysical aspects of Wabamun salt distribution in southern Alberta: Canadian Journal Exploration Geophysics 24, 166-178.

Baar, C.A., 1977, Applied salt-rock mechanics 1: Elsevier Scientific Publishing Company, 294 p.

Carter, N.L. and Hansen, F.D., 1983, Creep of rock salt: Tectonophysics 92, 275-333.

Davies, P.B., 1989, Assessing deep-seated dissolution-subsidence hazards at radioactive-waste repository sites in bedded salt, *in*

Ege, J.R., 1979, Surface subsidence and collapse in relation to extraction of salt and other soluable evaporites; USGS Open-file Report 79-1666.

Jackson, M.P.A. and Talbot, C.J., 1986, External shapes, strain rates, and dynamics of salt structures: Bulletin Geological Society of America 97, 305-323.

Keary, P. and Brooks, M., 1984, An introduction to geophysical exploration: Blackwell Scientific Publications, Boston, 296 p.

Meijer Drees, N.C., 1986, Evaporitic deposits of western Canada: Geological Survey of Canada Paper 85-20, 118 p.

O'Brien, J.J. and Lerche, I., 1984, The influence of salt domes on paleo-temperature distributions, Geophysics 49, 2032-2043.

Oliver, J.A. and Cowper, N.W., 1983, Wabamun salt removal and shale compaction effects, Rumsey area, Alberta: Bulletin Canadian Society Petroleum Geology 31, 161-168.

Richter-Bernburg, G., 1987, Deformation within salt bodies: Dynamical Geology of Salt and Related Structures, 39-75.

Rokar, R.B. and Staudtmeister, K., 1985, Creep rupture criteria for rock salt, *in* Schreiber, B.C. and Harner, H.L., Eds., Sixth International Symposium on Salt: Salt Institute Inc., Virginia, 1, 455-462.

Talbot, C.J. and Jarvis, R.J., 1984, Age, budget and dynamics of an active salt extrusion in Iran: Journal Structural Geology 6, 521-533.

Urai, J.L., Spiers, C.J., Zwart, H.J. and Lister, G.S., 1986, Weakening of rock salt by water during long-term creep: Nature 324, 554-557.

VI: CASE HISTORIES

1) EXAMPLES FROM THE NORTH SEA

According to Jenyon and Cresswell (1987), the sub-sea level desert surface of the Lower Permian (Rottliegendes) Basin was subjected to the rapid ingress of oceanic water (Figure VI:1:1). At the time of this Zechstein transgression, the climate in the area was probably changing from highly arid to semi-arid. Such conditions, when combined with intermittent cessation and re-establishment of the flow of oceanic water into the basin, were favourable to evaporite formation. The subsequent history of the Zechstein is one of repetition of cycles of evaporation, from Z1 to Z4 (Figure VI:1:2).

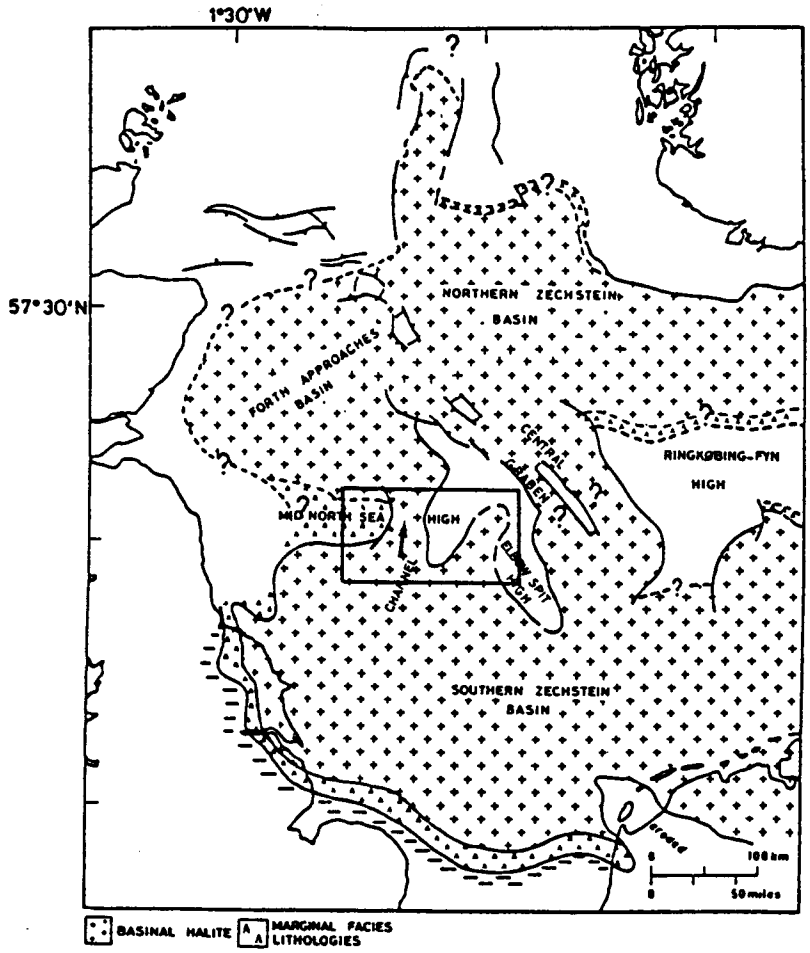

Fig. 1. Sketch-map showing principal features at the western end of the Zechstein Basin. Study area bounded by heavy lines. Modified from Jenyon *et al.*, 1984 , after Taylor, 1984.

Figure VI:1:1 (Figure 1; Jenyon, 1987)

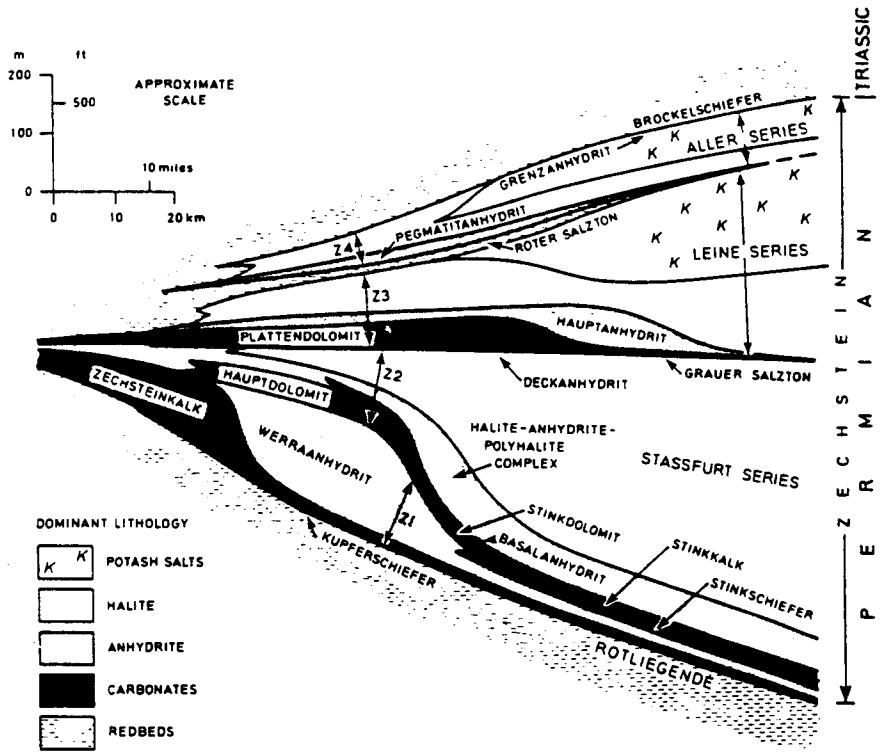

Fig. 3.4 Generalised shelf-to-basin section of the Zechstein evaporite cycles in the Southern North Sea. Note the three major carbonate units (Zechsteinkalk, Hauptdolomit, Plattendolomit), each overlain by a massive ramp of anhydrite prograding into the basin. This situation is difficult to reconcile with, particularly, the deep desiccating basin model in its basic form (Fig. 3.5c). (From Taylor, 1984, courtesy of the author and Blackwell Scientific Publications.)

Figure VI:1:2 (Figure 3.4; Jenyon, 1986)

The Zechstein cycles ideally consist of a basal clastic member representing the products of the initial transgression, folowed by carbonates (limestones and dolomites), anhydrite, halite, bittern salts, and a "regressive" anhydrite. In practice many interruptions or even reversals occur due to variations in the salinity gradient.

The massive Z2 halite may have exceeded 1400 m in thickness in the basin depocenter. Much thinner halites are present in cycles Z3 and Z4 which have a combined thickness of some 200 m.

These halites are thought to have become active as early as the Early Triassic and to have reached a peak of movement activity in the Late Cimmerian (Late Jurassic to Early Cretaceous).

Jenyon and co-workers in a series of papers describe some collapse features associated with the dissolution of the Zecchstein salts. In one particularly

interesting case study (Figures VI:1:3 and VI:1:4), Jenyon (1986) describes the localized dissolution of salt in response to synclinal stress-zoning.

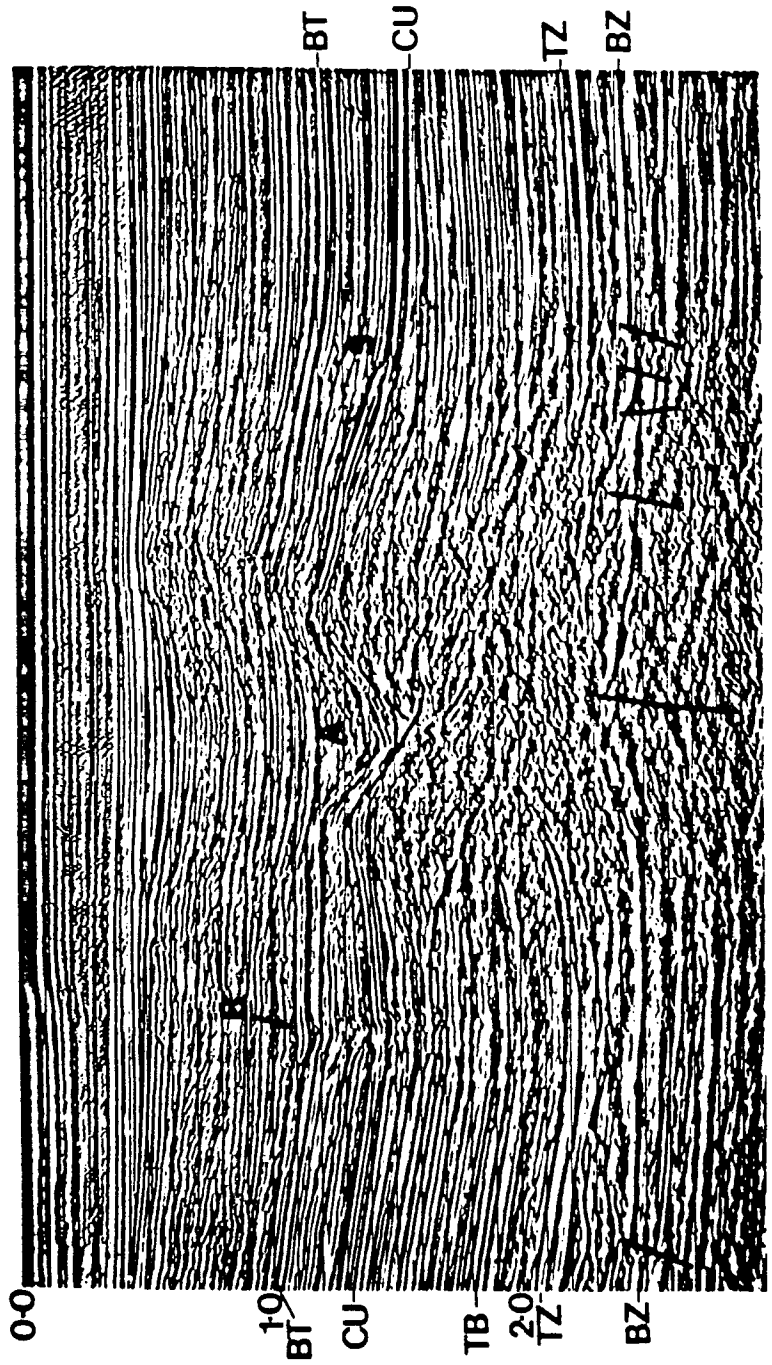

Fig. 6.16 Major (A) and minor (B) collapse features, discussed in the text. S is a thrust produced by salt uplift deformation which has led to bed repetition as seen by the events in the CU zone. BZ-TZ is the salt interval. TB is the Top Bacton horizon. CU, unconformity. BT, Base Tertiary. (Courtesy of SS(E)L.)

Figure VI:1:3 (Figure 6.16; Jenyon, 1986)

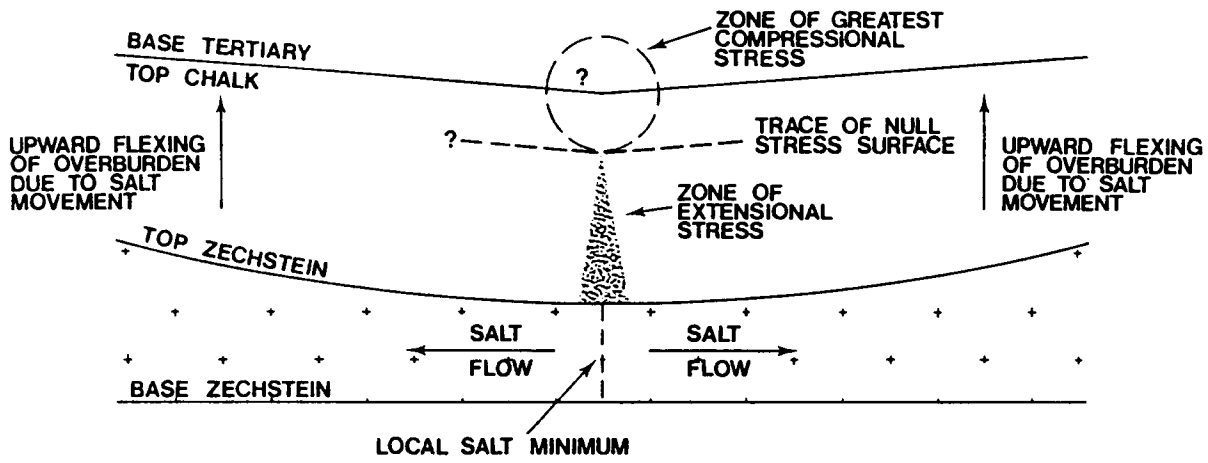

Fig. 6.17 Schematic showing an interpretation of the minor collapse features discussed in the text.

Figure VI:1:4 (Figure 6.17; Jenyon, 1986)

According to Jenyon (1986), the small collapse feature at B (Figures VI:1:3 and VI:1:4) is an example of a subtle and complex type of salt dissolution. Jenyon states that the small synform shape that occurs at the Base Tertiary/Top Chalk boundary BT seems to indicate that the basal Tertiary sediments have collapsed into the Top Chalk surface. He notes that vertically below, e.g. at the CU level and deeper, there are signs of rather wider and shallower graben-like collapse effects and that superficially, there appears to be no connection between these features and the salt interval (BZ-TZ) below.

This author reports that a number of features of this type are present in this general area of the southern Zechstein Basin of the North Sea. His interpretation is that they are produced by linear collapse channels (seen in cross-section in Figures VI:1:3 and VI:1:4), which are narrow, but very long and persistent for such small features. According to Jenyon, one of them has been traced for over 100 km whilst retaining an almost uniform width of about 0.5 km. He notes that they are parallel to the main tectonic trend in the area, which is also imposed on the major salt structures, that they normally occur at places where the underlying Zechstein is *relatively* thin (the local thinning of the salt is often very subtle, but exists) and that following from this, the salt thickens laterally away from this minimum in both directions. As a result, there is commanly a distinct dip change in the post-Zechstein bedding reflections so that a shallow V-shaped overburden feature is formed in contrast to the shallow U-shape of the top salt locally.

Jenyon's interpretation of these channels is as follows. "Due to late, very minor salt movement, synclinal stress zoning has occured in the post-Zechstein sequences at these loacations, with the compressed fold-core being approximately at the Base Tertiary/Top Chalk boundary. The schematic illustration in Figure VI:1:3

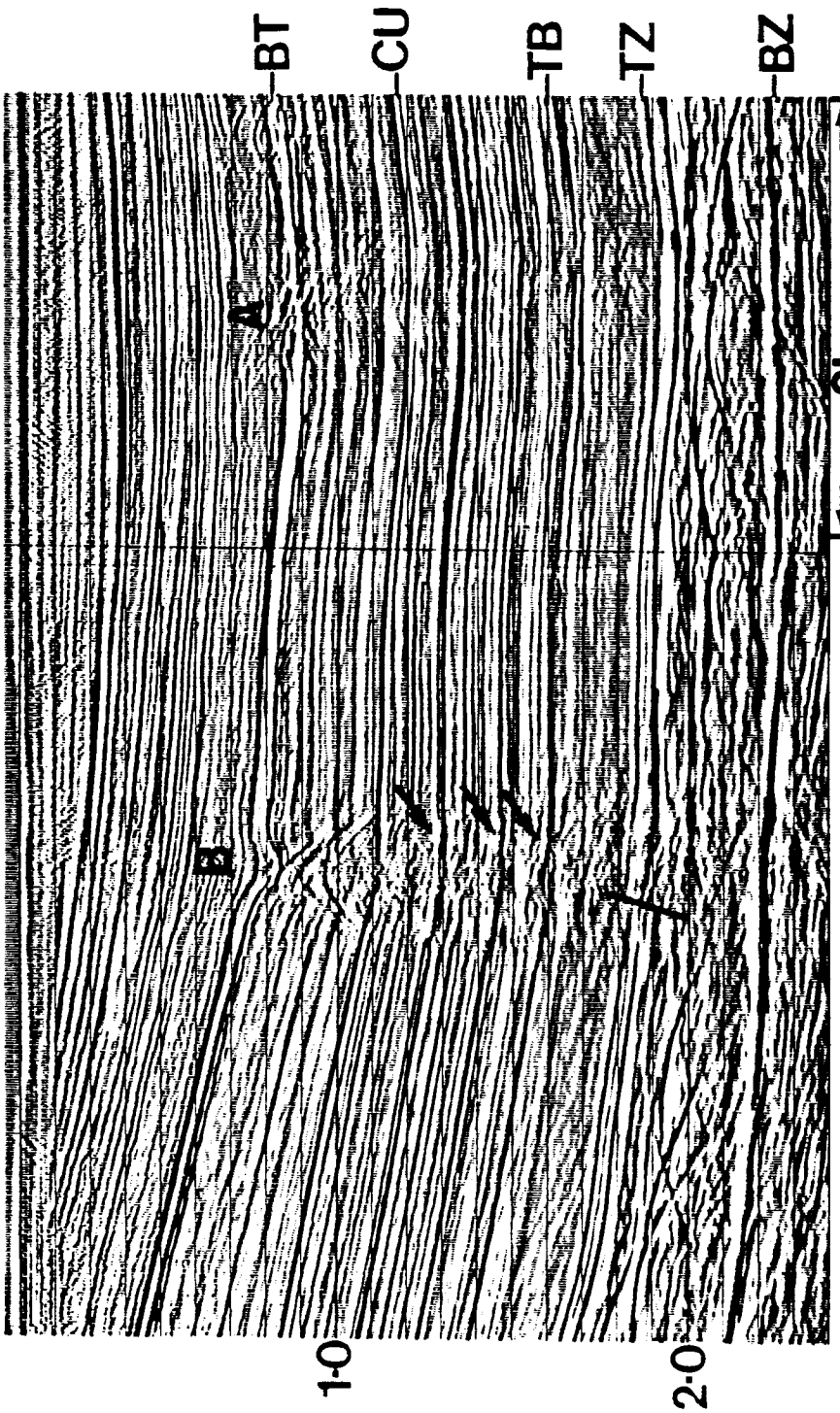

Fig. 6.18 Unmigrated section. Another example of a well-developed minor collapse feature (B), and an incipient feature of the same type (A). See text for explanation. Key is as for Fig. 6.16. (Courtesy of SS(E)L.)

Figure VI:1:5 (Figure 6.18; Jenyon, 1986)

illustrates the situation envisaged. The compressional stress acting at this boundary appears to have caused severe fracturing at the top of the Chalk. The compressional stress decreases vertically downwards probably quite rapidly to a surface of null stress, below which a zone of increasing extensional stress is present. It appears that undersaturated water has percolated downwards through the fracture system resulting, and dissolved the disrupted top of the Chalk to produce a sink channel into which basal Tertiary sediments have collapsed. It shoul be noted that in the schematic diagram the radius of the zone of greatest compressional stress, the position of the trace of the null stress surface, and the location and width of the zone of extensional stress are suggestions only, since precise indications cannot be given from the seismic data alone.

It seems that vertically below the sink channel, the zone of extensional tress has caused micro- and macro-fracturing. Further dissolution - in this scase, of several thin Middle/Upper Triassic evaporite units and also possibly some thin carbonate intervals - appears to have occurred from the observed evidence on the seismic sections.

Another point of interest is the short time interval within which the collapse effects die out in the overlying basal Tertiary strata reflections, usually within a TWT interval of 100-200 ms. This suggests that the minor localised salt movements which probably caused these features can be dated to within quite narrow limits as having occurred shortly after the deposition of the basl Tertiary beds.

In Figure VI:1:5 is shown at B another well-developed feature of this type; in this instance, the example is of an unmigrated seismic section, which leaves visible the strong hyperbolas which are being produced by the basal shape of the collapse at the Tertiary/Chalk boundary. The zone of extensional stress below B has led to the development of several wider but time-resticted collapse events, three of which are indicated by the arrows. Within this part of the section, three thin Triassic salt intervals are known to exist - the Rot, Muschelkalk and Keuper halites - and it is also possible that thin carbonate intervals may have been affected by dissolution. The extensional stress is also likely to be the cause of the normal fault at the top of the BZ-TZ interval which includes the main Zechstein salts.

Indicated at A in this same example is an incipient feature of the same type, where the zone of compression has begun to develop with thickenining and disruption of the event at BT level which marks the top of the Chalk. As yet the extensional stress zone has not developed. Note particularly the subtle but visible localised thinning of the BZ-TZ salt interval below both A and B, bearing in mind that it is the upwards flexing of the overburden sequences in both directions laterally away from the salt minima such as these that is causing the synclinal stress zoning in the overlying sequences."

Jenyon (1986) concludes his discussion by stating that features of this type may be of importance in hydrocarbon exploration, since the breaching of an otherwise impermeable seal formation may result, providing an upwards migratory route for hydrocarbons into the shallower section. This may be either good or bad news

depending on the reservoir/trap/seal situation.

2) CANADIAN RIVER VALLEY, TEXAS

According to Gustavson (1986), the development of the Canadian River Valley in the Texas Panhandle resulted mainly from regional subsidence related to the dissolution of Permian salts (Clear Forks, Glorietta, San Andres and Seven Rivers formations; Figures VI:2:1-VI:2:3). Gustavson demonstrates that the Canadian River Valley follows a zone of subsidence for more than 200 km, and that dissolution and subsidence is still active.

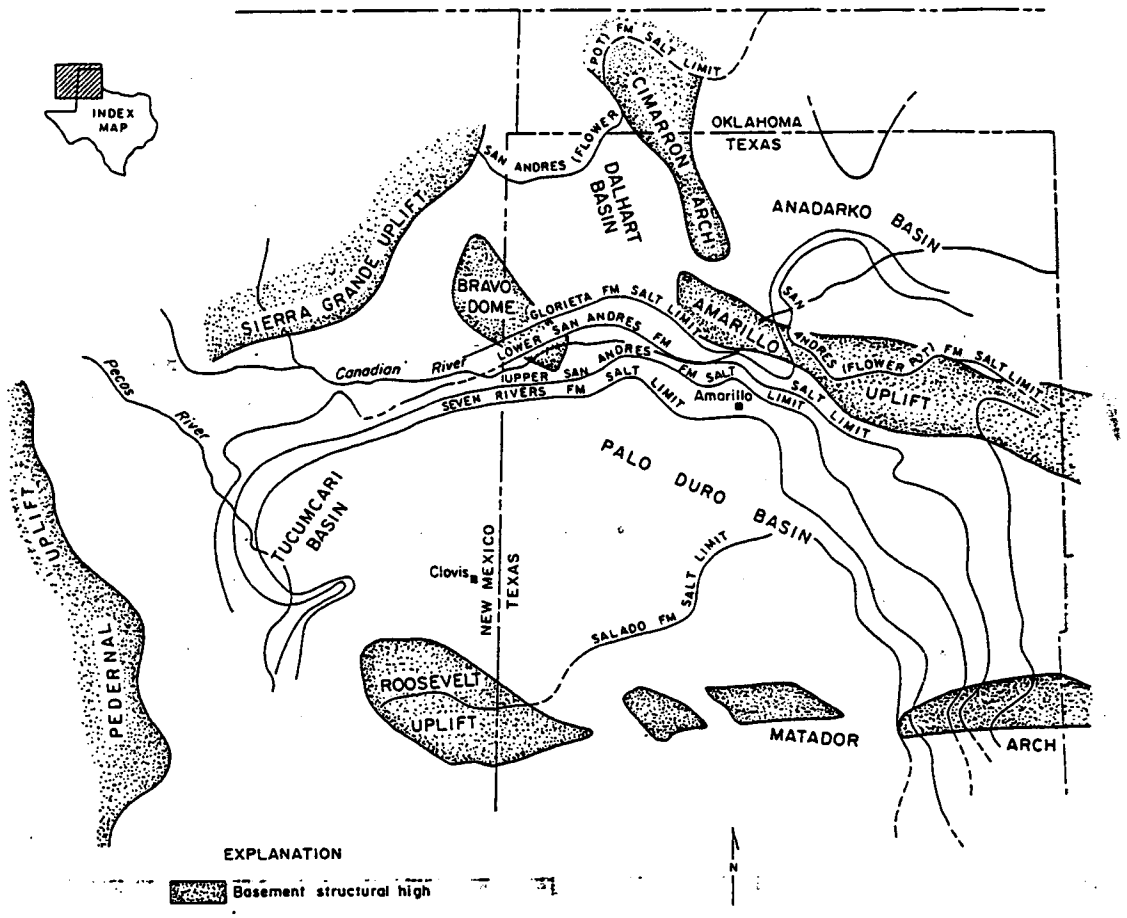

Figure 2. Regional structural elements, Texas Panhandle and eastern New Mexico. The peripheral salt dissolution zone in the Palo Duro and Anadarko Basins, along the margins of the Glorieta through Seven Rivers salt limit lines, follows the upturned edges of Permian strata along the basin margins, which illustrates that dissolution of salt tends to occur in structurally high areas where salts are nearest to the surface. The study area occurs along the Amarillo Uplift and Bravo Dome.

Figure VI:2:1 (Figure 2; Gustavson, 1986)

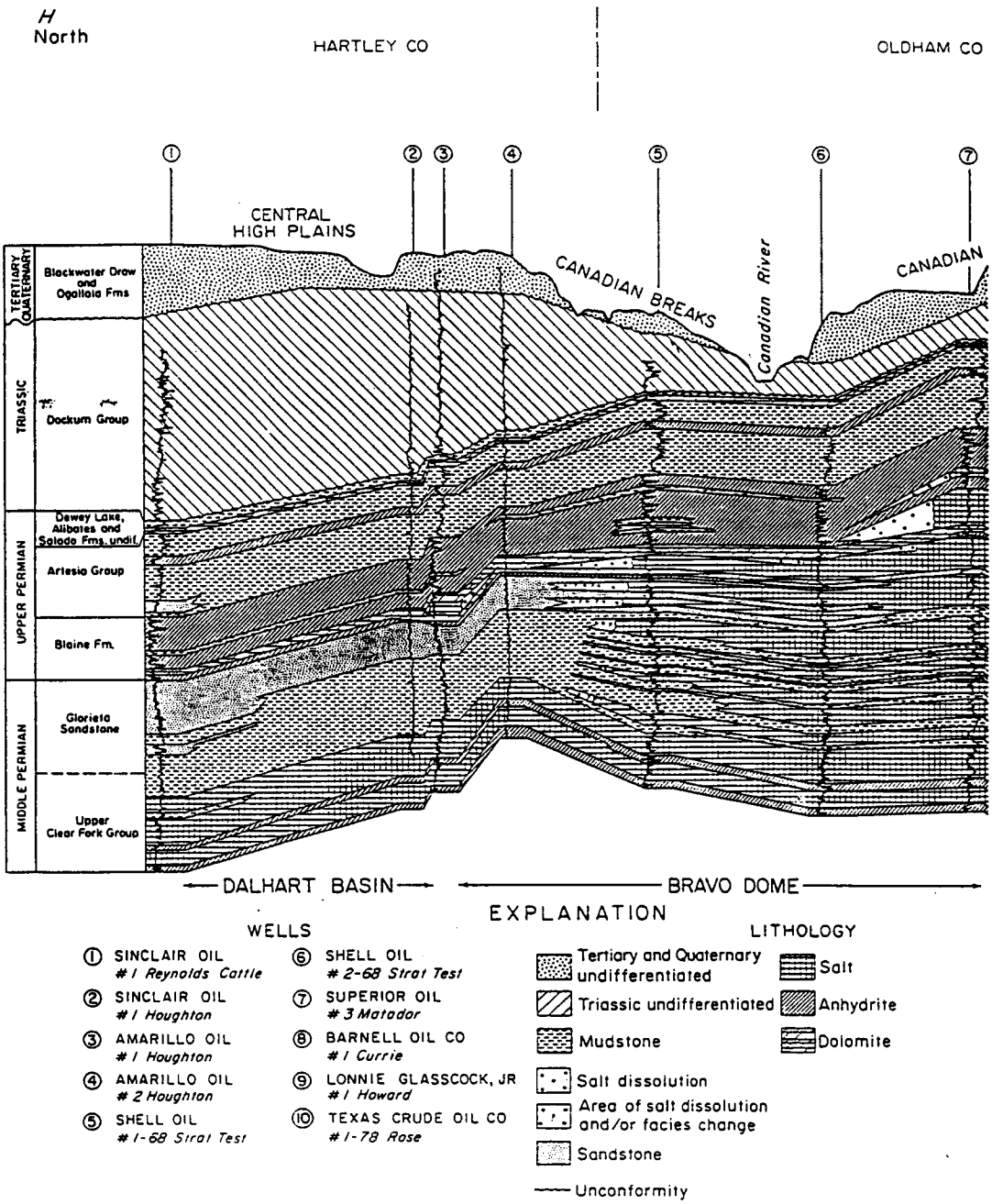

Figure 4. Stratigraphic cross section H–H′ illustrates the loss of >200 m (600 ft) of salt along the northern margin of the Palo Duro Basin. Structural collapse of overlying units and the continuation of nonsalt evaporite units in the upper part of the section across the structurally high Bravo Dome without significant change suggests that salts have thinned because of dissolution and not because of facies change. A facies change from salt to sandstone occurs in the upper Glorieta Formation. See Figure 5 for the location of cross section H–H′. Cross section modified from McGookey and others (1985).

Figure VI:2:2 (Figure 4; Gustavson, 1986)

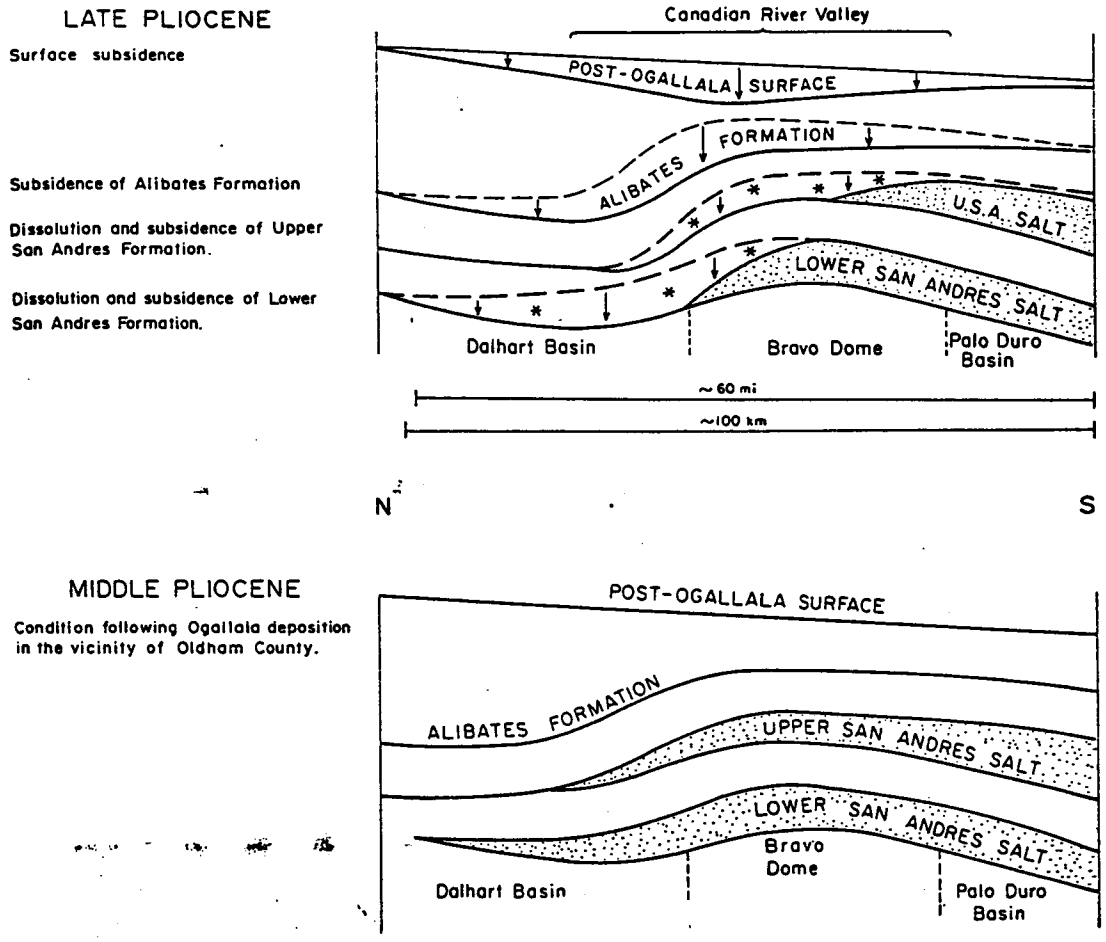

Figure 10. Dissolution of salt in the late Tertiary and early Pleistocene in structurally high areas resulted in subsidence of overlying strata. Areas undergoing dissolution and subsidence were roughly lens-shaped in cross section. Surface subsidence resulted in the development of the Canadian River Valley and accounts, in part, for the depth of the valley.

Figure VI:2:3 (Figure 10; Gustavson, 1986)

3) WINK SINK, TEXAS

According to Johnson (1989), the Wink Sink, in Winkler County, Texas (Figure VI:3:1), is a collapse feature that formed in June 1980 when an underground dissolution cavity migrated upward by successive roof failures until it breached the land surface (Figure VI:3:1). He suggests that the original cavity developed in the Permian Salado Formation salt beds more than 400 m below ground level. According to Johnson (1989), although natural dissolution of the Salado salts occurred in the sinkhole study area in the past, it appears likely that the Wink Sink was influenced by petroleum production activity in the immediate area. He concludes that the drilling, completion, and plugging procedures used on an abandoned oil well at the site of the sink appear to have created a conduit that enabled water to circulate down the borehole and dissolve the salt. When the dissolution cavity became large enough, the roof failed and the overlying rocks collapsed into the cavity.

4) KNACKSTEDT, KANSAS

Geological control from drilling indicates that the Hutchinson salt (Permian Wellington Formation; Figure VI:4:1) is preserved throughout central and south-central Kansas as a more-or-less continuous body with net thicknesses of up to 170 m. This salt has been extensively dissolved along its eastern margin due to access to the Tertary, Quaternary, and present water tables. To the west of the main dissolutional edge, localized leaching that is probably associated with subsurface flow systems related to structural features such as fractures and faults has occurred in the past, and in some areas is presently occurring. Such sites are characterized by surface sinkholes and/or subsurface cavities. The more recent sinkholes (last 100 years) are often associated with either salt mining or saltwater disposal and in some instances surface expressions developed in a matter of only hours or days (Walters, 1978).

Basinward of the present day main edge of the Hutchinson salt, subsurface cavities have been discovered that are associated with saltwater disposal wells in oil and gas fields. Some of these have led to catastrophic surface collapse. It is anticipated that many of these cavities will eventually collapse and that sinkholes will develop at those sites where bridging of overlying strata does not prevent the collapse features from manifesting themselves at the surface. Structural features and associated flow of subsurface waters may play an important part in the dissolution rate and resultant size of cavities formed around artificial penetrations.

The Hutchinson Salt in the Knackstedt study area, Kansas (Township 20 South, Range 5 West), extends from approximately 135 m to 210 m below the ground surface. The prominent part of the lost-circulation or salt-solution zone in the Wellington Formation lies approximately 13 km to the east, based on a map of Gogel (1981). At a saltwater disposal well site in the study area, an air-filled, subsurface cavity (Figure VI:4:2), which is not manifested at the surface as a

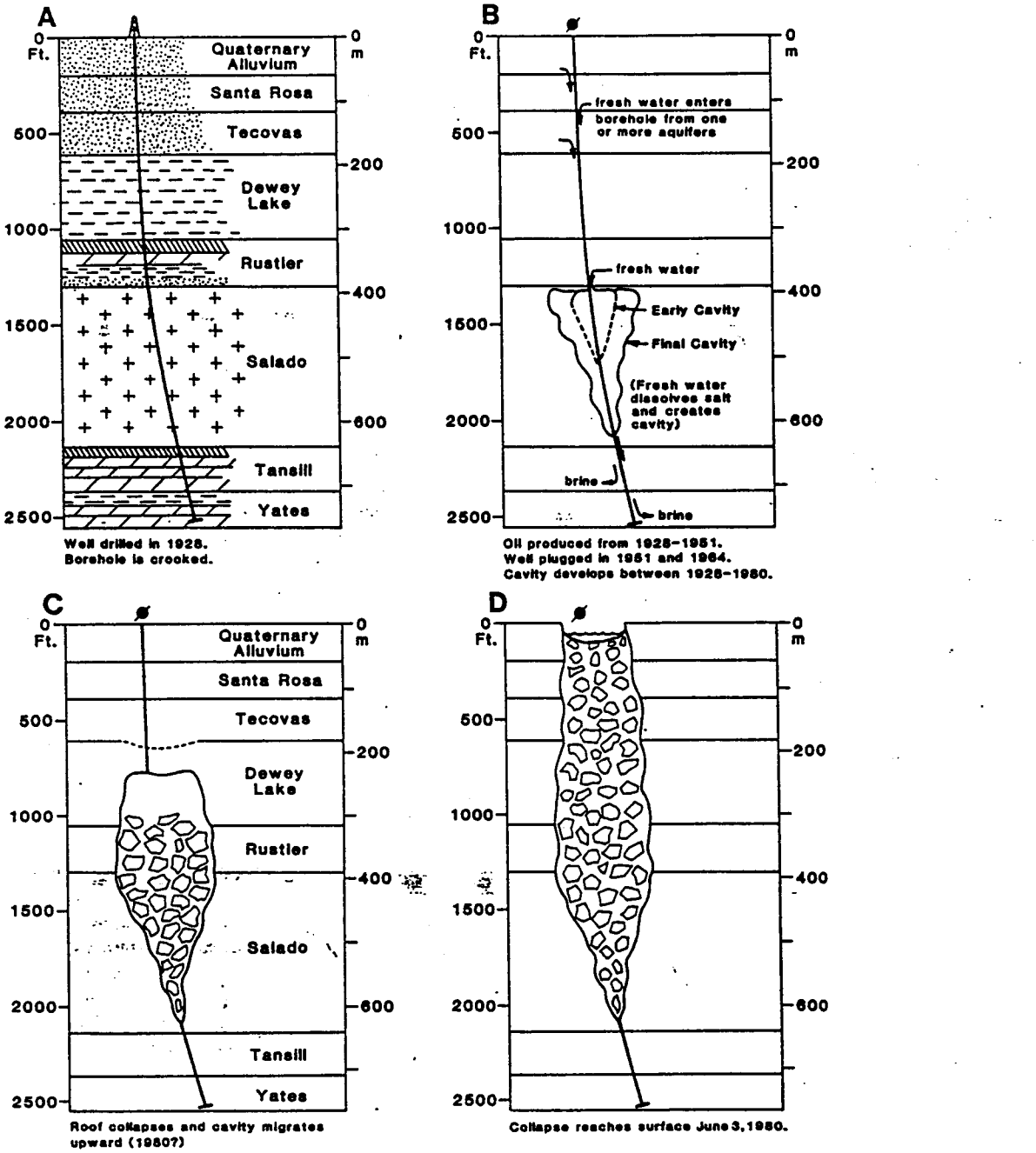

Figure 8. East–west cross section through the Hendrick Well 10-A showing possible relationship of well to development of the Wink Sink. Freshwater may have circulated down the borehole to dissolve the salt and create a cavity; by successive roof failures, the cavity migrated upward to the land surface.

Figure VI:3:1 (Figure 8; Johnson, 1989)

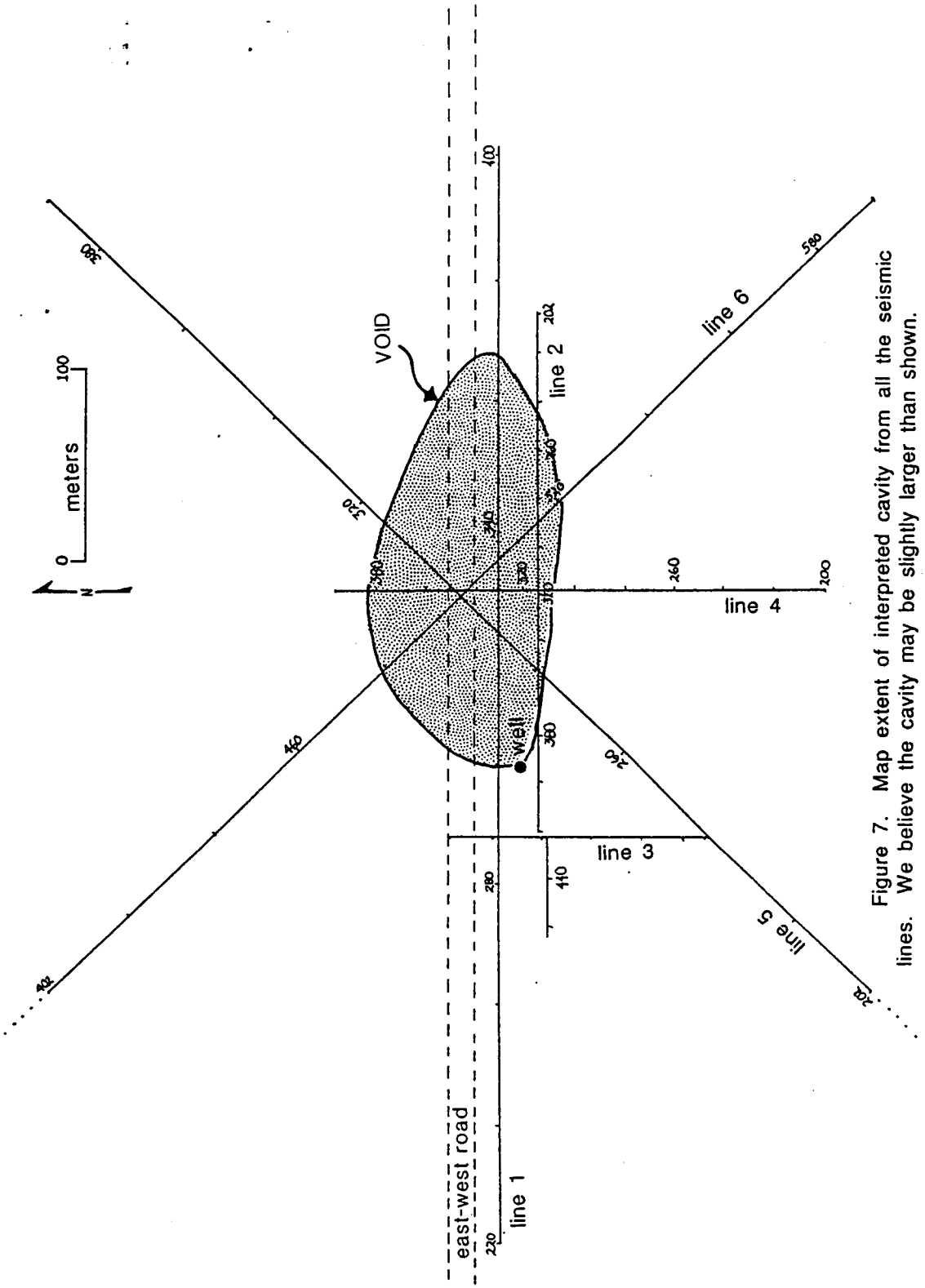

Figure 7. Map extent of interpreted cavity from all the seismic lines. We believe the cavity may be slightly larger than shown.

Figure VI:4:1 (Figure 8; Miller et al., 1988)

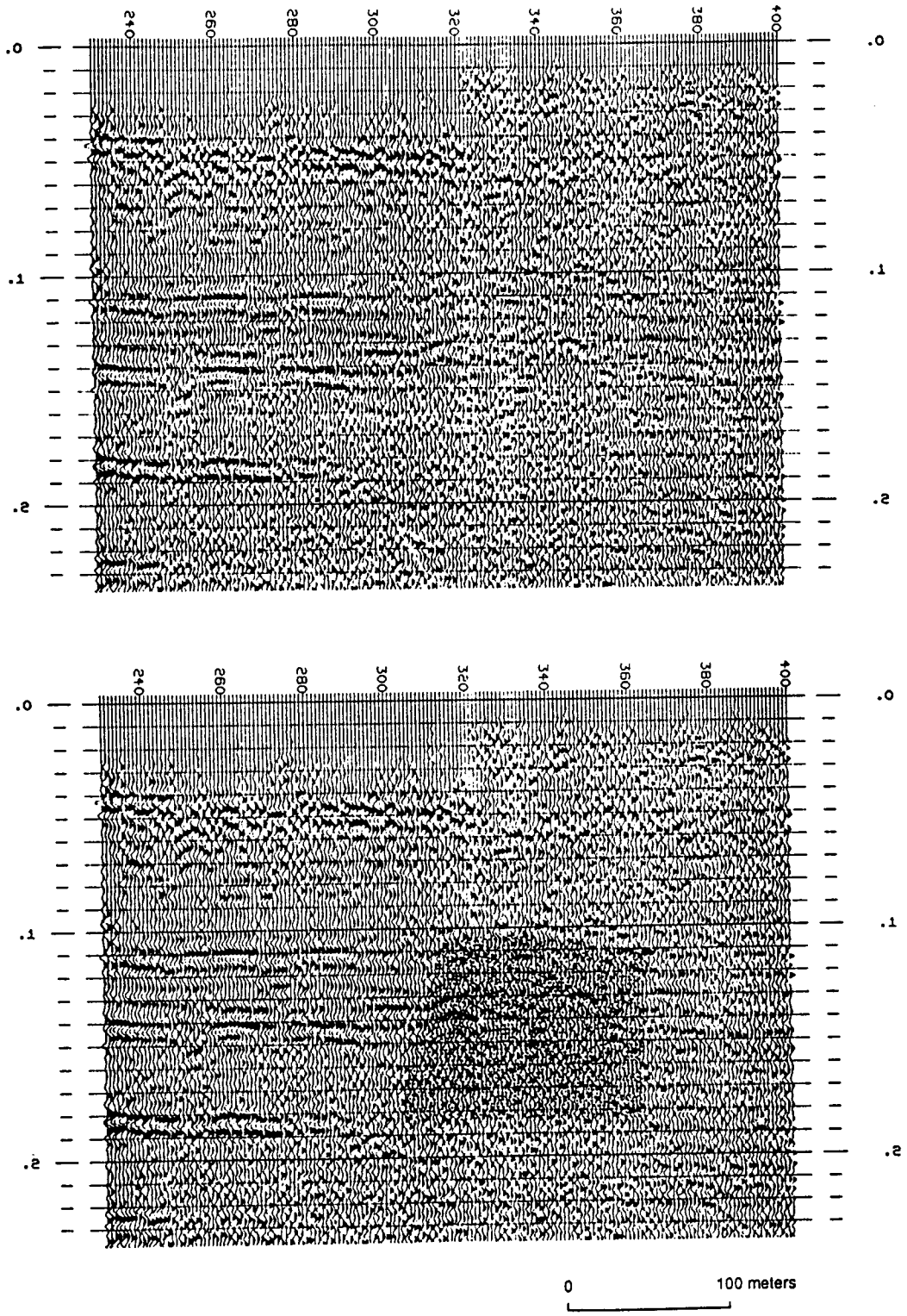

Figure 2. Seismic section for line 1. Interpreted cavity is from locations 305 to 365 on this line. The upper seismic section is uninterpreted, and the lower section has light stippling covering the location of the cavity.

Figure VI:4:2 (Figure 2; Miller et al., 1988)

sinkhole, was discovered when investigations into the loss of static water level resulted in a wireline video inspection of the well casing. The video discovered the absence of casing as well as any borehole walls between 97 m and 146 m in depth. The bottom of the borehole, which originally extended over 900 m, was plugged with neat cement. In an attempt to fill the void, 8400 m^3 of gravel were poured into the well from the surface, raising the floor of the cavity from 160 m to 135 m.

During the filling process, the hole was occasionally flushed with a saturated brine solution in an attempt to level the coning of the pile of material directly beneath the borehole opening in the ceiling of the void. No static fluid level was ever recorded after a brine solution flush. The absence of a measurable water level in the hole at any time during the past several years, even though the alluvial sediments on the overlying shale roof contain a relatively shallow water level, suggests that the void is hydraulically connected by a large conduit to an aquifer with a hydrostatic head at least 160 m below the earth's surface. The aquifer could either be the intended oil-brine disposal horizon (several hundred meters below the salt) or a salt-solution zone extending laterally from the cavity location.

The source of the waters causing most of the dissolution was probably oil brine that escaped from the failed injection casing. Shallow ground waters could have been slowly flowing to and dissolving the salt in a structural fracture system in the area prior to the drilling of the borehole. Ground waters unsaturated with respect to halite could have been and are probably presently entering the large cavity, and therefore could be causing further dissolution expansion of its dimensions.

5) SALT GLACIERS

According to Talbot and Jarvis (1983), the Hormuz salt of Kuh-e-Namak, Iran began rising through its Phanerozoic cover in Jurassic times and had surfaced by Cretaceous times. In Miocene times, the still-active Zagros folds began to develop and the salt is still extruding to feed a massive topographic dome and two surface flows of salt called namakiers (salt glaciers;).

These authors calculated two crude but independent estimates for the rate of salt extrusion (on the assumption that the current salt dynamics are assumed to be in steady state). Their first estimate was based on the calculation that to replace the extrusive salt likely to be lost in solution in the annual rainfall, the salt must rise at an average velocity of about 11 cm a^{-1}. Their second independant estimate was based on their analysis of the foliation pattern within the rock salt which shows that the extruding (and partially dissolved) salt column spreads under its own weight. According to these authors, the maximum height of the salt dome is consistent with a viscous fluid with a viscosity of 2.6 X 10^{17} poises extruding from its orifice at a rate of almost 17 cm a^{-1}. Both estimates are consistent in indicating that salt can extrude onto the surface 42-85 times faster than the average long term rate at which salt diapirs rise to the surface.

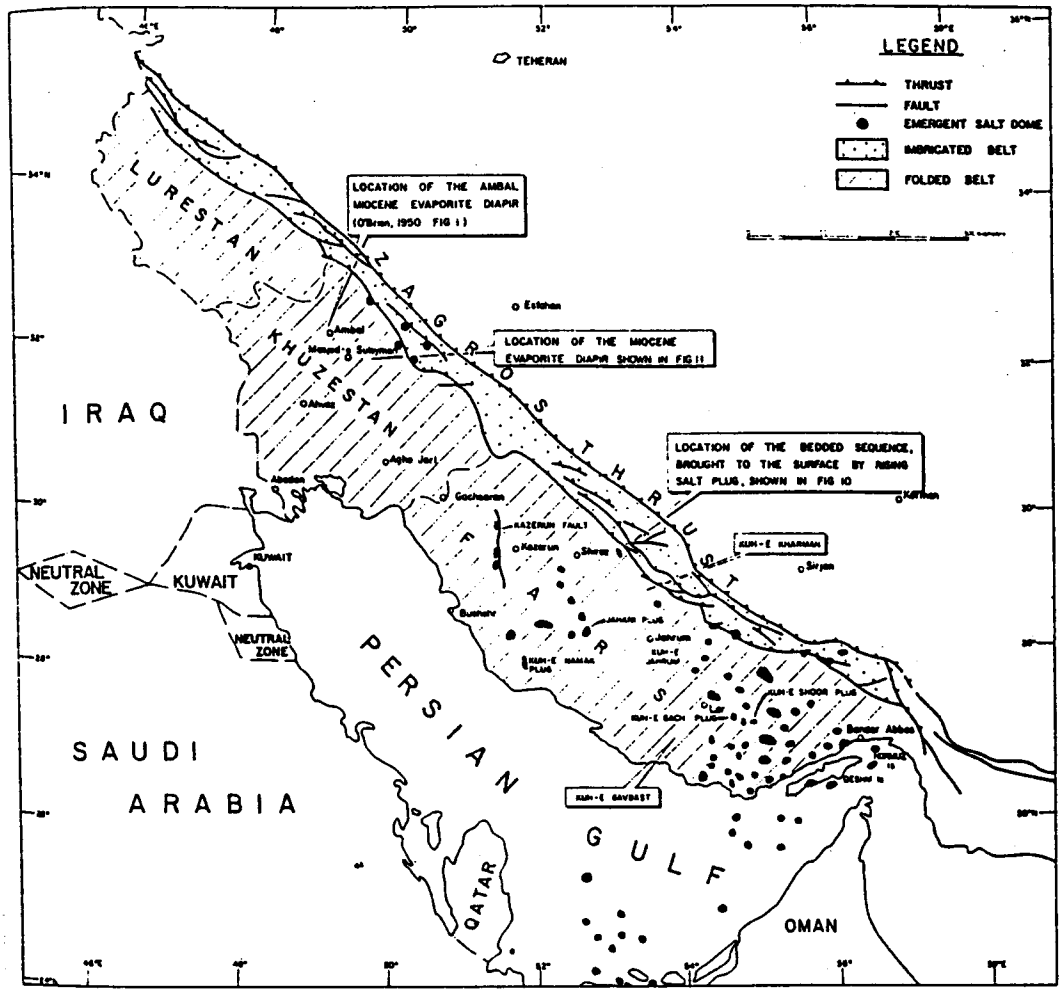

FIG. 1—Distribution of salt domes in southern Iran and Persian Gulf.

Figure VI:5:1 (Figure 1; Ala, 1974)

According to Talbot and Jarvis (1983), the structure, fabrics, textures and deformation mechanisms of the impure halite all change along the path of the extrusive salt from the dome down the length of both namakiers. They note that such changes tend to occur when the flowing salt encounters changes in its boundary conditions, and the recognition of buried namakiers is discussed in the light of such observations. Episodes of salt flow at a rate of 0.5 m per day have been measured along the margin of the namakier after significant rain showers. Such brief episodes of rapid flow alternate with long periods when the namakier is dry and stationary. Although the reported annual rainfall has the potential of dissolving both namakiers in about 2000 years, a superimposed thin marine cover may protect static parts of them for as long as 30,000 to 300,000 years (Talbot and Jarvis, 1983).

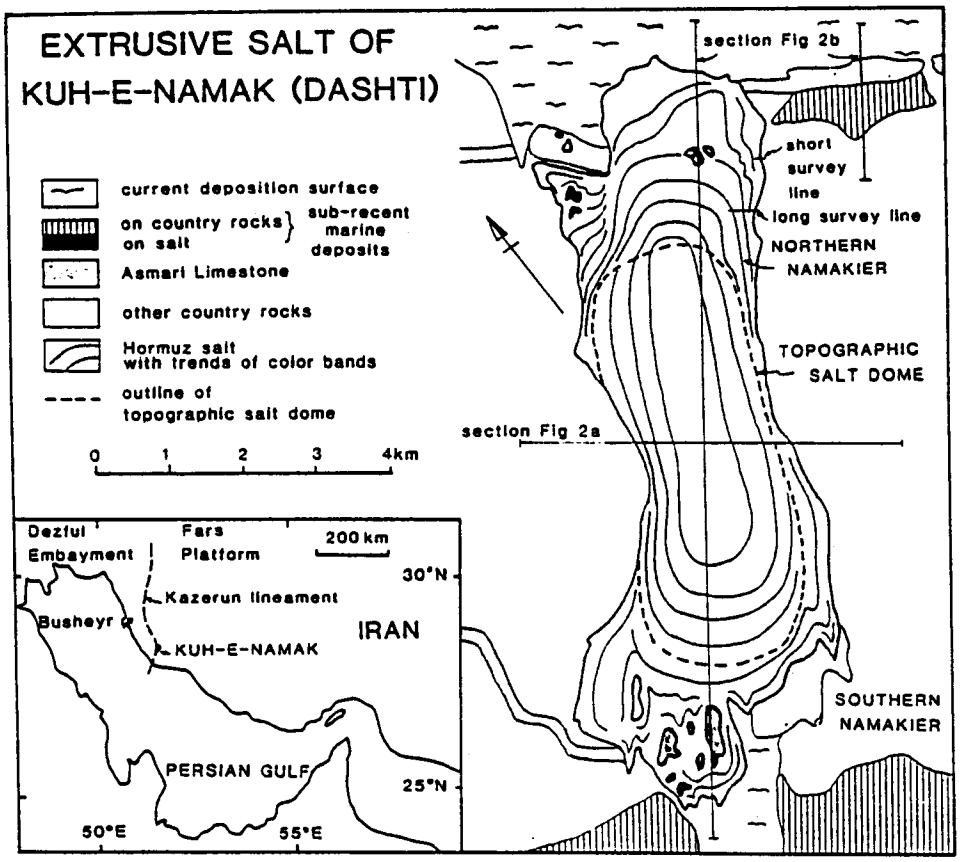

Fig. 1. Geological sketch map of the salt extrusives at Kuh-e-Namak (Dashti) showing locations of profiles in Fig. 2.

Figure VI:5:2 (Figure 1; Talbot and Jarvis, 1984)

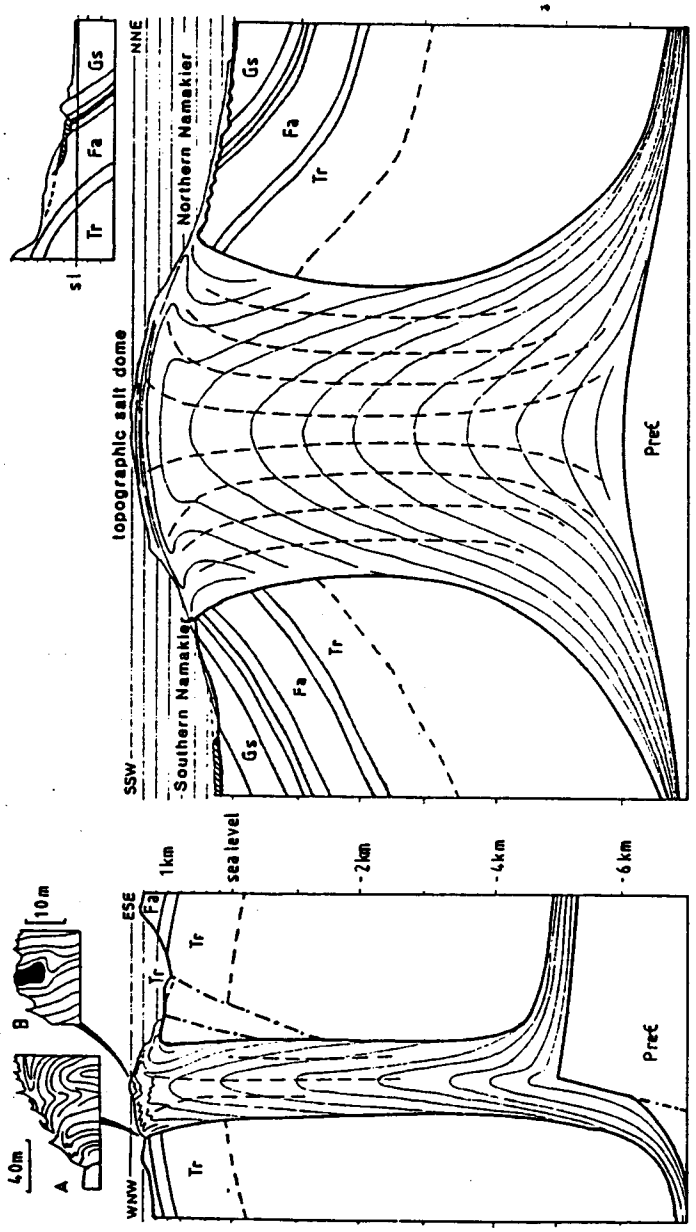

Fig. 2. Vertical cross (a) and longitudinal (b) sections of the Hormuz (= Eocambrian) salt mass showing the geometry of the flow profiles inferred from surface exposure. Locations of profiles are shown on Fig. 1. The colour banding (= bedding?) is shown in solid lines while the trace of the foliation (= stream lines) is indicated by dashed lines. Country rocks are: Pre€, Precambrian; Tr, Trias; Fa, Fahliyan-Surmeh Formation (Cretaceous); Grs, Gachsaran Formation (Miocene).

Inserts on Fig. 2(a): (A) The subvertical axial surface of mature folds inherited from depth curl to parallel the top free surface of the salt dome on its flank. These are joined or refolded by immature folds with axial planes which also curl to parallel the free surface but are too small-scale to illustrate (see Talbot 1979, fig. 8). (B) Occasional large blocks of insoluble Hormuz material (e.g. black limestone) are incorporated in the salt emerging in the dome. These are milled and dispersed in the halite if they are carried towards the distal portions of the namakiers in (rather than on) the salt.

Insert on Fig. 2(b): Cross section 1.5 km east of N namakier (see Fig. 1 for location) to show recent marine deposits (oblique ruling) and marine bevel (dashed) which define a recent surface (33,000–283,000 BP?) already showing significant folding. The same deposits and bevel can be seen to define the south limb of the recent increment of the Kuh-e-Namak anticline on the main longitudinal profile (Fig. 2b).

Figure VI:5:3 (Figure 2; Talbot and Jarvis, 1984)

6) REFERENCES

Ala, M.A., 1974, Salt diapirism in southern Iran: Bulletin American Association of Petroleum Geologists 58, 1758-1770.

Gustavson, T.G., 1986, Geomorphic development of the Canadian River Valley, Texas Panhandle: An example of regional salt dissolution and subsidence: Geol. Soc. Am. Bull. 97, 459-472.

Jenyon, M.K., 1986, Salt tectonics: Elsevier Applied Science Publishers, 191 p.

Johnson, K.S., 1989, Development of the Wink Sink in West Texas, U.S.A., due to salt dissolution and collapse: Environmental Geology and Water Science 2, 81-92.

Miller, R.D., Steeples, D.W., Myers, P. and Somanas, D., 1988, Seismic reflection surveys at the Knackstedt salt-water disposal well: Kansas Geological Survey Open File Report 88-31.

Talbot, C.J. and Jarvis, R.J., 1984, Age, budget and dynamics of an active salt extrusion in Iran: Journal Structural Geology 6, 521-533.

Walters, R.F., 1978, Land subsidence in central Kansas related to salt dissolution: Kansas Geological Survey Bulletin 214, 82p.

VII: DEVONIAN SALTS IN WESTERN CANADA

1) OVERVIEW

There are six main Devonian salts in Alberta, those of the Lotsberg Formation, Cold Lake Formation, Prairie Evaporite Formation (and equivalents), Beaverhill Lake Group, Leduc Formation and Wabamun Group (Figures VII:1:1-VII:1:4). Each of these salts is different: some are thick (>160 m) - others are thin (<45 m); some are massive - others are bedded; some are areally extensive - others are areally restricted. Yet, each of these salts have one comman characteristic; they have all been extensively dissolved in places.

The leaching of these salts is of significant interest to the explorationist for several reasons: 1) stratigraphic traps can form where reservoir facies were either preferentially deposited or preserved in salt-dissolution lows; 2) reservoir facies can develop in high energy environments such as topographic highs that are controlled by salt edges or remnants; 3) structural traps can form where reservoir facies are draped across salt remnants or collapse features; and 4) salt remnants can be misinterpreted as reefs, faults or other structural features (Chapter II).

In an effort to elucidate the leaching of the Devonian salts in western Canada, we present in this chapter: 1) an overview of the present-day distribution of the main Devonian salts in Alberta; and 2) illustrative discussions of the methodology we used to reconstruct the paleo-distribution of some of the Devonian salts in the Stettler, Youngstown and Lloydminster areas.

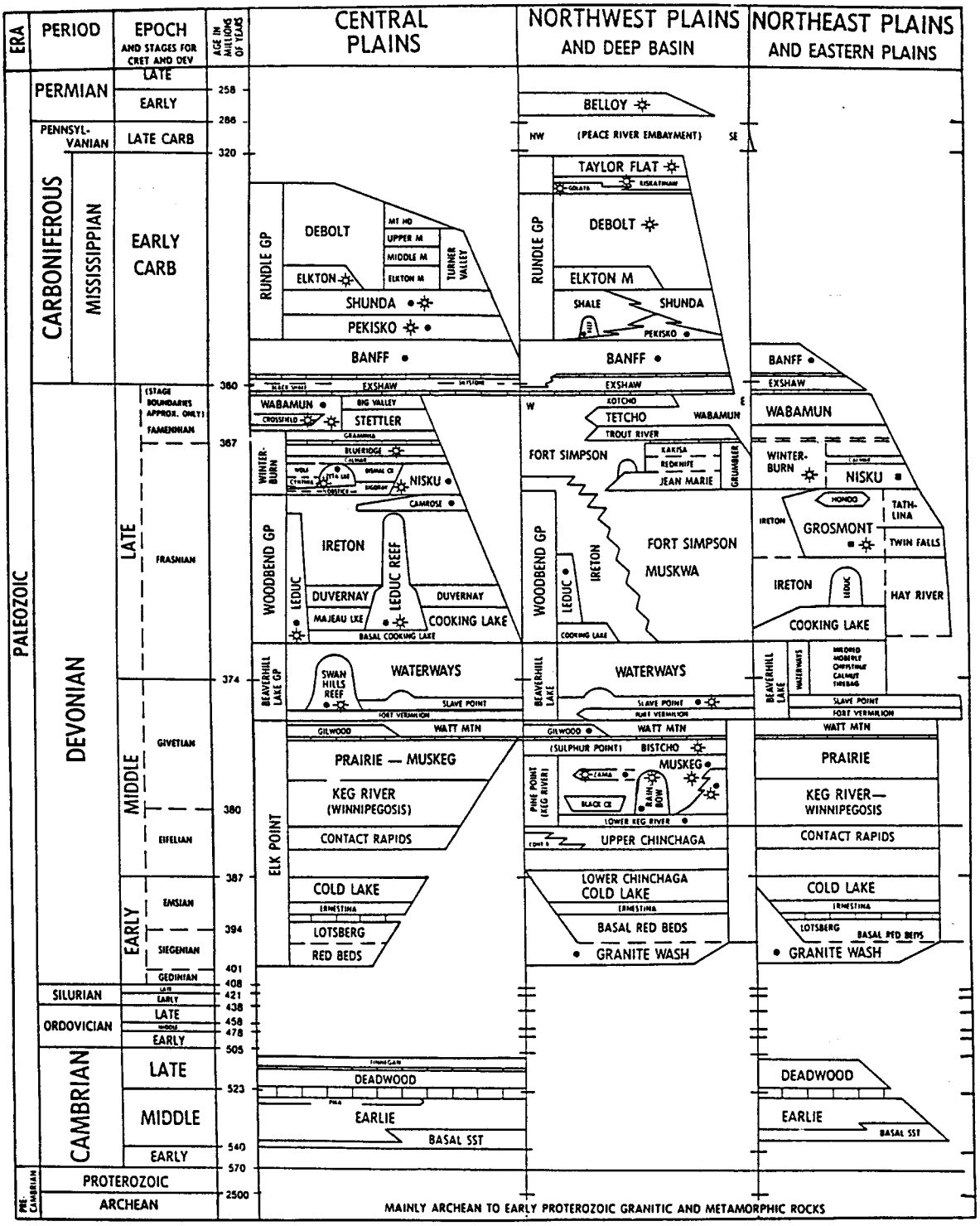

Figure VII:1:1 - Stratigraphic Chart for the Paleozoic of Central and Northern Alberta (after AGAT Laboratories, 1988).

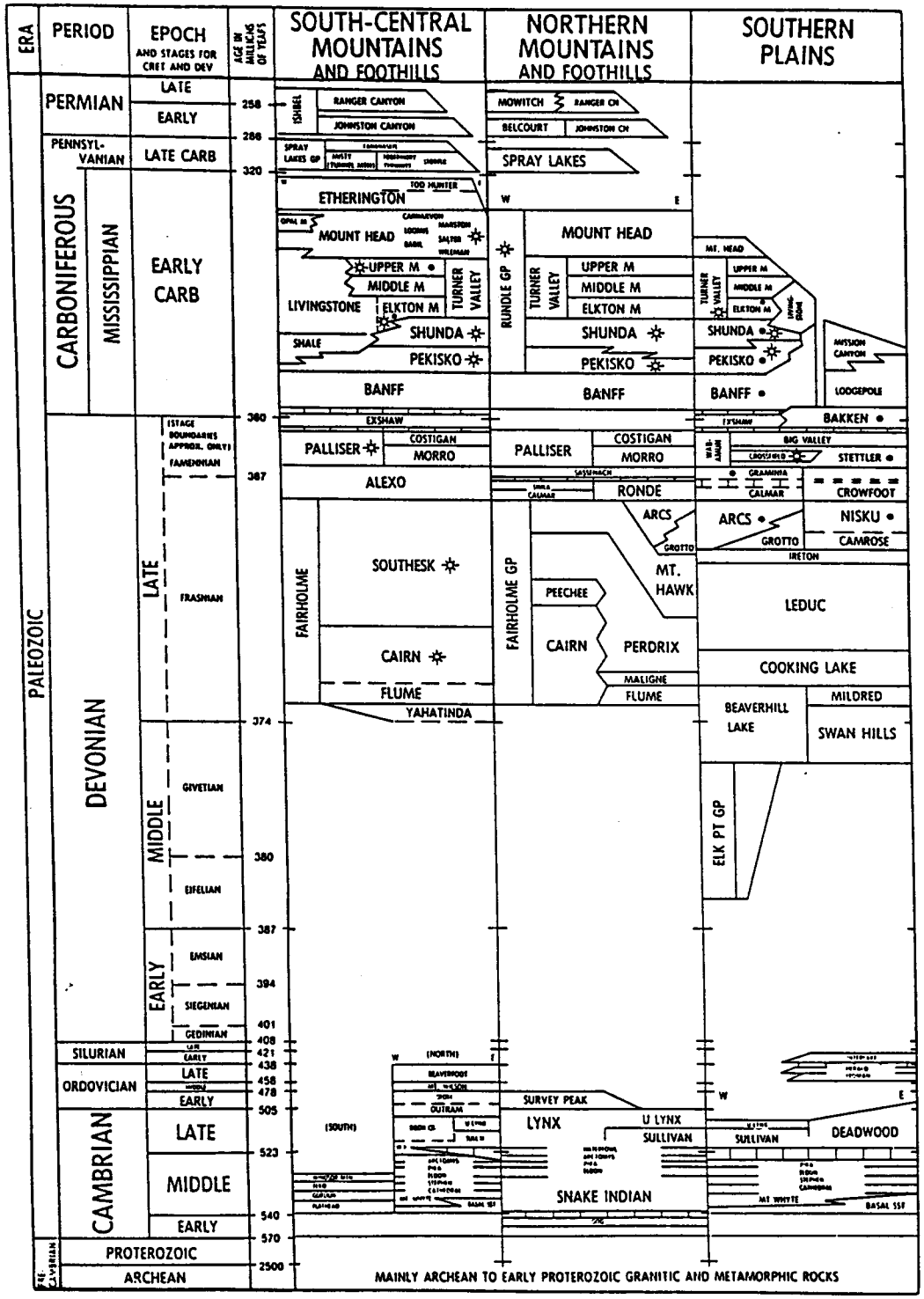

Figure VII:1:2 - Stratigraphic Chart for the Paleozoic of Southern and Western Alberta (after AGAT Laboratories, 1988).

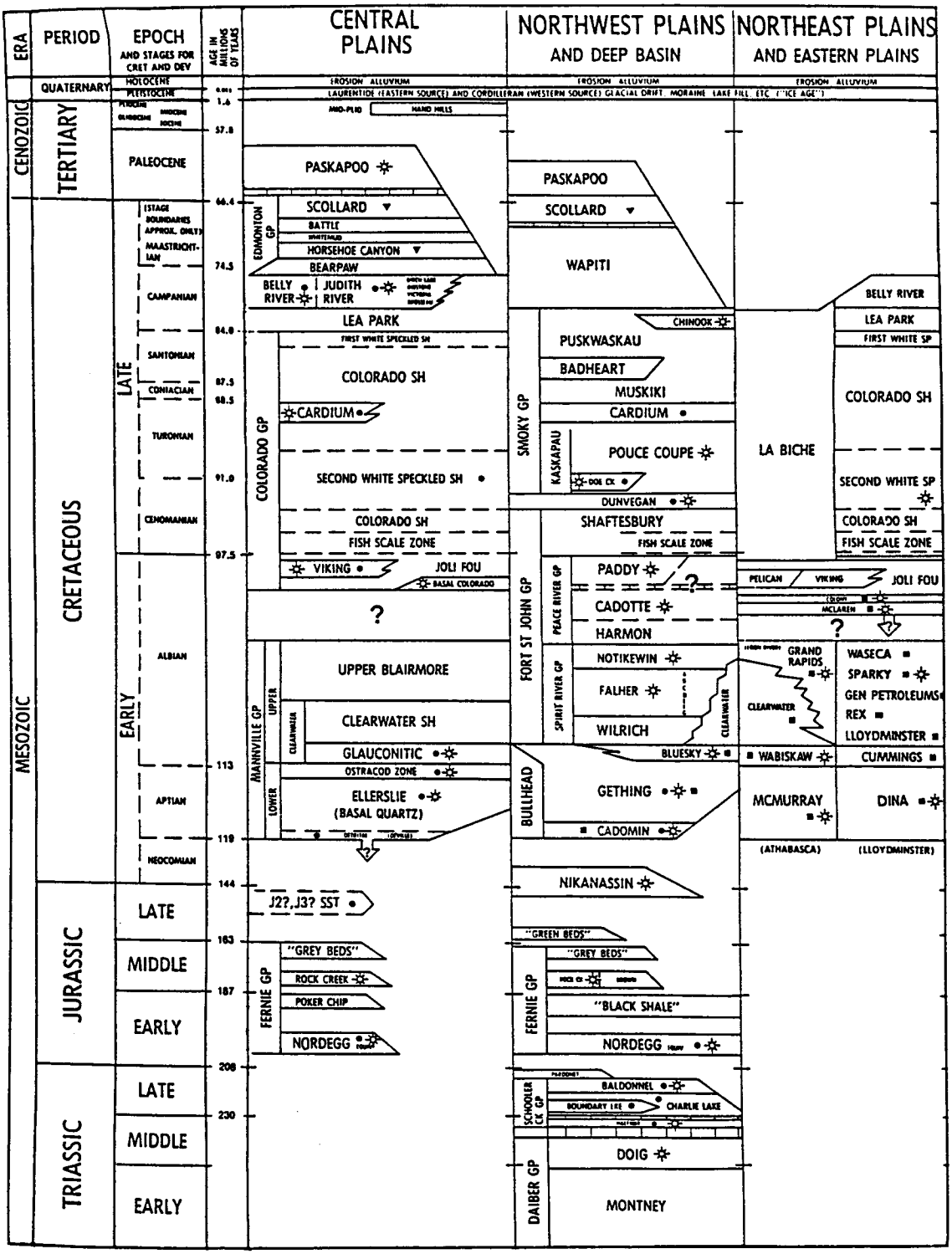

Figure VII:1:3 - Stratigraphic Chart for the Mesozoic of Central and Northern Alberta (after AGAT Laboratories, 1988).

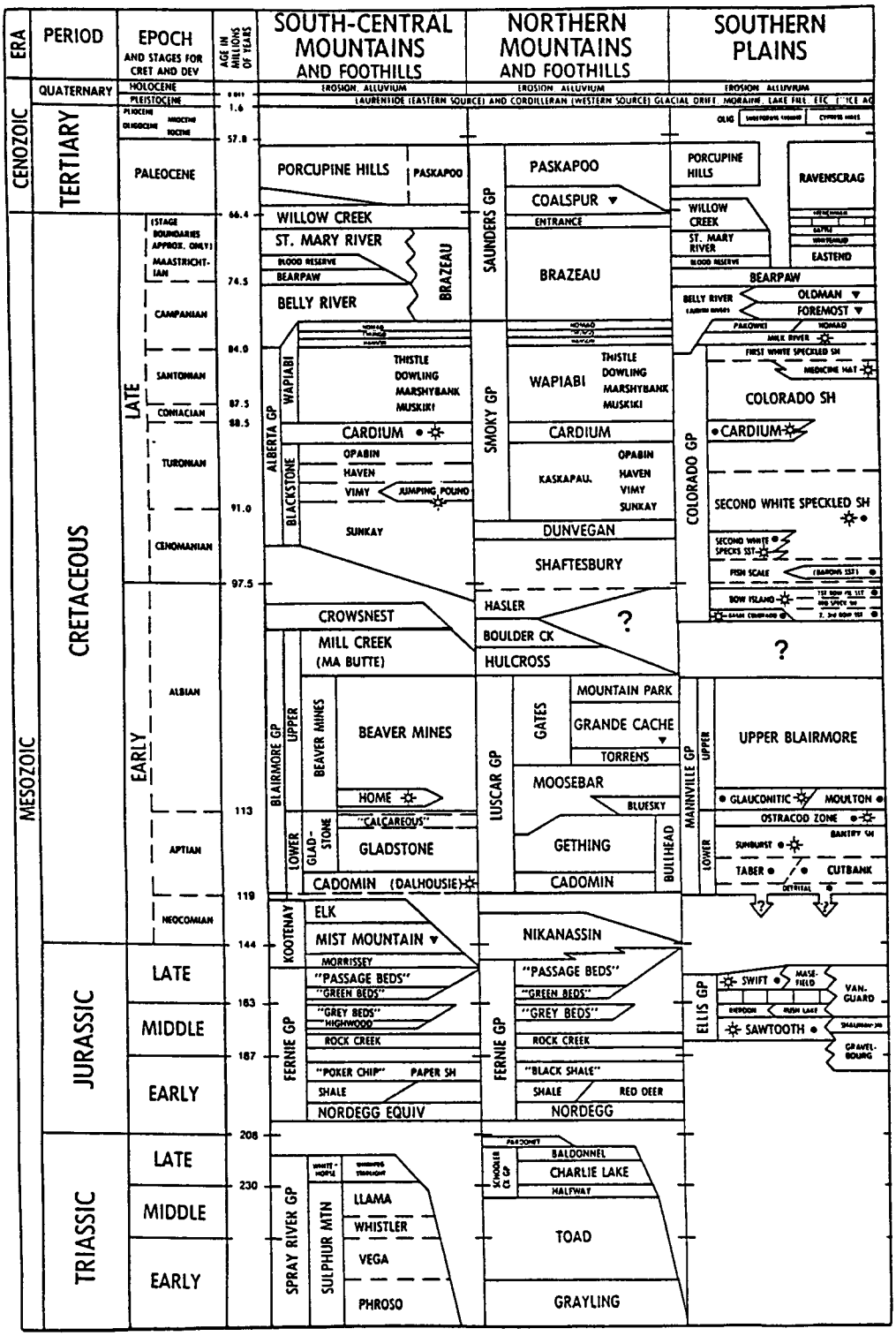

Figure VII:1:4 -Stratigraphic Chart for the Mesozoic of Southern and Western Alberta (after AGAT Laboratories, 1988).

2) DISTRIBUTION OF THE MAIN DEVONIAN SALTS IN ALBERTA

A) LOTSBERG FORMATION SALT

Geological Overview:

The type section for the Lotsberg Formation (Sherwin, 1962) is located between the depths of 1058 and 1225 m (3470 and 4020 ft) in the Canadian Seaboard Ernestina Lake (10-13-60-4W4) well (Figures VII:1:1-VII:1:2 and VII:2:1). The Lotsberg in this well consists of almost pure halite. It is underlain by the Basal Red Beds unit and overlain by the Ernestina Lake Formation. Hamilton (1971) subdivided the Lotsberg Formation into Lower and Upper Lotsberg members. These are separated by an shale facies (unnamed) described by Sherwin (1962), Hamilton (1971) and Meijer Drees (1986).

Lower Lotsberg Member:

The Lower Lotsberg ranges in thickness from 0 to about 60 m and overlies the Basal Red Beds. This salt was cored in the Imperial Grosmont No. 1 (13-17-67-23W4) well where it is composed of clear, commonly reddish-tinted, coarse crystalline halite, with variable amounts of red shale between the crystals and, rarely, as discontinuous interbeds (Meijer Drees, 1986).

Upper Lotsberg Member:

The Upper Lotsberg, which in places is up to 150 m thick, was completely cored in the Anglo Home C & E Elk Point No. 2 (3-14-57-6W4) well, where it is described as predominantly clear, often colorless, pink or amber, coarse crystalline halite. Red shale occurs between salt crystals and as thin interbeds (Meijer Drees, 1986). The Upper Lotsberg is overlain by the Ernestina Lake Formation.

Middle Shale Unit:

The Lower and Upper Lotsberg salts, where both are present, are separated by an unnamed red shale. Where the lower salt is absent, this shale grades into the Basal Red Beds unit.

Distribution of the Lotsberg Salts:

The general distribution of the Lower and Upper Lotsberg salts is depicted, in Figures VII:2:2-VII:2:3, respectively. These salts are confined to the basinal area bounded by the Meadow Lake Escarpment, the West Alberta Ridge and an

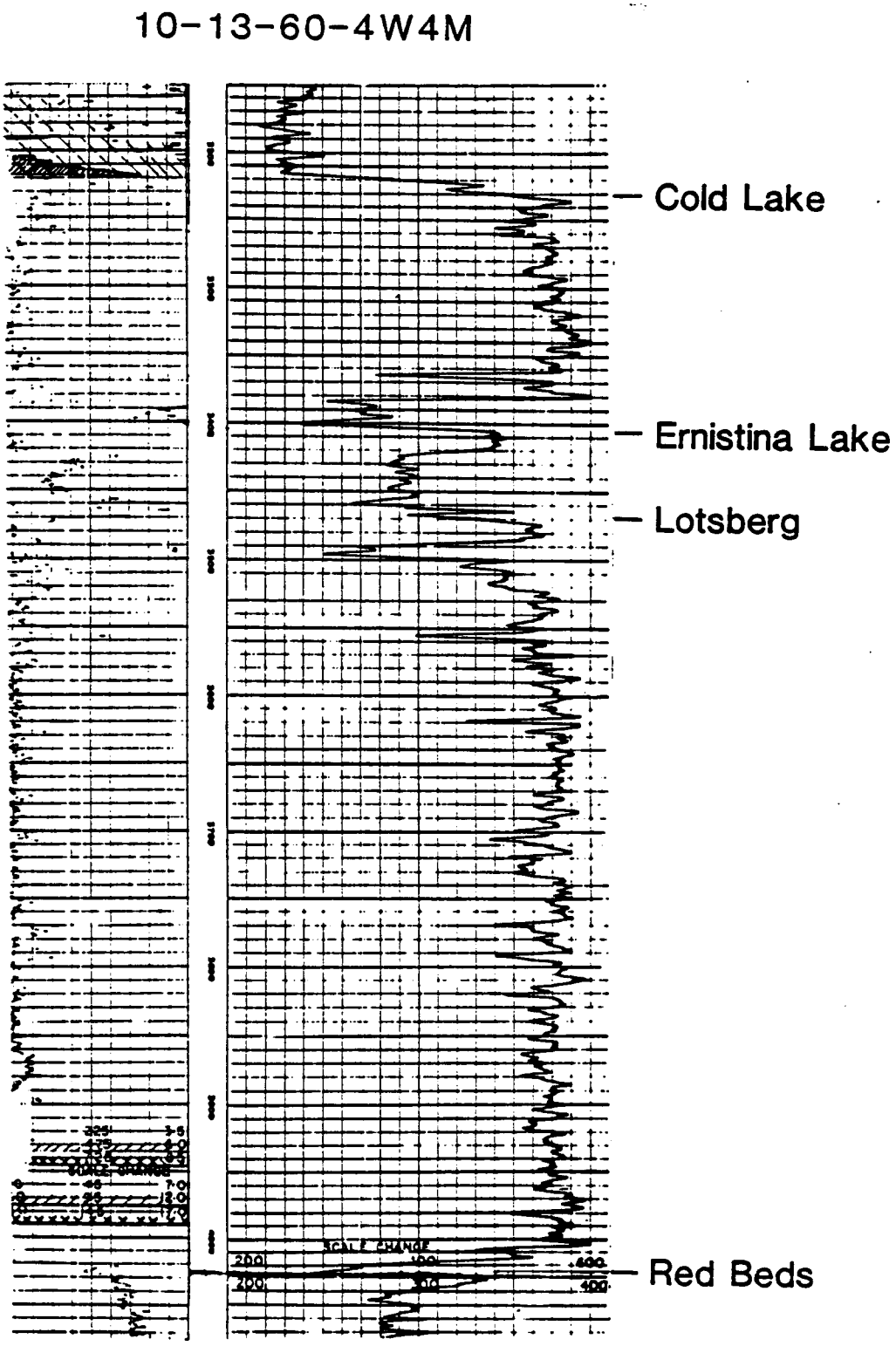

Figure VII:2:1: Gamma-ray and neutron logs of the type section for both the Lotsberg and Cold Lake Formation, (10-13-60-4W4 well).

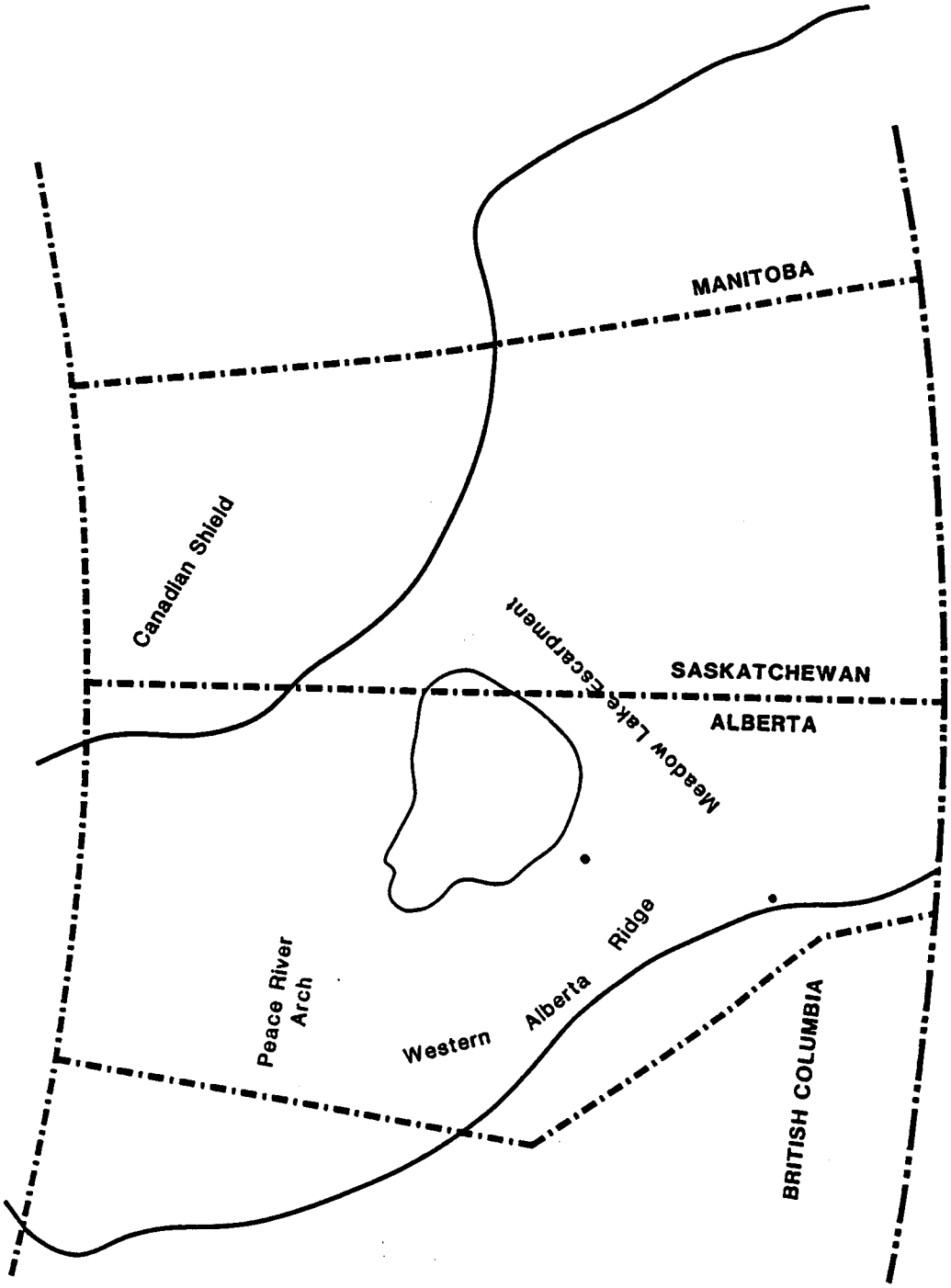

Figure VII:2:2: Map showing the (closed) areal extent of the Lower Lotsberg salt (modified after Meijer Drees, 1986).

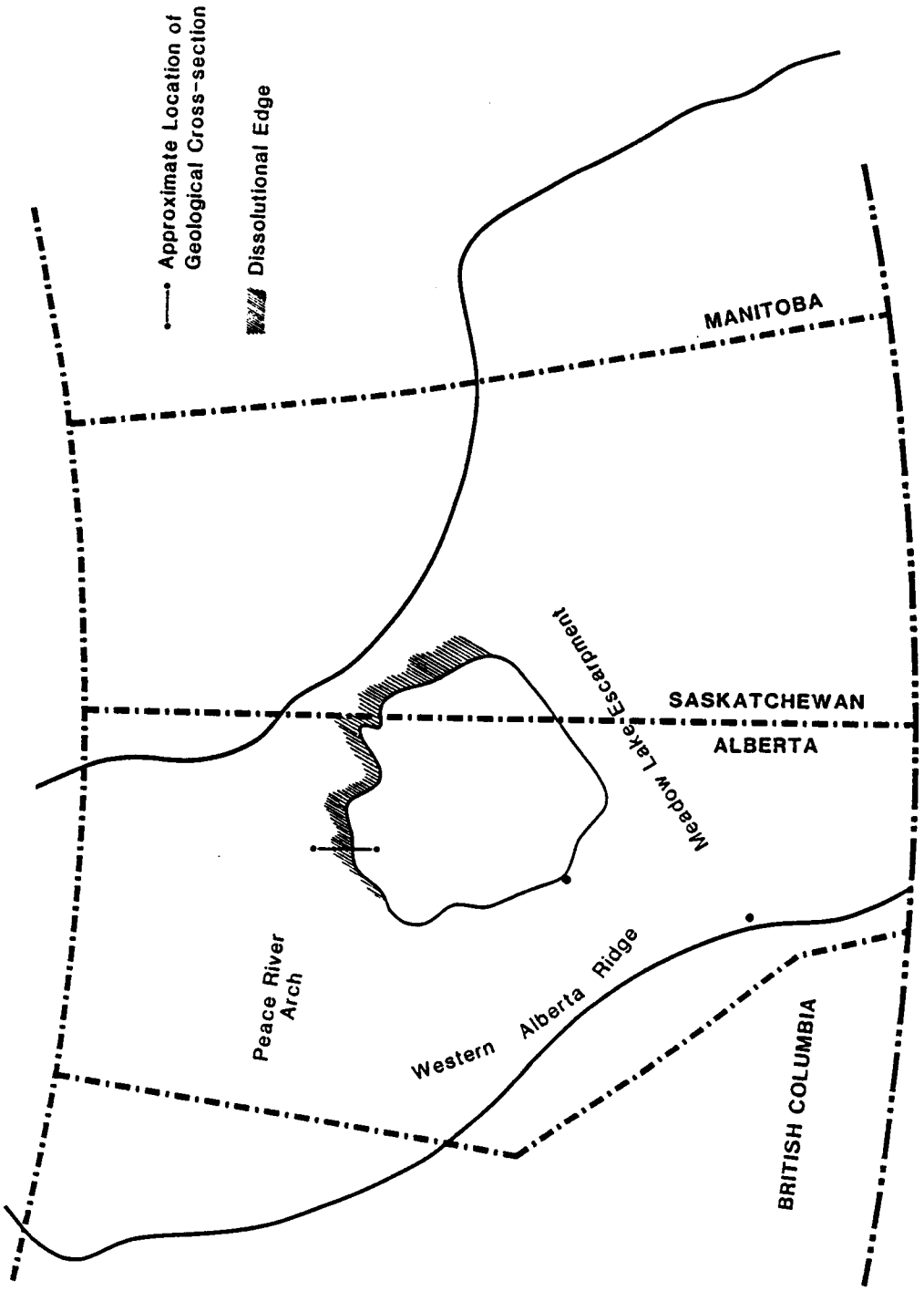

Figure VII:2:3: Map showing the (closed) areal extent of the Upper Lotsberg salt (modified after Meijer Drees, 1986).

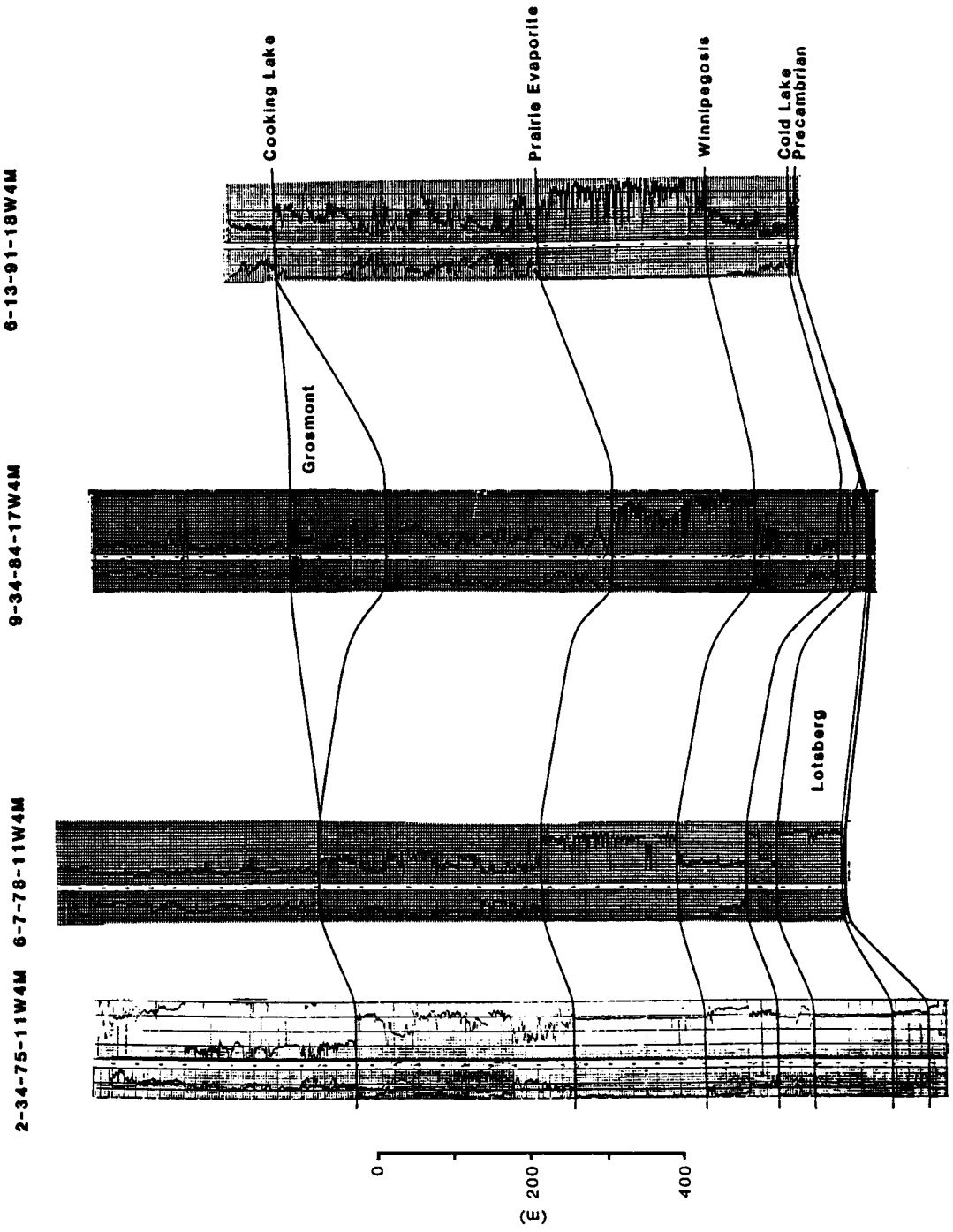

Figure VII:2:4: Geologic cross-section illustrating the northern dissolutional edge of the Upper Lotsberg salt.

eastern extension of the Peace River Arch. As shown in Figure VII:2:2, the edge of the Lower Lotsberg salt is interpreted as depositional. In contrast, as shown in Figure VII:2:3, the northern and eastern edges of the Upper Lotsberg salts are principally dissolutional. The 6-7 well, as shown on the geologic cross-section of Figure VII:2:4, encountered about 85 m of the Upper Lotsberg salt. These salts are not present in the 6-36 well, presumably as a result of dissolution. This geologic cross-section suggests that the edge of the salt is relatively abrupt and that dissolution occurred in the vicinity of the 6-36 well principally during pre-Cretaceous time. In places, dissolution has probably occurred more or less continuously from the time of deposition. On the geologic cross-section, the Cooking Lake Formation is shown to be preferentially preserved in a salt-dissolution low.

B) COLD LAKE FORMATION SALT

Geological Overview:

The type section for the Cold Lake Formation (Sherwin, 1962) is located between the depths of 981 m and 1037 m (3220 ft and 3403 ft) in the Canadian Seaboard Ernestina Lake (10-13-60-4W4) well. The unit consists of 6 m of red, calcareous basal shale and 50 m of overlying salt (Figures VII:1:1, VII:1:2 and VII:2:1). The Cold Lake is underlain and overlain by the Ernestina Lake and Contact Rapids Formations, respectively.

According to Meijer Drees (1986), the lithology of the Cold Lake Formation does not show much variation. The basal red shale is almost always present, being absent only in the Horn Plateau area (Northwest Territories) where the salt member overlies greyish bedded anhydrites or brown dolostone. The salt member is described from core as a reddish brown, semitranslucent, coarsely crystalline halite containing varying amounts of red-brown shale and interbeds of red-brown dolomitic shale. Where the salt-member is absent, the lower shale is mapped as part of the Contact Rapids Formation.

Distribution of the Cold Lake Salt:

Figure VII:2:5 is a generalized Cold Lake salt distribution map. As indicated, the salt is present as two bodies separated by an eastern extension of the Peace River Arch. The southern body attains a maximum thickness of approximately 50 m, the northern body about 75 m. The eastern edges of these salts are principally dissolutional; the southern, western and northern edges primarily depositional.

The geologic cross-section of Figure VII:2:6 illustrates the dissolutional character of the eastern edge of the southern body of salt. The 10-2 well encountered about 35 m of Cold Lake salt which is not present at either the 8-11 or 12-34 locations, presumably as a result of dissolution as opposed to

nondeposition. The geologic cross-section suggests that dissolution occurred principally during the Cretaceous.

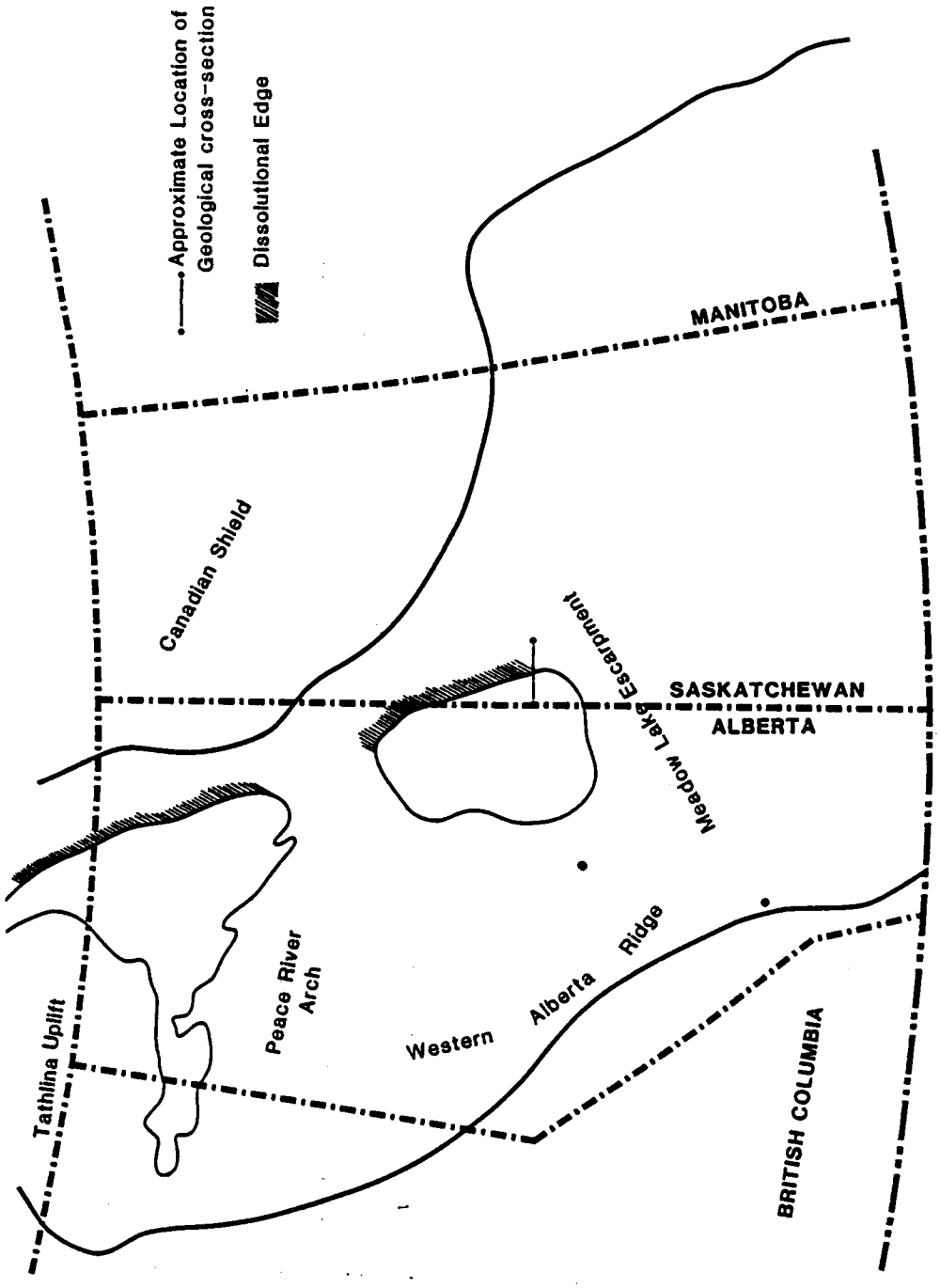

Figure VII:2:5. Map showing the areal extent (two bodies) of the Cold Lake salt (modified after Meijer Drees, 1986).

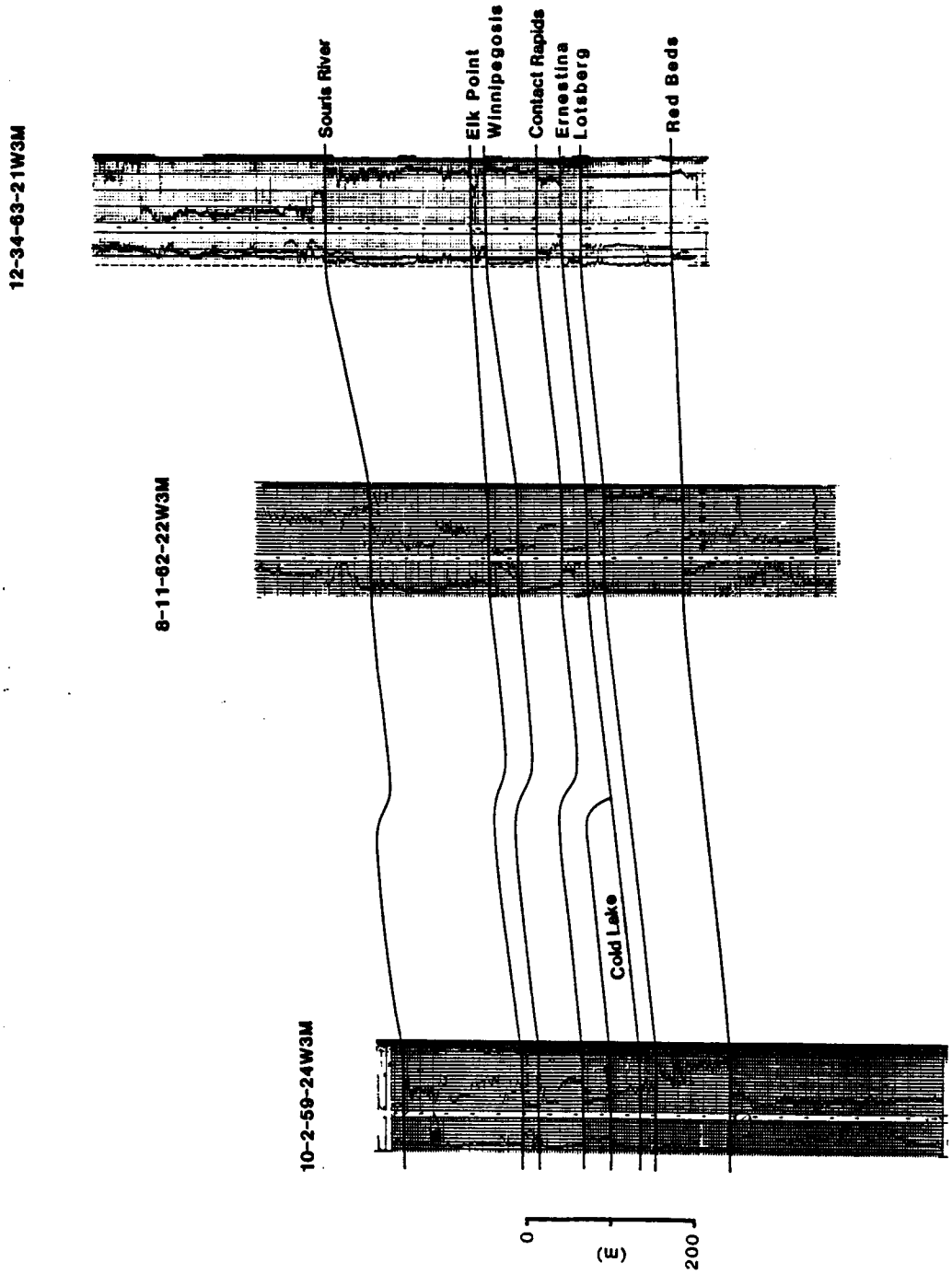

Figure VII:2:6 Geologic cross-section illustrating the eastern dissolutional edge of the southern body of the Cold Lake salt.

C) SALTS OF THE PRAIRIE FORMATION AND EQUIVALENTS

Geological Overview:

The type section for the Prairie Formation (Baillie, 1953) is located between the depths of 1326 and 1524 m (4352 and 5000 ft) in the Imperial Davidson No. 1 (16-8-27-1W3) well. Because borehole logs and samples are missing and only two short cores are available, Holter (1969) established a reference section in the White Rose et al. Drake No. 4-29 (4-29-32-22W2) well (Figures VII:1:1, VII:1:2 and VII:2:7) between the depths of 993 and 1187 m (3259 to 3894 ft). In Alberta, the Prairie Evaporite is overlain by the shales of the Watt Mountain Formation and underlain by the carbonates of either the Winnipegosis or Keg River Formation.

The Prairie Formation is an interbedded succession of halite, sylvite, bedded anhydrite and minor anhydritic dolostones which grade westwards into shales, carbonates and anhydrites. It was informally subdivided (Jordan, 1967) into lower (Whitkow) and upper (Leofnard) salt members separated by the Shell Lake member. These members are further described by Jordan (1968) and Reinson and Wardlaw (1972), who formally subdivided the lower Prairie into the Whitkow and Shell Lake Members, and by Meijer Drees (1986).

Whitkow Member:

The Whitkow Member was defined (Reinson and Wardlaw, 1972) in the Tidewater Bryce Lake Crown No. 1 (1-14-25-16W2) well between the depths of 1371 and 1459 m (4497 to 4786 ft). It consists of halite with interbeds of anhydrite and includes a basal dolomitic anhydrite (Figure VII:2:7). The Whitkow is locally present in Saskatchewan and east-central Alberta where it forms the base of the Prairie Formation. It overlies the Ratner Member of the Winnipegosis Formation and underlies the Shell Lake Member of the Prairie Evaporite.

Shell Lake Member:

The Shell Lake Member was defined (Reinson and Wardlaw, 1972) in the White Rose et al. Drake No. 4-29 (4-29-32-22W2) well from 1106 to 1141 m depth (3629 to 3744 ft). It includes three dolomitic beds and, in those area where the Whitkow Member is absent, forms the base of the Prairie Formation. The Shell Lake Member is overlain by the Leofnard Member (Figure VII:2:7).

Leofnard Member:

The Leofnard Member (Jordan, 1967, 1968) as described by Meijer Drees (1986) consists of an interbedded succession of salt, anhydrite, and minor dolostone

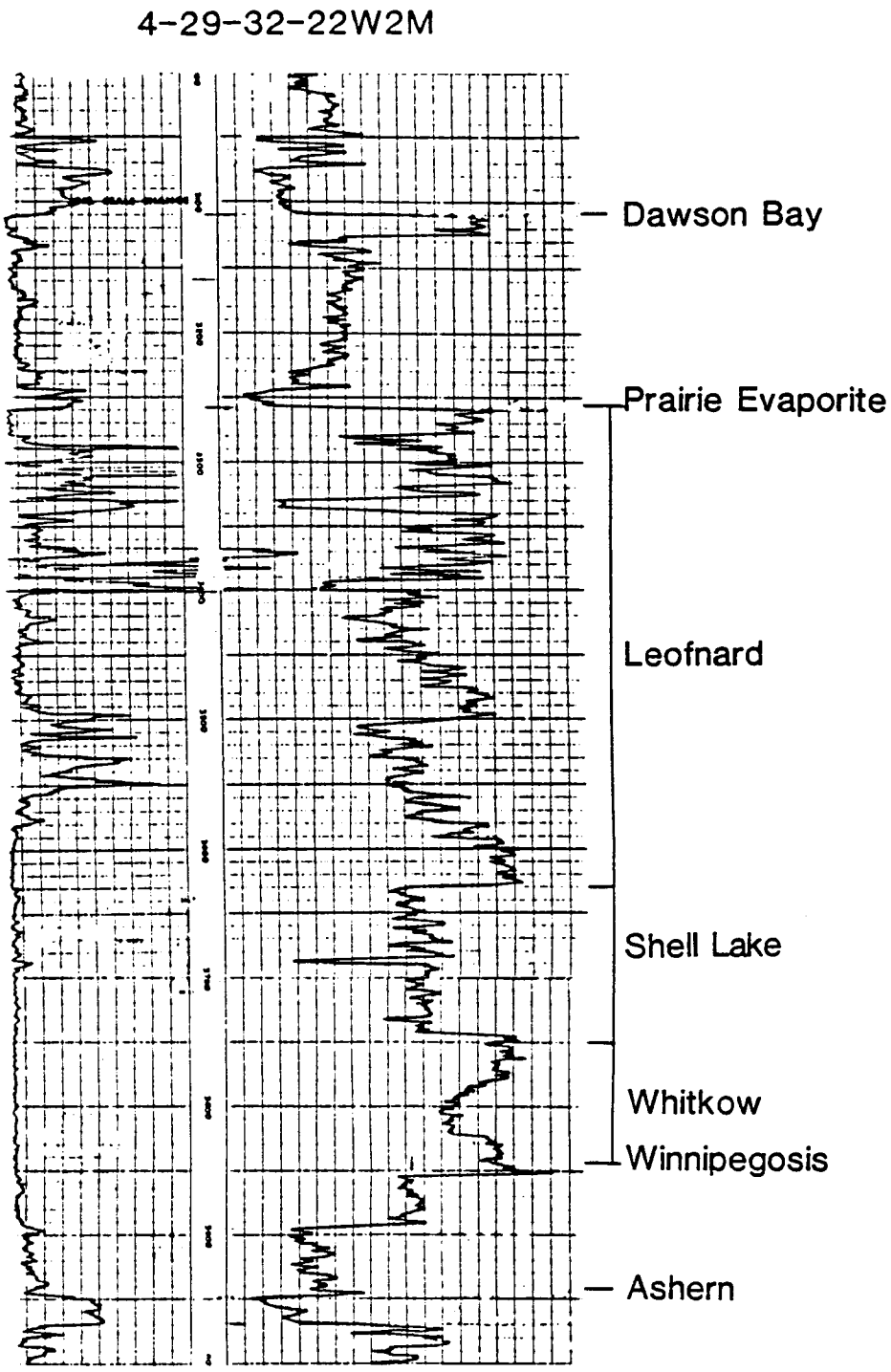

Figure VII:2:7. Gamma-ray and neutron logs of the reference section for the Prairie Formation (4-29-32-22W2 well).

and shale in the Prairie Formation, situated between the Shell Lake Member below and the Dawson Bay Formation above (Figure VII:2:7). The interval between depths of 1054 m and 1187 m (3457 and 3895 ft) in the Verbata No. 2 (7-24-41-24W3) well is designated by Meijer Drees (1986) as the type section.

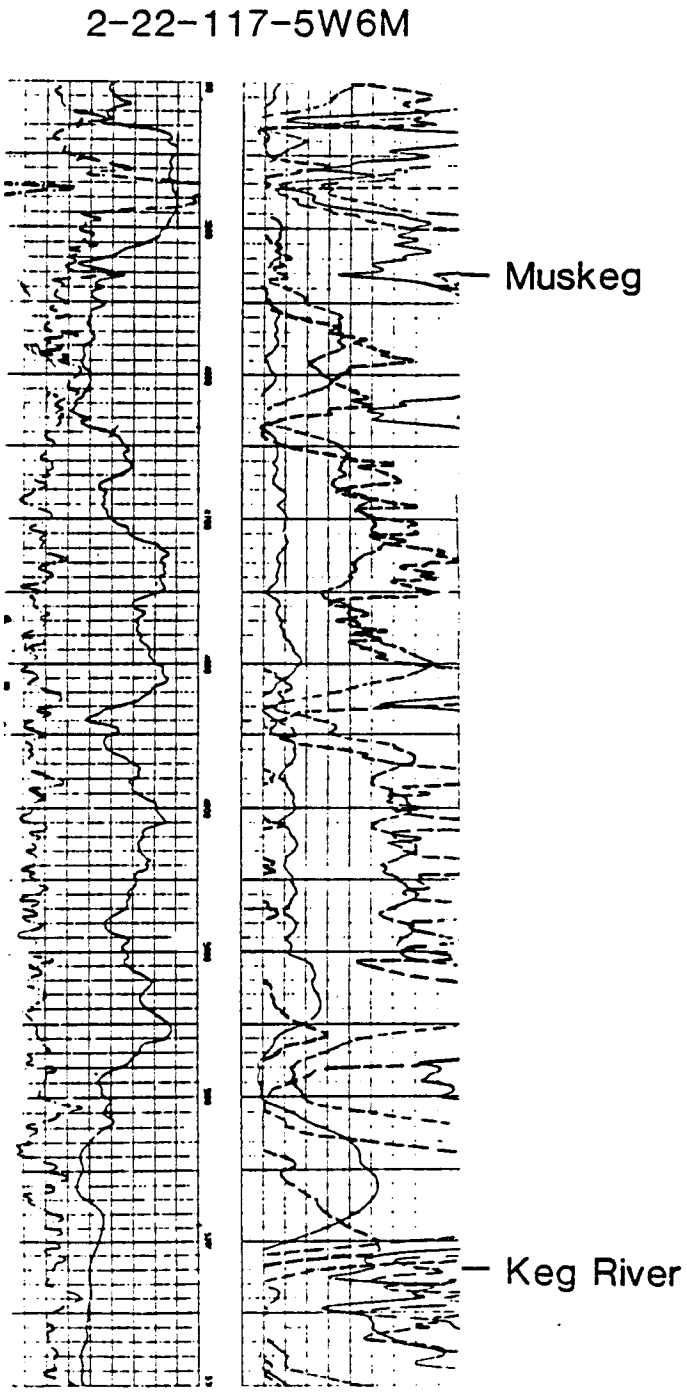

Figure VII:2:8. SP and resistivity logs of the type section for the Muskeg Formation (2-22-117-5W6 well).

Muskeg Formation:

The anhydritic equivalents of the Prairie and Dawson Bay Formations in northern and central Alberta are known as the Muskeg Formation. This unit

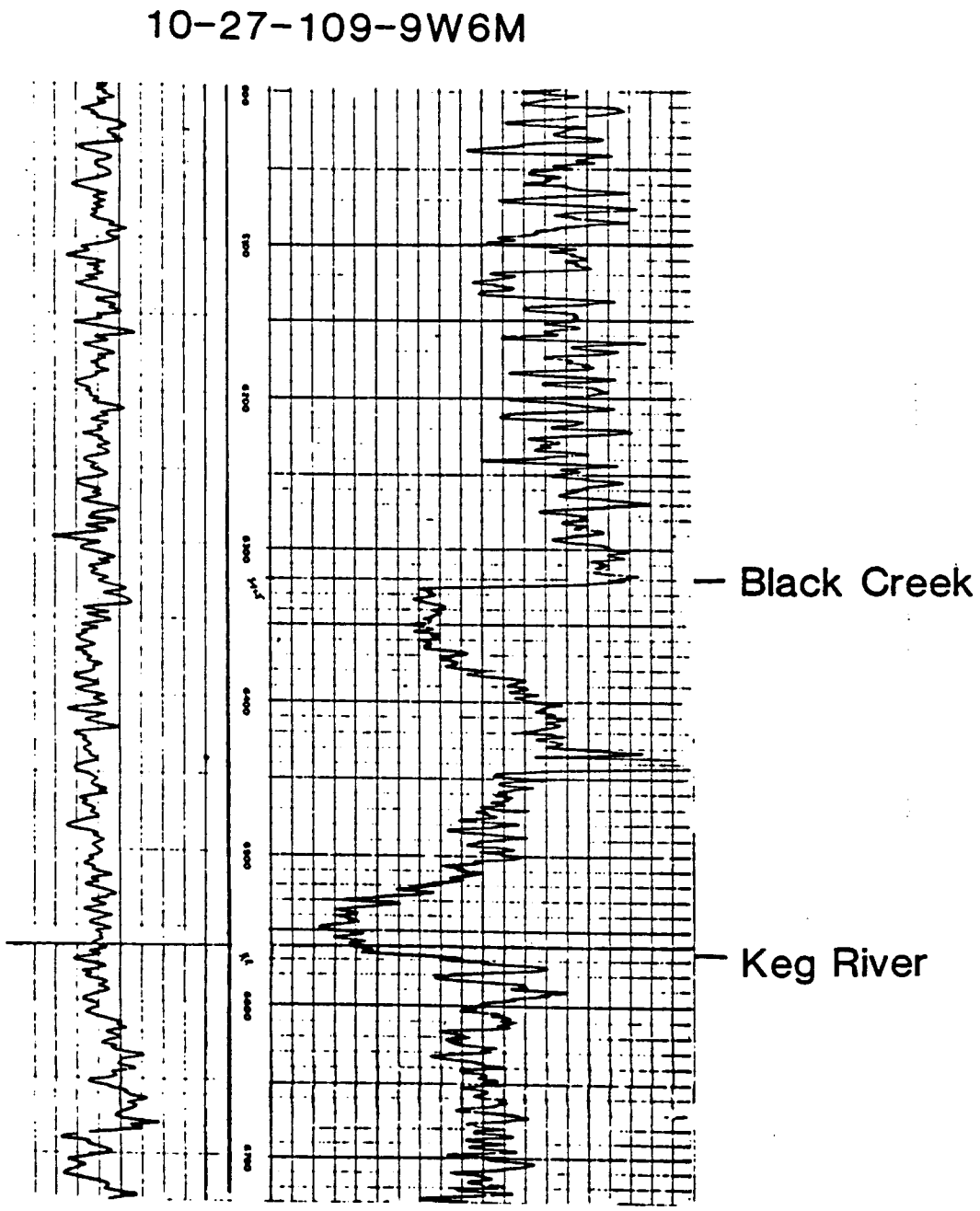

Figure VII:2:9. Gamma-ray and neutron logs from the 10-27-109-9W6 well for the Black Creek Member.

is bounded by the underlying Keg River and overlying Watt Mountain formations and described as a light-colored succession of interbedded white and grey salt, brown anhydrite, brownish grey dolostone and limestone (Meijer Drees, 1986). The type section (Law, 1955) for the Muskeg is the interval between depths of 1376 and 1588 m (4513 and 5210 ft) in the California Standard Steen River (2-22-117-5W6) well (Figure VII:2:8). The Muskeg grades to the south into the interbedded salt and anhydrite facies of the Prairie Evaporite.

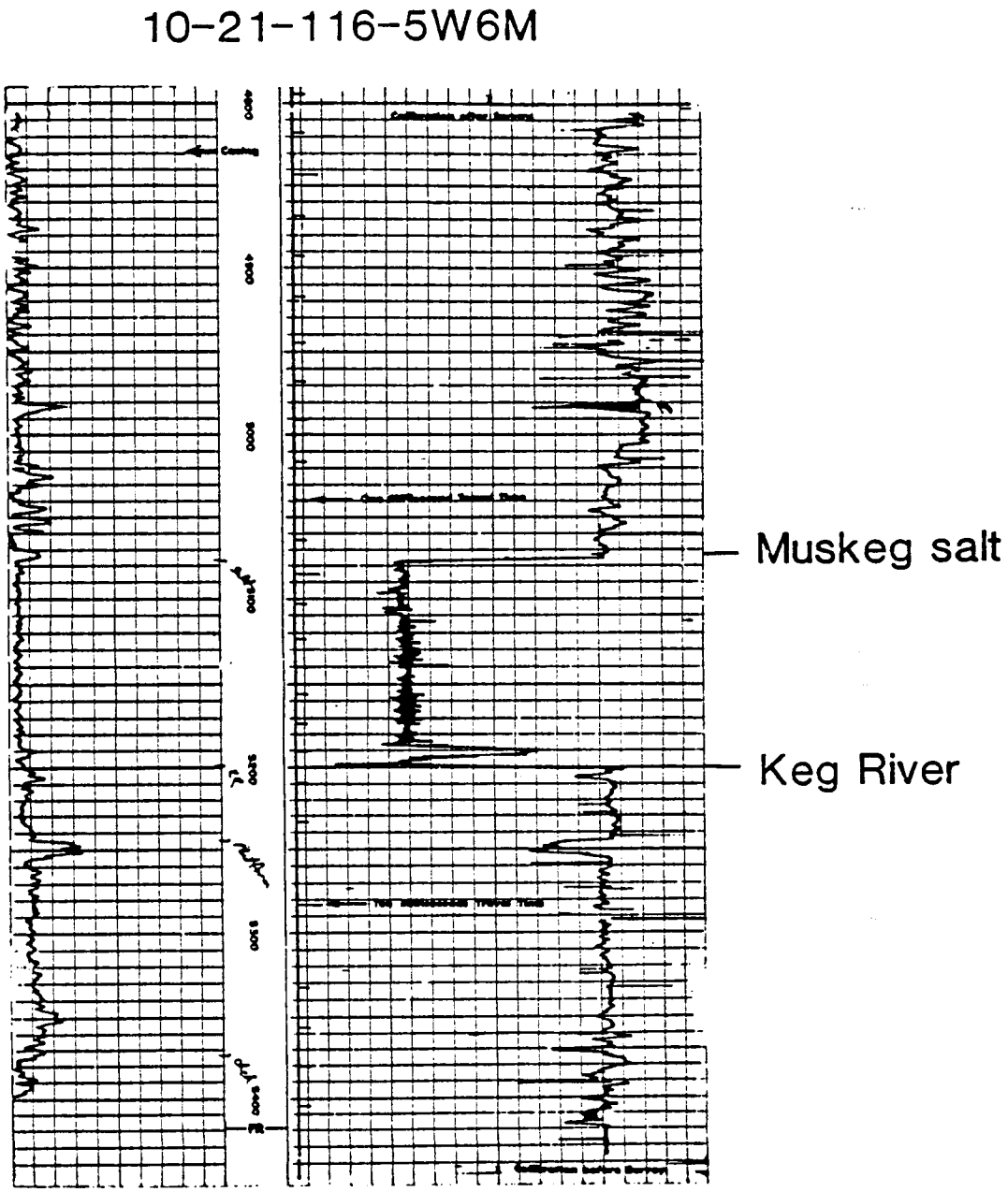

Figure VII:2:10. Gamma-ray and sonic logs; 10-21-116-5W6 well, Zama area.

Isolated Muskeg salt remnants are present in three areas in northern Alberta: Rainbow Lake, Zama Lake and Hay River. The salt at Rainbow Lake, the Black Creek Member, attains maximum thicknesses of about 75 m and is described from the 10-27-109-9W6 well as light-grey, semitranslucent, coarsely crystalline and containing thin stringers of anhydrite (Figure VII:2:9). The salt bed at Zama Lake (Figure VII:2:10) is present in only one well (10-21-116-5W6) where it is 38 m thick. The salt bed at Hay River, cored in the 5-18-113-22W5 well (Figure VII:2:11), is described as a clear and very coarsely crystalline halite with interbeds of anhydrite. Detailed regional correlations suggest that these three bodies are different salt deposits (Meijer Drees, 1986).

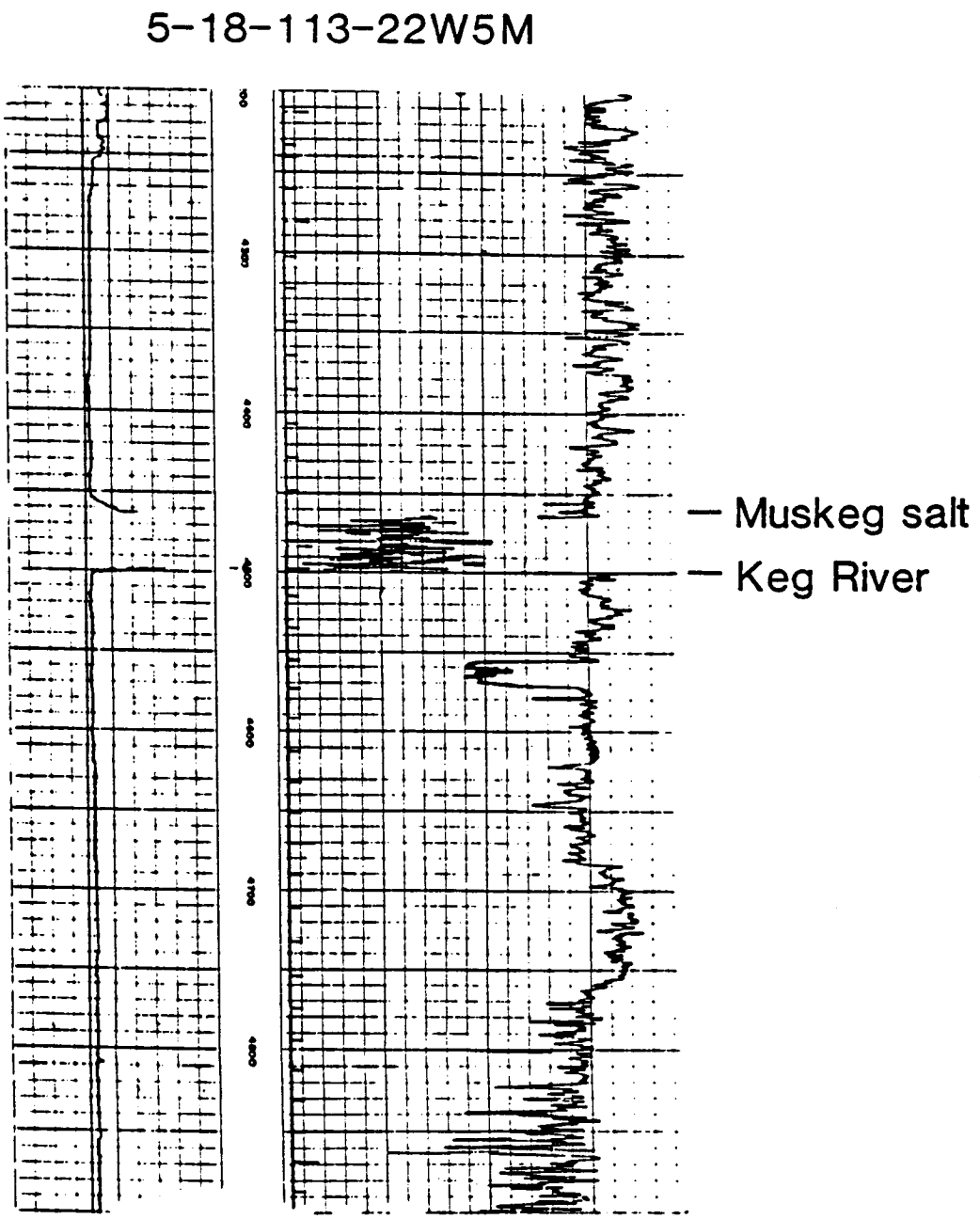

Figure VII:2:11. Gamma-ray and sonic logs; 5-18-113-22W5, Hay River area.

Salt distribution - Prairie and Muskeg Formations:

Figure VII:2:12 shows the generalized distribution of the Prairie and Muskeg salts as trending north-northwest through eastern and northern Alberta. The

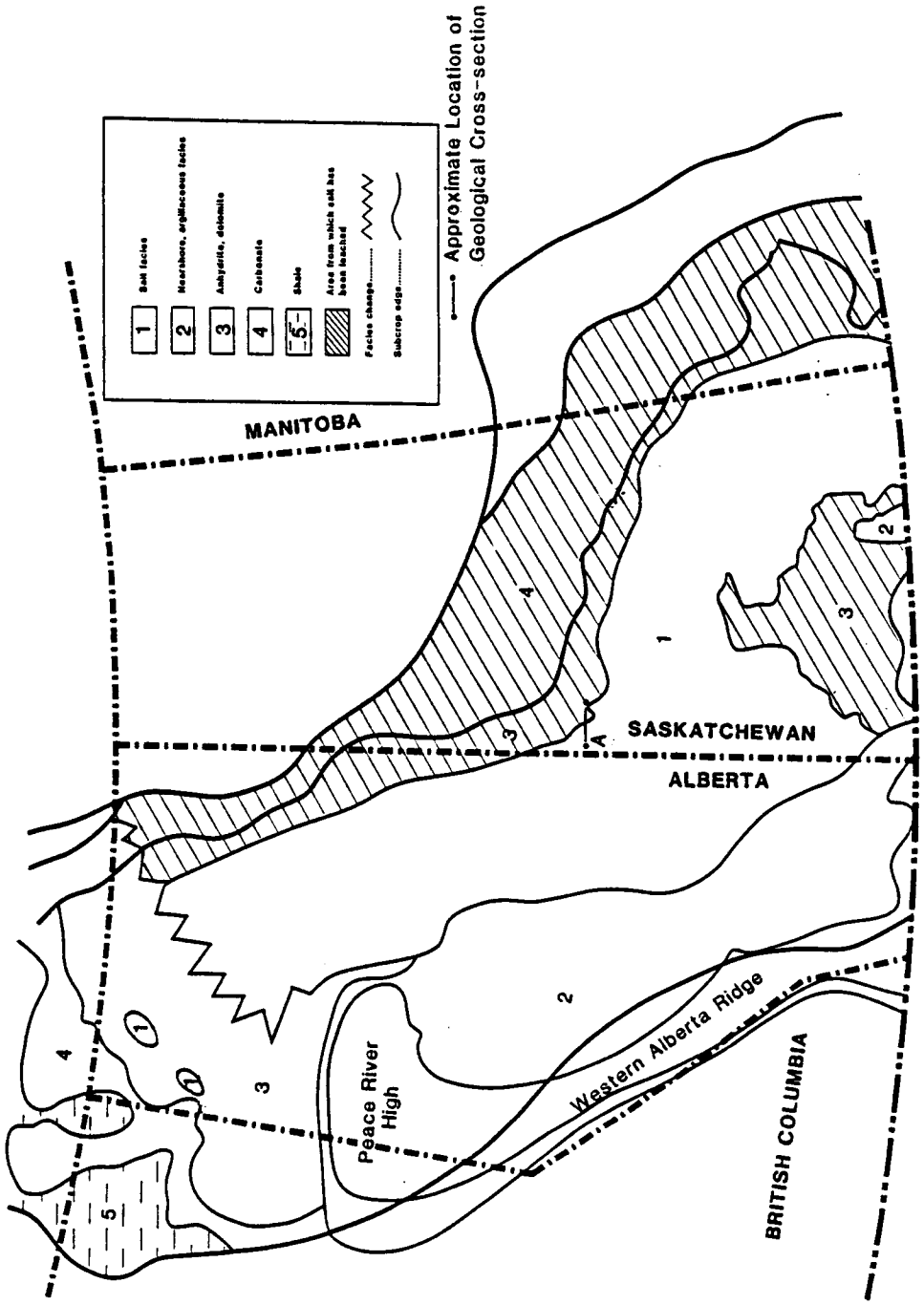

Figure VII:2:12. Facies distribution and paleogeography of the lower part of the Upper Elk Point and equivalents (after Meijer Drees, 1986).

salt thickness reaches in excess of 140 m near the Alberta-Saskatchewan border. Of principal interest to the explorationist is the question of where the salt edges are depositional and where they are dissolutional. As shown in Figure VII:2:12, the southern and eastern edges are primarily dissolutional, while the northern and western edges are principally depositional, although exceptions to these generalizations do occur. The suite of cross-sections of Figures VII:2:13-VII:2:16 shows that dissolution occurs along the western and eastern edge of the remnant rock salt, within the basin interior and within the Black Creek sub-basin. And Alcock and Benteau (1976) present evidence that dissolution of the Prairie salt has also occurred in the Nipisi area, which is located along the western margin of the main Elk Point basin and the eastern flank of the Peace River High.

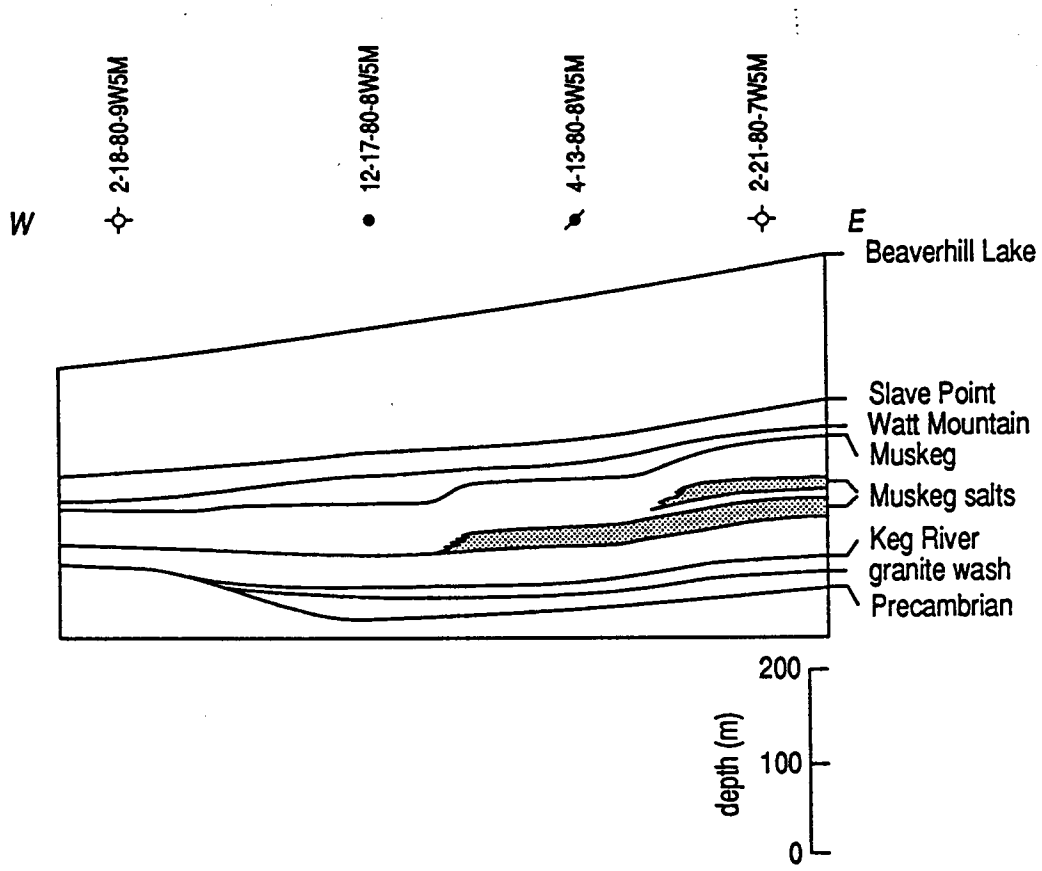

Figure VII:2:13. Geologic cross-section illustrating dissolution of the Muskeg salts in the Nipisi area.

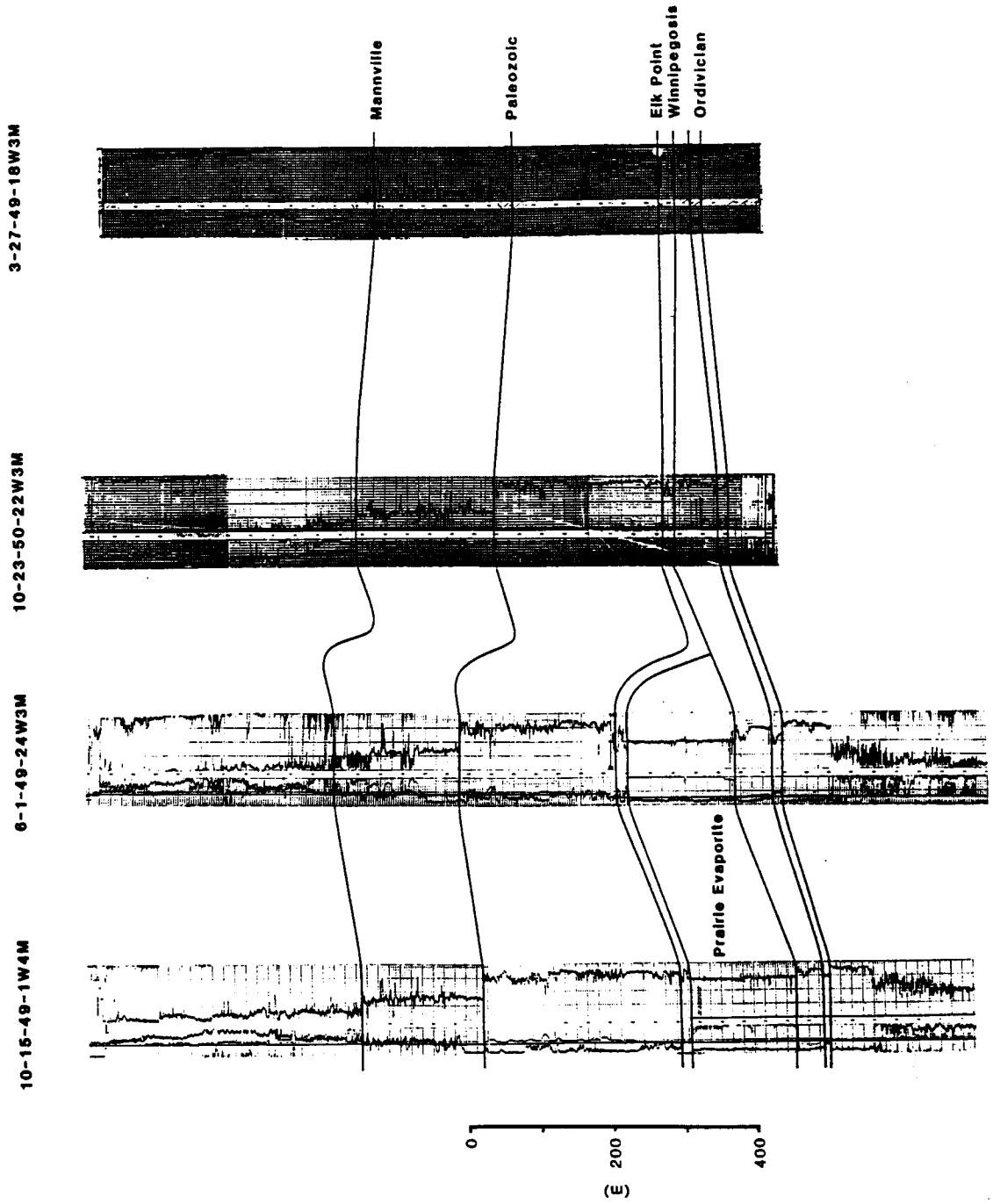

Figure VII:2:14. Geologic cross-section illustrating the eastern dissolutional edge of the Prairie Formation salt.

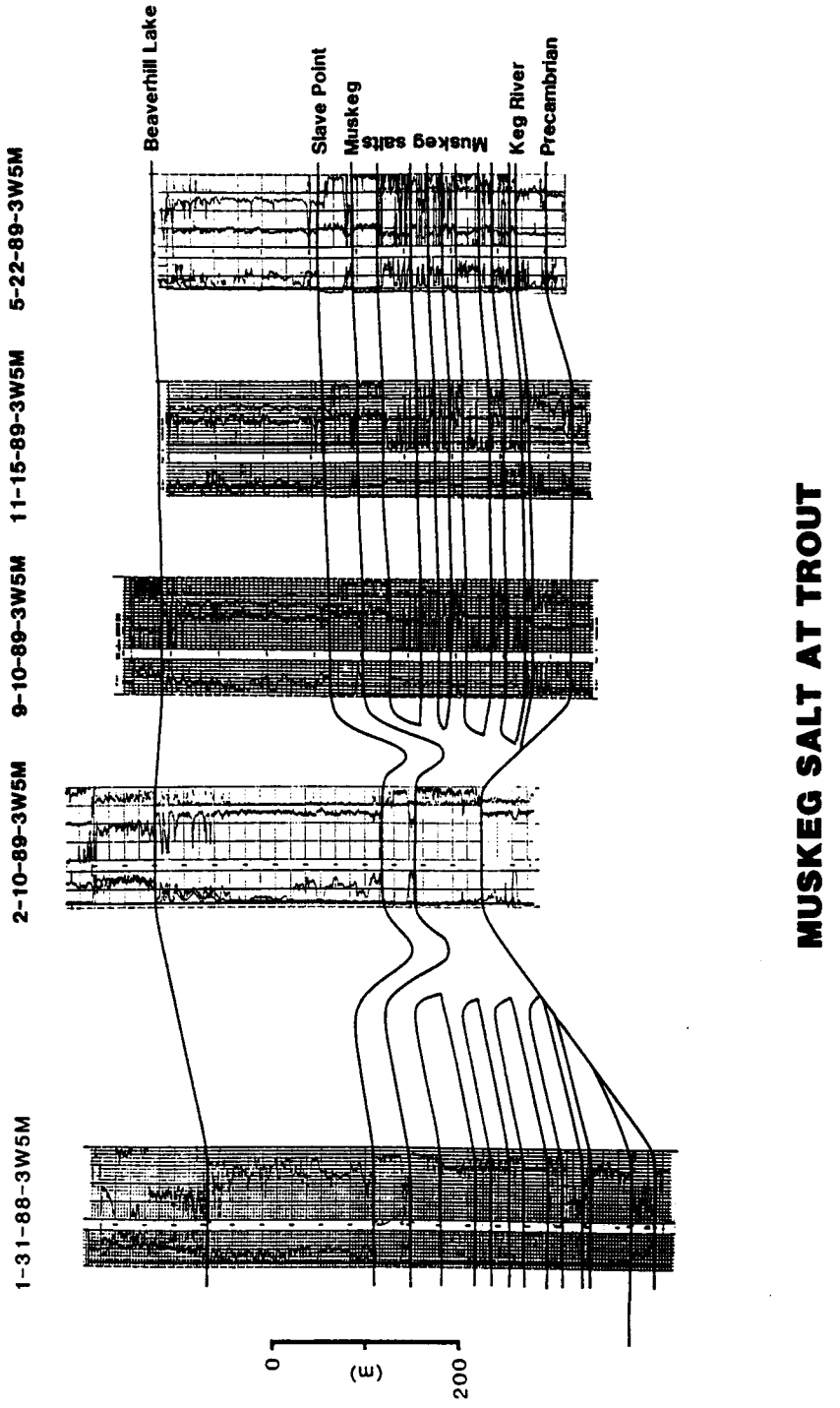

Figure VII:2:15. Geologic cross-section illustrating dissolution of the Muskeg salts in the Trout area.

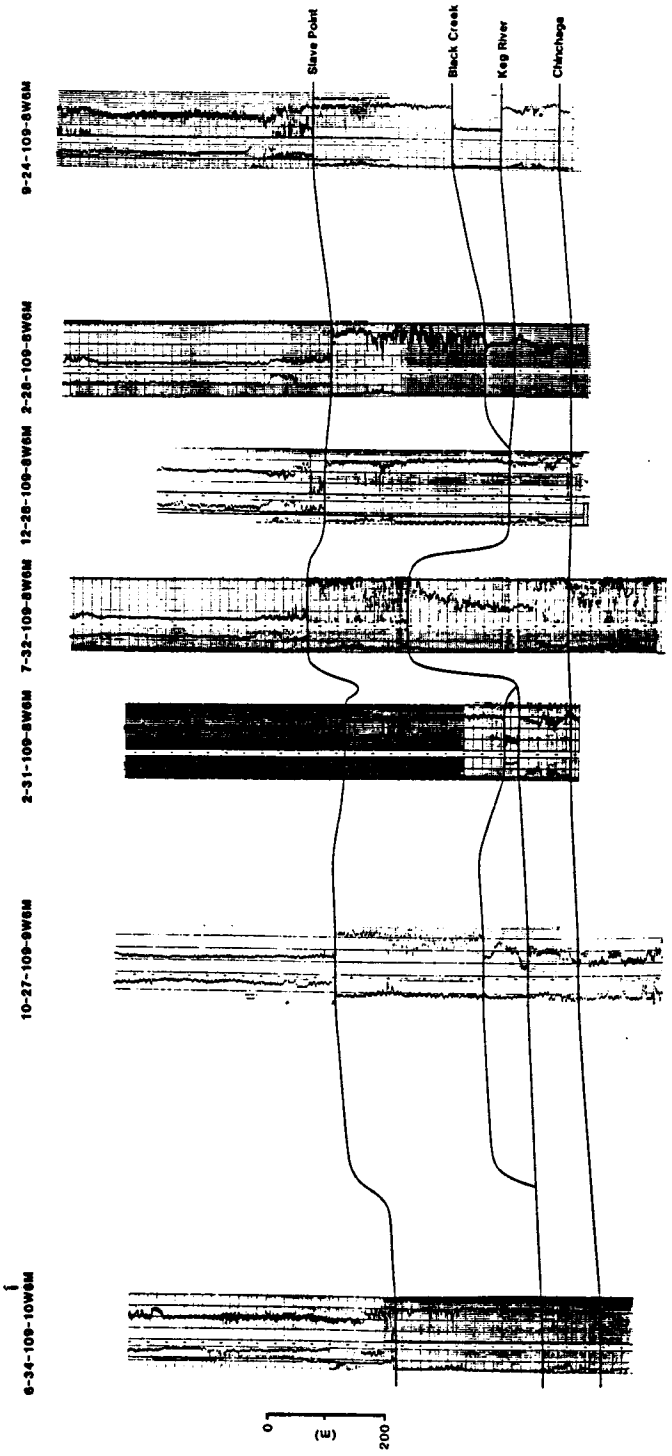

Figure VII:2:16. Geologic cross-section illustrating dissolution of the Black Creek salt in the Rainbow area.

D) CAIRN FORMATION SALT

Geological Overview:

The type section for the Cairn Formation (Figures VII:1:1, VII:1:2 and VII:2:17) as designated by McLaren (1955) is on the northern spur of Mount Dalhousie immediately south of the junction of the Southesk and Cairn rivers, about 35

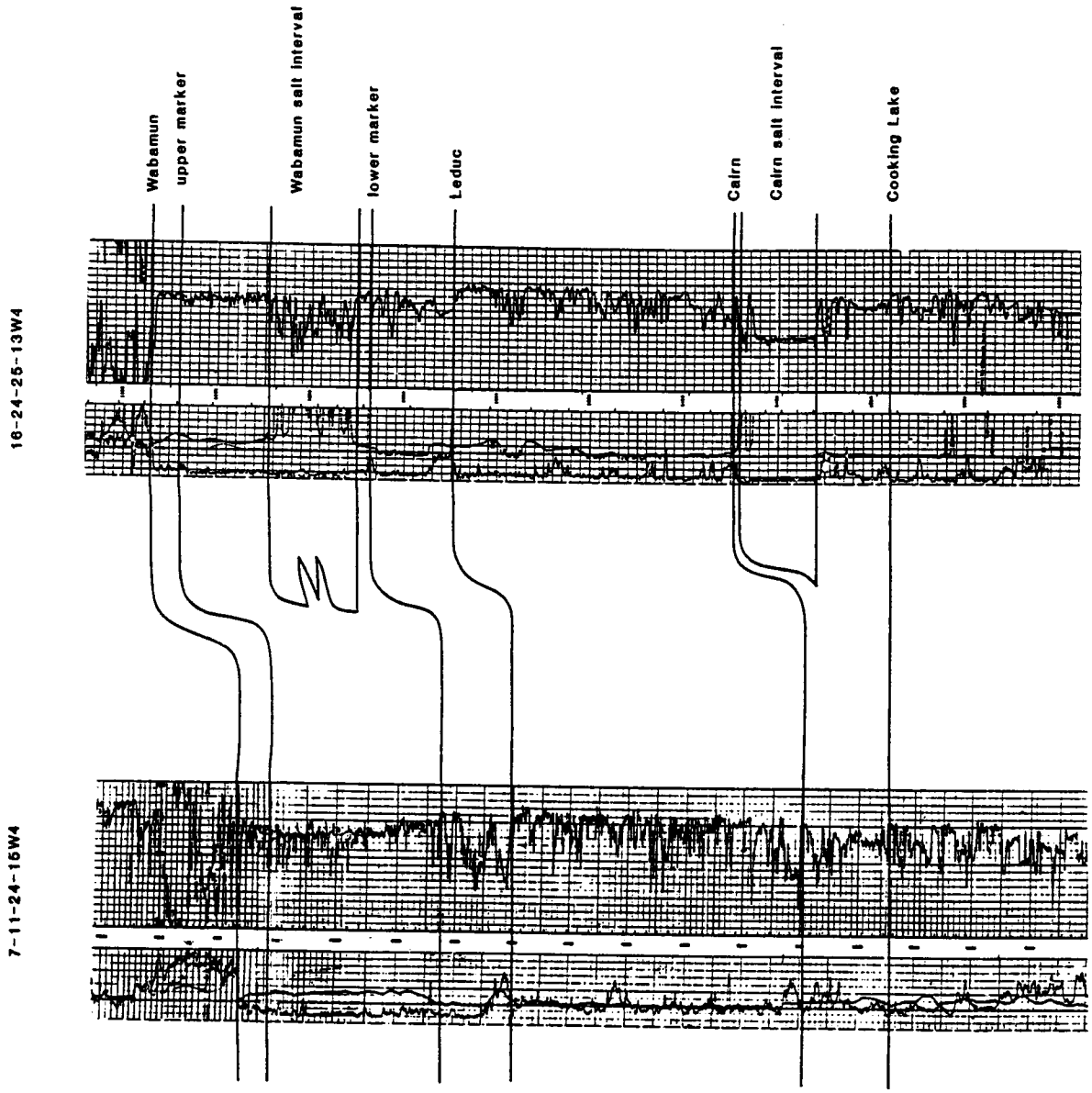

Figure VII:2:17. Gamma-ray and sonic logs from the 7-11-24-15W4 and 16-24-25-13W4 wells.

km southeast of the village of Mountain Park, Alberta. The well-log signature of the Cairn Formation is illustrated in Figure VII:2:17. In the 16-24-25-13W4 well, a thick remnant of salt was penetrated, while in the 7-11-24-15W4 well this salt has been postdepositionally dissolved.

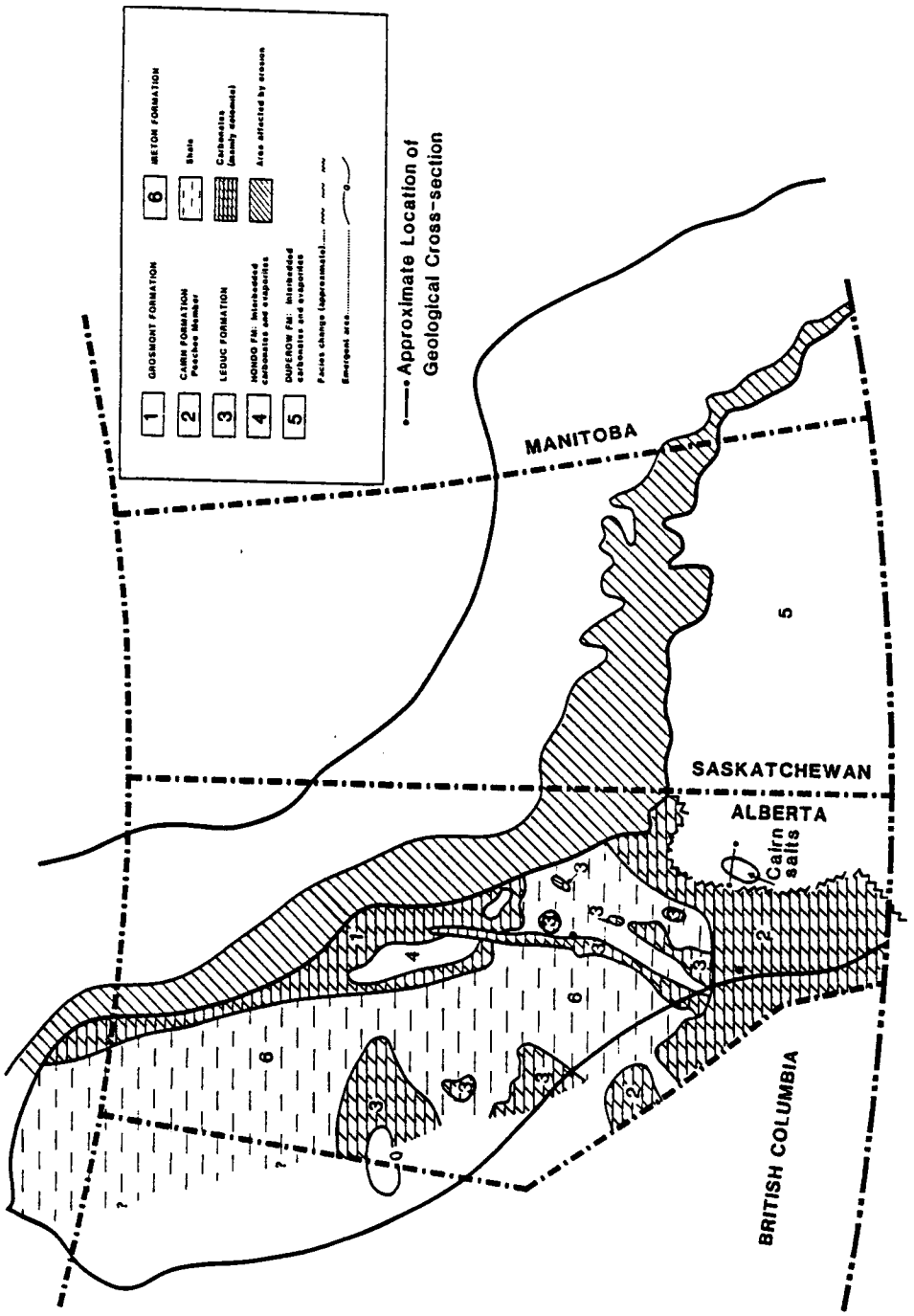

Figure VII:2:18: Distribution of the Grosmont Formation and equivalents, western Interior Plains (modified after Meijer Drees, 1986).

McLaren (1955) described the lower Cairn as dark-grey fine- to medium-grained dolomite with nodules, bands and stringers of chert, and the upper Cairn as grey to brown medium-grained dolomite, medium- and thick-bedded to massive and slightly argillaceous, with very abundant traces of organic remains. In southern Alberta, these carbonates locally encompass thick salt remnants.

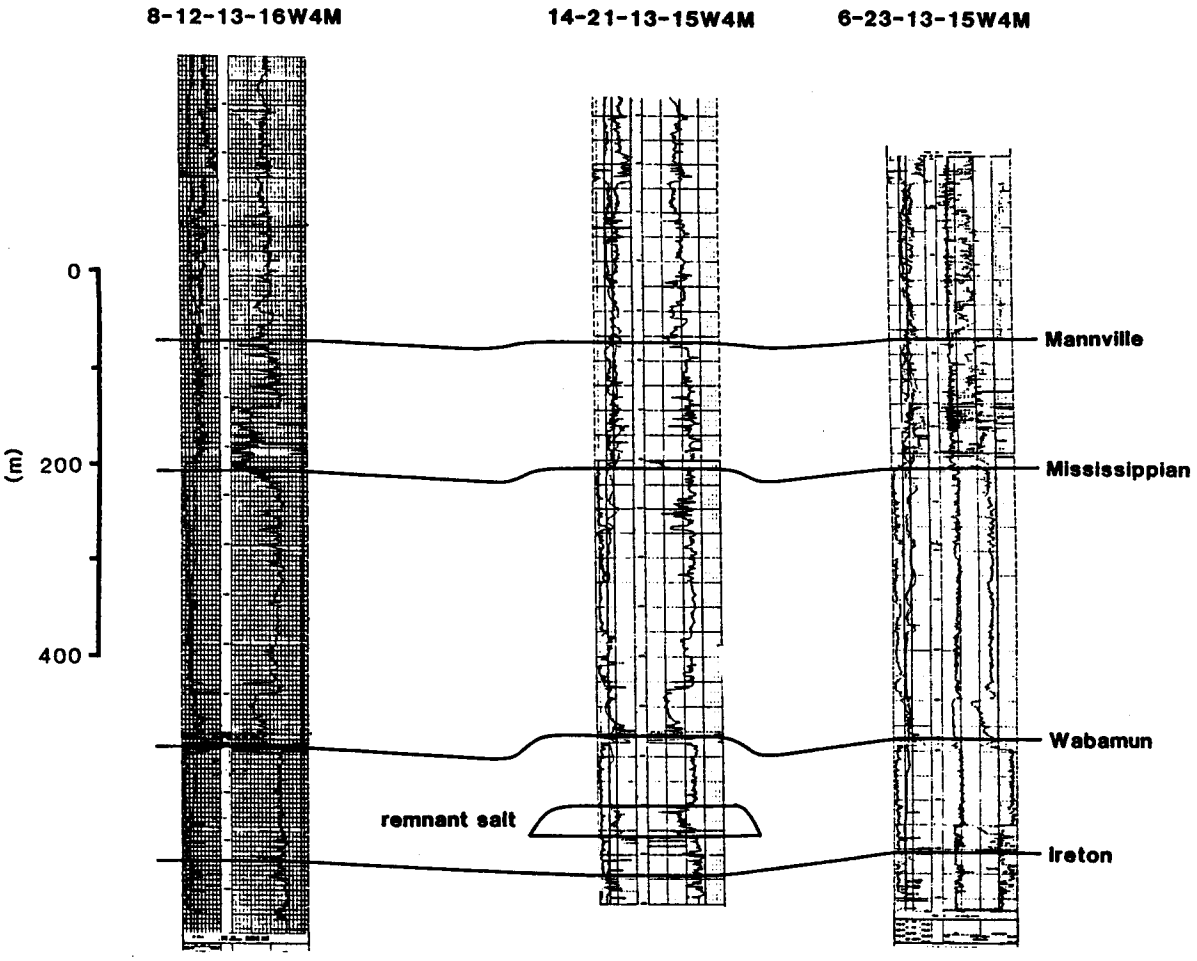

Figure VII:2:19: Dissolutional edges of the Cairn salt.

In the vicinity of these residual salt bodies, the Cairn Formation rests on the Beaverhill Lake Group and is overlain by the Southesk Formation (Figures VII:1:1 and VII:1:2). The lower Cairn is correlative with the Cooking Lake Formation whereas the overlying Peechee Member of the Southesk Formation is correlative with the Leduc Formation. Throughout the Cairn salt basin, the lower part of the Cairn Formation and the Peechee Member are frequently referred to as the Cooking Lake and Leduc Formations, respectively.

Distribution of the Cairn Salt:

A generalized Cairn salt map and a representative cross-section are shown in Figures VII:2:18 and VII:2:19, respectively. The salt, although depicted as a single continuous north-northeast trending body, could consist of two or more bodies. The salt attains a maximum thickness of about 45 m and thins abruptly near its edges. The Cairn Formation (Figure VII:2:19) is thick (typically 80-85 m) where salt remnants are present and generally thinner immediately outside the area of the salt (typically 45-50 m) indicating that the edges are dissolutional as opposed to depositional. Further from the salt edge, the upper Cairn is in some places thick and in others thin. The thins are interpreted as areas of extensive post-Cairn-time dissolution, the thicks either as zones of more or less contemporaneous deposition and dissolution or of nonbasinal (bank) or reefal areas.

E) WABAMUN GROUP SALT

Geological Overview:

The typical section for the Wabamun Group (Imperial Oil Ltd., 1950) is located between the depths of 1748 and 1919 m (5735 and 6297 ft) in the Anglo Canadian Wabamun Lake No. 1 (5-10-51-4W5) well. The well-log signature of the Wabamun in southern Alberta is illustrated by the two logs in Figure VII:2:19. The thick Wabamun salts that are present in the 16-24-25-13W4 well are absent in the 7-11-24-15W4 well, presumably due to postdepositional dissolution.

The Wabamun Group in east-central Alberta consists predominantly of limestone with dolomitic mottling and local accumulations of dolomite in the lower part. To the south, there is a gradual change from limestone first to interbedded limestone and dolomite, then to dolomite and anhydrite with local halite in the Stettler-Drumheller area. Wonfor and Andrichuk (1953) defined the evaporite sequence as the Stettler Formation, with the type section from 1411 to 1588 m (4630 to 5210 ft) in the Canadian Gulf Jerard No. 1 (16-34-37-20W4) well. Andrichuk and Wonfor (1953) named the overlying green shale and fossiliferous limestone as the Big Valley Formation (Figures VII:2:1 and VII:2:2).

The Wabamun Group overlies the Graminia Formation of the Winterburn

Group (Figures VII:1:1 and VII:1:2). Throughout much of the area, the Graminia cannot be mapped as a distinct unit and its equivalents are included in the lower part of the Stettler Formation (Belyea and McLaren, 1957; Belyea, 1966). Where erosion has not removed the overlying Mississippian strata, the Wabamun is overlain by the Exshaw Formation; elsewhere by the Lower Cretaceous.

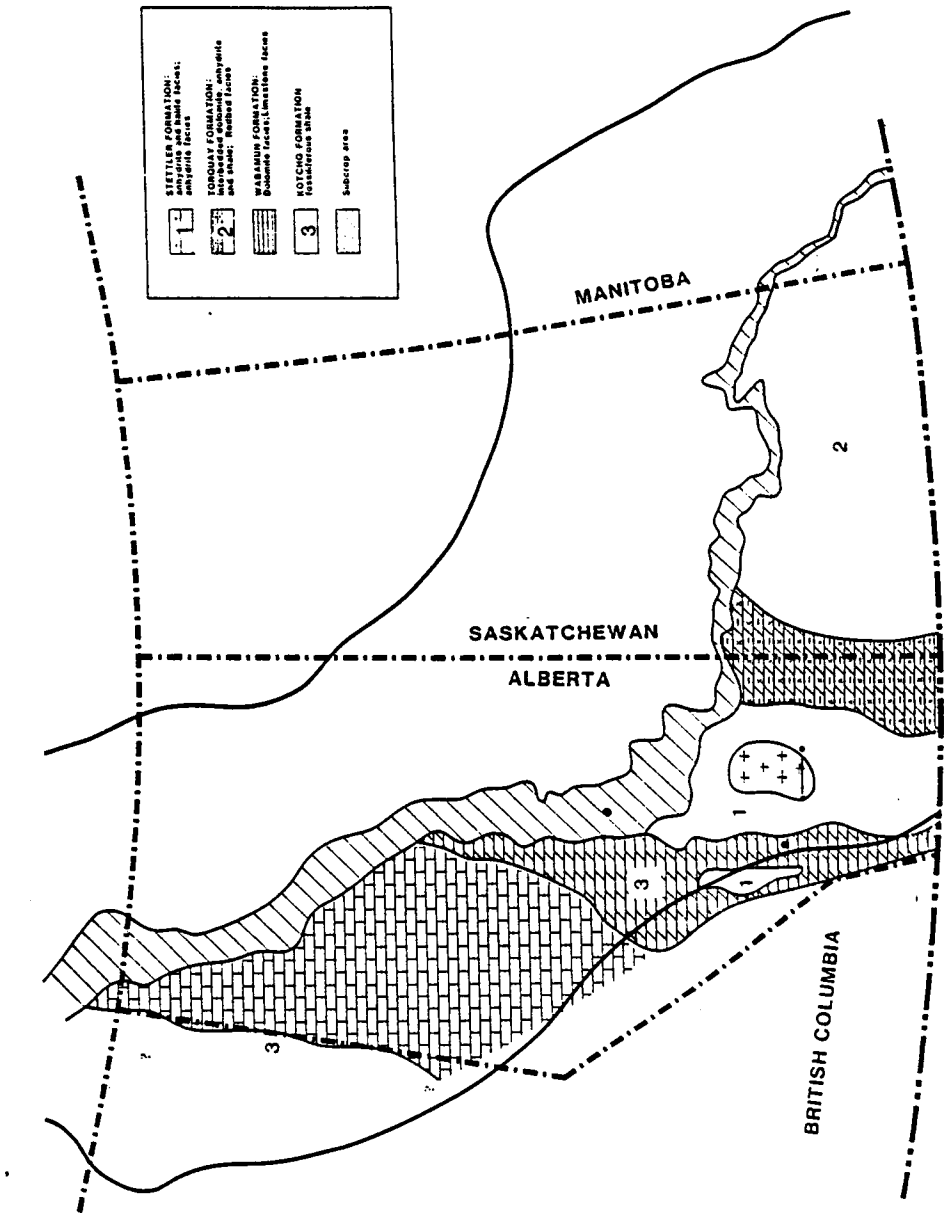

Figure 20: Distribution of the Stettler Formation (Wabamun Group) and its equivalents (modified after Meijer Drees, 1986).

Distribution of the Wabamun (Stettler) Salts:

In Figure VII:2:20, the generalized distribution of the remnants of Stettler Formation salt, commonly referred to as Wabamun salt, is depicted, and in Figure VII:2:21 a representative cross-section is shown. As indicated, these salts, which are about 17 m thick (net) on the cross-section, attain maximum net thicknesses of about 40 m and are much more areally extensive to the north of these wells (Anderson et al., 1988b). The cross-section illustrates that the Wabamun salt has been subjected to extensive postdepositional dissolution.

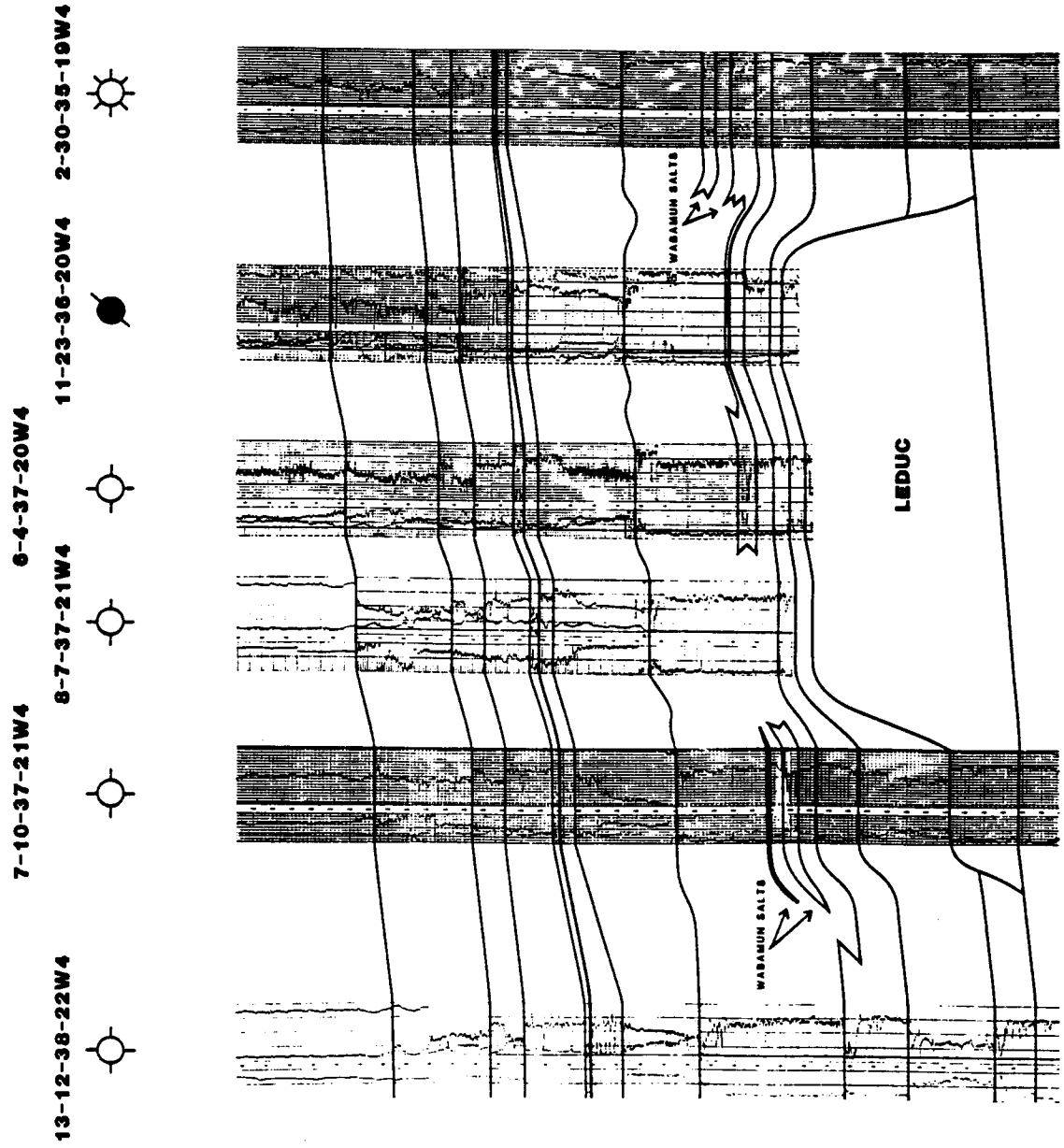

Figure VII:2:21. Geologic cross-section illustrating dissolutional edges of the Wabamun salt.

3) PALEO-RECONSTRUCTION OF SALT DISTRIBUTION

A) Overview (Anderson 1992b; Anderson and Brown, 1992)

The Upper Devonian Wabamun Group in southeastern Alberta is subdivided into the Stettler and Big Valley formations (Figures VII:1:1, VII:1:2, VII:2:19-VII:2:21). The Stettler consists predominantly of interlayered dolomites, anhydrites and isolated to contiguous remnants of halite; the Big Valley is composed of green shales and fossiliferous limestones (Belyea, 1964).

The Wabamun salts are preserved throughout southeastern Alberta, at subsurface depths of between 1000 and 2000 m, as isolated to contiguous bodies of irregular shape having maximum net thicknesses on the order of 40 m. Analysis of collapse features and anomalous variations in the structure of overlying strata associated with these salts suggests that they were widely distributed, uniformly deposited, and extensively leached (Figure VII:3:1).

We have identified correlation patterns involving the thickness of the Wabamun, structural relief at the Wabamun level, relief along post-Wabamun horizons, and the thickness of the salt remnants. On the basis of these relationships, we have mapped the distribution of the Wabamun Group salt in the Stettler area, southeastern Alberta (T30-T41, R10-R25 W4M) and reconstructed the distribution of these salts at selected intervals from late Paleozoic to the present. These maps are significant in that they elucidate the timing, the extent, and to some extent the mechanisms of dissolution.

B) Original distribution of the Wabamun salts

In order to estimate the original distribution of the Wabamun salt in the Stettler study area (original salt thickness (OST) map; Figure VII:3:2), we constructed three maps: 1) net salt (NS), based on sonic/density /caliper log control only (a modified version of this map, PST (present salt thickness), is shown as Figure VII:3:8); 2) present-day Wabamun (PDW) structure (Figure VII:3:9); and 3) restored Wabamun (RW) structure (Figure VII:3:10). (Ideally, the restored Wabamun map was created by replacing all of the dissolved salts). We also studied a proprietary Wabamun isopach map.

On the net salt (NS) map (similar to Figure VII:3:8), the halite remnants attain maximum thicknesses on the order of 40 m, suggesting that the initial thickness of the Wabamun salt was about 40 m. This estimate is supported by the Wabamun isopach map that we examined. More specifically, throughout most of the study area a direct, linear correlation can be made between the thickness of the salt and the thickness of the Wabamun interval, suggesting that about 40 m of salt were uniformly deposited. In the extreme northwestern part of the study area (T34-T41 R20-R25 W4M), progressively less correlation is observed, suggesting that the salts depositionally thin in this direction (OST map: Figure VII:3:2).

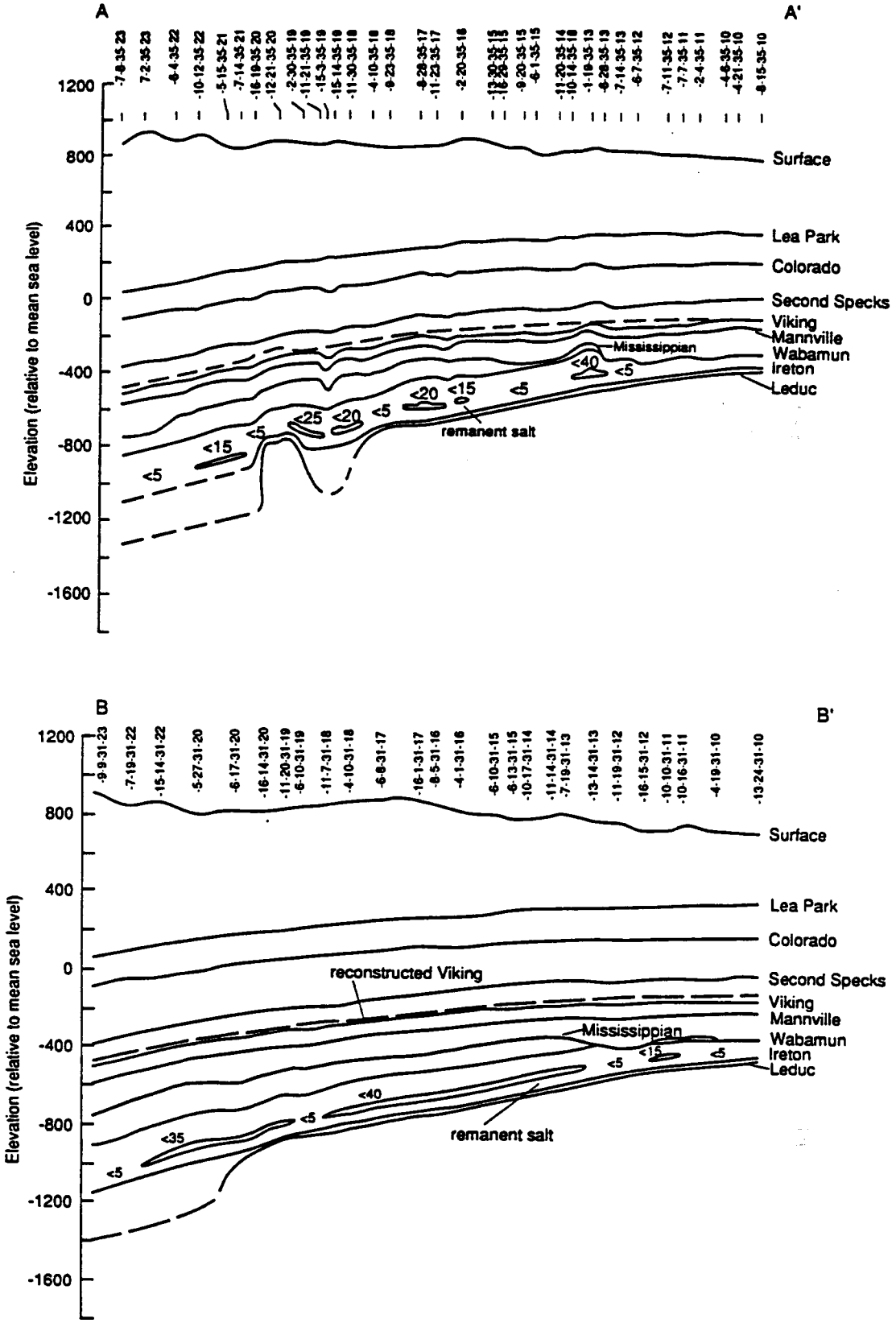

Figure VII:3:1. West-east geologic cross-sections illustrating the discontinuous nature of the Wabamun Group salts. (The maximun net thickness of these salts in the Stettler area is on the order of 40 m). Both present-day and reconstructed profiles for the Viking horizon are displayed.

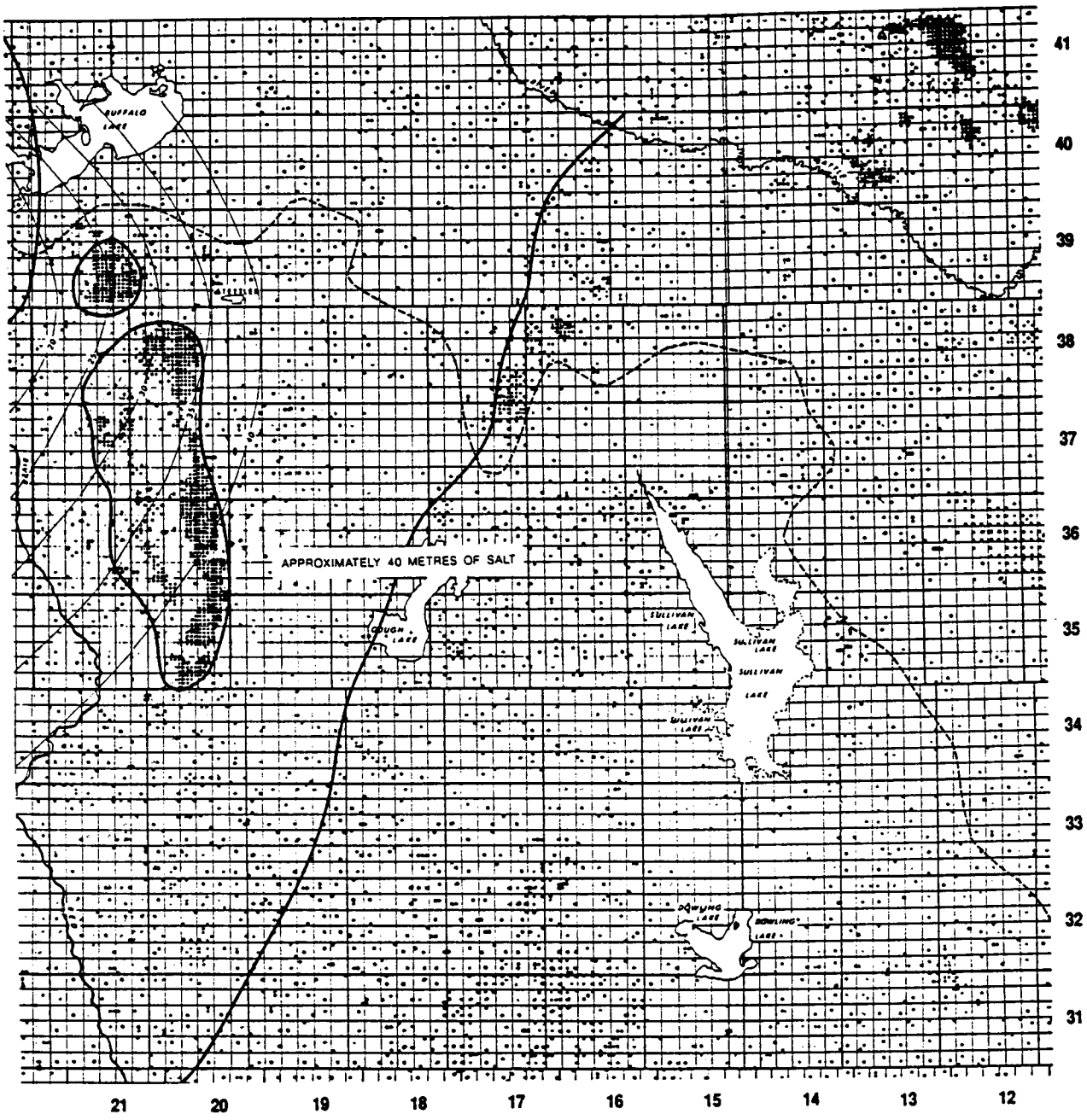

Figure VII:3:2. Contour map (m) depicting the original distribution (hypothesized) of the Wabamun Group salts (Stettler area). The dashed lines represent the Wabamun subcrop edge; the solid lines denote the edges of Leduc reef complexes.

The present-day (PDW; Figure VII:3:9) and restored (RW; Figure VII:3:10) Wabamun maps also support the theses: 1) that about 40 m of salt was uniformly deposited throughout most of the study area; and 2) that these salts depositionally thin to the northwest. More specifically, the difference in relief, at each control point, between these two maps is consistent with both the thickness of any preserved salt (NS) as well as the original salt distribution

map (OST; Figure VII:3:2). Exceptions to these relationships occur within the Cairn salt basin (including T30-T34, R12-R15). In this area, the underlying Cairn salt was partially dissolved in post-Wabamun time, a process which also resulted in the relative subsidence of post-Wabamun strata. (The superposed effects of the dissolution of the Cairn and Wabamun salts are difficult to differentiate in places.)

C) Present-day distribution of the Wabamun salts

In order to estimate the present-day distribution of the Wabamun salt (PST; Figure VII:3:8), we analyzed three maps: 1) original salt thickness (OST; Figure VII:3:2); 2) present-day Wabamun (PDW; Figure VII:3:9) structure; and 3) restored Wabamun (RW; Figure VII:3:10) structure. At each well control point, the original salt thickness, less the difference between the restored and present-day Wabamun structure values, is our present-day salt thickness (PST) estimate. We use the formula: (PST = (OST - (RW - PDW)). (In those areas where Wabamun control (deep well data) is sparse, contouring was constrained by apparent local trends and structural patterns along shallower horizons).

Note that these salt thickness estimates are based on the assumption that the dissolution of these salts occurred in post-Wabamun time. This thesis is supported by the present-day salt map (PST; Figure VII:3:8) which is consistent with: 1) the salt thicknesses (NS map; not shown) as determined directly from sonic/density/caliper log control; 2) the suite of reconstructed salt distribution maps (Figures VII:3:2-VII:3:7); and 3) the initial salt distribution map (OST; Figure VII:3:8).

D) Paleo-distribution of the Wabamun salts

The paleo-distribution of the Wabamun salt was estimated using the three steps outlined below:

Step 1) The subsea depths to the seven horizons listed below were determined at about 5000 well locations within the study area; (increasing depth and age, top to bottom):

A) top Lea Park
B) top Colorado
C) top Second Specks

D) top Viking
E) top Mannville
F) base Cretaceous
G) top Wabamun

Step 2) Both present-day (PD) and restored structure (R) maps were drafted for each of these seven data sets. (PD and R maps for the Wabamun (PDW and RW) and Lea Park (PDL and RL) are presented as Figures VII:3:9-VII:3:10, VII:3:11 and VII:3:12 respectively; Present-day (PDV) and reconstructed (RV) profiles for the Viking horizon are displayed on Figure VII:3:1). Ideally, the restored map for a particular unit represents the pattern of structural relief which would exist if we replaced all of the Wabamun salt that dissolved after deposition of the unit. Differences in structural relief, between corresponding present-day (PD) and restored structure maps (R), are therefor estimates of the thickness of salt removed after the deposition of the relevent strata.

The contouring of the restored structure maps (R) was constrained by: 1) well-log control; and 2) several key guidelines. The following key guidelines were used: 1) the contour patterns were to be both consistent with regional trends, and relatively smooth (implying uniform deposition); 2) the estimated thicknesses of dissolved salt were to be consistent with both the present-day (PST; Figure VII:3:8) and original (OST; Figure VII:3:2) salt thickness maps; and 3) the suite of present-day (PD) and restored structure (R) maps were to be compatible, such that the structural difference (PD - R) at a specific location on any horizon, was less than or equal to the difference at that location on any deeper level. For example, at any control point (RL - PDL) must be less than or equal to (RW - PDW).

Step 3) The paleo-distribution of the Wabamun salt was determined at the following times (Figures VII:3:2-VII:3:8, respectively):

A) end Wabamun (original distribution)
B) end Mannville
C) end Viking
D) end Second Specks
E) end Colorado
F) end Lea Park
G) present-day

The thickness of the salt remnants at these times was estimated on the basis of: 1) the original salt distribution map (OST); 2) the present-day structure maps (PD?); and 3) the restored structure maps (R?). For example, the present-day thickness of the salt (PST) was determined first, and estimated to be the original salt thickness (OST) less the difference between the restored (RW) and present-day (PDW) Wabamun structure maps: (PST = OST - (RW - PDW)). Similarly, the thickness of the salt at the end of Lea Park time (RLP) was calculated as the present-day (PDT)

thickness plus the difference between the restored (RL) and present-day (PDL) Lea Park structure maps: (PDT + RL - PDL). Salt thicknesses at the other selected times within the Cretaceous were determined in an analogous manner.

The present-day and paleo-distribution of the Wabamun salts is depicted in Figures VII:3:2-VII:3:8 (decreasing age). From these maps several significant conclusions can be drawn:

1) About 40 m of Wabamun salt was uniformly deposited throughout most of the study area. In the extreme northwestern part of the study area, the net depositional thicknesses of these salts uniformly thins to 0 m.

2) Dissolution was initiated and/or enhanced by some or all of four principal processes: 1) the near surface exposure of the salt, as a result of the erosion of the overlying Paleozoic sediment during the pre-Cretaceous hiatus; 2) the partial dissolution of the underlying Cairn salt in post-Wabamun time; 3) regional faulting/fracturing during the late Cretaceous; and 4) glacial unloading.

3) With respect to erosion, the earliest phases of dissolution occurred during the pre-Cretaceous along the projected salt outcrop edge. Later phases occurred successively further to the southwest, suggesting that leaching is a self-perpetuating process (Figures VII:3:2-VII:3:8).

4) Work by both the authors and Brown and Anderson (1991) has shown that the Cairn salt has been extensively dissolved in places, more-or-less continuously since the late Devonian. Indeed, in the southeastern part of the study area the effects of the leaching of the Wabamun and Cairn salts are difficult to differentiate. We conclude that, within the confines of the Cairn salt basin, the dissolution of the Wabamun salt could have been triggered by the leaching of the underlying Cairn. Such leaching could have occurred at any time after the deposition of the Wabamun salt. (Note on the suite of reconstructed maps that the leaching of the Wabamun salt in this area is shown as initiating during the Upper Cretaceous; additional detailed work is necessary to convincingly establish whether or not earlier phases of dissolution occurred).

5) The orthogonal patterns of dissolution shown on the suite of paleo-distribution maps strongly suggest that regional faulting/fracturing during the Upper Cretaceous initiated widespread leaching. These patterns also imply that the dissolution fronts, initiated along these fault/fracture planes, moved laterally thereafter. It is interesting to note that the Stettler reef (T35-38, R20W4M) is situated across a major lineament, and that the edges of both the main reefs, as well as the Cairn salt, are consistent with the hypothesized fault/fracture planes. (Perhaps the lineaments are reactivated planes of weakness.)

6) Several lakes (Buffalo, Gough, Sullivan and Dowling; Figure VII:3:8) are situated in areas where the salts are thin or absent, suggesting that significant leaching has occurred in post-glacial times, possibly in response to glacial loading and unloading.

7) Dissolution of the Wabamun salt has occurred at various times during the geologic past, supporting the thesis that dissolution, in places, has been more-or-less continuous since deposition. The correlation between the present-day drainage pattern and remnant salt suggests that significant leaching is still occurring.

8) Leaching is self-perpetuating: a process whereby the collapse of overlying strata enhances both their porosity and permeability, thereby providing a conduit for water, and facilitating further dissolution.

9) Several trigger mechanisms have been identified and it has been suggested that leaching is self-perpetuating. With respect to this self-perpetuating process, we note that the established dissolution fronts do not advance at a uniform rate. For example, particularly extensive dissolution has occurred near the western depositional edge of the salt, in the southwestern part of the study area, and across the Stettler reef. These observations suggest that a number of secondary factors influence salt dissolution. Consideration should be given to effects of the intenity and magnitude of faulting, regional tectonism, periods of emergence, underlying reefs, the differential compaction of pre-salt sediment, uneven loading and unloading, glaciation, post-glacial rebound, facies changes within both the salt and encompassing strata, the local hydrological and geochemical environment and changes therein, and the effects of wells.

E) Complicating factors

The methodology employed, is based on the premise that the dissolution of subsurface salt causes the contemporaneous collapse of the overlying strata. The thickness of leached salt and the magnitude of collapse are assumed to be equal. Although the methodology appears to be relatively robust, as evidenced by the suite of compatible, consistent, restored structure maps, it might not, in places, adequately account for processes such as: 1) non-uniform deposition or erosion; 2) lateral strain associated with collapse; 3) differential compaction of infill (compensation) sediments; 4) salt flow; 5) dissolution of underlying salts; and 6) faulting.

Primary deposition and secondary processes such as erosion and differential compaction (particularly across reefs) can create anomalous lateral variations in subsurface structure. Although we have attempted to incorporate drape across both known Leduc reefs and the sub-Cretaceous unconformity into our restored structure maps, we have probably attributed some minor components of such relief to salt dissolution. As evidenced by the suite of restored maps, the

timing of salt dissolution is difficult to estimate to the east of the Wabamun subcrop edge. Due to extreme relief at the Wabamun and post-Wabamun levels in this area, we had difficulties creating consistent restored maps. We were also unable to determine whether the paleo-topography is simply erosional in origin, or if it is partially attributable to the leaching of the Cairn salt.

Our methodology assumes that only vertical strain occurs in response to leaching and does not account for the the lateral movement of overlying strata. Although we recognize this source of error, previous work (Anderson and Brown, 1987) suggest that it should not affect our interpretations significantly. Similarly, the differential compaction between the sediments which infill the salt dissolution lows and the adjacent strata should not significantly compromise our results.

With respect to the mobilization of salt, we have found neither evidence of flow nor attempted to compensate for such processes. We do, however, recognize that the Cairn salt has been extensively leached in post-Wabamun time, in places. Due to a paucity of deep well control, the combined effects of the dissolution of the Cairn and Wabamun salts are difficult to differentiate. As a result, our reconstructed salt distribution maps have a greater degree of uncertainty in this area. We have not seen any evidence that the Prairie salt (Figure VII:1:1 and VII:1:2) has been leached in the area, however well control at this level is sparse.

The patterns of dissolution on the suite of reconstructed salt distribution maps (Figures VII:3:2-VII:3:8) suggest that leaching, in places, was initiated by widespread regional faulting and/or fracturing in the late Cretaceous (as opposed to localized slumping due to the dissolution of pre-Wabamun salts). Although there is no conclusive evidence of vertical displacement, significant movement (on the order of 10 m or more) could have occurred and may be incorrectly attributed to salt dissolution and/or drape across either reefs or the pre-Cretaceous subcrop. The relative absence of salt in the southwestern part of the study area suggests that the intensity of faulting might have been greater there.

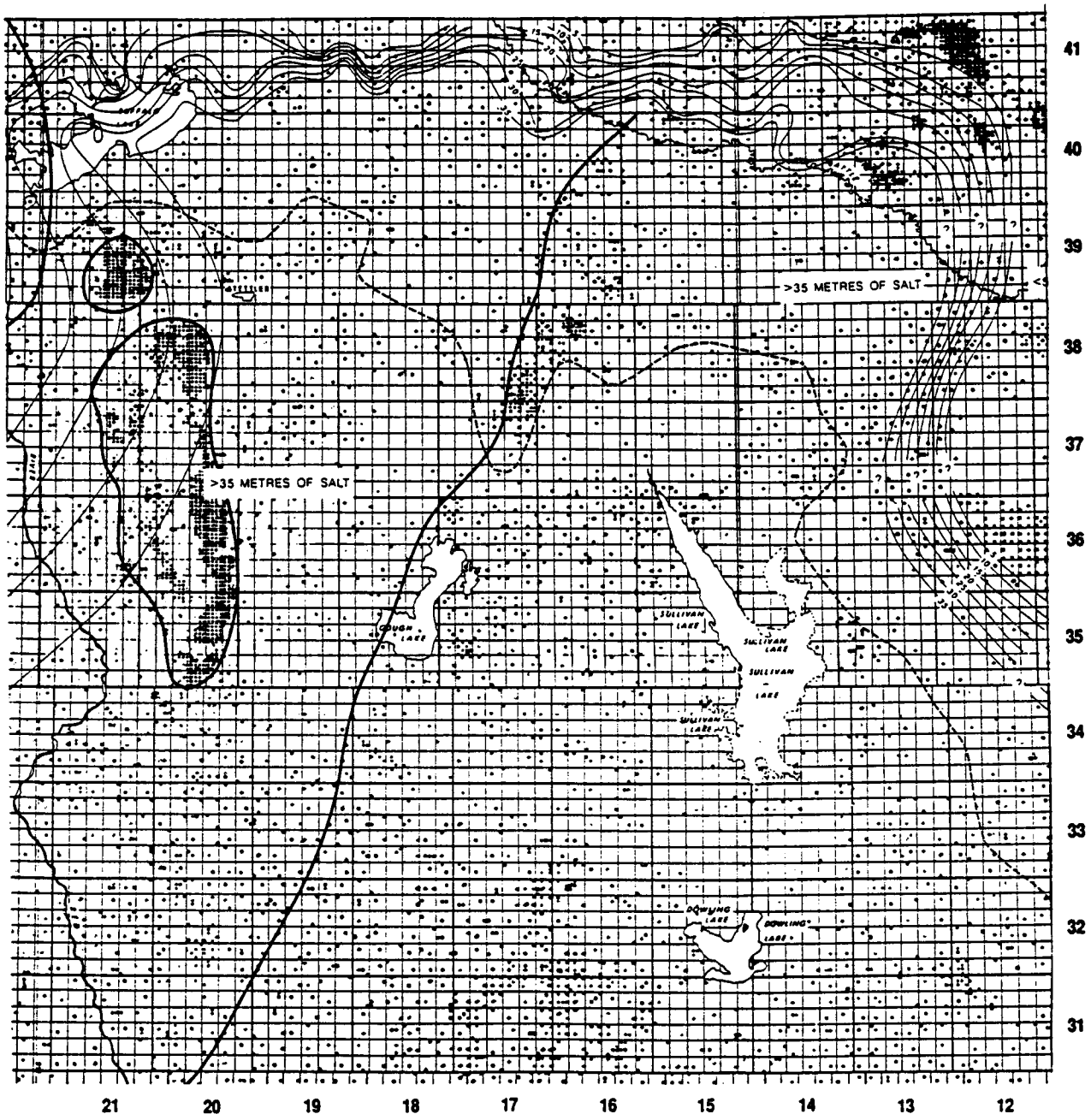

Figure VII:3:3. Contour map (in meters) showing the distribution (hypothesized) of the Wabamun salts at the end of Mannville time.

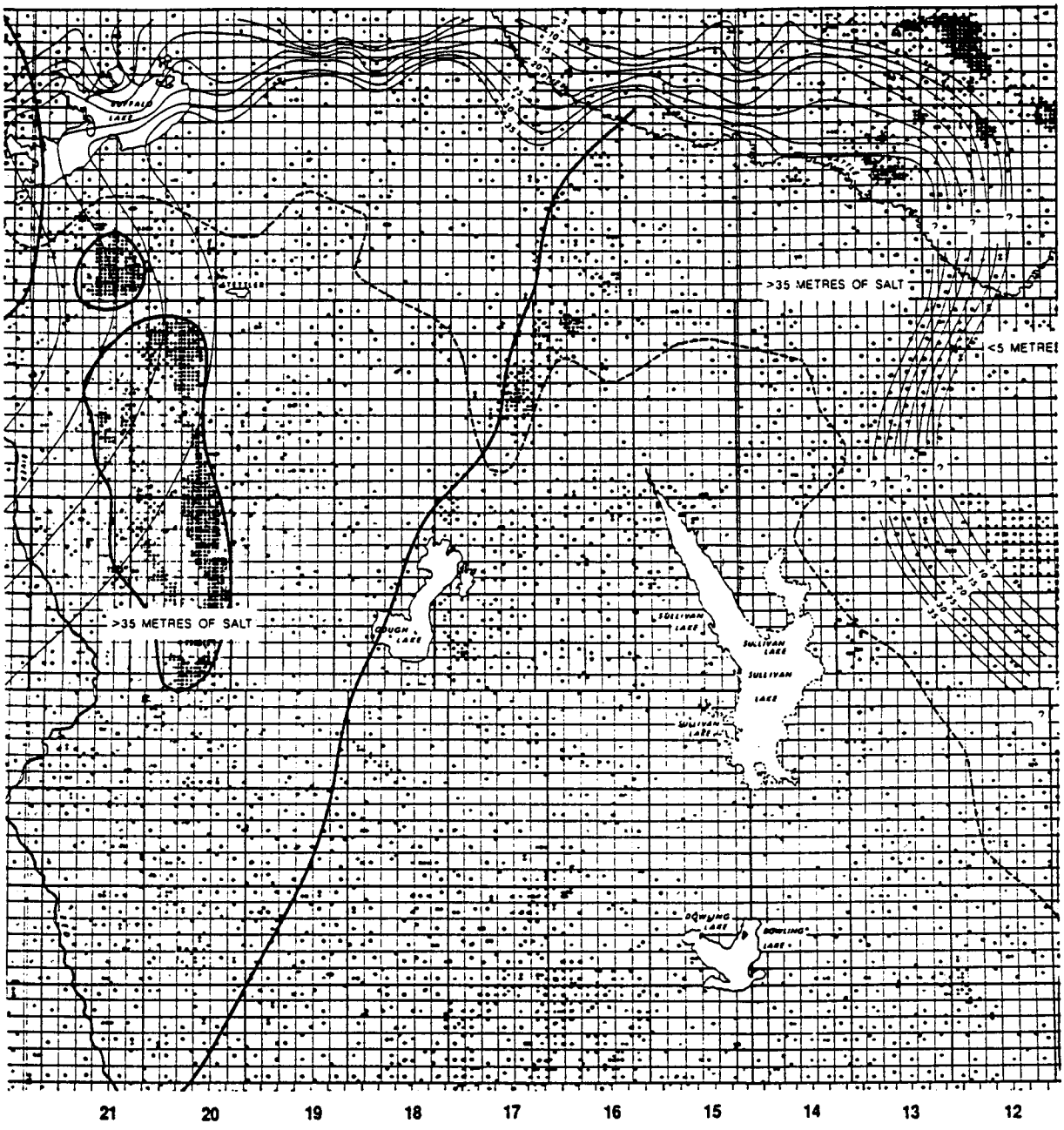

Figure VII:3:4. Contour map (in meters) showing the distribution (hypothesized) of the Wabamun salts at the end of Viking time.

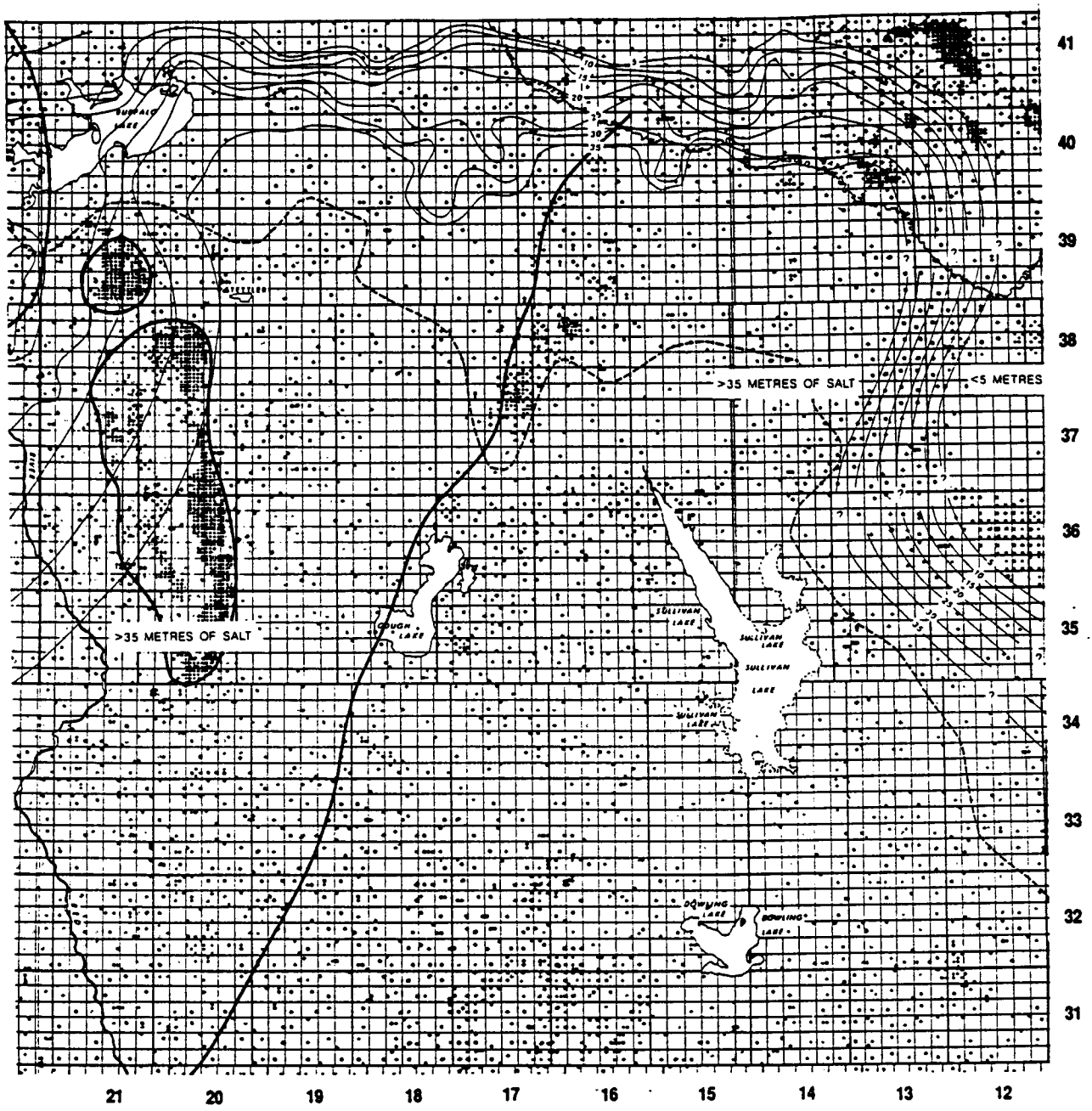

Figure VII:3:5. Contour map (in meters) showing the distribution (hypothesized) of the Wabamun salts at the end of Second Specks time.

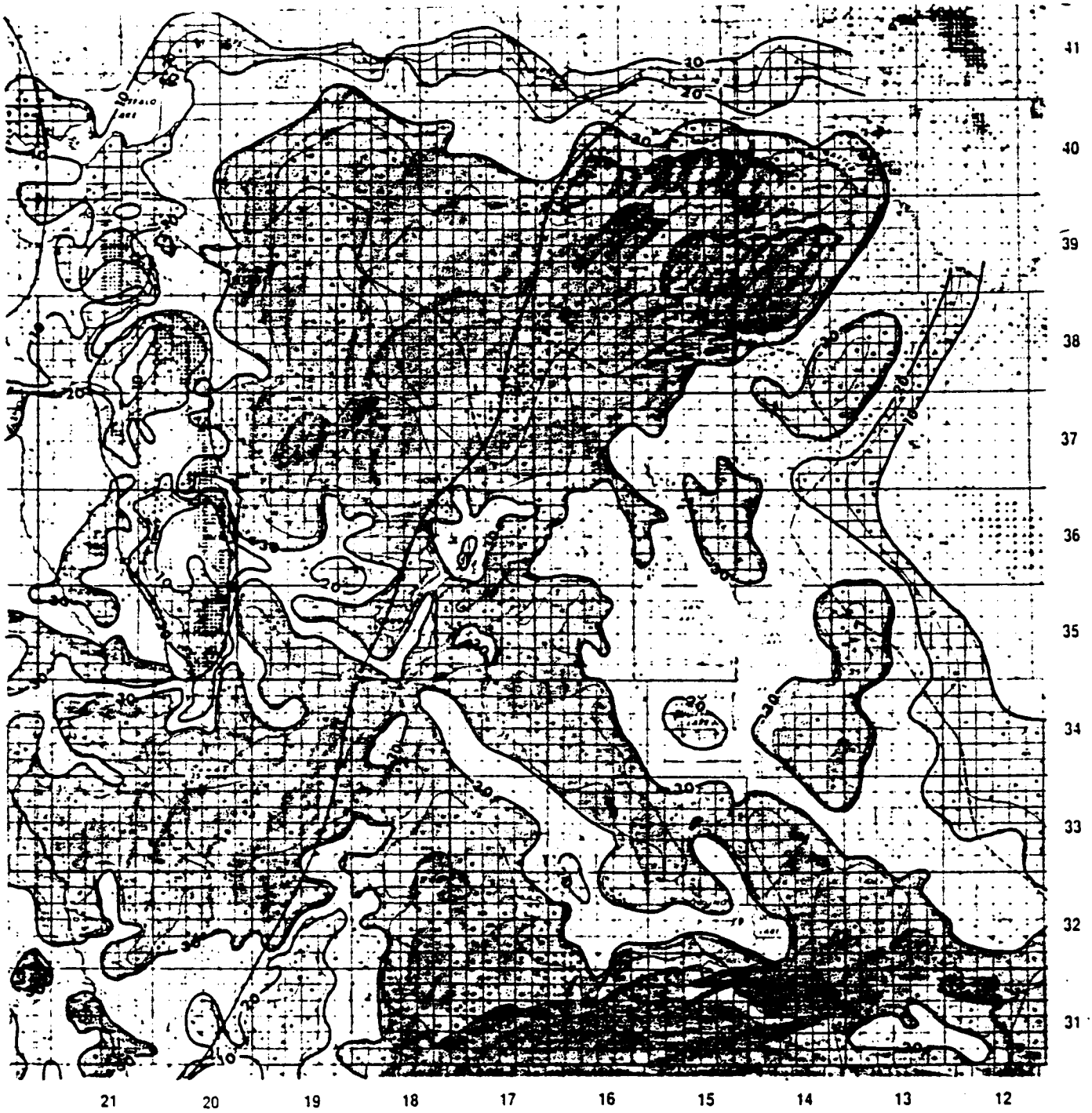

Figure VII:3:6. Contour map (in meters) showing the distribution (hypothesized) of the Wabamun salts at the end of Colorado time.

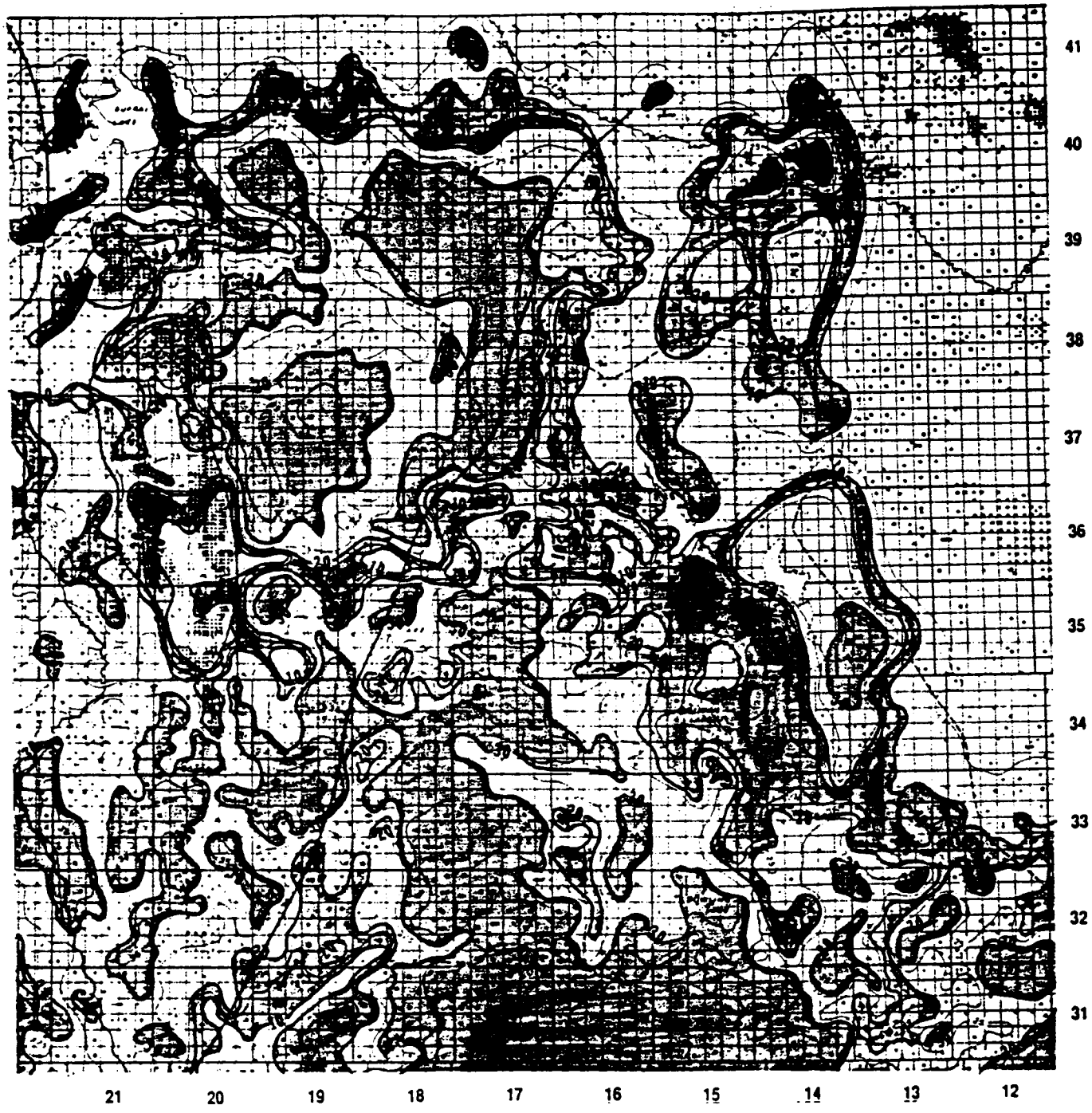

Figure VII:3:7. Contour map (in meters) showing the distribution (hypothesized) of the Wabamun salts at the end of Lea Park time.

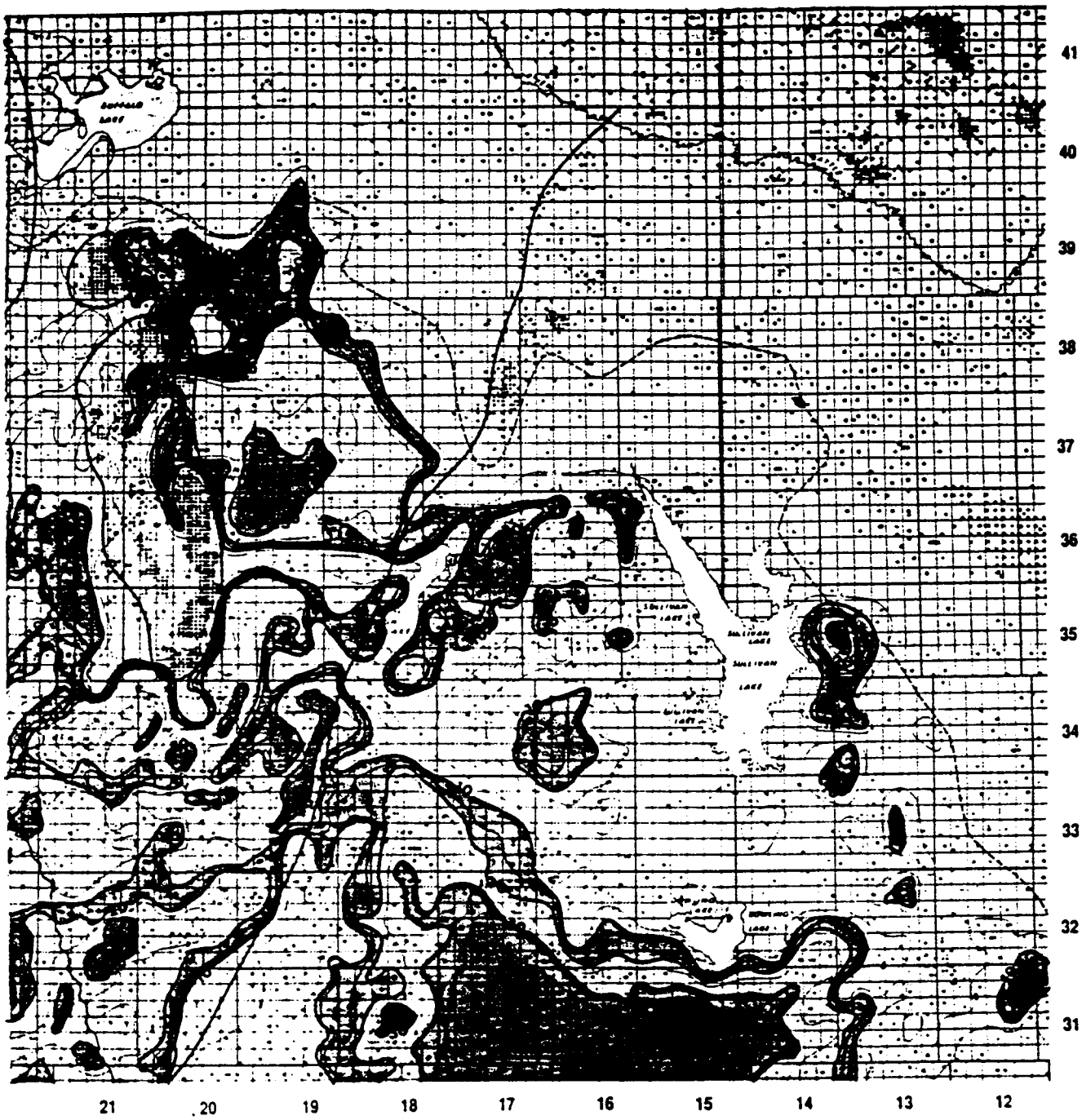

Figure VII:3:8. Contour map (in meters) depicting the present-day distribution of the Wabamun salts.

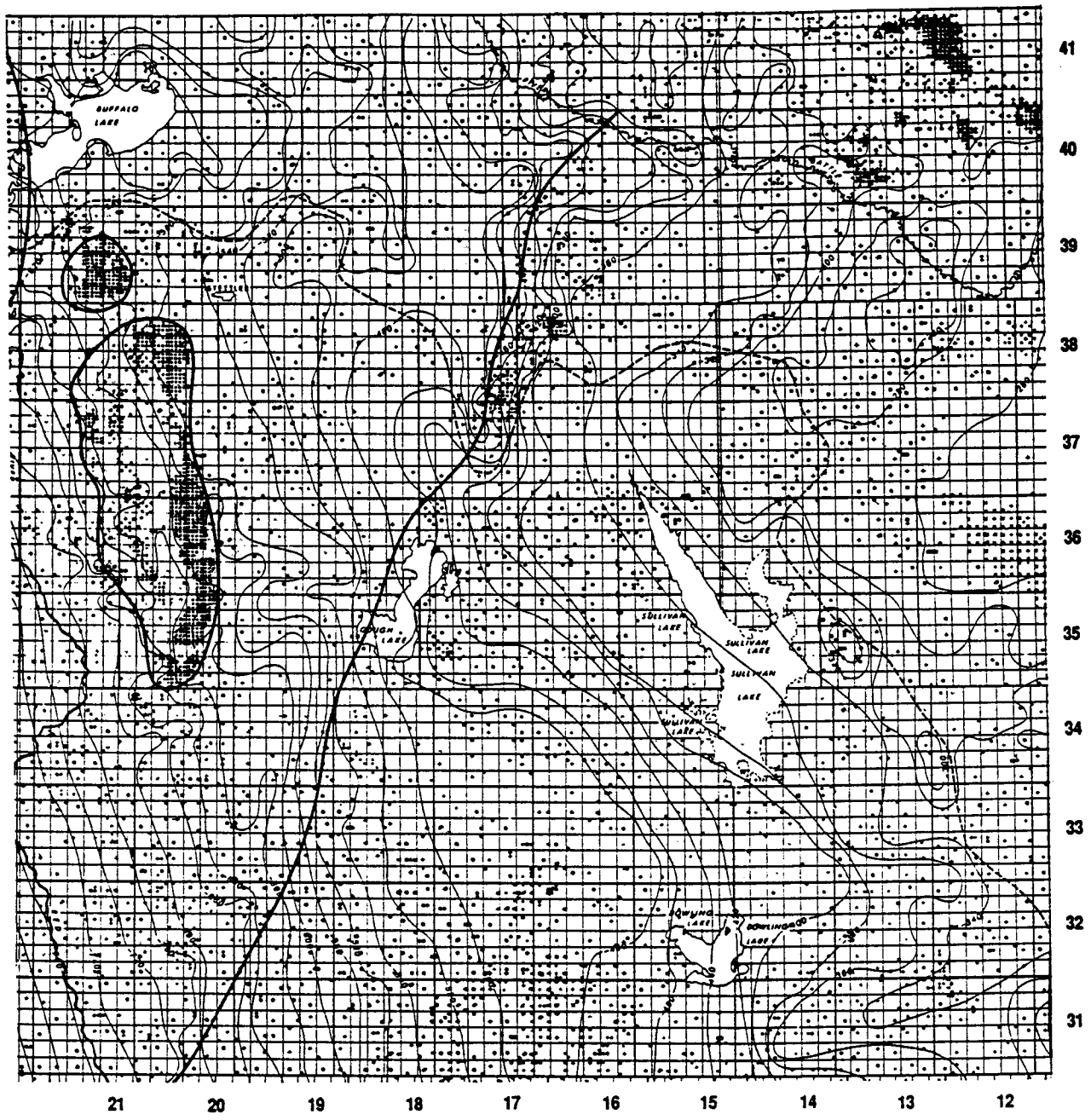

Figure VII:3:9. Contour map (in meters) of the subsea depth to the top of the Wabamun.

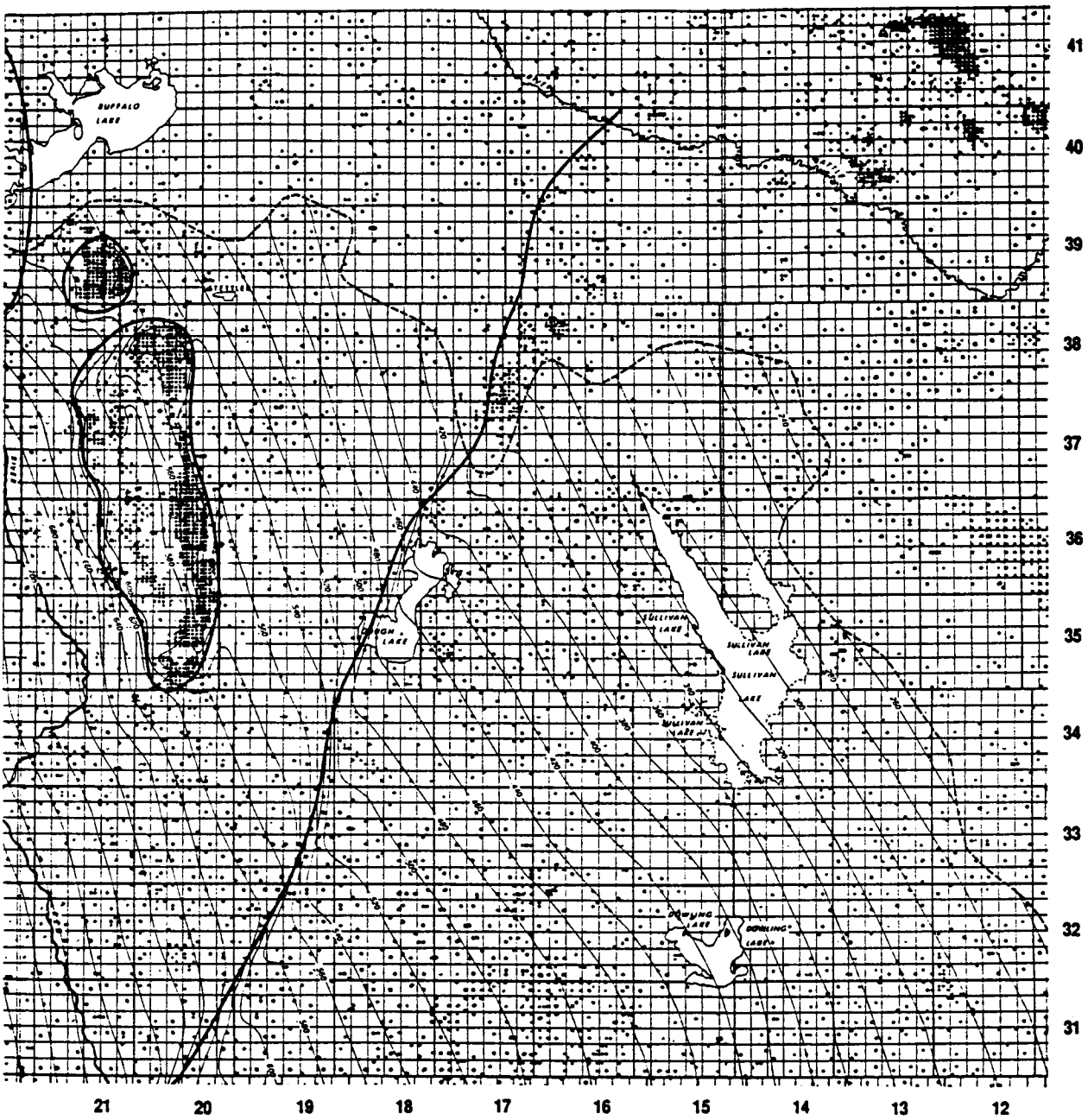

Figure VII:3:10. Restored contour map (m) depicting what the elevation of the Wabamun would be if dissolution had not occurred.

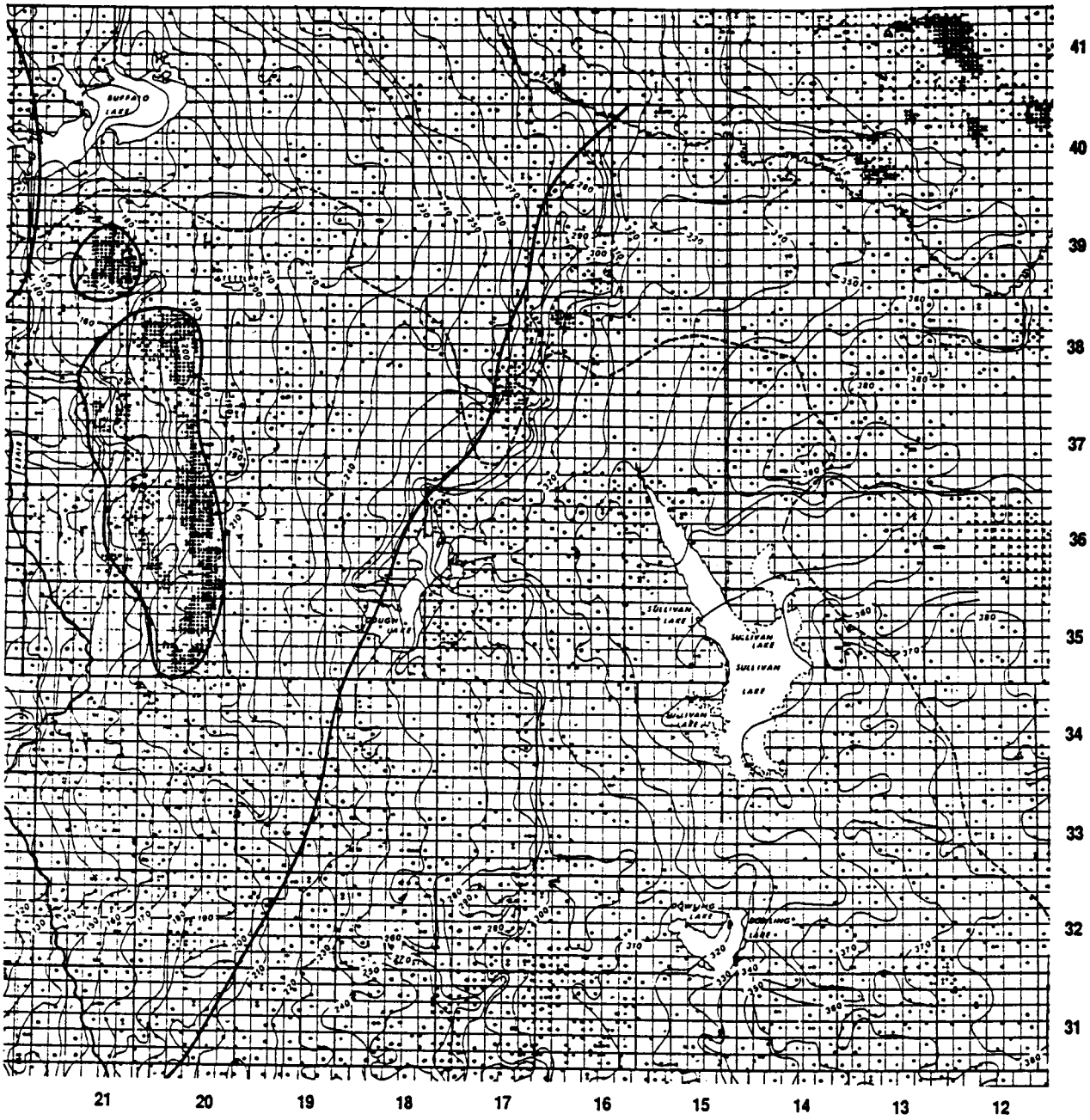

Figure VII:3:11. Contour map (in meters) of the subsea depth to the top of the Lea Park.

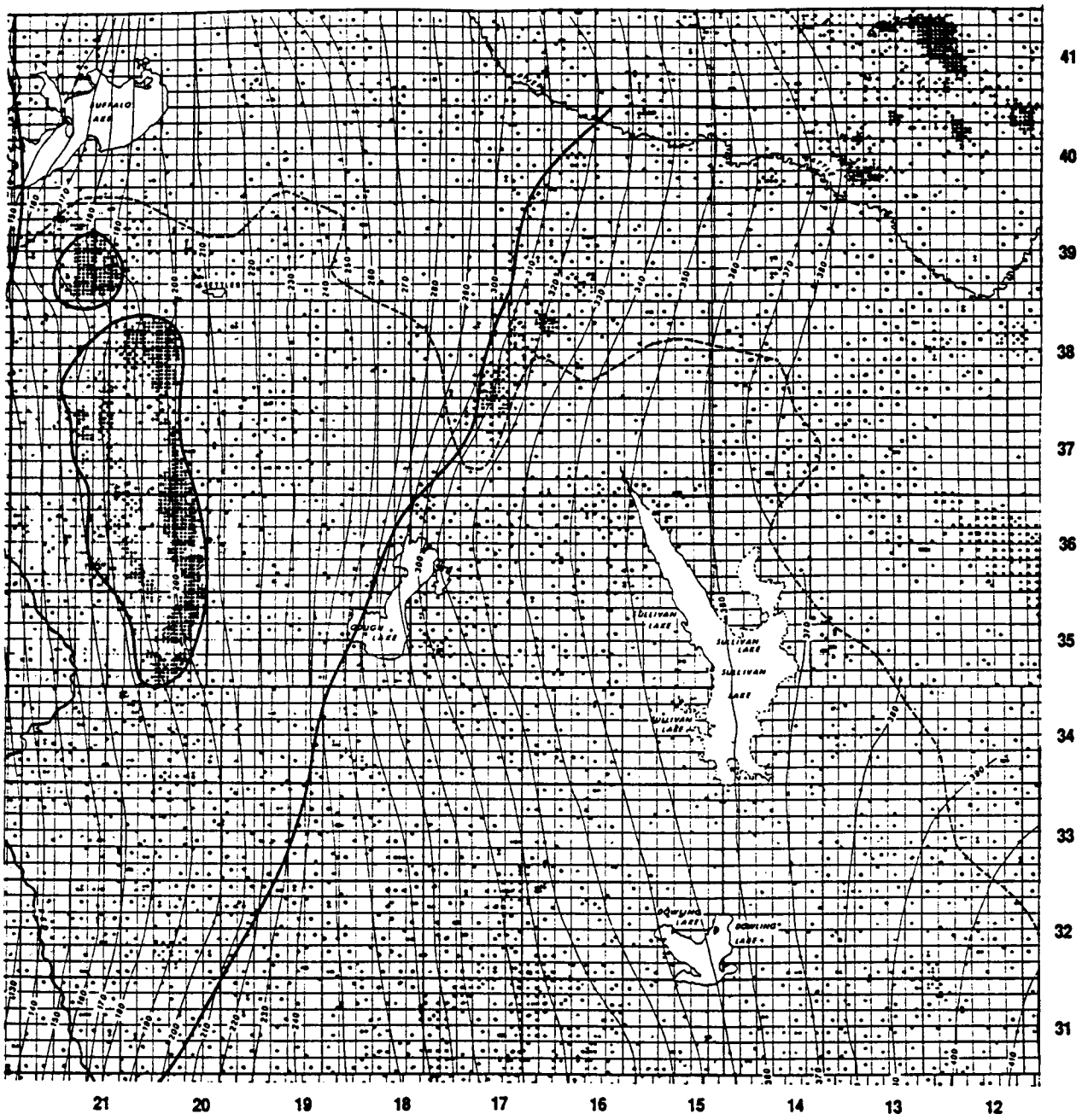

Figure VII:3:12. Restored contour map (m) depicting what the elevation of the Lea Park (hypothesized) would be if post-Lea Park dissolution had not occurred.

4) YOUNGSTOWN AREA: CASE STUDY

A) Overview

The halite salts of the Wabamun Group (Figures VII:1:1, VII:1:2, VII:2:17, and VII:2:19-VII:2:21) are preserved throughout much of southern Alberta as isolated to contiguous bodies of irregular shape, having maximum net thicknesses on the order of 40 m. The Leduc salts (Figures VII:1:1, VII:1:2 and VII:2:17-VII:2:19), in contrast, appear to be preserved only as a single, more-or-less contiguous body with a maximun net thickness on the order of 45 m. Both the Leduc and Wabamun salts are thought to have been more widely deposited than their present-day distribution might suggest, and both are believed to have been extensively leached (Anderson, 1991; Anderson and Brown, 1987, 1991a,b; Anderson et al., 1988, 1989; Hopkins et al., 1987; Meijer Drees, 1986 and Oliver and Cowper, 1983).

In an effort to elucidate the dissolution of these salts, we conducted a well-log based study of the Youngstown area (T25-T35, R5-R20W4M). We identified correlation patterns involving the thicknesses of the Wabamun and the Leduc intervals, structural relief at the Wabamun and Leduc levels, relief along post-Devonian horizons, and the thicknesses of the salt remnants. On the basis of these relationships, we reconstructed the distribution of these salts at selected times from late Paleozoic to the present. We conclude the following:

1) Up to 45 m of Leduc salt was deposited in each of two main sub-basins in the eastern part of the study area (on the shelfward side of the developing Leduc fringing reef complex).

2) About 40 m of Wabamun salt was uniformly deposited throughout the Youngstown study area.

3) Both the Wabamun and Leduc salts were extensively leached subsequent to deposition. The dissolution of these salts was initiated and/or enhanced by some or all of four principal processes: 1) the near-surface exposure of these salts, as a result of the erosion of the overlying Paleozoic sediment during the pre-Cretaceous hiatus; 2) the partial dissolution of underlying salts; 3) regional faulting/fracturing during the mid-Late Cretaceous; and 4) glacial loading and unloading.

4) The leaching of both salts appears to have been self-perpetuating; a process whereby fractures, created by the collapse of overlying strata, provide conduits for water thereby facilitating further dissolution.

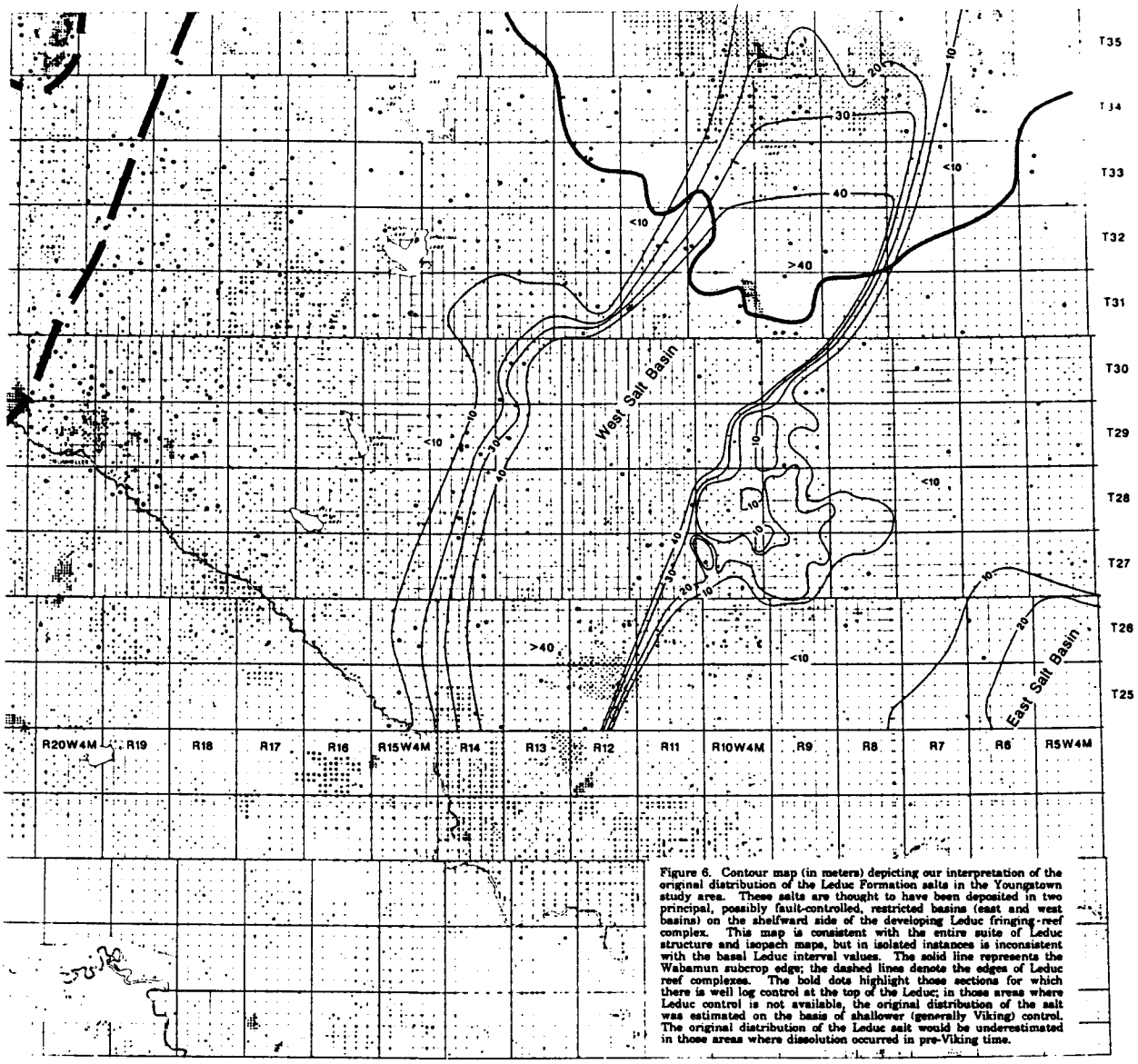

Figure 6. Contour map (in meters) depicting our interpretation of the original distribution of the Leduc Formation salts in the Youngstown study area. These salts are thought to have been deposited in two principal, possibly (salt-controlled, restricted basins (east and west basins) on the shelfward side of the developing Leduc fringing-reef complex. This map is consistent with the entire suite of Leduc structure and isopach maps, but in isolated instances is inconsistent with the basal Leduc interval values. The solid line represents the Wabamun subcrop edge; the dashed lines denote the edges of Leduc reef complexes. The bold dots highlight those sections for which there is well log control at the top of the Leduc; in those areas where Leduc control is not available, the original distribution of the salt was estimated on the basis of shallower (generally Viking) control. The original distribution of the Leduc salt would be underestimated in those areas where dissolution occurred in pre-Viking time.

Figure VII:4:1. Contour map (m) depicting the original distribution of the Leduc Formation salts. These salts are thought to have been deposited in two principal, possibly fault-controlled, restricted basins (east and west basins). The solid line represents the Wabamun subcrop edge; the dashed lines denote the edges of Leduc reef complexes. The bold dots highlight well-log control at the Leduc level.

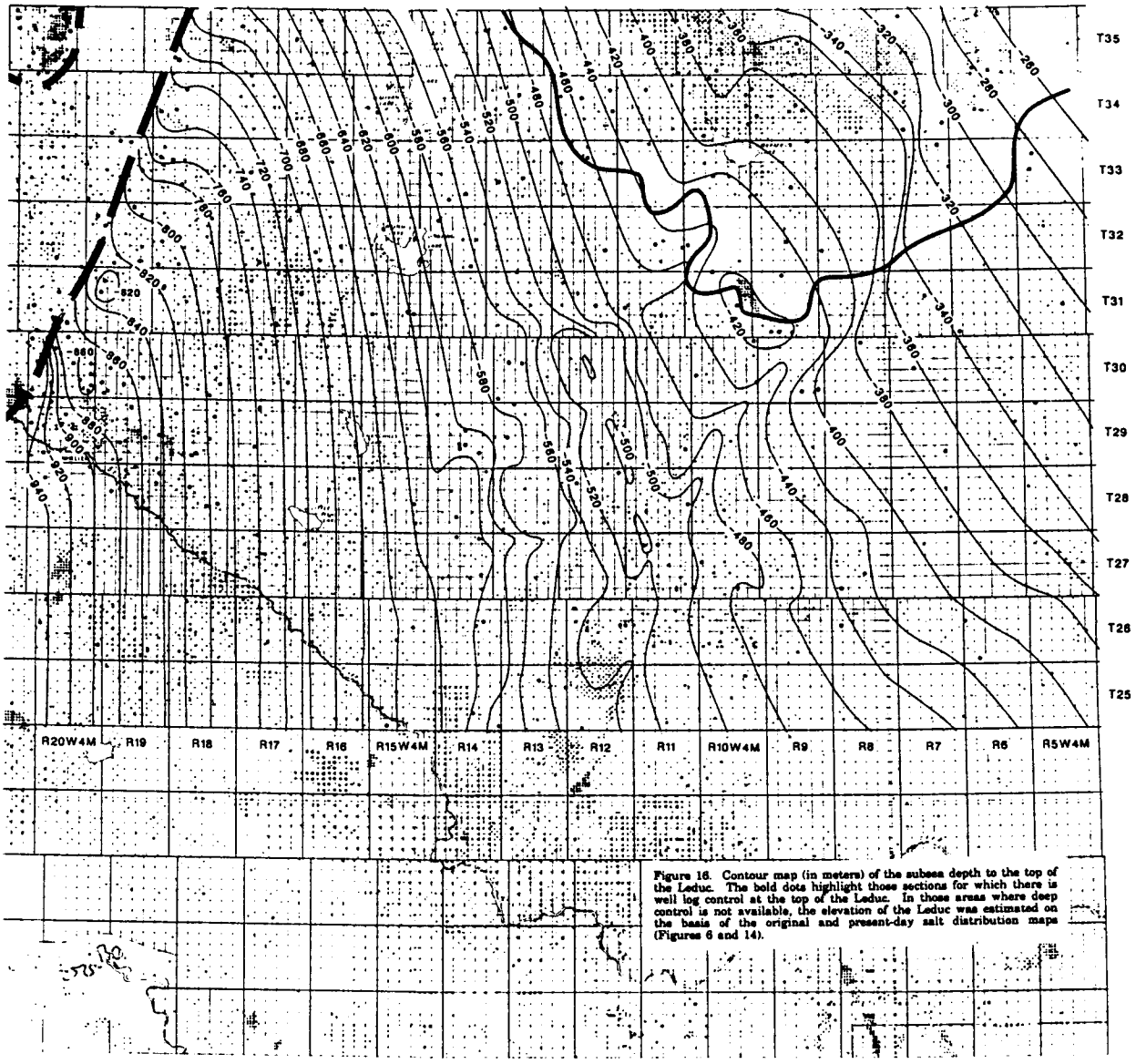

Figure 16. Contour map (in meters) of the subsea depth to the top of the Leduc. The bold dots highlight those sections for which there is well log control at the top of the Leduc. In those areas where deep control is not available, the elevation of the Leduc was estimated on the basis of the original and present-day salt distribution maps (Figures 6 and 14).

Figure VII:4:2. Contour map (m) of the subsea depth to the top of the Leduc. The bold dots highlight Leduc well-log control. In those areas where deep well control is absent, the contouring of the present-day Leduc structure map was constrained by apparent local trends and structural patterns along shallower horizons.

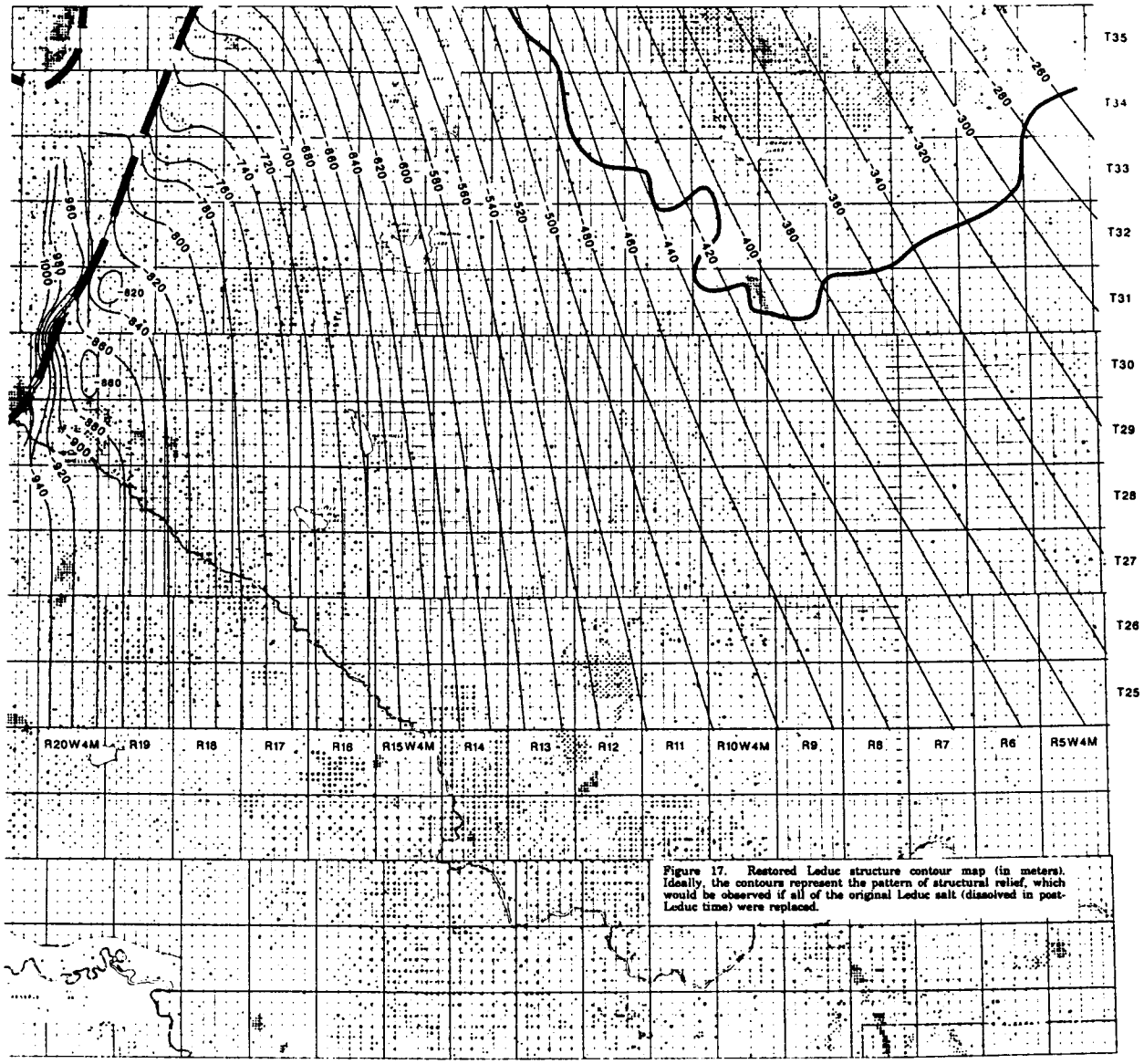

Figure VII:4:3. Restored Leduc structure contour map (m). Ideally, the contours represent the pattern of structural relief, that would be observed if all of the original Leduc salt (dissolved in post-Leduc time) were replaced.

B) Original distribution of the Leduc salts

The lithology of the Upper Devonian age, Leduc Formation in the Youngstown area of Alberta varies significantly. Near the edge of the East Ireton Shale Basin, the Leduc is dolomitized and described as fringing reef. Shelfward (to the east in the study area) of this fringing reef complex, the Leduc becomes increasingly evaporitic and consists predominantly of interlayered dolomites, anhydrites and in places a basal halite unit. From a facies perspective, the Leduc Formation in the eastern part of the study area is equivalent to the evaporitic Duperow Formation of southwestern Saskatchewan.

In order to estimate the original (end of Leduc time; Figure VII:4:1) distribution of the Leduc salts in the Youngstown study area and following the methodology described by Anderson and Brown (1992), we initially constructed a suite of four maps: 1) net Leduc salt, based on sonic/density/caliper log control only; 2) Leduc-isopach; 3) present-day Leduc-structure (Figure VII:4:2); and 4) restored Leduc-structure (Figure VII:4:3).

Our analysis of this map suite indicates that there is a direct, linear correlation between the structure at the top of the Leduc and the thickness of the Leduc interval. We also conclude that there is a direct correlation between these values and the thickness of Leduc salt that was dissolved in post-Leduc time.

Outside of the postulated Leduc salt sub-basins (Figure VII:4:1) for example, the top of the Leduc is consistent with the restored Leduc-structure map, suggesting that little, if any, Leduc salt was either deposited and/or dissolved in post-Leduc time. Within the sub-basins however, the present-day structure values are lower than the restored structure values, except at those well locations where thick remnant salt is preserved. Our conclusion is that these relative structural lows can provide a direct and reasonable estimate of the thickness of Leduc salt that was dissolved in post-Leduc time. It is on the basis of the apparent correlations between these data, that we have reconstructed the original distribution of the Leduc salt within the Youngstown study area.

C) Original distribution of the Wabamun salts

The Upper Devonian Wabamun Group in the Youngstown area is subdivided into the Stettler and Big Valley formations (southern plains area, Alberta; Figure VII:1:1 and VII:1:2). The Stettler consists predominantly of interlayered dolomites, anhydrites and isolated to contiguous remnants of halite; the Big Valley is composed of green shales and fossiliferous limestones.

The salts of the Wabamun Group (Stettler Formation) have been mapped in detail by Anderson et al. (1988) and Anderson and Brown (1991) over the Stettler area (T30-T45, R10-R25W4M). These authors concluded that about 40 meters of these halites were deposited throughout much of southeastern

Alberta and subsequently leached (Figure VII:4:4).

In order to estimate the original distribution of the Wabamun salt in the Youngstown study area, we constructed four maps: 1) net salt, based on sonic/density/caliper log control only; 2) Wabamun-isopach; 3) present-day Wabamun-structure; and 4) restored Wabamun-structure (Figure VII:4:5).

Our analysis of this map suite indicates that outside of the postulated Leduc sub-basins, there is a direct, linear correlation between the structure at the top of the Wabamun and the thickness of the Wabamun interval. We have also concluded that there is a direct correlation between these values and the thickness of Wabamun salt that was dissolved in post-Wabamun time. These relationship supports our thesis that about 40 m of Wabamun salt were uniformly deposited within the Youngstown study area (Figure VII:4:5).

D) Present-day distribution of the Leduc salts

In order to estimate the present-day distribution of the Leduc salts (Figure VII:4:6), we analyzed three maps: 1) original salt-thickness (Figure VII:4:1); 2) present-day Leduc-structure (Figure VII:4:2); and 3) restored Leduc-structure (Figure VII:4:3). At each well control point, our present-day salt-thickness estimate (A) is equal to the original (end Leduc time) salt-thickness (B) less the difference between the restored (C) and present-day (D) Leduc-structure values (Figure VII:4:7 and VII:4:8). Following Anderson and Brown (1991b), we use the formula:

$$A = B - (C - D).$$

In those areas where deep well control is absent, the contouring of the present-day Leduc-structure map was constrained by apparent local trends and structural patterns along shallower horizons. At all available deep well control points, our present-day salt-thickness estimate (A) and the actual thickness of the remnant salt (as per the well-log data) were effectively the same.

The original and present-day thicknesses of the Wabamun salts were estimated concurrently with our analysis of the Leduc salts. This was necessary in order to ensure that our paleo-distribution maps were compatible.

E) Present-day distribution of the Wabamun salts

In order to estimate the present-day distribution of the Wabamun salt (Figure VII:4:9), we analyzed three maps: 1) original salt-thickness (Figure VII:4:4); 2) present-day Wabamun-structure; and 3) restored Wabamun-structure. At each well control point our present-day salt-thickness estimate (A) is equal to the original salt-thickness (40 m) plus our estimate of the thickness of Leduc salt dissolved in post-Wabamun time (B) less the difference between the restored

(C) and present-day (D) Wabamun-structure values. We use the formula:

$$A = 40\ m + B - (C - D).$$

At all available deep well control points, our present-day salt-thickness estimate (A) and the actual thickness of the remnant Wabamun salt (as per the well-log data) were effectively the same. In those areas where Wabamun control is sparse, the contouring of the present-day Wabamun-structure map was constrained by apparent local trends and structural patterns along shallower horizons).

F) Paleo-distribution of the Leduc and Wabamun salts

The paleo-distributions of the Leduc and Wabamun salts were estimated following for the following times using the methodology described by Anderson and Brown (1991).

A) end Leduc
B) end Wabamun
C) end Mannville
D) end Viking (Figures VII:4:10 and VII:4:11)
E) end Second Specks
F) end Colorado
G) end Lea Park
H) present-day

On the basis of these maps we have concluded.

1) The Leduc salts in the study area (Figure VII:4:12) are thought to have been deposited in two, possibly interconnected, fault/fracture controlled, restricted basins on the shelfward side of the developing Leduc fringing-reef complex. The maximum thickness of the Leduc salt in the study area was probably on the order of 45 m.

There are several reasons for sugesting that the Leduc salt-basins were fault/fracture-controlled: 1) prominent diffraction patterns and vertical offsets are clearly visible along near-basement events (pre-Leduc) on seismic data from the Leduc salt-basin areas (unfortunately we do not have access to enough data to conclusively establish the orientation of these lineaments); the original, postulated salt-basins are oriented more-or-less parallel to the edge of the fringing-reef complex, suggesting that both features could have been influenced by the reactivation of pre-existing planes of weakness (a near-orthogonal pattern of faulting/fracturing can satisfactorily explain any observed non-linearities in the shape of the basin); 3) the western depositional edges of the Leduc salt are interpreted as being abrupt rather than gradational, a feature more characteristic of a

fault-controlled basin than of a gradual environmental change; 4) the dissolution of both the Wabamun and Leduc salts appears to have initiated along an orthogonal set of lineaments, that possibly represent pre-existing faults and/or fractures; and 5) with respect to the western salt-basin, dissolution of the Leduc salts has been most extensive near the basin margins, perhaps as a result of the reactivation of the fractures/faults that influenced the development of the basin originally.

2) About 40 m of Wabamun salt were uniformly deposited throughout the Youngstown study area. This conclusion is based on our observation that there is a direct, linear correlation between the structure at the top of the Wabamun, the thickness of the Wabamun interval, and the thickness of Wabamun salt that was dissolved in post-Wabamun time. All three values vary, in a relative sense, by 40 m or less.

3) The dissolution of the Leduc and Wabamun salts was initiated and/or enhanced by some or all of four principal processes: 1) near-surface exposure, as a result of the erosion during the pre-Cretaceous hiatus; 2) regional faulting/fracturing during the mid-Late Cretaceous; 3) glacial loading and unloading; 4) the partial dissolution of the underlying salts.

4) With respect to erosion during the pre-Cretaceous, the earliest phases of Wabamun salt dissolution appear to have occurred along the projected Wabamun outcrop edge during the pre-Cretaceous. As indicated on the suite of reconstructed maps, the dissolution front, that was established along the subcrop edge, appears to have migrated over time to the southwest, suggesting that leaching is a self-perpetuating process. Minor dissolution of the Leduc salt along the margins of the postulated sub-basins could have occurred during the post-Leduc/pre-Viking interval. This apparent phase of leaching could have been initiated during the pre-Cretaceous hiatus, and in response to an influx of unsaturated water along the Leduc outcrop to the northeast of the study area.

5) The orthogonal pattern displayed on the suite of Wabamun and Leduc salt paleo-distribution maps strongly suggest that dissolution fronts developed along a suite of more-or-less orthogonally-oriented (NNE-WNW) regional fault/fracture planes during the mid-Late Cretaceous. The apparent expansion of these areas of dissolution over time, implies that the dissolution fronts migrated laterally. It is interesting to note that the edge of the fringing reef complex, as well as edges of the postulated Leduc sub-basins, are consistent with the hypothesized fault/fracture planes. Perhaps these lineaments are reactivated planes of weakness.

6) Several lakes to the west of the postulated Leduc sub-basins (Gough, Sullivan and Dowling) are situated in areas where the Wabamun salts are thin or absent; all of the larger lakes in the Leduc sub-basin area (Plover, Antelope, Goose, Gopher, Contracosta, Coleman, Oakland, and the Berry Reservoir) are situated in areas where the Leduc salts have been

extensively leached. These relationships suggest that a significant salt leaching occurred in post-glacial times, possibly in response to glacial loading and unloading and an influx of unsaturated glacial melt water. It is very possible that leaching is still occurring.

7) Elk Point (Cold Lake and Prairie Evaporite) salts are present within the study area. Although we have found no evidence that these salts have been leached in the study area, it is possible that the dissolution of these underlying halites could have triggered the leaching of the Wabamun and/or Leduc salt. Within the confines of the postulated Leduc sub-basins, the dissolution of the Wabamun salt could have been triggered by the leaching of the underlying Leduc salt. Such leaching could have occurred at any time after the deposition of the Wabamun salt.

8) The dissolution of the Leduc and Wabamun salts has occurred at various times during the geologic past, supporting the thesis that dissolution, in places, has been more-or-less continuous since deposition. Several trigger mechanisms have been identified and it has been suggested that leaching is self-perpetuating. With respect to this self-perpetuating process, we note that the established dissolution fronts do not advance at a uniform rate. These observations suggest that a number of secondary factors influence salt dissolution. Consideration should be given to effects of features and/or processes such as regional tectonism, periods of emergence, underlying reefs, the differential compaction of pre-salt sediment, uneven loading and unloading, gypsum to anhydrite conversion (and vice-versa), facies changes within both the salt and encompassing strata, the local hydrological and geochemical environment and changes therein, and the effects of oil and gas wells.

9) The timing of salt dissolution is of significance to the explorationist for several reasons: 1) stratigraphic traps can form where reservoir facies were either preferentially deposited or preserved in salt-dissolution lows; 2) reservoir facies can develop in high energy environments such as topographic highs that are controlled by salt edges or remnants; 3) structural traps can form where reservoir facies are draped across salt remnants or collapse features; and 4) salt remnants can be misinterpreted as reefs, faults or other structural features.

10) The methodology employed in this study (Anderson and Brown, 1991b), is based on the premise that the dissolution of subsurface salt causes the contemporaneous collapse of the overlying strata. The thickness of leached salt and the magnitude of collapse are assumed to be equal. Although the methodology appears to be relatively robust, as evidenced by the suite of compatible, consistent, restored structure maps, it might not, in places, adequately account for processes such as: 1) non-uniform primary deposition; 2) erosion; 3) differential compaction; 4) horizontal strain associated with collapse; 5) differential compaction of infill (compensation) sediments; 6) salt flow; 7) dissolution of underlying salts; and 8) faulting.

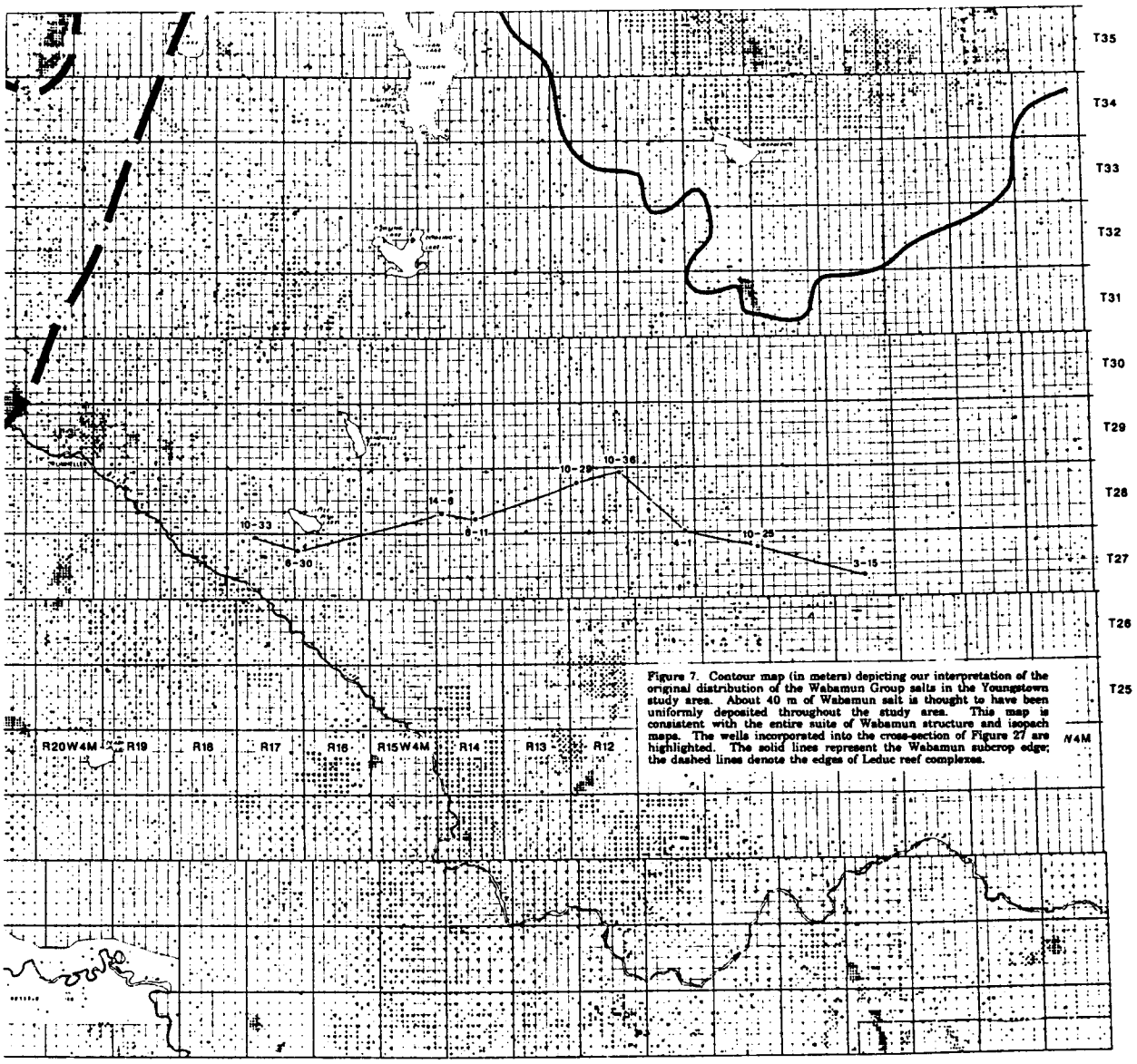

Figure VII:4:4. Contour map (m) depicting the original distribution of the Wabamun Group salts. About 40 m of Wabamun salt is thought to have been uniformly deposited throughout the study area. The wells incorporated into the cross-section of Figure VII:4:11 are highlighted.

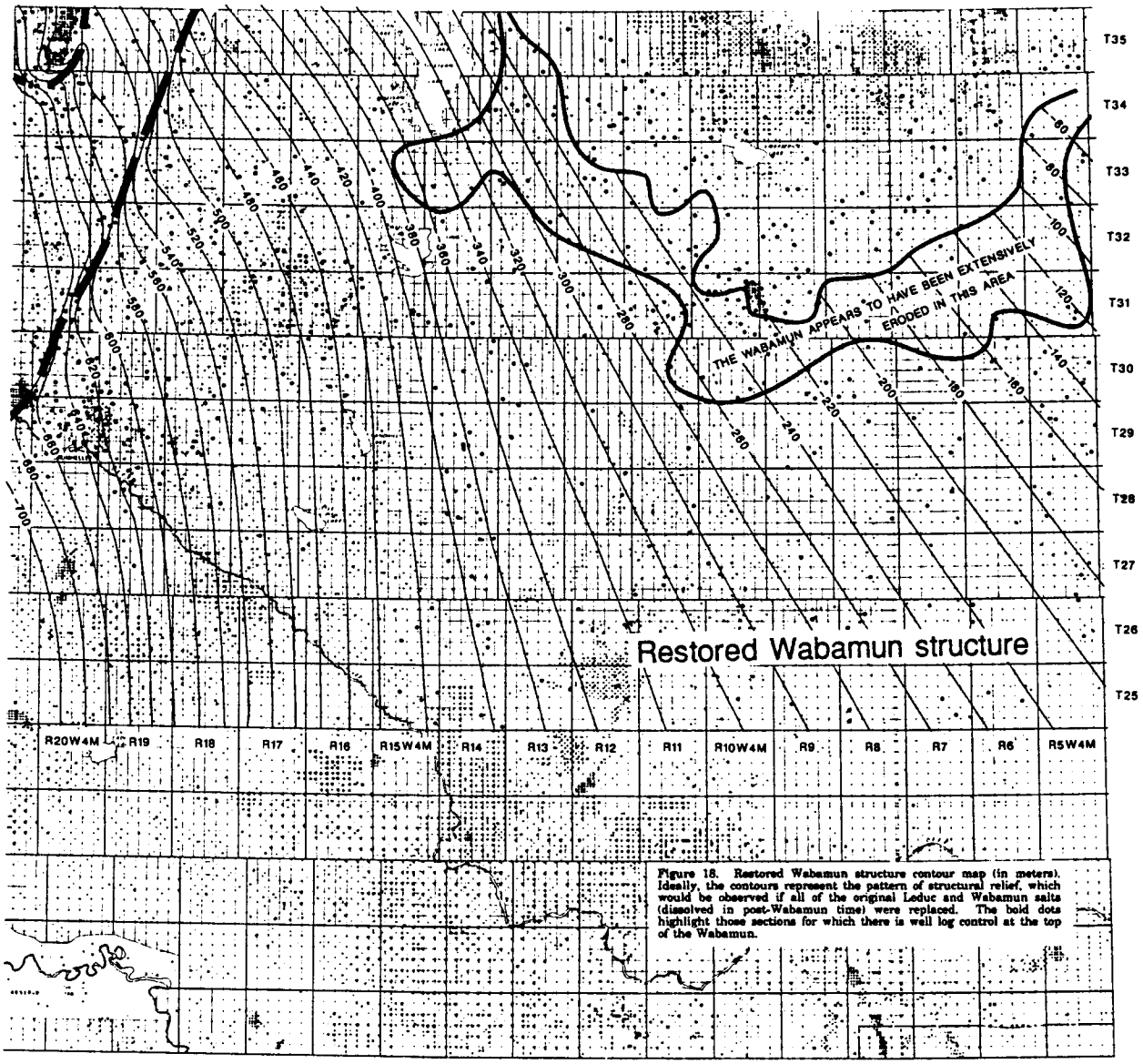

Figure VII:4:5. Restored Wabamun structure contour map (m). Ideally, the contours represent the pattern of structural relief, that would be observed if all of the original Leduc and Wabamun salts (dissolved in post-Wabamun time) were replaced.

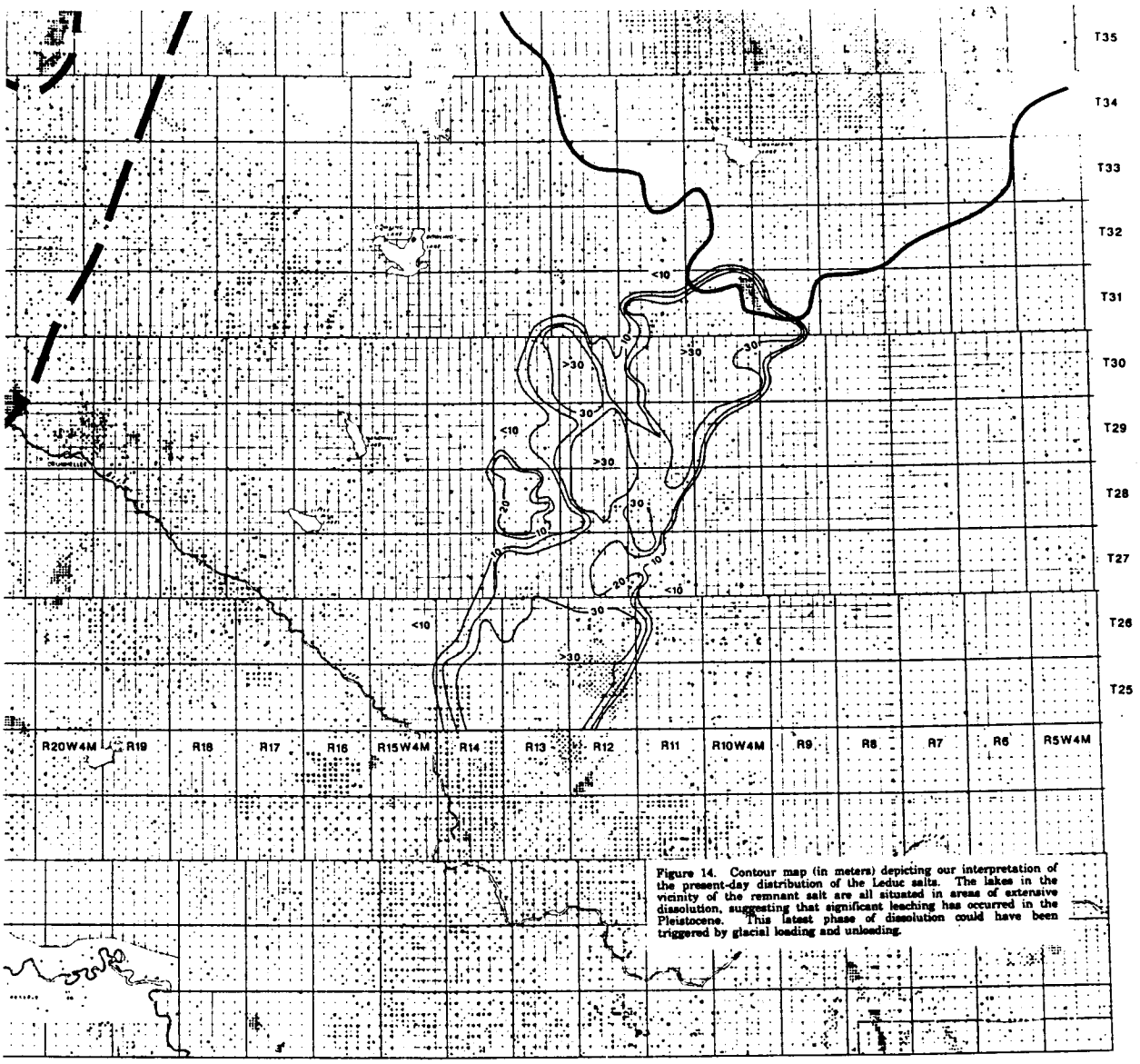

Figure VII:4:6. Contour map (m) depicting the present-day distribution of the Leduc salts. The lakes in the vicinity of the remnant salt are all situated in areas of extensive dissolution, suggesting that significant leaching has occurred in the post-Pleistocene. This latest phase of dissolution could have been triggered by glacial loading and unloading.

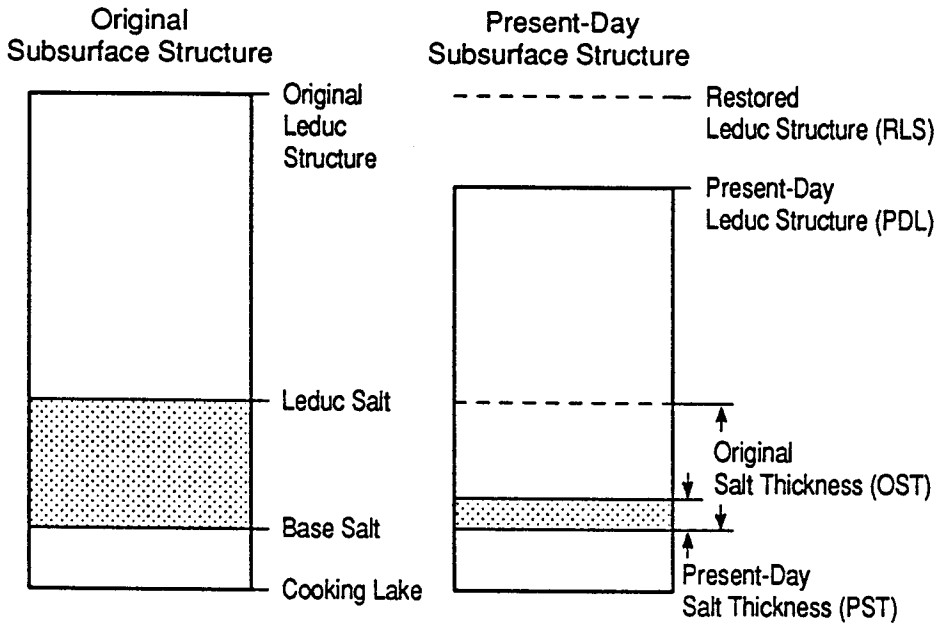

Figure VII:4:7. Schematic diagram illustrating the technique used to calculate the present-day thickness of the Leduc salt. At each control point, our present-day salt-thickness estimate PST (A) equals the original salt-thickness OST (B) less the difference between the restored RLS (C) and present-day PDL (D) Leduc structure values. We use the formula: A = B + (C - D).

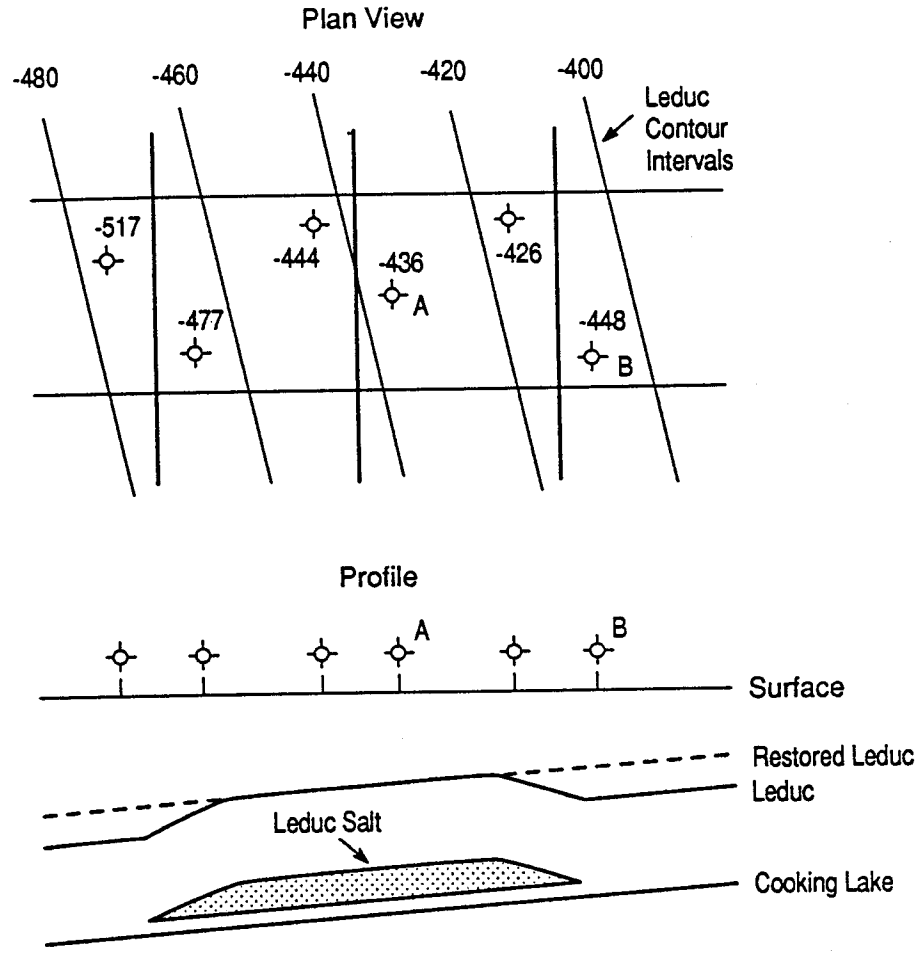

Figure VII:4:8. Schematic diagram illustrating the technique used to calculate the thickness of leached Leduc salt (post-Leduc dissolution). On the map the top of the Leduc at each control point has been noted and the restored Leduc structure has been contoured; on the section both the restored and present-day Leduc tops have been correlated. At each well control point, the thickness of salt dissolved in post-Leduc time is equal to the difference between the restored and present-day Leduc structure values. For example at wells A and B, 0 m (-444 m - (-444 m)) and 20 m (-428 m - (-448 m)) of salt have been dissolved respectively.

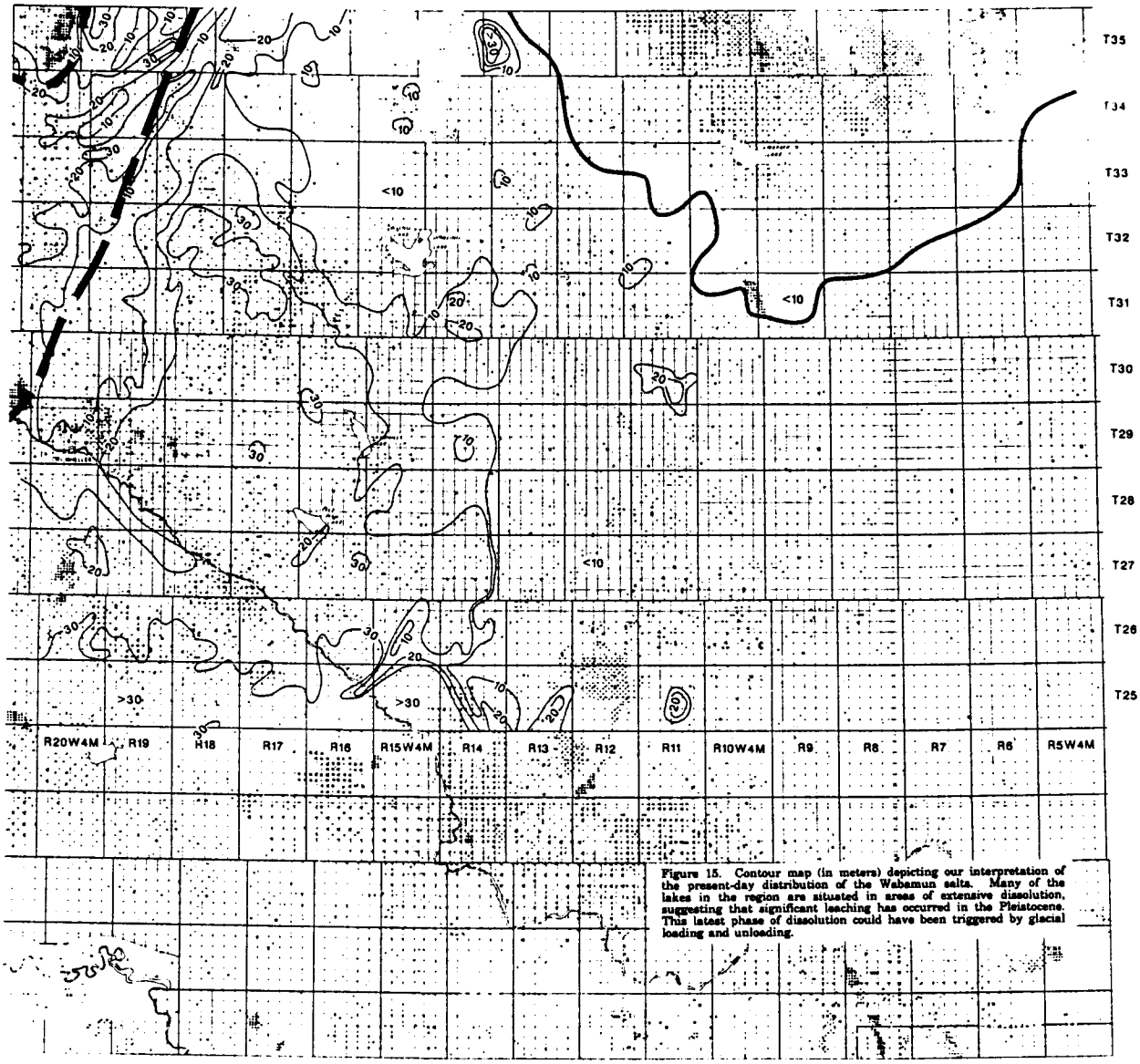

Figure VII:4:9. Contour map (m) depicting the present-day distribution of the Wabamun salts. Many of the lakes in the region are situated in areas of extensive dissolution, suggesting that significant leaching has occurred in the post-Pleistocene. This latest phase of dissolution could have been triggered by glacial loading and unloading.

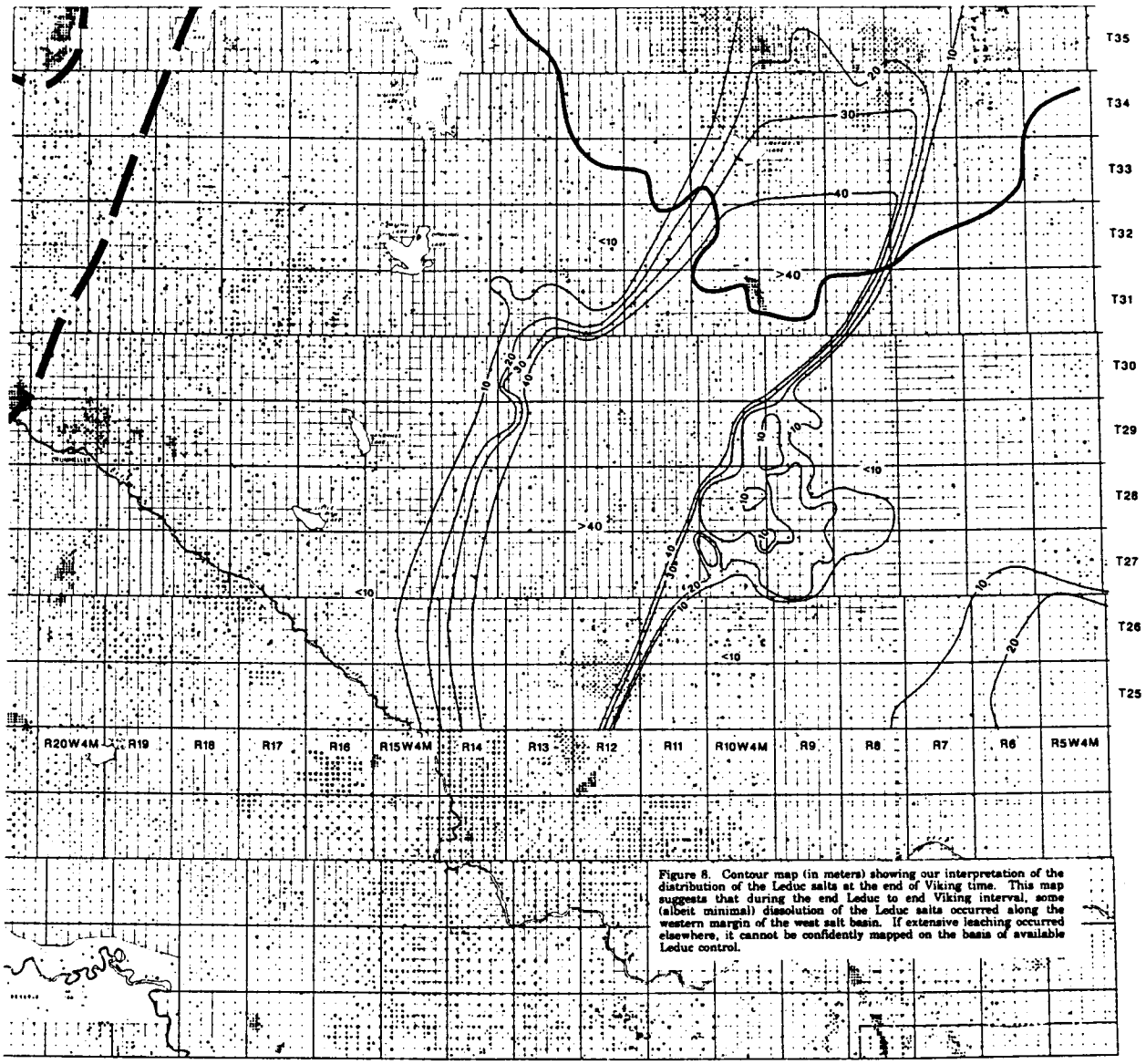

Figure VII:4:10. Contour map (m) showing the distribution of the Leduc salts at the end of Viking time. This map suggests that during the end Leduc to end Viking interval, some (albeit minimal) dissolution of the Leduc salts occurred along the western margin of the west salt-basin. If extensive leaching occurred elsewhere, it cannot be confidently mapped on the basis of available well-log control.

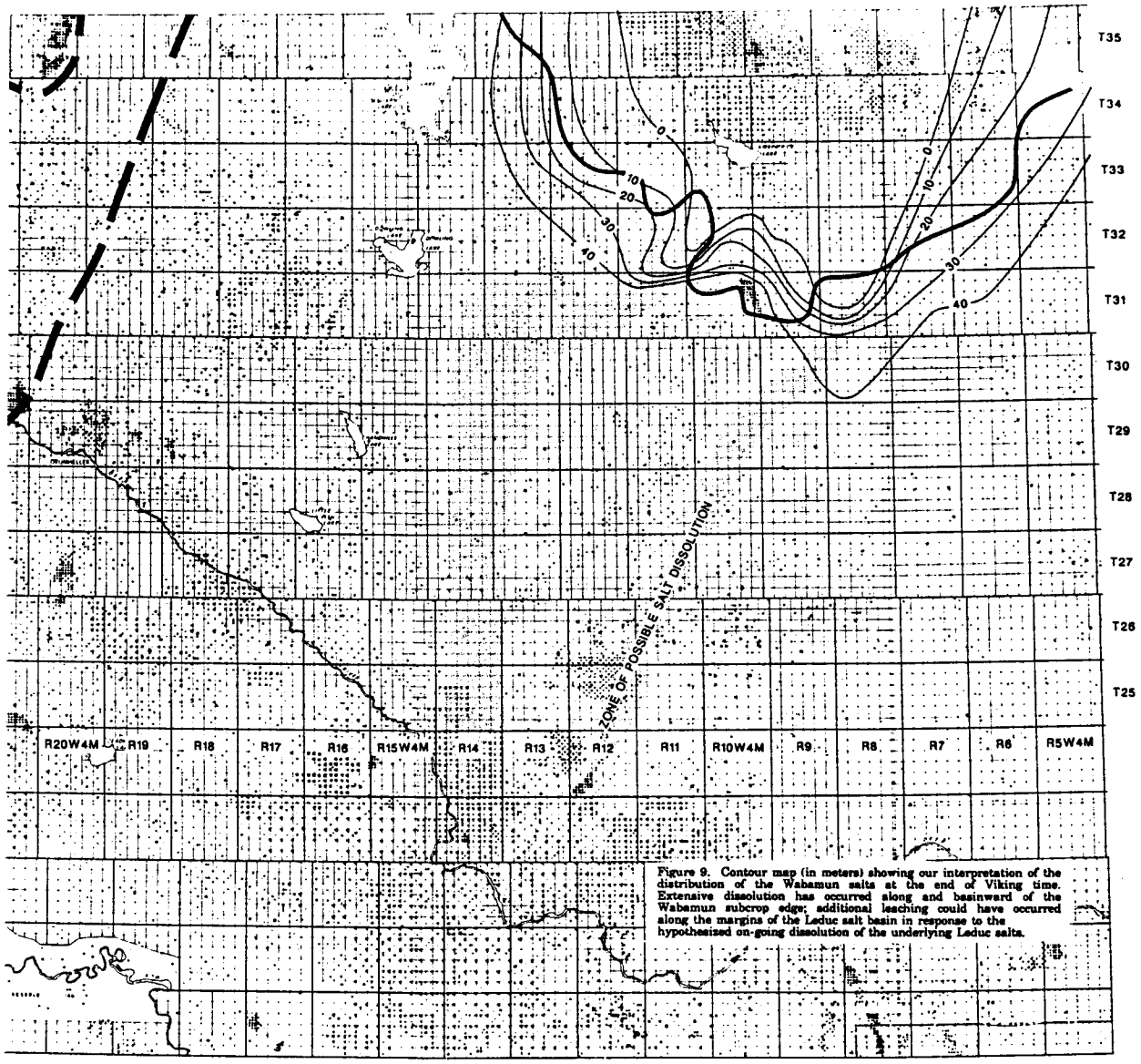

Figure VII:4:11. Contour map (m) showing the distribution of the Wabamun salts at the end of Viking time. Extensive dissolution has occurred along and basinward of the Wabamun subcrop edge; additional leaching could have occurred along the margins of the Leduc salt-basin in response to the hypothesized dissolution of the underlying Leduc salts.

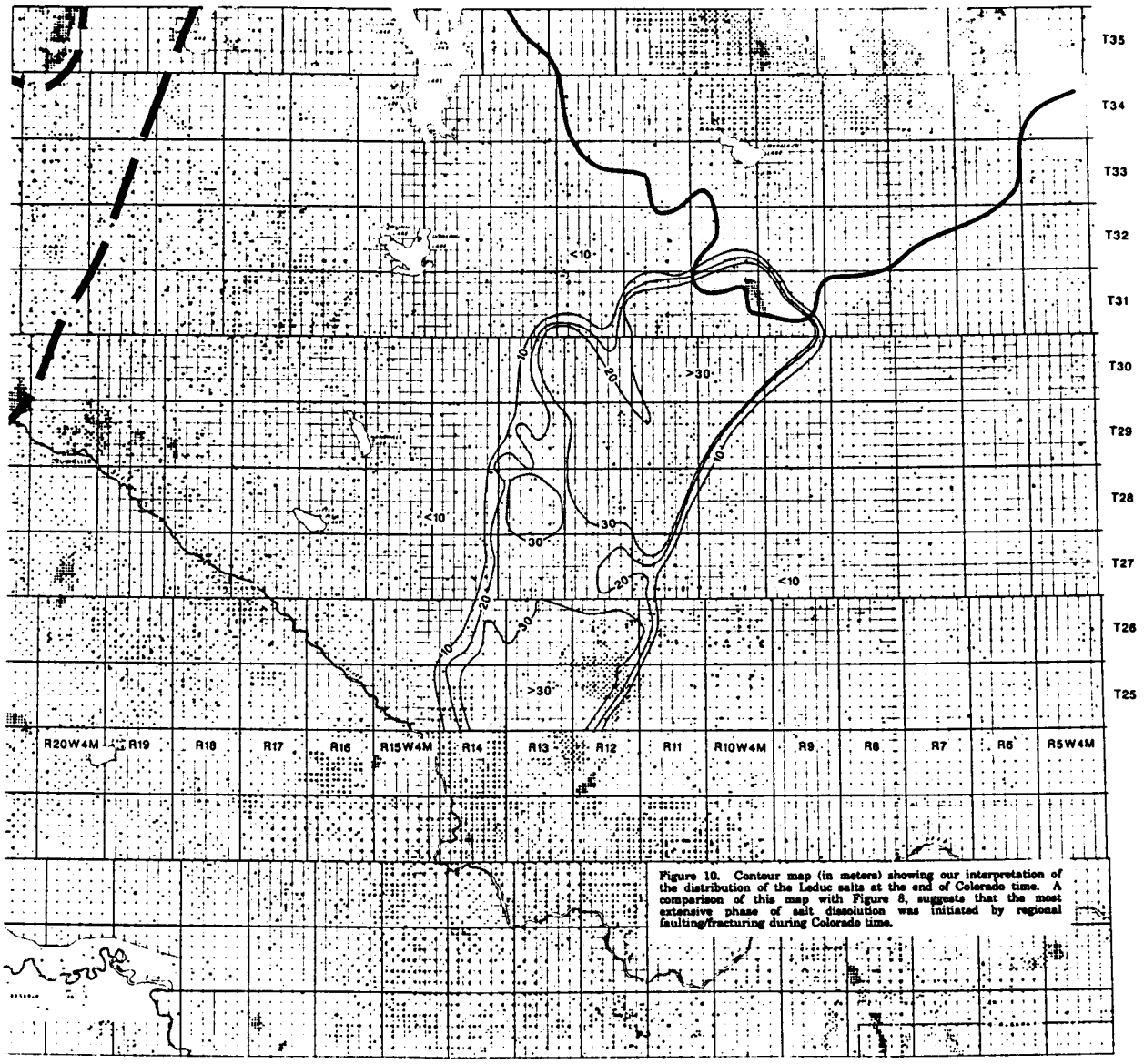

Figure VII:4:12. Contour map (m) showing the distribution of the Leduc salts at the end of Colorado time. A comparison of this map with Figure VII:4:10, suggests that an extensive phase of salt dissolution was initiated by regional faulting/fracturing during Colorado time.

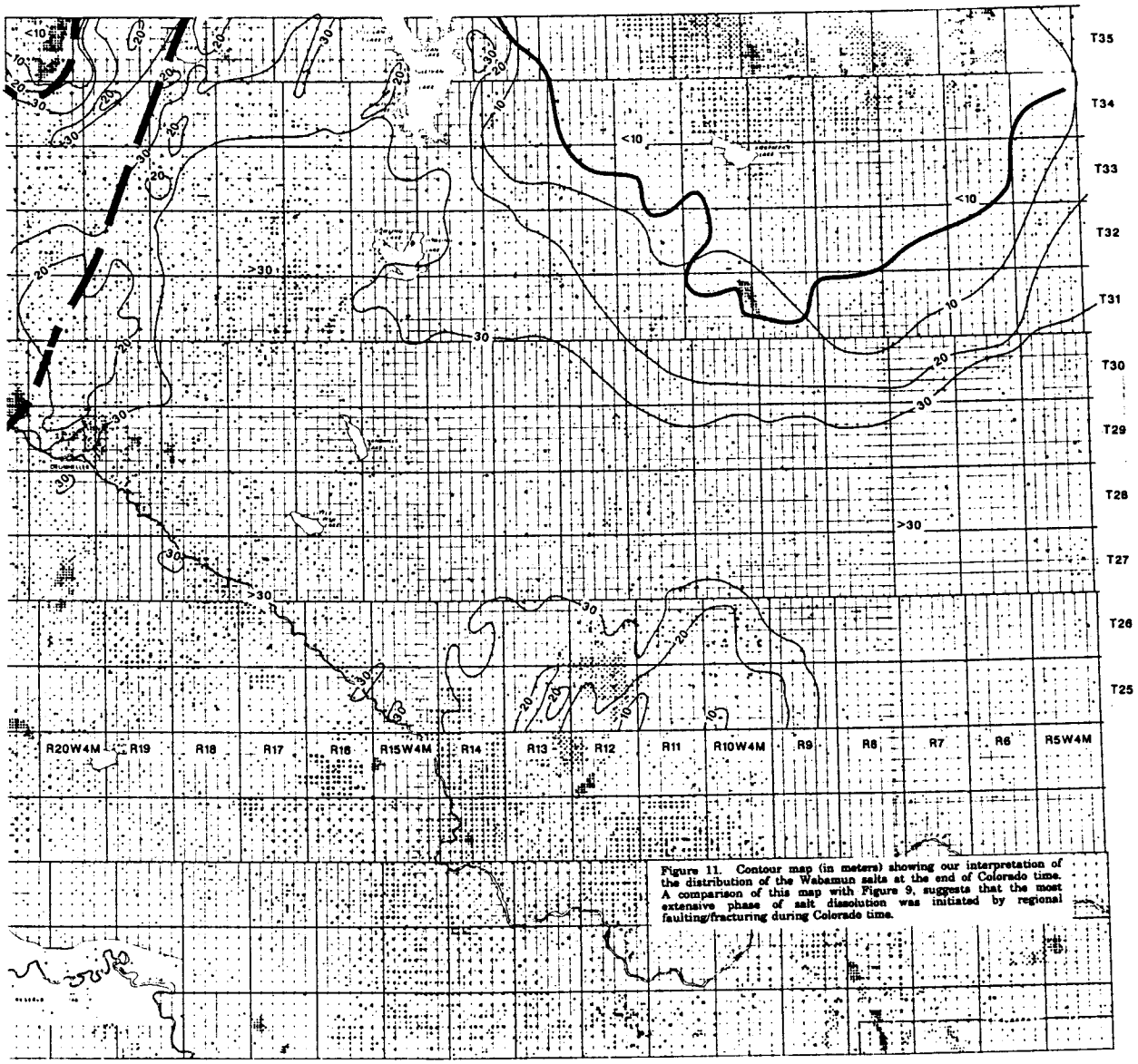

Figure VII:4:13. Contour map (m) showing our the distribution of the Wabamun salts at the end of Colorado time. A comparison of this map with Figure VII:4:11, suggests that an extensive phase of salt dissolution was initiated by regional faulting/fracturing during Colorado time.

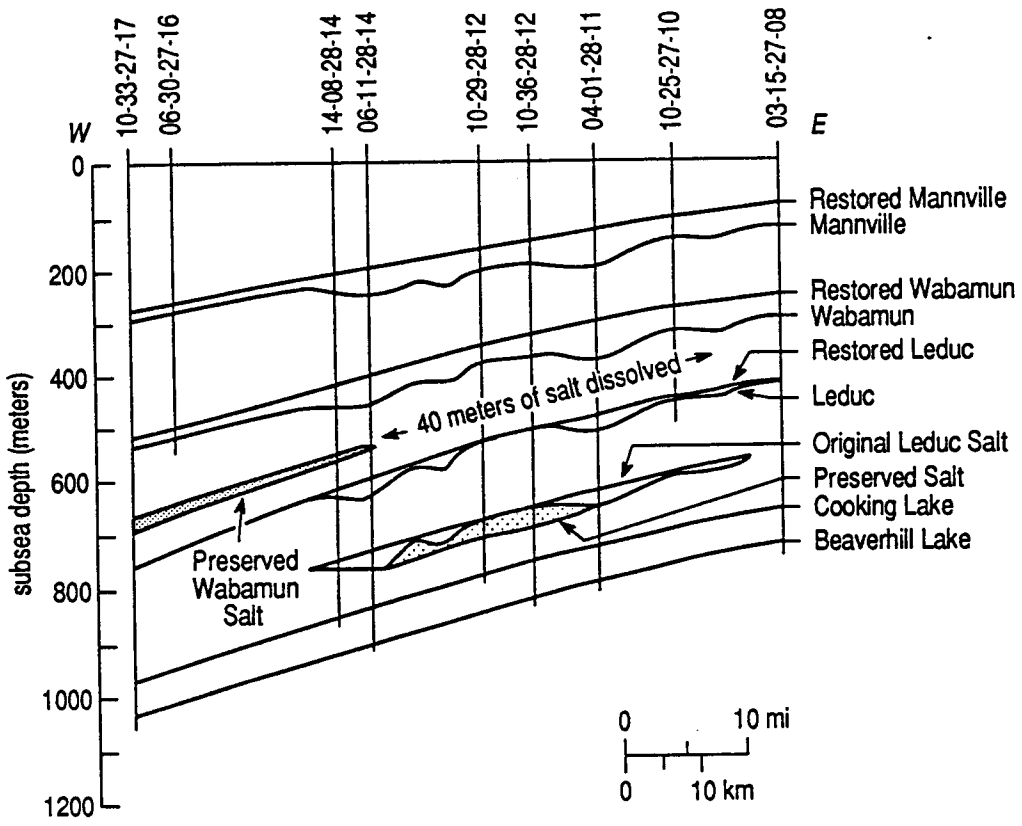

Figure VII:4:14. West-to-east geologic cross-section from the Youngstown study area illustrating the discontinuous nature of the Wabamun and Leduc salts. Both present-day and reconstructed profiles are displayed on the cross-section. The wells incorporated into the cross-section are highlighted on Figure VII:4:4.

5) PRAIRIE EVAPORITE SALT: LLOYDMINSTER AREA

A) Overview

There are five main Elk Point Group (Lower/Middle Devonian age) salts in the Lloydminster study area (T50-T65, R15W3M-R10W4M): those of the Leofnard Member (Prairie Evaporite Formation), Cold Lake Formation, upper Lotsberg Formation and lower Lotsberg Formation (Figures VII:1:1-VII:1:2, VII:2:1-VII:2:17). Within the study area, the eastern edges of the Leofnard Member, Cold Lake, and upper Lotsberg salts appear to be dissolutional and relatively abrupt. In contrast, the salts lower Lotsberg Formation do not appear to have been extensively leached within the study area. Whitkow Member salt (Prairie Evaporite Formation) does not appear to have been deposited within the study area.

In an effort to elucidate the dissolution of the Elk Point salts and in order to map their present-day distribution in the Lloydminster area (T50-T65, R15W3M-R10W4M), we conducted a regional, well-log based study (with limited seismic and gravity control). In particular, we analyzed: 1) variations in the thicknesses of the remnant Prairie Evaporite, Cold Lake and Lotsberg salts; 2) variations in the thicknesses of the stratigraphic units which encompass these salts; 3) the patterns of structural relief in the subsurface; 4) gravity profiles; and 5) collapse features on seismic data. We identified correlation patterns involving the thicknesses of the Prairie Evaporite, Cold Lake and Lotsberg intervals, structural relief at the Prairie Evaporite, Cold Lake and Lotsberg levels, relief along post-Elk Point horizons, and the thicknesses of the remnant salts. On the basis of these relationships (and following the methodology outlined by Anderson and Brown, 1992), we estimated the present-day distribution of the Elk Point salts in the study area and reconstructed the distribution of these evaporites at selected times from late Paleozoic to the present (Figures VII:5:1-VII:5:5).

A) end Lotsberg
B) end Cold Lake
C) end Prairie Evaporite
D) end base Cretaceous
E) end Mannville
F) end Viking
G) end Second Specks
H) present-day

These maps are significant in that they elucidate the timing, the magnitude, and to some extent, the mechanisms of dissolution. From these maps several significant conclusions can be drawn or reconfirmed:

1) The salts of the Leofnard Member (upper unit of the Prairie Evaporite Formation) were uniformly deposited throughout the Lloydminster study area. The net thickness (depositional) of these salts varied from a high of about 150 m (northern and eastern parts of the study area) to a low of about 80 m (southwestern part of the study area; Figure VII:5:7-VII:5:9). The salts of the Whitkow Member (lower unit of the Prairie Evaporite Formation) are not present in the study area and do not appear to have been extensively leached from any of the Elk Point test wells in the study area. This strongly suggests that these salts were not deposited in the study area;

2) The most extensive phases of Leofnard salt dissolution occurred during the pre-Cretaceous hiatus and post-Second Specks intervals. During the pre-Cretaceous, the main salt dissolution front is thought to have migrated westward from the projected subcrop edge into the study area. This conclusion is based on our analysis of the Souris River and sub-Cretaceous structure maps from which we infer that dissolution of the Elk Point salts in the study area was initiated in the post-Souris River/pre-Cretaceous interval. (Note: in the northeastern part of the study the Souris River is the pre-Cretaceous subcrop.) The second major phase of dissolution appears to have occurred in the post-Second Specks interval. This inference is based on the similarity in the patterns of structural relief at the Mannville, Viking and Second Specks levels. These maps suggest that the dissolution front migrated to the west relatively slowly during the Mannville/Second Specks interval and then more rapidly sometime thereafter. We have had difficulty further refining the timing of this later phase because the Late Cretaceous subcrops throughout the study area.

3) The dissolution of the Leofnard salt appears to have been initiated and/or enhanced by some or all of six principal processes: 1) the near-surface exposure of these salts, as a result of the erosion of the overlying Paleozoic sediment during the post-Paleozoic hiatus; 2) the influx of meteoric water, which could have been introduced into the system along the Elk Point outcrop/subcrop to the east; 3) the partial dissolution of the underlying Cold Lake and upper Lotsberg salt; 4) faulting/fracturing during or after the mid-Late Cretaceous; 5) salt movement; and 6) glacial loading and unloading;

4) With respect to erosion during post-Paleozoic time, the earliest phases of Leofnard salt dissolution probably occurred along the Prairie Evaporite outcrop edge (to the east of the study area) during the post-Paleozoic hiatus. As indicated on the suite of reconstructed maps, the dissolution front, which was established along the outcrop edge, appears to have migrated over time to the west, suggesting that leaching is a self-perpetuating process.

5) With respect to the influx of meteoric water, it is probable that the westward migration of the main salt edge was initiated and/or accentuated

by the westward flow of fresh water through the adjacent sediment. These waters could have entered the system along the Elk Point outcrop/subcrop to the east of the study area.

6) The dissolution of the Leofnard salt could have been triggered by the leaching of the underlying Cold Lake and/or upper Lotsberg salt (Figure VII:5:7-VII:5:9). Such leaching could have occurred at any time after the deposition of the Prairie Evaporite.

7) The patterns displayed on the suite of Leofnard salt paleo-distribution maps suggest that dissolution could have been influenced by the reactivated of pre-existing, more-or-less orthogonally oriented (NNW/ESE), regional fault/fracture planes during or after the mid-Late Cretaceous. The orientation of these hypothetical fault/fracture planes is more-or-less parallel/orthogonal to the southern edge of the Meadow Lake Escarpment in the study area, suggesting that postulated lineaments could have influenced the development of the Lower Elk Point Basin. (In the Stettler area of Alberta, the authors have attributed the extensive dissolution of the Wabamun salts in Colorado time to regional faulting/fracturing at this time).

8) The pattern displayed on the suite of Leofnard salt paleo-distribution maps suggest that some movement of these salts may have occurred in the vicinity of the main salt edge during or after the mid-Late Cretaceous. Such movement (envisioned by the authors as analogous to growth-fault type slumping/salt flow) could have been caused by excessive overburden pressure and/or glacial loading. This process could have been triggered by regional faulting/fracturing and enhanced by pre-existing fault/fracture planes and/or an influx of meteoric water.

9) Several lakes and rivers (Jackfish Lake, Murray Lake, Birch Lake, Helene Lake, Midnight Lake, Stony Lake, Turtle Lake, Brightsand Lake, Bronson Lake, Cold Lake, Marie Lake, and Saskatchewan River) are situated in areas where the Leofnard salts are thin or absent, suggesting that a significant amount of leaching has occurred in post-glacial times, possibly in response to glacial loading and unloading.

10) The Cold Lake salts in the study area were widely deposited only to the north of the Meadow Lake Escarpment (Early Elk Point Basin; Figure VII:5:6). The Cold Lake salt is thought to have attained a maximum thickness of about 50 m in the northwestern part of the study area and depositionally thinned to the east (Figure VII:5:2).

11) The most extensive phases of Cold Lake salt dissolution appears to have occurred during the pre-Cretaceous hiatus and post-Second Specks intervals. During the pre-Cretaceous, the main salt dissolution front is thought to have migrated westward from the projected outcrop edge into the study area. This conclusion is based on our analysis of the Souris

River and sub-Cretaceous structure maps from which we infer that dissolution of the Elk Point salts in the study area was initiated in the post-Souris River/pre-Cretaceous interval. (Note: in the northeastern part of the study the Souris River is the pre-Cretaceous subcrop.) A second major phase of dissolution appears to have occurred in the post-Second Specks interval. This inference is based on the similarity in the patterns of structural relief at the Mannville, Viking and Second Specks levels. These maps suggest that the dissolution front migrated to the west relatively slowly during the Mannville/Second Specks interval and then more rapidly sometime thereafter. We have had difficulty further refining the timing of this later phase because the Late Cretaceous subcrops throughout the study area.

12) The leaching of the Cold Lake salt is thought to have been initiated and/or enhanced by five principal processes: 1) the near-surface exposure of these salts, as a result of the erosion of the overlying Paleozoic sediment during the post-Paleozoic hiatus; 2) the influx of meteoric water, which could have been introduced into the system along the Elk Point outcrop/subcrop to the east; 3) the partial dissolution of the underlying upper Lotsberg salt; 4) regional faulting/fracturing during or after the mid-Late Cretaceous; and 5) glacial loading and unloading.

13) With respect to erosion during post-Paleozoic time, the earliest phases of Cold Lake salt dissolution probably occurred during the post-Paleozoic hiatus and closer to the Elk Point outcrop edge (to the east of the study area).

14) With respect to the influx of meteoric water, it is very possible that the westward migration of the main Cold Lake salt edge was initiated and/or accentuated by the westward flow of fresh water through the adjacent sediment. These waters could have entered the system along the Elk Point outcrop/subcrop to the east.

15) The dissolution of the Cold Lake salt could also have been triggered by the leaching of the underlying upper Lotsberg salt. Such leaching could have occurred at any time after the deposition of the Cold Lake salt.

16) If the dissolution of the Leofnard salt was influenced by regional faulting/fracturing during or after the mid-Late Cretaceous, then it is likely that the Cold Lake salts would have been similarly affected. Due to the paucity of deep well control near the edge of this salt, the characteristics of the dissolution front (orientation, abruptness, etc) cannot be conclusively established.

17) Several of the larger lakes in the Lower Elk Point Basin area (Lac Des Iles, Big Head, Pierce Lake, Cold Lake, Makwa) are situated in areas where the Cold Lake salts have been extensively leached, suggesting that a significant amount of dissolution has occurred in post-glacial times, possibly

in response to glacial loading and unloading.

18) The upper Lotsberg salts in the study area were widely deposited only to the north of the Meadow Lake Escarpment (Lower Elk Point Basin; Figure VII:5:10). These salts attained maximum thickness of about 150 m in the northwestern part of the study area and depositionally thinned to the east (Figure VII:5:7). The salts of the lower Lotsberg (lower unit of the Lotsberg Formation) were deposited only in the northwestern part of the study area (north of the Meadow Lake Escarpment; Figure VII:5:6). These salts were encountered in only three wells (16-28-56-8W4M, 12-19-61-8W4M and 6-13-63-8W4M) and attained maximum thicknesses on the order of 50 m. They do not appear to have been leached from any of the Elk Point test wells in the study area;

19) The most extensive phases of upper Lotsberg salt dissolution appears to have occurred during the pre-Cretaceous hiatus and post-Second Specks intervals. During the pre-Cretaceous, the main salt dissolution front is thought to have migrated westward from the projected outcrop edge into the study area. This conclusion is based on our analysis of the Souris River and sub-Cretaceous structure maps from which we infer that dissolution of the Elk Point salts in the study area was initiated in the post-Souris River/pre-Cretaceous interval. (Note: in the northeastern part of the study the Souris River is the pre-Cretaceous subcrop.) A second major phase of dissolution appears to have occurred in the post-Second Specks interval. This inference is based on the similarity in the patterns of structural relief at the Mannville, Viking and Second Specks levels. These maps suggest that the dissolution front migrated to the west relatively slowly during the Mannville/Second Specks interval and then more rapidly sometime thereafter. We have had difficulty further refining the timing of this later phase because the Late Cretaceous subcrops throughout the study area.

20) The leaching of the upper Lotsberg salt is thought to have been initiated and/or enhanced by four principal processes: 1) the near-surface exposure of these salts, as a result of the erosion of the overlying Paleozoic sediment during the post-Paleozoic hiatus; 2) the influx of meteoric water, which could have been introduced into the system along the Elk Point outcrop/subcrop to the east; 3) regional faulting/fracturing during or after the mid-Late Cretaceous; and 4) glacial unloading.

21) With respect to erosion during post-Paleozoic time, the earliest phases of Cold Lake salt dissolution probably occurred during the post-Paleozoic hiatus and closer to the Elk Point outcrop edge (to the east of the study area).

22) With respect to the influx of meteoric water, it is very possible that the westward migration of the main upper Lotsberg salt edge was initiated and/or accentuated by the westward flow of fresh water through the

adjacent sediment. These waters could have entered the system along the Elk Point outcrop/subcrop to the east.

23) If the dissolution of the Leofnard salt was influenced by regional faulting/fracturing during or after the mid-Late Cretaceous, then it is likely that the upper Lotsberg salts would have been similarly affected. Due to the paucity of deep well control near the edge of these salts, the characteristics of the dissolution front (orientation, abruptness, etc.) cannot be conclusively established.

24) Several of the larger lakes in the Lower Elk Point Basin area (Makwa, Flotten Lake, Greig Lake, Waterhen Lake, and Meadow Lake) are situated in areas where the upper Lotsberg salts have been extensively leached, suggesting that a significant amount of dissolution has occurred in post-glacial times, possibly in response to glacial loading and unloading.

25) Salt leaching appears to be self-perpetuating: a process whereby the collapse of overlying strata enhances both their porosity and permeability, thereby providing a conduit for water and facilitating further dissolution.

26) The dissolution of the Leofnard, Cold Lake and upper Lotsberg salts has occurred at various times during the geologic past, supporting the thesis that dissolution, in places, has been more-or-less continuous since deposition. The correlation between the present-day drainage pattern and salt dissolution fronts suggests that significant leaching is still occurring.

27) Several potential triggering mechanisms have been identified and it has been suggested that leaching is self-perpetuating. With respect to this self-perpetuating process, we note that the established dissolution fronts do not advance at a uniform rate. These observations suggest that a number of secondary factors influence salt dissolution. Consideration should be given to effects of the intensity and magnitude of faulting, regional tectonism, periods of emergence, underlying reefs, the differential compaction of pre-salt sediment, uneven loading and unloading, glaciation, dewatering of shales, gypsum to anhydrite conversions and vice versa, facies changes within both the salt and encompassing strata, the local hydrological and geochemical environment and changes therein, and the effects of oil and gas wells.

28) The timing of salt dissolution is of significance to the explorationist for several reasons: 1) stratigraphic traps can form where reservoir facies were either preferentially deposited or preserved in salt-dissolution lows; 2) reservoir facies can develop in high energy environments such as topographic highs that are controlled by salt edges or remnants; 3) structural traps can form where reservoir facies are draped across salt remnants or collapse features; and 4) salt remnants can be misinterpreted as reefs, faults or other structural features.

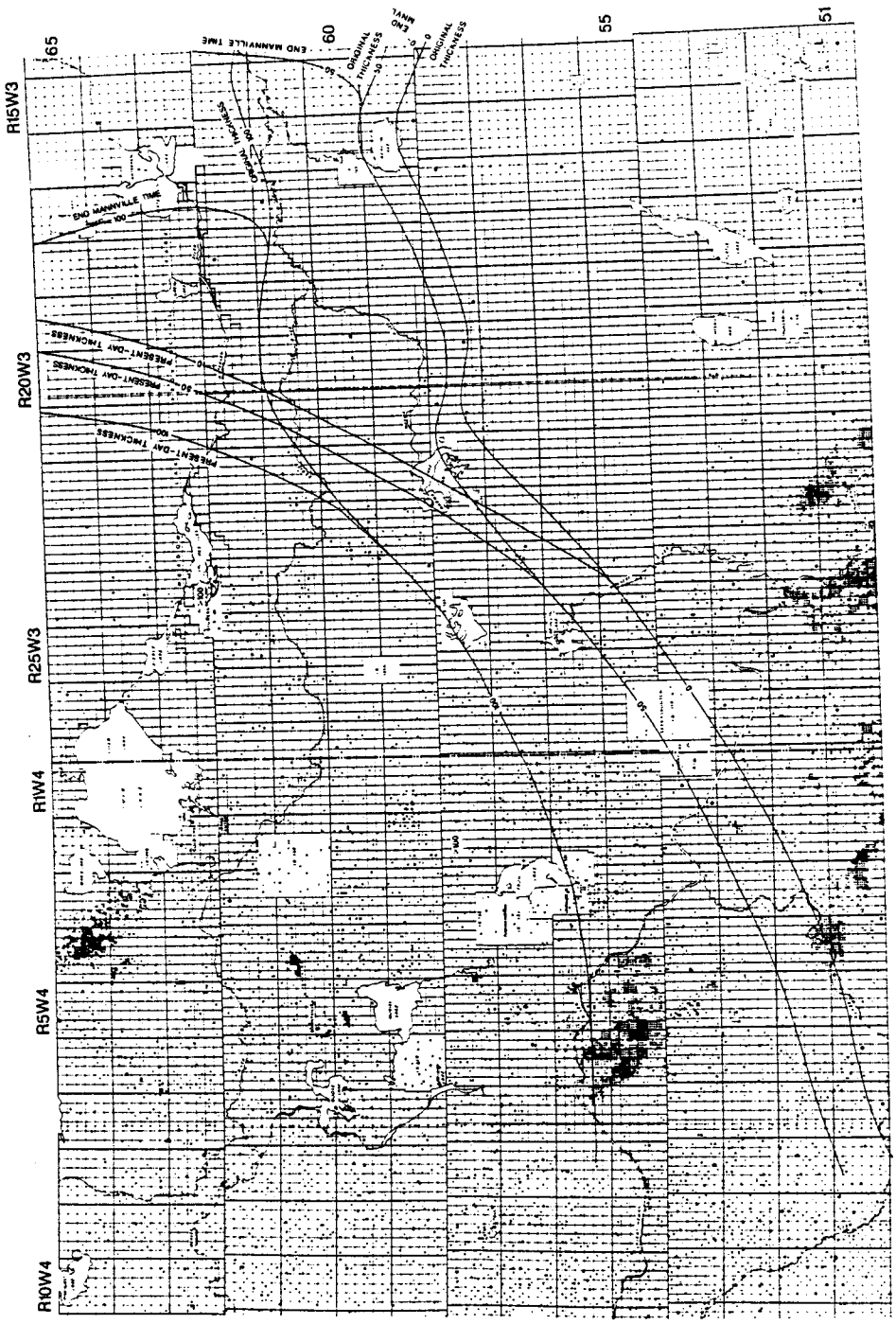

Figure VII:5:1. Contour map (m) depicting the distribution of the upper Lotsberg salt in the Lloydminster study area at three selected times: original distribution; distibution at the end of Mannville time; and present-day distribution. The bold dots highlight those sections for which there is well log control at the top of the Lotsberg.

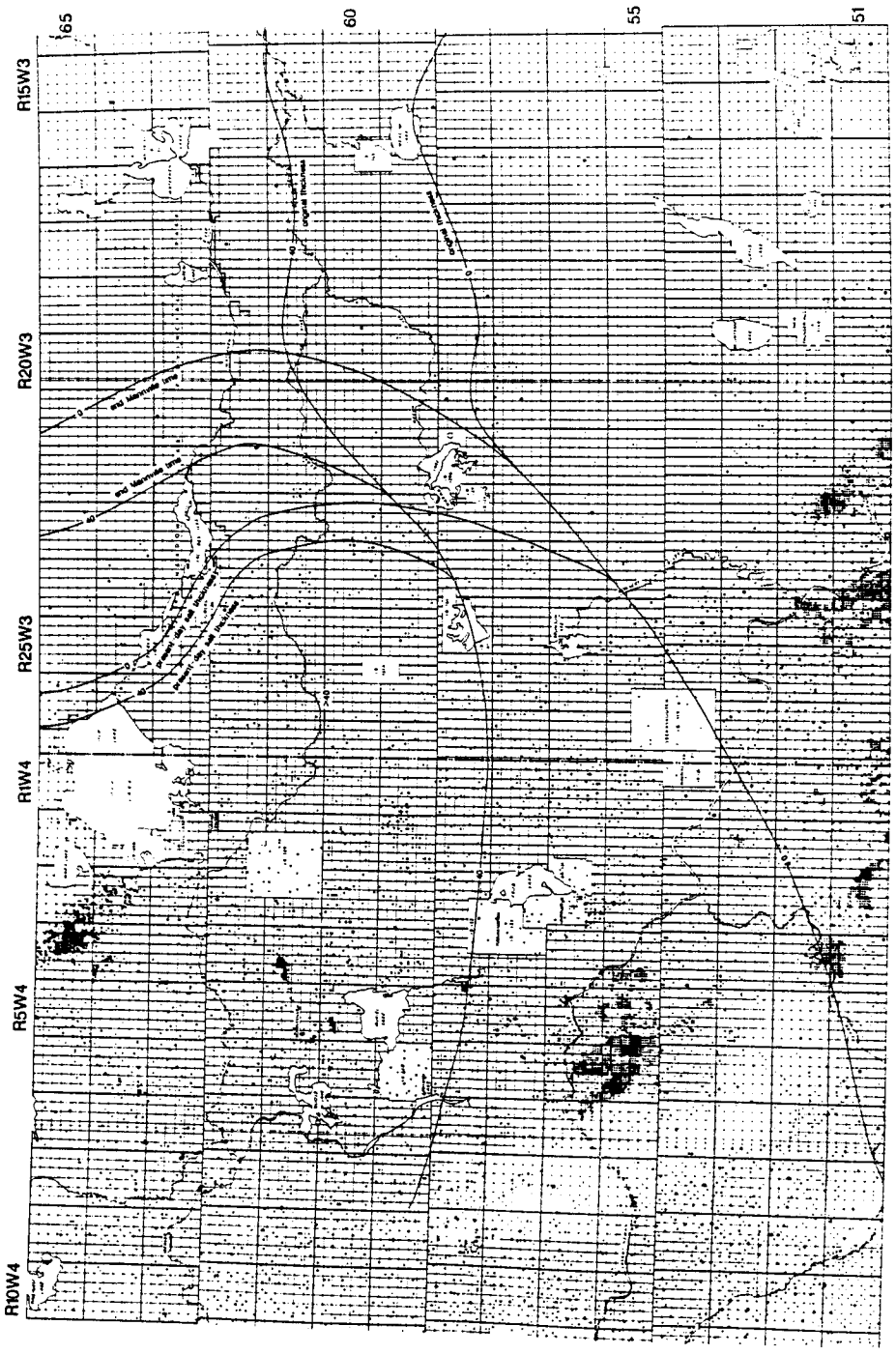

Figure VII:5:2. Contour map (m) depicting the distribution of the Cold Lake Formation salts at three selected times: original distribution; distibution at the end of Mannville time; and present-day distribution. These salts were widely distributed only in that area to the north of the Meadow Lake Escarpment (Early Elk Point Basin). The bold dots highlight those sections for which there is well log control at the top of the Cold Lake.

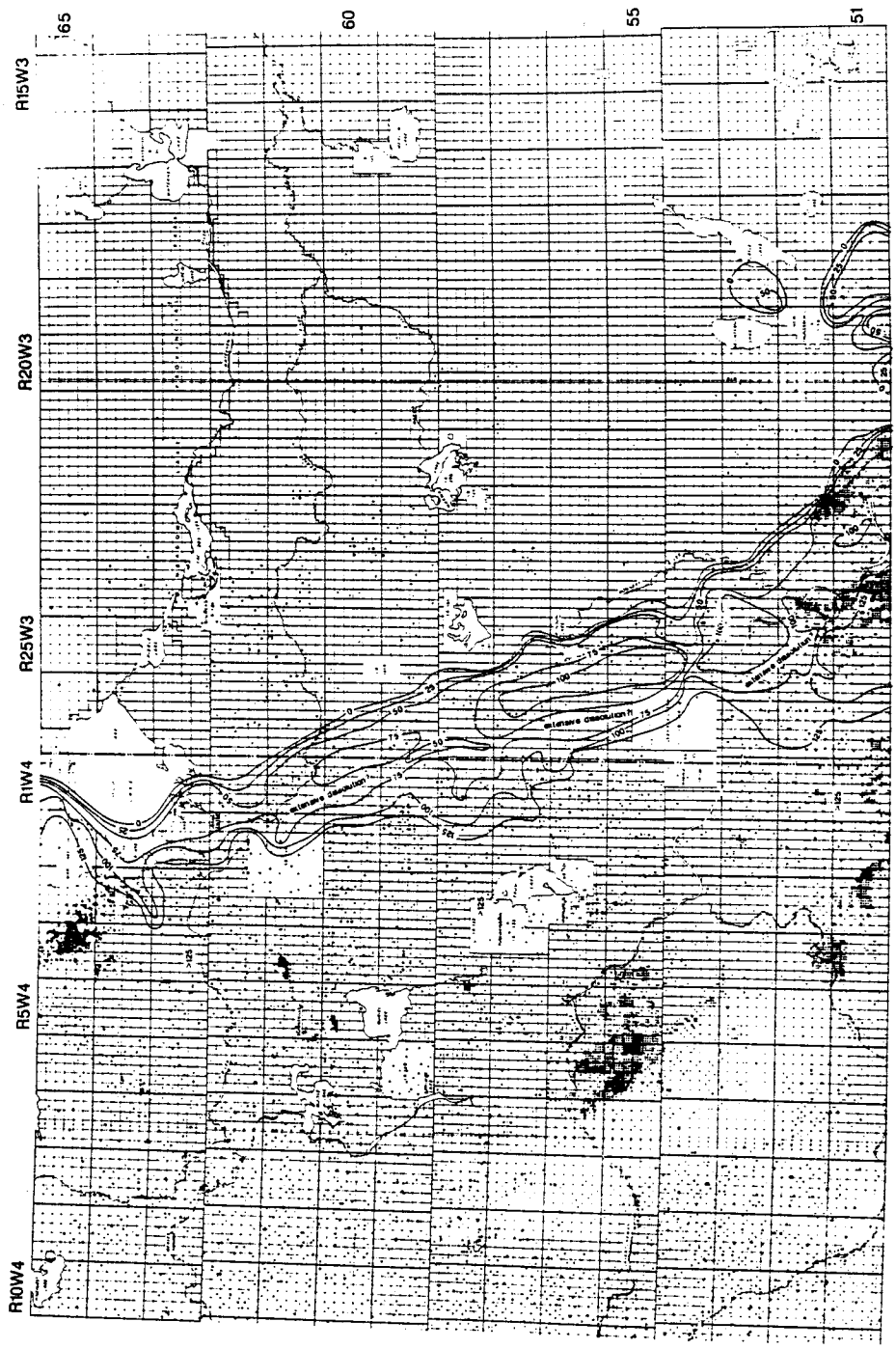

Figure VII:5:3. Contour map (m) depicting the present-day distribution of the Leofnard salts. Many of the lakes in the region are situated in areas of extensive dissolution, suggesting that significant leaching has occurred in the Pleistocene. This latest phase of dissolution could have been triggered by glacial loading and unloading.

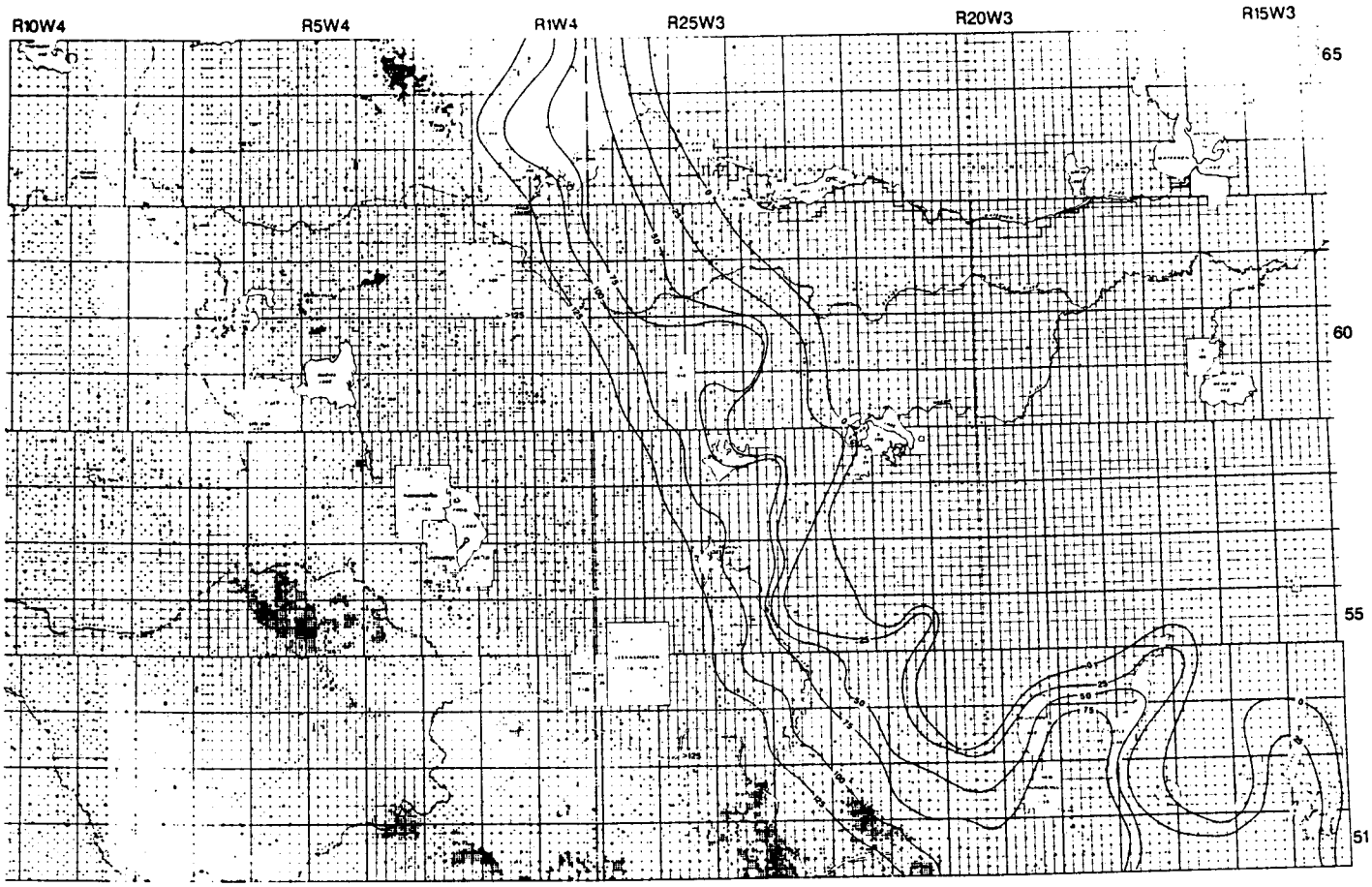

Figure VII:5:4. Contour map (m) showing the distribution of the Leofnard salts at the end of Mannville time. The Leofnard salts had been relatively stable until the onset of the pre-Cretaceous hiatus at which time the eastern edge of these salts receded rapidly westwards across the study area. This established dissolution front appears to have migrated slowly westward from Early Cretaceous until mid-Late Cretaceous. The migration rate of the dissolution front increased sometime thereafter. The timing of this accelerated migration has not be conclusively established throughout the study due to the fact that the top of the Late Cretaceous is an erosional surface and well log tops control at this level is sparse.

Figure VII:5:5. Contour map (m) depicting the original distribution of the Leofnard salts in the Lloydminster study area. Our data suggest that about 150 m were precipitated in the study area. These salts appear to have been relatively stable until the pre-Cretaceous hiatus at which time the eastern edge of these salts receded westwards across the study area.

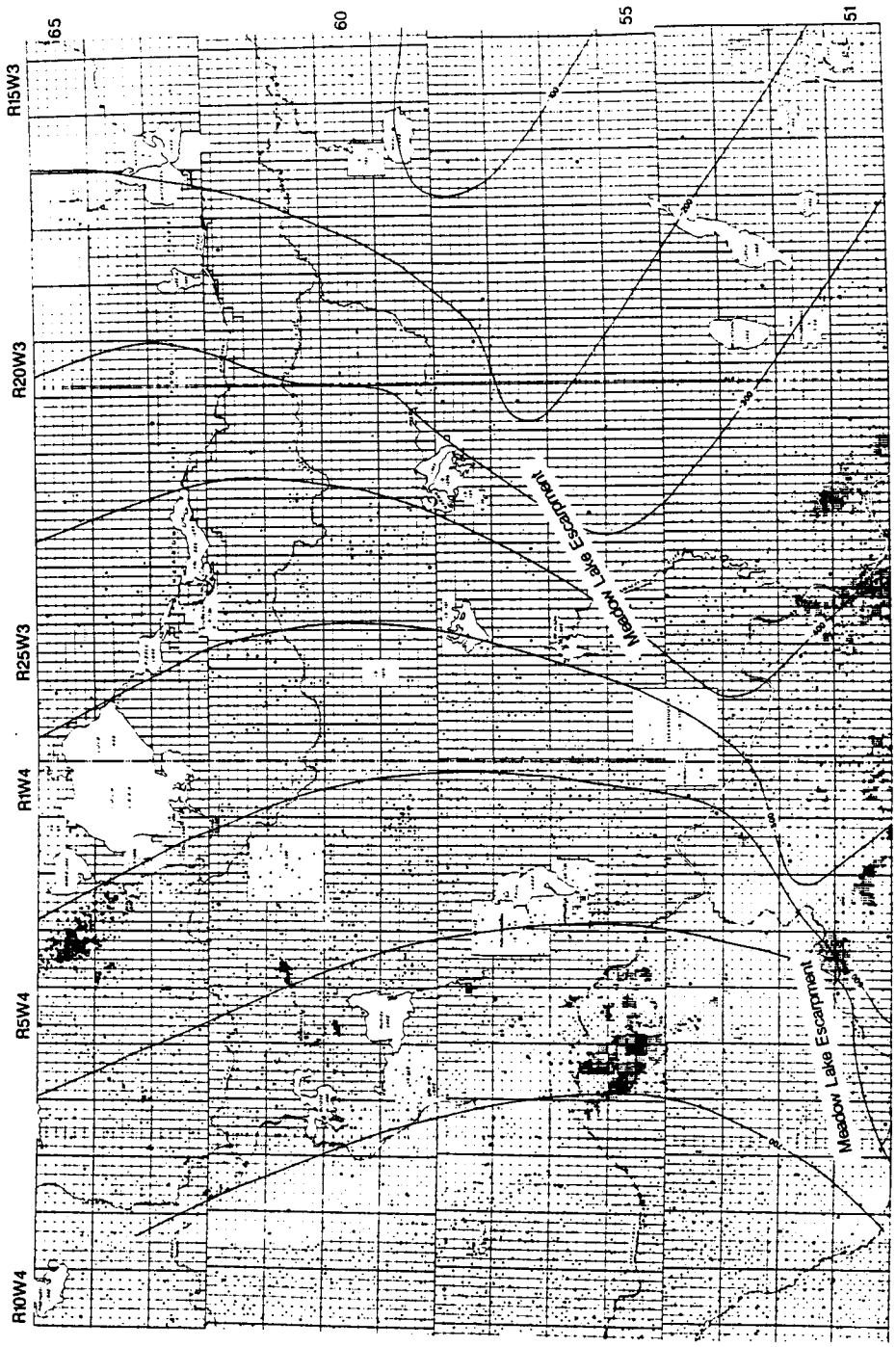

Figure VII:5:6. Contour map (m) of the subsea depth to the top of the base of the Elk Point (base Devonian). The bold dots highlight those sections for which there is well log control. The salts of the Lotsberg and Cold Lake formation (in the Lloydminster study area) were widely distributed only in that area to the north of the Meadow Lake Escarpment.

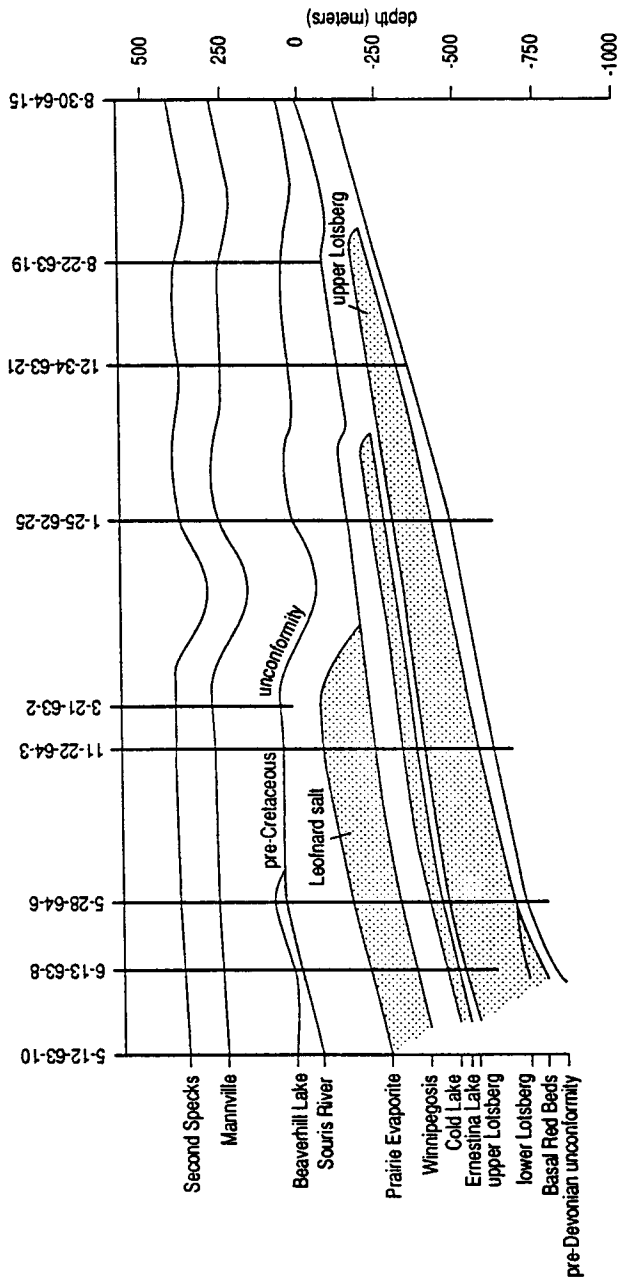

Figure VII:5:7. West-to-east geologic cross-section from the northern part of the Lloydminster study area illustrating the discontinuous nature of the Prairie Evaporite, Cold Lake and Lotsberg salts.

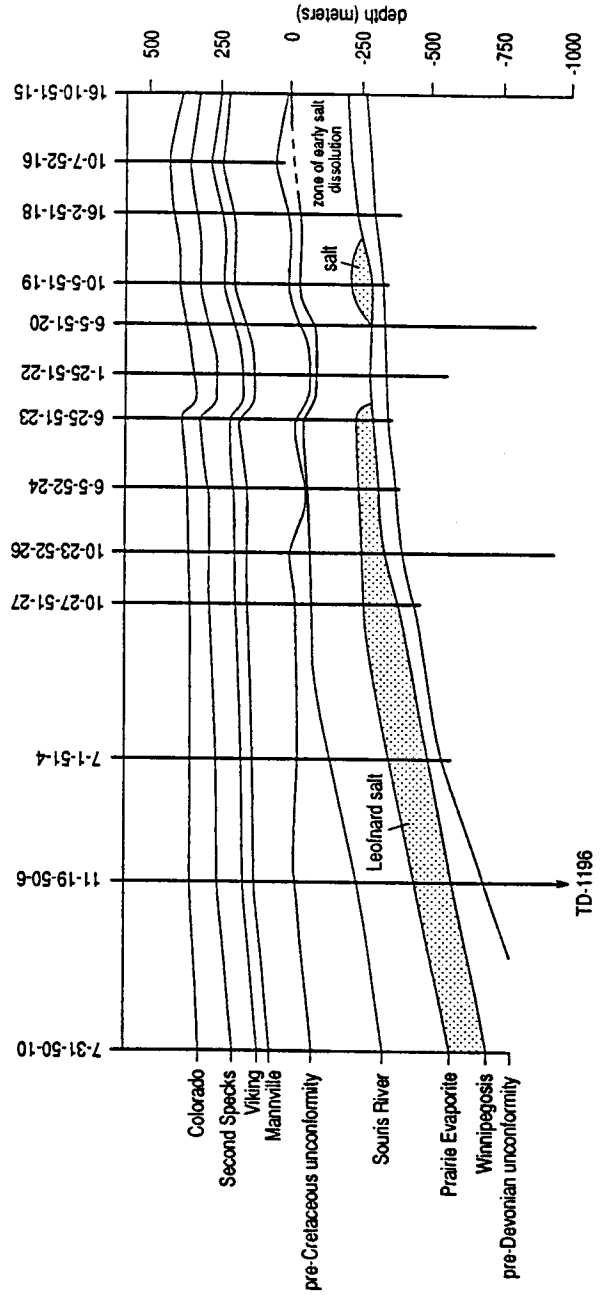

Figure VII:5:8. West-to-east geologic cross-section from the central part of the Lloydminster study area illustrating the discontinuous nature of the Prairie Evaporite salt.

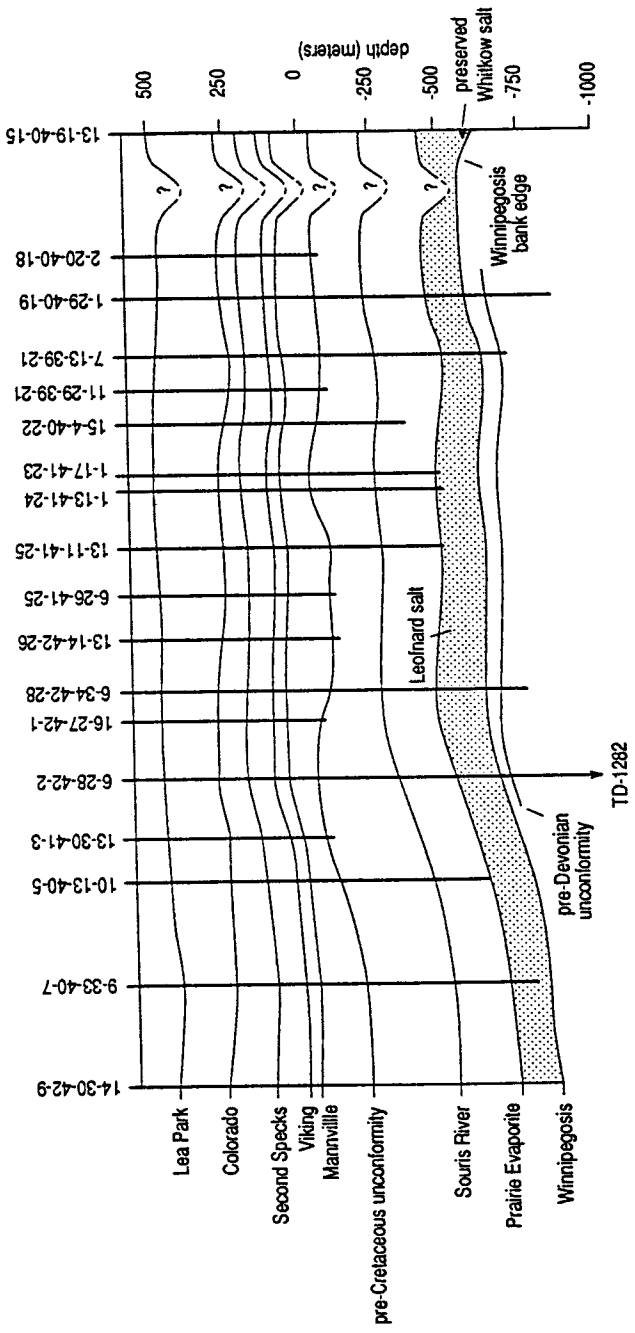

Figure VII:5:9. West-to-east geologic cross-section from the southern part of the Lloydminster study area illustrating the discontinuous nature of the Prairie Evaporite salt.

6) REFERENCES

AGAT Laboratories, 1988, Table of formations of Alberta: AGAT Laboratories, Calgary.

Alcock, F.G. and Benteau, R.I., 1976, Nipisi field - a middle Devonian clastic reservoir, *in* Lerand, M.M., Ed., The sedimentology of selected oil and gas reservoirs in Alberta: Canadian Society Petroleum Geologists, 1-24.

Anderson, N.L., 1987, Clastic seismology: Petrel Robertson, Calgary, Alberta, 277 p. (Available through the University of Calgary Geology Library).

Anderson, N.L., 1990a, An overview of some of the large scale mechanisms of salt dissolution: Kansas Geological Survey Open File Report 90-39.

Anderson, N.L., 1990b, Exploration implications of salt dissolution: Kansas Geological Survey Open File Report 90-37.

Anderson, N.L., 1990c, Hydrological, geological, biological, environmental, and exploration implications of salt dissolution: Kansas Geological Survey Open File Report 90-38.

Anderson, N.L., 1990d, Paleo-restoration of leached salts: an overview of the methodology used in the reconstruction of the Wabamun salt, southern Alberta, Canada: Kansas Geological Survey Open File Report 90-36.

Anderson, N.L., 1991a, Reconstruction of the Elk Point salts in the Lloydminster area (T50-T65, R15W3-R10W4M): Kansas Geological Survey Open File Report 91-56

Anderson, N.L., 1991b, Large scale mechanisms of salt dissolution: illustrated case histories: Kansas Geological Survey Open File Report 91-57

Anderson, N.L., 1992a, Reconstruction of the Leduc (Cairn) and Wabamun salts, Youngstown area, southern Alberta (T25-T35, R5-R20W4M): Kansas Geological Survey Open File Report 92-3.

Anderson, N.L., 1992b, Dissolution of the Wabamun Group salt: exploration implications, *in* Cavanaugh, T.D., Ed., Integrated exploration case histories, North America: The Geophysical Society of Tulsa Special Publication, in press.

Anderson, N.L. and Brown, R.J., 1987, The seismic signatures of some western Canadian Devonian reefs: Journal Canadian Society Exploration Geophysicists 1, 7-26.

Anderson, N.L. and Brown, R.J., 1992, Reconstruction of the Wabamun Group salts, southern Alberta, Canada, *in* Cavanaugh, T.D., Ed., Integrated exploration case histories, North America: The Geophysical Society of Tulsa Special Publication,

in press.

Anderson, N.L. and Brown, R.J., 1991, Dissolution of the Wabamun and Black Creek salts: a seismic analysis: Geophysics 56, 618-627.

Anderson, N.L., Brown, R.J. and Hinds, R.C., 1988a, A seismic perspective on the Panny and Trout fields of north-central Alberta: Canadian Journal Exploration Geophysics 24, 154-165.

Anderson, N.L., Brown, R.J. and Hinds, R.C., 1988b, Geophysical aspects of Wabamun salt distribution in southern Alberta: Canadian Journal Exploration Geophysics 24, 166-178.

Anderson, N.L., Brown, R.J. and Hinds, R.C., 1989a, Upper Elk Point reservoirs, *in* Anderson, N.L., Hills, L.V. and Cederwall, D.A., Eds., Geophysical atlas of western Canadian hydrocarbon pools: Canadian Society Exploration Geophysicists and Canadian Society Petroleum Geologists Special Publication, 27-66.

Anderson, N.L., Chapman, J. and Brown, R.J., 1990, Paleo-reconstruction of the Wabamun Group salt in southern Alberta, Canada: report to the Geological Survey of Canada.

Anderson, N.L., Cederwall, D.A. and Hills, L.V., 1986, Carbonate seismology: Sigma Exploration Ltd., Calgary, Alberta, 194 p. (Available through the University of Calgary Geology Library).

Anderson, N.L. and Chappell, F., 1987b, Devonian salts and hydrocarbon traps: Petrel-Robertson, Calgary, Alberta, 113 p. (Available through the University of Calgary Geology Library).

Anderson, N.L., Brown, R.J., Gendzwill, D.J., Hinds, R.C. and Lundberg, R.N., 1989a, Elk Point Group reservoirs, *in* Anderson, N.L., Hills, L.V. and Cederwall, D.A., Eds., The geophysical atlas of western Canadian hydrocarbon pools: Canadian Society Exploration Geophysicists and Canadian Society Petroleum Geologists Special Publication, 27-66.

Anderson, N.L. and Franseen, E.K., 1991, Differential compaction of Winnipegosis reefs: a seismic analysis: Geophysics 56, 142 -147.

Anderson, N.L. and Knapp, R.W., 1992, An overview of some large-scale mechanisms of salt dissolution: submitted to Geophysics, in review.

Anderson, N.L., White, D.G. and Hinds, R.C., 1989b, Woodbend Group Reservoirs, *in* Anderson, N.L., Hills, L.V. and Cederwall, D.A., Eds., Geophysical atlas of western Canadian hydrocarbon pools: Canadian Society Exploration Geophysicists and Canadian Society Petroleum Geologists Special Publication, 101-132.

Andrichuk, J.M. and Wonfor, J.S., 1953, Late Devonian geologic history in Stettler

area, Alberta, Canada: Alberta Society of Petroleum Geologists, News Bulletin 1, 3-5.

Baillie, A.D., 1953, Devonian System of the Williston basin area: Manitoba Mines Branch Publication 52-5.

Barss, D.L., Copland, A.B. and Ritchie, W.D., 1970, Geology of Middle Devonian reefs, Rainbow area, Alberta, Canada, *in* Halbouty, M.T., Ed., Geology of giant petroleum fields: AAPG Memoir 14, 19-49.

Bathurst, R.G.C., 1975, Carbonate sediments and their diagenesis: Developments in Sedimentology 12, Elsevier, Amsterdam, 685 p.

Belyea, H.R. 1966, Woodbend, Winterburn and Wabamun Groups, *in* McCrossan, R.G. and Glaister, R.P., Eds., Geological history of western Canada, 2nd edition: Alberta Society Petroleum Geologists, 66-88.

Belyea, H.R. and Mclaren, D.J., 1957, Upper Devonian nomenclature in southern Alberta: Journal of Alberta Society of Petroleum Geologists 5, 166-182.

Bishop, 1974, Hummingbird structure, Saskatchewan, single vs multiple stage salt soultion-collapse, *in* Parslow, G.R., Ed., Fuels: a geologic appraisal: Saskatchewan Geological Society Special Publication 2, 179-197.

Bond, G.C. and Kominz, M.A., 1984, Construction of tectonic subsidence curves for the early Paleozoic miogeocline, southern Canadian Rocky Mountains: Implications for subsidence mechanisms, age of breakup, and crustal thinning: Bulletin Geological Society America 95, 155-173.

Brown, R.J. and Anderson, N.L., 1991, On the question of lateral velocity variations over Leduc and Rainbow reefs: Canadian Journal Exploration Geophysics 27, 43-52.

Brown, R. J. and Anderson, N. L., 1992, An overview of salt dissolution and related hydrocarbon trapping potential in western Canada: AAPG Bulletin, submitted.

Brown, R.J., Anderson, N.L. and Hills, L.V., 1990, The seismic interpretation of Upper Elk Point (Givetian) carbonate reservoirs of western Canada: Geophysical Prospecting 38, 719-736.

Cederwall, D.A. and Anderson, N.L., 1991a, A seismic and gravity study of salt dissolution at the Westhazel General Petroleums Pool, west-central Saskatchewan, Canada: Kansas Geological Survey Open File Report 90-46.

Cederwall, D.A. and Anderson, N.L., 1991b, Westhazel General Petroleums Pool, east-central Alberta, Canada: SEG Annual Meeting Expanded Technical Program Abstracts, 184-187.

Christianson, E.A., 1971, Geology of the Crater Lake collapse structure in south-

eastern Saskatchewan: Canadian Journal Earth Science 8, 1505-1513.

Ehrets, J.R. and Kissling, D.L., 1987, Winnipegosis platform margin and pinnacle reef reservoirs, northwest North Dakota, in Fischer, D.W., Ed., Core workshop volume, Fifth international Williston Basins symposium, North Dakota Geological Survey, Miscellaneous Series 69, 1-31.

Gendzwill, D.J., 1978, Winnipegosis mounds and Prairie Evaporite Formation of Saskatchewan seismic study: AAPG Bulletin 62, 73-86.

Gendzwill, D.J. and Hajnal, Z., 1971, Seismic investigation of the Crater Lake collapse structure in southeastern Saskatchewan: Canadian Journal Earth Science 8, 1514-1524.

Gendzwill, D.J. and Lundberg, R.M., 1989, Upper Elk Point carbonate reservoirs, part B: Winnipegosis carbonates, *in* Anderson, N.L., Hills, L.V. and Cederwall, D.A., Eds., Geophysical atlas of western Canadian hydrocarbon pools: Canadian Society Exploration Geophysicists and Canadian Society Petroleum Geologists Special Publication, 52-66.

Gendzwill, D.J. and Wilson, N.L., 1987, Form and distribution of Winnipegosis mounds in Saskatchewan, *in* Peterson, J.A., Kent, D.M., Anderson, S.B., Pilatzke, R.H. and Longman, M.W., Eds.,Williston Basin; Anatomy of a Cratonic Oil Province: Rocky Mountain Association Geologists, Denver, 109-117.

Gorrel, H.A. and Alderman, G.R., 1968, Elk Point Group saline basins of Alberta, Saskatchewan and Manitoba, Canada, *in* Mattox, R.B., Ed., Saline Deposits: Geological Society America Special Paper 88, 291-317.

Hamilton, W.N., 1971, Salt in east-central Alberta: Research Council Alberta Bulletin 29.

Holter, M.E., 1969, The Middle Devonian Prairie Evaporite of Saskatchewan: Saskatchewan Department Mineral Resources Report 123.

Hopkins, J. C.,1987, Contemporaneous subsidence and fluvial channel sedimentation: Upper Mannville C pool, Berry field, Lower Cretaceous of Alberta: AAPG Bulletin 71, 334-345.

Hriskevich, M.E., 1970, Middle Devonian reef production, Rainbow area, Alberta, Canada: AAPG Bulletin 54, 2260-2281.

Imperial Oil Ltd., Western Division, Geological Staff, 1950, Devonian nomenclature in Edmonton area, Alberta, Canada: AAPG Bulletin 34, 1807-1825.

Jones, l., 1965, The Middle Devonian Winnipegosis Formation of Saskatchewan: Saskatchewan Department Mineral Resources report 98, 101 p.

Jordan, S.P., 1967, Saskatchewan reef trend looks big: Oilweek, 17, 10-12.

Jordan, S.P., 1968, Will Zama be duplicated at Quill Lake Saskatchewan: Oilweek, 19, 10-12.

Law, J., 1955, Geology of northwestern Alberta and adjacent areas (with Discussion and Reply): AAPG Bulletin 39, 1927-1978.

McCrossan, R.G. and Glaister, R.P., 1966, Geological history of western Canada, 2nd edition: Alberta Society of Petroleum Geologists.

McLaren, D.J., 1955, Devonian formations in the Alberta Rocky Mountains between Bow and Athabasca Rivers: Geological Survey of Canada, Bulletin 35, 59 p.

Meijer Drees, N.C., 1986, Evaporitic deposits of western Canada: Geological Survey of Canada Paper 85-20, 118 p.

Mossop, G.D., 1972, Origin of the peripheral rim, Redwater reef, Alberta: Bulletin Canadian Society Petroleum Geology 20, 238-280.

Oliver, J.A. and Cowper, N.W., 1983, Wabamun salt removal and shale compaction effects, Rumsey area, Alberta: Bulletin Canadian Society Petroleum Geology 31, 161-168.

Perrin, N.A.,1982, Environments of deposition and diagenesis of the Winnipegosis Formation (Middle Devonian), Williston Basin, North Dakota, *in* Christopher, J.E. and Kaldi, J, Eds., Proceedings of the Fourth International Williston Basin Symposium, 51-66.

Perrodon, A., 1983, Dynamics of oil and gas accumulation: Elf Aquitaine, France, 369 p.

Pray, L.C., 1960, Compaction in calcilutites: Bulletin Geological Society America 71, 1946.

Precht, G.D., 1983, Reservoir development and hydrocarbon potential of Winnipegosis (Middle Devonian) pinnacle reefs, southern Elk Point Basin, North Dakota, *in* Carbonates and Evaporites: Northeastern Science Foundation, 1, 83-99.

Reinson, G.E. and Wardlaw, N.C., 1972, Nomenclature and stratigraphic relationships, Winnipegosis and Prairie Evaporite formations, central Saskatchewan: Bulletin Canadian Petroleum Geology 20, 301-320.

Ricken, W., 1986, Diagenetic bedding: A model for marl-limestone alternations: Lecture Notes in Earth Sciences, Springer-Verlag, New York, 210 p.

Sherwin, D.F., 1962, Lower Elk Point section in east-central Alberta: Journal of the Alberta Society of Petroleum Geologists 10, 185-191.

Shinn, E.A. and Robbin, D.M., 1983, Mechanical and chemical compaction in fine-grained shallow-water limestones: Journal Sedimentary Petrology 53, 595-618.

Shinn, E.A, Halley, R.B., Hudson, J.H. and Lidz, B.H., 1977, Limestone compaction: An enigma: Geology 5, 21-24.

Smith, D.G. and Pullen, J.R., 1967, Hummingbird structure of southeast Saskatchewan: Bulletin Canadian Petroleum Geology 15, 468-482.

Wardlaw, N.C. and Reinson, G.E., 1971, Carbonate and evaporite deposition and diagenesis, Middle Devonian Winnipegosis and Prairie Evaporite formations of south-central Saskatchewan: AAPG Bulletin 55, 1759-1786.

Williams, G.K., 1977, The Hay River Formation and its relationship to adjacent formations, Slave River map-area, N.W.T.: Geological Survey of Canada Paper 75-12, 17 p.

Wilmot, B.R., 1985, The geology of the Lower Cretaceous Mannville Group, Edam, Saskatchewan: M.Sc. thesis, University of Calgary, 160 p.

Wilson, N.L., 1984, The Winnipegosis Formation of south-central Saskatchewan, in Lorsong, J.A. and Wilson, M.A., Eds., Oil and Gas in Saskatchewan: Saskatchewan Geological Society Special Publication 7, 13-15.

Wirnkar, F.T. and Anderson, N.L., 1989, Seismic analysis of the differential compaction of reef and off-reef sediments: Expanded abstracts, SEG Annual Meeting, 888-890.

Wonfor, J.S. and Andrichuk, J.M., 1953, Upper Devonian in the Stettler area, Alberta, Canada: Alberta Society of Petroleum Geologists News Bulletin 1, 3-6.

VIII: WESTERN CANADA - CASE HISTORIES

1) OVERVIEW

There are six main Devonian salts in Alberta, those of the Lotsberg Formation, Cold Lake Formation, Prairie Evaporite Formation (and equivalents), Beaverhill Lake Group, Leduc Formation and Wabamun Group. Each of these salts is different: some are thick (>160 m) - others are thin (<45 m); some are massive - others are bedded; some are areally extensive - others are areally restricted. Yet, each of these salts have one comman characteristic; they have all been extensively dissolved in places.

The leaching of these salts is of significant interest to the explorationist for several reasons: 1) stratigraphic traps can form where reservoir facies were either preferentially deposited or preserved in salt-dissolution lows; 2) reservoir facies can develop in high energy environments such as topographic highs that are controlled by salt edges or remnants; 3) structural traps can form where reservoir facies are draped across salt remnants or collapse features; and 4) salt remnants can be misinterpreted as reefs, faults or other structural features.

In an effort to elucidate the leaching of the Devonian salts in western Canada, we present in this chapter nine case histories of salt dissolution in western Canada.

2) RAINBOW AREA: CASE STUDY

The Muskeg Formation in the Rainbow area is subdivided into the basal Black Creek Member salt and the upper anhydritic member (Figures VIII:2:1 and VIII:2:2). The Black Creek salt attains a maximum thickness of about 80 m, and is described as light-grey, semi-transluscent, coursely crystalline, and containing thin stringers of anhydrite. These salts are thought to have been widely distributed and uniformly deposited within the Rainbow area. As a result of extensive post-depositional dissolution the distribution of these salts is not what it once was.

According to Hriskevich (1970), Anderson et al. (1989), Brown et al. (1990), and Anderson and Brown (1991) the dissolution of the Black Creek salt in the Rainbow area initiated shortly after deposition and continued into the post-Mississippian. Their concept is supported by the geologic and seismic data of Figures VIII:2:3 and VIII:2:4, respectively. Specifically, note that the salt collapse features decrease in amplitude going upward in the stratigraphic section, but that the rate of decrease in amplitude varies laterally. This implies that dissolution has occurred at varying times in different places even on this local scale, and supports the thesis that leaching has occurred, in places, more-or-less continuously since deposition.

Anderson et al. (1989), Brown et al. (1990), and Anderson and Brown (1991) suggest that the dissolution of the Black Creek salt in the Rainbow area was initiated about the peripheries of the isolated reefs and along the margins of the reef-fringed Black Creek sub-basin shortly after deposition (upper Muskeg time). These authors suggested that leaching was initiated at those places where the salts were proximal to relatively porous and permeable reefal carbonates. These authors concluded that salt dissolution is, at least in some instances, a self-perpetuating process and that these salt dissolution fronts, once established, would migrate laterally. These authors also indicated that they had mapped a NNE-trending, salt-dissolution lineament on seismic data in the Black Creek area. They state that the lineament effectively parallels the Hay River fault, and that it is characterized by both a relatively narrow zone of extensive leaching and vertical displacement of post-salt strata. They concluded that some of the leaching in the Rainbow area, could have been caused by the reactivation of pre-existing planes of weakness.

These postulated processes of dissolution in the Rainbow study area, are consistent with two of the previously cited (Chapter II) large-scale mechanisms of dissolution: centrifugal flow and regional fracturing/faulting.

1) The observation that the earliest phases of leaching occurred in proximity to reef is consistent with the thesis of centrifugal fluid flow through these porous and permeable carbonates. During upper Muskeg time, anhydites and carbonates were deposited in the inter-reef areas. Diagenetic processes at depth could have resulted in the expulsion of interstitial waters. It is conceivable that the reefs acted as a conduit for such fluids, and that such fluids dissolved the proximal salts. These established salt-dissolution fronts could have migrated away from the reefs in a self-perpetuating manner (Figure VIII:2:5).

2) The 12 km long, NNE-trending salt-dissolution lineament on seismic data is strong (though not conclusive) evidence of regional faulting/fracturing, particularly in that it is consistent with the orientation of the Hay River fault. The pattern could also have been caused by preferential pathways along an advancing salt-dissolution front.

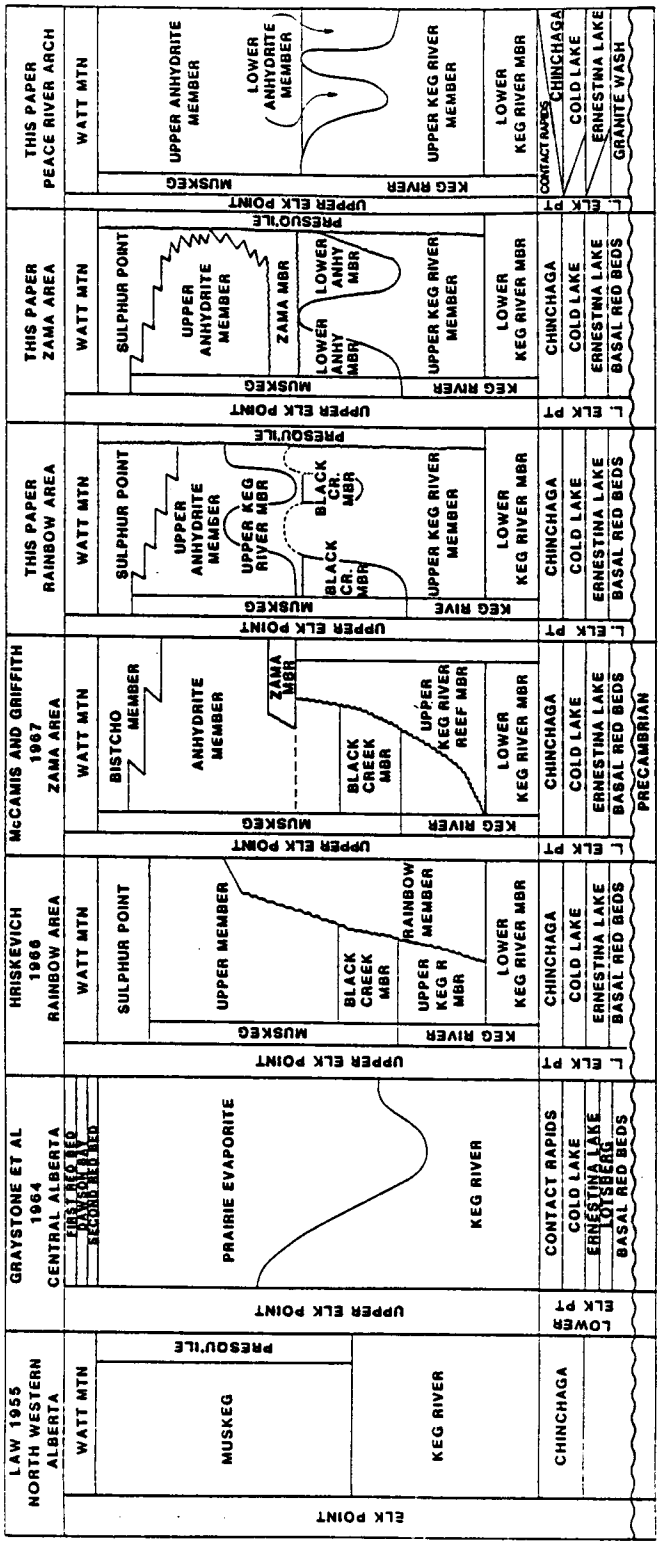

Figure VIII:2:1. Stratigraphic chart for the Elk Point Group, northern Alberta.

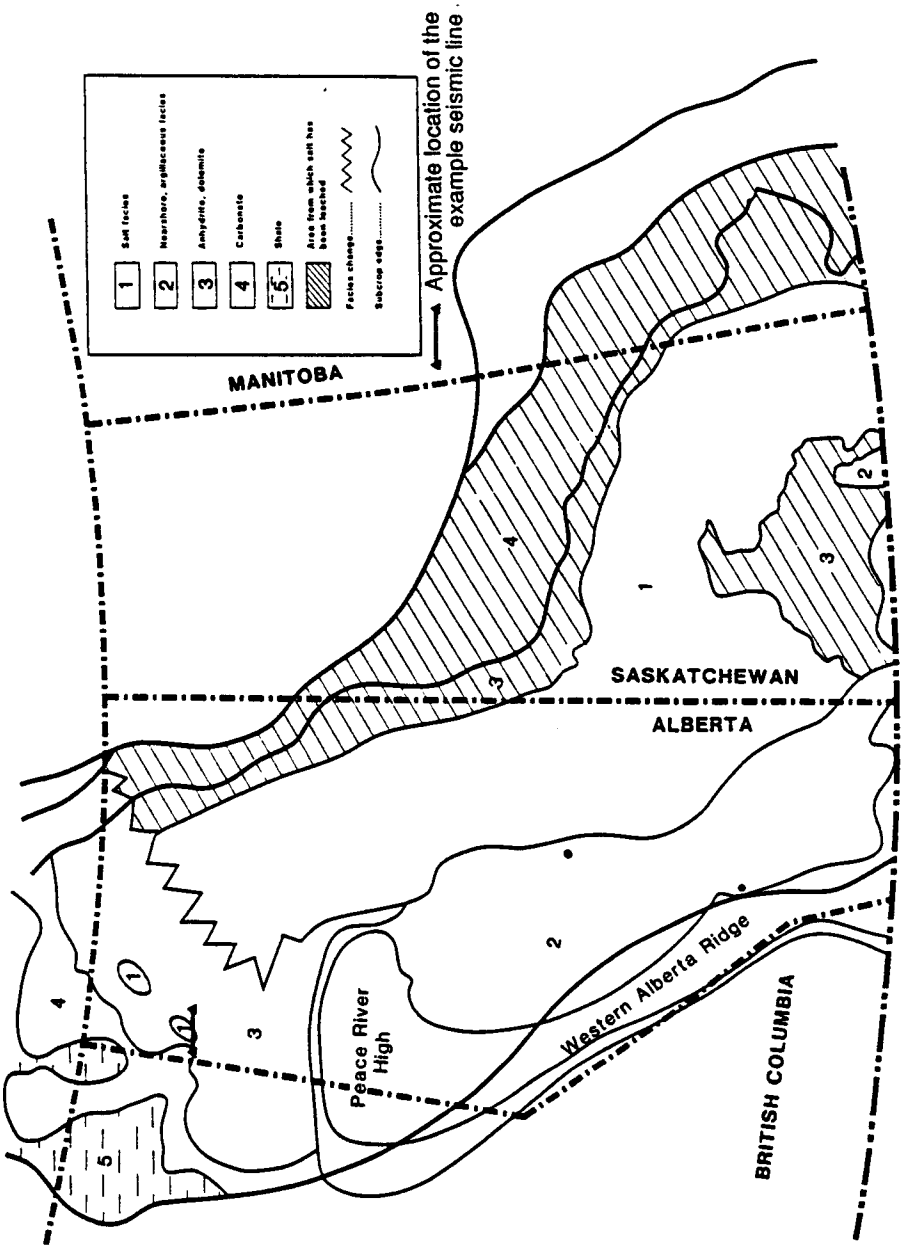

Figure VIII:2:2. Facies distribution and paleogeography of the lower part of the Upper Elk Point and equivalents (after Meijer Drees, 1986).

Figure VIII:2:3. Synthetic seismogram, Rainbow study area.

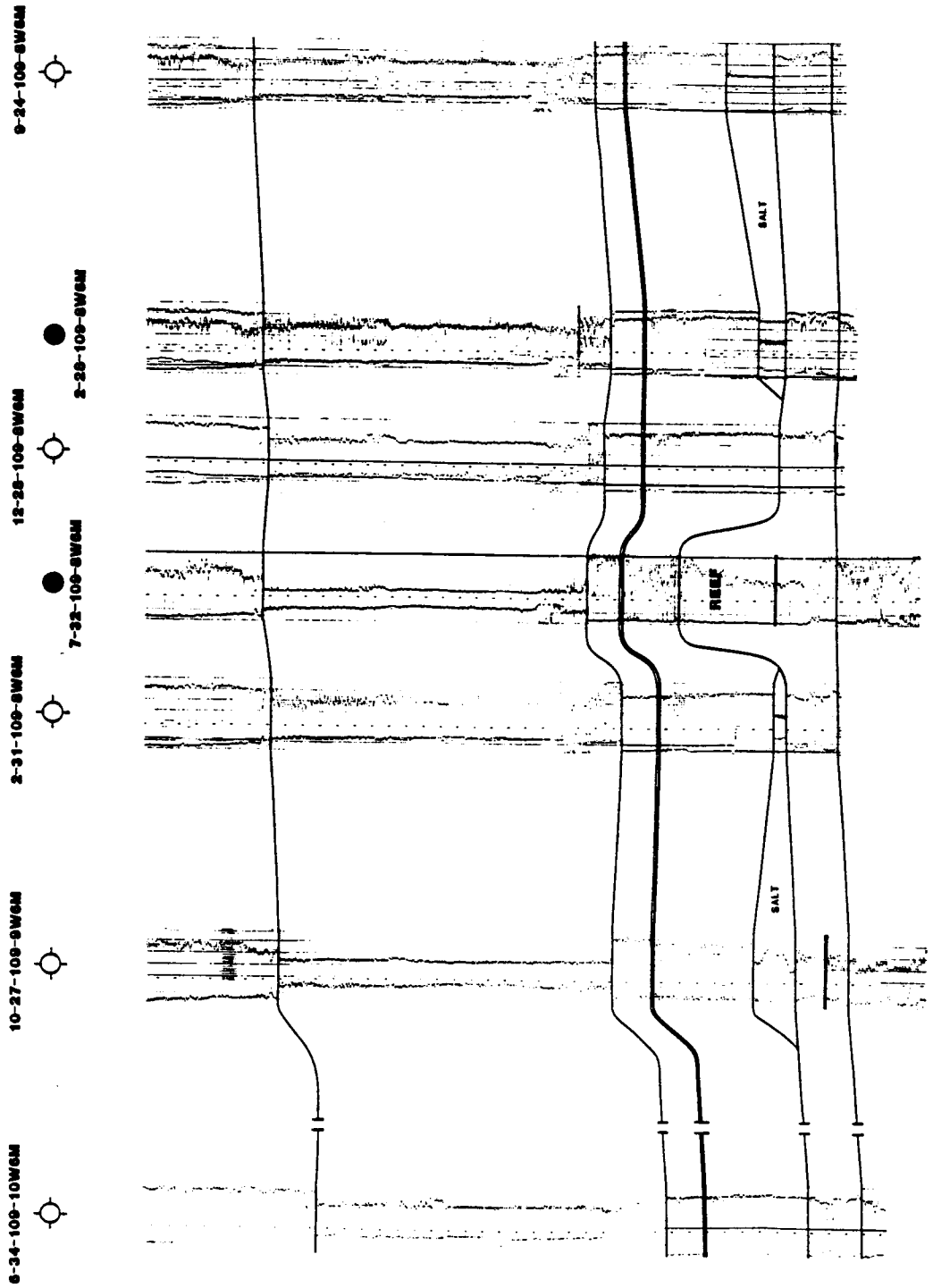

Figure VIII:2:4. Geologic section across the Keg River reef (Rainbow Member) at Rainbow A pool. Remnant Muskeg salts (Black Creek Member) are preserved in the 9-24, 2-28, 2-31, and 10-27 wells; these salts have been leached at the 12-28 and 6-34 locations.

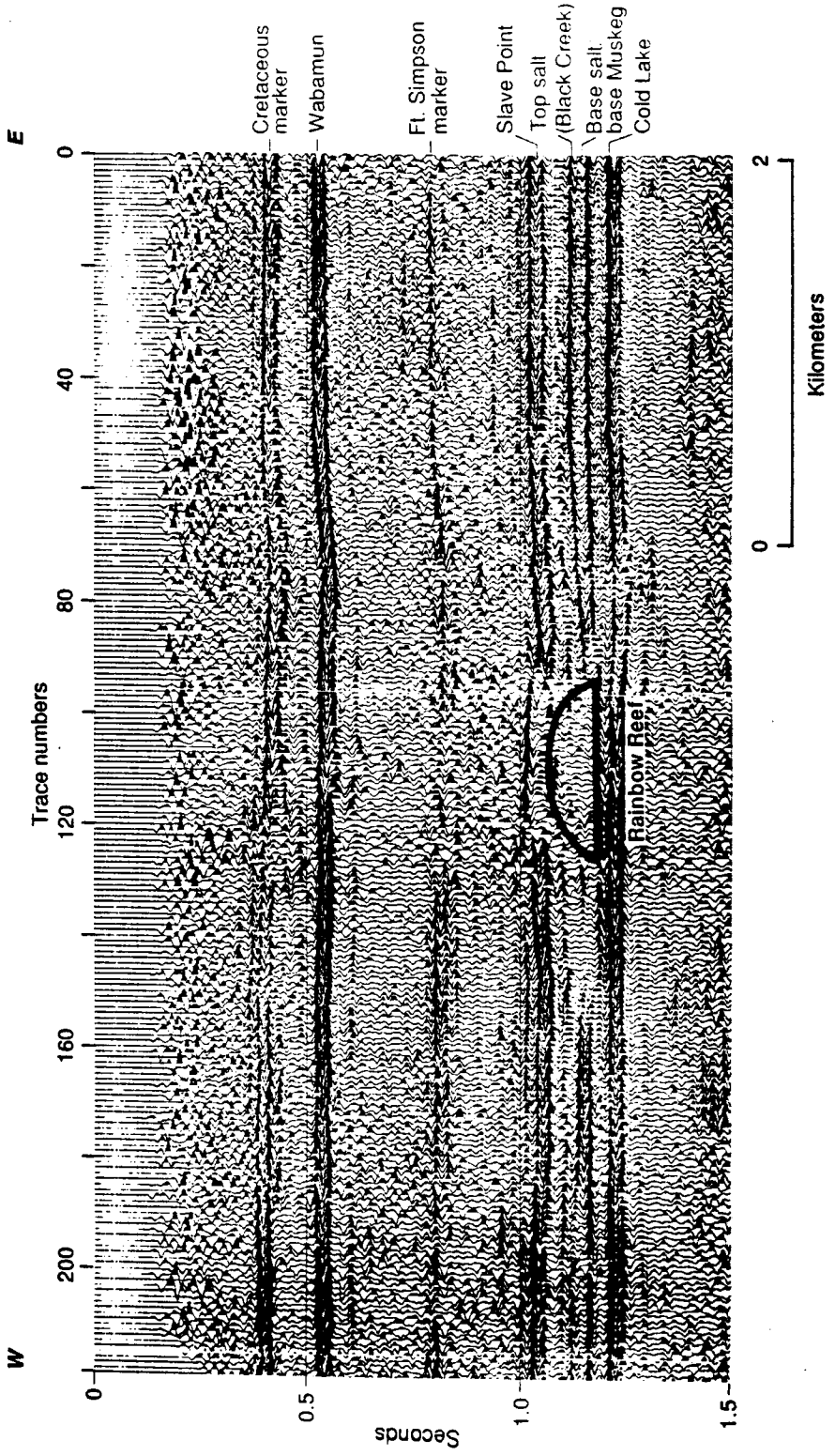

Figure VIII:2:5. Seismic line across the Keg River reef (Rainbow Member) at Rainbow A pool (Anderson and Brown, 1991). Up to 80 m of salt is imaged at the eastern and western edges of the seismic line.

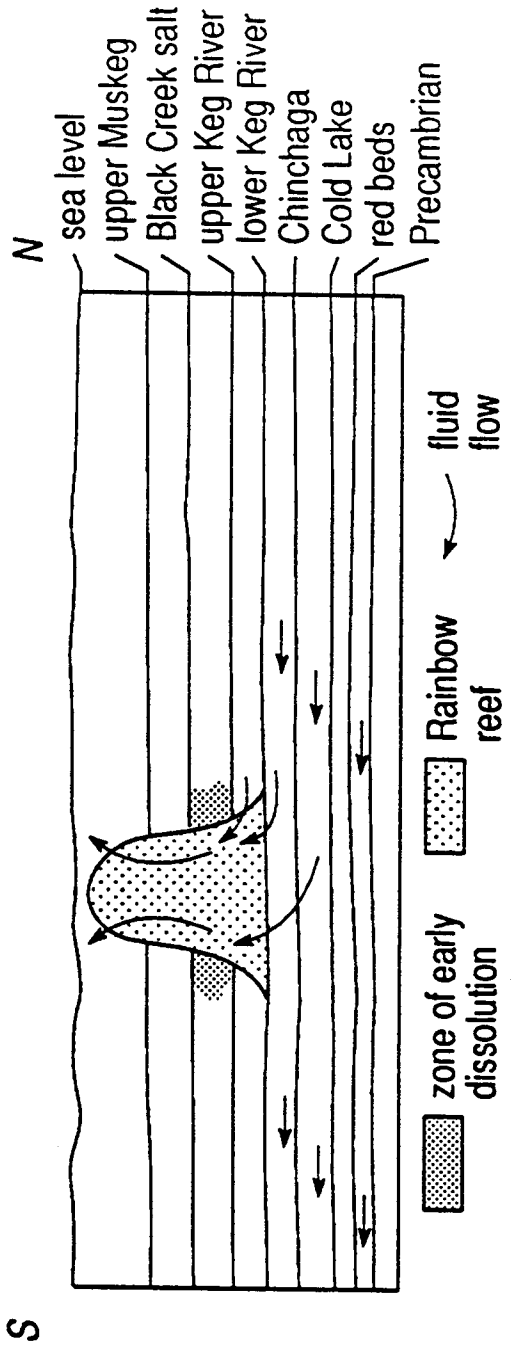

Figure VIII:2:6. The observation that the earliest phases of leaching occurred in proximity to reef is most easily attributed to centrifugal fluid flow through these porous and permeable carbonates. During upper Muskeg time, anhydites and carbonates were deposited in the inter-reef areas. Concurrent diagenetic processes could have resulted in the expulsion of interstitial waters through the reefs.

3) TROUT AREA: CASE STUDY (ANDERSON AND KNAPP)

The anhydritic equivalent of the Prairie Evaporite in northern Alberta is known as the Muskeg Formation (Figure VIII:2:1 and VIII:2:2). It is described by Meijer Drees (1986) as a light coloured succesion of interbedded white and grey salt, brown anhydrite, brownish gray dolostone and limestone. In the Trout area, salt comprises about one-half of the Muskeg section, with the exception of those isolated places where extensive dissolution has occurred.

Anderson and Brown (1988), and Anderson et al. (1989) interpret seismic and geologic data from the Trout field study area (Figures VIII:3:1-VIII:3:3) with a view to documenting the seismic signature of the dual Keg River/Granite Wash reservoir and elucidating the localized dissolution of Muskeg salts. These authors conclude that the Keg River reservoir facies (Figure VIII:3:1) depositionally pinchout against the flanks of the pre-existing Precambrian structure penetrated by the 2-10 well, and are now structurally closed as a result of differential compaction on and off-structure. The authors also note that the salts of the Muskeg Formation have been extensively leached from the 2-10 well site, apparently during the deposition of the upper Beaverhill Lake Group. They indicate that the area of extensive leaching is proximal to the more-or-less circular and closed crystalline basement high and suggest that the dissolution was focused by this underlying structure. Their conclusions are supported by a suite of plan view maps, geologic sections and seismic control from the region.

We have followed up this earlier work in an effort to elucidate some of the large-scale mechanisms of leaching in the Trout area. Our preferred thesis is that the dissolution at the 2-10 well site was triggered and/or accentuated by two principal causes: centrifugal flow and localized fracturing/pressure dissolution. Our rational is as follows.

1) During the early Late-Devonian, the transgressive sediments of the Beaverhill Lake Group were being deposited on a regional scale. As a result of burial and the associated diagenetic changes, interstitial fluids were being expelled from the relatively thin veneer of underlying Elk Point strata.

2) Contemporaneously, at the Trout site and elsewhere, significant differential compaction was occurring between crystalline basement structures (2-10 well) and the off-structure, infilling clastic/carbonate/evaporite facies. We suggest that the process of differential compaction resulted in the localized pressure dissolution of the Muskeg salts and stress and/or collapse-related fracture permeability in the vicinity of the 2-10 well site. This zone of increased permeability provided conduits for the over-pressured, interstitial waters within the underlying Elk Point strata, thereby facilitating additional leaching (Figure VIII:3:4).

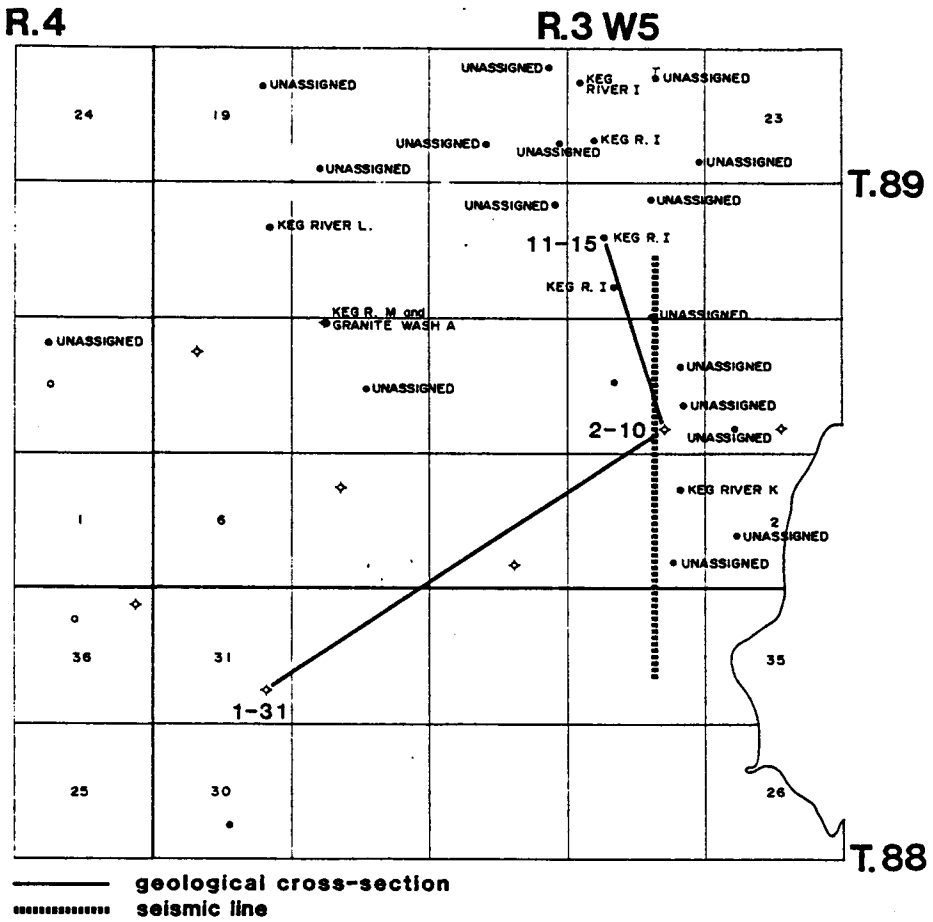

Figure 2.42. Trout study area. Pool outlines, the three wells incorporated into the geological cross-section and the location of the seismic line are shown.

Figure VIII:3:1. Trout study area.

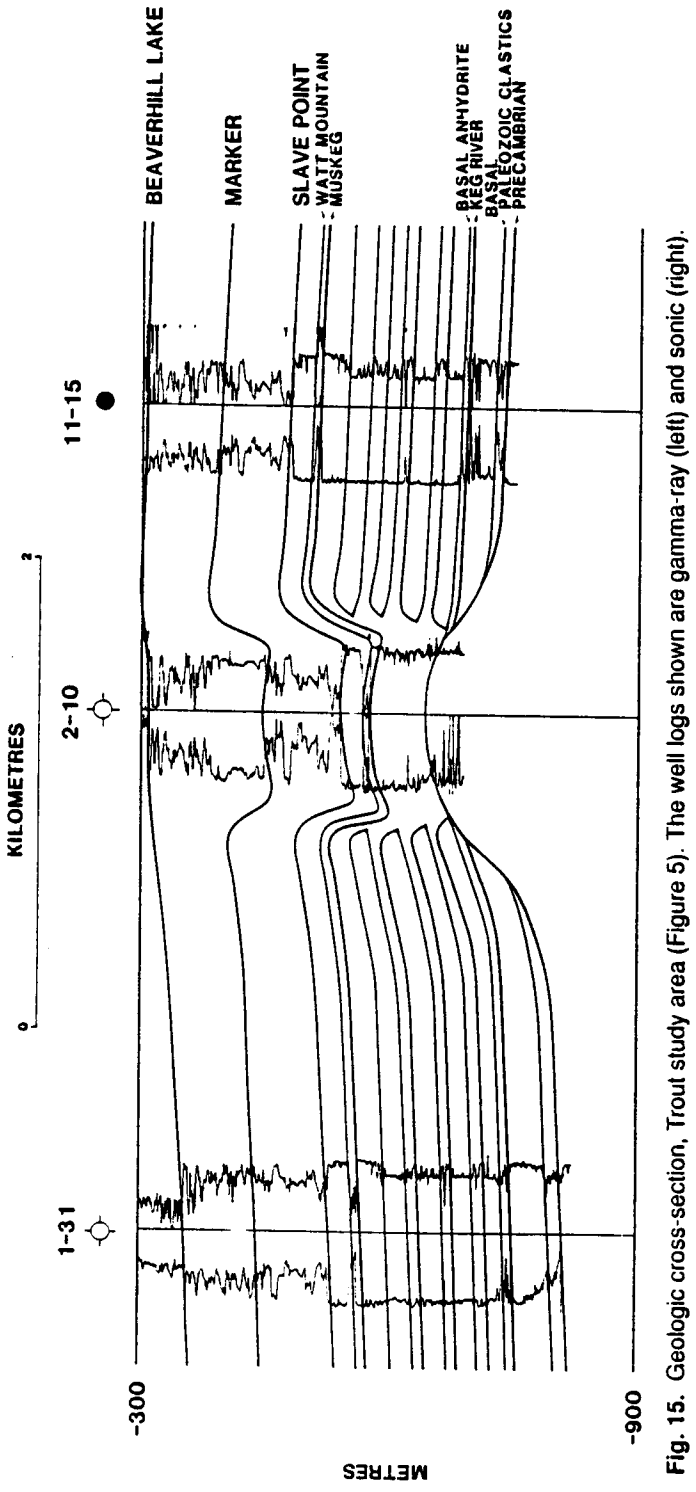

Fig. 15. Geologic cross-section, Trout study area (Figure 5). The well logs shown are gamma-ray (left) and sonic (right).

Figure VIII:3:2. Geologic section across the crystalline basement structural high in the Trout study area. Thick remnant Muskeg salts are preserved in the 1-31 and 5-22 wells. The salts have been leached at 2-10.

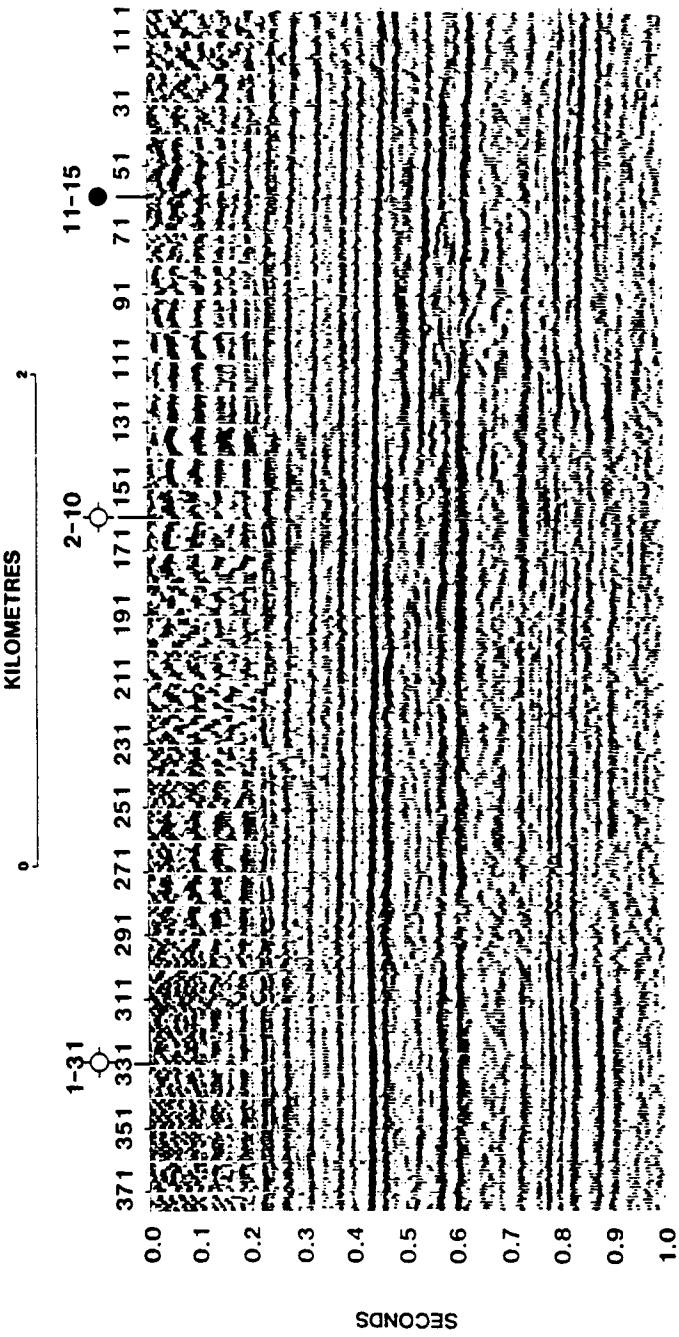

Fig. 16. Normal-polarity seismic section, Trout study area; see Figure 5 for well locations relative to the seismic line. The TD point for each one of these wells is in the Precambrian.

Figure VIII:3:3. Seismic line across the crystalline basement structural high in the Trout study area (Anderson et al., 1988b).

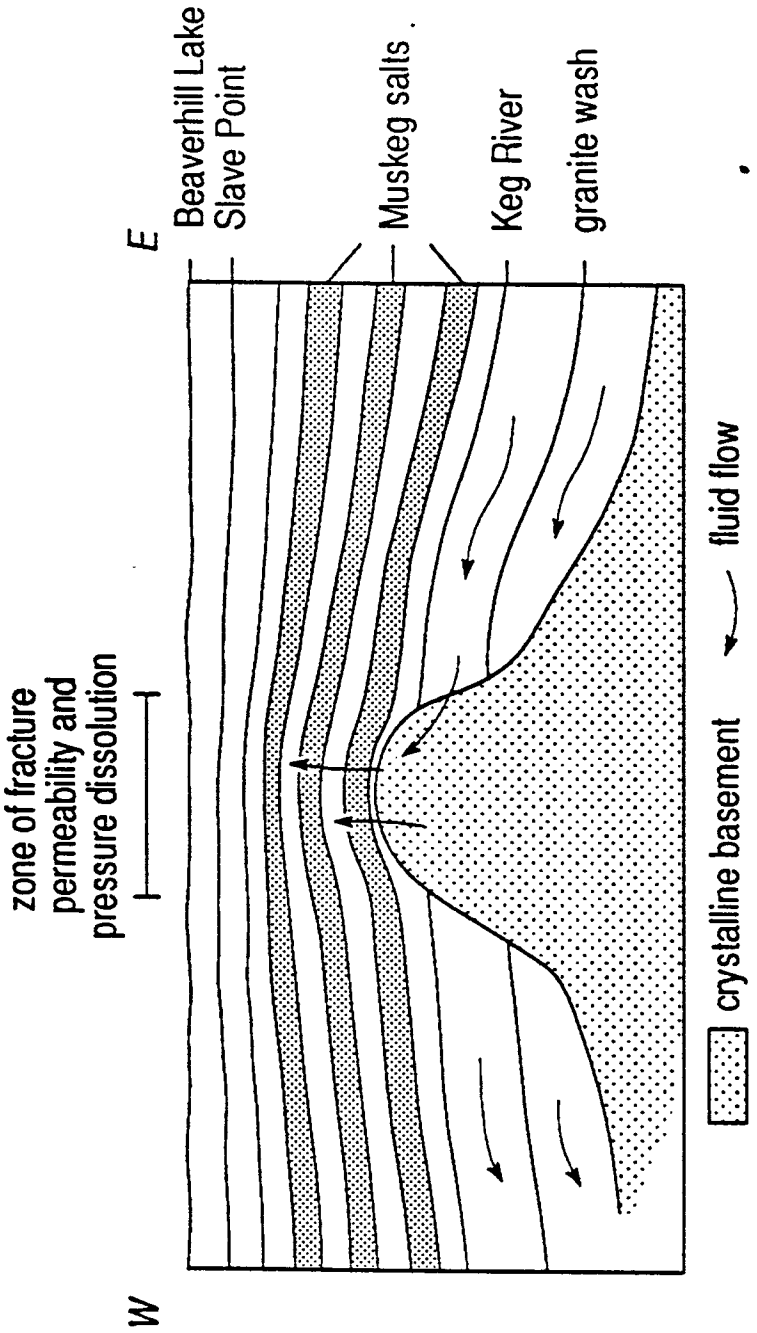

Figure VIII:3:4. **At the Trout study area and elsewhere, differential compaction between crystalline basement (2-10 well) and adjacent strata could have resulted in the localized pressure dissolution of the Muskeg salts, and stress and/or collapse-related fracture permeability in the vicinity of the 2-10 well site. This zone of increased permeability could have provided conduits for the over-pressured, interstitial waters within the underlying Elk Point strata, thereby facilitating additional leaching.**

4) LLOYDMINSTER AREA: CASE STUDY (ANDERSON AND KNAPP)

The Prairie Formation (Figures VII:2:1 and VII:2:2) is subdivided into three units: the basal Whitkow Member salt, the Shell Lake Member anhydrite, and the upper Leofnard Member salt. In the Lloydminster study area (T45-T55, R20W3M-R5W4M) of Cederwall and Anderson (1991), only the Leofnard salt was deposited; it consists of interbedded massive salts and thin anhydrite, with minor dolostone and shale (Meijer Drees, 1986).

The author in an unpublished study of the Prairie salts (T35-T65, R15W3M-R10W4M), and Cederwall and Anderson (1991) conclude that about 150 m of Leofnard Member salt (Prairie Formation) was uniformly deposited in the Lloydminster study area. However as a result of post-depositional dissolution, the distribution of the Leofnard is not what it once was; the present-day net thickness of these salts varies from 0 m to in excess of 145 m.

Our study of the Prairie and the published literature, suggests that the leaching of the these salts was triggered and/or accentuated by some or all of six principal processes: A) the near-surface exposure of these salts, as a result of the erosion of the overlying Paleozoic sediment during the pre-Cretaceous hiatus; B) the influx of meteoric water, which could have been introduced into the system along the Elk Point outcrop/subcrop to the east; C) the partial dissolution of the underlying Cold Lake and upper Lotsberg salt; D) faulting/fracturing during or after the mid-Late Cretaceous; E) salt movement; and F) glacial loading and unloading. In support for some of these conclusions, the geologic, seismic, and gravity sections of Figures VIII:4:1-VIII:4:4, respectively are presented. These sections cross the main eastern dissolutional edge of the Prairie salt.

The postulated process of dissolution in and to the east of the Lloydminster study area as outlined below, is consistent with the previously cited large-scale mechanisms of dissolution.

1) Dissolution is thought to have initiated, during pre-Cretaceous time as a result of the near-surface exposure of these salts along the Elk Point subcrop edge (Figures VIII:4:5 and VIII:4:6).

As a result of erosion during the pre-Cretaceous hiatus, the Elk Point Group subcrops to the east of the Lloydminster study area. The consensus in the literature is that Prairie Evaporite salts were initially deposited within the subcropping section, but were leached when exposed to a near-surface environment. Our work on the paleo-reconstruction of the Prairie suggests that the main salt dissolution front, that was established adjacent to the Elk Point outcrop during the pre-Cretaceous, migrated basinward (westward) thereafter.

2) The established dissolution front is believed to have migrated basinward and relatively rapidly during the pre-Cretaceous hiatus. The rate of advance appears to have slowed significantly during the Early to mid-Late Cretaceous

interval. With respect to the seismic and geologic sections, we submit that the main salt dissolution front was situated to the east of these lines prior to the deposition of the upper Colorado (mid-Late Cretaceous time), and that most of the leaching in these vicinities occurred thereafter. As a consequence, the regional southwesterly dip of the Colorado has been locally reversed.

These conclusions are consistent with accelerated centripetal flow as a result of uplift and unloading during the pre-Cretaceous, and deccelerated flow as a result of renewed subsidence thereafter. Another point to consider is that with the onset of Cretaceous sedimentation, the Elk Point outcrop would be covered with clastic deposits and in hydrologic contact with marine water. The influx of water would be additionally slowed, and the dissolution potential of such water would be diminished.

3) As evidenced by the seismic and geologic sections, the rate of salt dissolution increased markedly in mid-Late Cretaceous time. Similar observations have been reported by Anderson (1991) and Anderson and Brown (1991a) for the Wabamun and Leduc salts in the Stettler area of Alberta. These authors have identified lineaments on reconstructed salt distribution maps, and suggest that they were caused by regional faulting and/or fracturing during the mid-Late Cretaceous. The proximity of the Stettler and Lloydminster area and the linearity of the main Prairie salt edge suggests that a similar mechanism could have affected leaching here.

4) The nature of the main Prairie salt edge is consistent with the thesis that significant movement (creep) of these salts has occurred during or after the mid-Late Cretaceous. Such movement could have been triggered by dissolution, the postulated regional faulting/fracturing, and/or glacial loading and unloading. This process could have been and enhanced by pre-existing fault/fracture planes and/or an influx of meteoric water.

5) Several lakes and rivers (Jackfish Lake, Murray Lake, Birch Lake, Helene Lake, Midnight Lake, Stony Lake, Turtle Lake, Brightsand Lake, Bronson Lake, Cold Lake, Marie Lake, and Saskatchewan River) in our regional Prairie study area (T35-T65, R15W3M-R10W4M) are situated in areas where the Leofnard salts are thin or absent, suggesting that a significant amount of leaching has occurred in post-glacial times, possibly in response to glacial loading and unloading.

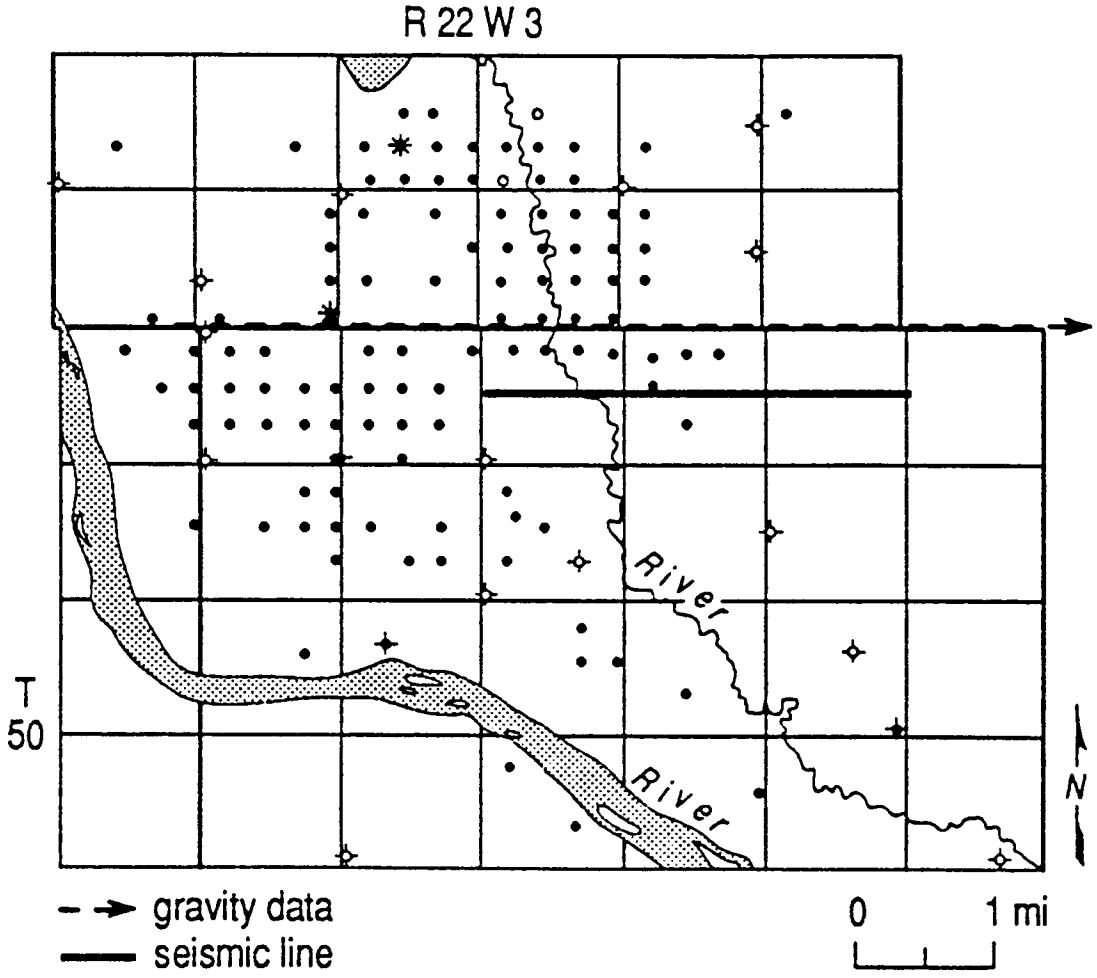

Figure VIII:4:1. Lloydminster study area.

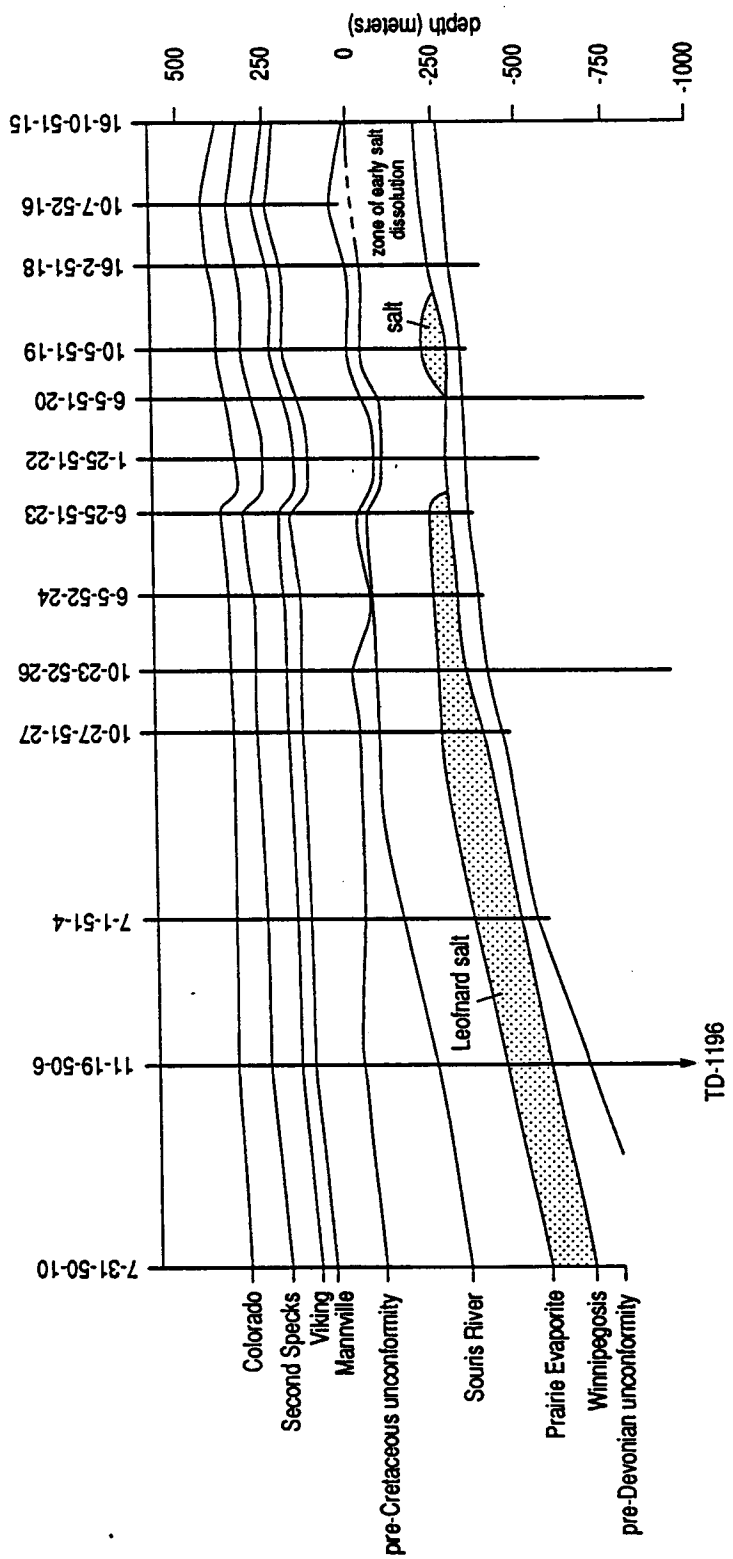

Figure VIII:4:2. Geologic section across the main dissolutional edge of the Leofnard salt.

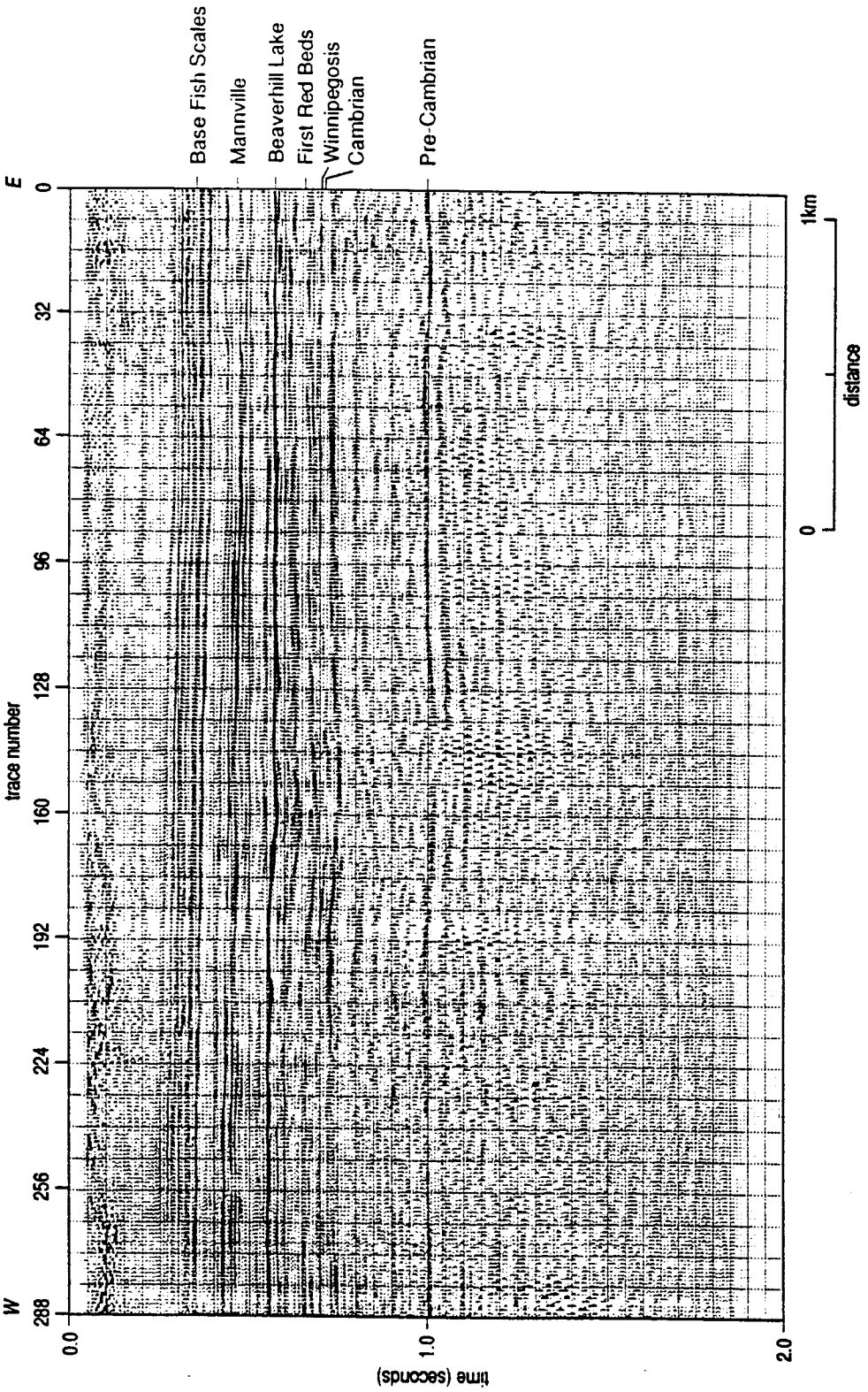

Figure VIII:4:3. Seismic line across the main dissolutional edge of the Leofnard salt. The Leofnard salt has been totally leached to the east of shotpoint 160; up to 80 m of salt are preserved to the west. These data could be variously misinterpreted as indicative of reefs, faults, and/or extreme relief at the pre-Cretaceous subcrop. Up to 145 m of salt is preserved several kilometers to the west of the seismic line (Cederwall and Anderson, 1991).

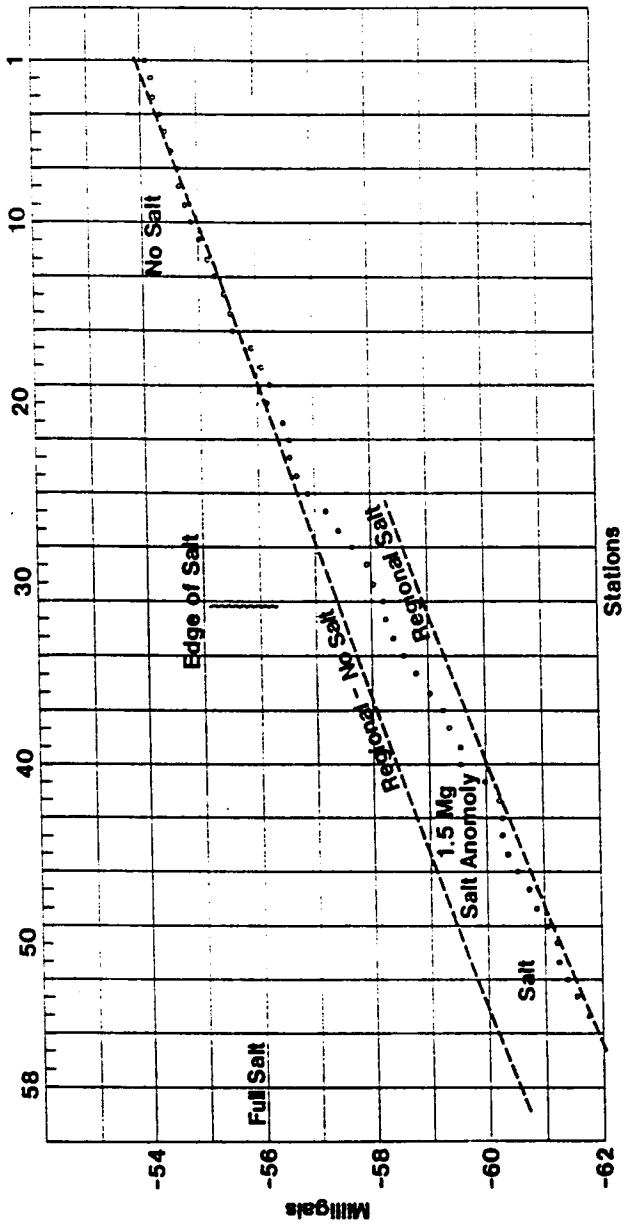

Figure VIII:4:4. Gravity profile #1. These data are part of a suite of lines acquired across the main dissolutional edge of the Leofnard salt. The Leofnard salt has been totally leached to the east of station 25; up to 80 m of salt are preserved to the west. These data could be variously misinterpreted as indicative of reefs, faults, and/or extreme relief at the pre-Cretaceous subcrop. Up to 145 m of salt is preserved several kilometers to the west of the study area (Cederwall and Anderson 1991).

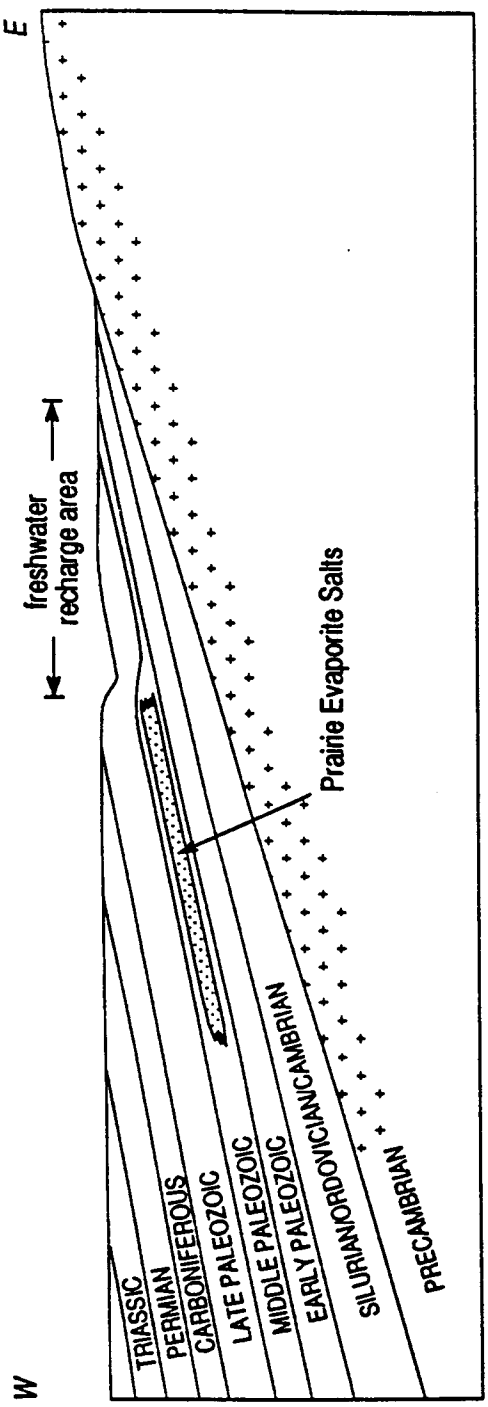

Figure VIII:4:5. Schematic cross-section depicting the east-central part of the Western Canadian Sedimentary Basin prior to the onset of Cretaceous sedimentation.

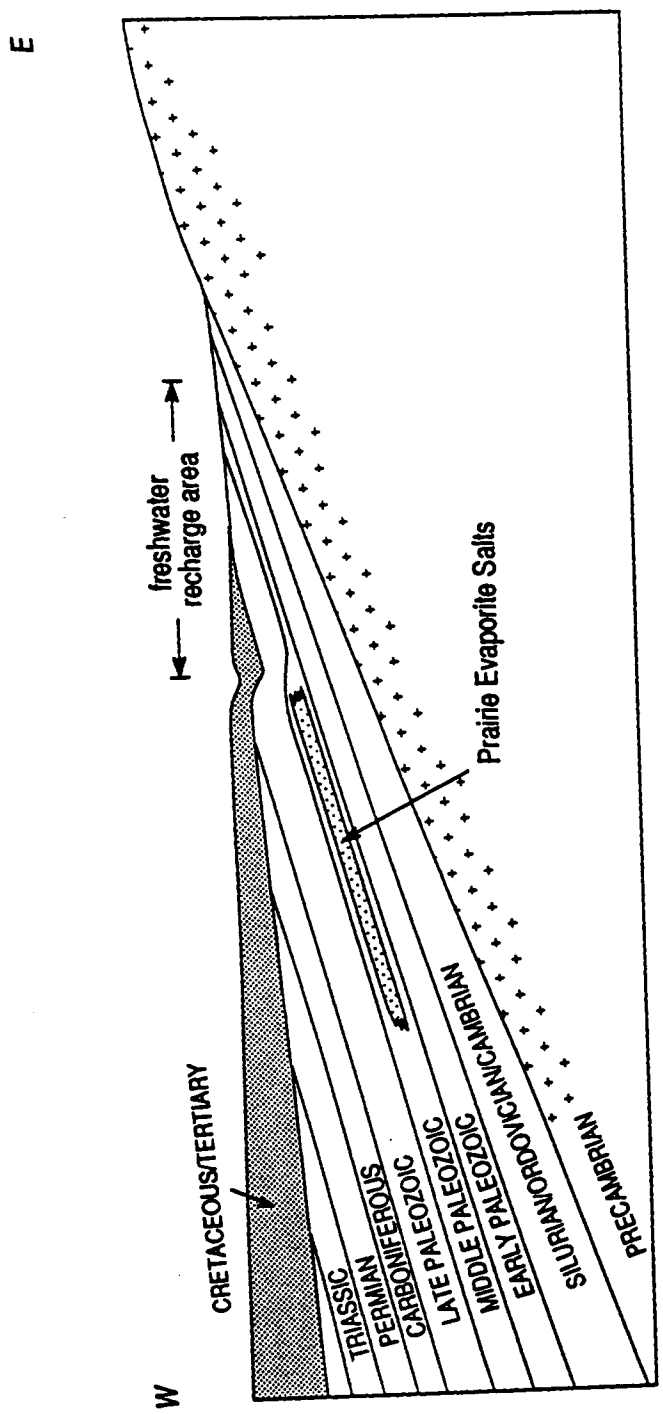

Figure VIII:4:6. Schematic cross-section depicting the east-central part of the Western Canadian Sedimentary Basin prior to the deposition of the thin veneer of Quaternary glacial sediment.

5) STETTLER AREA: CASE STUDY

A) Geological Overview

The Upper Devonian Wabamun Group in the Stettler area of Alberta is subdivided into the Stettler and Big Valley formations (Figure VII:1:1 and VII:1:2). The Stettler consists predominantly of interlayered dolomites, anhydrites and isolated to contiguous remnants of halite; the Big Valley is composed of green shales and fossiliferous limestones.

The salts of the Wabamun Group (Stettler Formation) have been mapped in detail by Anderson et al. (1988b, 1991) over most of the Stettler area. These authors conclude that a 40 meter thick interval of these halites was uniformly deposited throughout much of southeastern Alberta (Chapter VII) and subsequently leached. The discontinuous nature of these salts is illustrated in Figure VIII:5:1.

B) Example seismic line

In Figure VIII:5:2, the approximate location (T33, R20-R21W4M) of the example seismic line is superposed on a map showing the geographical distribution of the Wabamun salts (Stettler Formation equivalent). These reverse-polarity, nonmigrated data were acquired using a dynamite source and a 40 meter group interval. In Figures VIII:5:3 and VIII:5:4 interpreted versions of this seismic line are presented.

The reflections from the tops of both the Ireton and Wabamun are high amplitude and laterally continuous across the seismic line as shown by synthetic seismic modeling (Figure VIII:5:5). To the east of trace 80 and to the west of trace 240, this interval is consistently about 90 ms thick. In between these two positions, the Ireton-Wabamun interval thins, reaching a minimum of about 75 ms at trace 136. The thickness of the salt interval similarily decreases by about 15 ms. These variations are consistent with the dissolution of 40 meters of halite. Inasmuch as the maximun known thickness of salt in the area is about 40 meters (Anderson et al., 1988b, 1991), the inferences are that about 40 meters of salt are present to the east and west of traces 80 and 240, respectively, and that there is little, if any, salt in the vicinity of trace 136. The 35 ms time-structural low observed along the Wabamun at trace 136, relative to traces 80 and 240 also supports the thesis that about 40 meters of salt have been dissolved and replaced by post-Viking clastics (average P-wave velocities on the order of 2500 m/s).

As a consequence of the leaching, time-structural relief is observed along both pre- and post-Wabamun reflections. For example, the Mississippian and Viking events are about 35 ms lower in the vicinity of trace 136 relative to their apparent regional time-depth, indicating that at least some leaching occurred in post-Viking time. Successively less time-structure is present along progressively younger strata suggesting that dissolution occurred over an

extended period of time and supporting the conclusion of Anderson et al. (1988b) that leaching has been, and is, an ongoing process.

Structural relief is also observed at pre-Wabamun levels. Note, for example, that the Elk Point reflectors are pushed down by about 10 ms in the vicinity of trace 136. This pattern is consistent with the replacement of 40 meters of salt (P-wave velocity of about 4,400 m/s) with 40 meters of interlayered mudstones and shales (P-wave velocity of 2,500 m/s).

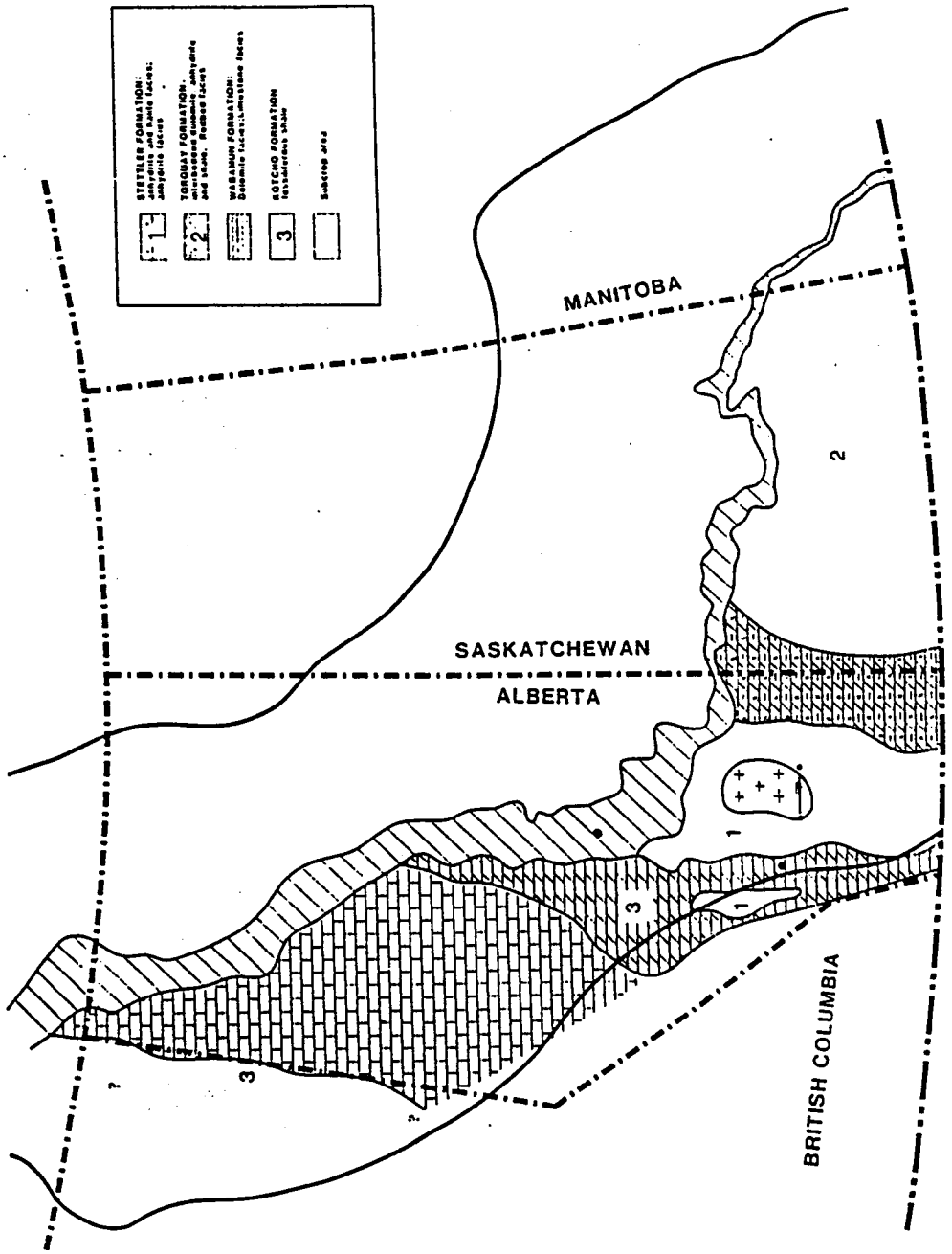

Figure 4. Distribution of the Stettler Formation (basal Wabamun Group) and its equivalents within the western Canadian interior plains (modified after Belyea, 1964; Meijer Drees, 1986). The approximate time equivalents are: 1 = Stettler Formation (white: anhydrite: crosses: halite and anhydrite; 2 = Wabamun Group (diagonal hatching: dolomite; vertical hatching: limestone); 3 = Torquay Formation (white: redbeds; hatching: dolomite, anhydrite and shale) and 4 = Kotcho Formation (fossiliferous shale). In addition 5 = the Wabamun (and equivalents) subcrop area

Figure VIII:5:1. Stettler study area.

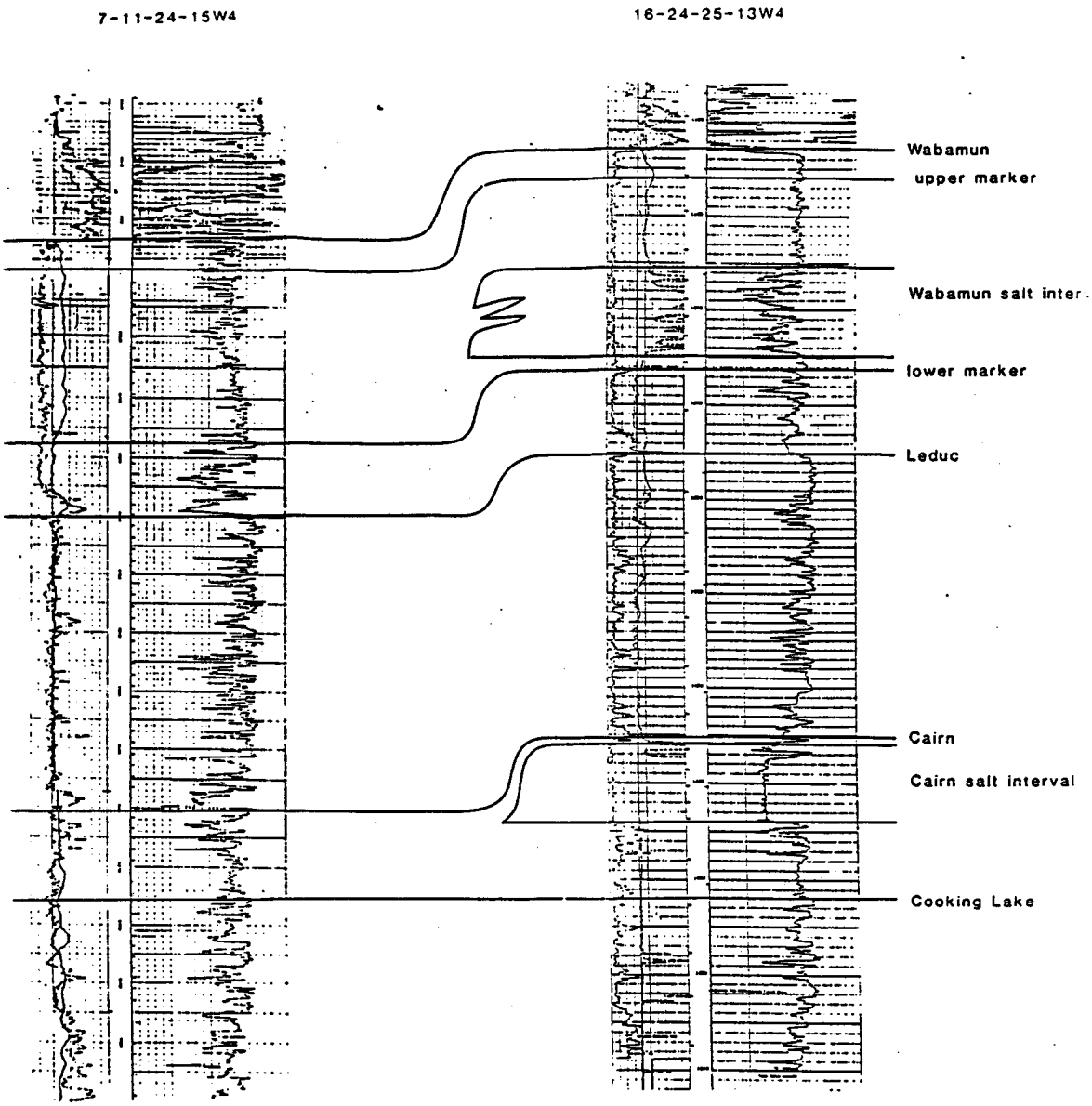

Figure 3. Gamma-ray and sonic logs for the Wabamun to Cooking Lake intervals in the 17-11 and 16-24 wells. (Note: 1) this cross-section has been flattened at the top of the Cooking Lake; and 2) in the report, the Cairn salt and the Cairn/Cooking Lake intervals are referred to as the Leduc salt and lower Leduc intervals respectively.) The remnant Leduc and Wabamun salts are 36 m and 20 m thick in the 16-24-25-13W4M well; these salts have been leached from the 7-11-24-15W4M well.

Figure VIII:5:2. Cross-section illustrating the log signature of the Wabamun salt.

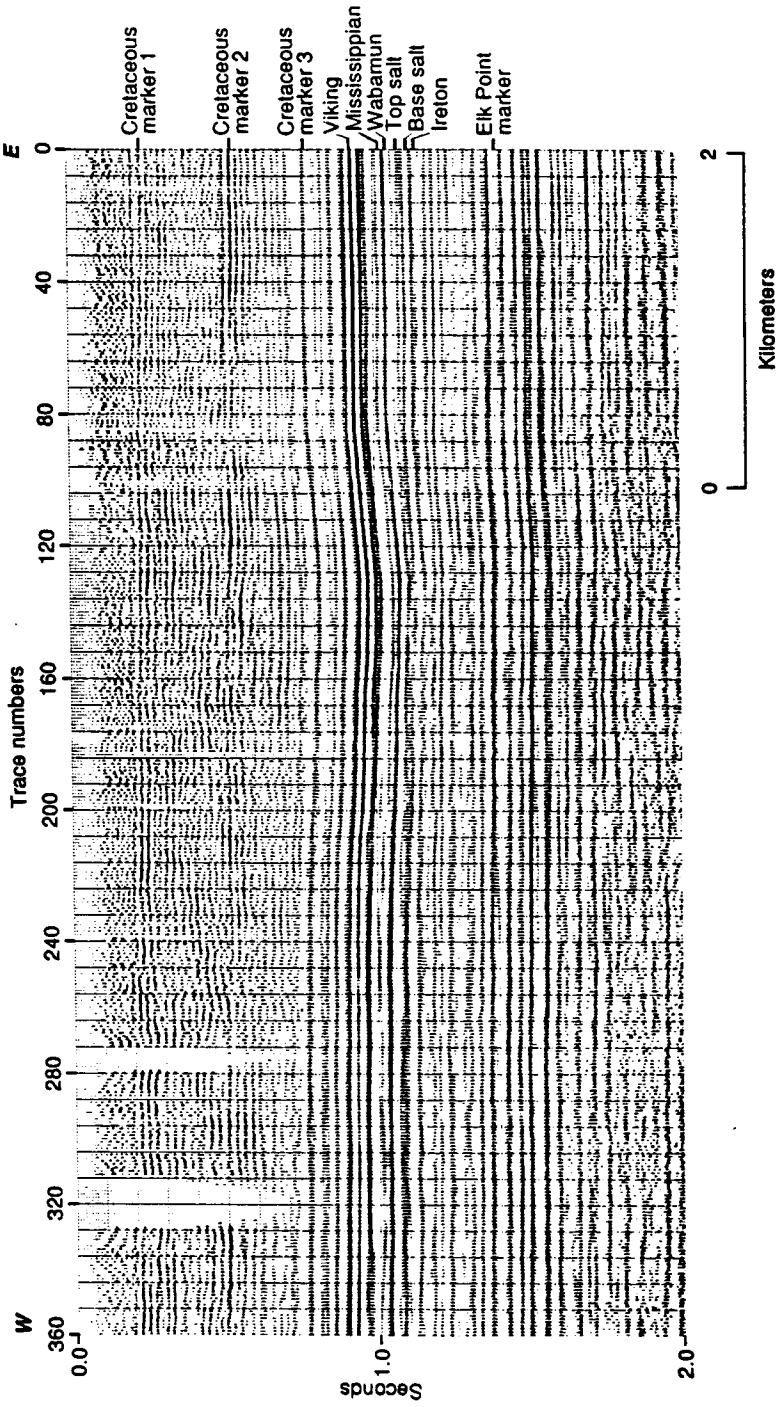

Figure VIII:5:3. Reverse-polarity, nonmigrated seismic line, located in Figure VIII:5:1, depicting the signature of remnant Wabamun salt.

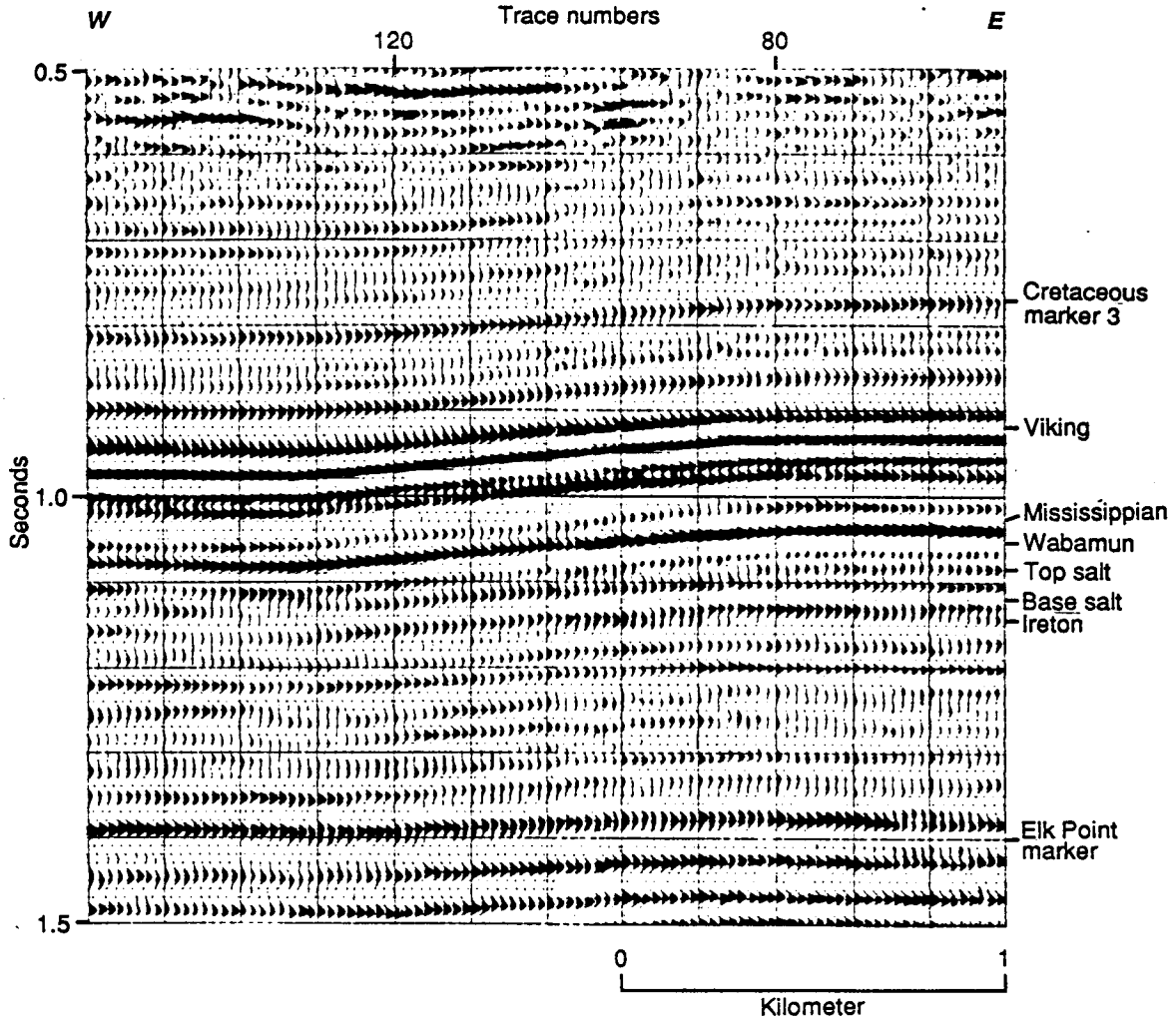

Figure VIII:5:4. Enlargement of a portion of the example seismic line.

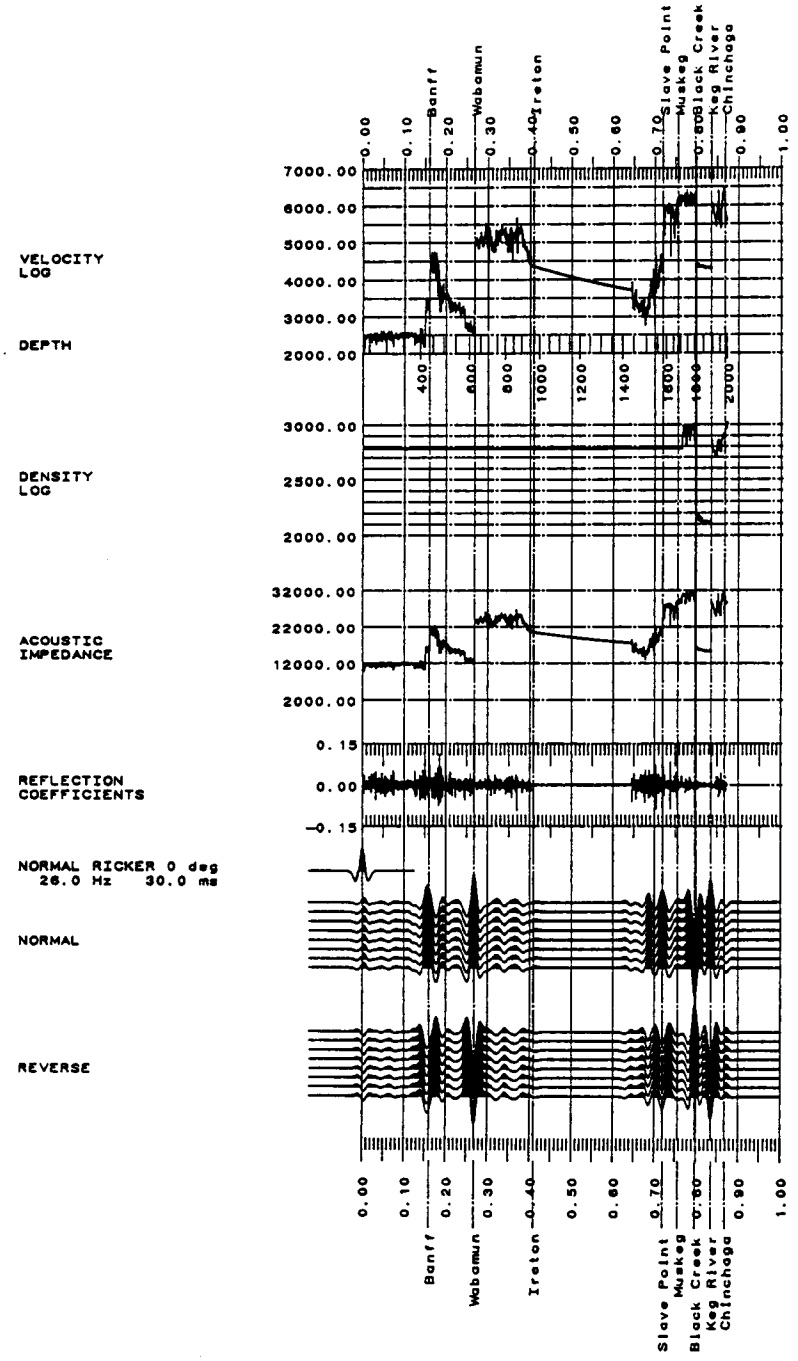

FIG. 6. Synthetic seismogram and related logs for the 9-24-109-8W6M well. This well encountered 82 meters of Black Creek salt. Note that the transit times for the 950 to 1450 meter interval (Ireton shale) were not reliably logged. This log ties the seismic section (Figure 5) reasonably well at trace 210.

Figure VIII:5:5. Synthetic seismogram for the 10-34-32-21W4M well. This well encountered about 25 meters of Wabamun salt. Note that it is about 9 kilometers south of the seismic line and penetrated a thick Banff interval (relative to that seen in the seismic line).

C) Exploration implications

The dissolution of salts has both positive and negative implications for the explorationist. From a positive perspective, leaching can create both structural traps and stratigraphic traps; from a negative perspective, dissolutional features can be mistaken for either deep-seated structures or reefs.

Structural traps can develop where reservoir facies are draped across collapse features or the updip edge of remnant salts. The potential for such entrapment is illustrated by the seismic line (Figure VIII:5:5). Note for example, that post-salt strata drape across the edge of the remnants.

Stratigraphic traps may develop where reservoir facies are either preferentially deposited or preserved in salt-dissolution lows. Such traps could have developed within our study area in those locations where salts have been extensively leached. Preliminary and ongoing work in the study area (Anderson et al., 1988b) suggests that the progressive leaching of salt influenced paleo-structure and drainage patterns. If this thesis is correct, play fairways could be defined on the basis of paleo-dissolutional patterns.

D) Misinterpretation

Dissolution can cause time-structual relief along both reflections that are pre-salt (velocity pull-up or push-down) and on those that are post-salt (collapse structure). As suggested by Figure VIII:5:7, such relief could be misinterpreted as indicative of reefal buildups or deep-seated structure. The explorationist, working in an area of salt dissolution, must carefully evaluate the seismic data, keeping in mind the several possible interpretations - and testing each - in order to determine the most probable cause of any time-structural relief.

In Figure VIII:5:8, a modified version of Figure VIII:5:4 is presented. Manual static corrections were applied to these data by a processor who was not aware that spectacular collapse features occurred in this area. Had it not been for both the anomolous relief at a two-way traveltime of about 20 milliseconds and the discontinuity near trace 102, this processing error might have gone unchallenged by the interpreter. In any case it is not difficult to conceive of seismic sections that are equally misprocessed but do not display such telltale evidence of it. These data (Figures VIII:5:7 or VIII:5:8), on the basis of apparent velocity pullup and the thinning of the Wabamun to Ireton interval, could have been misinterpreted as indicative of reef and/or faults, resulting possibly in the acquisition of additional seismic control, an acreage position, and/or unwarranted drilling.

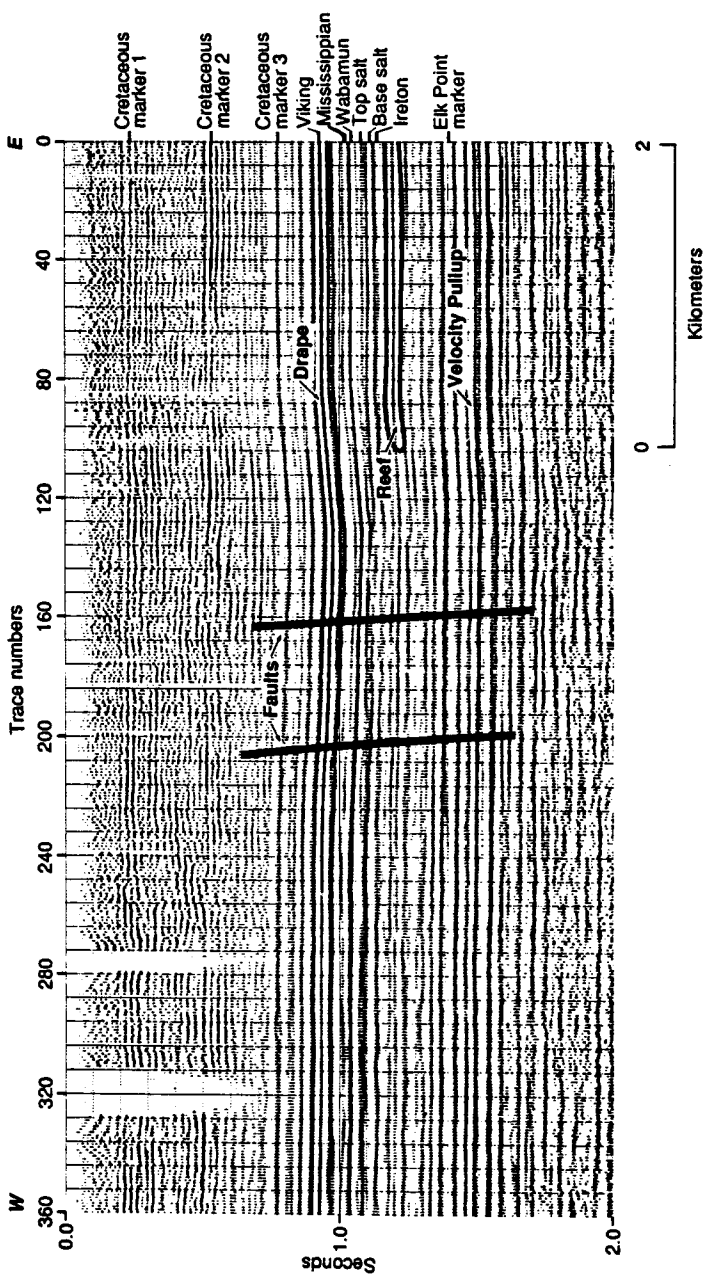

FIG. 17. Intentionally misinterpreted version of the example seismic line (Figure 10), illustrating the similarities among the seismic signatures of salt collapse features, reefs, and faults.

Figure VIII:5:6. Intentionally misinterpreted version of Figure VIII:5:3.

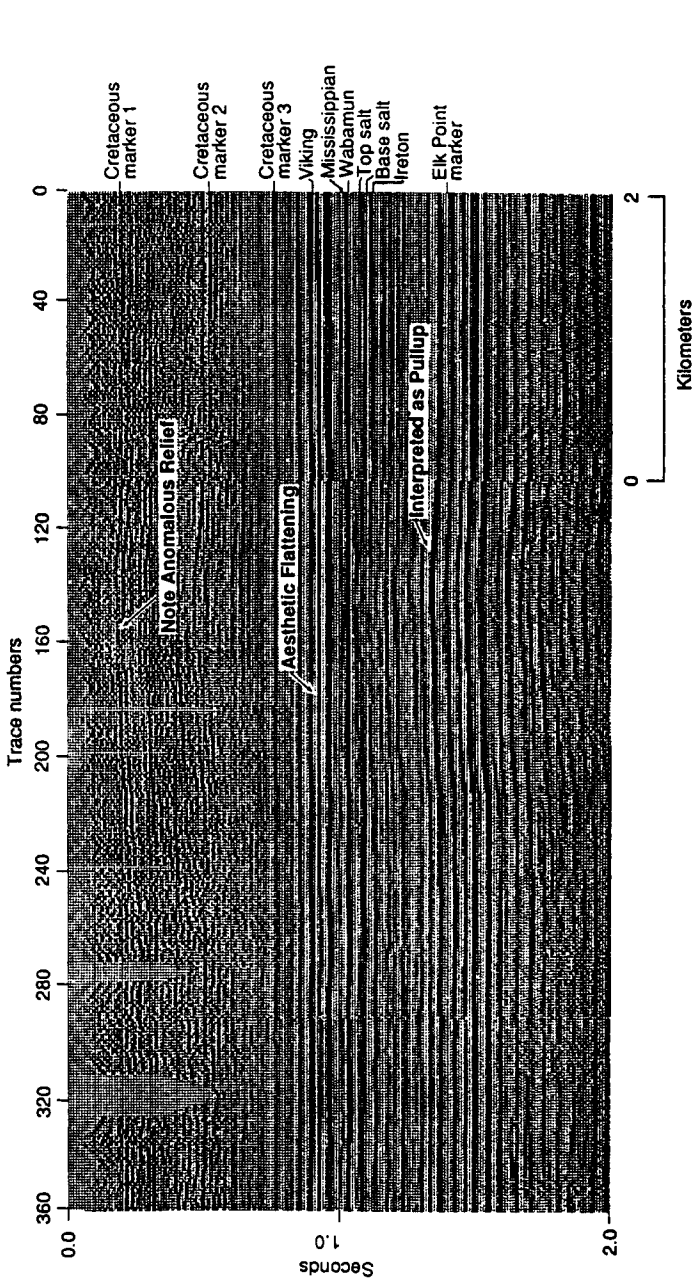

FIG. 18. Improperly processed version of the example seismic section. This line was arbitrarily smoothed at the Viking level by the processor.

Figure VIII:5:7. Improperly processed version of Figure VIII:5:3.

6) RICH AREA: CASE STUDY (ANDERSON ET AL., 1988)

A) Introduction

Rich field (Figures VIII:6:1 and VIII:6:2) is located in the southern part of the east Ireton shale basin, southwest of the Fenn-Big Valley reef complex, west of the southern Alberta shelf carbonate complex, and east of the Bashaw reef complex. In the study area, which includes the southwest edge of the Fenn-Big Valley field, there are 10 assigned and unassigned pools. Eight of these pools are in the Rich field and two are in the Fenn-Big Valley field. Two of the seven pools in the Rich field, D-3A and D-2A, are Devonian reservoirs (Leduc Formation and Nisku Formation, respectively). Four of the pools, the Glauconite B, Glauconite C, Belly River B, and Viking A are Cretaceous reservoirs. The unassigned pool is a shut-in potential gas well capable of producing from the Mannville. The D-3A pool produces from the Rumsey 9-36 Leduc pinnacle reef well and the D-2A pool produces from the biostromal Nisku Formation which drapes across this Leduc pinnacle.

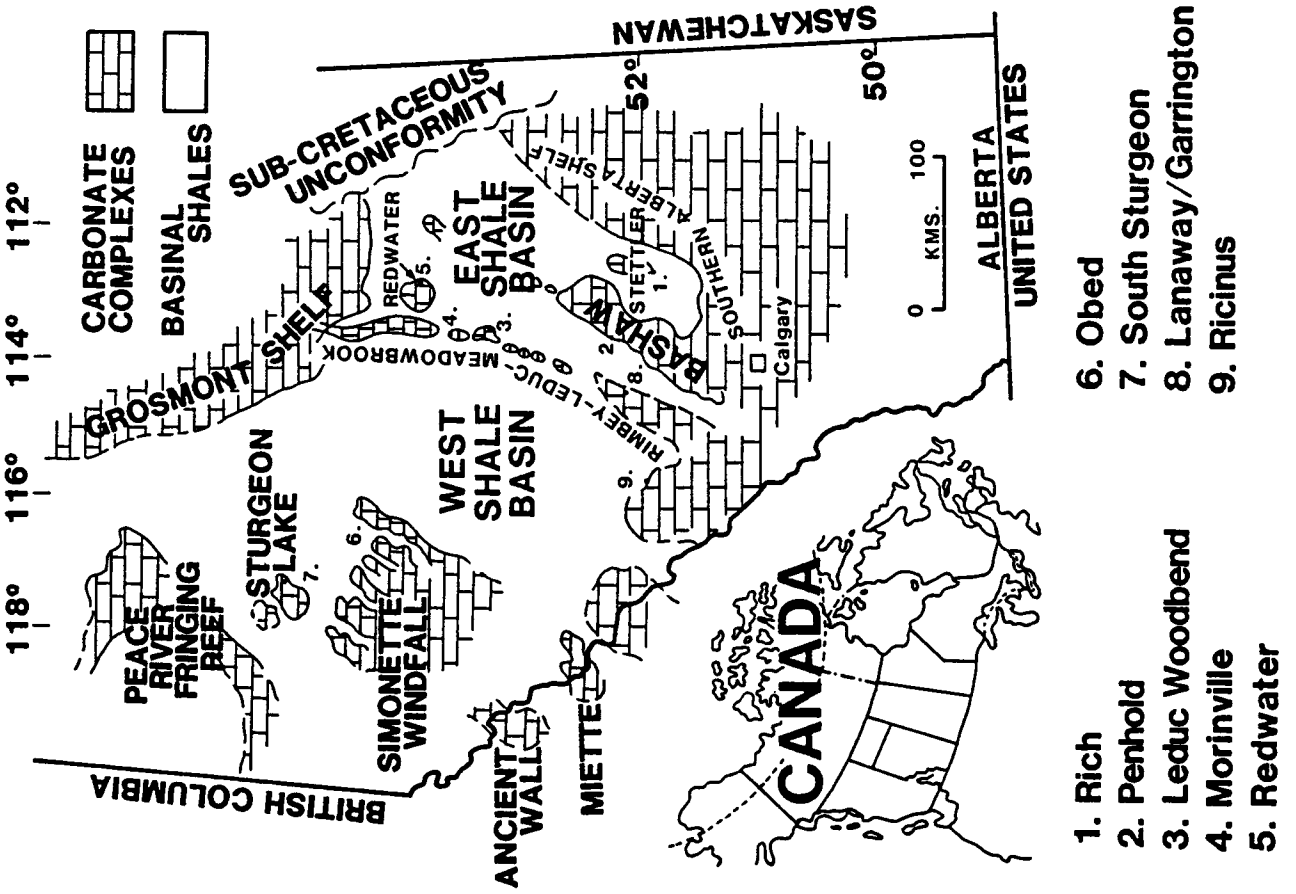

Figure VIII:6:1. Rich study area (Anderson et al., 1989).

Figure 4.2. Distribution of the Woodbend Gp carbonate complexes (modified after Stoakes, 1980).

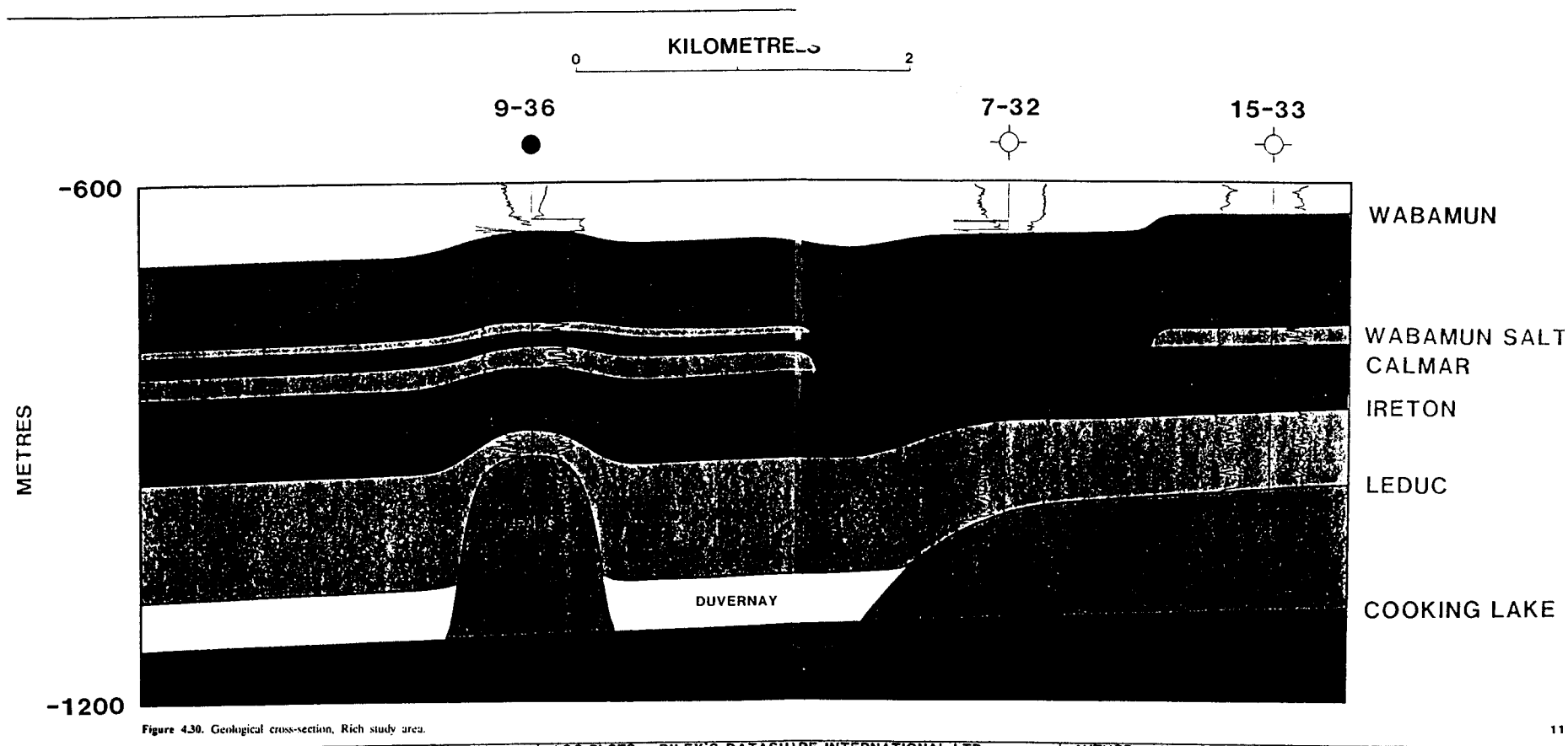

Figure 4.30. Geological cross-section, Rich study area.

Figure VIII:6:2. Rich study area (Anderson et al., 1989).

The Leduc Formation in the area developed as isolated pinnacles and larger atolls. The Rich field pinnacle (D-3A pool) is located basinward of the Fenn-Big Valley Leduc reef complex. Pinnacles in this area typically attain heights of 200 m and are overlain by Ireton Formation shales. The Rich field was selected as an example Woodbend Group reservoir for three reasons:

(1) The Leduc Formation, D-3A pool is a significant reservoir from an economic perspective. Production as of December 1987 from this pinnacle and from the overlying D-2A pool was 574 x 10^3 m^3 of oil and 30,000 X 10^3 m^3 of gas; and 36 x 10^3 m^3 of oil and 18,000 x 10^3 m^3 of gas, respectively;

(2) The seismic line displays a significant variation in the seismic signature of the Wabamun salts (due to partial dissolution); and

(3) The seismic line is well orientated for illustrative purposes, crossing the D-3A pinnacle and the southeastern edge of the Fenn-Big Valley Leduc reef complex.

B) Geologic cross-section

Figure VIII:6:2 gives the locations of the three wells incorporated into the geological cross-section (Figure VIII:6:3) and the seismic section (Figure VIII:6:4). Two of the wells are approximately 500 m from the seismic line, whereas the third lies on the seismic line. Such extrapolation is necessary for interpretation purposes as the geological cross-section illustrates the 25 m (minimum) variation of the thickness of the Wabamun salts in the area and demonstrates the effect of dissolution; particularly in the vicinity of the 7-32 well. The top of the Wabamun Group in this well is 20 m structurally low relative to many of the surrounding wells. Relief due to salt dissolution is complicated as a result of drape across underlying Leduc reefs.

The contoured Leduc/Cooking Lake structure map is shown as Figure VIII:6:6. The Leduc D-3A pinnacle is isolated from the Fenn-Big Valley reef complex to the northeast. The inner contour of -900 m sub-sea across the pinnacle is 50 m lower than the Fenn-Big Valley reef contour of -850 m suggesting that the 9-36 well may not have penetrated the apex of the pinnacle. The Leduc is overlain by the upper Ireton Formation and the Winterburn Groupp. In off-reef areas the Ireton overlies the Duvernay Formation shale. The Calmar Formation structure map shows that the Calmar drapes across both the pinnacle and the reef complex.

Without the effect of partial salt dissolution, the Wabamun, more typically, would drape across both the D-3A pinnacle reef and Fen-Big Valley reef complex. The Wabamun is 7 m lower immediately to the east of the 9-36 well than in this well. However, the Wabamun top is 25 m lower (-659 versus -634 m sub-sea) at the 7-32 well than at the neighboring reef complex well, 15-33. This could be interpreted as drape due to differential compaction except for the fact that the Calmar depth values in the same two wells differ by only 13 m

(Figure VIII:6:7). Wabamun structure, therefore, must be related to partial dissolution of the Wabamun salts.

The Glauconite B, C, Viking A and Belly River pools overlie relative structural lows at the Wabamun and Banff levels (Figure VIII:6:8). The Belly River B pool in the 10-32 well appears to lie within the structural low caused by the salt dissolution in the area of the 7-32 well. The Viking A pool lies across the Leduc D-3A pinnacle and appears to be influenced by the drape due to differential compaction. The other two pools do not appear to be associated with anomalous Wabamun structure.

C) Seismic section

Figure VIII:6:4 shows the location of the seismic line which crosses the D-3A pinnacle reef and extends onto the southwestern edge of the Fenn-Big Valley reef complex. These seismic data were acquired using the Vibroseis source (4 in-line with a 12-second 90-10-Hz sweep length), a 1530-m split spread, 120-m shot spacing and a 30-m group interval.

Figure VIII:6:5 is a seismogram for a pinnacle reef (9-36-34-21W4M). The Cooking Lake Formation is not penetrated by the 9-36 well, and regional seismic control as well as other synthetics were used for the interpretation of this marker on the seismic data. On the seismic section, the Cooking Lake event is as much as 20 ms time-structurally higher beneath the pinnacle than off-reef, due primarily to lateral variations in the thicknesses of Leduc and Wabamun salts. Less pull-up is observed beneath the Fenn-Big Valley reef complex at the eastern end of the seismic line probably due to the fact that the reef complex is relatively thin in this area.

The Ireton shale event, off-reef, is a strong peak on the seismic section. On-reef, this reflection diminishes in amplitude and undergoes a character change due to interference with the Nisku event. It is difficult to interpret variations of Nisku porosity on seismic data because of these interference effects.

Drape at the Wabamun (on the order of 5 ms) is affected by the presence or absence of the Wabamun salts. The salt affects the seismic interpretation in that the drape across reefs due to compaction of reef and off-reef strata may be affected by the discontinuous nature of these salts (Anderson et al., 1988a). For example, drape across the D-3A pool reef is accented by the thinning of the salt from the 9-36 well to the 2-31 well (to the east). In contrast, drape at the Wabamun level on the eastern part of the seismic section is diminished by the absence of salt in the 7-32 well (at the edge of the reef complex) and the presence of salt off-reef.

The Cretaceous markers exhibit closure across the reef that could be affected by the dissolution of the Wabamun salts. Above the pinnacle D-3A pool reef the Viking marker drapes some 10 ms and does not exhibit closure until the

area of the 73-32 well. East of the 7-32 well, the Viking drapes across the edge of remnant salt. This abrupt change in relief along the Cretaceous (Viking) could be misinterpreted as drape across of an underlying Leduc reef. The presence of the more or less continuous Ireton marker below the salt dissolution allows the identification of off-reef shale in the seismic section.

Interpretation of the seismic data in those areas where remnant Wabamun salts are present is done in two steps:

(1) Estimate the relative thickness of the Wabamun; and

(2) After mapping the salts, analyze the seismic data for features characteristic of Leduc reefs. Such features would include pull-up, drape, lateral variations in the seismic image of the Woodbend and lateral amplitude changes along specific seismic events.

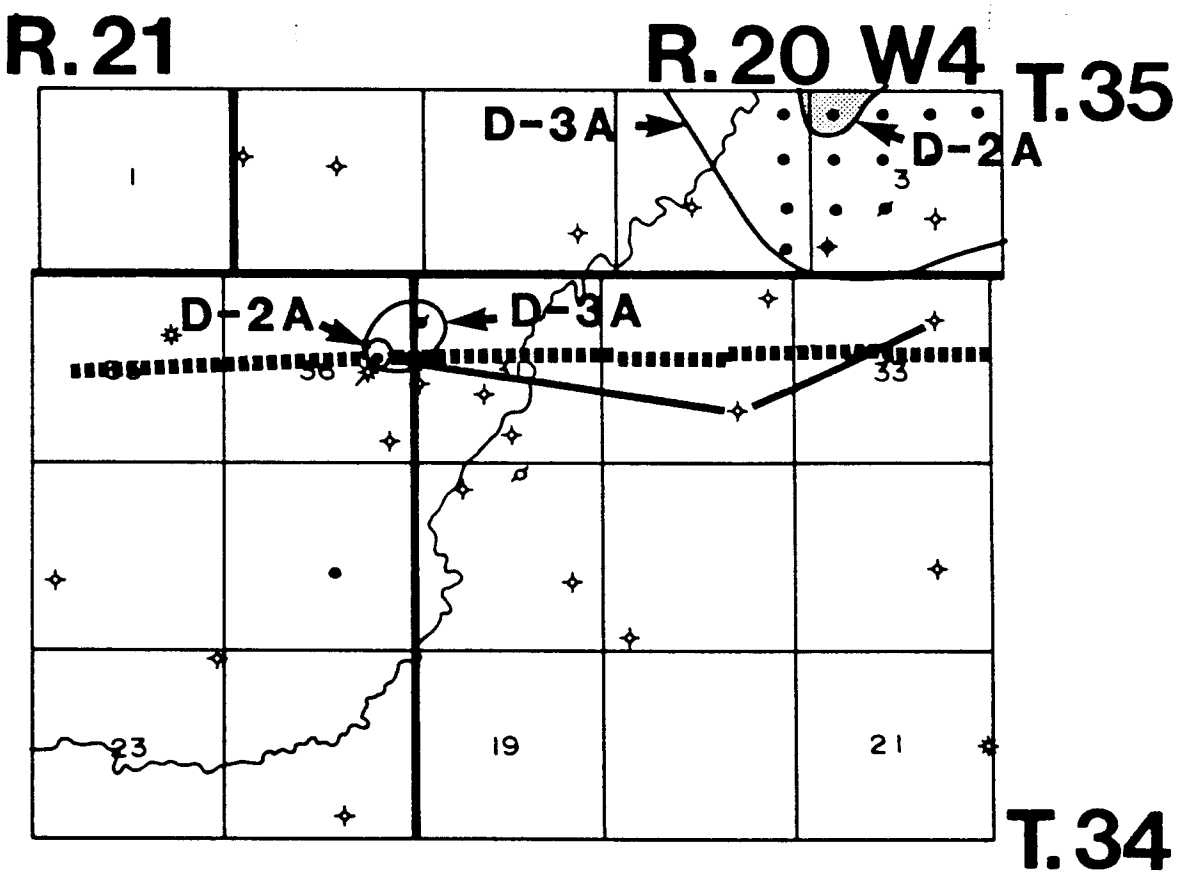

Figure 4.29. Rich study area. Pool outlines, the three wells incorporated into the geological cross-section and the approximate

Figure VIII:6:3. Geologic section (Anderson et al., 1988).

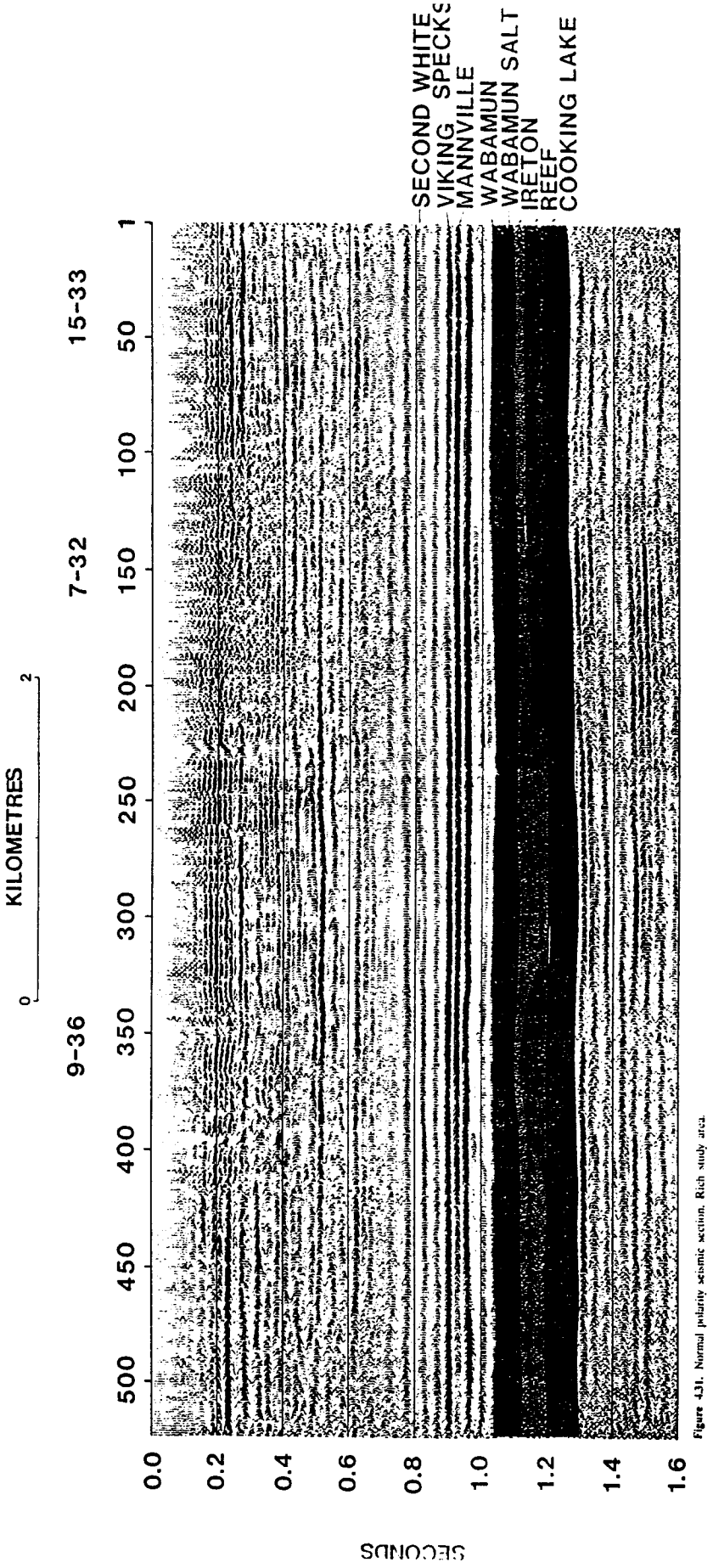

Figure VIII:6:4. Seismic section (Anderson et al., 1988).

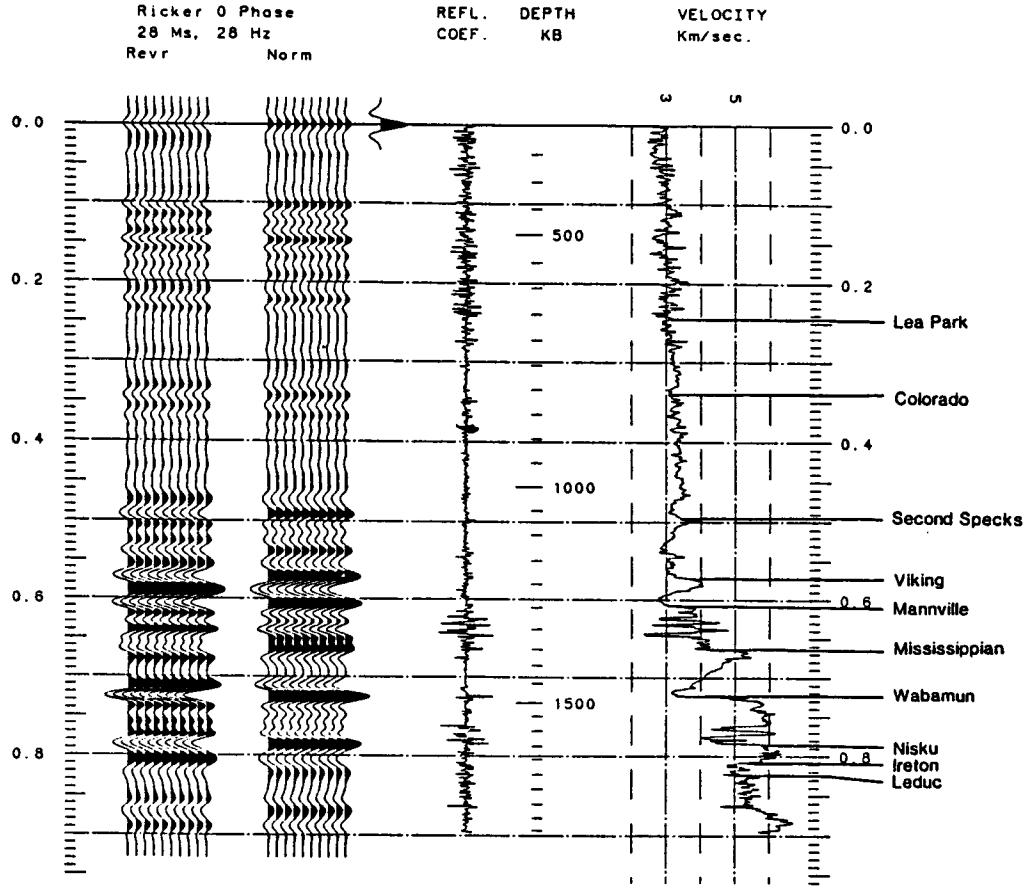

Figure 4.36. Seismogram for the 9-36-34-21W4M well.

Figure VIII:6:5. Synthetic seismogram (Anderson et al., 1988).

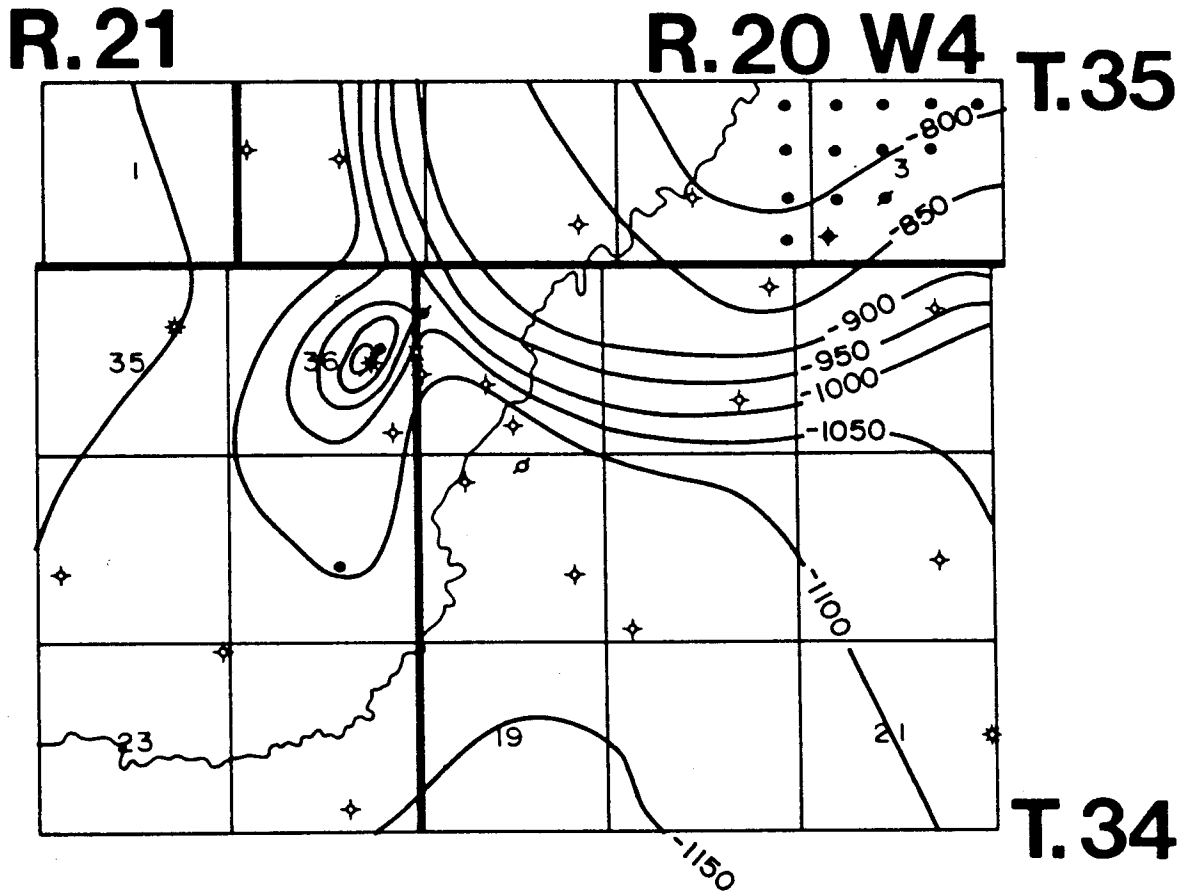

Figure 4.32. Contour map (in metres relative to mean sea level) of the Leduc Fm (or in its absence, the Cooking Lake Fm).

Figure VIII:6:6. Leduc/Cooking Lake structure map (Anderson et al., 1988).

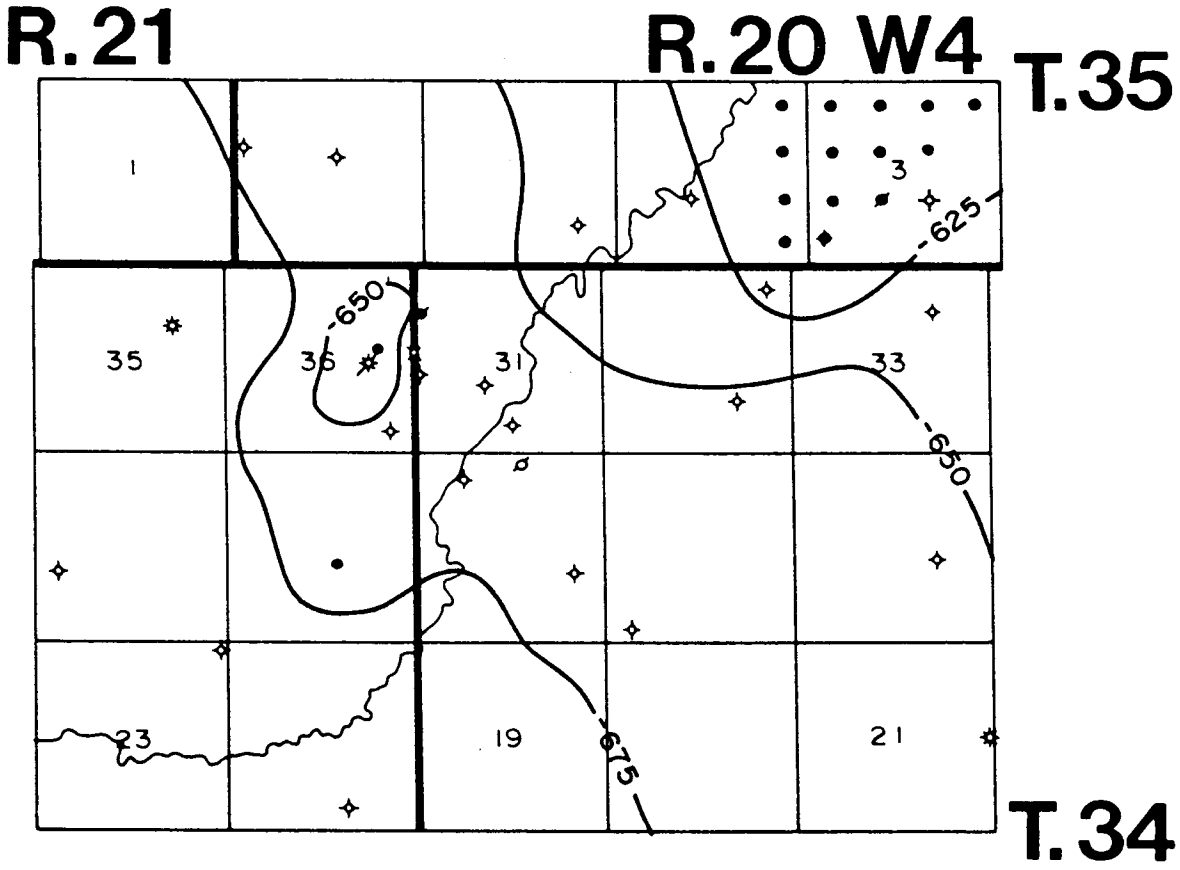

Figure 4.34. Contour map (in metres relative to mean sea level) of the Wabamun Fm.

Figure VIII:6:7. Wabamun structure map (Anderson et al., 1988).

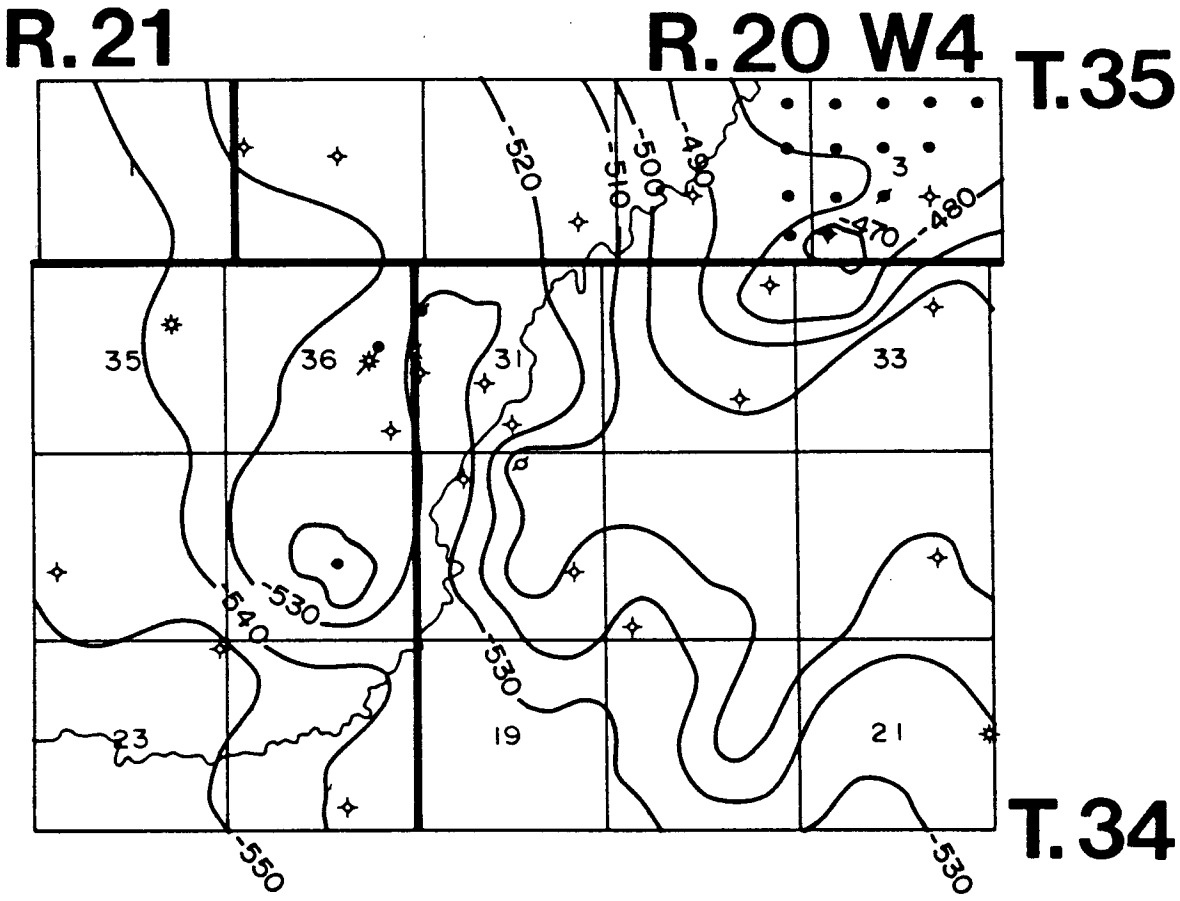

Figure 4.35. Contour map (in metres relative to mean sea level) of the Banff Fm.

Figure VIII:6:8. Banff structure map (Anderson et al., 1988).

7) WINNIPEGOSIS REEFS (ANDERSON AND FRANSEEN)

A) Introduction

Upper Winnipegosis Formation buildups are scattered throughout the Middle Devonian Elk Point basin (Figure VIII:7:1). These dolomitized carbonates have been variously described as reefs or as mounds, due to an apparent absence of framebuilding or binding organisms in cores (Gendzwill, 1978; Gendzwill and Lundberg, 1989; Gendzwill and Wilson, 1987; Walter, 1969; Jones, 1965; Perrin, 1982; Precht, 1983; Reinson and Wardlaw, 1972; Wardlaw and Reinson, 1971; and Wilson, 1984). The Upper Winnipegosis buildup, herein referred to as a reef, exhibits a raised rim on the example seismic data, mostly a secondary compactional feature characteristic of Devonian reefs in western Canada

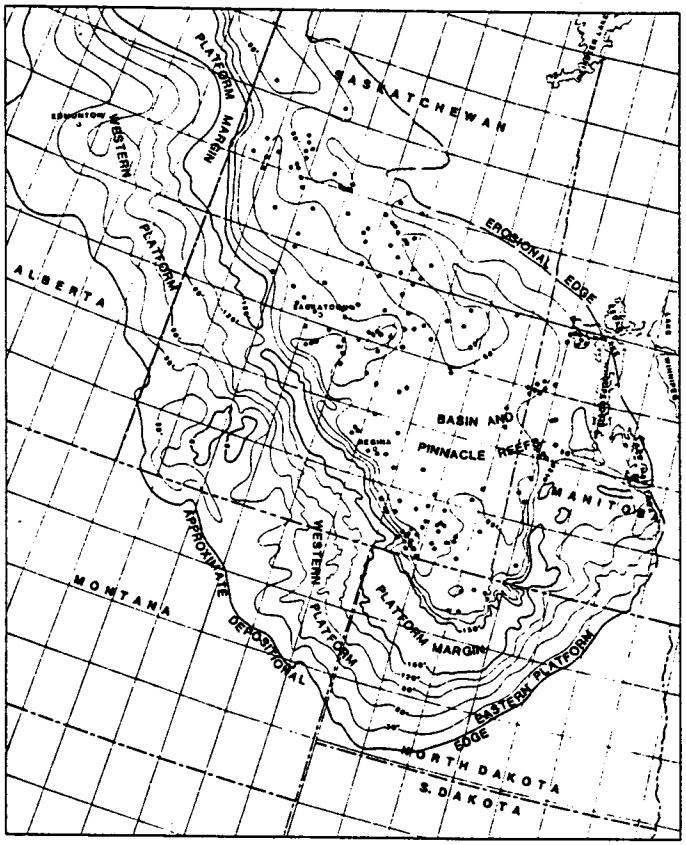

FIG. 1. Regional map showing the Elk Point basin, the thickness of the Winnipegosis, and some known mounds (dots). Contour interval, 30 ft (9.1 m) (Ehrets and Kissling, 1987).

Figure VIII:7:1 (Anderson and Franseen, 1991)

(Anderson and Brown, 1987; Anderson et al., 1986; Anderson et al., 1989; Brown et al., 1990; Mossop, 1972; and Wirnkar and Anderson, 1989). The raised rim could also reflect an original buildup morphology with a margin that was topographically higher than the interior, possibly due to framebuilding organisms and/or submarine cementation.

The Winnipegosis reef example of this paper is encased in the salts of the Prairie Evaporite Formation (Figure VIII:7:2) which appear to be relatively incompressible compared to carbonates. The top of these salts, on the example seismic line, is structurally lower on top of the reef than in the adjacent offreef areas. This structural low and the pattern of relief as the beds are traced across the top of the reef itself are consistent with the thesis of post-depositional compaction of the reef.

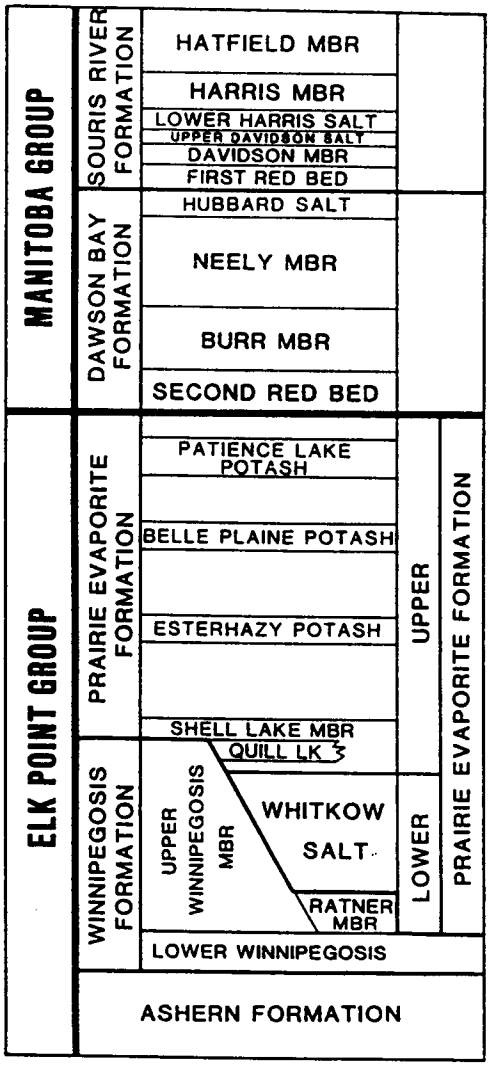

FIG. 2. Detailed stratigraphy of the Elk Point group of southern Saskatchewan (modified after Gendzwill and Lundberg, 1989).

Figure VIII:7:2 (Anderson and Franseen, 1991)

If the Prairie Evaporite was uniformly deposited in the study area, as appears to be the case, then the relief observed across the tops of the reef and the salts are estimates of differential compaction within the different reef environments, and between the reef and the salts, respectively. If the salts are assumed to be effectively incompressible (as a minimizing assumption), then the extent to which this reef was compacted can be quantifiably estimated.

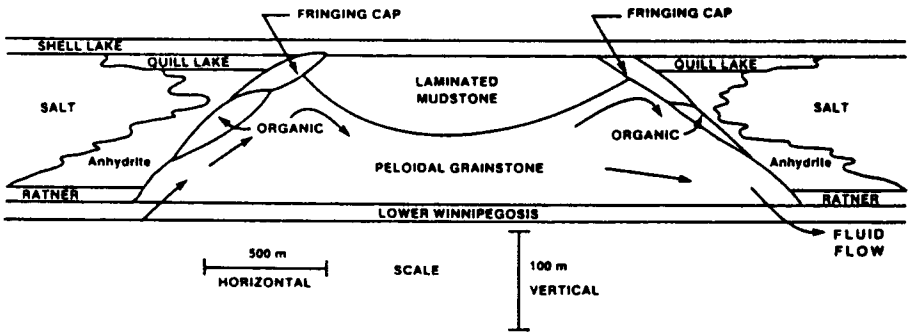

FIG. 3. Conceptual model of a Winnipegosis mound showing the four principal units of the upper Winnipegosis: peloidal grainstone, laminated mudstone, an organic unit, and fringing cap unit (Gendzwill and Lundberg, 1989).

Figure VIII:7:3 (Anderson and Franseen, 1991)

B) The Elk Point Group

The Elk Point Group in Saskatchewan (Figure VIII:7:2) is subdivided into three formations: 1) the Ashern, a basal shale unit; 2) the Winnipegosis, a dolomitized carbonate unit; and 3) the Prairie Evaporite, a thick rock salt.

The Ashern is typically composed of thin bedded, red, green, and grey shale, dolomitic siltstone, and argillaceous dolomite. This unit was deposited unconformably above Silurian strata in a shallow-marine environment during the initial transgression of the Devonian sea across southern Saskatchewan. The Ashern has an unconformable contact with the overlying Winnipegosis (Perrin, 1982).

The Winnipegosis consists of platform (lower Winnipegosis), reef (upper Winnipegosis), and inter-reef (Ratner Member) carbonates (Figure VIII:7:2). The lower Winnipegosis is described as a dolomitized fossiliferous packstone (Jones, 1965) that has a gradational upper contact. The overlying upper Winnipegosis reefs are composed of dolomitized carbonates (Gendzwill and Wilson, 1987) that Wilson (1984) subdivided into four main units from base to top: 1) peloidal grainstone; 2) laminated carbonate mudstone; 3) an "organic" unit; and 4) a fringing cap unit (Figure VIII:7:3). The organic (stromatoporoids, oncolites, and shell fragments) and fringing cap (pisolites, peloids, and

intraclasts in micrite matrix) units are thought to have been deposited as reef-margin facies in relatively high-energy environments around the outer edge of the reef. The laminated carbonate mudstone (locally with anhydrite in the upper portion) was deposited in an interior (lagoon to sabkha?) environment, behind and likely sheltered by the organic and fringing cap units.

The structural relief observed across the top of the reef in the seismic line in Figures VIII:7:4 and VIII:7:5, is largely a result of the differential compaction of these different reef facies. As evidenced by the example seismic data, the reef in the study area attains a maximum thickness, including the underlying platform facies, of about 95 m and is about 1.4 km wide. The inter-reef Ratner Member (Figure VIII:7:3), described as carbonate mudstone and/or anhydrite, is about 45 m thick (including the thickness of the underlying platform facies).

The Prairie Evaporite overlies the Winnipegosis Formation and, in the study area, attains maximum thicknesses of about 140 m in areas adjacent to the reefs (Gendzwell and Lundberg, 1989).

C) Example seismic line

The interpreted, reverse polarity, example seismic line and enlargement of the same, are presented as Figures VIII:7:4 and VIII:7:5, respectively. These 12-fold, dynamite data were acquired using a 25-m group interval. In Figure VIII:7:6, these data are correlated to a 1-D synthetic seismogram for the 13-24-02-3W217 well (about 6 kilometres off-line).

These data have been hand inverted and a compatible depth/velocity cross-section has been created (Figure VIII:7:7). The model in Figure VIII:7:7 also supports the thesis of differential compaction within the reef and illustrates many of the interpretational concepts discussed below.

The reflection from the top of the Winnipegosis (base Prairie Evaporite) is high amplitude and can be confidently correlated (Figures VIII:7:4 and VIII:7:5). The reflection from the base is not easily correlated, being effectively masked by the Silurian (base Ashern) event. Despite the absence of a reflection from the base of the Winnipegosis, the thickness of the Winnipegosis Formation can be estimated. For example, if the thickness of the Ashern, on-line, is assumed to be 16 m as in the 13-24-2-3W2M well, then the thicknesses of the Winnipegosis (including the Ratner where present) at traces 266, 296 and 180 are calculated to be 93, 85 and 60 metres respectively. These estimates are based on Winnipegosis/Silurian intervals of 41ms, 39ms and 28ms respectively, and average Ashern and Winnipegosis velocities of 5300 m/s. The reef (traces 240 to 360), is characterized by: 1) positive relief at the Winnipegosis level (20ms/45m at trace 266; 16ms/36m at trace 296) relative to adjacent offreef locations; negative relief along the Prairie Evaporite event ; and 3) pull-up along pre-Devonian horizons (8ms at trace 296; 5ms at trace 266). Note that the reef exhibits a well-defined raised rim (traces 260-275 and 310-330) and a 4ms/9m structurally lower interior area (traces 275-310).

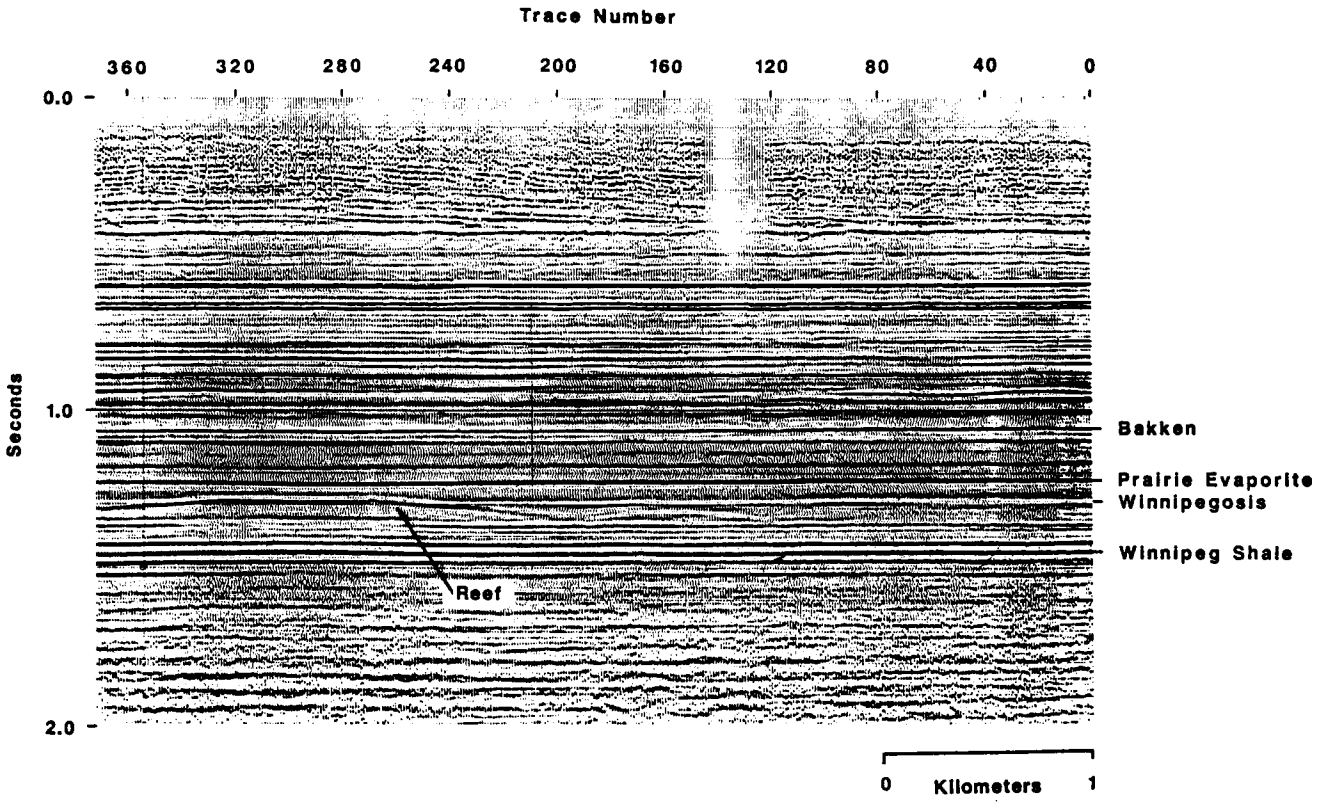

FIG. 4. Seismic line across a Winnipegosis reef (traces 240–360 at about 1.3 s).

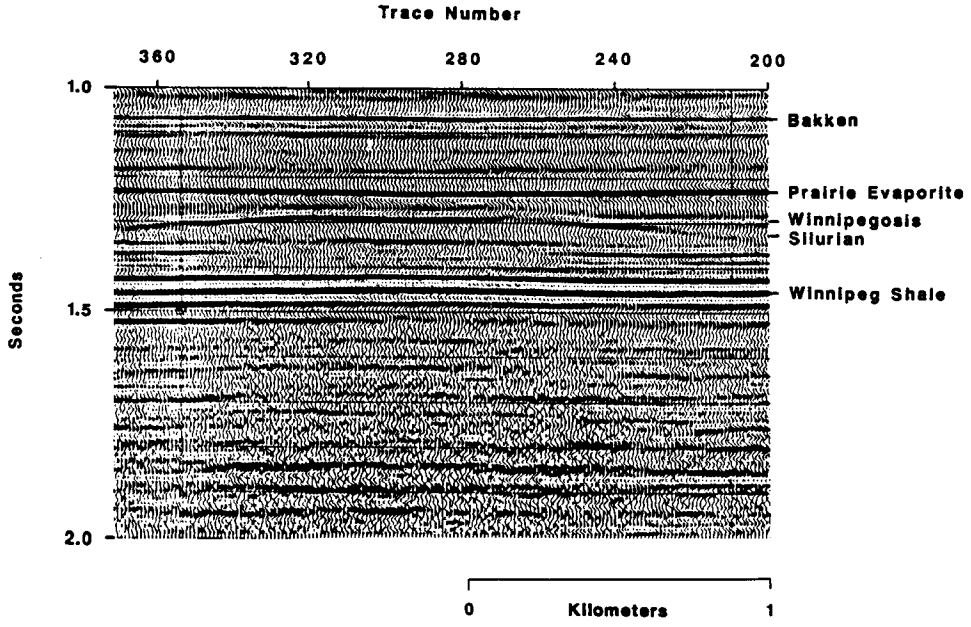

FIG. 5. Enlargement of Figure 4. The raised rim (traces 260–275 and 310–330) and the interior backreef environment (275–310) are clearly visible.

Figures VIII:7:4 and VIII:7:5 (Anderson and Franseen, 1991)

The reflections from the top and base (top Winnipegosis) of the Prairie Evaporite are high amplitude (Figures VIII:7:4 and VIII:7:5). On the basis of this interval, the thicknesses of the Prairie Evaporite at traces 180, 266 and 296 are estimated to be 140m, 88 and 95m respectively. Note that the Prairie Evaporite event is low across the reef (7ms/20m at trace 296 and 4ms/12m at trace 266) relative to trace 180 in an offreef area, presumably as a result of differential compaction within the reef and due to the relative incompressibility of the salts.

The two lowest events identified on the seismic section are the reflections from the Winnipeg Shale and the underlying Silurian. All three events are pulled up by about 7ms beneath the reef interior (trace 296) and about 5 ms below the raised rim (trace 266). These estimates are consistent with reef velocities on the order of 5300m/s, salt velocities on the order of 4200 m/s, and the geological model of Figure VIII:7:7.

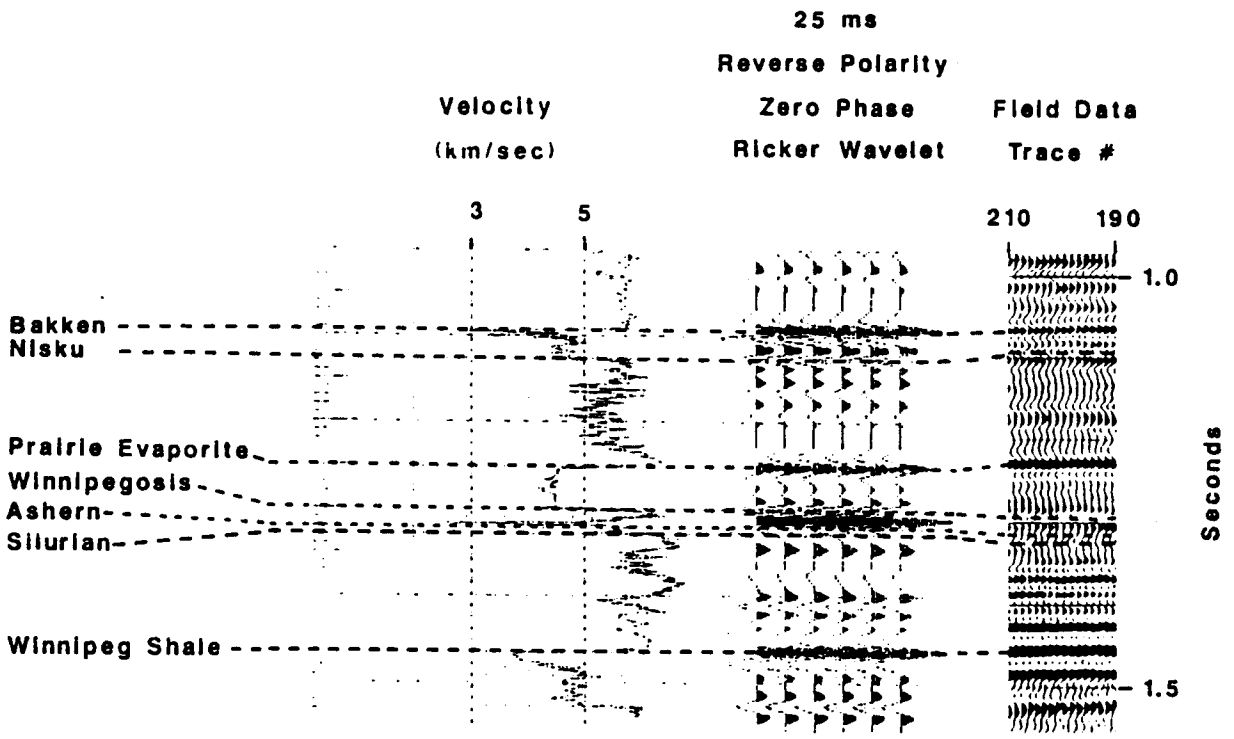

FIG. 6. Correlation of the synthetic seismogram for the 13-24-02-3W2M well and the seismic data.

Figure VIII:7:6 (Anderson and Franseen, 1991)

D) Discussion

The Winnipegosis reef example of this paper is characterized by: 1) a pronounced raised rim and a structurally lower interior lagoon; 2) negative drape along the Prairie Evaporite horizon; and 3) pull-up at pre-reef levels (Figures VIII:7:4, VIII:7:5 and VIII:7:7). The raised rim, the structurally lower lagoon, and the negative drape at the Prairie Evaporite level are attributed mostly to differential compaction within the reef, possibly enhancing original depositional morphologies of the reef environments and/or cementation (or rigid frame-building) characteristics of the different facies, and to the relatively incompressible nature of the encasing salt. These structural features are illustrated in the depth/velocity cross-section of Figure VIII:7:7.

Figure VIII:7:8 is a reconstructed version of the geologic model, created by flattening the top of the Prairie Evaporite. This reconstructed model removes the effects of the post-Elk Point compaction of that portion of the reef above the Ratner Member. Several particularly interesting relationships can be deduced by comparing these before- and after-decompaction models.

1) The interior of the reef at the end of Prairie Evaporite time was about 45 m higher than the inter-reef Winnipegosis (top Ratner). It is now about 25 m higher, indicating that these interior reef facies (laminated carbonate mudstone unit) have been compacted by at least 44 percent. This represents a minimum estimate in that some compaction probably occurred prior to the end of Prairie Evaporite time. Gendzwill (1978) describes differential thickening of salt layers over Winnipegosis mounds and attributes these features to early compaction within the reef.

2) The rim of the reef at the end of Prairie Evaporite time stood about 50 m above the inter-reef Ratner deposits. It is now some 35 m higher than the Ratner, indicating that the rim was compacted by about 30 percent. This is also a minimum estimate, as some compaction probably occurred prior to the end of Prairie Evaporite time.

3) The decompaction exercise indicates that at the end of Prairie Evaporite time the interior of the reef was slightly lower (5 m or less) than the reef rim, thus illustrating the usefulness of this method to determine original reef morphology. As a result of compaction, the reef interior area is now about 10 m lower than the reef rim.

These estimated compactional factors are probably reasonable estimates of the overall compaction of the reef if the salts are indeed incompressible and have not undergone selective dissolution along their on-reef trace, if the Ratner and basal reef were compacted to a similar degree, and if most of the compaction of the Winnipegosis occurred after the deposition of the Prairie Evaporite. Most likely, some compaction occurred prior to the end of Prairie Evaporite time, meaning that our compaction factors represent minimum estimates.

Mossop (1972), in a study of the Devonian Redwater Leduc reef complex, pointed out that compaction by stylolitization through pressure-solution of carbonate mineral matter was an important process resulting in volume loss in carbonate rocks. He reported rim and reef-interior compactional factors of 13 and 24 percent, respectively, based on measurements of stylolites. Mossop (1972) cautioned that the percentages were likely minimum estimates and that numerous factors bias their reliability as precise indicators of the amount of carbonate removed. The different values in Mossop's estimates of compaction are also attributable to the differences in susceptibility to compaction of the reef rim and reef interior facies. Our study also confirms the differences in compactibility of the reef rim and reef interior facies. This is likely to be at least partly due to the cementation or lithification history (early cements are more likely in the reef rim facies), selective dolomitization (possibly more dolomite in the interior reef area related to the anhydrite) or the presence of relatively more non-carbonate mud (or other insoluble material) in the reef-interior facies (Wilson, 1984). Core examination of the different reef environments may confirm which, if any, of the above were important factors for the compactional differences of the reef environments.

Much remains to be learned about the compaction of carbonate sediments. Many carbonate sediments, including carbonate mud, have been typically interpreted to be relatively noncompactible (e.g. Pray, 1960; Bathurst, 1975; Ricken, 1986). When restoring sections (backstripping) in some basin analysis modeling studies, the burial compaction of carbonates is interpreted to be essentially zero, with the reduction of porosity in the carbonates attributed solely to the addition of cement from an outside source (e.g. Bond and Kominz, 1984).

However, Shinn et al. (1977) and Shinn and Robbin (1983) showed through experiments that some Recent carbonate sediments (originally mud-supported) could be compacted up to 75% without showing much lithologic evidence. Thus, it is possible that some ancient carbonates could have been similarly compacted prior to lithification without revealing much lithologic evidence of such compaction.

The consideration of compaction in carbonate rocks is important, but it may require the integration of several methods to derive an accurate estimate for the amount of compaction in ancient carbonate rocks. Our study, utilizing seismic data, indicates that some carbonates, similar to those of the Redwater Reef, were compacted by as much as 45%. Other case studies will add to the information on what types of carbonates are most susceptible to compaction and, importantly, more details on the timing and mechanisms of compaction.

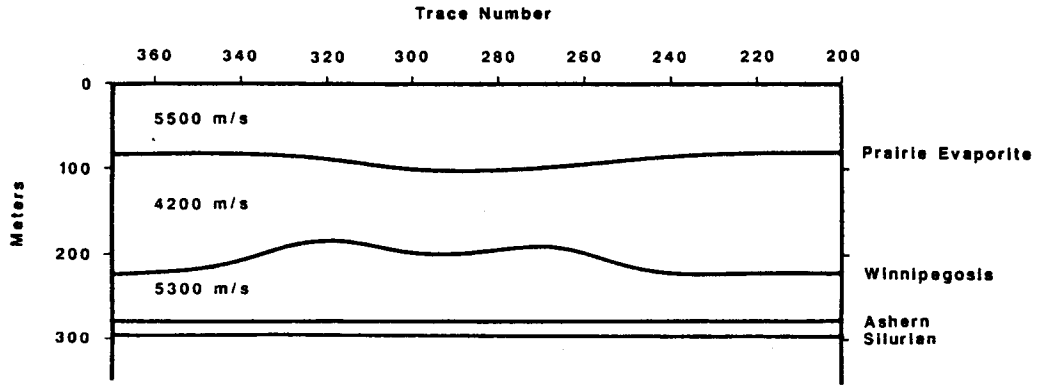

FIG. 7. Geologic model for the Elk Point. This geologic section is an inverted representation of the seismic line of Figure 5. Datum is at 1.2 s.

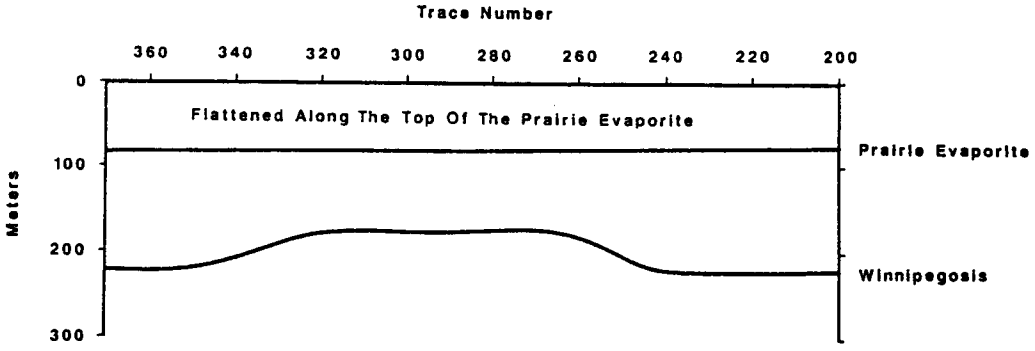

FIG. 8. Reconstructed version of the Elk Point model, created by flattening Figure 7 along the Prairie Evaporite horizon. Ideally this model represents the morphology of the reef at the end of Prairie Evaporite time.

Figure VIII:7:7 and VIII:7:8 (Anderson and Franseen, 1991)

8) HUMMINGBIRD (based principally on Reimer, 1989)

a) Introduction

Hummingbird Field, situated approximately 70 km southwest of Weyburn, Saskatchewan is small, barely 250 ha in size, but has been quite prolific. It currently produces from three zones; the Devonian Birdbear Formation, and the Mississippian Bakken Formation and Ratcliffe Member (Charles Formation). In the literature, the field is described as the result of multiple stage salt dissolution and collapse.

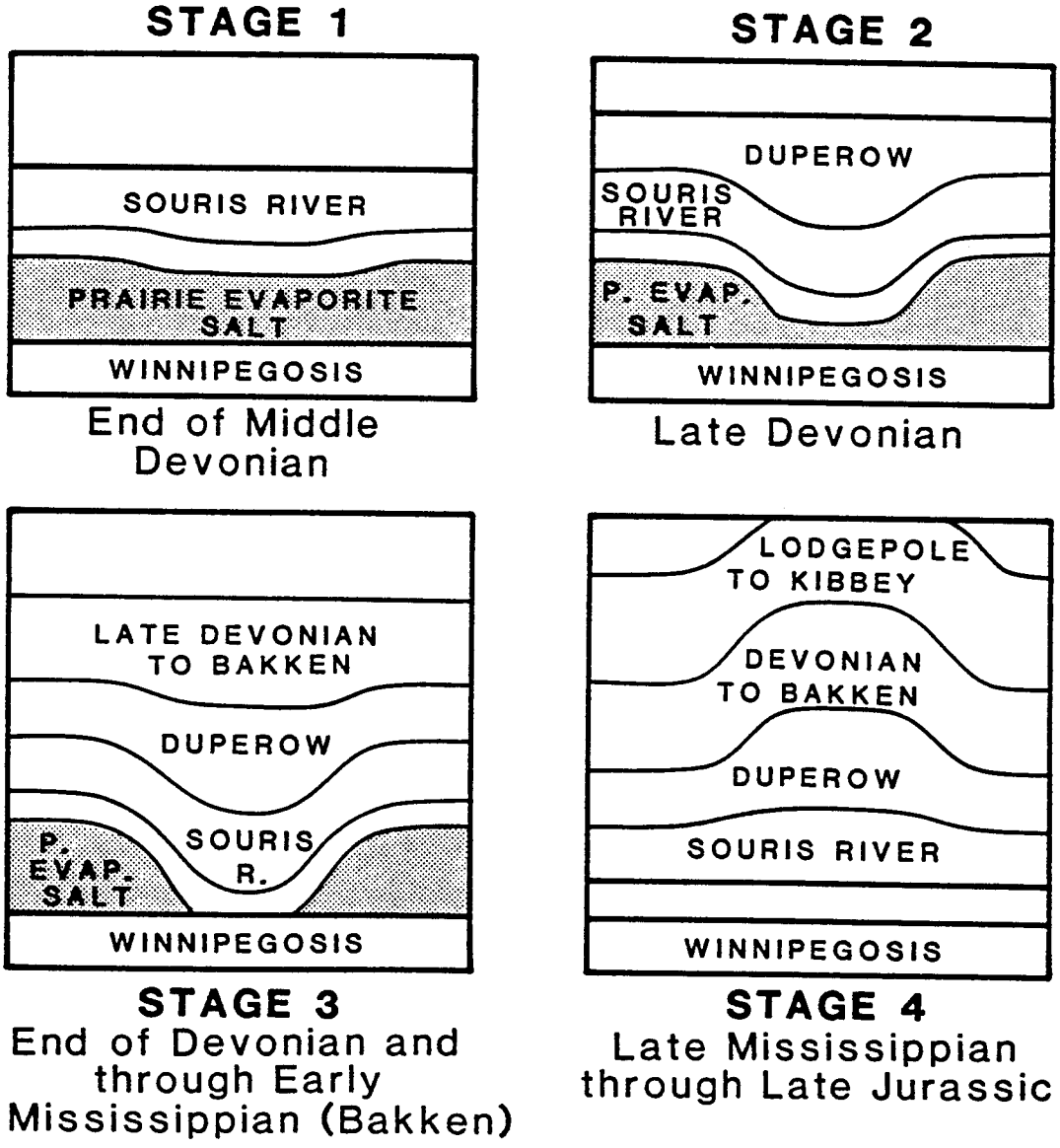

Figure 6.29. Stages of differential salt dissolution.

Figure VIII:8:1. (Reimer, 1989)

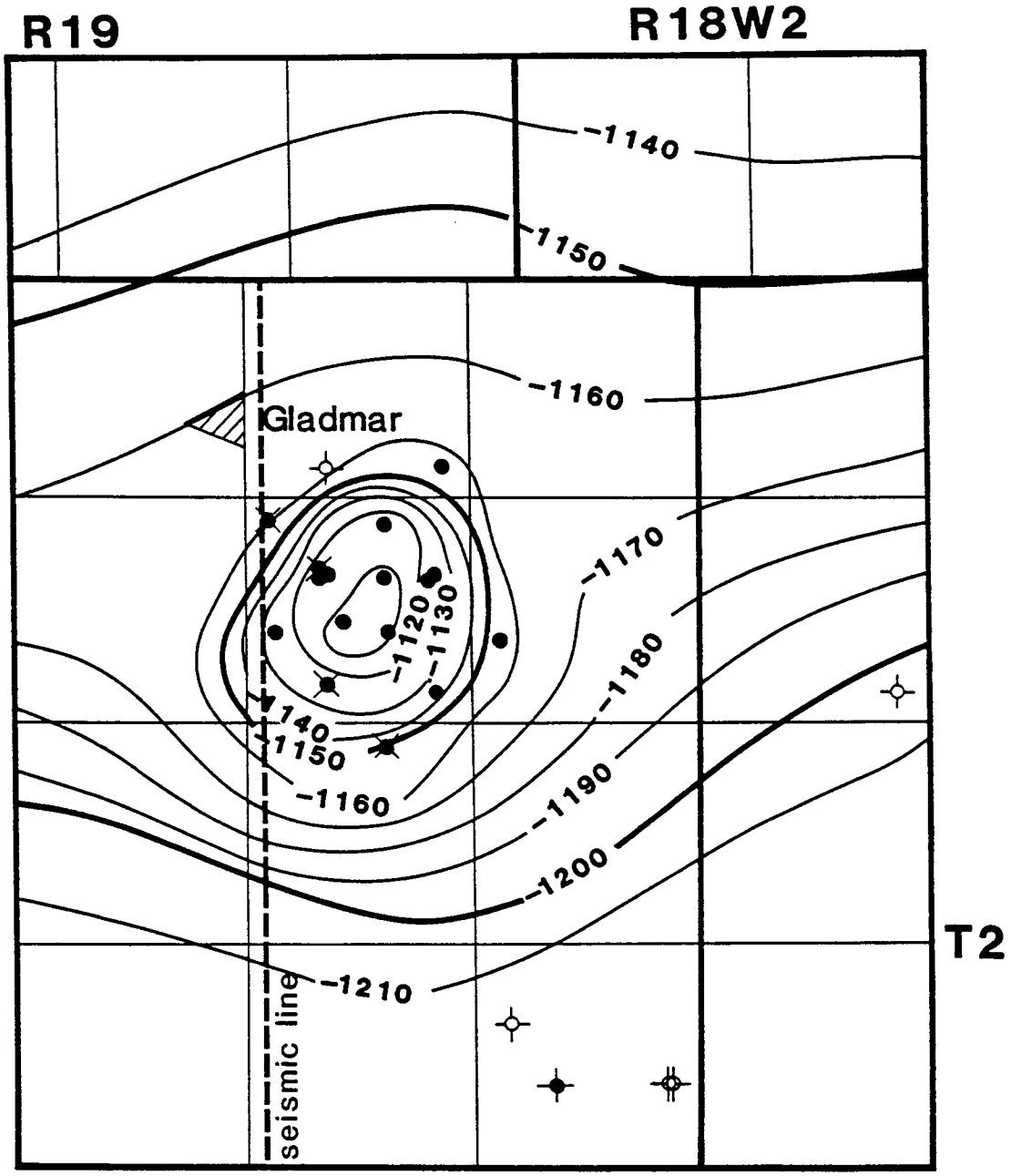

Figure 6.30. Structure contour map of the Ratcliffe Mbr, Hummingbird field. Seismic line (dashed) lies along the west flank of feature (contour interval 10 m).

Figure VIII:8:2. (Reimer, 1989)

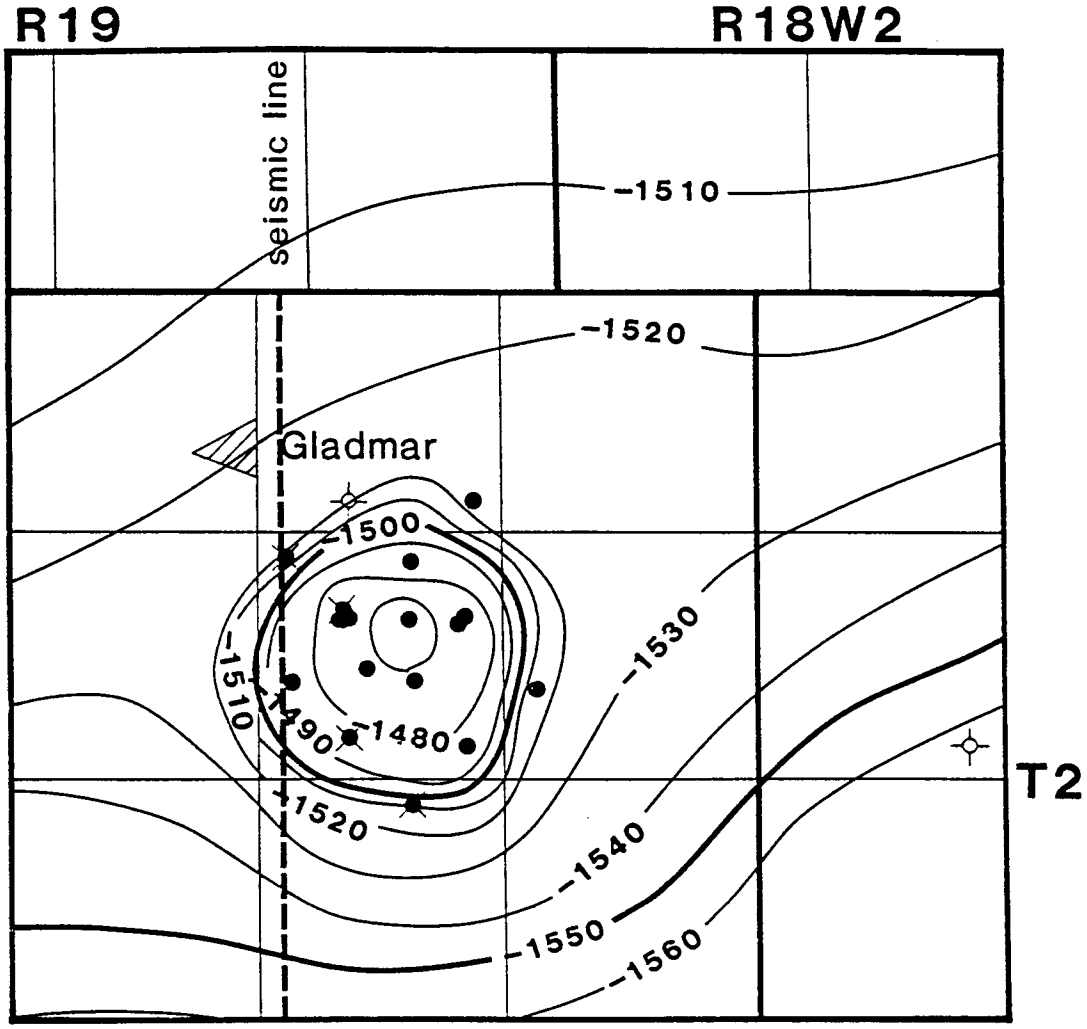

Figure 6.31. Structure contour map Bakken Fm, Hummingbird field. Structure is steep-sided relative to the Shallower Ratcliffe Mbr structure (contour interval 10 m).

Figure VIII:8:3. (Reimer, 1989)

Hummingbird Field lies in the northwest quadrant of the Williston Basin, an ancestral structural low more than 600 km in diameter. The Williston Basin actively subsided during the Ordovician and Silurian, and remained relatively stable during Devonian. Active subsidence occurred throughout the remainder of the Paleozoic time, and continued until the Late Jurassic (Smith and Pullen, 1967).

During Devonian time, Prairie Evaporite Formation salts were deposited in the Hummingbird area (and indeed throughout a large part of the Elk Point Basin; Chapter VII). In the Hummingbird Field area, these salts were subsequently leached to the extent that none of the wells drilled within the confines of the field encountered salt, thus supporting a salt dissolution origin. The original thickness of the Prairie Evaporite salt in the Hummingbird area cannot be directly determined, but evidence suggests that at least 90 m of salt was initially present. The nearest well with residual Prairie Evaporite Formation salt (9-9-3-18 W2M; 6 km to the northeast) penetrated about 85 m of rock salt (Reimer, 1989).

Seismic and geological data suggest that the dissolution of Prairie Evaporite salt occurred episodically; leaching appears to have been initiated towards the end of the Middle Devonian, with most loss occurring in the Late Devonian. During the course of the deposition of the Bakken (uppermost Devonian/lowermost Mississippian), additional salt was removed and as much as 20 m of additional Bakken sandstone accumulated in the associated structural lows. Salt dissolution in those areas immediately adjacent to the Hummingbird Field occurred during the Jurassic. As a consequence, the anomalously thick Devonian intervals, such as that of Bakken Formation, are now relatively structurally high. As a result of this differential salt dissolution and differential compaction, the deeper post-salt sediments drape across the anomalously thick Devonian-age strata at Humminbird and variously act as reservoirs or seals (Figure VIII:8:1; Reimer, 1989).

Structure maps for the Ratcliffe Member (Figure VIII:8:2) and Bakken Formation (Figure VIII:8:3) are similar. Both exhibit about 50 m of closure, with the former being less steep-sided.

b) Seismic data

The reverse-polarity seismic section (Fig. 6.34) was acquired along the west flank of the Hummingbird field (Fig. 6.31) and parallels the geological cross-section. These 12 fold seismic were recorded in the winter of 1983 using a 2-kg dynamite source, single 18 m deep holes, a source interval of 132 m, and a group interval of 33 m. A nest of 9-14 Hz geophones with 4 m separation was used.

The following events have been identified on the seismic data: the Winnipegosis Formation (a strong peak); the Bakken Fm (a peak); the Ratcliffe Member (a moderate-amplitude peak); the top of the Mississippian (a trough), and the Jurassic Shaunavon Formation (a trough).

Structure is evident on all the Mississippian events. In addition, the Bakken Fm reflection changes from a low-frequency peak to a high-frequency doublet, the result

of a thicker sandstone between traces 305 and 350. At its thickest, the sandstone gives rise to a reflection from both its top and base.

The Ratcliffe Mbr also shows character change as it dims over the structure. This is attributed to its greater thickness off structure and is the effect of tuning whereby the velocity-frequency content of the seismic interfere constructively in the thicker beds but destructively in the thinner beds. The top Mississippian event is nearly regional, dipping from north to south. The isochron from top Mississippian to Ratcliffe Mbr is much thicker off the Ratcliffe structure. This isochron change indicates that much of this zone was eroded in the vicinity of the anomaly. The Shaunavon Fm has only minor structure.

c) Conclusions

Until the Hummingbird structure was tested, multi-stage salt dissolution had not been proven in Western Canada. The discovery and development of this feature became one of the more exciting success stories of the early 1960's where geology and geophysics were used to complement each other. Other similar features in the area, smaller than Hummingbird, have also been identified and successfully developed. Thus, Hummingbird became one of the key geological and geophysical models for multi-stage salt dissolution features in the Paleozoic.

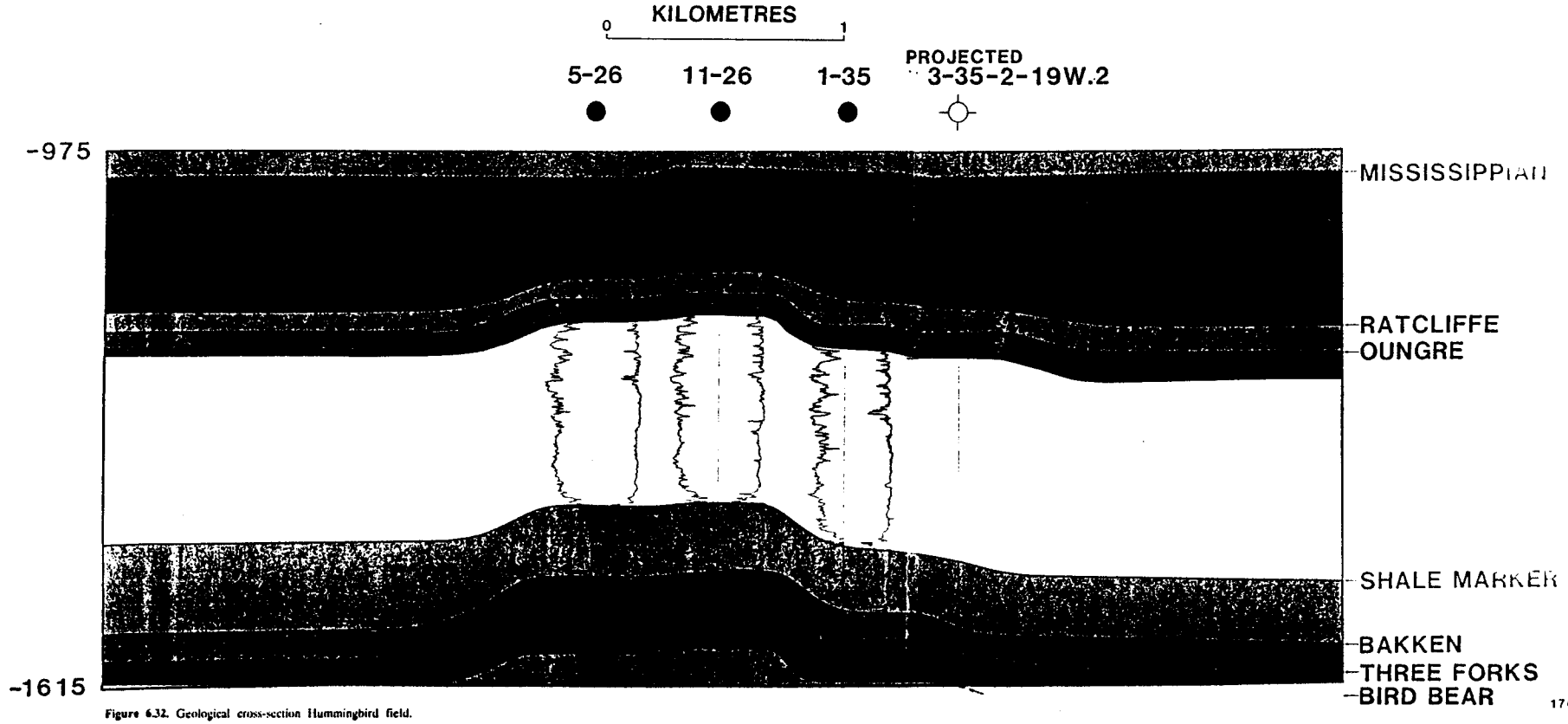

Figure 6.32. Geological cross-section Hummingbird field.

Figure VIII:8:4. (Reimer, 1989)

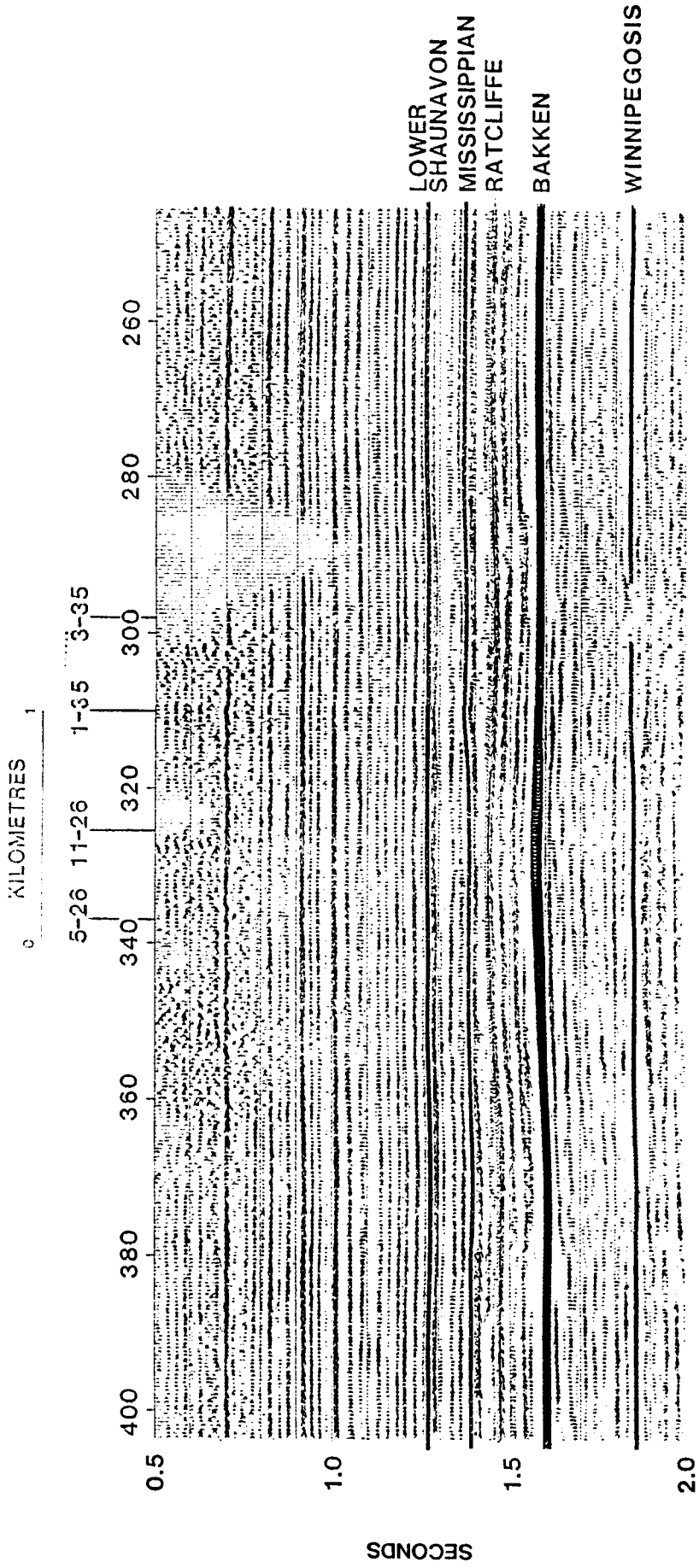

Figure VIII:8:5. (Reimer, 1989)

9) CRATER LAKE (after Christianson, 1971)

The Crater Lake depression is the surface expression of the Crater Lake collapse structure (Christianson, 1971; Figures VIII:9:1-VIII:9:3). The structure comprises 2 main concentric fault zones forming an inner and outer cylinder of collapse beneath Crater Lake. The inner cylinder, which is about 90 m in diameter, was downfaulted about 43 m in Late Cretaceous-Tertiary-Early Pleistocene time and the outer cylinder, which is about 213 m in diameter, was downfaulted 15-30 m during the last deglaciation about 13,600 years ago. According to Christianson (1971) the Crater Lake structure was formed by collapse as a result of the removal of salt from the Prairie Formation by groundwater.

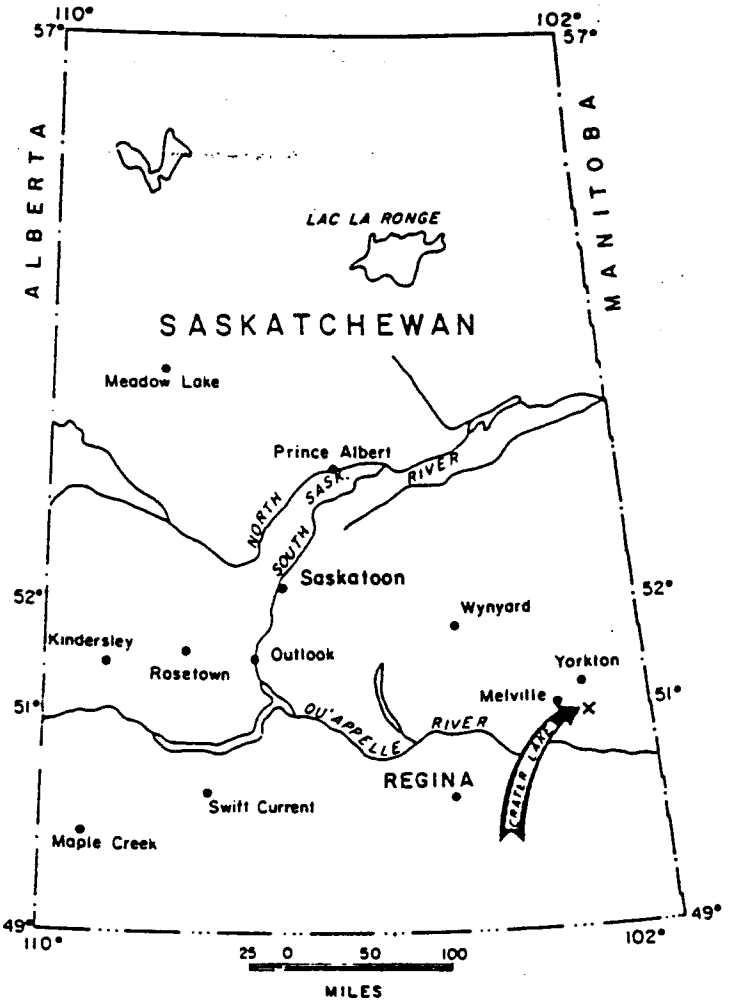

FIG. 1. Location of the Crater Lake structure.

Figure VIII:9:1. (Christianson, 1971)

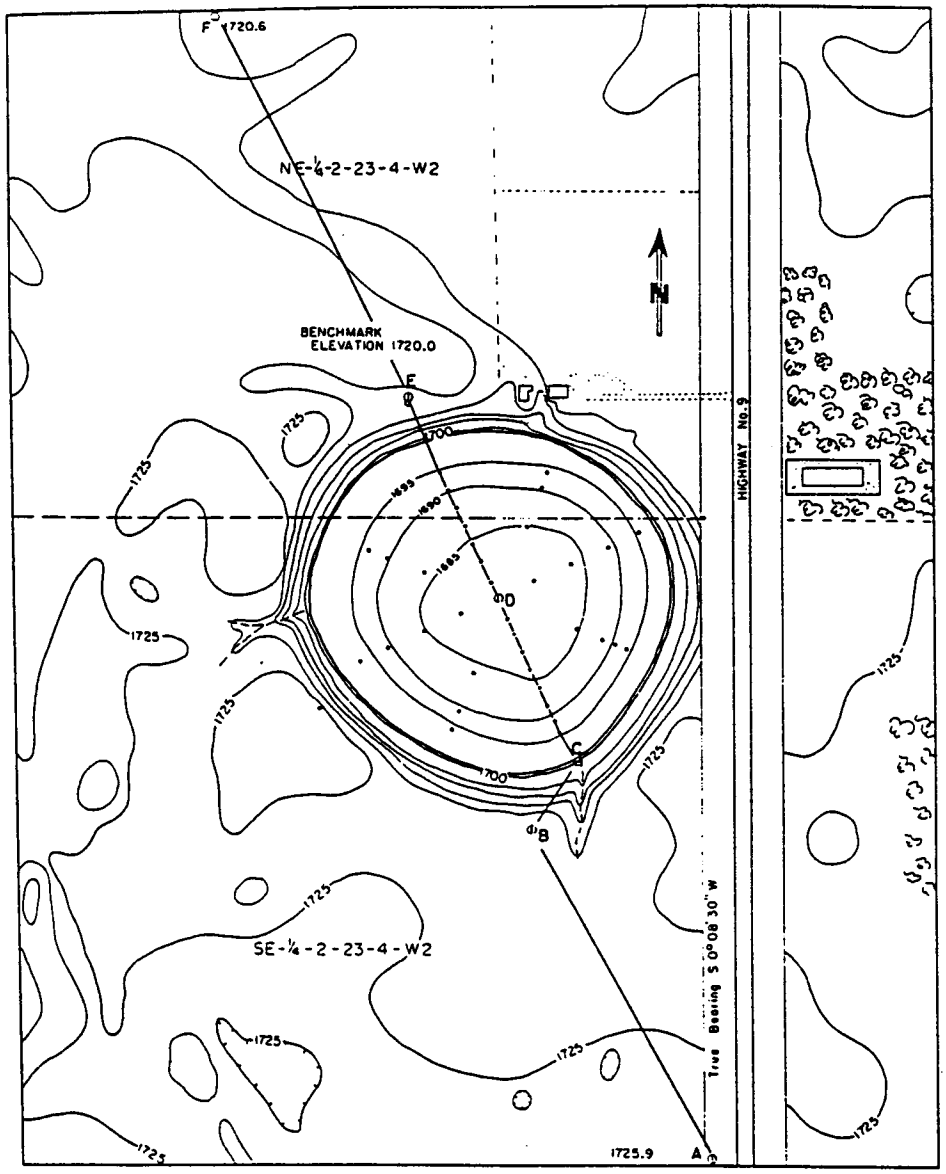

FIG. 2. Topography of Crater Lake bottom and adjacent upland. Soundings were taken by F. M. Atton, Sask. Fisheries Br., September 15, 1969, and the topographic map of the adjacent upland was surveyed and compiled by W. A. Meneley.

Figure VIII:9:2. (Christianson, 1971)

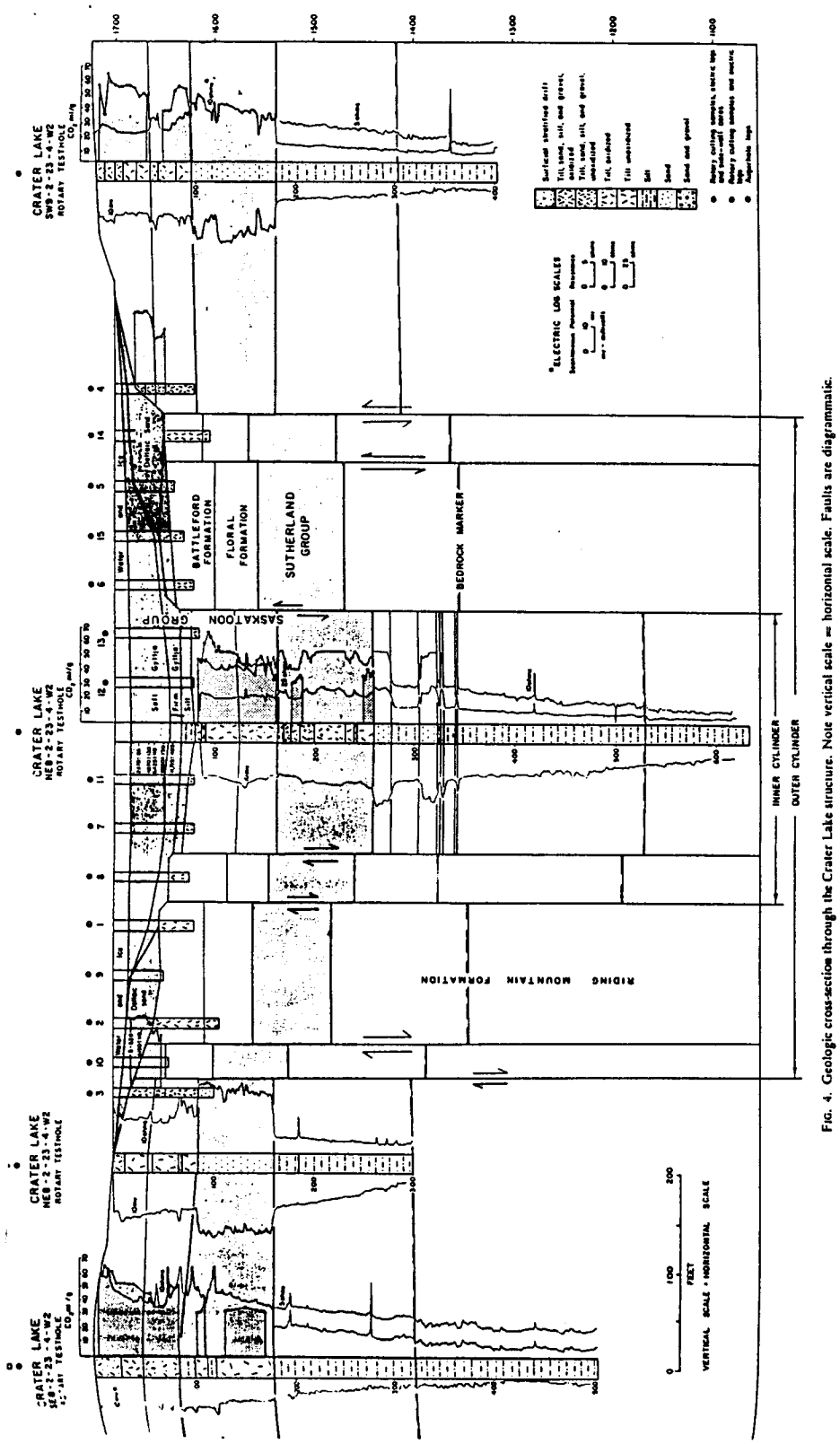

FIG. 4. Geologic cross-section through the Crater Lake structure. Note vertical scale = horizontal scale. Faults are diagrammatic.

Figure VIII:9:3. (Christianson, 1971)

10) NIPISI (based on Alcock and Benteau, 1976)

Nipisi Field is situated within the northern part of the Alberta Basin on the eastern flank of the Peace River High (Figures VIII:10:1 and VIII:10:2). The reservoir (Gilwood Member, Watt Mountain Formation) is considered to be stratigraphically trapped; the sandstones shaleout in an updip direction (Figure VIII:10:3). The overlying shales and evaporites of the Ft. Vermilion Formation provides a highly effective seal to vertical oil migration.

The Gilwood Member is interpreted as having been deposited in a fan-like deltaic system that prograded eastward from the Peace River high during Watt Mountain time (Figure VIII:10:4; Alcock and Benteau, 1976). These deltaic sediments are thought to have been preferentially deposited and/or preferentially preserved within a structural depression at the Muskeg surface. The structural low is attributed to the contemporaneous dissolution of the rock salts within the underlying Muskeg Formation (Figures VII:2:15, VIII:10:5 and VIII:10:6).

Three main facies have been described by these authors: 1) alluvial plain - tributary channel facies; 2) delta plain - distributary channel facies; and 3) delta front - marine destructive facies. The recognition of these facies was based on: 1) paleostructural patterns of the underlying Muskeg Formation; 2) Gilwood sandstone-body geometry; 3) paleotology in vertical and areal sequences; and 4) internal sedimentary structures. Porosity and permeability within the field are partially cement-controlled. The areal distribution of different types of cements appear to be related to depositional environment. According to Alcock and Benteau, the best oil reservoir rocks are the channel sandstones of the delta-plain facies where the intensity of cementation is lowest. The sandstones of the delta front-destructive facies in contrast, are well cemented by anhydrite and siliceous cements, creating potential permeability barriers.

Seismic data from the Nipisi area can be interpreted as supporting the thesis that the Gilwood Member was preferentially deposited and/or preserved in structural depressions at the Muskeg surface (Angus et al., 1989). These lows very conceivably are related to the contemporaneous dissolution of the Muskeg salts.

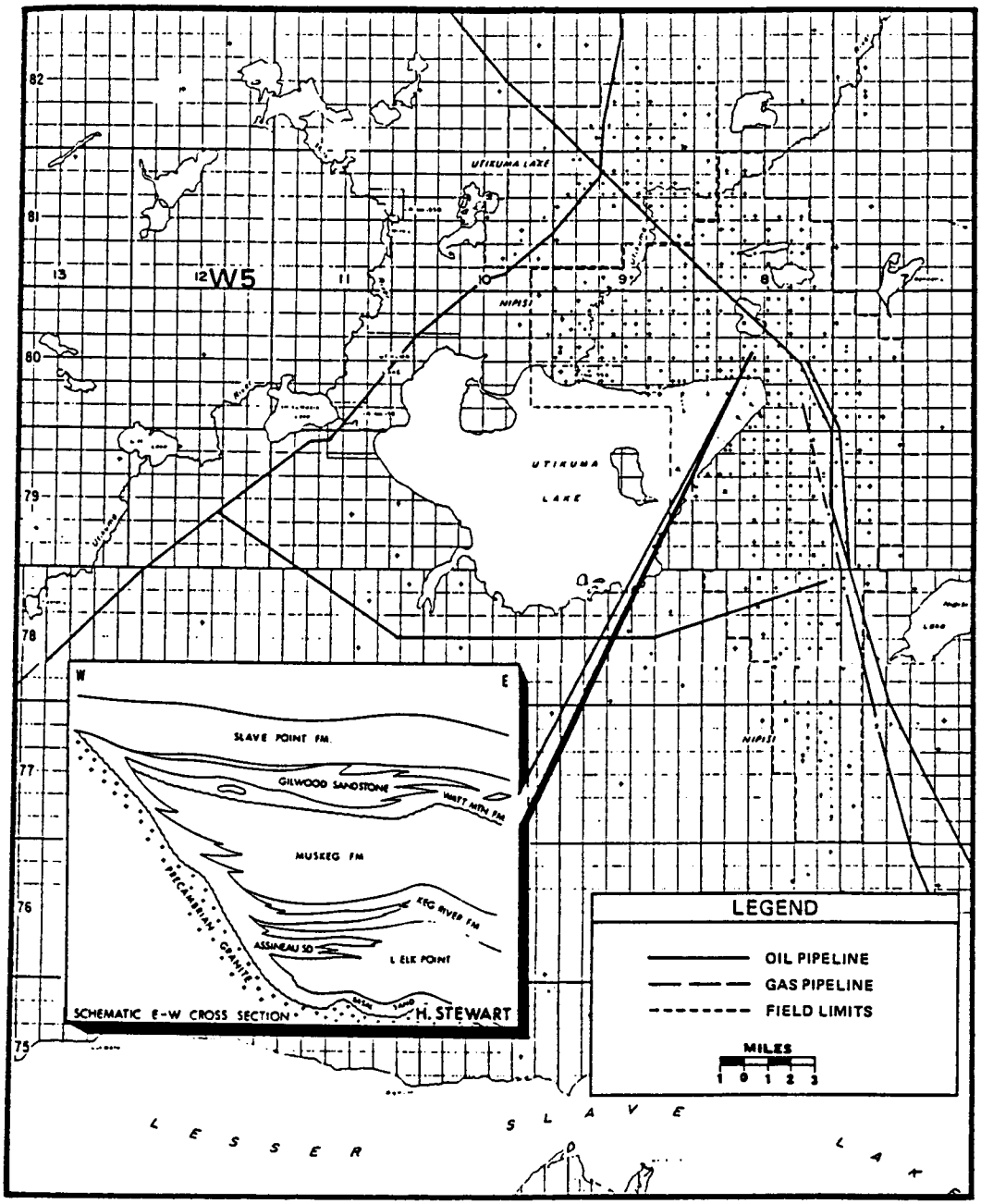

FIGURE 1.

— INDEX MAP —

Figure VIII:10:1. (Alcock and Benteau, 1976)

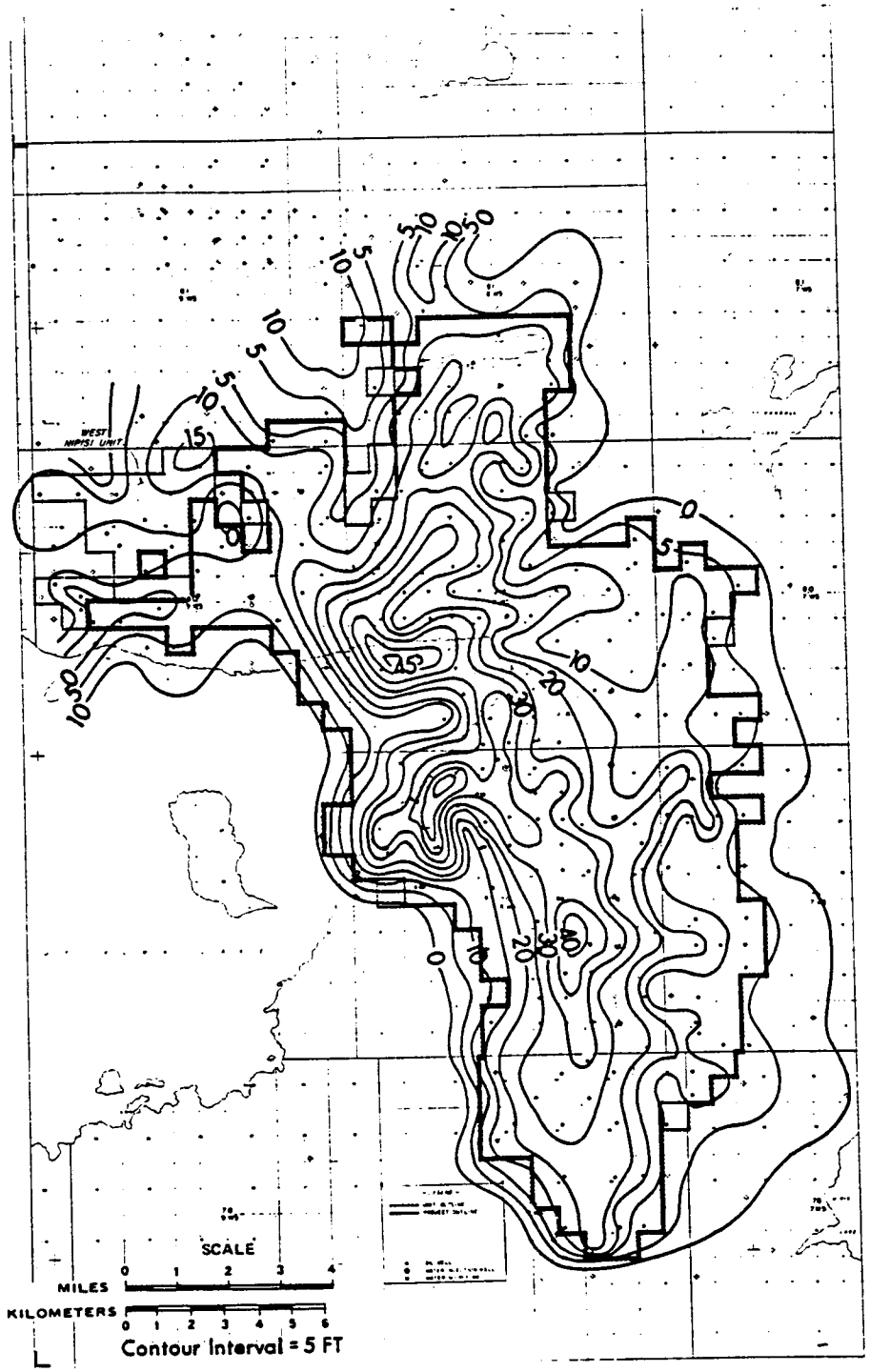

FIGURE 2
GILWOOD NET OIL PAY ISOPACH

Figure VIII:10:2. (Alcock and Benteau, 1976)

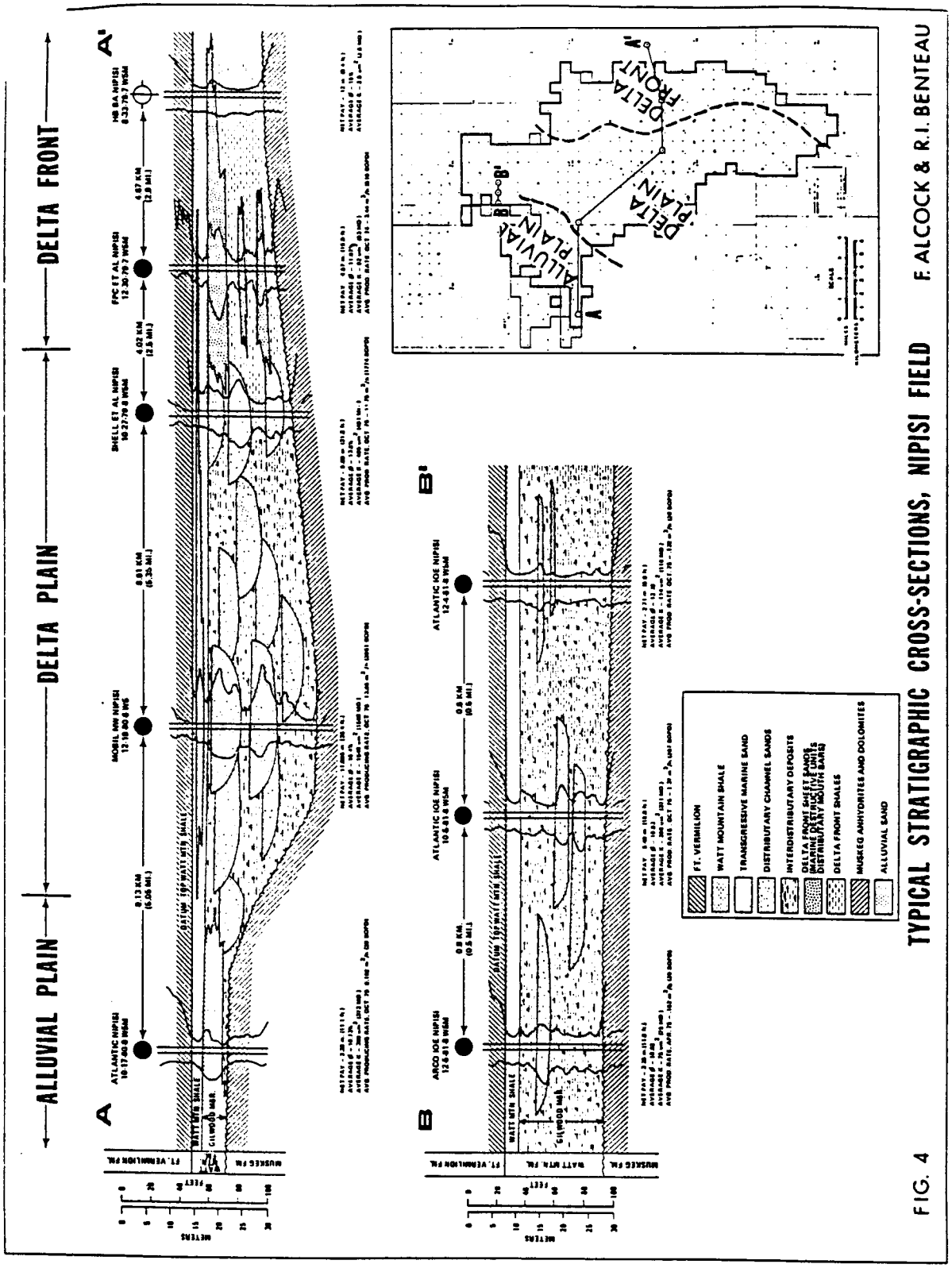

Figure VIII:10:3. (Alcock and Benteau, 1976)

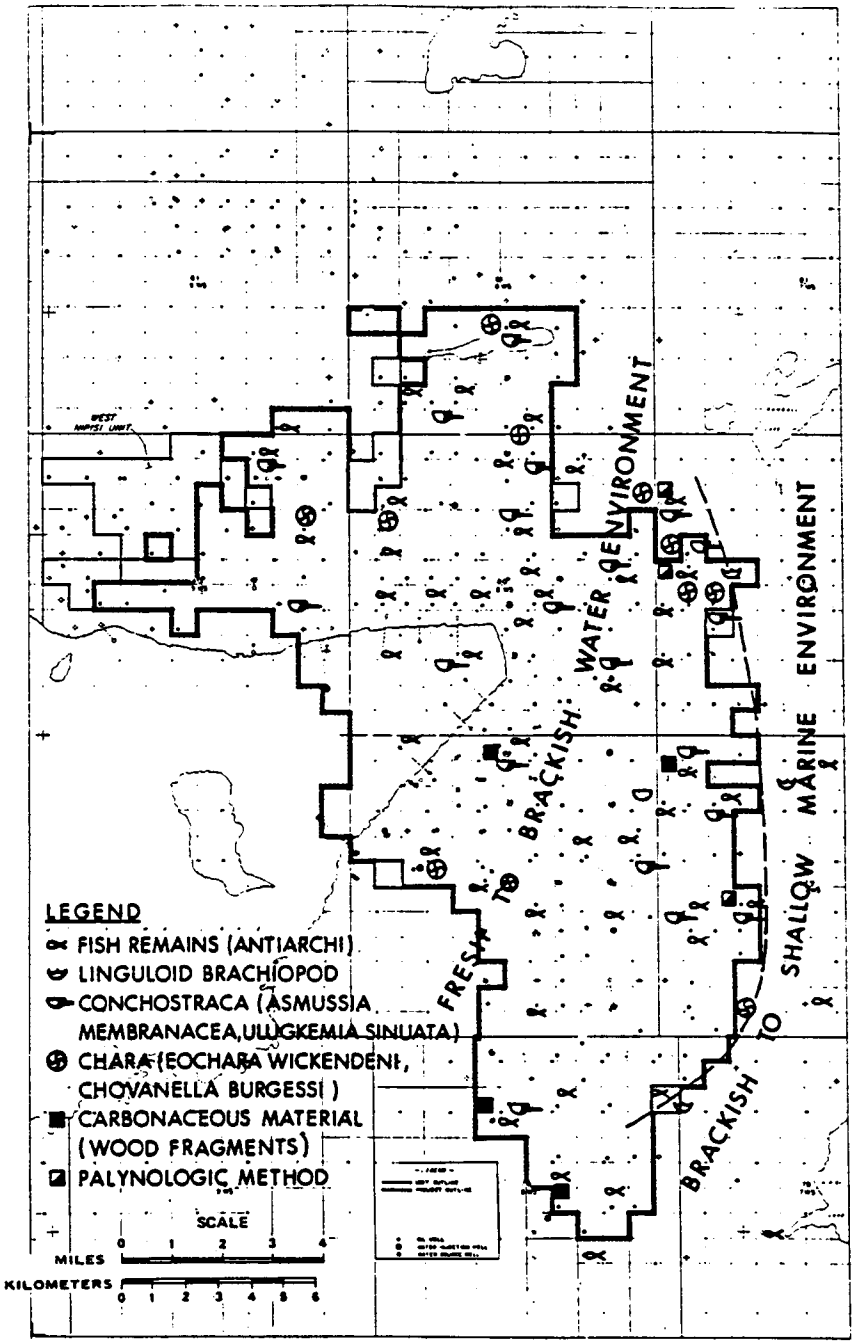

FIGURE 9

PRELIMINARY FAUNAL DISTRIBUTION AND GENERALIZED PALEOENVIRONMENTS

Figure VIII:10:4. (Alcock and Benteau, 1976)

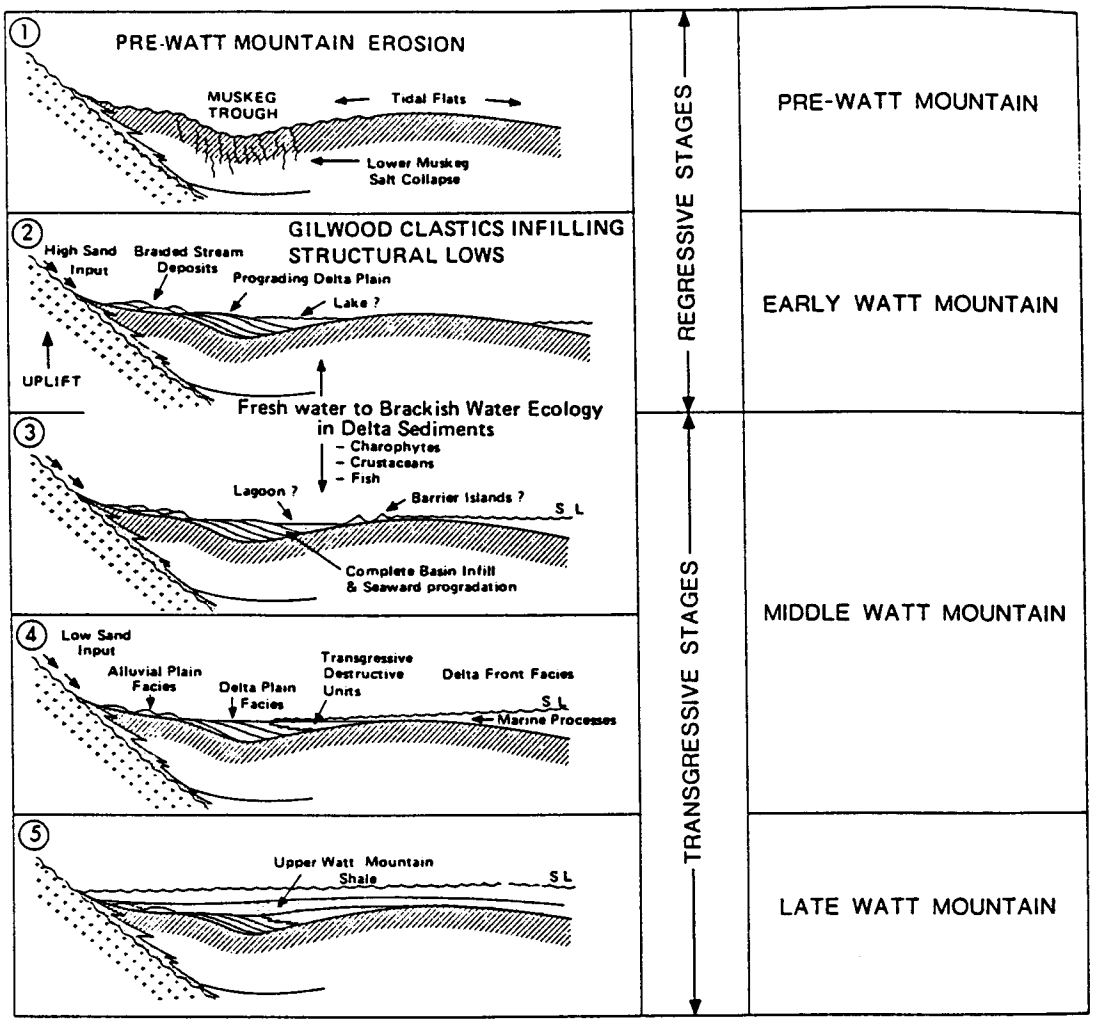

Figure 10

DIAGRAMMATIC SECTIONS ILLUSTRATING THE DEPOSITIONAL HISTORY OF THE WATT MOUNTAIN FORMATION

Figure VIII:10:5. (Alcock and Benteau, 1976)

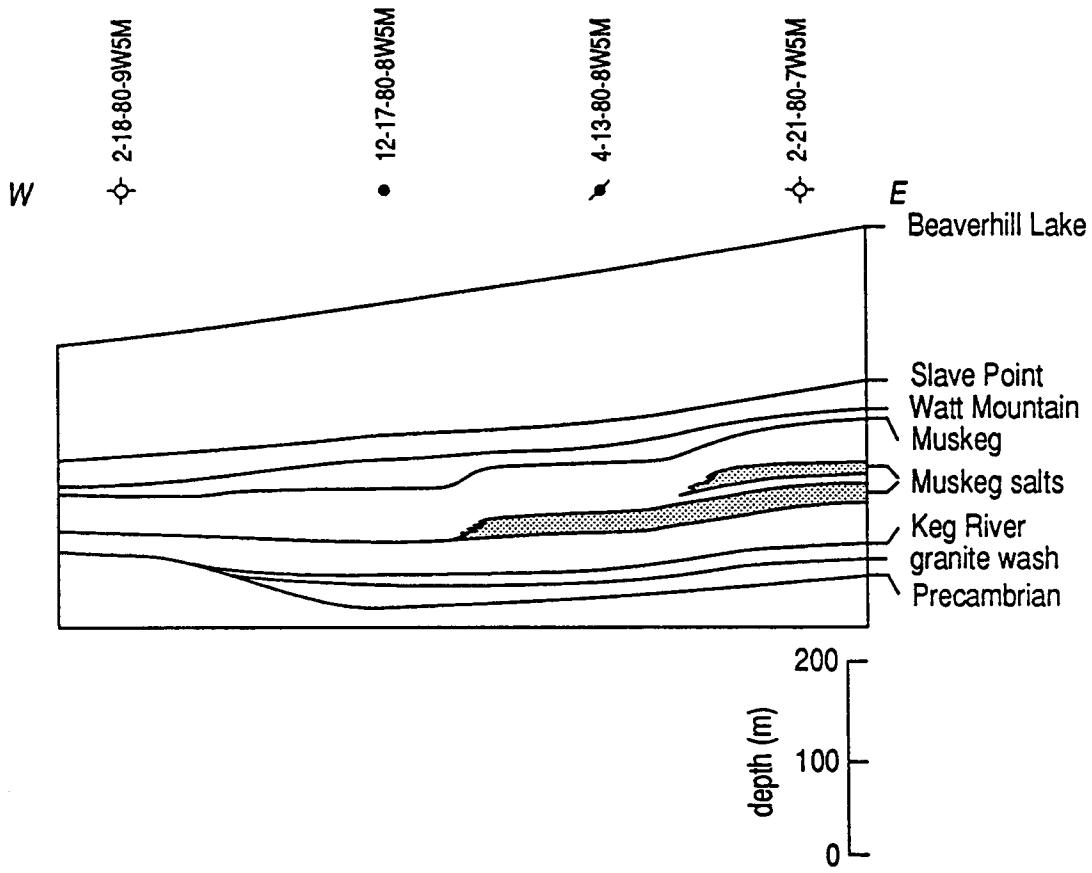

Figure VIII:10:6. (Anderson and Knapp))

11) REFERENCES

AGAT Laboratories, 1988, Table of formations of Alberta: AGAT Laboratories, Calgary.

Alcock, F.G. and Benteau, R.I., 1976, Nipisi field - a middle Devonian clastic reservoir, *in* Lerand, M.M., Ed., The sedimentology of selected oil and gas reservoirs in Alberta: Canadian Society Petroleum Geologists, 1-24.

Anderson, N.L., 1987, Clastic seismology: Petrel Robertson, Calgary, Alberta, 277 p. (Available through the University of Calgary Geology Library).

Anderson, N.L., 1990a, An overview of some of the large scale mechanisms of salt dissolution: Kansas Geological Survey Open File Report 90-39.

Anderson, N.L., 1990b, Exploration implications of salt dissolution: Kansas Geological Survey Open File Report 90-37.

Anderson, N.L., 1990c, Hydrological, geological, biological, environmental, and exploration implications of salt dissolution: Kansas Geological Survey Open File Report 90-38.

Anderson, N.L., 1990d, Paleo-restoration of leached salts: an overview of the methodology used in the reconstruction of the Wabamun salt, southern Alberta, Canada: Kansas Geological Survey Open File Report 90-36.

Anderson, N.L., 1991a, Reconstruction of the Elk Point salts in the Lloydminster area (T50-T65, R15W3-R10W4M): Kansas Geological Survey Open File Report 91-56

Anderson, N.L., 1991b, Large scale mechanisms of salt dissolution: illustrated case histories: Kansas Geological Survey Open File Report 91-57

Anderson, N.L., 1992a, Reconstruction of the Leduc (Cairn) and Wabamun salts, Youngstown area, southern Alberta (T25-T35, R5-R20W4M): Kansas Geological Survey Open File Report 92-3.

Anderson, N.L., 1992b, Dissolution of the Wabamun Group salt: exploration implications, *in* Cavanaugh, T.D., Ed., Integrated exploration case histories, North America: The Geophysical Society of Tulsa Special Publication, in press.

Anderson, N.L. and Brown, R.J., 1987, The seismic signatures of some western Canadian Devonian reefs: Journal Canadian Society Exploration Geophysicists 1, 7-26.

Anderson, N.L. and Brown, R.J., 1992, Reconstruction of the Wabamun Group salts, southern Alberta, Canada, *in* Cavanaugh, T.D., Ed., Integrated exploration case histories, North America: The Geophysical Society of Tulsa Special Publication,

in press.

Anderson, N.L. and Brown, R.J., 1991, Dissolution of the Wabamun and Black Creek salts: a seismic analysis: Geophysics 56, 618-627.

Anderson, N.L., Brown, R.J. and Hinds, R.C., 1988a, A seismic perspective on the Panny and Trout fields of north-central Alberta: Canadian Journal Exploration Geophysics 24, 154-165.

Anderson, N.L., Brown, R.J. and Hinds, R.C., 1988b, Geophysical aspects of Wabamun salt distribution in southern Alberta: Canadian Journal Exploration Geophysics 24, 166-178.

Anderson, N.L., Brown, R.J. and Hinds, R.C., 1989a, Upper Elk Point reservoirs, *in* Anderson, N.L., Hills, L.V. and Cederwall, D.A., Eds., Geophysical atlas of western Canadian hydrocarbon pools: Canadian Society Exploration Geophysicists and Canadian Society Petroleum Geologists Special Publication, 27-66.

Anderson, N.L., Chapman, J. and Brown, R.J., 1990, Paleo-reconstruction of the Wabamun Group salt in southern Alberta, Canada: report to the Geological Survey of Canada.

Anderson, N.L., Cederwall, D.A. and Hills, L.V., 1986, Carbonate seismology: Sigma Exploration Ltd., Calgary, Alberta, 194 p. (Available through the University of Calgary Geology Library).

Anderson, N.L. and Chappell, F., 1987b, Devonian salts and hydrocarbon traps: Petrel-Robertson, Calgary, Alberta, 113 p. (Available through the University of Calgary Geology Library).

Anderson, N.L., Brown, R.J., Gendzwill, D.J., Hinds, R.C. and Lundberg, R.N., 1989a, Elk Point Group reservoirs, *in* Anderson, N.L., Hills, L.V. and Cederwall, D.A., Eds., The geophysical atlas of western Canadian hydrocarbon pools: Canadian Society Exploration Geophysicists and Canadian Society Petroleum Geologists Special Publication, 27-66.

Anderson, N.L. and Franseen, E.K., 1991, Differential compaction of Winnipegosis reefs: a seismic analysis: Geophysics 56, 142 -147.

Anderson, N.L. and Knapp, R.W., 1992, An overview of some large-scale mechanisms of salt dissolution: submitted to Geophysics, in review.

Anderson, N.L., White, D.G. and Hinds, R.C., 1989b, Woodbend Group Reservoirs, *in* Anderson, N.L., Hills, L.V. and Cederwall, D.A., Eds., Geophysical atlas of western Canadian hydrocarbon pools: Canadian Society Exploration Geophysicists and Canadian Society Petroleum Geologists Special Publication, 101-132.

Andrichuk, J.M. and Wonfor, J.S., 1953, Late Devonian geologic history in Stettler

area, Alberta, Canada: Alberta Society of Petroleum Geologists, News Bulletin 1, 3-5.

Angus, K., Wylie, J., McCloskey, W. and Noble, D., Paleozoic clastic reservoirs, *in* Anderson, N.L., Hills, L.V. and Cederwall, D.A., Eds., Geophysical atlas of western Canadian hydrocarbon pools: Canadian Society Exploration Geophysicists and Canadian Society Petroleum Geologists Special Publication, 1-26.

Baillie, A.D., 1953, Devonian System of the Williston basin area: Manitoba Mines Branch Publication 52-5.

Barss, D.L., Copland, A.B. and Ritchie, W.D., 1970, Geology of Middle Devonian reefs, Rainbow area, Alberta, Canada, *in* Halbouty, M.T., Ed., Geology of giant petroleum fields: AAPG Memoir 14, 19-49.

Bathurst, R.G.C., 1975, Carbonate sediments and their diagenesis: Developments in Sedimentology 12, Elsevier, Amsterdam, 685 p.

Belyea, H.R. 1966, Woodbend, Winterburn and Wabamun Groups, *in* McCrossan, R.G. and Glaister, R.P., Eds., Geological history of western Canada, 2nd edition: Alberta Society Petroleum Geologists, 66-88.

Belyea, H.R. and Mclaren, D.J., 1957, Upper Devonian nomenclature in southern Alberta: Journal of Alberta Society of Petroleum Geologists 5, 166-182.

Bishop, 1974, Hummingbird structure, Saskatchewan, single vs multiple stage salt soultion-collapse, *in* Parslow, G.R., Ed., Fuels: a geologic appraisal: Saskatchewan Geological Society Special Publication 2, 179-197.

Bond, G.C. and Kominz, M.A., 1984, Construction of tectonic subsidence curves for the early Paleozoic miogeocline, southern Canadian Rocky Mountains: Implications for subsidence mechanisms, age of breakup, and crustal thinning: Bulletin Geological Society America 95, 155-173.

Brown, R.J. and Anderson, N.L., 1991, On the question of lateral velocity variations over Leduc and Rainbow reefs: Canadian Journal Exploration Geophysics 27, 43-52.

Brown, R. J. and Anderson, N. L., 1992, An overview of salt dissolution and related hydrocarbon trapping potential in western Canada: AAPG Bulletin, submitted.

Brown, R.J., Anderson, N.L. and Hills, L.V., 1990, The seismic interpretation of Upper Elk Point (Givetian) carbonate reservoirs of western Canada: Geophysical Prospecting 38, 719-736.

Cederwall, D.A. and Anderson, N.L., 1991a, A seismic and gravity study of salt dissolution at the Westhazel General Petroleums Pool, west-central Saskatchewan, Canada: Kansas Geological Survey Open File Report 90-46.

Cederwall, D.A. and Anderson, N.L., 1991b, Westhazel General Petroleums Pool, east-central Alberta, Canada: SEG Annual Meeting Expanded Technical Program Abstracts, 184-187.

Christianson, E.A., 1971, Geology of the Crater Lake collapse structure in southeastern Saskatchewan: Canadian Journal Earth Science 8, 1505-1513.

Ehrets, J.R. and Kissling, D.L., 1987, Winnipegosis platform margin and pinnacle reef reservoirs, northwest North Dakota, in Fischer, D.W., Ed., Core workshop volume, Fifth international Williston Basins symposium, North Dakota Geological Survey, Miscellaneous Series 69, 1-31.

Gendzwill, D.J., 1978, Winnipegosis mounds and Prairie Evaporite Formation of Saskatchewan seismic study: AAPG Bulletin 62, 73-86.

Gendzwill, D.J. and Hajnal, Z., 1971, Seismic investigation of the Crater Lake collapse structure in southeastern Saskatchewan: Canadian Journal Earth Science 8, 1514-1524.

Gendzwill, D.J. and Lundberg, R.M., 1989, Upper Elk Point carbonate reservoirs, part B: Winnipegosis carbonates, *in* Anderson, N.L., Hills, L.V. and Cederwall, D.A., Eds., Geophysical atlas of western Canadian hydrocarbon pools: Canadian Society Exploration Geophysicists and Canadian Society Petroleum Geologists Special Publication, 52-66.

Gendzwill, D.J. and Wilson, N.L., 1987, Form and distribution of Winnipegosis mounds in Saskatchewan, *in* Peterson, J.A., Kent, D.M., Anderson, S.B., Pilatzke, R.H. and Longman, M.W., Eds.,Williston Basin; Anatomy of a Cratonic Oil Province: Rocky Mountain Association Geologists, Denver, 109-117.

Gorrel, H.A. and Alderman, G.R., 1968, Elk Point Group saline basins of Alberta, Saskatchewan and Manitoba, Canada, *in* Mattox, R.B., Ed., Saline Deposits: Geological Society America Special Paper 88, 291-317.

Hamilton, W.N., 1971, Salt in east-central Alberta: Research Council Alberta Bulletin 29.

Holter, M.E., 1969, The Middle Devonian Prairie Evaporite of Saskatchewan: Saskatchewan Department Mineral Resources Report 123.

Hopkins, J. C.,1987, Contemporaneous subsidence and fluvial channel sedimentation: Upper Mannville C pool, Berry field, Lower Cretaceous of Alberta: AAPG Bulletin 71, 334-345.

Hriskevich, M.E., 1970, Middle Devonian reef production, Rainbow area, Alberta, Canada: AAPG Bulletin 54, 2260-2281.

Imperial Oil Ltd., Western Division, Geological Staff, 1950, Devonian nomenclature

in Edmonton area, Alberta, Canada: AAPG Bulletin 34, 1807-1825.

Jones, l., 1965, The Middle Devonian Winnipegosis Formation of Saskatchewan: Saskatchewan Department Mineral Resources report 98, 101 p.

Jordan, S.P., 1967, Saskatchewan reef trend looks big: Oilweek, 17, 10-12.

Jordan, S.P., 1968, Will Zama be duplicated at Quill Lake Saskatchewan: Oilweek, 19, 10-12.

Law, J., 1955, Geology of northwestern Alberta and adjacent areas (with Discussion and Reply): AAPG Bulletin 39, 1927-1978.

McCrosson, R.G. and Glaister, R.P., 1966, Geological history of western Canada, 2nd edition: Alberta Society of Petroleum Geologists.

McLaren, D.J., 1955, Devonian formations in the Alberta Rocky Mountains between Bow and Athabasca Rivers: Geological Survey of Canada, Bulletin 35, 59 p.

Meijer Drees, N.C., 1986, Evaporitic deposits of western Canada: Geological Survey of Canada Paper 85-20, 118 p.

Mossop, G.D., 1972, Origin of the peripheral rim, Redwater reef, Alberta: Bulletin Canadian Society Petroleum Geology 20, 238-280.

Oliver, J.A. and Cowper, N.W., 1983, Wabamun salt removal and shale compaction effects, Rumsey area, Alberta: Bulletin Canadian Society Petroleum Geology 31, 161-168.

Perrin, N.A.,1982, Environments of deposition and diagenesis of the Winnipegosis Formation (Middle Devonian), Williston Basin, North Dakota, *in* Christopher, J.E. and Kaldi, J, Eds., Proceedings of the Fourth International Williston Basin Symposium, 51-66.

Perrodon, A., 1983, Dynamics of oil and gas accumulation: Elf Aquitaine, France, 369 p.

Pray, L.C., 1960, Compaction in calcilutites: Bulletin Geological Society America 71, 1946.

Precht, G.D., 1983, Reservoir development and hydrocarbon potential of Winnipegosis (Middle Devonian) pinnacle reefs, southern Elk Point Basin, North Dakota, *in* Carbonates and Evaporites: Northeastern Science Foundation, 1, 83-99.

Reinson, G.E. and Wardlaw, N.C., 1972, Nomenclature and stratigraphic relationships, Winnipegosis and Prairie Evaporite formations, central Saskatchewan: Bulletin Canadian Petroleum Geology 20, 301-320.

Ricken, W., 1986, Diagenetic bedding: A model for marl-limestone alternations: Lecture Notes in Earth Sciences, Springer-Verlag, New York, 210 p.

Sherwin, D.F., 1962, Lower Elk Point section in east-central Alberta: Journal of the Alberta Society of Petroleum Geologists 10, 185-191.

Shinn, E.A. and Robbin, D.M., 1983, Mechanical and chemical compaction in fine-grained shallow-water limestones: Journal Sedimentary Petrology 53, 595-618.

Shinn, E.A, Halley, R.B., Hudson, J.H. and Lidz, B.H., 1977, Limestone compaction: An enigma: Geology 5, 21-24.

Smith, D.G. and Pullen, J.R., 1967, Hummingbird structure of southeast Saskatchewan: Bulletin Canadian Petroleum Geology 15, 468-482.

Wardlaw, N.C. and Reinson, G.E., 1971, Carbonate and evaporite deposition and diagenesis, Middle Devonian Winnipegosis and Prairie Evaporite formations of south-central Saskatchewan: AAPG Bulletin 55, 1759-1786.

Williams, G.K., 1977, The Hay River Formation and its relationship to adjacent formations, Slave River map-area, N.W.T.: Geological Survey of Canada Paper 75-12, 17 p.

Wilmot, B.R., 1985, The geology of the Lower Cretaceous Mannville Group, Edam, Saskatchewan: M.Sc. thesis, University of Calgary, 160 p.

Wilson, N.L., 1984, The Winnipegosis Formation of south-central Saskatchewan, in Lorsong, J.A. and Wilson, M.A., Eds., Oil and Gas in Saskatchewan: Saskatchewan Geological Society Special Publication 7, 13-15.

Wirnkar, F.T. and Anderson, N.L., 1989, Seismic analysis of the differential compaction of reef and off-reef sediments: Expanded abstracts, SEG Annual Meeting, 888-890.

Wonfor, J.S. and Andrichuk, J.M., 1953, Upper Devonian in the Stettler area, Alberta, Canada: Alberta Society of Petroleum Geologists News Bulletin 1, 3-6.

IX: SELECTED BIBLIOGRAPHY

AGAT Laboratories, 1988, Table of formations of Alberta: AGAT Laboratories, Calgary.

Ala, M.A., 1974, Salt diapirism in southern Iran: Bulletin American Association of Petroleum Geologists 58, 1758-1770.

Alcock, F.G. and Benteau, R.I., 1976, Nipisi field - a middle Devonian clastic reservoir, *in* Lerand, M.M., Ed., The sedimentology of selected oil and gas reservoirs in Alberta: Canadian Society Petroleum Geologists, 1-24.

Anderson, N.L., 1986, An integrated geophysical/geological analysis of the seismic signatures of some western Canadian Devonian reefs: unpublished Ph.D. thesis, University of Calgary, 333 p.

Anderson, N.L., 1987, Clastic seismology: Petrel Robertson, Calgary, Alberta, 277 p. (Available through The University of Calgary Geology Library).

Anderson, N.L., 1990, An overview of some of the large scale mechanisms of salt dissolution: Kansas Geological Survey Open File Report 90-39.

Anderson, N.L., 1990, Exploration implications of salt dissolution: Kansas Geological Survey Open File Report 90-37.

Anderson, N.L., 1990, Hydrological, geological, biological, environmental, and exploration implications of salt dissolution: Kansas Geological Survey Open File Report 90-38.

Anderson, N.L., 1990, Paleo-restoration of leached salts: an overview of the methodology used in the reconstruction of the Wabamun salt, southern Alberta, Canada: Kansas Geological Survey Open File Report 90-36.

Anderson, N.L., 1992, Dissolution of the Wabamun Group salt: exploration implications, *in* Cavanaugh, T.D., Ed., Integrated exploration case histories, North America: The Geophysical Society of Tulsa Special Publication, in press.

Anderson, N.L., 1991, Reconstruction of the Elk Point salts in the Lloydminster area (T50-65, R15W3-R10W4M): Kansas Geological Survey Open File Report 91-56.

Anderson, N.L., 1991, Large scale mechanisms of salt dissolution: illustrated case histories: Kansas Geological Survey Open File Report 91-57.

Anderson, N.L., 1992, Reconstruction of the Leduc (Cairn) and Wabamun salts, Youngstown area, southern Alberta (T25-35, R5-20W4M): Kansas Geological Survey Open File Report 92-2.

Anderson, N.L. and Brown, R.J., 1987, The seismic signatures of some western

Canadian Devonian reefs: Journal Canadian Society Exploration Geophysics 1, 7-26.

Anderson, N.L. and Brown, R.J., 1992, Reconstruction of the Wabamun Group salts, southern Alberta, Canada, *in* Cavanaugh, T.D., Ed., Integrated exploration case histories, North America: The Geophysical Society of Tulsa Special Publication, in press.

Anderson, N.L. and Brown, R.J., 1991, Dissolution of the Wabamun and Black Creek salts: a seismic analysis: Geophysics 56, 618-627.

Anderson, N.L., Brown, R.J., Gendzwill, D.J., Hinds, R.C. and Lundberg, R.N., 1989, Elk Point carbonate reservoirs, *in* Anderson, N.L., Hills, L.V. and Cederwall, D.A., Eds., The geophysical atlas of western Canadian hydrocarbon pools: Canadian Society Exploration Geophysicists and Canadian Society Petroleum Geologists Special Publication, 27-66.

Anderson, N.L., Brown, R.J. and Hinds, R.C., 1988, A seismic perspective on the Panny and Trout fields of north-central Alberta: Canadian Journal Exploration Geophysics 24, 154-165.

Anderson, N.L., Brown, R.J. and Hinds, R.C., 1988, Geophysical aspects of Wabamun salt distribution in southern Alberta: Canadian Journal Exploration Geophysics 24, 166-178.

Anderson, N.L., Cederwall, D.A. and Hills, L.V., 1986, Carbonate seismology: Sigma Exploration Ltd., Calgary, Alberta. 194 p. (Available through the University of Calgary Geology Library).

Anderson, N.L., Chapman, J. and Brown, R.J., 1990, Paleo- reconstruction of the Wabamun Group salt in southern Alberta, Canada: report to the Geological Survey of Canada.

Anderson, N.L. and Chappell, F., 1987, Devonian salts and hydrocarbon traps: Petrel-Robertson, Calgary, Alberta, 113 p. (Available through The University of Calgary Geology Library).

Anderson, N.L. and Franseen, E.K., 1991, Differential compaction of Winnipegosis reefs: a seismic analysis: Geophysics 56, 142-147.

Anderson, N.L., White, D.G. and Hinds, R.C., 1989, Woodbend Group Reservoirs, *in* Anderson, N.L., Hills, L.V. and Cederwall, D.A., Eds., Geophysical atlas of western Canadian hydrocarbon pools: Canadian Society Exploration Geophysicists and Canadian Society Petroleum Geologists Special Publication, 101-132.

Anderson, R.Y. and Kirkland, D.W., 1980, Dissolution of salt deposits by brine density flow: Geology 8, 66-69.

Andrichuk, J.M. and Wonfor, J.S., 1953, Late Devonian geologic history in Stettler area, Alberta, Canada: Alberta Society of Petroleum Geologists News Bulletin 1, 3-5.

Angus, K., Wylie, J., McCloskey, W. and Noble, D., Paleozoic clastic reservoirs, *in* Anderson, N.L., Hills, L.V. and Cederwall, D.A., Eds., Geophysical atlas of western Canadian hydrocarbon pools: Canadian Society Exploration Geophysicists and Canadian Society Petroleum Geologists Special Publication, 1-26.

Baar C.A., 1974, Geological problems in Saskatchewan potash mining due to peculiar conditions during deposition of potash beds: Fourth Symposium on Salt, 2, 101-118.

Baar, C.A., 1977, Applied salt-rock mechanics 1: Elsevier Scientific Publishing Company, 294 p.

Baillie, A.D., 1953, Devonian System of the Williston basin area: Manitoba Mines Branch Publication 52-5.

Barrows, L. and Fett, J.D., 1985, A high-precision gravity survey in the Delaware Basin of southeastern New Mexico: Geophysics 50, 825-833.

Barss, D.L., Copland, A.B. and Ritchie, W.D., 1970, Geology of Middle Devonian reefs, Rainbow area, Alberta, Canada, *in* Halbouty, M.Y., Ed., Geology of giant petroleum fields: AAPG Memoir 14, 19-49.

Bathurst, R.G.C., 1975, Carbonate sediments and their diagenesis: Developments in Sedimentology 12, Elsevier, Amsterdam, 685 p.

Belyea, H.R., 1966, Woodbend, Winterburn and Wabamun Groups, *in* McCrossan, R.G. and Glaister, R.P., Eds., Geological history of western Canada, 2nd edition: Alberta Society Petroleum Geologists, 66-88.

Belyea, H.R. and Mclaren, D.J., 1957, Upper Devonian nomenclature in southern Alberta: Journal of Alberta Society of Petroleum Geologists 5, 166-182.

Bishop, 1974, Hummingbird structure, Saskatchewan, single vs multiple stage salt soultion-collapse, *in* Parslow, G.R., Ed., Fuels: a geologic appraisal: Saskatchewan Geological Society Special Publication, 2, 179-197.

Bishop, R.S., 1978, Mechanism for emplacement of piercement diapirs: Bulletin American Association of Petroleum Geologists 62, 1561-1583.

Boehner, R.C., 1985, Windsor Group salt and potash in Nova Scotia, Canada, *in* Schreiber, B.C. and Harner, H.L., Eds., Sixth International Symposium on Salt: Salt Institute Inc., Virginia, 1, 115-129.

Bond, G.C. and Kominz, M.A., 1984, Construction of tectonic subsidence curves for

the early Paleozoic miogeocline, southern Canadian Rocky Mountains: Implications for subsidence mechanisms, age of breakup, and crustal thinning: Bulletin Geological Society America 95, 155-173.

Braitsch, O., 1971, Salt deposits - their origin and composition: Springer, 297 p.

Brink, A.H., 1974, Petroleum geology of Gabon: AAPG Bulletin 58, 216-235.

Brown, R.J. and Anderson, N.L., 1991, On the question of lateral velocity variations over Leduc and Rainbow reefs: Journal Canadian Society Exploration Geophysics 27, 43-52.

Brown, R.J. and Anderson, N.L., 1992, An overview of salt dissolution and related hydrocarbon trapping potential in western Canada: AAPG Bulletin, submitted.

Brown, R.J., Anderson, N.L. and Hills, L.V., 1990, The seismic interpretation of Upper Elk Point (Givetian) carbonate reservoirs of western Canada: Geophysical Prospecting 38, 719-736.

Camsell, C., 1917, Salt and gypsum deposits of the region between Peace and Slave rivers, northern Alberta: Geological Survey, Sessional Paper 26, 134-145.

Carter, N.L. and Hansen, F.D., 1983, Creep of rock salt: Tectonophysics 92, 275-333.

Cederwall, D.A. and Anderson, N.L., 1991, A seismic and gravity study of salt dissolution at the Westhazel General Petroleums Pool, west-central Saskatchewan, Canada: Kansas Geological Survey Open File Report 90-46.

Cederwall, D.A. and Anderson, N.L., 1991, Westhazel General Petroleums Pool, east-central Alberta, Canada: SEG Annual Meeting Expanded Technical Program Abstracts, 184-187.

Christiansen, E.A., 1967, Collapse structures near Saskatoon, Saskatchewan, Canada: Canadian Journal of Earth Sciences 4, 757-767.

Christianson, E.A., 1971, Geology of the Crater Lake collapse structure in southeastern Saskatchewan: Canadian Journal Earth Science 8, 1505-1513.

Coates, G.K., Lee, C.A., McClain, W.C. and Senseny, P.E., 1985, Closure and collapse of man-made cavities in salt, *in* Schreiber, B.C. and Harner, H.L., Eds., Sixth International Symposium on Salt: Salt Institute Inc., Virginia, 2, 139-157.

Crandall, S.H., Dahl, N.C. and Lardner, T.J., 1972, An Introduction to the Mechanics of Solids: McGraw-Hill, New York, 628 p.

Czapowski, G., 1987, Sedimentary facies of the oldest rock salt (Na1) of the Leba elevation (northern Poland), *in* Peryt, T.M., Ed., The Zechstein facies in Europe:

Springer-Verlag, New York, 207-224.

Davies, P.B., 1985, Structural characteristics of a deep-seated dissolution-subsidence chimney in bedded salt, in Sixth International Symposium on Salt: The Salt Institute, Alexandria, Virginia, 1, 331-350.

Davies, P.B., 1989, Assessing deep-seated dissolution-subsidence hazards at radioactive-waste repository sites in bedded salt, *in* Johnson, A.M., Burnham, C.W., Allen, C.R. and Muehlberger, W., Eds., Richard H. Jahns Memorial Volume: Engineering Geology 27, 467-487.

Davis, D.M., 1987, Thin-skinned deformation over salt: Dynamical Geology of Salt and Related Structures, 301-337.

Dellwig, L.F., 1963, Environment and mechanics of deposition of the Permian Hutchinson Salt Member of the Wellington Shale, *in* Symposium on salt: Northern Ohio Geological Society, Cleveland, 74-85.

DeMille, G., Shouldice, J.R. and Nelson, H.W., 1964, Collapse structures related to evaporites of the Prairie Formation, Saskatchewan: Bulletin Geological Society of America 75, 307-316.

Dibner, V.D., Mitin, N.Y., Rozhdestvenskaya, I.I., Seryakov, M.M. and Ustinova, L.A., 1986, Geologic structure and halokinesis on the continental margin of Angola: International Geology Review, 444-448.

Dutton, A.R., 1989, Hydrogeochemical processes involved in salt-dissolution zones, Texas Panhandle, U.S.A.: Hydrological Processes 3, 75-89.

Dutton, A.R., 1987, Hydrogeologic and hydrochemical properties of salt-dissolution zones, Palo Duro Basin. Texas Panhandle - preliminary assessment: Bureau of Economic Geology, The University of Texas at Austin, Geological Circular 87-2, 32 p.

Dutton, A.R., 1989, Hydrochemical processes involved in salt-dissolution zones, Texas Panhandle, U.S.A.: Hydrological Processes 3, 75-89.

Ege, J.R., 1979, Surface subsidence and collapse in relation to extraction of salt and other soluable evaporites; USGS Open-file Report 79-1666.

Ehrets, J.R. and Kissling, D.L., 1987, Winnipegosis platform margin and pinnacle reef reservoirs, northwest North Dakota, *in* Fischer, D.W., Ed., Core workshop volume, Fifth international Williston Basins symposium, North Dakota Geological Survey, Miscellaneous Series 69, 1-31.

Evans, R., 1987, Pathways of migration of oil and gas in the South Mississippi Salt Basin: Transactions Gulf Coast Association Geological Societies 37, 75-86.

Fader, S.W., 1975, Land subsidence caused by dissolution of salt near four oil and gas wells in central Kansas: U.S. Geological Survey, Water Resources Investigations 27-75, 28 p.

Friedman, G.M., 1978, Principles of sedimentology: John Wiley and Sons, 792 p.

Garfunkel, Z. and Almagor, G., 1987, Active salt dome development in the Levant Basin, southeast Mediterranean: Dynamical Geology of Salt and Related Structures, 263-300.

Gendzwill, D.J., 1978, Winnipegosis mounds and Prairie Evaporite Formation of Saskatchewan seismic study: AAPG Bulletin 62, 73-86.

Gendzwill, D.J. and Hajnal, Z., 1971, Seismic investigation of the Crater Lake collapse structure in southeastern Saskatchewan: Canadian Journal Earth Science 8, 1514-1524.

Gendzwill, D.J. and Lundberg, R.M., 1989, Upper Elk Point carbonate reservoirs, part B: Winnipegosis carbonates, *in* Anderson, N.L., Hills, L.V. and Cederwall, D.A., Eds., Geophysical atlas of western Canadian hydrocarbon pools: Canadian Society Exploration Geophysicists and Canadian Society Petroleum Geologists Special Publication, 52-66.

Gendzwill, D.J. and Wilson, N.L., 1987, Form and distribution of Winnipegosis mounds in Saskatchewan, *in* Peterson, J.A., Kent, D.M., Anderson, S.B., Pilatzke, R.H. and Longman, M.W., Eds., Williston Basin; Anatomy of a Cratonic Oil Province: Rocky Mountain Association Geologists, Denver, 109-117.

Gobran, G.R and Miyamoto, S., 1985, Dissolution rate of gypsyum in aqueous salt solutions: Soil Science 140, 2, 89-93.

Gogel, T., 1981, Discharge of saltwater from Permian rocks: Kansas Geological Survey Chemical Quality Series 9, 60 p.

Goldstein, A.G., 1981, Brittle deformation associated with salt dissolution, Palo Duro Basin, *in* Gustavsan, T.C. and others, Eds., Geology and Geohydrology of the Palo Duro Basin, Texas Panhandle, University of Texas (Austin), Bureau of Economic Geology Geological Circular 82-7, p 18-27.

Gorrel, H.A. and Alderman, G.R., 1968, Elk Point Group saline basins of Alberta, Saskatchewan and Manitoba, Canada, *in* Mattox, R.B., Ed., Saline Deposits: Geological Society America Special Paper 88, 291-317.

Goudie, A.S., (Undated), Salt tectonics and geomorphology: University of Oxford, 597-605.

Gravenor, C.P., Green, R. and Godfrey, J.D., 1960, Karst topography, in Air photographs of Alberta, Bulletin Research Council of Alberta 5, 21-22.

Gulliver, T.W., 1985, Saline dissolution collapse in the Piceance Creek Basin: Colorado School of Mines, 47-57.

Gustavson, T.C., 1986, Geomorphic development of the Canadian River Valley, Texas Panhandle: An example of regional salt dissolution and subsidence: Bulletin Geological Society of America 97, 459-472.

Gustavson, T.C., Simpkins, W.W., Alhades, A. and Hoadley, A., 1982, Evaporite dissolution and development of karst features on the rolling plains of the Texas Panhandle: Earth Surface Processes and Landforms 7, 545-563.

Gustin, J.D., 1985, Energy storage in salt, *in* Schreiber, B.C. and Harner, H.L., Eds., Sixth International Symposium on Salt: Salt Institute Inc., Virginia, 2, 177-182.

Hamilton, W.N., 1971, Salt in east-central Alberta: Research Council Alberta Bulletin 29.

Haddenhorst, H.G., Quast, P., 1985, Underground storage of natural gas in West Germany, *in* Schreiber, B.C. and Harner, H.L., Eds., Sixth International Symposium on Salt: Salt Institute Inc., Virginia, 2, 203-210.

Halbouty, M.T., 1979, Salt domes: Gulf Publishing Company, Houston, 561 p.

Hamilton, W.N., 1971, Salt in east-central Alberta: Research Council of Alberta Bulletin 29, 53 p.

Hitchon, B., 1969, Fluid flow in the western Canada sedimentary basin: Water Resources Research 5, 186-195.

Holdoway, K.A., 1978, Deposition of evaporites and red beds of the Nipewalla Group, Permian, western Kansas: Kansas Geological Survey Bulletin 215.

Holter, M.E., 1969, The Middle Devonian Prairie Evaporite of Saskatchewan: Saskatchewan Department Mineral Resources Report 123.

Hopkins, J.C.,1987, Contemporaneous subsidence and fluvial channel sedimentation: Upper Mannville C pool, Berry field, Lower Cretaceous of Alberta: AAPG Bulletin 71, 334-345.

Horner, R.B. and Hasegawa, H.S., 1987, The seismotectonics of southern Saskatchewan: Canadian Journal Earth Science 15, 1341-1355.

Hriskevich, M.E., 1970, Middle Devonian reef production, Rainbow area, Alberta, Canada: AAPG Bulletin 54, 2260-2281.

Hsu, K.J., Cita, M.B. and Ryan, W.B.F., 1973, The origin of the Mediterranean

evaporites, *in* Initial Reports of the Deep Sea Drilling Project, 13: U.S. Government Printing Office, Washington, D.C., 1203-1233.

Huh, J.M., Briggs, L.I. and Gill, D., 1977, Depositional environments of pinnacle reefs, Niagara and Salina groups, northern shelf, Michigan Basin, *in* Fisher, J.H., Ed., Reefs and evaporites - concepts and depositional models: AAPG Studies in Geology No. 5, 1-21.

Humphris, Jr., C.C., 1979, Salt movement on continental slope, northern Gulf of Mexico: Bulletin American Association of Petroleum Geologists 63, 782-798.

Imperial Oil Ltd., Western Division, Geological Staff, 1950, Devonian nomenclature in Edmonton area, Alberta, Canada: AAPG Bulletin 34, 1807-1825.

Jackson, M.P.A. and Talbot, C.J., 1986, External shapes, strain rates, and dynamics of salt structures: Bulletin Geological Society of America 97, 305-323.

Jackson, M.P.A. and Talbot, C.J., 1985, Reinterpretation of the internal structure of Palangana Salt Dome, South Texas: Bulletin, South Texas Geological Society 25, 37-48.

Jenyon, M.K., 1984, Seismic response to collapse structures in the Southern North Sea: Marine and Petroleum Geology 1, 27-36.

Jenyon, M.K., 1985, Basin-edge diapirism and updip salt flow in Zechstein of southern North Sea: Bulletin American Association Petroleum Geologists 69, 53-64.

Jenyon, M.K., 1985, Fault-associated salt flow and mass movement: Journal Geological Society 142, 547-553.

Jenyon, M.K., 1986, Some consequences of faulting in the presence of a salt rock interval: Journal of Petroleum Geology 9, 29-52.

Jenyon, M.K., 1986, Salt tectonics: Elsevier Applied Science Publishers, 191 p.

Jenyon, M.K., 1987, The development by salt diapirs of superficial overhang features, and effects on associated sediments: Dynamical Geology of Salt and Related Structures, 679-709.

Jenyon, M.K., 1988, Fault-salt wall relationships, southern N. Sea: Oil & Gas Journal, 76-81.

Jenyon, M.K., 1988, Seismic expression of salt dissolution-related features in the North Sea: Bulletin Canadian Petroleum Geology 36, 274-283.

Jenyon, M.K., 1989, Plastic flow and contraflow in superposed Zechstein salt sequences: Journal of Petroleum Geology 12, 477-486.

Jenyon, M.K. and Cresswell, P.M., 1987, The Southern Zechstein salt basin of the British North Sea, as observed in regional seismic traverses: Petroleum Geology North West Europe, 277-292.

Jenyon, M.K., Cresswell, P.M. and Taylor, J.C.M., 1984, Nature of the connection between the Northern and Southern Zechstein Basins across the Mid North Sea High: Marine and Petroleum Geology 1, 355-363.

Jenyon, M.K. and Goudswaard, W. 1989, Geological concepts and seismic interpretation examples from the EAEG Seismic Atlas: First Break 7, 437-446.

Jenyon, M.K. and Taylor, J.C.M., 1987, *in* Peryt, T.M., Ed., The Zechstein facies in Europe: Springer-Verlag, New York, 51-76.

Johnson, K.S., 1981, Dissolution of salt on the east flank of the Permian Basin in the southwestern U.S.A.: Journal of Hydrology 54, 75-93.

Johnson, K.S., 1989, Development of the Wink Sink in West Texas, U.S.A., due to salt dissolution and collapse: Environmental Geology and Water Science 2, 81-92.

Johnson, R.B. and DeGraff, J.V., 1988, Principles of Engineering Geology: John Wiley and Sons, New York, 497 p.

Jones, l., 1965, The Middle Devonian Winnipegosis Formation of Saskatchewan: Saskatchewan Department Mineral Resources Report 98, 101 p.

Jordan, S.P., 1967, Saskatchewan reef trend looks big: Oilweek, 17, 10-12.

Jordan, S.P., 1968, Will Zama be duplicated at Quill Lake Saskatchewan: Oilweek, 19, 10-12.

Karably, L.S., 1985, High integrity isolation of industrial waste in salt, *in* Schreiber, B.C. and Harner, H.L., Eds., Sixth International Symposium on Salt: Salt Institute Inc., Virginia, 2, 211-216.

Kashfi, M.S., 1985, The pre-Zagros integrity of the Iranian platform, Journal Petroleum Geology 8, 353-360.

Keary, P. and Brooks, M., 1984, An introduction to geophysical exploration: Blackwell Scientific Publications, Boston, 296 p.

Knapp, R.W. and Steeples, D.W., 1981, Investigation of salt dissolution collapse using high-resolution MiniSOSIE reflection seismology: EOS, Transactions American Geophysical Union 62, 954-955.

Knapp, R.W., Steeples, D.W., Miller, R.D. and McElwee, C.D., 1989, Seismic reflection at sinkholes; *in* Steeples, D.W., Ed., Geophysics in Kansas: Kansas Geological Survey Bulletin 226, 95-116.

Knuth, M., Jackson, J.L. and Whittemore, D.O., 1990, An integrated approach to identifying the salinity source contaminating a ground-water supply: Ground Water 28, 207-214.

Koestler, A.G. and Ehrmann, W.U., 1987, Fractured chalk overburden of a salt diapir, Laegerdorf, NW Germany - exposed example of a possible hydrocarbon reservoir: Dynamical Geology of Salt and Related Structures, 457-477.

Kupfer, D.H., 1989, Gypsum dehydration, agent of salt diapirism: Transactions Gulf Coast Association of Geological Societies 34, 171-181.

Langbein, R., 1987, The Zechstein sulfates: the state of the art, *in* Peryt, T.M., Ed., The Zechstein facies in Europe: Springer-Verlag, New York, 143-188.

Langstroth, W.T., 1971, Seismic study along a portion of the Devonian salt front in North Dakota: Geophysics 36, 330-338.

Law, J., 1955, Geology of northwestern Alberta and adjacent areas (with Discussion and Reply): AAPG Bulletin 39, 1927-1978.

Lerche, I. and O'Brien, J.J., 1987, Modelling of buoyant salt diapirism: Dynamical Geology of Salt and Related Structures, 129-259.

Light, M.P.R. and Posey, H.H., 1987, Model for the origins of geopressured brines, hydrocarbons, cap rocks and metallic mineral deposits: Gulf Coast, U.S.A.: Dynamical Geology of Salt and Related Structures, 787-830.

Lindsay, J.F., 1977, Salt tectonism and the evolution of the Sigsbee Scarp, Gulf of Mexico: Tectonophysics 39, 607-619.

Lindsay, J.F., 1987, Upper Proterozoic evaporites in the Amedeus Basin, central Australia, and their role in basin tectonics: Geological Society of America Bulletin 99, 852-865.

Lohmann, H.H., 1972, Salt dissolution in subsurface of British North Sea as interpreted from seismograms: AAPG Bulletin 56, 3, 472-479.

Lohmann, H.H., 1979, Seismic recognition of salt diapirs: AAPG Bulletin 63, 2097-2102.

Martinez, J.D., 1985, Energy programs - a contribution to salt dome knowledge, *in* Schreiber, B.C. and Harner, H.L., Eds., Sixth International Symposium on Salt: Salt Institute Inc., Virginia, 2, 235-248.

McCrossan, R.G. and Glaister, R.P., 1966, Geological history of western Canada, 2nd ed.: Alberta Society of Petroleum Geologists.

McLaren, D.J., 1955, Devonian formations in the Alberta Rocky Mountains between Bow and Athabasca Rivers: Geological Survey of Canada Bulletin 35, 59 p.

McTavish, G.J. and Vigrass, L.W., 1987, Salt dissolution and tectonics, south-central Saskatchewan: Saskatchewan Geological Society, Fifth International Williston Basin Symposium 9, 157-168.

Meijer Drees, N.C., 1986, Evaporitic deposits of western Canada: Geological Survey of Canada Paper 85-20, 118 p.

Melvin, J.L. (Editor), 1991, Evaporites, Petroleum and Mineral Resources; Elsevier, New York, 556 p.

Merriam, D.F., 1963, The Geologic History of Kansas: Kansas Geological Survey Bulletin 162, 317 p.

Miller, R.D., Steeples, D.W., Myers, P. and Somanas, D., 1988, Seismic reflection surveys at the Knackstedt salt-water disposal well: Kansas Geological Survey Open File Report 88-31.

Miller, R.D., Steeples, D.W. and Treadway, J.A., 1985, Seismic reflection survey at a sinkhole in Ellsworth County, Kansas: Society of Exploration Geophysicists, 55th annual meeting, Washington D.C., 154-156.

Mossop, G.D., 1972, Origin of the peripheral rim, Redwater reef, Alberta: Bulletin Canadian Society Petroleum Geology 20, 238-280.

Mylroie, J.E. and Carew, J.L., 1990, The flank margin model for dissolution cave development in carbonate platforms: Earth Surface Processes and Landforms 15, 413-424.

Nieto, A.S., Stump, D. and Russell, D.G., 1985, A mechanism for sinkhole development above brine cavities in the Windsor-Detroit area, *in* Schreiber, B.C. and Harner, H.L., Eds., Sixth International Symposium on Salt: Salt Institute Inc., Virginia, 1, 351-367.

Nurmi, R.D. and Friedman, G.M., 1977, Sedimentology and depositional environments of basin-center evaporites, Lower Salina Group (Upper Silurian), Michigan Basin, *in* Fisher, J.H., Ed., Reefs and evaporites - concepts and depositional models: AAPG Studies in Geology No. 5, 23-52.

O'Brien, J.J. and Lerche, I., 1984, The influence of salt domes on paleo-temperature distributions, Geophysics 49, 2032-2043.

O'Brien, J.J. and Lerche, I., 1987, Heat flow and thermal maturation near salt diapirs: Dynamical Geology of Salt and Related Structures, 711-749.

O'Brien, J.J. and Lerche, I., 1987, Modelling of the deformation and faulting of

formations overlying an uprising salt dome: Dynamical Geology of Salt and Related Structures, 419-455.

O'Brien, J.J. and Lerche, I., 1988, Impact of heat flux anomalies around salt diapirs and salt sheets in the Gulf Coast on hydrocarbon maturity: models and observations: Transactions Gulf Coast Association of Geological Societies 38, 231-243.

Oliver, J.A. and Cowper, N.W., 1983, Wabamun salt removal and shale compaction effects, Rumsey area, Alberta: Bulletin Canadian Society Petroleum Geology 31, 161-168.

Orchard, D.M., 1987, Structural history of Poplar Dome and the dissolution of Charles Formation salt, Roosevelt County, Montana, Saskatchewan Geological Society, Fifth International Williston Basin Symposium, 169-177.

Parker, J.M., 1967, Salt solution and subsidence structures, Wyoming, North Dakota, and Montana: Bulletin American Association of Petroleum Geologists 51, 1929-1947.

Perrin, N.A.,1982, Environments of deposition and diagenesis of the Winnipegosis Formation (Middle Devonian), Williston Basin, North Dakota, *in* Christopher, J.E. and Kaldi, J, Eds., Proceedings of the Fourth International Williston Basin Symposium, 51-66.

Perrodon, A., 1983, Dynamics of oil and gas accumulations: Elf-Aquitaine, France, 368 p.

Peryt, T.M., Introduction, *in* Peryt, T.M., Ed., The Zechstein facies in Europe: Springer-Verlag, New York, 143-188.

Pfiffner, O.A. and Ramsay, J.G., 1982, Constraints on geological strain rates: arguments from finite strain states of naturally deformed rocks: Journal Geophysical Research 87, 311-321.

Posey, H.H., 1986, Isotope geochemistry of the Hockley Dome cap rock, *in* Comparison of cap rocks, mineral resources, and surface features of salt domes in the Houston diapir province: Geological Society of America and Society of Economic Geology Special Publication, 185-207.

Posey, H.H, Kyle, J. R., Jackson, T.J. and Hurst, S.D., 1987, Multiple fluid components of salt diapirs and salt dome cap rocks, Gulf Coast, U.S.A.: Applied Geochemistry 2, 523-534.

Prats, M., 1966, The effect of horizontal fluid flow on thermally induced convection currents in porous mediums: Journal of Geophysical Research 71, 4835-4838.

Pray, L.C., 1960, Compaction in calcilutites: Bulletin Geological Society America 71,

1946.

Precht, G.D., 1983, Reservoir development and hydrocarbon potential of Winnipegosis (Middle Devonian) pinnacle reefs, southern Elk Point Basin, North Dakota, *in* Carbonates and Evaporites: Northeastern Science Foundation, 1, 83-99

Preece, D.S. and Foley, J.T., 1985, Finite element analysis of salt caverns employed in the strategic petroleum reserve, *in* Schreiber, B.C. and Harner, H.L., Eds., Sixth International Symposium on Salt: Salt Institute Inc., Virginia, 2, 49-64.

Quast, P. and Schmidt, M.W., 1985, Disposal of medium- and low-level radioactive waste (MLW/LLW) in leached caverns, *in* Schreiber, B.C. and Harner, H.L., Eds., Sixth International Symposium on Salt: Salt Institute Inc., Virginia, 2, 217-234.

Ramberg, H., 1968, Fluid dynamics of layered systems in the field of gravity, a theoretical basis for certain global structures and isostatic adjustment: Physics of the Earth and Planetary Interiors 1, 63-87.

Ranade, D.H. and Gupta, Ram K., 1990, Prediction of water requirement for gypsum dissolution in a calcareous clay soil and evaluation of dissolution rate constant: Journal Indian Society Soil Science 38, 353-354.

Reimer, D.A., 1989, Mississippian reservoirs, *in* Anderson, N.L., Hills, L.V. and Cederwall, D.A., Eds., The geophysical atlas of western Canadian hydrocarbon pools: Canadian Society Exploration Geophysicists and Canadian Society Petroleum Geologists Special Publication, 187-216.

Reinson, G.E. and Wardlaw, N.C., 1972, Nomenclature and stratigraphic relationships, Winnipegosis and Prairie Evaporite formations, central Saskatchewan: Bulletin Canadian Petroleum Geology 20, 301-320.

Ricken, W., 1986, Diagenetic bedding: A model for marl-limestone alternations: Lecture Notes in Earth Sciences, Springer-Verlag, New York, 210 p.

Richter-Bernburg, G., 1987, Deformation within salt bodies: Dynamical Geology of Salt and Related Structures, 39-75.

Robson, S.G. and Saulnier, G.J., 1981, Hydrochemistry and simulated solute transport, Piceance Basin, Northwest Colorado: Geological Survey Professional Paper 1196, United States Government Printing Office, Washington, 65 p.

Rokar, R.B. and Staudtmeister, K., Creep rupture criteria for rock salt, *in* Schreiber, B.C. and Harner, H.L., Eds., Sixth International Symposium on Salt: Salt Institute Inc., Virginia, 1, 455-462.

Romer, M.M. and Neugebauer, H.J., 1991, The salt dome problem: a multilayered approach: Journal of Geophysical Research, 96, 2389-2396.

Roulston, B.V. and Waugh, D.C.E., 1985, Stratigraphic comparison of the Mississippian potash deposits in New Brunswick, Canada, *in* Schreiber, B.C. and Harner, H.L., Eds., Sixth International Symposium on Salt: Salt Institute Inc., Virginia, 1, 115-129.

Russo, A.J., 1985, Solution mining calculations for SPR caverns, *in* Schreiber, B.C. and Harner, H.L., Eds., Sixth International Symposium on Salt: Salt Institute Inc., Virginia, 1, 101-109.

Schreiber, B.C. and Harner, H.L., Eds., Sixth International Symposium on Salt, Salt Institute Inc., Virginia, 1, 99-113.

Schwerdtner, W.M., 1986, Identification of evaporite diapirs formed under the influence of horizontal compression: Bulletin Canadian Petroleum Geology 34, 271-276.

Schwerdtner, W.M., Torrance, J.G. and van Berkel, J.T., 1989, Pattern of apparent total strain in the bedded anhydrite cap of a folded salt wall: Canadian Journal Earth Science 26, 983-992.

Seni, S.J. and Jackson, M.P.A., 1984, Sedimentary record of Cretaceous and Tertiary salt movement, East Texas Basin: Times, rates, and volumes of salt flow and their implications to nuclear wate isolation and petroleum exploration: The University of Texas at Austin Bureau of Economic Geology Report of Investigations 139, 89 p.

Sherwin, D.F., 1962, Lower Elk Point section in east-central Alberta: Journal of the Alberta Society of Petroleum Geologists 10, 185-191.

Shinn, E.A. and Robbin, D.M., 1983, Mechanical and chemical compaction in fine-grained shallow-water limestones: Journal Sedimentary Petrology 53, 595-618.

Shinn, E.A, Halley, R.B., Hudson, J.H. and Lidz, B.H., 1977, Limestone compaction: An enigma: Geology 5, 21-24.

Simpkins, W.W., Gustavson, T.C., Alhades, A.B. and Hoadley, A.D., 1981, Impact of evaporite dissolution and collapse on highways and other cultural features in the Texas Panhandle and eastern New Mexico: Bureau of Economic Geology, Geological Circular 81-4, 23 p.

Simpson, F., 1984, Potential for additional hydrocarbon recovery from the Colorado and Montana groups (Cretaceous) of Saskatchewanin Lorsong, J.A. and Wilson, M.A., Eds., Oil and Gas in Saskatchewan, Special Publication 7, Saskatchewan Geological Society, 211-244.

Smith, D.G. and Pullen, J.R., 1967, Hummingbird structure of southeast Saskatchewan: Bulletin Canadian Petroleum Geology 15, 468-482.

Spiers, C.J., Urai, J.L. and Lister, G.S., 1984, the effect of brine (inherent or added) on rheology and deformation mechanisms in salt rock in Mechanical behavior of salt Federal Institue for Geosciences and Natural Resources, Hanover, Federal Republic of Germany, 89-101.

Steeples, D.W., Knapp, R.W. and McElwee, C.D., 1983, Seismic reflection surveys of a catastrophically collapsed sinkhole, Ellis County, Kansas: SEG Expanded Abstracts, 296-298.

Steeples, D.W., Knapp, R.W. and McElwee, C.D, 1986, Seismic reflection investigations of sinkholes beneath interstate highway 70 in Kansas: Geophysics 51, 295-301.

Steeples, D.W., Knapp, R.W. and Miller, R.D., 1984, Examination of sinkholes by reflection seismology, *in* Beck, B.F., Ed., Sinkholes - their geology, Engineering and Environmental Impact: Proceedings of the First Multidisciplinary Conference on Sinkholes, Orlando, Florida, 15-17 October, 217-223.

Steeples, D. and Miller R.D., 1987, Direct detection of shallow subsurface voids using high-resolution seismic-refleciton techniques, *in* Beck, B.F. and Wilson, W.L., Eds., Karst hydrogeology: engineering and environmental applications: Second Multidisciplinary Conference on Sinkholes and Environmental Impacts of Karsts, 179-183.

Stormont, J.C., 1990, Discontinuous behaviour near excavations in a bedded salt formation: International Journal of Mining and Geological Engineering, 8, 35-56.

Talbot, C.J. and Jackson, M.P.A., 1987, Internal Kinematics of salt diapirs: Bulletin American Association Petroleum Geologists 71, 1068-1093.

Talbot, C.J. and Jarvis, R.J., 1984, Age, budget and dynamics of an active salt extrusion in Iran: Journal Structural Geology 6, 521-533.

Talbot, C.J., Koyi, H., Sokoutis, D. and Mulugeta, G., 1988, Identification of evaporite diapirs formed under the influence of horizontal compression: a discussion: Bulletin Canadian Petroleum Geology 36, 91-95.

Thomas, G.E., 1974, Lineament-block tectonics: Williston-Blood Creek basin: Bulletin American Association Petroleum Geologists 58, 1305-1322.

Thurston, D.K. and Lothamer, R.T., 1991, Seismic evidence of evaporite diapirs in the Chukchi Sea, Alaska: Geology 19, 477-480.

Tùth, J., 1978, Gravity-induced cross-formational flow of formation fluids, red earth region, Alberta, Canada: analysis, patterns, and evolution: Water Resources Research 14, 805-843.

Tùth, J., 1963, A theoretical analysis of groundwater flow in small drainage basins:

Journal of Geophysical Research 68, 4795-4812.

Tùth, J., 1962, A theory of groundwater motion in small drainage basins in central Alberta, Canada 67, 4375-4387.

Urai, J.L., Spiers, C.J., Zwart, H.J. and Lister, G.S., 1986, Weakening of rock salt by water during long-term creep: Nature 324, 554-557.

Walters, R.F., 1978, Land subsidence in central Kansas related to salt dissolution: Kansas Geological Survey Bulletin 214, 82p.

Wassmann, T.H., 1985, Cavity utilization in the Netherlands, *in* Schreiber, B.C. and Harner, H.L., Eds., Sixth International Symposium on Salt: Salt Institute Inc., Virginia, 2, 191-201.

Wardlaw, N.C. and Reinson, G.E., 1971, Carbonate and evaporite deposition and diagenesis, Middle Devonian Winnipegosis and Prairie Evaporite formations of south-central Saskatchewan: AAPG Bulletin 55, 1759-1786.

Warren, J.K., 1989, Evaporite Sedimentology: Prentice-Hall, Eaglewood Cliffs, N.J., p.

Waugh, D.C.E. and Urquhart, B.R., 1985, The geology of Denison-Potcan's New Brunswick potash deposit, *in* Schreiber, B.C. and Harner, H.L., Eds., Sixth International Symposium on Salt: Salt Institute Inc., Virginia, 1, 85-98.

White, W.M. and Spiers, C.A., 1985, Characterization of salt domes for storage and waste disposal, *in* Schreiber, B.C. and Harner, H.L., Eds., Sixth Inter-national Symposium on Salt: Salt Institute Inc., Virginia, 1, 511-544.

Williams, G.K., 1977, The Hay River Formation and its relationship to adjacent formations, Slave River map-area, N.W.T.: Geological Survey of Canada Paper 75-12, 17 p.

Wilmot, B.R., 1985, The geology of the Lower Cretaceous Mannville Group, Edam, Saskatchewan: unpublished M.Sc. thesis, University of Calgary, 160 p.

Wilson, N.L., 1984, The Winnipegosis Formation of south-central Saskatchewan, in Lorsong, J.A. and Wilson, M.A., Eds., Oil and Gas in Saskatchewan: Saskatchewan Geological Society Special Publication 7, 13-15.

Wirnkar, F.T. and Anderson, N.L., 1989, Seismic analysis of the differential compaction of reef and off-reef sediments: Expanded Abstracts, SEG Annual Meeting, 888-890.

Wonfor, J.S. and Andrichuk, J.M., 1953, Upper Devonian in the Stettler area, Alberta, Canada: Alberta Society of Petroleum Geologists News Bulletin 1, 3-6.

Yuanxiong, L. and Ghengxun, N., 1985, Technical development of solution mining in thinly bedded rock salt deposits of Ziliujing, Sichuan, China, *in* Schreiber, B.C. and Harner, H.L., Eds., Sixth International Symposium on Salt: Salt Institute Inc., Virginia, 1, 87-99.

Yanshin, A.L., Ed., 1984, Paleozoic Salt Bearing Formations of the World: Springer-Verlag, 427 p. (Original text authored by Zharkov, M.A.)